Mediators of Inflammation

The Role of Inflammation in the Pathophysiology of Cardiovascular Diseases

Lead Guest Editor: Azizah Ugusman
Guest Editors: Simon Kennedy, Amilia Aminuddin, and Dominik Skiba

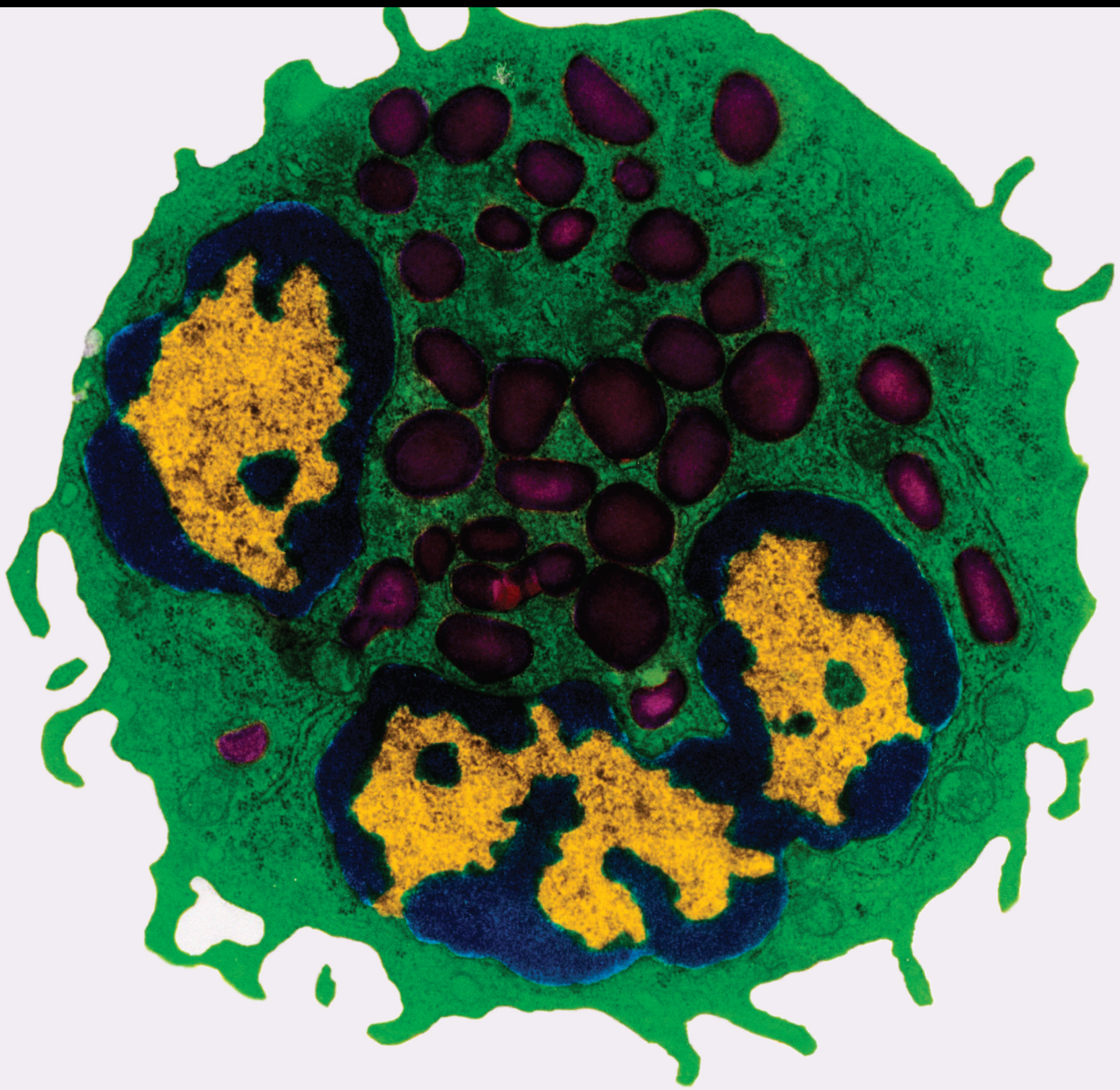

The Role of Inflammation in the Pathophysiology of Cardiovascular Diseases

The Role of Inflammation in the Pathophysiology of Cardiovascular Diseases

Lead Guest Editor: Azizah Ugusman
Guest Editors: Simon Kennedy, Amilia Aminuddin, and Dominik Skiba

Contents

Hindawi
Mediators of Inflammation
Volume 2022, Article ID 2734321, 16 pages
https://doi.org/10.1155/2022/2734321

Review Article

Exploring the Relationship of Perivascular Adipose Tissue Inflammation and the Development of Vascular Pathologies

Afifah Zahirah Abd Rami,[1] **Adila A. Hamid**,[1] **Nur Najmi Mohamad Anuar**,[2] **Amilia Aminuddin**,[1] **and Azizah Ugusman**[1]

[1]*Department of Physiology, Faculty of Medicine, Universiti Kebangsaan Malaysia, Jalan Yaacob Latif, Cheras, 56000 Kuala Lumpur, Malaysia*
[2]*Center for Toxicology & Health Risk Studies, Faculty of Health Sciences, Universiti Kebangsaan Malaysia, Jalan Raja Muda Abd Aziz, 50300 Kuala Lumpur, Malaysia*

Correspondence should be addressed to Amilia Aminuddin; amilia@ppukm.ukm.edu.my and Azizah Ugusman; dr.azizah@ppukm.ukm.edu.my

Received 1 October 2021; Revised 11 January 2022; Accepted 21 January 2022; Published 8 February 2022

Academic Editor: Agnieszka Dobrzyn

Initially thought to only provide mechanical support for the underlying blood vessels, perivascular adipose tissue (PVAT) has now emerged as a regulator of vascular function. A healthy PVAT exerts anticontractile and anti-inflammatory actions on the underlying vasculature via the release of adipocytokines such as adiponectin, nitric oxide, and omentin. However, dysfunctional PVAT produces more proinflammatory adipocytokines such as leptin, resistin, interleukin- (IL-) 6, IL-1β, and tumor necrosis factor-alpha, thus inducing an inflammatory response that contributes to the pathogenesis of vascular diseases. In this review, current knowledge on the role of PVAT inflammation in the development of vascular pathologies such as atherosclerosis and hypertension was discussed.

1. Introduction

Cardiovascular diseases (CVD) have been widely known for decades as the leading cause of mortality worldwide. According to the World Health Organization (WHO), in 2019, an estimated 17.9 million deaths due to CVD were recorded, representing 32% of global deaths [1]. This alarming situation raises the importance of investigating the pathophysiological aspects of CVD. Perivascular adipose tissue (PVAT) surrounds most blood vessels and has been implicated in the pathophysiology of CVD due to its proximity and crosstalk with the underlying vasculature, with PVAT inflammation suggested to be contributing to the development of vascular diseases. A link between PVAT, inflammation, and CVD was first discovered two decades ago when a study showed an increase in leukocyte infiltration in the PVAT in response to coronary angioplasty [2]. This signifies the role of PVAT inflammation in the pathophysiology of CVD and as a potential future therapeutic target.

2. Perivascular Adipose Tissue

PVAT consists of adipocytes that surround most systemic blood vessels, except the cerebral vasculature [3]. Structurally, PVAT consists of adipocytes, fibroblasts, stem cells, lymphocytes, and macrophages. The characteristics of PVAT differ in different anatomical sites. For example, thoracic aorta PVAT (tPVAT) and abdominal aorta PVAT (aPVAT) are two subtypes of PVAT which possess different phenotypes and functions. In rodents, tPVAT's characteristics are more similar to brown adipose tissue (BAT), while aPVAT is phenotypically a mixture of white adipose tissue (WAT) and BAT, whereas in humans, coronary PVAT's characteristics are more similar to WAT [4–6]. tPVAT is mainly

involved in lipolysis and heat generation and facilitates vascular relaxation via adipokine release, whereas aPVAT is involved in lipid storage and cytokine secretion and contains more macrophages and immune cells [7]. Hence, aPVAT is regarded to be more prone to proinflammatory activity and is proatherogenic compared to tPVAT.

Studies have shown that each type of adipocyte is derived from a specific precursor and is differentiated at separate times during embryogenesis [8, 9]. Most white adipocytes are differentiated from $Myf5^+$ and $PAX3^+$ precursors or $Myf5^-/Pax3^+$, while brown adipocytes are derived from paraxial mesoderm $Myf5^+/Pax3^+/Pax7^+/En1^+$, a common precursor of myocytes [10]. Peroxisome proliferator-activated receptor- (PPAR-) γ is a transcription factor that is involved in the regulation of gene expression and differentiation of adipocytes [11]. Deletion of PPAR-γ during BAT adipogenesis impairs PVAT development and increases local inflammation, which often leads to the progression of atheromatous plaque and myocardial injury in vivo [12, 13]. The activation of PPAR-γ has been shown to attenuate arterial stiffening and reduce inflammatory and oxidative stress in the PVAT of obese mice [14]. These findings highlight the significant role of PPAR-γ in PVAT in modulating inflammation and risk of vascular diseases.

Although PVAT was initially regarded as a structural support organ for the vasculature, recent findings have demonstrated its physiological importance, especially in regulating vascular tone and function [15]. In healthy subjects, PVAT functions as an endocrine and paracrine organ that secrets more anti-inflammatory, antiatherogenic, and vasorelaxant adipokines such as adiponectin, omentin, vaspin, angiotensin 1-7, methyl palmitate, and nitric oxide (NO), which contribute to its anticontractile, anti-inflammatory, and antiatherogenic actions [16, 17]. However, in the presence of vascular diseases such as hypertension, atherosclerosis, and obesity, PVAT becomes dysfunctional. A dysfunctional PVAT secretes less anti-inflammatory adipocytokines and more proinflammatory adipocytokines such as leptin, interleukin- (IL-) 6, tumor necrosis factor-alpha (TNF-α), and monocyte chemoattractant protein-1 (MCP-1) [18, 19]. These trigger inflammatory responses that lead to vascular dysfunction and an increased risk of developing CVD (Figure 1).

3. PVAT-Derived Anti-Inflammatory Adipocytokines

Adiponectin is one of the most abundant adipokines secreted by PVAT with anticontractile and anti-inflammatory effects on the vascular wall. Adiponectin acts via two types of receptors: adiponectin receptor 1 (AdipoR1) and adiponectin receptor 2 (AdipoR2) [20]. Adiponectin exerts its anti-inflammatory effects by decreasing the expression of proinflammatory cytokines such as IL-6 and TNF-α and suppressing the production of cellular adhesion molecules by inhibiting the nuclear factor kappa-B (NF-κB) pathway [21]. Moreover, hypoadiponectinemia results in endothelial dysfunction, and this is mediated by Nod-like receptor family pyrin domain-containing 3 (NLRP3) inflammasome activation [22]. Adiponectin knock-out mice showed an increase in the gene expression of inflammatory markers such as TNF-α and MCP-1. This further proves the anti-inflammatory action of adiponectin [23].

Omentin secreted by PVAT also has an anti-inflammatory effect. In obese mice, omentin reduces the expression of proinflammatory cytokines such as IL-6, IL-1β, and TNF-α and increases the secretion of other anti-inflammatory adipocytokines such as adiponectin and IL-10 through the inhibition of thioredoxin-interacting protein (TXNIP)/NLTP3 signaling pathway [24]. Furthermore, omentin reduces oxidative stress, mitochondrial dysfunction, proinflammatory cytokines (IL-6, IL-8, and MCP-1), cyclooxygenase-2 (COX), and prostaglandin E2 (PGE2) in lipopolysaccharide-induced macrophages [25]. Omentin protects against vascular endothelial dysfunction by suppressing endoplasmic reticulum (ER) and oxidative stress. This is achieved through the activation of AMP-activated protein kinase (AMPK)/PPAR-δ pathway that stimulates NO release [26]. In free fatty acid-induced endothelial cells, omentin decreases proinflammatory agents (MCP-1, IL-6, IL-1, ICAM-1, TNF-α) and NF-κB activation [27].

Fibroblast growth factor-21 (FGF-21) is a growth factor expressed in multiple tissues and organs such as adipose tissue, liver, and pancreas that regulates insulin signaling, glucose, and lipid metabolism [28]. FGF-21 exerts anti-inflammatory effects in macrophages and obese adipose tissue via various inflammatory signaling pathways [29, 30]. Treatment of apolipoprotein E-deficient ($ApoE^{-/-}$) mice with FGF-21 reduced atherosclerosis formation by increasing adiponectin expression and inhibiting ER stress, NLRP3 inflammasome activation, and factor-associated suicide (FAS) signaling [31–33]. FGF-21 also improves oxidative-stress-induced endothelial dysfunction by activating the calcium/calmodulin-dependent protein kinase kinase 2 (CaMKK2)/AMPKα pathway [34].

Vaspin, which is also known as visceral adipose tissue-derived serine protease inhibitor, is an anti-inflammatory adipokine that improves insulin sensitivity [35]. A study has reported that vaspin inhibits the gene expression of leptin receptor, production of TNF-α, and NF-κB activation in leptin-induced rat chondrocytes [36] This suggests an important role of vaspin produced by PVAT in modulating inflammatory reactions. Meanwhile, interleukin-10, which is produced by T cells, B cells, and macrophages in the PVAT, plays a significant role in preventing inflammation [37]. IL-10 suppresses proinflammatory cytokine secretion and prevents macrophage and dendritic cell maturation [38]. IL-10 acts on heterodimeric IL-10 receptors (IL-10R1, IL-10R2), which activates the Janus kinase (JAK)/STAT signaling pathway. This leads to inhibition of proinflammatory mediator production [39].

Another PVAT-derived anti-inflammatory factor is NO. Vascular NO is produced mainly by endothelial NO synthase (eNOS) [40]. NO inhibits vascular smooth muscle proliferation and migration, platelet aggregation, leukocyte adhesion, and inflammation [41]. eNOS, which is mainly expressed in the endothelium, has also been found to be present in PVAT [42]. PVAT-derived adiponectin increases

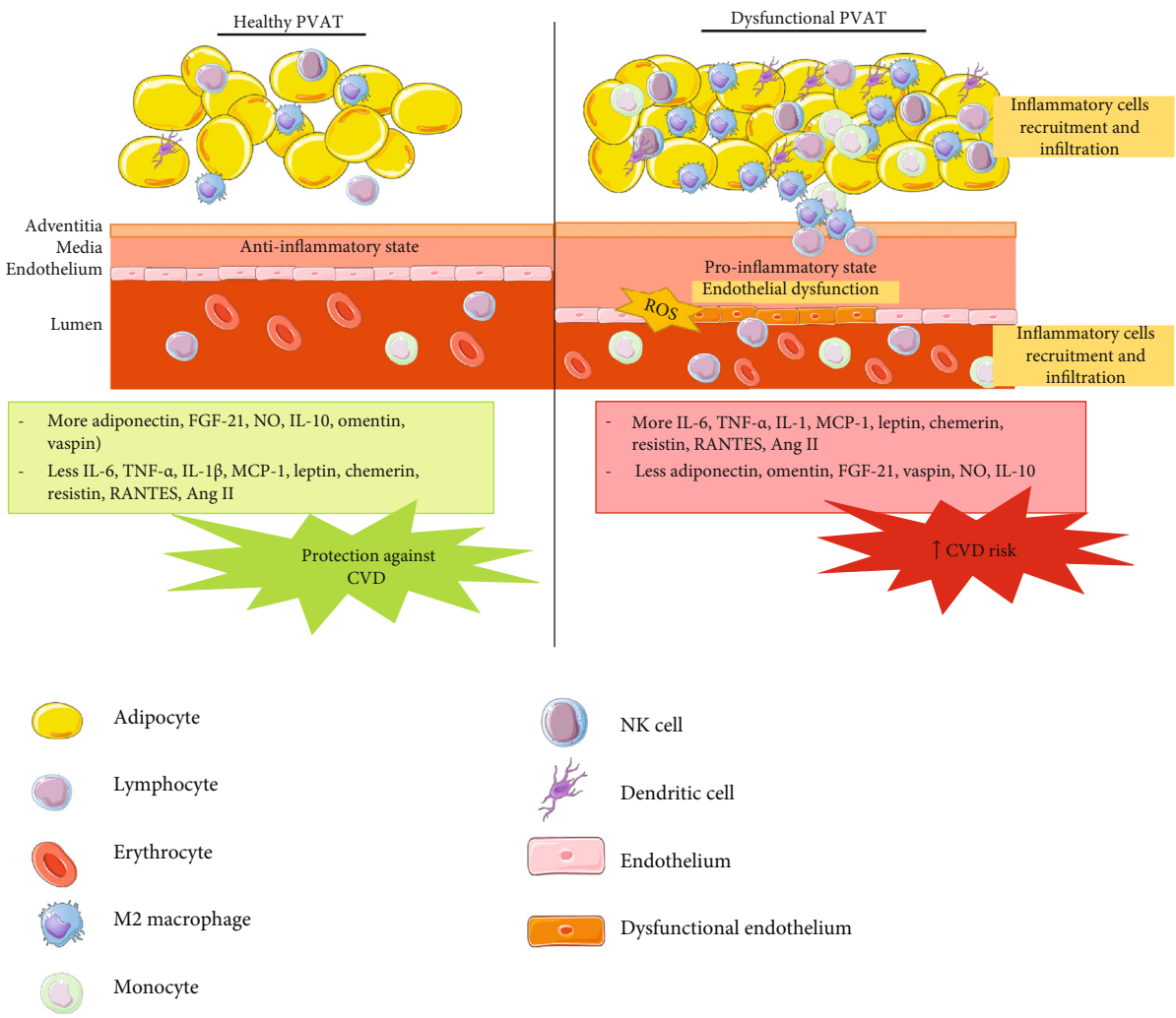

Figure 1: The anti-inflammatory state of healthy perivascular adipose tissue (PVAT) compared to the proinflammatory state of dysfunctional PVAT. CVD: cardiovascular diseases; FGF-21: fibroblast growth factor-21; IL: interleukin; MCP-1: monocyte chemoattractant protein-1; NO: nitric oxide; RANTES: regulated on activation, normal T cell expressed, and secreted; ROS: reactive oxygen species; TNF-α: tumor necrosis factor-alpha.

eNOS phosphorylation, thus enhancing NO production. Endothelial dysfunction is characterized by the reduction of NO bioavailability, and this is associated with inflammation and development of atherosclerosis and hypertension [42].

4. PVAT-Derived Proinflammatory Adpocytokines

IL-6 is one of the most studied proinflammatory cytokines secreted by PVAT. IL-6 can directly act on endothelial cells to increase superoxide production, thus leading to endothelial dysfunction [18]. Another prominent cytokine that modulates PVAT inflammatory response is TNF-α. TNF-α is released by a few types of cells including monocytes, vascular cells, and adipocytes. It inhibits the eNOS expression and stimulates the production of reactive oxygen species (ROS) via activation of the NF-κB pathway [18]. Other proinflammatory cytokines released by PVAT include MCP-1 and IL-1β. MCP-1 plays a crucial role in facilitating the infiltration of macrophages into the vascular wall and is often associated with the pathogenesis of atherosclerosis [43]. Meanwhile, IL-1β induces the MCP-1 expression via NF-κB and activator protein-1 (AP-1) activation [44].

Chemerin, also known as tazarotene-induced gene 2 (TIG2), is a chemoattractant protein that regulates the immune response, metabolism, and inflammation. Although some studies have associated chemerin with anti-inflammatory actions, its function is mainly considered as proinflammatory [45]. Chemerin is expressed in adipose tissue including PVAT and visceral adipose tissue [46, 47]. Both chemerin and its receptor, CMKLR1, are upregulated in obesity [48]. Furthermore, chemerin recruits dendritic cells into adipose tissue, thus increasing the inflammatory reaction in adipocytes [49]. Chemerin also stimulates the recruitment and retention of macrophages at inflammation sites by inducing macrophage adhesion to extracellular matrix proteins and adhesion molecules [50]. The level of

chemerin is closely correlated with the level of other proinflammatory cytokines such as TNF-α, C-reactive protein (CRP), and IL-6, which further supports chemerin's proinflammatory action [51].

Leptin has been suggested as a PVAT-derived proinflammatory factor as its expression can be stimulated by other proinflammatory mediators such as IL-1 and TNF-α, and its concentration increases during pathological conditions such as fever and sepsis [52]. Leptin activates monocytes, leukocytes, and macrophages to secrete TNF-α, IL-6, and IL-12, increases CC-chemokine ligand production in macrophages, and stimulates ROS generation [38]. Additionally, leptin causes endothelial dysfunction [53] by inducing CRP production, cellular adhesion molecules, and platelet tissue factors in endothelial cells [54].

Resistin is another proinflammatory adipokine released by PVAT that enhances the expression of IL-6, IL-1β, and TNF-α via NF-κB signaling [55]. Other than adipocytes, resistin is released by immune cells including monocytes and macrophages, and this suggests its role in atherogenesis. Moreover, resistin causes endothelial dysfunction by enhancing proinflammatory markers such as MCP-1, TNF-α, IL-6, long pentraxin 3, IL-1β, vascular cell adhesion molecule-1 (VCAM-1), and intercellular adhesion molecule-1 (ICAM-1). Besides, resistin promotes oxidative stress and ER stress, thus leading to mitochondrial dysfunction and redox imbalance [56, 57].

The components of the renin angiotensin aldosterone system are expressed in PVAT. Its bioactive peptide, angiotensin II (Ang II), exerts its inflammatory effect by stimulating the expression of adhesion molecules and cytokines such as MCP-1 and IL-6 [58]. Ang II is also reported to induce immune cells including T lymphocytes, M1 and M2 macrophages, and dendritic cell infiltration in PVAT [59, 60]. Interestingly, a large proportion of these cells, particularly T lymphocytes, bear regulated on activation, normal T cell expressed, and secreted (RANTES) CC chemokine receptor (CCR)1, CCR3, and CCR5 receptors. Expression of RANTES chemokine receptors is stimulated by Ang II [61]. RANTES, also known as CC chemokine ligand 5 (CCL5), is present in both human and mouse adipose tissue. RANTES acts as a chemoattractant for inflammatory cells, particularly T cells, and it is associated with the development of atherosclerosis and hypertension [62]. The summary of anti- and proinflammatory adipocytokines secreted by PVAT and its involvement in vascular diseases is summarized in Table 1.

5. PVAT Inflammation in Vascular Diseases

5.1. Atherosclerosis. Atherosclerosis is an inflammatory disease involving the formation of fibrofatty plaques in the arterial wall that can progress to several chronic diseases such as coronary artery disease (CAD), stroke, and peripheral artery disease [63]. The atherosclerotic plaque consists of the accumulation of fatty substances, cholesterol, calcium, cellular waste products, and fibrin [64]. Several risk factors are closely related to atherosclerosis, including hypertension, tobacco smoking, obesity, and diabetes [65]. Traditionally, the pathogenesis of atherosclerosis has been described as an "inside-to-outside" model that starts with endothelial dysfunction, inflammation, and formation of foam cells [66]. However, in most vascular studies, PVAT was removed from the underlying blood vessels prior to experiments as PVAT was considered to be a nonvascular and inactive tissue [67].

Interestingly, more current studies propose that the crosstalk between PVAT and the underlying vasculature happens in two directions, with an "outside-to-inside" inflammatory signaling activated by the dysfunctional PVAT [68–70]. For example, it was demonstrated that inflammation in the PVAT and adventitial layer happened prior to the development of endothelial dysfunction and formation of atherosclerotic plaques in apolipoprotein E-deficient ($ApoE^{-/-}$) mice [71]. Perivascular adipocytes send signals to both immune cells and endothelial cells via the release of adipocytokines to modulate the inflammatory crosstalk in atherogenesis [72]. PVAT plays a crucial role in the pathogenesis of atherosclerosis through mechanisms involving endothelial dysfunction and inflammatory cell recruitment and infiltration [70, 73].

Immune cell infiltration is an important step in PVAT inflammation and atherosclerosis. T cell infiltration in PVAT may occur prior to macrophage infiltration in mice [74]. Both proatherogenic ($CD4^+$ T helper (Th), $CD8^+$ T cytotoxic (Tc)), and atheroprotective (T regulatory (Treg)) T cells are found in PVAT [75–77]. Th1, Tc1, and Th17 cells release proinflammatory cytokines such as interferon-γ (IFN-γ), IL-7, and TNF-α, whereas Treg cells secrete anti-inflammatory cytokine, IL-10 [78, 79]. Subpopulation of T cells such as natural killer T cells also release IFN-γ and TNF-α in PVAT [80].

5.2. Mechanisms Linking PVAT Inflammation to Atherosclerosis. The endothelium acts as a physical barrier between blood and the vascular wall. Besides, the endothelium also secretes bioactive molecules involved in the regulation of vascular tone, vascular remodeling, inflammatory process, and thrombosis [81]. NO produced by eNOS is an important antiatherogenic molecule, and reduced NO bioavailability is the hallmark of endothelial dysfunction [82]. Endothelial dysfunction is well established as the precursor of atherosclerosis. A dysfunctional endothelium loses its physiological characteristics and transforms into a proinflammatory, prothrombotic, and vasoconstrictor state, thus promoting atherosclerosis [83].

As described earlier, in physiological condition, PVAT produces a range of vasoprotective adipocytokines with antiatherogenic effects such as adiponectin, NO, and hydrogen sulfide (H_2S) [84]. Reduced NO and H_2S have been shown to worsen atherosclerosis progression [82, 85]. Unsurprisingly, since atherosclerosis is closely related to obesity, PVAT-derived NO, H_2S, and adiponectin levels were reduced in obese animals [86–89]. It is postulated that in obesity, increased PVAT mass and hyperthrophic adipocytes in PVAT promote endothelial dysfunction and atherosclerosis through increased oxidative stress and inflammation [90, 91].

Breakdown of fat in hypertrophic PVAT releases free fatty acids (FFA) into the vasculature. FFA causes

Table 1: Anti- and proinflammatory adipocytokines secreted by PVAT and its involvement in vascular diseases.

Adipokine/cytokine	Effect on vasculature	Association with vascular diseases
Anti-inflammatory adipocytokines		
Adiponectin	(i) Vasodilator [169] (ii) ↓ adhesion molecule expression [170] (iii) ↓ oxidative stress [171]	(i) ↓ production in obesity [172] and hypertension [173]
Omentin	(i) ↓ oxidative stress [25] (ii) ↓ mitochondrial dysfunction [25] (iii) ↑ NO [174]	(i) ↓ expression in obesity [175] and CAD [176]
FGF-21	(i) ↓ oxidative stress [177] (ii) ↑ vasorelaxation [178]	(i) Improves vascular dysfunction in hypertension [179]
Vaspin	(i) ↑ insulin sensitivity [35] (ii) ↑ cytokine production [35]	(i) ↓ production in atherosclerosis [180]
Nitric oxide	(i) Vasorelaxant [167]	(i) ↓ production in atherosclerosis [181] and hypertension [182]
IL-10	(i) ↓ immune cell infiltration [37]	(i) ↓ in atherosclerosis [183]
Proinflammatory adipocytokines		
IL-6, TNF-α, IL-1, MCP-1	(i) ↑ immune cell infiltration [184] (ii) Endothelial dysfunction [90] (iii) ↑ ROS [185]	(i) ↑ production in obesity [184] and atherosclerosis [186, 187]
Chemerin	(i) ↑ immune cell infiltration [188] (ii) ↑ adhesion molecule expression [189]	(i) ↑ production in obesity and diabetes [190]
Leptin	(i) ↑ immune cell infiltration [54] (ii) ↑ ROS [191] (iii) endothelial dysfunction [192]	(i) ↑ production in obesity, hypertension [192], and CAD [193]
Resistin	(i) ↑ ROS [56] (ii) ↑ macrophage infiltration [56]	(i) ↑ production in atherosclerosis [194]
RANTES, Ang II	(i) ↑ immune cell infiltration [62]	(i) ↓ production in atherosclerosis [195] and hypertension [196]

Abbreviations: Ang II: angiotensin II; CAD: coronary artery disease; IL: interleukin; MCP: monocyte chemoattractant protein; NO: nitric oxide; ROS: reactive oxygen species; TNF-α: tumor necrosis factor-alpha.

phosphorylation of insulin receptor substrate 1 (IRS-1) present in PVAT and other vascular cells by activating NF-κB, protein kinase C (PKC), and Toll-like receptors [92]. This decreases the activation of downstream PI3K/Akt signaling, leading to inhibition of eNOS expression and NO synthesis [93]. Besides, PKC activation by FFA causes eNOS coupling, resulting in further reduction in NO synthesis and production of reactive oxygen species (ROS) [7, 94]. Furthermore, PKC induces the synthesis of endothelin-1 (ET-1), which is a potent vasoconstrictor. Reduced NO bioavailability, increased vasoconstrictor, and ROS accumulation result in endothelial dysfunction and enhance the development of atherosclerosis [92].

Subsequently, monocyte recruitment and activation ensue. Dysfunctional PVAT releases more pro-inflammatory adipocytokines such as TNF-α, leptin, and IL-6 that induce the expression of cellular adhesion molecules like VCAM-1 and ICAM-1 on the endothelial cells. Cellular adhesion molecules promote the adherence and migration of monocytes into the subendothelial layer [95–97]. The migrated monocytes transformed into macrophages that secrete proinflammatory cytokines such as MCP-1, TNF-α, IFN-γ, and IL-6, which further aggravate monocyte recruitment and low-density lipoprotein (LDL) oxidation [98].

The macrophages engulf oxidized LDL (oxLDL) through scavenger receptors including leptin-like oxLDL receptor-1 and CD36, leading to formation of foam cells. Foam cells are the hallmark of initial stage of atherosclerosis [98]. Furthermore, PVAT-derived adipocytokines such as leptin, TNF-α, visfatin, and IL-6 stimulate vascular smooth muscle cell (VSMC) proliferation and migration, which is an important step in neointima formation [99, 100]. Recent evidence demonstrates that in animal models, infiltration of macrophages in the PVAT and adventitial layer is more marked compared to the intimal layer [101, 102]. This further supports the notion that PVAT inflammation plays a significant role in atherosclerosis development.

Proinflammatory chemokines such as macrophage inflammatory protein 1-α (MIP-1α or CCL3), MCP-1, and RANTES attract immune cells to the site of perivascular inflammation in atherosclerotic ApoE$^{-/-}$ mice [103–105]. PVAT of ApoE$^{-/-}$ mice was also found to have increased levels of IL-6 and IL-1 as well as macrophages and T cell infiltration [106]. However, there was a decrease in the number of B-1 cells that secrete antiatherosclerotic IgM in ApoE$^{-/-}$ mouse PVAT. This further worsens the atherosclerotic lesion formation in the mouse coronary artery and aorta [107]. Additionally, microRNA-19b in endothelial cell-derived microparticles promotes atherosclerosis progression in ApoE$^{-/-}$ mice by increasing the secretion of proinflammatory cytokines (IL-6, IL-10, and TNF-α) and inducing macrophage infiltration in PVAT [108].

Interestingly, transplantation of normal PVAT from wild-type mice decreased the size of atherosclerotic plaque

in ApoE$^{-/-}$ mice. This effect was mediated by the anti-inflammatory action of transforming growth factor (TGF)-β1 [109]. Besides, adiponectin obtained from PVAT decreased carotid collar-induced atherosclerosis by stimulating macrophage autophagy [110]. A study demonstrated that xenotropic and polytropic retrovirus receptor 1 (Xpr1), a macrophage regulator, and TATA-box binding protein associated factor 3 (Taf3), a core transcription factor, were upregulated in the PVAT of ApoE$^{-/-}$ mice. Furthermore, an upregulation of the Taf3 and Xpr1 expression was also detected in human atherosclerotic plaques [111]. This suggests that Taf3 and Xpr1 have a role in modulating the chronic inflammatory phenotype of PVAT.

Data from human studies demonstrated that PVAT derived from patients with CVD have increased expression of proinflammatory genes and decreased expression of anti-inflammatory adiponectin [112–114]. For instance, the epicardial adipose tissue of patients with coronary atherosclerosis showed increased expression of IL-1β, IL-6, and TNF-α [113] and lower expression of adiponectin [114]. The levels of inflammatory mediators such as IL-1β, IL-6, and IL-10 were elevated in the pericoronary PVAT of patients with CAD compared to patients without CAD [115]. This suggests the influence of PVAT inflammation on atherosclerosis development through an outside-to-inside manner.

Besides, the levels of protein inhibitor of activated STAT1 (PIAS1), a key negative regulator of inflammation, were reduced in PVAT obtained from patients with atherosclerotic vessel disease [116]. PIAS1 downregulates inflammation by inhibiting STAT1 and NF-κB signaling pathways [117, 118]. Besides, the number of macrophages in the PVAT correlates with the number of immune cells in the atherosclerotic plaque [119–121].

Unstable plaque is an important culprit for the occurrence of acute coronary syndrome. Apart from the established factors that influence plaque stability such as intraplaque neovascularization, inflammation, and intraplaque protease activity [122], PVAT inflammation has also been suggested to affect plaque stability. The number of macrophages was higher in PVAT near unstable plaques compared to the PVAT near stable plaques [123]. Furthermore, endoplasmic reticulum (ER) stress transforms adipose tissue to a proinflammatory phenotype [124]. ER stress in PVAT contributes to plaque instability by stimulating a proinflammatory factor, granulocyte macrophage colony-stimulating factor (GM-CSF), via NF-κB activation [125]. GM-CSF causes adipose tissue inflammation by recruiting and activating M1 macrophages [126]. The mechanisms linking PVAT inflammation and atherosclerosis are summarized in Figure 2.

6. Hypertension

There are several mechanisms involving PVAT that contribute to hypertension, such as loss of PVAT anticontractile effect, increase in PVAT proinflammatory adipocytokines, decrease in PVAT anti-inflammatory adipocytokines, immune cell infiltration, activation of local RAAS, and increase in vascular oxidative stress [12]. The initial site of inflammation during the development of hypertension is in the PVAT and in the border between the PVAT and the adventitial layer [61, 127, 128].

6.1. Mechanisms Linking PVAT Inflammation to Hypertension. In hypertension, PVAT releases more proinflammatory adipocytokines such as IL-6, IL-17, IL-8, IL-23, IL-1β, TNF-α, and TGF-β [129] and less anti-inflammatory adipocytokines such as adiponectin, IL-10, and IL-4 [129, 130]. Consequently, there is infiltration of immune cells in the PVAT, loss of PVAT anti-contractile action, and increased vascular resistance [19]. These events are mediated by numerous inflammatory cells and cytokines. For example, complement C5a mediates the reduction in PVAT adiponectin release [131], RANTES mediates the invasion of lymphocyte T cells into the perivascular space [38], and IFN-γ is released by CD8$^+$ cells that invade the PVAT [132]. All these changes intensify PVAT dysfunction and proinflammatory crosstalk between PVAT and the underlying hypertensive vessels.

A study involving spontaneously hypertensive mice induced by perilipin-1 deletion showed that the mice had higher aortic blood pressure, loss of PVAT anti-contractile effect, and decreased adiponectin expression. These findings are associated with increased expression of MCP-1, TNF-α, and IL-6 in the aorta [133]. Meanwhile, PVAT of DOCA-salt hypertensive mice displayed an increase in the complement C3 expression, leading to increased proinflammatory M1 macrophages and decreased anti-inflammatory M2 macrophage expression in the PVAT [134]. Recruitment of proinflammatory macrophages in the PVAT of DOCA-salt hypertensive mice enhances complement activation and promotes TNF-α release, thereby reducing adiponectin expression [135].

During the progression of hypertension, accumulation of immune cells has been reported in the PVAT surrounding both the aorta and mesenteric arteries of hypertensive animals [18]. Hypertension is associated with a significant increase in T cell infiltration in the PVAT. This promotes inflammation and endothelial disyfunction via NF-κB-dependent, Notch ligand Jagged 1-regulated integrin, and adhesion molecule expression [136, 137]. Additionally, both CD4$^+$ and CD8$^+$ T cell subpopulations are increased in the PVAT of hypertensive mice. T cell- and monocyte-deficient mice exposed to various hypertensive stimuli showed reduced perivascular inflammatory reaction [75, 138].

Macrophage infiltration in PVAT is also significantly increased in hypertension, and this is regulated by T cell-dependent mechanisms [61]. Depriving the lymphocyte adaptor protein (Lnk) gene that encodes the negative regulator of T cell activation promotes PVAT inflammation, as the number of macrophages increase in both aorta and adipocytes [139]. The increase in blood pressure also corresponds with the expression of macrophage chemokine receptors CCR2 and its ligands such as CCL2, CCL7, CCL8, and CCL12 in the PVAT [140]. Moreover, the expression of proinflammatory M1 macrophage is increased in hypertension compared to healthy condition, whereby the anti-inflammatory M2 macrophage is more dominant [61].

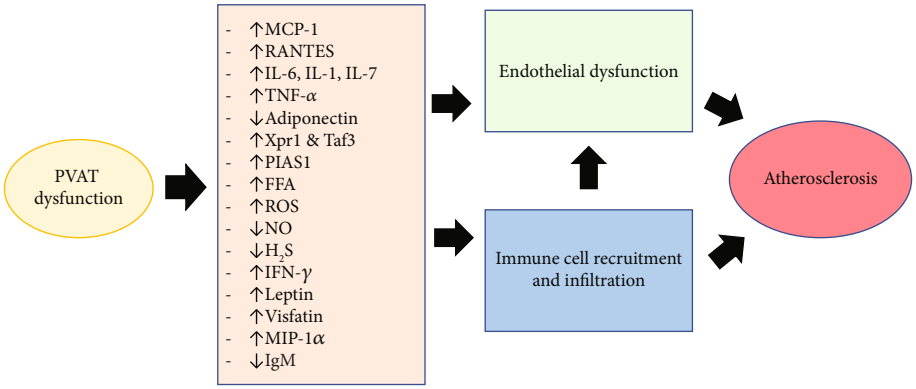

Figure 2: Pathways involving perivascular adipose tissue (PVAT) inflammation in atherosclerosis. FFA: free fatty acid; H_2S: hydrogen sulfide; IFN-γ: interferon-γ; IL: interleukin; IgM: immunoglobulin M; MCP-1: monocyte chemoattractant protein-1; MIP-1α: macrophage inflammatory protein 1-α; NO: nitric oxide; PIAS1: protein inhibitor of activated STAT1; RANTES: regulated on activation, normal T cell expressed, and secreted; ROS: reactive oxygen species; Taf3: TATA-box binding protein associated factor 3; TNF-α: tumor necrosis factor-alpha; Xpr1: xenotropic and polytropic retrovirus receptor 1.

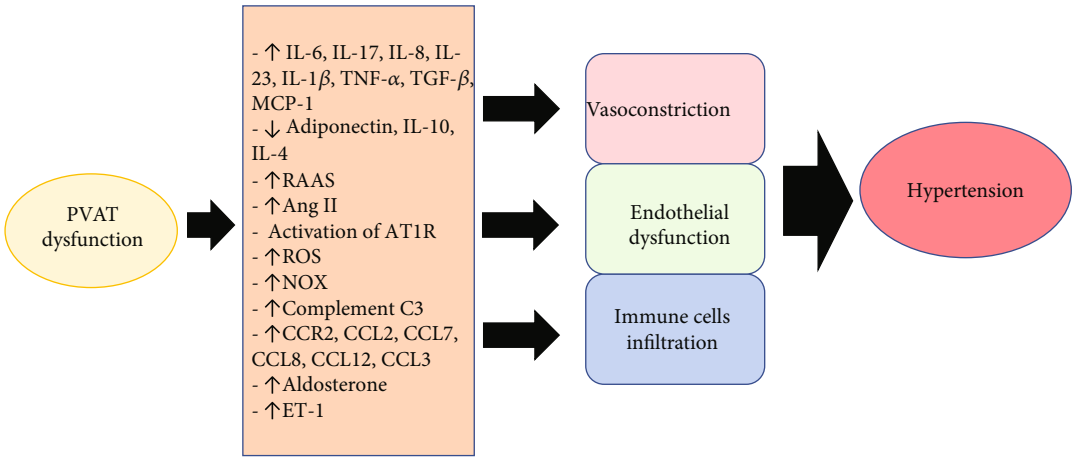

Figure 3: Pathways involving perivascular adipose tissue (PVAT) inflammation in hypertension. Ang II: angiotensin II; AT1R: angiotensin II type 1 receptor; C3: component 3; CCR: CC chemokine receptor; CCL: CC chemokine ligand; ET-1: endothelin-1; IL: interleukin; MCP-1: monocyte chemoattractant protein-1; NOX: NADPH oxidase; RAAS: renin-angiotensin-aldosterone system; ROS: reactive oxygen species.

Overactivation of RAAS is critical to the development of hypertension. Adipose tissue has been suggested as one of the main sites of RAAS activation in hypertensive patients [92]. In obese hypertensive patients, adipose tissues are the major source of RAAS [141]. All components of RAAS can be found in PVAT except renin [142, 143]. Angiotensinogen and Ang II levels in PVAT were significantly increased in SHR [144]. Knockout of angiotensinogen gene in PVAT successfully decreased local Ang II production in mice PVAT [145].

PVAT of Ang II-induced hypertensive mice displayed a higher number of immune cells such as macrophages, leukocytes, T cells, and dendritic cells. Ang II induction also enhances RANTES, MCP-1, and CCL3 expression in the periaortic PVAT and the aortic wall of the mice [61, 146]. Moreover, activation of angiotensin II type 1 receptor (AT1R) in PVAT promotes vascular inflammation and endothelial dysfunction [147].

Sirtuin-3 (SIRT3), a mitochondrial NAD^+-dependent deacetylase that regulates multiple metabolic enzymes, plays a significant role in Ang II-related PVAT inflammation. It was reported that Ang II promotes PVAT inflammation and fibrosis by stimulating NLRP3/IL-Iβ pathway in myeloid SIRT3 knockout mice [148]. Activation of NLRP3 inflammasome is involved in vascular inflammation and its blockade has been proven to reduce adipose tissue inflammation and fibrosis (P. [149, 150]). SIRT3 is therefore a potential therapeutic target to inhibit NLRP3-related PVAT inflammation and fibrosis [148].

In addition to the direct actions of Ang II, aldosterone that is released in response to Ang II stimulation also has a proinflammatory action on PVAT [151]. Treatment with aldosterone receptor antagonists improves endothelial function, reduces oxidative stress, and decreases blood pressure [152, 153]. Meanwhile, treatment with angiotensin receptor blockers lower the release of Ang II from PVAT. This leads

Table 2: Changes related to PVAT inflammation in atherosclerosis and hypertension.

Atherosclerosis	Hypertension
(i) ↑ MCP-1 [197]	(i) ↑ IL-6, IL-17, IL-8, IL-23, IL-1β, TNF-α, TGF-β, MCP-1 [198–200]
(ii) ↑ RANTES [201]	(ii) ↓ adiponectin, IL-10, IL-4 [202]
(iii) ↑ IL-6, IL-1, IL-7 [203–205]	(iii) ↑ RAAS, aldosterone, and Ang II [206]
(iv) ↑ TNF-α [207]	(iv) ↑ activation of AT1R [208]
(v) ↓ adiponectin [209]	(v) ↑ ROS [210]
(vi) ↑ Xpr1 & Taf3 [111]	(vi) ↑ NOX [211]
(vii) ↑ PIAS1 [212]	(vii) ↑ complement C3 [213]
(viii) ↑ FFA [214]	(viii) ↑ CCR2, CCL2, CCL7, CCL8, CCL12, CCL3 [140]
(ix) ↑ ROS [215]	(ix) ↑ ET-1 [210]
(x) ↓ NO [216]	
(xi) ↓ H_2S [217]	
(xii) ↑ IFN-γ [218]	
(xiii) ↑ Leptin [219]	
(xiv) ↑ Visfatin [220]	
(xv) ↑ MIP-1α [221]	
(xvi) ↓ IgM [222]	

Abbreviations: Ang II: angiotensin II; AT1R: angiotensin II type 1 receptor; C3: component 3; CCR: CC chemokine receptor; CCL: CC chemokine ligand; ET-1: endothelin-1; FFA: free fatty acid; H_2S: hydrogen sulfide; IFN-γ: interferon-γ; IL: interleukin; IgM: immunoglobulin M; MCP-1: monocyte chemoattractant protein-1; MIP-1α: macrophage inflammatory protein 1-α; NO: nitric oxide; NOX: NADPH oxidase; PIAS1: protein inhibitor of activated STAT1; RAAS: renin-angiotensin-aldosterone system; RANTES: regulated on activation, normal T cell expressed, and secreted; ROS: reactive oxygen species; Taf3: TATA-box binding protein-associated factor 3; TNF-α: tumor necrosis factor-alpha; Xpr1: xenotropic and polytropic retrovirus receptor 1.

to the release of PVAT-derived relaxing factors that stimulate vasodilation through the opening of voltage-gated potassium channels in the vascular smooth muscle cells [147, 154, 155].

A complex reactive oxygen species (ROS) machinery containing NADPH oxidase (Nox) and antioxidative enzymes are also expressed in PVAT [156, 157]. Chronic oxidative stress enhances vascular inflammation in hypertension, with Nox being the main source of superoxide in the vasculature [158]. ROS derived from Nox in PVAT induces endothelial dysfunction by scavenging endothelial NO and modulating perivascular inflammation [90, 159].

SHR showed greater T cell accumulation in the PVAT and higher mRNA expression of Nox1 and Nox 4 in the vessels, an effect that was exacerbated with aging [160]. Mice with the overexpression of Nox p22phox catalytic subunit have enhanced vascular superoxide production and increased PVAT leukocyte infiltration that worsens hypertension progression [161]. Meanwhile, mice with loss of Nox subunit such as p47phox, Nox1, and Nox4 show protection against hypertension [162, 163]. Surprisingly, treatment of SHR with GKT137831, a dual inhibitor of Nox1/4, raised both blood pressure and PVAT macrophage infiltration and accelerated vascular aging. This observation was associated with increased expression of proinflammatory chemokine expression (CCL2 and CCL5) in the PVAT [160]. Therefore, these changes need to be considered when designing a therapy that targets Nox to treat hypertension.

Hypertension is more common in people who are obese compared to people who are lean [164]. Animal studies showed that obesity leads to increased PVAT mass and adipocyte hypertrophy with signs of PVAT inflammation, endothelial dysfunction, and altered release of adipocytokines. The release of proinflammatory cytokines such as TNF-α, MCP-1, IL-6, and IL-8 is markedly enhanced, whereas the anti-inflammatory adipokine, adiponectin, is markedly reduced [90, 91]. TNF-α inhibits adiponectin and NO production and stimulates ET-1 release. Imbalance between the vasoconstrictor ET-1 and the vasodilators such as NO and adiponectin is implicated in obesity-induced endothelial dysfunction and hypertension [42]. Adiponectin level is restored in hypertensive patients who received antihypertensive agents to control their blood pressure, which signifies the beneficial effect of adiponectin in hypertension [165].

PVAT inflammation and altered adipocytokine profile in obesity have significant effects on the anticontractile effect of PVAT and blood pressure [166]. Obesity causes the loss of anticontractile function of PVAT [90] and impairs endothelium-dependent vasorelaxation which contribute to hypertension [167]. The loss of anticontractile function of PVAT correlates with the increase in blood pressure in rodent models of diet-induced obesity [87]. Like obese animal models, the anticontractile effect of PVAT is lost in obese patients [168]. TNF-α expression is also elevated in the vascular wall and PVAT isolated from the small arteries of obese patients [42]. Six months following bariatric surgery, reduction in the body

weight of obese patients is accompanied by improvement in their PVAT adipocytokine profile, PVAT anticontractile function, and blood pressure [168]. The mechanisms linking PVAT inflammation and hypertension are summarized in Figure 3.

7. Conclusion

PVAT inflammation plays a mechanistic role in the pathogenesis of vascular diseases such as atherosclerosis and hypertension (Table 2). The vicinity of PVAT as an active endocrine and paracrine organ that produces various adipocytokines as well as the related changes in this tissue supports the idea that alteration in PVAT phenotype contributes to disease processes in the adjacent vascular wall. Inflammation leads to PVAT dysfunction through the release of various proinflammatory adipocytokines and immune cell infiltration. Although the mechanisms on how PVAT inflammation is linked to vascular diseases are not entirely clear, hence the need for more mechanistic studies to explore this matter, the available evidence shows that PVAT inflammation occurs at the initial part of vascular pathology in a tightly regulated manner. Therefore, further studies are needed to explore the potential of PVAT as a target for the prevention and treatment of vascular diseases.

Conflicts of Interest

The authors declare no conflict of interest.

Acknowledgments

This project is supported by the Faculty of Medicine, Universiti Kebangsaan Malaysia (project code FF-2021-146).

References

[1] World Health Organization, "Cardiovascular Diseases (CVD)," 2021, https://www.who.int/news-room/fact-sheets/detail/cardiovascular-diseases-(cvds).

[2] E. Okamoto, T. Couse, H. de Leon et al., "Perivascular inflammation after balloon angioplasty of porcine coronary arteries," *Circulation*, vol. 104, no. 18, pp. 2228–2235, 2001.

[3] S. N. Saxton, A. M. Heagerty, and S. B. Withers, "Perivascular adipose tissue: an immune cell metropolis," *Experimental Physiology*, vol. 105, no. 9, pp. 1440–1443, 2020.

[4] M. S. Fernández-Alfonso, B. Somoza, D. Tsvetkov, A. Kuczmanski, M. Dashwood, and M. Gil-Ortega, "Role of perivascular adipose tissue in health and disease," in *Comprehensive Physiology*, pp. 23–59, 2017.

[5] K.-V. Tran, T. Fitzgibbons, S. Y. Min, T. DeSouza, and S. Corvera, "Distinct adipocyte progenitor cells are associated with regional phenotypes of perivascular aortic fat in mice," *Molecular Metabolism*, vol. 9, pp. 199–206, 2018.

[6] W. Xiong, X. Zhao, L. Villacorta et al., "Brown Adipocyte-Specific PPARγ (Peroxisome Proliferator-Activated Receptor γ) deletion impairs Perivascular Adipose Tissue development and enhances atherosclerosis in mice," *Arteriosclerosis, Thrombosis, and Vascular Biology*, vol. 38, no. 8, pp. 1738–1747, 2018.

[7] X. Y. Qi, S. L. Qu, W. H. Xiong, O. Rom, L. Chang, and Z. S. Jiang, "Perivascular adipose tissue (PVAT) in atherosclerosis: a double-edged sword," *Cardiovascular Diabetology*, vol. 17, no. 1, p. 134, 2018.

[8] L. Chang, L. Villacorta, R. Li et al., "Loss of perivascular adipose tissue on peroxisome proliferator-activated receptor-γ deletion in smooth muscle cells impairs intravascular thermoregulation and enhances atherosclerosis," *Circulation*, vol. 126, no. 9, pp. 1067–1078, 2012.

[9] S. Hildebrand, J. Stümer, and A. Pfeifer, "PVAT and Its Relation to Brown, Beige, and White Adipose Tissue in Development and Function," *Frontiers in Physiology*, vol. 9, p. 70, 2018.

[10] V. Pellegrinelli, S. Carobbio, and A. Vidal-Puig, "Adipose tissue plasticity: how fat depots respond differently to pathophysiological cues," *Diabetologia*, vol. 59, no. 6, pp. 1075–1088, 2016.

[11] I. Akoumianakis, A. Tarun, and C. Antoniades, "Perivascular adipose tissue as a regulator of vascular disease pathogenesis: identifying novel therapeutic targets," *British Journal of Pharmacology*, vol. 174, no. 20, pp. 3411–3424, 2017.

[12] A. Grigoras, C. Amalinei, R. A. Balan, S. E. Giusca, and I. D. Caruntu, "Perivascular adipose tissue in cardiovascular diseases-an update," *Anatolian Journal of Cardiology*, vol. 22, no. 5, pp. 219–231, 2019.

[13] M. J. Hobson, P. W. Hake, M. O'Connor et al., "Conditional deletion of cardiomyocyte peroxisome proliferator-activated receptor γ enhances myocardial ischemia-reperfusion injury in mice," *Shock (Augusta, Ga.)*, vol. 41, no. 1, pp. 40–47, 2014.

[14] J. Y. Chen, Y. P. Wu, C. Y. Li et al., "PPARγ activation improves the microenvironment of perivascular adipose tissue and attenuates aortic stiffening in obesity," *Journal of Biomedical Science*, vol. 28, no. 1, p. 22, 2021.

[15] T. P. Mikołajczyk and T. J. Guzik, "Perivascular adipose tissue as the secret behind resistance to atherosclerosis exhibited by the human internal mammary artery," *Kardiologia Polska*, vol. 78, no. 12, pp. 1194–1196, 2020.

[16] A. Sowka and P. Dobrzyn, "Role of perivascular adipose tissue-derived adiponectin in vascular homeostasis," *Cells*, vol. 10, no. 6, p. 1485, 2021.

[17] S. B. Withers, C. E. Bussey, S. N. Saxton, H. M. Melrose, A. E. Watkins, and A. M. Heagerty, "Mechanisms of adiponectin-associated perivascular function in vascular disease," *Arteriosclerosis, Thrombosis, and Vascular Biology*, vol. 34, no. 8, pp. 1637–1642, 2014.

[18] R. Nosalski and T. J. Guzik, "Perivascular adipose tissue inflammation in vascular disease," *British Journal of Pharmacology*, vol. 174, no. 20, pp. 3496–3513, 2017.

[19] J. G. Ramirez, E. J. O'Malley, and W. S. V. Ho, "Pro-contractile effects of perivascular fat in health and disease," *British Journal of Pharmacology*, vol. 174, no. 20, pp. 3482–3495, 2017.

[20] H. Yanai and H. Yoshida, "Beneficial effects of adiponectin on glucose and lipid metabolism and atherosclerotic progression: mechanisms and perspectives," *International Journal of Molecular Sciences*, vol. 20, no. 5, p. 1190, 2019.

[21] S. Feijóo-Bandín, A. Aragón-Herrera, S. Moraña-Fernández et al., "Adipokines and inflammation: focus on cardiovascular diseases," *International Journal of Molecular Sciences*, vol. 21, no. 20, pp. 7711–7734, 2020.

[22] J. Zhang, L. Xia, F. Zhang et al., "A novel mechanism of diabetic vascular endothelial dysfunction: hypoadiponectinemia-induced NLRP3 inflammasome activation," *Biochimica et Biophysica Acta-Molecular Basis of Disease*, vol. 1863, no. 6, pp. 1556–1567, 2017.

[23] Y. Hou, X. F. Wang, Z. Q. Lang et al., "Adiponectin is protective against endoplasmic reticulum stress-induced apoptosis of endothelial cells in sepsis," *Brazilian Journal of Medical and Biological Research = Revista Brasileira de Pesquisas Medicas e Biologicas*, vol. 51, no. 12, article e7747, 2018.

[24] H. Zhou, Z. Zhang, G. Qian, and J. Zhou, "Omentin-1 attenuates adipose tissue inflammation via restoration of TXNIP/NLRP3 signaling in high-fat diet-induced obese mice," *Fundamental & Clinical Pharmacology*, vol. 34, no. 6, pp. 721–735, 2020.

[25] J. Wang, Y. Gao, F. Lin, K. Han, and X. Wang, "Omentin-1 attenuates lipopolysaccharide (LPS)-induced U937 macrophages activation by inhibiting the TLR4/MyD88/NF-κB signaling," *Archives of Biochemistry and Biophysics*, vol. 679, article 108187, 2020.

[26] F. Liu, S. Fang, X. Liu et al., "Omentin-1 protects against high glucose-induced endothelial dysfunction via the AMPK/PPARδ signaling pathway," *Biochemical Pharmacology*, vol. 174, article 113830, 2020.

[27] H. Yamawaki, J. Kuramoto, S. Kameshima, T. Usui, M. Okada, and Y. Hara, "Omentin, a novel adipocytokine inhibits TNF-induced vascular inflammation in human endothelial cells," *Biochemical and Biophysical Research Communications*, vol. 408, no. 2, pp. 339–343, 2011.

[28] F. M. Fisher and E. Maratos-Flier, "Understanding the physiology of FGF21," *Annual Review of Physiology*, vol. 78, no. 1, pp. 223–241, 2016.

[29] N. Wang, J. Y. Li, S. Li et al., "Fibroblast growth factor 21 regulates foam cells formation and inflammatory response in Ox-LDL-induced THP-1 macrophages," *Biomedicine & Pharmacotherapy = Biomedecine & Pharmacotherapie*, vol. 108, pp. 1825–1834, 2018.

[30] N. Wang, T. T. Zhao, S. M. Li et al., "Fibroblast growth factor 21 exerts its anti-inflammatory effects on multiple cell types of adipose tissue in obesity," *Obesity (Silver Spring, Md.)*, vol. 27, no. 3, pp. 399–408, 2019.

[31] X. Wu, Y. F. Qi, J. R. Chang et al., "Possible role of fibroblast growth factor 21 on atherosclerosis via amelioration of endoplasmic reticulum stress-mediated apoptosis in apoE(-/-) mice," *Heart and Vessels*, vol. 30, no. 5, pp. 657–668, 2015.

[32] X. Yan, Z. Gou, Y. Li et al., "Fibroblast growth factor 21 inhibits atherosclerosis in apoE−/− mice by ameliorating Fas-mediated apoptosis," *Lipids in Health and Disease*, vol. 17, no. 1, p. 203, 2018.

[33] Z. Zeng, Q. Zheng, J. Chen et al., "FGF21 mitigates atherosclerosis via inhibition of NLRP3 inflammasome-mediated vascular endothelial cells pyroptosis," *Experimental Cell Research*, vol. 393, no. 2, article 112108, 2020.

[34] L. Ying, N. Li, Z. He et al., "Fibroblast growth factor 21 ameliorates diabetes-induced endothelial dysfunction in mouse aorta via activation of the CaMKK2/AMPKα signaling pathway," *Cell Death & Disease*, vol. 10, no. 9, p. 665, 2019.

[35] K. I. Maijer, E. Neumann, U. Müller-Ladner et al., "Serum vaspin levels are associated with the development of clinically manifest arthritis in autoantibody-positive individuals," *PLoS One*, vol. 10, no. 12, article e0144932, 2015.

[36] J. Bao, L. H. Xu, J. S. Ran, Y. Xiong, and L. D. Wu, "Vaspin prevents leptin-induced inflammation and catabolism by inhibiting the activation of nuclear factor-κB in rat chondrocytes," *Molecular Medicine Reports*, vol. 16, no. 3, pp. 2925–2930, 2017.

[37] S. S. Iyer, A. A. Ghaffari, and G. Cheng, "Lipopolysaccharide-mediated IL-10 transcriptional regulation requires sequential induction of type I IFNs and IL-27 in macrophages," *Journal of Immunology (Baltimore, Md. : 1950)*, vol. 185, no. 11, pp. 6599–6607, 2010.

[38] T. J. Guzik, D. S. Skiba, R. M. Touyz, and D. G. Harrison, "The role of infiltrating immune cells in dysfunctional adipose tissue," *Cardiovascular Research*, vol. 113, no. 9, pp. 1009–1023, 2017.

[39] S. S. Iyer and G. Cheng, "Role of interleukin 10 transcriptional regulation in inflammation and autoimmune disease," *Critical Reviews in Immunology*, vol. 32, no. 1, pp. 23–63, 2012.

[40] U. M. Sundar, A. Ugusman, H. K. Chua, J. Latip, and A. Aminuddin, "*Piper sarmentosum* promotes endothelial nitric oxide production by reducing asymmetric dimethylarginine in tumor necrosis factor-α-induced human umbilical vein endothelial cells," *Frontiers in Pharmacology*, vol. 10, p. 1033, 2019.

[41] U. Forstermann and W. C. Sessa, "Nitric oxide synthases: regulation and function," *European Heart Journal*, vol. 33, no. 7, pp. 829–837, 2012.

[42] A. Virdis, E. Duranti, C. Rossi et al., "Tumour necrosis factor-alpha participates on the endothelin-1/nitric oxide imbalance in small arteries from obese patients: role of perivascular adipose tissue," *European Heart Journal*, vol. 36, no. 13, pp. 784–794, 2015.

[43] J. H. Lim, H. J. Um, J. W. Park, I. K. Lee, and T. K. Kwon, "Interleukin-1β promotes the expression of monocyte chemoattractant protein-1 in human aorta smooth muscle cells via multiple signaling pathways," *Experimental & Molecular Medicine*, vol. 41, no. 10, pp. 757–764, 2009.

[44] N. Kaneko, M. Kurata, T. Yamamoto, S. Morikawa, and J. Masumoto, "The role of interleukin-1 in general pathology," *Inflammation and Regeneration*, vol. 39, no. 1, p. 12, 2019.

[45] J. L. Rourke, H. J. Dranse, and C. J. Sinal, "Towards an integrative approach to understanding the role of chemerin in human health and disease," *Obesity Reviews*, vol. 14, no. 3, pp. 245–262, 2013.

[46] C. G. Kostopoulos, S. G. Spiroglou, J. N. Varakis, E. Apostolakis, and H. H. Papadaki, "Chemerin and CMKLR1 expression in human arteries and periadventitial fat: a possible role for local chemerin in atherosclerosis?," *BMC Cardiovascular Disorders*, vol. 14, no. 1, p. 56, 2014.

[47] S. Zylla, M. Pietzner, J. P. Kühn et al., "Serum chemerin is associated with inflammatory and metabolic parameters-results of a population-based study," *Obesity (Silver Spring, Md.)*, vol. 25, no. 2, pp. 468–475, 2017.

[48] V. Catalán, J. Gómez-Ambrosi, A. Rodríguez et al., "Increased levels of chemerin and its receptor, chemokine-like receptor-1, in obesity are related to inflammation: tumor necrosis factor-α stimulates mRNA levels of chemerin in visceral adipocytes from obese patients," *Surgery for Obesity and Related Diseases*, vol. 9, no. 2, pp. 306–314, 2013.

[49] A. R. Ghosh, R. Bhattacharya, S. Bhattacharya et al., "Adipose Recruitment and Activation of Plasmacytoid Dendritic Cells Fuel Metaflammation," *Diabetes*, vol. 65, no. 11, pp. 3440–3452, 2016.

[50] R. Hart and D. R. Greaves, "Chemerin contributes to inflammation by promoting macrophage adhesion to VCAM-1 and fibronectin through clustering of VLA-4 and VLA-5," *Journal of Immunology (Baltimore, Md. : 1950)*, vol. 185, no. 6, pp. 3728–3739, 2010.

[51] K. Sawicka, M. Michalska-Jakubus, E. Potembska, M. Kowal, A. Pietrzak, and D. Krasowska, "Visfatin and chemerin levels correspond with inflammation and might reflect the bridge between metabolism, inflammation and fibrosis in patients with systemic sclerosis," *Postepy Dermatologii i Alergologii*, vol. 36, no. 5, pp. 551–565, 2019.

[52] O. Gruzdeva, D. Borodkina, E. Uchasova, Y. Dyleva, and O. Barbarash, "Leptin resistance: underlying mechanisms and diagnosis," *Diabetes, Metabolic Syndrome and Obesity: Targets and Therapy*, vol. 12, pp. 191–198, 2019.

[53] B. Liu, J. Qiao, J. Hu et al., "Leptin promotes endothelial dysfunction in chronic kidney disease by modulating the MTA1-mediated WNT/β-catenin pathway," *Molecular and Cellular Biochemistry*, vol. 473, no. 1–2, pp. 155–166, 2020.

[54] I. Drosos, G. Chalikias, M. Pavlaki et al., "Differences between perivascular adipose tissue surrounding the heart and the internal mammary artery: possible role for the leptin-inflammation-fibrosis-hypoxia axis," *Clinical Research in Cardiology*, vol. 105, no. 11, pp. 887–900, 2016.

[55] M. Bokarewa, I. Nagaev, L. Dahlberg, U. Smith, and A. Tarkowski, "Resistin, an adipokine with potent proinflammatory properties," *Journal of Immunology (Baltimore, Md. : 1950)*, vol. 174, no. 9, pp. 5789–5795, 2005.

[56] C. Chen, J. Jiang, J. M. Lü et al., "Resistin decreases expression of endothelial nitric oxide synthase through oxidative stress in human coronary artery endothelial cells," *American Journal of Physiology-Heart and Circulatory Physiology*, vol. 299, no. 1, pp. H193–H201, 2010.

[57] J. Luo, L. Huang, A. Wang et al., "Resistin-induced endoplasmic reticulum stress contributes to the impairment of insulin signaling in endothelium," *Frontiers in Pharmacology*, vol. 9, p. 1226, 2018.

[58] R. S. de Lima, J. C. . S. Silva, C. T. Lima et al., "Proinflammatory role of angiotensin II in the aorta of normotensive mice," *BioMed Research International*, vol. 2019, Article ID 9326896, 11 pages, 2019.

[59] H. Pons, A. Ferrebuz, Y. Quiroz et al., "Immune reactivity to heat shock protein 70 expressed in the kidney is cause of salt-sensitive hypertension," *American Journal of Physiology Renal Physiology*, vol. 304, no. 3, pp. F289–F299, 2013.

[60] B. Rodriguez-Iturbe, "Autoimmunity in the pathogenesis of hypertension," *Hypertension*, vol. 67, no. 3, pp. 477–483, 2016.

[61] T. P. Mikolajczyk, R. Nosalski, P. Szczepaniak et al., "Role of chemokine RANTES in the regulation of perivascular inflammation, T-cell accumulation, and vascular dysfunction in hypertension," *FASEB Journal*, vol. 30, no. 5, pp. 1987–1999, 2016.

[62] L. Markó, H. Kvakan, J. K. Park et al., "Interferon-γ signaling inhibition ameliorates angiotensin II-induced cardiac damage," *Hypertension (Dallas, Tex. : 1979)*, vol. 60, no. 6, pp. 1430–1436, 2012.

[63] P. Libby, J. E. Buring, L. Badimon et al., "Atherosclerosis," *Nature Reviews Disease Primers*, vol. 5, no. 1, p. 56, 2019.

[64] A. Chroni, G. Leondaritis, and H. Karlsson, "Lipids and lipoproteins in atherosclerosis," *Journal of Lipids*, vol. 2011, Article ID 160104, 2 pages, 2011.

[65] M. Rafieian-Kopaei, M. Setorki, M. Doudi, A. Baradaran, and H. Nasri, "Atherosclerosis: process, indicators, risk factors and new hopes," *International Journal of Preventive Medicine*, vol. 5, no. 8, pp. 927–946, 2014.

[66] D. Tousoulis, E. Oikonomou, E. K. Economou, F. Crea, and J. C. Kaski, "Inflammatory cytokines in atherosclerosis: current therapeutic approaches," *European Heart Journal*, vol. 37, no. 22, pp. 1723–1732, 2016.

[67] E. Nava and S. Llorens, "The local regulation of vascular function: from an inside-outside to an outside-inside model," *Frontiers in Physiology*, vol. 10, p. 729, 2019.

[68] T. K. Chatterjee, L. L. Stoll, G. M. Denning et al., "Proinflammatory phenotype of perivascular adipocytes: influence of high-fat feeding," *Circulation Research*, vol. 104, no. 4, pp. 541–549, 2009.

[69] J. Mancio, E. K. Oikonomou, and C. Antoniades, "Perivascular adipose tissue and coronary atherosclerosis," *Heart (British Cardiac Society)*, vol. 104, no. 20, pp. 1654–1662, 2018.

[70] A. Omar, T. K. Chatterjee, Y. Tang, D. Y. Hui, and N. L. Weintraub, "Proinflammatory phenotype of perivascular adipocytes," *Arteriosclerosis, Thrombosis, and Vascular Biology*, vol. 34, no. 8, pp. 1631–1636, 2014.

[71] D. S. Skiba, R. Nosalski, T. P. Mikolajczyk et al., "Anti-atherosclerotic effect of the angiotensin 1–7 mimetic AVE0991 is mediated by inhibition of perivascular and plaque inflammation in early atherosclerosis," *British Journal of Pharmacology*, vol. 174, no. 22, pp. 4055–4069, 2017.

[72] T. K. Chatterjee, B. J. Aronow, W. S. Tong et al., "Human coronary artery perivascular adipocytes overexpress genes responsible for regulating vascular morphology, inflammation, and hemostasis," *Physiological Genomics*, vol. 45, no. 16, pp. 697–709, 2013.

[73] A. Virdis, "Endothelial dysfunction in obesity: role of inflammation," *High Blood Pressure & Cardiovascular Prevention*, vol. 23, no. 2, pp. 83–85, 2016.

[74] H. Wu, S. Ghosh, X. D. Perrard et al., "T-cell accumulation and regulated on activation, normal T cell expressed and secreted upregulation in adipose tissue in obesity," *Circulation*, vol. 115, no. 8, pp. 1029–1038, 2007.

[75] T. J. Guzik, N. E. Hoch, K. A. Brown et al., "Role of the T cell in the genesis of angiotensin II induced hypertension and vascular dysfunction," *The Journal of Experimental Medicine*, vol. 204, no. 10, pp. 2449–2460, 2007.

[76] P. Lesnik, C. A. Haskell, and I. F. Charo, "Decreased atherosclerosis in CX3CR1-/- mice reveals a role for fractalkine in atherogenesis," *The Journal of Clinical Investigation*, vol. 111, no. 3, pp. 333–340, 2003.

[77] S. Sakaguchi, M. Miyara, C. M. Costantino, and D. A. Hafler, "FOXP3^{+} regulatory T cells in the human immune system," *Nature Reviews Immunology*, vol. 10, no. 7, pp. 490–500, 2010.

[78] H. A. Itani, W. G. McMaster Jr., M. A. Saleh et al., "Activation of Human T Cells in Hypertension: Studies of Humanized Mice and Hypertensive Humans," *Hypertension (Dallas, Tex. : 1979)*, vol. 68, no. 1, pp. 123–132, 2016.

[79] D. A. Kasal, T. Barhoumi, M. W. Li et al., "T regulatory lymphocytes prevent aldosterone-induced vascular injury," *Hypertension (Dallas, Tex. : 1979)*, vol. 59, no. 2, pp. 324–330, 2012.

[80] L. Wu, V. V. Parekh, C. L. Gabriel et al., "Activation of invariant natural killer T cells by lipid excess promotes tissue inflammation, insulin resistance, and hepatic steatosis in obese mice," *Proceedings of the National Academy of Sciences of the United States of America*, vol. 109, no. 19, pp. E1143–E1152, 2012.

[81] A. Ugusman, J. Kumar, and A. Aminuddin, "Endothelial function and dysfunction: Impact of sodium-glucose

cotransporter 2 inhibitors," *Pharmacology & Therapeutics*, vol. 224, article 107832, 2021.

[82] J. Chen, Z. X. Ye, X. F. Wang et al., "Nitric oxide bioavailability dysfunction involves in atherosclerosis," *Biomedicine & Pharmacotherapy*, vol. 97, pp. 423–428, 2018.

[83] M. Mudau, A. Genis, A. Lochner, and H. Strijdom, "Endothelial dysfunction: the early predictor of atherosclerosis," *Cardiovascular Journal of Africa*, vol. 23, no. 4, pp. 222–231, 2012.

[84] M. Gil-Ortega, B. Somoza, Y. Huang, M. Gollasch, and M. S. Fernández-Alfonso, "Regional differences in perivascular adipose tissue impacting vascular homeostasis," *Trends in Endocrinology & Metabolism*, vol. 26, no. 7, pp. 367–375, 2015.

[85] Z. J. Wang, J. Wu, W. Guo, and Y. Z. Zhu, "Atherosclerosis and the hydrogen sulfide signaling pathway - therapeutic approaches to disease prevention," *Cellular Physiology and Biochemistry*, vol. 42, no. 3, pp. 859–875, 2017.

[86] C. Agabiti-Rosei, C. de Ciuceis, C. Rossini et al., "Anticontractile activity of perivascular fat in obese mice and the effect of long-term treatment with melatonin," *Journal of Hypertension*, vol. 32, no. 6, pp. 1264–1274, 2014.

[87] R. Aghamohammadzadeh, R. D. Unwin, A. S. Greenstein, and A. M. Heagerty, "Effects of obesity on perivascular adipose tissue vasorelaxant function: nitric oxide, inflammation and elevated systemic blood pressure," *Journal of Vascular Research*, vol. 52, no. 5, pp. 299–305, 2015.

[88] T. Almabrouk, A. D. White, A. B. Ugusman et al., "High fat diet attenuates the anticontractile activity of aortic PVAT via a mechanism involving AMPK and reduced adiponectin secretion," *Frontiers in Physiology*, vol. 9, p. 51, 2018.

[89] J. Bełtowski, "Endogenous hydrogen sulfide in perivascular adipose tissue: role in the regulation of vascular tone in physiology and pathology," *Canadian Journal of Physiology and Pharmacology*, vol. 91, no. 11, pp. 889–898, 2013.

[90] J. Ketonen, J. Shi, E. Martonen, and E. Mervaala, "Periadventitial adipose tissue promotes endothelial dysfunction via oxidative stress in diet-induced obese C57Bl/6 mice," *Circulation Journal*, vol. 74, no. 7, pp. 1479–1487, 2010.

[91] C. Marchesi, T. Ebrahimian, O. Angulo, P. Paradis, and E. L. Schiffrin, "Endothelial nitric oxide synthase uncoupling and perivascular adipose oxidative stress and inflammation contribute to vascular dysfunction in a rodent model of metabolic syndrome," *Hypertension (Dallas, Tex. : 1979)*, vol. 54, no. 6, pp. 1384–1392, 2009.

[92] H. Hu, M. Garcia-Barrio, Z. S. Jiang, Y. E. Chen, and L. Chang, "Roles of perivascular adipose tissue in hypertension and atherosclerosis," *Antioxidants and Redox Signaling*, vol. 34, no. 9, pp. 736–749, 2021.

[93] M. Federici, A. Pandolfi, E. A. de Filippis et al., "G972R IRS-1 variant impairs insulin regulation of endothelial nitric oxide synthase in cultured human Endothelial cells," *Circulation*, vol. 109, no. 3, pp. 399–405, 2004.

[94] P. Geraldes and G. L. King, "Activation of protein kinase C isoforms and its impact on diabetic complications," *Circulation Research*, vol. 106, no. 8, pp. 1319–1331, 2010.

[95] M. Barton, "Prevention and endothelial therapy of coronary artery disease," *Current Opinion in Pharmacology*, vol. 13, no. 2, pp. 226–241, 2013.

[96] N. D. Brunetti, G. Salvemini, A. Cuculo et al., "Coronary artery ectasia is related to coronary slow flow and inflammatory activation," *Atherosclerosis*, vol. 233, no. 2, pp. 636–640, 2014.

[97] A. Zernecke and C. Weber, "Chemokines in the vascular inflammatory response of atherosclerosis," *Cardiovascular Research*, vol. 86, no. 2, pp. 192–201, 2010.

[98] I. Tabas, G. García-Cardeña, and G. K. Owens, "Recent insights into the cellular biology of atherosclerosis," *The Journal of Cell Biology*, vol. 209, no. 1, pp. 13–22, 2015.

[99] C.-Y. Miao and Z. Y. Li, "The role of perivascular adipose tissue in vascular smooth muscle cell growth," *British Journal of Pharmacology*, vol. 165, no. 3, pp. 643–658, 2012.

[100] K. T. Moe, T. M. Naylynn, N. O. Yin et al., "Tumor necrosis factor-α induces aortic intima-media thickening via perivascular adipose tissue inflammation," *Journal of Vascular Research*, vol. 50, no. 3, pp. 228–237, 2013.

[101] Z. Ding, A. M. Mizeracki, C. Hu, and J. L. Mehta, "LOX-1 deletion and macrophage trafficking in atherosclerosis," *Biochemical and Biophysical Research Communications*, vol. 440, no. 2, pp. 210–214, 2013.

[102] A. Yamashita, K. Shoji, T. Tsuruda et al., "Medial and adventitial macrophages are associated with expansive atherosclerotic remodeling in rabbit femoral artery," *Histology and Histopathology*, vol. 23, no. 2, pp. 127–136, 2008.

[103] D. Manka, T. K. Chatterjee, L. L. Stoll et al., "Transplanted perivascular adipose tissue accelerates injury-induced neointimal hyperplasia: role of monocyte chemoattractant protein-1," *Arteriosclerosis, Thrombosis, and Vascular Biology*, vol. 34, no. 8, pp. 1723–1730, 2014.

[104] M. P. W. Moos, N. John, R. Gräbner et al., "The lamina adventitia is the major site of immune cell accumulation in standard chow-fed apolipoprotein E–Deficient mice," *Arteriosclerosis, Thrombosis, and Vascular Biology*, vol. 25, no. 11, pp. 2386–2391, 2005.

[105] S. Sakamoto, T. Tsuruda, K. Hatakeyama, T. Imamura, Y. Asada, and K. Kitamura, "Impact of age-dependent adventitia inflammation on structural alteration of abdominal aorta in hyperlipidemic mice," *PLoS One*, vol. 9, no. 8, article e105739, 2014.

[106] C. Lohmann, N. Schäfer, T. von Lukowicz et al., "Atherosclerotic mice exhibit systemic inflammation in periadventitial and visceral adipose tissue, liver, and pancreatic islets," *Atherosclerosis*, vol. 207, no. 2, pp. 360–367, 2009.

[107] P. Srikakulapu, A. Upadhye, F. Drago et al., "Chemokine receptor-6 promotes B-1 cell trafficking to perivascular adipose tissue, local IgM production and atheroprotection," *Frontiers in Immunology*, vol. 12, pp. 1–13, 2021.

[108] C. Li, S. Li, F. Zhang et al., "Endothelial microparticles-mediated transfer of microRNA-19b promotes atherosclerosis via activating perivascular adipose tissue inflammation in apoE$^{-/-}$ mice," *Biochemical and Biophysical Research Communications*, vol. 495, no. 2, pp. 1922–1929, 2017.

[109] K. Terada, H. Yamada, M. Kikai et al., "Transplantation of periaortic adipose tissue inhibits atherosclerosis in *apoE*$^{-/-}$ mice by evoking TGF-β1-mediated anti- inflammatory response in transplanted graft," *Biochemical and Biophysical Research Communications*, vol. 501, no. 1, pp. 145–151, 2018.

[110] C. Li, Z. Wang, C. Wang, Q. Ma, and Y. Zhao, "Perivascular adipose tissue-derived adiponectin inhibits collar-induced carotid atherosclerosis by promoting macrophage autophagy," *PLoS One*, vol. 10, no. 5, article e0124031, 2015.

[111] M. Hueso, L. de Ramon, E. Navarro et al., "Silencing of *CD40 in vivo* reduces progression of experimental atherogenesis through an NF-κB/miR-125b axis and reveals new potential mediators in the pathogenesis of atherosclerosis," *Atherosclerosis*, vol. 255, pp. 80–89, 2016.

[112] A. R. Baker, N. F. da Silva, D. W. Quinn et al., "Human epicardial adipose tissue expresses a pathogenic profile of adipocytokines in patients with cardiovascular disease," *Cardiovascular Diabetology*, vol. 5, no. 1, p. 1, 2006.

[113] G. Iacobellis, D. Pistilli, M. Gucciardo et al., "Adiponectin expression in human epicardial adipose tissue in vivo is lower in patients with coronary artery disease," *Cytokine*, vol. 29, no. 6, pp. 251–255, 2005.

[114] T. Mazurek, L. F. Zhang, A. Zalewski et al., "Human epicardial adipose tissue is a source of inflammatory mediators," *Circulation*, vol. 108, no. 20, pp. 2460–2466, 2003.

[115] T. Suzuki, H. Ogita, A. Sato, N. Minamidate, and K. Hachiro, "Differences between patients with and without atherosclerosis in expression levels of inflammatory mediators in the adipose tissue around the coronary artery," *International Heart Journal*, vol. 62, no. 2, pp. 390–395, 2021.

[116] E. Schütz, R. Gogiraju, M. Pavlaki et al., *Age-Dependent and -Independent E ff ects of Perivascular Adipose Tissue and Its Paracrine Activities during Neointima Formation*, pp. 1–20, 2020.

[117] B. Liu, J. Liao, X. Rao et al., "Inhibition of Stat1-mediated gene activation by PIAS1," *Proceedings of the National Academy of Sciences of the United States of America*, vol. 95, no. 18, pp. 10626–10631, 1998.

[118] B. Liu, R. Yang, K. A. Wong et al., "Negative regulation of NF-kappaB signaling by PIAS1," *Molecular and Cellular Biology*, vol. 25, no. 3, pp. 1113–1123, 2005.

[119] I. Kralova Lesna, Z. Tonar, I. Malek et al., "Is the amount of coronary perivascular fat related to atherosclerosis?," *Physiological Research*, vol. 64, Supplement 3, pp. S435–S443, 2015.

[120] F. Tavora, R. Kutys, L. Li, M. Ripple, D. Fowler, and A. Burke, "Adventitial lymphocytic inflammation in human coronary arteries with intimal atherosclerosis," *Cardiovascular Pathology*, vol. 19, no. 3, pp. e61–e68, 2010.

[121] S. N. Verhagen, A. Vink, Y. van der Graaf, and F. L. J. Visseren, "Coronary perivascular adipose tissue characteristics are related to atherosclerotic plaque size and composition. A post-mortem study," *Atherosclerosis*, vol. 225, no. 1, pp. 99–104, 2012.

[122] D. A. Chistiakov, A. N. Orekhov, and Y. V. Bobryshev, "Contribution of neovascularization and intraplaque haemorrhage to atherosclerotic plaque progression and instability," *Acta Physiologica (Oxford, England)*, vol. 213, no. 3, pp. 539–553, 2015.

[123] D. S. Farias-Itao, C. A. Pasqualucci, A. Nishizawa et al., "B lymphocytes and macrophages in the perivascular adipose tissue are associated with coronary atherosclerosis: an autopsy study," *Journal of the American Heart Association*, vol. 8, no. 24, article e013793, 2019.

[124] N. Kawasaki, R. Asada, A. Saito, S. Kanemoto, and K. Imaizumi, "Obesity-induced endoplasmic reticulum stress causes chronic inflammation in adipose tissue," *Scientific Reports*, vol. 2, no. 1, p. 799, 2012.

[125] R. Ying, S. W. Li, J. Y. Chen et al., "Endoplasmic reticulum stress in perivascular adipose tissue promotes destabilization of atherosclerotic plaque by regulating GM-CSF paracrine," *Journal of Translational Medicine*, vol. 16, no. 1, pp. 1–13, 2018.

[126] D.-H. Kim, D. Sandoval, J. A. Reed et al., "The role of GM-CSF in adipose tissue inflammation," *American Journal of Physiology. Endocrinology and Metabolism*, vol. 295, no. 5, pp. E1038–E1046, 2008.

[127] D. G. Harrison, T. J. Guzik, H. E. Lob et al., "Inflammation, immunity, and hypertension," *Hypertension (Dallas, Tex. : 1979)*, vol. 57, no. 2, pp. 132–140, 2011.

[128] A. Kirabo, V. Fontana, A. P. C. de Faria et al., "DC isoketal-modified proteins activate T cells and promote hypertension," *The Journal of Clinical Investigation*, vol. 124, no. 10, pp. 4642–4656, 2014.

[129] D. M. Tanase, E. M. Gosav, S. Radu et al., "Arterial hypertension and interleukins: potential therapeutic target or future diagnostic marker?," *International Journal of Hypertension*, vol. 2019, Article ID 3159283, 17 pages, 2019.

[130] R. Supriya, B. Y. Yung, A. P. Yu et al., "Adipokine profiling in adult women with central obesity and hypertension," *Frontiers in Physiology*, vol. 9, p. 294, 2018.

[131] C.-C. Ruan, Y. Ma, Q. Ge et al., "Complement-mediated inhibition of adiponectin regulates perivascular inflammation and vascular injury in hypertension," *FASEB Journal*, vol. 31, no. 3, pp. 1120–1129, 2017.

[132] S. Kossmann, M. Schwenk, M. Hausding et al., "Angiotensin II-induced vascular dysfunction depends on interferon-γ-driven immune cell recruitment and mutual activation of monocytes and NK-cells," *Arteriosclerosis, Thrombosis, and Vascular Biology*, vol. 33, no. 6, pp. 1313–1319, 2013.

[133] L. Zou, W. Wang, S. Liu et al., "Spontaneous hypertension occurs with adipose tissue dysfunction in perilipin-1 null mice," *Biochimica et Biophysica Acta*, vol. 1862, no. 2, pp. 182–191, 2016.

[134] C.-C. Ruan, D. L. Zhu, Q. Z. Chen et al., "Perivascular adipose tissue-derived complement 3 is required for adventitial fibroblast functions and adventitial remodeling in deoxycorticosterone acetate-salt hypertensive rats," *Arteriosclerosis, Thrombosis, and Vascular Biology*, vol. 30, no. 12, pp. 2568–2574, 2010.

[135] C.-C. Ruan, Q. Ge, Y. Li et al., "Complement-mediated macrophage polarization in perivascular adipose tissue contributes to vascular injury in deoxycorticosterone acetate-salt mice," *Arteriosclerosis, Thrombosis, and Vascular Biology*, vol. 35, no. 3, pp. 598–606, 2015.

[136] T. Minami, K. Satoh, M. Nogi et al., "Statins up-regulate SmgGDS through β1-integrin/Akt1 pathway in endothelial cells," *Cardiovascular Research*, vol. 109, no. 1, pp. 151–161, 2016.

[137] M. Nus, B. Martínez-Poveda, D. MacGrogan et al., "Endothelial Jag1-RBPJ signalling promotes inflammatory leucocyte recruitment and atherosclerosis," *Cardiovascular Research*, vol. 112, no. 2, pp. 568–580, 2016.

[138] P. Wenzel, M. Knorr, S. Kossmann et al., "Lysozyme M-positive monocytes mediate angiotensin II-induced arterial hypertension and vascular dysfunction," *Circulation*, vol. 124, no. 12, pp. 1370–1381, 2011.

[139] M. A. Saleh, W. G. McMaster, J. Wu et al., "Lymphocyte adaptor protein LNK deficiency exacerbates hypertension and end-organ inflammation," *The Journal of Clinical Investigation*, vol. 125, no. 3, pp. 1189–1202, 2015.

[140] C. T. Chan, J. P. Moore, K. Budzyn et al., "Reversal of vascular macrophage accumulation and hypertension by a CCR2 antagonist in deoxycorticosterone/salt-treated mice," *Hypertension (Dallas, Tex. : 1979)*, vol. 60, no. 5, pp. 1207–1212, 2012.

[141] L. A. Cassis, S. B. Police, F. Yiannikouris, and S. E. Thatcher, "Local adipose tissue renin-angiotensin system," *Current Hypertension Reports*, vol. 10, no. 2, pp. 93–98, 2008.

[142] B. Gálvez-Prieto, J. Bolbrinker, P. Stucchi et al., "Comparative expression analysis of the renin-angiotensin system components between white and brown perivascular adipose tissue," *The Journal of Endocrinology*, vol. 197, no. 1, pp. 55–64, 2008.

[143] A. Nguyen Dinh Cat and R. M. Touyz, "A new look at the renin-angiotensin system–focusing on the vascular system," *Peptides*, vol. 32, no. 10, pp. 2141–2150, 2011.

[144] L. te Riet, J. H. M. van Esch, A. J. M. Roks, A. H. van den Meiracker, and A. H. J. Danser, "Hypertension," *Circulation Research*, vol. 116, no. 6, pp. 960–975, 2015.

[145] L. Chang, W. Xiong, X. Zhao et al., "Bmal 1 in perivascular adipose tissue regulates resting-phase blood pressure through transcriptional regulation of angiotensinogen," *Circulation*, vol. 138, no. 1, pp. 67–79, 2018.

[146] T. P. Mikolajczyk, R. Nosalski, D. S. Skiba et al., "1,2,3,4,6-Penta-O-galloyl-β-d-glucose modulates perivascular inflammation and prevents vascular dysfunction in angiotensin II-induced hypertension," *British Journal of Pharmacology*, vol. 176, no. 12, pp. 1951–1965, 2019.

[147] S. Kagota, K. Maruyama-Fumoto, M. Shimari, J. J. McGuire, and K. Shinozuka, "Angiotensin II type 1 receptor antagonist azilsartan restores vascular reactivity through a perivascular adipose tissue-independent mechanism in rats with metabolic syndrome," *Cardiovascular Drugs and Therapy*, vol. 33, no. 5, pp. 501–509, 2019.

[148] T. Wei, J. Gao, C. Huang, B. Song, M. Sun, and W. Shen, "SIRT3 (Sirtuin-3) Prevents Ang II (Angiotensin II)-Induced Macrophage Metabolic Switch Improving Perivascular Adipose Tissue Function," *Arteriosclerosis, Thrombosis, and Vascular Biology*, vol. 41, no. 2, pp. 714–730, 2021.

[149] P. Liu, Q. Xie, T. Wei, Y. Chen, H. Chen, and W. Shen, "Activation of the NLRP3 inflammasome induces vascular dysfunction in obese OLETF rats," *Biochemical and Biophysical Research Communications*, vol. 468, no. 1–2, pp. 319–325, 2015.

[150] X. Unamuno, J. Gómez-Ambrosi, B. Ramírez et al., "NLRP3 inflammasome blockade reduces adipose tissue inflammation and extracellular matrix remodeling," *Cellular & Molecular Immunology*, vol. 18, no. 4, pp. 1045–1057, 2019.

[151] N. S. Ferreira, R. C. Tostes, P. Paradis, and E. L. Schiffrin, "Aldosterone, inflammation, immune system, and hypertension," *American Journal of Hypertension*, vol. 34, no. 1, pp. 15–27, 2021.

[152] F. Mayyas, K. H. Alzoubi, and D. R. van Wagoner, "Impact of aldosterone antagonists on the substrate for atrial fibrillation: aldosterone promotes oxidative stress and atrial structural/electrical remodeling," *International Journal of Cardiology*, vol. 168, no. 6, pp. 5135–5142, 2013.

[153] I. Sudano, F. Ruschitzka, G. Noll, and T. F. Luscher, "Endothelial function and the effects of aldosterone blockade," *European Heart Journal Supplements*, vol. 13, Supplement_B, pp. B21–B26, 2011.

[154] A. M. Briones, A. Nguyen Dinh Cat, G. E. Callera et al., "Adipocytes produce aldosterone through calcineurin-dependent signaling pathways," *Hypertension*, vol. 59, no. 5, pp. 1069–1078, 2012.

[155] Y.-C. Lee, H. H. Chang, C. L. Chiang et al., "Role of perivascular adipose tissue-derived methyl palmitate in vascular tone regulation and pathogenesis of hypertension," *Circulation*, vol. 124, no. 10, pp. 1160–1171, 2011.

[156] T. J. Guzik, R. Olszanecki, J. Sadowski et al., "Superoxide dismutase activity and expression in human venous and arterial bypass graft vessels," *Journal of Physiology and Pharmacology*, vol. 56, no. 2, pp. 313–323, 2005.

[157] T. Szasz, G. F. Bomfim, and R. C. Webb, "The influence of perivascular adipose tissue on vascular homeostasis," *Vascular Health and Risk Management*, vol. 9, pp. 105–116, 2013.

[158] C. M. Sena, A. Leandro, L. Azul, R. Seiça, and G. Perry, "Vascular oxidative stress: impact and therapeutic approaches," *Frontiers in Physiology*, vol. 9, p. 1668, 2018.

[159] S. E. L. Even, M. G. Dulak-Lis, R. M. Touyz, and A. Nguyen Dinh Cat, "Crosstalk between adipose tissue and blood vessels in cardiometabolic syndrome: implication of steroid hormone receptors (MR/GR)," *Hormone Molecular Biology and Clinical Investigation*, vol. 19, no. 2, pp. 89–101, 2014.

[160] R. Nosalski, T. Mikolajczyk, M. Siedlinski et al., "Nox1/4 inhibition exacerbates age dependent perivascular inflammation and fibrosis in a model of spontaneous hypertension," *Pharmacological Research*, vol. 161, article 105235, 2020.

[161] J. Wu, M. A. Saleh, A. Kirabo et al., "Immune activation caused by vascular oxidation promotes fibrosis and hypertension," *The Journal of Clinical Investigation*, vol. 126, no. 1, pp. 50–67, 2016.

[162] U. Landmesser, H. Cai, S. Dikalov et al., "Role of p47phoxin vascular oxidative stress and hypertension caused by angiotensin II," *Hypertension (Dallas, Tex. : 1979)*, vol. 40, no. 4, pp. 511–515, 2002.

[163] K. Matsuno, H. Yamada, K. Iwata et al., "Nox1 is involved in angiotensin II-mediated hypertension: a study in Nox1-deficient mice," *Circulation*, vol. 112, no. 17, pp. 2677–2685, 2005.

[164] S.-Z. Jiang, W. Lu, X. F. Zong, H. Y. Ruan, and Y. Liu, "Obesity and hypertension," *Experimental and Therapeutic Medicine*, vol. 12, no. 4, pp. 2395–2399, 2016.

[165] M. I. Yilmaz, A. Sonmez, K. Caglar et al., "Effect of antihypertensive agents on plasma adiponectin levels in hypertensive patients with metabolic syndrome," *Nephrology (Carlton, Vic.)*, vol. 12, no. 2, pp. 147–153, 2007.

[166] A. S. Greenstein, K. Khavandi, S. B. Withers et al., "Local inflammation and hypoxia abolish the protective anticontractile properties of perivascular fat in obese patients," *Circulation*, vol. 119, no. 12, pp. 1661–1670, 2009.

[167] N. Xia, S. Horke, A. Habermeier et al., "Uncoupling of endothelial nitric oxide synthase in perivascular adipose tissue of diet-induced obese mice," *Arteriosclerosis, Thrombosis, and Vascular Biology*, vol. 36, no. 1, pp. 78–85, 2016.

[168] R. Aghamohammadzadeh, A. S. Greenstein, R. Yadav et al., "Effects of bariatric surgery on human small artery function: evidence for reduction in perivascular adipocyte inflammation, and the restoration of normal anticontractile activity despite persistent obesity," *Journal of the American College of Cardiology*, vol. 62, no. 2, pp. 128–135, 2013.

[169] H. Chen, M. Montagnani, T. Funahashi, I. Shimomura, and M. J. Quon, "Adiponectin Stimulates Production of Nitric

Oxide in Vascular Endothelial Cells," *The Journal of Biological Chemistry*, vol. 278, no. 45, pp. 45021–45026, 2003.

[170] H. Vaverkova, D. Karasek, D. Novotny et al., "Positive association of adiponectin with soluble vascular cell adhesion molecule sVCAM-1 levels in patients with vascular disease or dyslipidemia," *Atherosclerosis*, vol. 197, no. 2, pp. 725–731, 2008.

[171] S. Nakanishi, K. Yamane, N. Kamei, H. Nojima, M. Okubo, and N. Kohno, "A protective effect of adiponectin against oxidative stress in Japanese Americans: the association between adiponectin or leptin and urinary isoprostane," *Metabolism*, vol. 54, no. 2, pp. 194–199, 2005.

[172] P. A. Kern, G. B. di Gregorio, T. Lu, N. Rassouli, and G. Ranganathan, "Adiponectin expression from human adipose tissue," *Diabetes*, vol. 52, no. 7, pp. 1779–1785, 2003.

[173] M. Adamczak, A. Wiecek, T. Funahashi, J. Chudek, F. Kokot, and Y. Matsuzawa, "Decreased plasma adiponectin concentration in patients with essential hypertension," *American Journal of Hypertension*, vol. 16, no. 1, pp. 72–75, 2003.

[174] S. Maruyama, R. Shibata, R. Kikuchi et al., "Fat-derived Factor Omentin Stimulates Endothelial Cell Function and Ischemia- induced Revascularization via Endothelial Nitric Oxide Synthase-dependent Mechanism," *The Journal of Biological Chemistry*, vol. 287, no. 1, pp. 408–417, 2012.

[175] C. M. de Souza Batista, R. Z. Yang, M. J. Lee et al., "Omentin plasma levels and gene expression are decreased in obesity," *Diabetes*, vol. 56, no. 6, pp. 1655–1661, 2007.

[176] Y. Du, Q. Ji, L. Cai et al., "Association between omentin-1 expression in human epicardial adipose tissue and coronary atherosclerosis," *Cardiovascular Diabetology*, vol. 15, no. 1, p. 90, 2016.

[177] A. Planavila, I. Redondo-Angulo, F. Ribas et al., "Fibroblast growth factor 21 protects the heart from oxidative stress," *Cardiovascular Research*, vol. 106, no. 1, pp. 19–31, 2015.

[178] Y. Zhang, Z. Liu, M. Zhou, and C. Liu, "Therapeutic effects of fibroblast growth factor-21 against atherosclerosis via the NF-κB pathway," *Molecular Medicine Reports*, vol. 17, no. 1, pp. 1453–1460, 2018.

[179] X. Pan, Y. Shao, F. Wu et al., "FGF21 Prevents Angiotensin II-Induced Hypertension and Vascular Dysfunction by Activation of ACE2/Angiotensin-(1-7) Axis in Mice," *Cell Metabolism*, vol. 27, no. 6, pp. 1323–1337.e5, 2018.

[180] J. Rueda-Gotor, R. López-Mejías, S. Remuzgo-Martínez et al., "Vaspin in atherosclerotic disease and cardiovascular risk in axial spondyloarthritis: a genetic and serological study," *Arthritis Research & Therapy*, vol. 23, no. 1, p. 111, 2021.

[181] K. Kauser, V. da Cunha, R. Fitch, C. Mallari, and G. M. Rubanyi, "Role of endogenous nitric oxide in progression of atherosclerosis in apolipoprotein E-deficient mice," *American Journal of Physiology-Heart and Circulatory Physiology*, vol. 278, no. 5, pp. H1679–H1685, 2000.

[182] T. Quaschning, F. Voss, K. Relle et al., "Lack of endothelial nitric oxide synthase promotes endothelin-induced hypertension: lessons from endothelin-1 transgenic/endothelial nitric oxide synthase knockout mice," *Journal of the American Society of Nephrology*, vol. 18, no. 3, pp. 730–740, 2007.

[183] L. T. Fourman, C. F. Saylor, L. Cheru et al., "Anti-Inflammatory interleukin 10 inversely relates to coronary atherosclerosis in persons with human immunodeficiency virus," *The Journal of Infectious Diseases*, vol. 221, no. 4, pp. 510–515, 2019.

[184] J. Mauer, B. Chaurasia, J. Goldau et al., "Signaling by IL-6 promotes alternative activation of macrophages to limit endotoxemia and obesity-associated resistance to insulin," *Nature Immunology*, vol. 15, no. 5, pp. 423–430, 2014.

[185] R. M. da Costa, R. S. Fais, C. R. P. Dechandt et al., "Increased mitochondrial ROS generation mediates the loss of the anticontractile effects of perivascular adipose tissue in high-fat diet obese mice," *British Journal of Pharmacology*, vol. 174, no. 20, pp. 3527–3541, 2017.

[186] H. Kirii, T. Niwa, Y. Yamada et al., "Lack of Interleukin-1β decreases the severity of atherosclerosis in ApoE-Deficient mice," *Arteriosclerosis, Thrombosis, and Vascular Biology*, vol. 23, no. 4, pp. 656–660, 2003.

[187] B. Schieffer, T. Selle, A. Hilfiker et al., "Impact of interleukin-6 on plaque development and morphology in experimental atherosclerosis," *Circulation*, vol. 110, no. 22, pp. 3493–3500, 2004.

[188] E. S. Darios, B. M. Winner, T. Charvat, A. Krasinksi, S. Punna, and S. W. Watts, "The adipokine chemerin amplifies electrical field-stimulated contraction in the isolated rat superior mesenteric artery," *American Journal of Physiology-Heart and Circulatory Physiology*, vol. 311, no. 2, pp. H498–H507, 2016.

[189] G. K. Dimitriadis, J. Kaur, R. Adya et al., "Chemerin induces endothelial cell inflammation: activation of nuclear factor-kappa beta and monocyte-endothelial adhesion," *Oncotarget*, vol. 9, no. 24, pp. 16678–16690, 2018.

[190] M. C. Ernst, M. Issa, K. B. Goralski, and C. J. Sinal, "Chemerin exacerbates glucose intolerance in mouse models of obesity and diabetes," *Endocrinology*, vol. 151, no. 5, pp. 1998–2007, 2010.

[191] S. I. Yamagishi, D. Edelstein, X. L. Du, Y. Kaneda, M. Guzmán, and M. Brownlee, "Leptin Induces Mitochondrial Superoxide Production and Monocyte Chemoattractant Protein-1 Expression in Aortic Endothelial Cells by Increasing Fatty Acid Oxidation via Protein Kinase A," *The Journal of Biological Chemistry*, vol. 276, no. 27, pp. 25096–25100, 2001.

[192] B. Gálvez-Prieto, B. Somoza, M. Gil-Ortega et al., "Anticontractile effect of perivascular adipose tissue and leptin are reduced in hypertension," *Frontiers in Pharmacology*, vol. 3, p. 103, 2012.

[193] M. R. Schroeter, N. Eschholz, S. Herzberg et al., "Leptin-dependent and leptin-independent paracrine effects of perivascular adipose tissue on neointima formation," *Arteriosclerosis, Thrombosis, and Vascular Biology*, vol. 33, no. 5, pp. 980–987, 2013.

[194] M. P. Reilly, M. Lehrke, M. L. Wolfe, A. Rohatgi, M. A. Lazar, and D. J. Rader, "Resistin is an inflammatory marker of atherosclerosis in humans," *Circulation*, vol. 111, no. 7, pp. 932–939, 2005.

[195] Y.-B. Lv, J. Jing, J. M. Li, J. P. Zhong, L. Fang, and B. Yang, "Assessment of RANTES levels as the indicators of plaque vulnerability in rabbit models of atherosclerosis," *Pathology, Research and Practice*, vol. 210, no. 12, pp. 1031–1037, 2014.

[196] P. Dorfmüller, V. Zarka, I. Durand-Gasselin et al., "Chemokine RANTES in severe pulmonary arterial hypertension," *American Journal of Respiratory and Critical Care Medicine*, vol. 165, no. 4, pp. 534–539, 2002.

[197] R. J. Aiello, P. A. K. Bourassa, S. Lindsey et al., "Monocyte chemoattractant protein-1 accelerates atherosclerosis in

apolipoprotein E-deficient mice," *Arteriosclerosis, Thrombosis, and Vascular Biology*, vol. 19, no. 6, pp. 1518–1525, 1999.

[198] J. Podolec, G. Kopec, L. Niewiara et al., "Chemokine RANTES is increased at early stages of coronary artery disease," *Journal of Physiology and Pharmacology*, vol. 67, no. 2, pp. 321–328, 2016.

[199] J. Chamberlain, S. Francis, Z. Brookes et al., "Interleukin-1 regulates multiple atherogenic mechanisms in response to fat feeding," *PLoS One*, vol. 4, no. 4, article e5073, 2009.

[200] R. Li, A. Paul, K. W. S. Ko et al., "Interleukin-7 induces recruitment of monocytes/macrophages to endothelium," *European Heart Journal*, vol. 33, no. 24, pp. 3114–3123, 2012.

[201] L. Ziegler, J. Lundqvist, K. Dreij et al., "Expression of Interleukin 6 signaling receptors in carotid atherosclerosis," *Vascular Medicine*, vol. 26, no. 1, pp. 3–10, 2020.

[202] Y. Zhang, X. Yang, F. Bian et al., "TNF-α promotes early atherosclerosis by increasing transcytosis of LDL across endothelial cells: crosstalk between NF-κB and PPAR-γ," *Journal of Molecular and Cellular Cardiology*, vol. 72, pp. 85–94, 2014.

[203] U. C. Broedl, C. Lebherz, M. Lehrke et al., "Low adiponectin levels are an independent predictor of mixed and non-calcified coronary atherosclerotic plaques," *PLoS One*, vol. 4, no. 3, article e4733, 2009.

[204] Z. Wang, C. Li, X. Sun et al., "Hypermethylation of miR-181b in monocytes is associated with coronary artery disease and promotes M1 polarized phenotype via PIAS1-KLF4 axis," *Cardiovascular Diagnosis and Therapy*, vol. 10, no. 4, pp. 738–751, 2020.

[205] M.-H. Zhang, Y. X. Cao, L. G. Wu et al., "Association of plasma free fatty acids levels with the presence and severity of coronary and carotid atherosclerotic plaque in patients with type 2 diabetes mellitus," *BMC Endocrine Disorders*, vol. 20, no. 1, p. 156, 2020.

[206] T. A. Jacinto, G. S. Meireles, A. T. Dias et al., "Increased ROS production and DNA damage in monocytes are biomarkers of aging and atherosclerosis," *Biological Research*, vol. 51, no. 1, p. 33, 2018.

[207] A. G. Herman and S. Moncada, "Therapeutic potential of nitric oxide donors in the prevention and treatment of atherosclerosis," *European Heart Journal*, vol. 26, no. 19, pp. 1945–1955, 2005.

[208] Y. Lin, H. Zeng, L. Gao, T. Gu, C. Wang, and H. Zhang, "Hydrogen Sulfide attenuates atherosclerosis in a partially ligated carotid artery mouse model via regulating angiotensin converting enzyme 2 expression," *Frontiers in Physiology*, vol. 8, p. 782, 2017.

[209] C. Buono, C. E. Come, G. Stavrakis, G. F. Maguire, P. W. Connelly, and A. H. Lichtman, "Influence of Interferon-γ on the Extent and Phenotype of Diet-Induced Atherosclerosis in the LDLR-Deficient Mouse," *Arteriosclerosis, Thrombosis, and Vascular Biology*, vol. 23, no. 3, pp. 454–460, 2003.

[210] P. F. Bodary, S. Gu, Y. Shen, A. H. Hasty, J. M. Buckler, and D. T. Eitzman, "Recombinant leptin promotes atherosclerosis and thrombosis in apolipoprotein E–deficient mice," *Arteriosclerosis, Thrombosis, and Vascular Biology*, vol. 25, no. 8, pp. e119–e122, 2005.

[211] T. B. Dahl, A. Yndestad, M. Skjelland et al., "Increased expression of visfatin in macrophages of human unstable carotid and coronary atherosclerosis," *Circulation*, vol. 115, no. 8, pp. 972–980, 2007.

[212] S. C. A. de Jager, A. O. Kraaijeveld, R. W. Grauss et al., "CCL3 (MIP-1α) levels are elevated during acute coronary syndromes and show strong prognostic power for future ischemic events," *Journal of Molecular and Cellular Cardiology*, vol. 45, no. 3, pp. 446–452, 2008.

[213] D. Tsiantoulas, I. Bot, M. Ozsvar-Kozma et al., "Increased plasma IgE accelerate atherosclerosis in secreted IgM deficiency," *Circulation Research*, vol. 120, no. 1, pp. 78–84, 2017.

[214] L. E. Bautista, L. M. Vera, I. A. Arenas, and G. Gamarra, "Independent association between inflammatory markers (C-reactive protein, interleukin-6, and TNF-α) and essential hypertension," *Journal of Human Hypertension*, vol. 19, no. 2, pp. 149–154, 2005.

[215] M. Buemi, D. Marino, F. Floccari et al., "Effect of interleukin 8 and ICAM-1 on calcium-dependent outflow of K+ in erythrocytes from subjects with essential hypertension," *Current Medical Research and Opinion*, vol. 20, no. 1, pp. 19–24, 2004.

[216] A. Cortez and E. Muxfeldt, "Proteina 1 quimioatrayente de monocitos e hipertension: generalidades," *Hipertensión y Riesgo Vascular*, vol. 38, no. 4, 2021.

[217] P. Chatterjee, V. L. Chiasson, G. Seerangan et al., "Cotreatment with interleukin 4 and interleukin 10 modulates immune cells and prevents hypertension in pregnant mice," *American Journal of Hypertension*, vol. 28, no. 1, pp. 135–142, 2015.

[218] S. D. Crowley, S. B. Gurley, M. J. Herrera et al., "Angiotensin II causes hypertension and cardiac hypertrophy through its receptors in the kidney," *Proceedings of the National Academy of Sciences of the United States of America*, vol. 103, no. 47, pp. 17985–17990, 2006.

[219] M. A. Sparks, J. Stegbauer, D. Chen et al., "Vascular type 1A angiotensin II receptors control BP by regulating renal blood flow and urinary sodium excretion," *Journal of the American Society of Nephrology*, vol. 26, no. 12, pp. 2953–2962, 2015.

[220] S. Cottone, G. Mule, M. Guarneri et al., "Endothelin-1 and F2-isoprostane relate to and predict renal dysfunction in hypertensive patients," *Nephrology, Dialysis, Transplantation*, vol. 24, no. 2, pp. 497–503, 2009.

[221] A. Troia, R. H. Knutsen, C. M. Halabi et al., "Inhibition of NOX1 Mitigates Blood Pressure Increases in Elastin Insufficiency," *Function*, vol. 2, no. 3, article zqab015, 2021.

[222] G. Engström, B. Hedblad, G. Berglund, L. Janzon, and F. Lindgärde, "Plasma levels of complement C3 is associated with development of hypertension: a longitudinal cohort study," *Journal of Human Hypertension*, vol. 21, no. 4, pp. 276–282, 2007.

Hindawi
Mediators of Inflammation
Volume 2022, Article ID 6979117, 18 pages
https://doi.org/10.1155/2022/6979117

Research Article

lnc-MRGPRF-6:1 Promotes M1 Polarization of Macrophage and Inflammatory Response through the TLR4-MyD88-MAPK Pathway

Dan Hu,[1] Yuzhong Wang,[2] Zhihuan You,[1] Yingfei Lu,[3] and Caihong Liang[1]

[1]*Department of Cardiology, The Affiliated Jiangning Hospital of Nanjing Medical University, Nanjing 210000, China*
[2]*Department of Geriatrics, The Affiliated Jiangning Hospital of Nanjing Medical University, Nanjing 210000, China*
[3]*Central Laboratory, Translational Medicine Research Center, The Affiliated Jiangning Hospital of Nanjing Medical University, Nanjing 210000, China*

Correspondence should be addressed to Yingfei Lu; emma_0614@163.com and Caihong Liang; lch@njmu.edu.cn

Received 10 August 2021; Revised 2 December 2021; Accepted 21 December 2021; Published 28 January 2022

Academic Editor: Simon Kennedy

Background. Macrophage-mediated inflammation plays an essential role in the development of atherosclerosis (AS). Long noncoding RNAs (lncRNAs), as crucial regulators, participate in this process. We identified that lnc-MRGPRF-6:1 was significantly upregulated in the plasma exosomes of coronary atherosclerotic disease (CAD) patients in a preliminary work. In the present study, we aim to assess the role of lnc-MRGPRF-6:1 in macrophage-mediated inflammatory process of AS. *Methods*. The correlation between lnc-MRGPRF-6:1 and inflammatory factors was estimated firstly in plasma exosomes of CAD patients. Subsequently, we established lnc-MRGPRF-6:1 knockout macrophage model via the CRISPR/Cas9 system. We then investigated the regulatory effects of lnc-MRGPRF-6:1 on macrophage polarization and foam cell formation. Eventually, transcriptome analysis by RNA sequencing was carried out to explore the contribution of differential genes and signaling pathways in this process. *Results*. lnc-MRGPRF-6:1 was highly expressed in the plasma exosomes of CAD patients and was positively correlated with the expression of inflammatory cytokines in plasma. lnc-MRGPRF-6:1 inhibition significantly reduced the formation of foam cells. The expression of lnc-MRGPRF-6:1 was upregulated in M1 macrophage, and lnc-MRGPRF-6:1 knockout decreased the polarization of M1 macrophage. lnc-MRGPRF-6:1 regulates macrophage polarization via the TLR4-MyD88-MAPK signaling pathway. *Conclusions*. lnc-MRGPRF-6:1 knockdown can inhibit M1 polarization of macrophage and inflammatory response through the TLR4-MyD88-MAPK signaling pathway. lnc-MRGPRF-6:1 is a vital regulator in macrophage-mediated inflammatory process of AS.

1. Introduction

Coronary atherosclerotic disease (CAD) is a serious threat to human health, which is also one of the leading causes of human death worldwide [1]. Atherosclerosis (AS) is the pathological basis of CAD [2]. AS is a chronic inflammatory vascular disease, and macrophage plays a key role in the occurrence and development of AS. Apoptosis of macrophage is the process of forming necrotic core, and it is an inducer of long-term low-level inflammation of the intima, which can further promote the occurrence of AS [3]. Macrophage can secrete a variety of proinflammatory factors and chemokines to regulate the development of AS. After lipopolysaccharide (LPS) stimulation, macrophages initiate a series of inflammatory responses by activating a specific signaling cascade and releasing preinflammatory cytokines and mediators, including interleukin- (IL-) 6, tumor necrosis factor- (TNF-) α, reactive oxygen species (ROS), nitric oxide (NO), and prostaglandin E2 (PGE2) [4].

Long noncoding RNAs (lncRNAs) are a class of noncoding RNAs with a length of more than 200 nucleotides, which have important functions in many biological processes [5]. Previous studies show that lncRNAs are specifically expressed in various diseases, such as cancer, diabetes,

cardiovascular disease, lung disease, and tissue fibrosis [6–8]. It is demonstrated that lncRNAs play important regulatory roles in inflammatory diseases by regulating macrophage function. It was reported that IL-7-AS promotes the expression of several inflammatory genes, including CCL2, CCL5, CCL7, and IL-6, by regulating NF-κB and MAPK signaling pathways in macrophages [9]. FOXP1-IT1 overexpression attenuates THP-1 cell differentiation and inhibits inflammatory development [10]. Therefore, lncRNA is an important regulator of macrophage activation. In our preliminary work, we identified that lnc-MRGPRF-6:1 was highly expressed in plasma exosomes of CAD patients. Interestingly, further research demonstrated lnc-MRGPRF-6:1 was positively correlated with TNF-α, TNF-β, and CXCL11 in CAD patients, which indicates that lnc-MRGPRF-6:1 may participate in the regulation of macrophage-mediated inflammation in AS.

Dysregulation of phenotypic transitions in macrophages prolongs inflammation and impedes tissue repair. There is evidence that the polarization imbalance of M1/M2 macrophage may contribute to inflammatory diseases, including AS [11]. The polarization of M1 and M2 macrophages largely determines the development direction of AS inflammation [12]. During the development of AS, M1 and M2 macrophages show different position preferences on the vascular wall. The plaque shoulder is dominated by atherogenic M1 cells, which are relatively fragile and prone to rupture but are rarely found in the fibrous cap area. The harmful effects of M1 macrophage were offset by the recovery of M2 macrophage and the protective effects of AS [13]. The plasticity of these subpopulations may have a considerable influence on the outcome of AS. Overactivation of M1 may preferentially promote persistent inflammation and plaque progression.

Coincidentally, several researches have indicated that lncRNAs are involved in the dysregulation of phenotypic transitions in macrophages. Cao et al. demonstrated that lncRNA-MM2P could affect macrophage M2 polarization by regulating the dephosphorylation of signal transducer and activator of transcription 6 (STAT6) [14]. Chi et al. suggested that lncRNA GAS5 could act as a ceRNA to facilitate SOCS3 expression by sponging miR-455-5p and result in macrophage M2 polarization in childhood pneumonia [15]. Li et al. proved that lnc-BAZ2B promoted M2 macrophage activation primarily by upregulating the transcription of interferon regulatory factor 4 (IRF4), a key transcription factor for M2 macrophage activation [16].

Taken together, the regulation of macrophage polarization largely determines macrophage-mediated inflammation development and AS progression, and maybe some lncRNAs are the keys to the lock of macrophage polarization. Therefore, in the present study, we aim to explore the role of lnc-MRGPRF-6:1 in macrophage polarization and macrophage-mediated inflammation.

2. Materials and Methods

2.1. Cell Lines and Cell Culture. THP-1 cells (purchased from Shanghai Institute of Cell Research, Chinese Academy of Sciences) were incubated in RPMI Medium 1640 (Invitrogen, 11875-093) with 10% fetal bovine serum (Invitrogen, 21985). All cells were cultured in a moist environment at 37°C and 5% CO_2.

2.2. Study Population. This study enrolled 20 CAD patients in the Cardiology Department of the Affiliated Jiangning Hospital of Nanjing Medical University. Inclusion criteria were patients undergoing coronary angiography for chest pain or suspected CAD. Coronary angiography of the patient showed a lesion stenosis $\geq 50\%$ in any coronary artery. And patients with congenital heart disease, cardiomyopathy, liver and kidney insufficiency, blood system diseases, malignant tumors, and other concomitant diseases were excluded. 20 healthy controls were selected from physical examination people during the same period. Plasma samples were collected and stored at liquid nitrogen immediately after collecting and centrifugation.

2.3. Exosome Isolation. Plasma exosomes were isolated using an exosome extraction kit (Invitrogen, 4484450). The enrichment of exosomes was identified using transmission electron microscopy (TEM).

2.4. Isolation of Human Monocyte. Human monocyte was isolated from venous blood by Ficoll (Solarbio, p8900). CD14 microbeads (Invitrogen, 11367D) and magnetic beads conjugated with antibodies against human CD14 were used for the monocyte separation.

2.5. Establishment of Macrophage Polarization and Repolarization Models. THP-1 cells (2×10^5/well) were inoculated in 24-well plates with 1 mL per well and incubated with PMA (Beyotime, S1819) with a final mass concentration of 100 ng/mL for 48 h. Human monocyte was incubated with macrophage colony-stimulating factor (M-CSF) (Beyotime, P5313) with a final mass concentration of 50 ng/mL for 7 days. M1 polarization of THP-1-derived macrophage and human monocyte-derived macrophage was performed using 20 ng/mL recombinant human IFN-γ (Beyotime, P5664) and 100 ng/mL LPS (Invitrogen, 00-4976). M2 polarization was performed using 20 ng/mL recombinant IL-4 (Beyotime, P5129). Nonpolarized PMA-activated cells were used as control. The polarization model of macrophage was established after 20 h of polarization. Based on the establishment of the macrophage polarization model, M1 macrophage was stimulated with 20 ng/ml IL-4 for 20 h and then induced to M2 polarization. M2 macrophage was induced to polarize toward M1 after 20 ng/mL IFN-γ and 100 ng/mL LPS stimulation for 20 h.

2.6. Establishment of Macrophage Foam Cell Model. As mentioned above, macrophage was activated from THP-1 cells by incubating with PMA. Macrophage-derived foam cell model was established by inducing 50 mg/L ox-LDL (Invitrogen, 2188176) for 24 h.

2.7. Generation and Infection of Lentivirus. CRISPR/Cas9 system was used to generate lnc-MRGPRF-6:1 knockout stable macrophage. The sgRNA targeting lnc-MRGPRF-6:1 was

designed using CRISPOR (http://crispor.tefor.net) [17]. Two targets were designed for each location, and two locations were designed for lnc-MRGPRF-6:1. Lentivirus encoding Cas9 nuclease and sgRNA targeting lnc-MRGPRF-6:1 or sgRNA control were constructed and packed by GENECHEM (Shanghai, China). Macrophages were infected by lentivirus for 24 h, and lnc-MRGPRF-6:1 knockout stable cells were sieved with a full medium containing puromycin for 72 h.

2.8. Activate TLR4-MyD88-MAPK Signaling Pathways. lnc-MRGPRF-6:1 knockout macrophage (KO) and control cells (1×10^6/well) were inoculated in 6-well plates with 2 mL per well and incubated with 100 ng/mL LPS for 24 h.

2.9. RNA Extraction and Quantitative Real-Time PCR. Total RNA was extracted from the cells using the RNeasy Plus Mini Kit (QIAGEN, 74134) , from the plasma using BIOG cfDNA Easy Kit (BIOG, 51028) and from exosomes by RNA Purification Kit (EZBioscience, EZB-EXO-RN1). Total RNA was reverse transcribed into cDNA by using PrimeScript™ RT Reagent Kit (Takara, RR037A). RT-qPCR was conducted using SYBR® Premix Ex Taq™ II (Takara, RR420A) on StepOnePlus Real-Time PCR System (ABI, USA). U6 was used as an internal reference. The primers of all genes were synthesized by GenScript (Nanjing, China). Primer sequences are listed in Table 1. Equation $2^{-\Delta\Delta CT}$ is used to analyze the relative expression data.

2.10. Cytokine Measurement via Enzyme-Linked Immunosorbent Assay (ELISA). The cell culture supernatant of each treatment group was collected, and the secretion of TNF-α (Beyotime, PI660), TNF-β (Beyotime, PT903), and IL-10 (Beyotime, PI528) in the cell culture medium was detected according to the protocols.

2.11. Flow Cytometry. Annexin-V-FITC apoptosis kit (KeyGEN BioTECH, KGA108) was utilized for apoptosis determination. 10^6 cells were dispersed with EDTA-free trypsin, washed with PBS, and resuspended in 500 μL binding buffer and were then stained with FITC-labeled annexin V and PI. Apoptotic cell rate (%) = annexin + /PI − cells (%) + annexin+/PI + cells (%). Flow cytometry was used to detect the fluorescence intensity of foam cell samples with ROS Assay Kit (Beyotime, S0033S), and average fluorescence intensity (MFI) represented ROS content.

2.12. Oil Red O Staining Test. THP-1 cells were induced to differentiate into foam cells. Dye with filtered solution of Oil Red O (Solarbio, G1262) was used for lipid staining in foam cells. The cells were finally observed and photographed microscopically.

2.13. Cell Counting Kit-8 (CCK-8) Assay. A CCK-8 assay tested the proliferation of cells (Dojindo, CK04). After 48 h of incubation, the supernatant was refreshed with RPMI-1640 medium containing CCK-8 for another 2 h. An automated microplate reader was used to read the optical density (OD) at 450 nm.

Table 1: The primer sequences in the present study.

Gene	Primer sequences (5′-3′)
TNF-α forward	AGGACACCATGAGCACTGAA
TNF-α reverse	CCGATCACTCCAAAGTGCAG
TNF-β forward	CTTCGTGCTTTGGACTACCG
TNF-β reverse	AGACGTTCAGGTGGTGTCAT
CXCL11 forward	CCTTGGCTGTGATATTGTGTGCTA
CXCL11 reverse	CCTATGCAAAGACAGCGTCCTC
CXCL10 forward	GGCCATCAAGAATTTACTGAAAGCA
CXCL10 reverse	TCTGTGTGGTCCATCCTTGGAA
CCL17 forward	CTTCTCTGCAGCACATCCAC
CCL17 reverse	TGGTACCACGTCTTCAGCTT
U6 forward	AACGCTTCACGAATTTGCGT
U6 reverse	CTCGCTTCGGCAGCACA
lnc-MRGPRF-6:1 forward	AGGGACAGGAAGATGGTTGGC
lnc-MRGPRF-6:1 reverse	GATGAGCAGAATGGTCGTGAGG
IL-1β forward	CTCTCTCCTTTCAGGGCCAA
IL-1β reverse	GCGGTTGCTCATCAGAATGT
ARG1 forward	GAAAGGCTGGTCTGCTTGAG
ARG1 reverse	CAGCACCAGGCTGATTCTTC
ERK forward	TTTCCTCTGGATCAGCGTGT
ERK reverse	GAGGCCTGTGAGCATTTCTG
JNK forward	GTTCCTGACGTGCACTCTTC
JNK reverse	GGATGCTTCTTTGCACACCA
TLR4 forward	GCCACATGTCAGGCCTTATG
TLR4 reverse	TTGGTTGAAATGCCCACCTG
MyD88 forward	CAGCTCTGAGCCATTCACAC
MyD88 reverse	CCAGCATGTAGTCCAGCAAC
P38 forward	AATCCTCACCATCCACAGCA
P38 reverse	GCTTAGAGTCCAGGCTTCCA

2.14. Western Blot. Protein samples were obtained by cleavage of cells using RIPA lysis buffer (Beyotime, P0013B). After being measured with bicinchoninic acid kit (Beyotime, P0010S), normalized volumes of protein samples were isolated on SDS-PAGE on a 10% gel and transferred onto polyvinylidene fluoride membranes. The transfer membrane was then washed in a wash buffer and sealed in 5% BSA TBST for 1 h, followed by overnight incubation with primary antibody at 4°C. Then, HRP-labeled goat anti-rabbit IgG was stained for 1 h. After the developer solution is added, the film is viewed under Bio-Rad chemiluminescence imaging system. The primary antibodies used in experiments were as follows: P38 (CST, 9252T), p-P38 (CST, 4511T), TLR4 (NOVUS, NB-100-56580), MyD88 (FineTest, FNab10314), GAPDH (Beyotime, AF1186), JNK (CST, 9252T), p-JNK (CST, 4668T), ERK (CST, 4695T), p-ERK (CST, 4370T), and Tubulin (Beyotime, AF1216).

2.15. RNA Sequencing and Data Analysis. Total RNA was extracted from the cells using Trizol (Invitrogen, 15596018). RNA-seq was performed by BGISEQ-500

platform of Beijing Genomics Institute (BGI). Data analyses were carried out with BGI Online platform (http://www.bgionline.cn).

2.16. Statistical Analysis. GraphPad Prism 7 (GraphPad Software, USA) software and WPS Office 3 (Kingsoft Software, China) were used for statistical analysis. Quantitative data between the two groups were evaluated using Student's t-test and Mann–Whitney U tests. Spearman correlation analysis confirmed the correlation. $P < 0.05$ was considered statistically significant.

3. Results

3.1. lnc-MRGPRF-6:1 Is Highly Expressed in the Plasma Exosomes of CAD Patients and Is Positively Correlated with the Expression of Inflammatory Cytokines in Plasma. We successfully isolated exosomes and characterized the vesicles by TEM. TEM shows the enriched fraction of exosome-like vesicles (Figure 1(e)). A total of 40 subjects (20 CAD patients and 20 healthy controls) were selected for the study. It was shown that the lnc-MRGPRF-6:1 levels in the plasma exosomes of CAD patients were significantly higher than those of the control group (Figure 1(a)). Compared with the control group, as shown in Table 2, mRNA levels of TNF-α, TNF-β, and CXCL11 in the plasma of CAD patients were significantly increased with U6 as an internal reference. Further research demonstrated that lnc-MRGPRF-6:1 was positively correlated with TNF-α (Spearman $r = 0.544$, $P = 0.001$), TNF-β (Spearman $r = 0.469$, $P = 0.005$), and CXCL11 (Spearman $r = 0.376$, $P = 0.018$) in plasma (Figures 1(b)–1(d)).

3.2. lnc-MRGPRF-6:1 Knockout Blocks ox-LDL-Induced Macrophage Foam Cell Formation. As mentioned above, THP-1 macrophage cells were used to establish lnc-MRGPRF-6:1 knockout macrophage model via the CRISPR/Cas9 system. It was confirmed that the expression of lnc-MRGPRF-6:1 was downregulated significantly in knockout macrophage (KO) compared with macrophage infected by control lentivirus (control) (Figure 2(a)). Subsequently, THP-1 macrophage foam cell model was established by using ox-LDL. Oil Red O staining analysis indicated lipid accumulation in ox-LDL-induced macrophage foam cells was reduced after lnc-MRGPRF-6:1 knockout (Figure 2(b)). Moreover, ROS generation was dramatically decreased in lnc-MRGPRF-6:1 knockout macrophage foam cells (Figure 2(d)). In addition, CCK-8 assay and flow cytometry suggested that knockdown of lnc-MRGPRF-6:1 decreased cell viability and inhibited cell apoptosis (Figures 2(c) and 2(e)).

3.3. lnc-MRGPRF-6:1 Is Significantly Upregulated in M1 Macrophage. After being induced by IFN-γ and LPS, both the levels of CXCL10, CXCL11, IL-1β, TNF-α, and TNF-β protein secretions were significantly increased in THP-1 macrophage, which suggested that THP-1 macrophage was polarized to M1 type (M1) successfully (Figures 3(a) and 3(b)). Concurrently, being treated with IL-4, both the levels of CCL17, ARG1, and IL-10 protein secretion were dramatically increased in THP-1 macrophage, which suggested that THP-1 macrophage was polarized to M2 type (M2) successfully (Figures 3(a) and 3(b)). It is worth noting that, compared with untreated THP-1 macrophage (M0), the expression of lnc-MRGPRF-6:1 in M1 was increased notably while the expression in M2 has no marked change (Figure 3(c)).

For further identification, we intend to analyze the expression of lnc-MRGPRF-6:1 in macrophage repolarization models. It was observed that the addition of IFN-γ and LPS in M2 (M2-M1) culture medium could increase the levels of M1-related cytokines CXCL10, CXCL11, IL-1β, TNF-α, and TNF-β and decrease the levels of M2-related cytokines CCL17, ARG1, and IL-10 (Figures 3(d) and 3(e)). Similarly, the addition of IL-4 in M1 (M1-M2) culture medium increased the levels of M2-related cytokines in macrophage, but decreased the levels of M1-related cytokines (Figures 3(d) and 3(e)). It was confirmed that macrophage repolarization models were constructed successfully. Unsurprisingly, lnc-MRGPRF-6:1 expression in M2-M1 was increased apparently (Figure 3(f)).

To further investigate the high expression of lnc-MRGPRF-6:1 in M1 macrophage, we induced human monocyte-derived macrophage to polarize M1 type using IFN-γ and LPS; lnc-MRGPRF-6:1 was still significantly elevated (Figures 3(g) and 3(h)). Moreover, the expression of lnc-MRGPRF-6:1 in M2-M1 was also increased in human monocyte-derived macrophage repolarization model (Figures 3(i) and 3(j)).

These facts suggest that the expression of lnc-MRGPRF-6:1 was upregulated in M1 macrophage, and the expression will change with the phenotype transformation of the macrophage.

3.4. lnc-MRGPRF-6:1 Knockout Inhibits the Polarization of M1 Macrophage. After being induced by IFN-γ and LPS, the levels of CXCL10, CXCL11, and IL-1β in both lnc-MRGPRF-6:1 knockout macrophage (KO) and control were significantly increased (Figures 4(a)–4(c)). Furthermore, the increases in KO were inferior to control. In the meantime, compared with control, TNF-α and TNF-β secretions were increased apparently in both KO and control, and the increasing levels in KO were also less than those in control (Figures 4(d) and 4(e)).

Meanwhile, induced by IL-4, the CCL17 and ARG1 levels in both KO and control were dramatically increased, and the increases in KO were great than those in the control group (Figures 4(g) and 4(h)). Similarly, the IL-10 secretions in both KO and control were also markedly increased (Figure 4(f)). Interestingly, the difference of IL-10 secretion level between KO and control was not statistically significant.

To further clarify whether lnc-MRGPRF-6:1 knockout inhibited M1 macrophage polarization, we infected human monocyte with lentivirus to knock out lnc-MRGPRF-6:1. After being induced into M1 and M2 macrophage, the increase of M1 markers (CXCL10, CXCL11, and IL-1β) after lnc-MRGPRF-6:1 knockout was significantly lower than that of the control group (Figures 4(i)–4(k)), while the increase of M2 markers (CCL17, ARG1) was higher (Figures 4(l) and 4(m)).

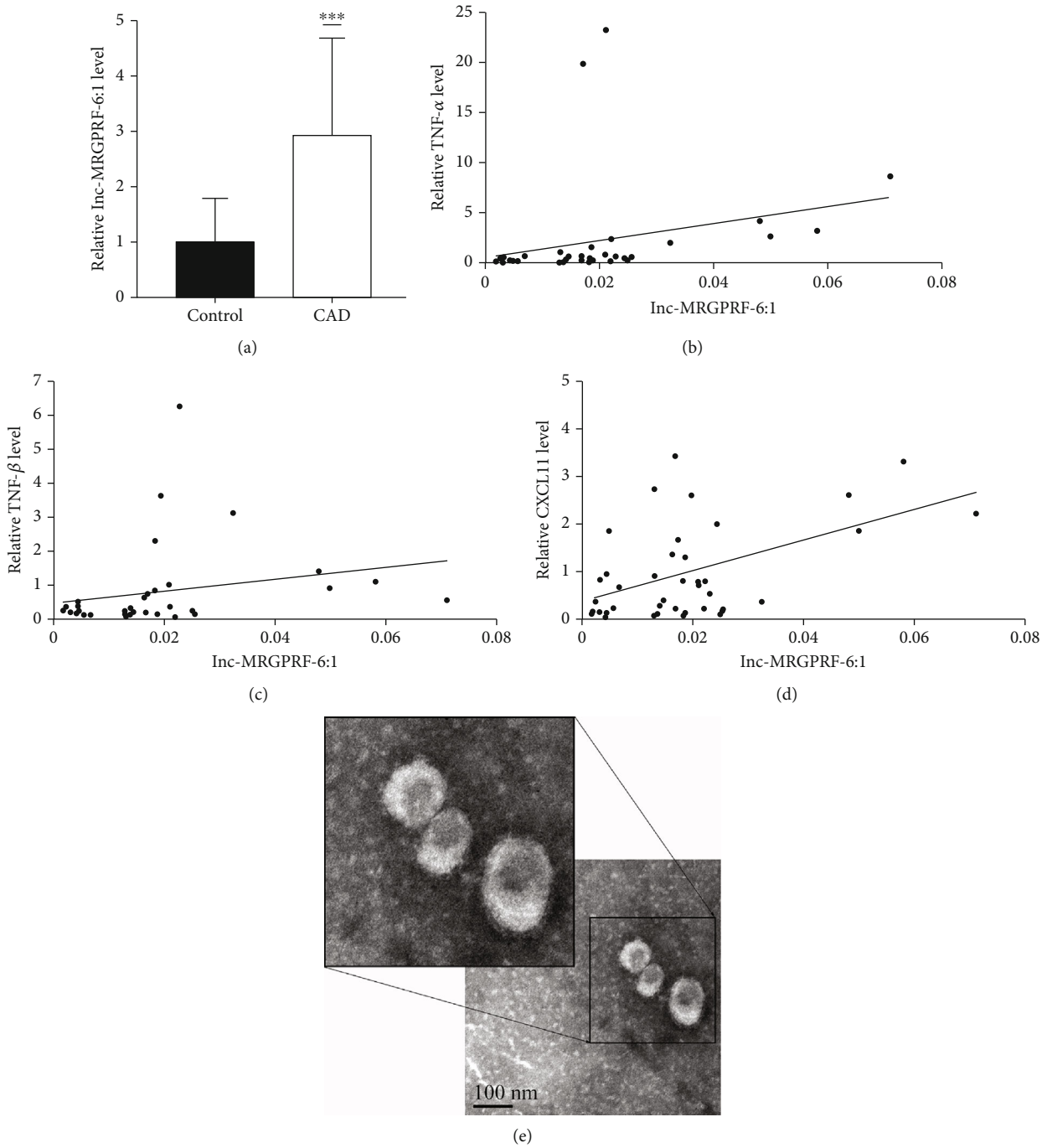

Figure 1: lnc-MRGPRF-6:1 significantly increased in plasma exosomes of CAD patients and was associated with inflammatory factors in plasma. (a) The mRNA level of lnc-MRGPRF-6:1 in the plasma exosomes was detected by RT-qPCR. (b–d) Scatter plot of Spearman correlation analysis between lnc-MRGPRF-6:1 and TNF-α (Spearman $r = 0.544$, $P = 0.001$), TNF-β (Spearman $r = 0.469$, $P = 0.005$), and CXCL11 (Spearman $r = 0.376$, $P = 0.018$) expression levels in plasma. (e) Electron microscopy image of exosome enrichment isolated from plasma (scale bar, 100 nm). CAD vs. control, $^{***}P < 0.001$. CAD: coronary atherosclerotic disease.

Table 2: Relative expressions of TNF-α, TNF-β, and CXCL11 at the transcription level between CAD patients and controls (U6 as an internal reference). The data were expressed as median (1st/3rd quartiles).

	TNF-α	TNF-β	CXCL11
Control ($n = 20$)	0.22 (0.14, 0.35)	0.23 (0.12, 0.27)	0.21 (0.11, 0.76)
CAD ($n = 20$)	1.52 (0.46, 3.85)	0.87 (0.43, 1.40)	1.40 (0.49, 2.62)
P	<0.001	<0.001	0.001

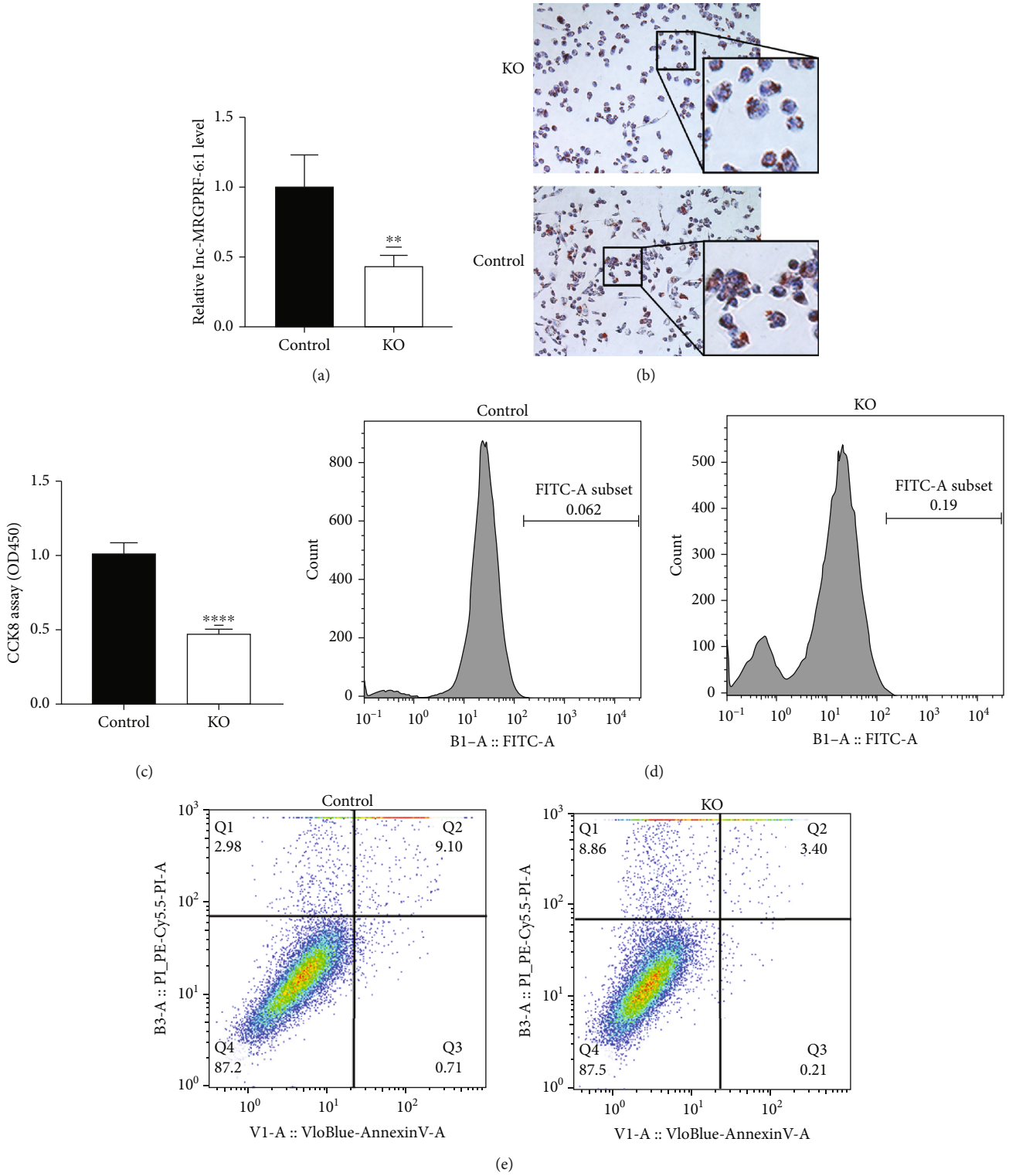

Figure 2: Knockout of lnc-MRGPRF-6:1 can reduce the lipid accumulation and ROS levels of foam cells, significantly increase the viability of macrophages, and inhibit cell apoptosis. After the lnc-MRGPRF-6:1 knockout macrophage was induced to differentiate with the control cells, the cells were stimulated with 50 mg/mL ox-LDL for 24 h. (a) The expression level of lnc-MRGPRF-6:1 between KO and control was detected by RT-qPCR. (b) Image of Oil Red O staining. (c) Viability of macrophage. (d) ROS levels in macrophage. (e) Apoptosis level of macrophage. KO vs. control, $^{*}P < 0.05$, $^{**}P < 0.01$, $^{***}P < 0.001$, and $^{****}P < 0.0001$. KO: lnc-MRGPRF-6:1 knockout macrophage; control: macrophage infected by control lentivirus.

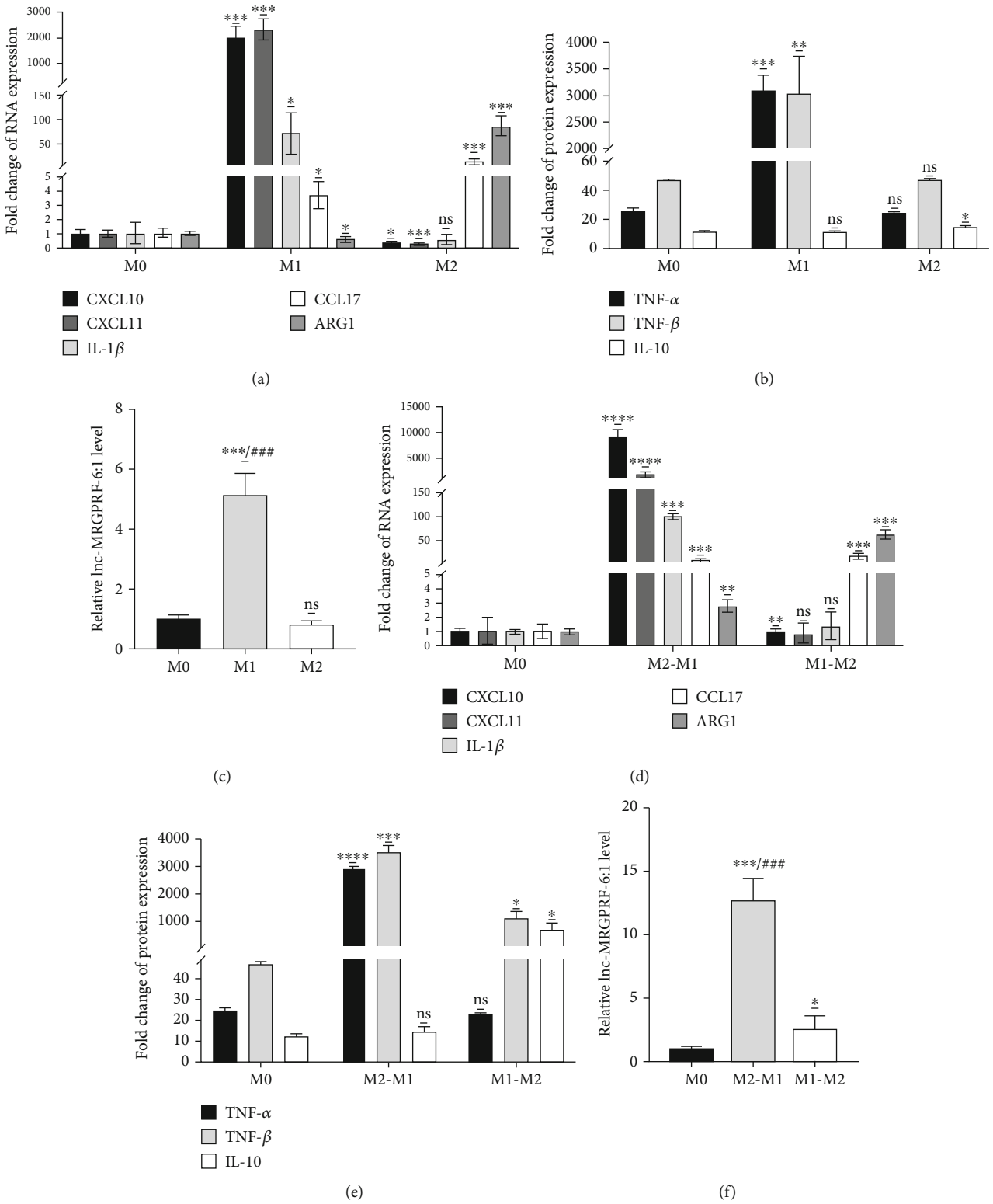

Figure 3: Continued.

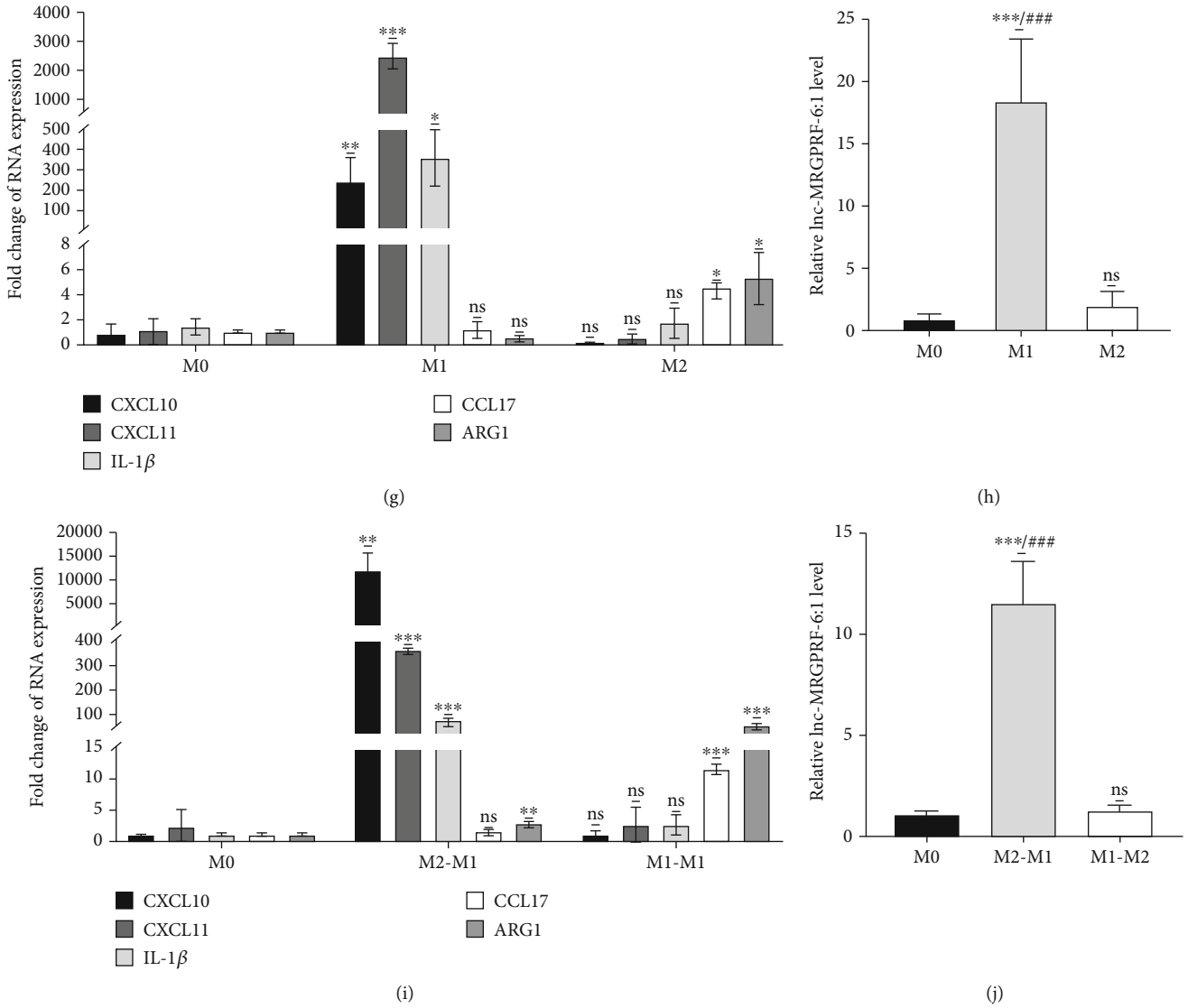

Figure 3: lnc-MRGPRF-6:1 was highly expressed in M1 macrophage. (a, b, g) M1 polarization was stimulated by IFN-γ/LPS, and M2 polarization was stimulated by IL-4. The levels of TNF-α, TNF-β, and IL-10 in the supernatant were detected by ELISA, and the mRNA levels of CXCL10, CXCL11, IL-1β, ARG1, and CCL17 were detected by RT-qPCR. (c, h) The expression levels of lnc-MRGPRF-6:1 in macrophages with different phenotypes were detected by RT-qPCR. (d, e, i) After repolarization, CXCL10, CXCL11, IL-1β, ARG1, and CCL17 levels were detected by RT-qPCR, and TNF-α, TNF-β, and IL-10 were detected by ELISA. (f, j) The expression levels of lnc-MRGPRF-6:1 in repolarization macrophages were detected by RT-qPCR. (a–c, g, h) M1/M2 vs. M0, ns: not statistically significant; $^{*}P < 0.05$, $^{**}P < 0.01$, $^{***}P < 0.001$, and $^{****}P < 0.0001$; M1 vs. M2, $^{\#\#\#}P < 0.001$; (d–f, i, j) M2-M1/M1-M2 vs. M0, ns: not statistically significant; $^{*}P < 0.05$, $^{**}P < 0.01$, $^{***}P < 0.001$, and $^{****}P < 0.0001$; M2-M1 vs. M1-M2, $^{\#\#}P < 0.01$.

These results suggest that lnc-MRGPRF-6:1 knockout effectively inhibits the polarization of M1 macrophage.

3.5. lnc-MRGPRF-6:1 May Regulate Macrophage Polarization via the TLR4-MyD88-MAPK Pathway. RNA sequencing was performed between lnc-MRGPRF-6:1 knockout macrophage (KO) and macrophage infected by control lentivirus (control). Transcriptome analysis showed that the expression levels of 32 genes were up-regulated and 191 down-regulated in THP-1 macrophage after lnc-MRGPRF-6:1 knockout with $|\mathrm{Log}_2\mathrm{FC}| > 1$ and $P < 0.05$ (Figure 5(a)). Gene Ontology (GO) and KEGG pathway enrichment analyses were then carried out for further analysis.

As shown in Figure 5(b), functions and processes associated with immune were enriched after lnc-MRGPRF-6:1 knockout, including *immune system processes*, *innate immune response*, and *inflammatory response*. In innate immunity, macrophages produce proinflammatory mediators by activating several receptors that recognize pathogens, including the toll-like receptor family (TLRs) [18]. Coincidentally, the toll-like receptor signaling pathway was enriched by KEGG pathway analysis (Figure 5(c)). After LPS stimulation, activated TLR4 can trigger the downstream MAPK signaling pathway through the MyD88-dependent pathway [19]. Fascinatingly, according to RNA sequencing data, expressions of TLR4, MyD88, and P38 were

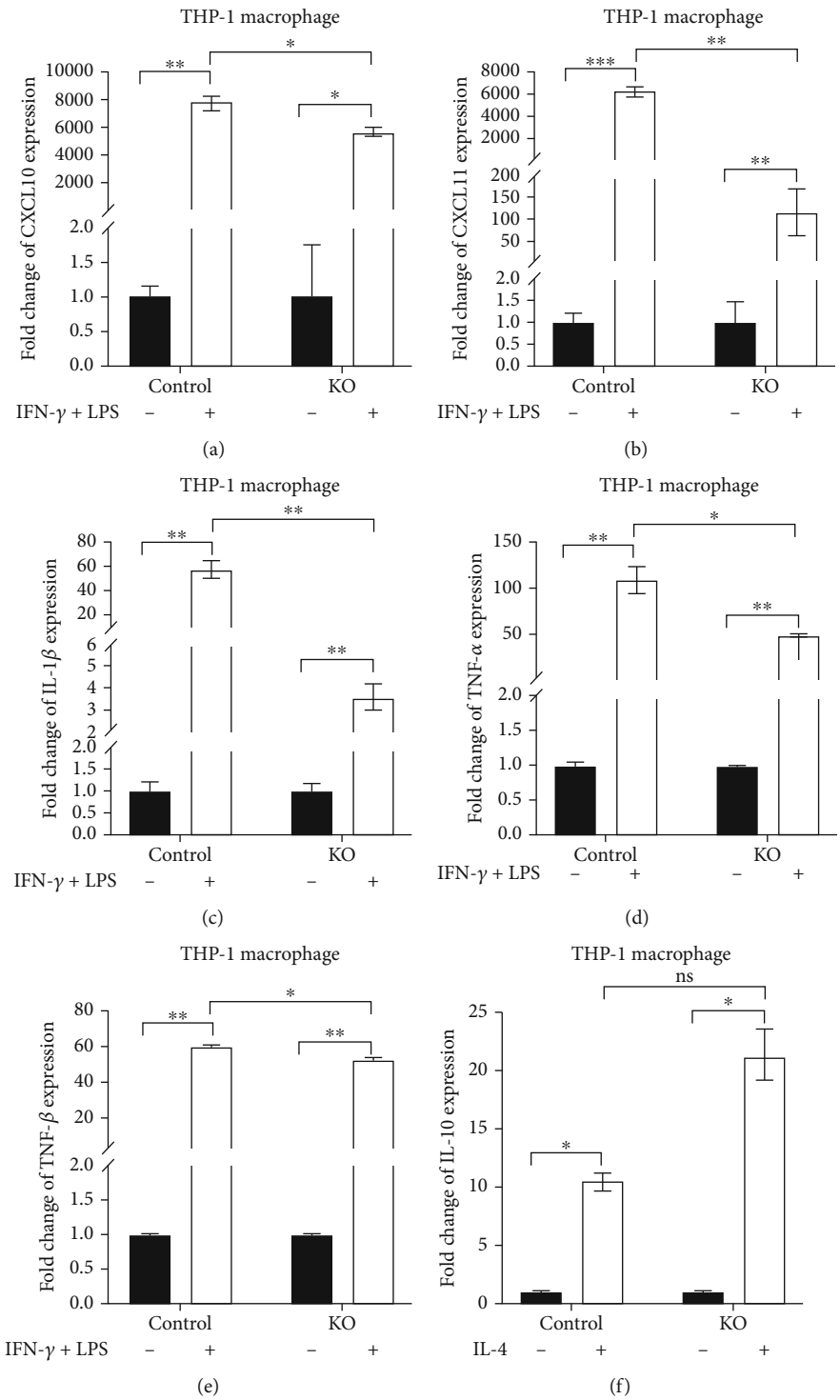

Figure 4: Continued.

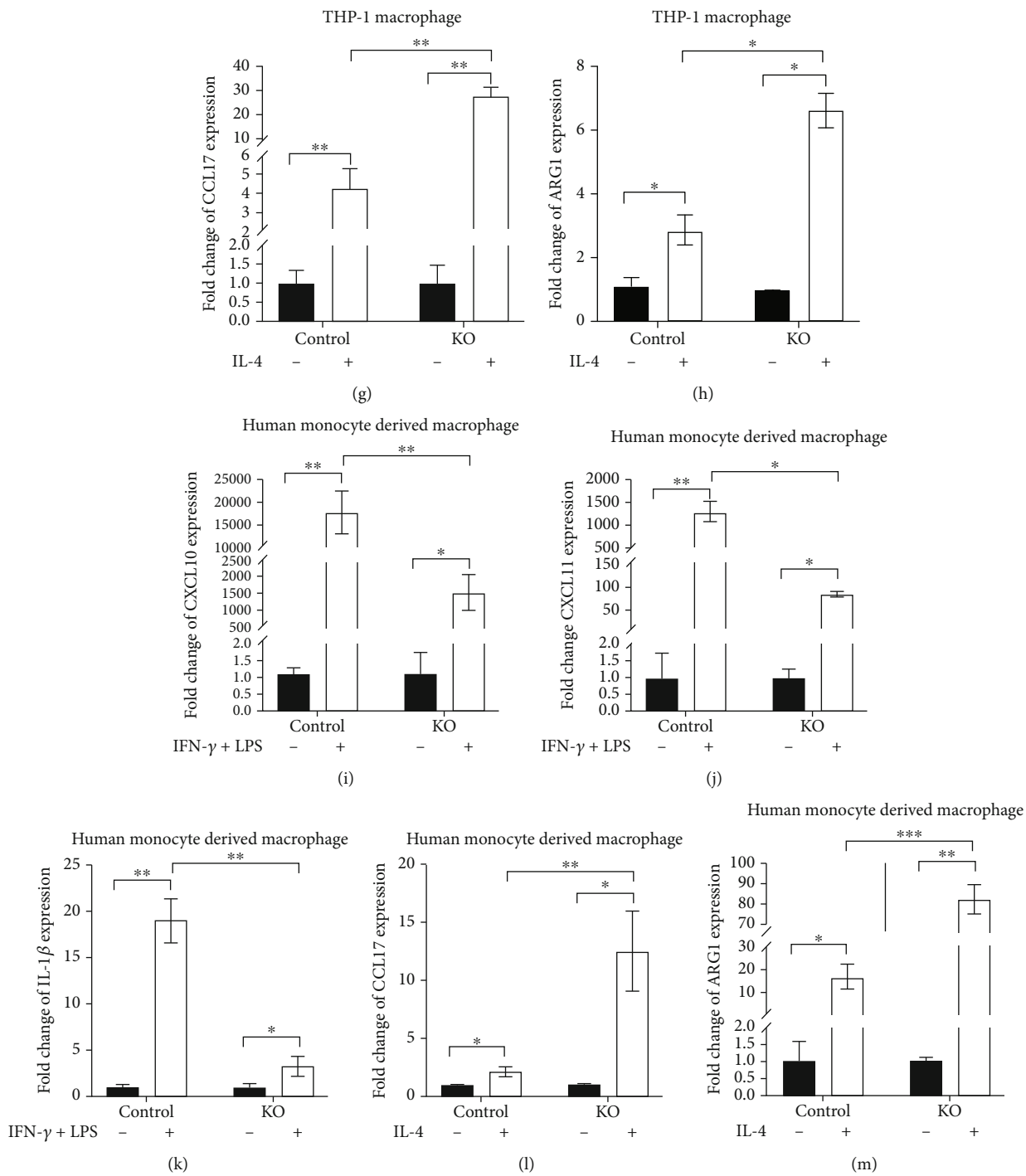

Figure 4: Knockout of lnc-MRGPRF-6:1 inhibits the formation of M1 macrophage and reduces the secretion of inflammatory cytokines. (a–c, i–k) The mRNA level of CXCL10, CXCL11, and IL-1β in M1-type macrophage was detected by RT-qPCR. (g, h, l, m) The expression of CCL17 and ARG1 in M2-type macrophage. (d, e) The protein levels of TNF-α and TNF-β in M1-type macrophage were detected by ELISA. (f) The expression of IL-10 in M2-type macrophage. ns: not statistically significant; $^{*}P < 0.05$, $^{**}P < 0.01$, $^{***}P < 0.001$, and $^{****}P < 0.0001$.

significantly changed after lnc-MRGPRF-6:1 knockout (Figure 5(d)).

Considering MAPK including JNK, ERK, and P38 signal transduction pathway, we still verified JNK and ERK pathways, although RNA-seq showed no significant changes in JNK and ERK expression in MAPK after lnc-MRGPRF-6:1 knockout.

Subsequently, we verified the expression of the genes above-mentioned by RT-PCR and Western blotting. In Figures 5(e)–5(i) and 5(m), TLR4, MyD88, P38, phosphorylation of P38, JNK, and phosphorylation of JNK expressions were decreased in both transcription and protein level after lnc-MRGPRF-6:1 knockout. Although ERK was decreased at the transcription level, there was no significant difference

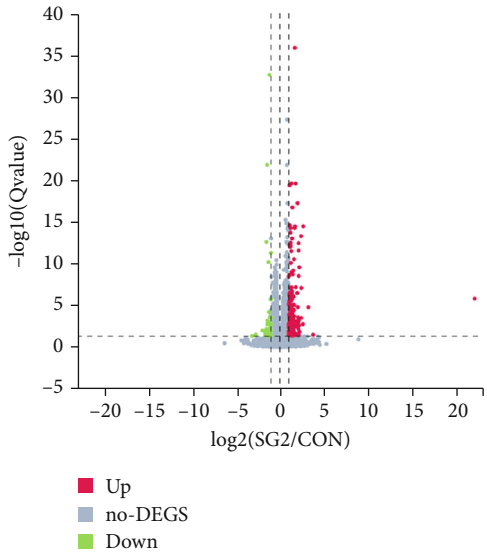

(a)

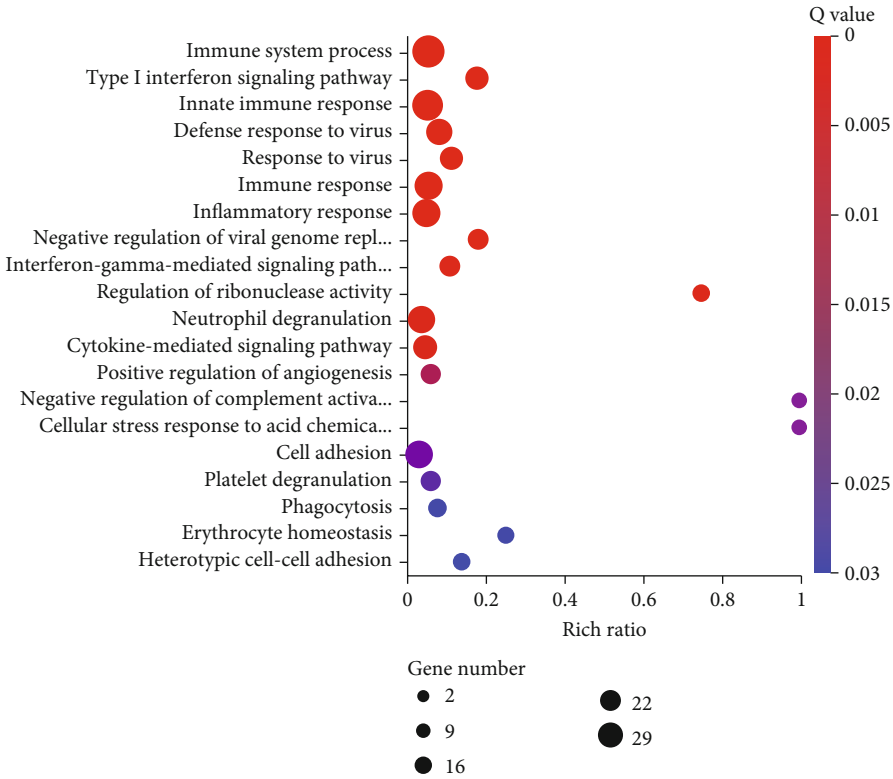

(b)

Figure 5: Continued.

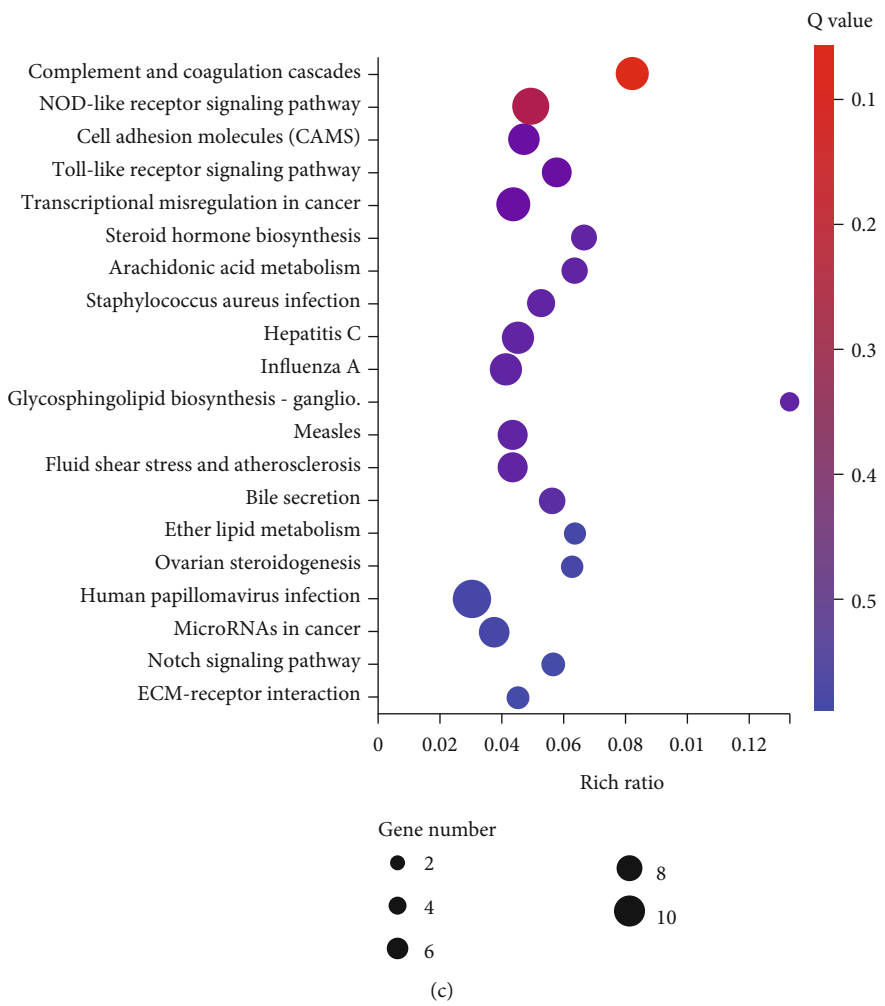

(c)

Figure 5: Continued.

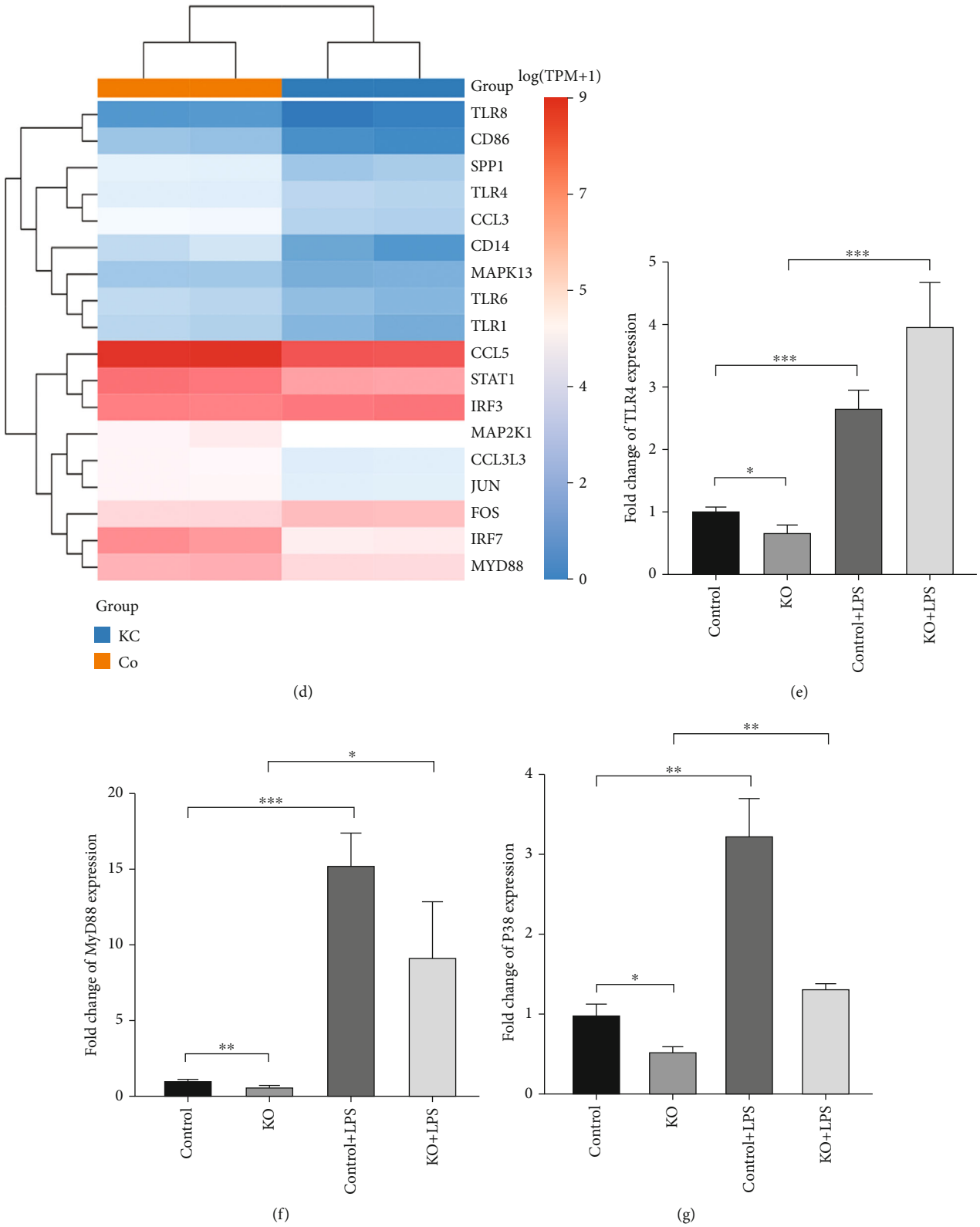

Figure 5: Continued.

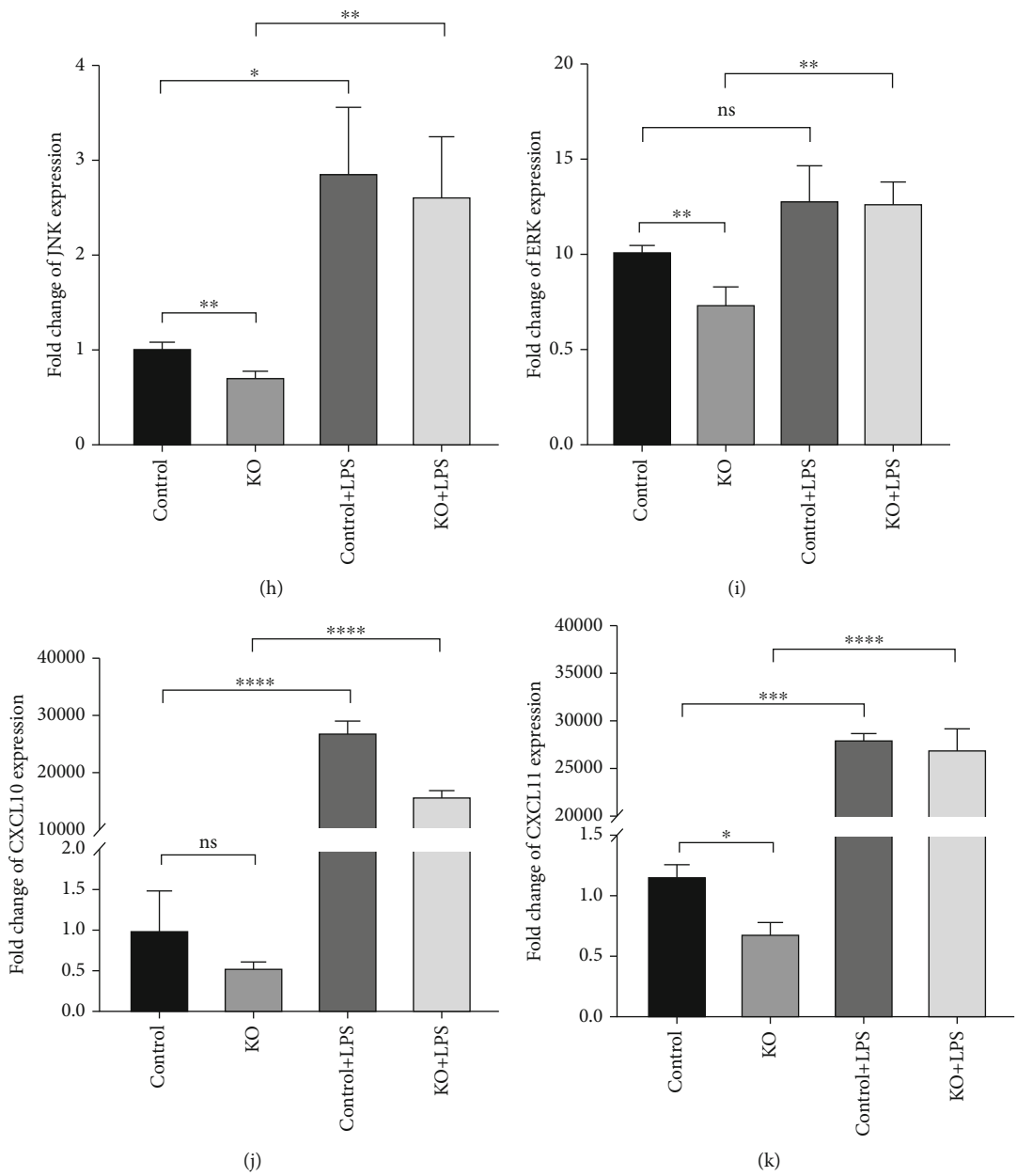

Figure 5: Continued.

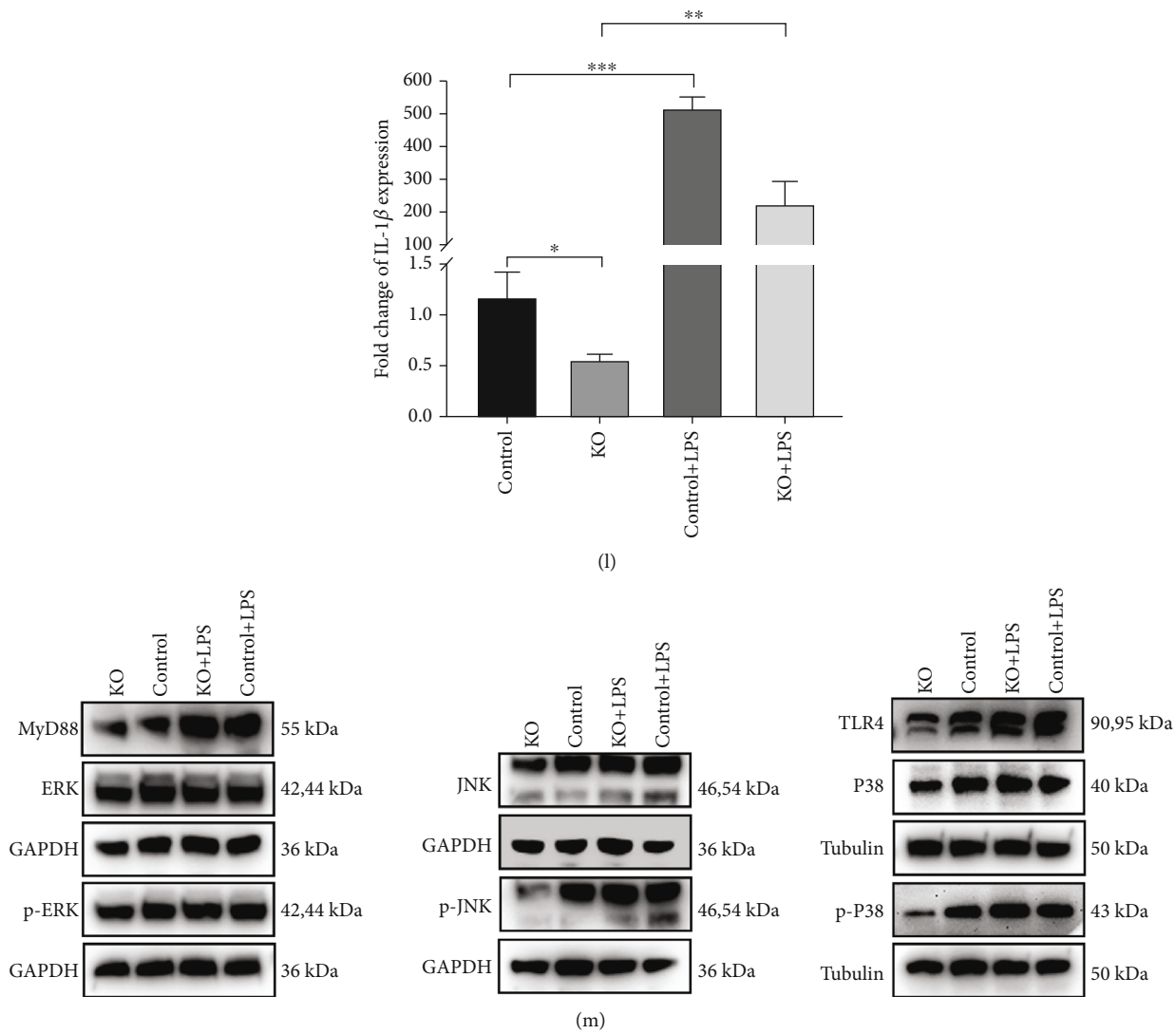

Figure 5: lnc-MRGPRF-6:1 may regulate macrophage polarization via the TLR4-MyD88-MAPK pathway. RNA sequencing was performed between lnc-MRGPRF-6:1 knockout macrophage (KO) and macrophage infected by control lentivirus (control). (a) Volcano plot shows differentially expressed genes between KO and control. (b, c) GO and KEGG analysis according to RNA sequencing data. (d) Hierarchical cluster analysis of differentially expressed mRNAs in KO compared to control (partially shown); (e–l) mRNA levels of TLR4, MyD88, P38, JNK, ERK, CXCL10, CXCL11, and IL-1β between KO, control, and after LPS induction were detected by RT-qPCR. (m) Expression of TLR4, MyD88, JNK, ERK, P38, p-P38, p-JNK, and p-ERK between KO and control were analyzed by Western blotting. KO: lnc-MRGPRF-6:1 knockout macrophage; control: macrophage infected by control lentivirus.

in the protein level, which suggested that lnc-MRGPRF-6:1 might regulate macrophage polarization through the TLR4-MyD88-MAPK signaling pathway.

To further investigate that lnc-MRGPRF-6:1 regulates macrophage polarization through the TLR4-MyD88-MAPK signaling pathway, we used LPS, the activator of TLR4, to activate this signaling pathway. LPS induced intense activation of TLR4, MyD88, P38, phosphorylation of P38, JNK, and phosphorylation of JNK in the KO group (Figures 5(e)–5(i) and 5(m)); meanwhile, M1 markers (CXCL10, CXCL11, and IL-1β) were significantly elevated in the KO group after LPS induction (Figures 5(g)–5(l)).

4. Discussion

AS, as a chronic inflammatory vascular disease, is the pathological basis of CAD, which is a serious threat to human health. It is demonstrated that lncRNAs play important regulatory roles in inflammatory diseases, including AS [20]. In a preliminary work, we identified that lnc-MRGPRF-6:1 was significantly upregulated in the plasma of CAD patients. We want to explore whether there is a relationship between lnc-MRGPRF-6:1 and AS.

Foam cells derived from macrophages are associated with the initial stage of AS [21]. Therefore, we investigated the effect of lnc-MRGPRF-6:1 expression on macrophage

foam cell formation. We first established lnc-MRGPRF-6:1 knockout macrophage model and then analyzed the lipid accumulation, ROS generation, viability, and apoptosis of model cells. The results show that lnc-MRGPRF-6:1 knockout blocks ox-LDL-induced macrophage foam cell formation, and lnc-MRGPRF-6:1 promotes the production of ROS, apoptosis, and viability loss of model cells. Foam cells derived from macrophages are the main cell type of early AS lesions [22]. Macrophages are Foam cells derived from macrophages are the main cell type of early AS lesions [22]. Macrophages are induced into foam cells after uptake of ox-LDL, which constitutes one of the important steps in the development of AS plaques [23]. In the present study, lnc-MRGPRF-6:1 promotes the production of ROS, which oxidizes LDL to form ox-LDL. Increased apoptosis and viability of macrophages can lead to lipid aggregation and further inflammation and promote the development of AS plaques [23]. These results suggest that lnc-MRGPRF-6:1 may play a crucial role in the development of AS.

Previous studies demonstrate that macrophage-mediated inflammation plays an essential role in the development of AS. After overtaking ox-LDL, macrophage transforms into foam cell under the intima of the coronary artery and recruits many proinflammatory factors to initiate the disease [24]. Afterwards, various inflammatory factors are released and lead to accelerating AS.

Interestingly, in our study, further research demonstrated lnc-MRGPRF-6:1 was positively correlated with TNF-α, TNF-β, and CXCL11 in CAD patients' plasma, which indicates that lnc-MRGPRF-6:1 may participate in the regulation of macrophage-mediated inflammation in AS.

Polarization is deeply involved in the regulation of macrophage-mediated inflammation [25, 26]. Macrophages could be polarized into classical activated M1 type and replacement activated M2 type. The M1 phenotype macrophage secretes inflammatory cytokines, which leads to recruiting inflammatory cells and aggravates inflammation and plaque formation [27]. In contrast, M2 phenotype macrophage, as an anti-inflammatory cell, could block the recruitment of inflammatory cells, inhibit the release of inflammatory cytokines, and reduce the formation of foam cells [28]. Therefore, the disbalance of macrophage polarization is closed related to the occurrence and development of AS.

Initially, we analyze the expression of lnc-MRGPRF-6:1 in both M1 and M2 phenotype macrophages. For further research, we analyze the expression of lnc-MRGPRF-6:1 in the repolarization models of M1 and M2 macrophages once again. lnc-MRGPRF-6:1 is significantly upregulated in M1 macrophage. It is worth noting that the unchanged thing is the expression of lnc-MRGPRF-6:1 which was upregulated in M1 macrophage. Moreover, we observe that lnc-MRGPRF-6:1 knockout inhibits the polarization of M1 macrophage. These facts suggest that lnc-MRGPRF-6:1 may modulate the macrophage-mediated inflammation through transforming its polarization.

However, the problem is how lnc-MRGPRF-6:1 regulates macrophage polarization. We conducted transcriptome sequencing between lnc-MRGPRF-6:1 knockout macrophage and control macrophage. Subsequently, GO enrichment analysis indicates that functions and processes associated with immune were enriched after lnc-MRGPRF-6:1 knockout. Coincidentally, the toll-like receptor signaling pathway, which is closely related to immune, was enriched by KEGG pathway analysis.

TLRs, regulating immune cell survival and proliferation, are involved in the first line of defense against invading pathogens in organisms and play important roles in inflammation [29]. TLRs play a central role in macrophage activation, differentiation, and polarization. In TLRs, TLR4 is a pattern recognition receptor in response to LPS. The binding of LPS to TLR4 induces phosphorylation of IRAK1, PI3K, or MAPKs, which are involved in host defense mechanisms by recognizing pathogens or acting as receptors for proinflammatory cytokines. The TLR-induced inflammatory response triggers the downstream MAPK signaling pathway through the MyD88 pathway [30]. MAPK consists of a group of serine/threonine protein kinases that mediate signaling from the cell surface to the nucleus following activation by various extracellular stimuli. The MAPK signaling pathway has been found in mammalian cells including JNK, ERK, and P38 pathways [19], and it can be induced by LPS-activated TLR4 [31].

Fascinatingly, expressions of TLR4, MyD88, and P38 were significantly changed after lnc-MRGPRF-6:1 knockout according to RNA sequencing data. Further analyses demonstrate that the expression levels of TLR4, MyD88, p-P38, and p-JNK were significantly decreased after knockout. After LPS induced lnc-MRGPRF-6:1 knockout macrophage model, the TLR4-MyD88-MAPK pathway was activated; meanwhile, CXCL10, CXCL11, and IL-1β, markers of M1, were also significantly increased.

Based on these findings, we speculate that lnc-MRGPRF-6:1 promotes macrophage-mediated inflammation through the TLR4-MyD88-MAPK signaling pathway which regulates macrophage M1 polarization.

In summary, the present study clarifies that lnc-MRGPRF-6:1 promotes macrophage-mediated inflammation by regulating macrophage M1 polarization, which may play a crucial role in the development of AS. Keeping the balance of macrophage polarization for reducing foam cell formation and alleviating inflammation has become the ideas for AS treatment strategies, and lnc-MRGPRF-6:1 might become a potential therapeutic target for AS.

Data Availability

The data used to support the findings of this study are included within the article.

Conflicts of Interest

The authors have no conflicts of interest.

Authors' Contributions

Dan Hu and Yuzhong Wang contributed equally to this work.

Acknowledgments

This work was supported by the National Natural Science Foundation of China (81800387) and Postgraduate Research & Practice Innovation Program of Jiangsu Province (SJCX20_0495).

References

[1] A. Sezaki, T. Imai, K. Miyamoto, F. Kawase, and H. Shimokata, "Mediterranean diet score and incidence of IHD: a global comparative study," *Public Health Nutrition*, vol. 22, pp. 1444–1450, 2019.

[2] L. Zhang, Y. Zhang, Y. Zhao et al., "Circulating miRNAs as biomarkers for early diagnosis of coronary artery disease," *Expert Opinion on Therapeutic Patents*, vol. 28, pp. 591–601, 2018.

[3] M. M. Kavurma, K. J. Rayner, and D. Karunakaran, "The walking dead: macrophage inflammation and death in atherosclerosis," *Current Opinion in Lipidology*, vol. 28, pp. 91–98, 2017.

[4] J. He, J. Li, H. Liu et al., "Scandoside exerts anti-inflammatory effect via suppressing NF-kappa B and MAPK signaling pathways in LPS-induced RAW 264.7 macrophages," *International Journal of Molecular Sciences*, vol. 19, 2018.

[5] W. X. Peng, P. Koirala, and Y. Y. Mo, "LncRNA-mediated regulation of cell signaling in cancer," *Oncogene*, vol. 36, pp. 5661–5667, 2017.

[6] N. Guo, Q. Zhou, X. Huang et al., "Identification of differentially expressed circulating exosomal lncRNAs in IgA nephropathy patients," *BMC Immunology*, vol. 21, p. 16, 2020.

[7] H. Jing, X. Qu, L. Liu, and H. Xia, "A novel long noncoding RNA (lncRNA), LL22NC03-N64E9.1, promotes the proliferation of lung cancer cells and is a potential prognostic molecular biomarker for lung cancer," *Medical Science Monitor*, vol. 24, pp. 4317–4323, 2018.

[8] B. Sun, M. Meng, J. Wei, and S. Wang, "Long noncoding RNA PVT1 contributes to vascular endothelial cell proliferation via inhibition of miR-190a-5p in diagnostic biomarker evaluation of chronic heart failure," *Experimental and Therapeutic Medicine*, vol. 19, pp. 3348–3354, 2020.

[9] X. Liu, Y. Lu, J. Zhu et al., "A long noncoding RNA, antisense IL-7, promotes inflammatory gene transcription through facilitating histone acetylation and switch/sucrose nonfermentable chromatin remodeling," *Journal of Immunology*, vol. 203, pp. 1548–1559, 2019.

[10] C. Shi, J. Miley, A. Nottingham, T. Morooka, D. A. Prosdocimo, and D. I. Simon, "Leukocyte integrin signaling regulates FOXP1 gene expression via FOXP1-IT1 long non-coding RNA-mediated IRAK1 pathway," *Biochimica et Biophysica Acta (BBA)-Gene Regulatory Mechanisms*, vol. 1862, pp. 493–508, 2019.

[11] A. Mantovani, S. Sozzani, M. Locati, P. Allavena, and A. Sica, "Macrophage polarization: tumor-associated macrophages as a paradigm for polarized M2 mononuclear phagocytes," *Trends in Immunology*, vol. 23, pp. 549–555, 2002.

[12] T. Wang, L. Zhang, J. Hu et al., "Mst1 participates in the atherosclerosis progression through macrophage autophagy inhibition and macrophage apoptosis enhancement," *Journal of Molecular and Cellular Cardiology*, vol. 98, pp. 108–116, 2016.

[13] S. Muhammad, S. R. Chaudhry, G. Dobreva, M. T. Lawton, M. Niemela, and D. Hanggi, "Vascular macrophages as therapeutic targets to treat intracranial aneurysms," *Frontiers in Immunology*, vol. 12, p. 630381, 2021.

[14] J. Cao, R. Dong, L. Jiang et al., "LncRNA-MM2P identified as a modulator of macrophage M2 polarization," *Cancer Immunology Research*, vol. 7, pp. 292–305, 2019.

[15] X. Chi, B. Ding, L. Zhang, J. Zhang, J. Wang, and W. Zhang, "lncRNA GAS5 promotes M1 macrophage polarization via miR-455-5p/SOCS3 pathway in childhood pneumonia," *Journal of Cellular Physiology*, vol. 234, pp. 13242–13251, 2019.

[16] L. Xia, X. Wang, L. Liu et al., "lnc-BAZ2B promotes M2 macrophage activation and inflammation in children with asthma through stabilizing BAZ2B pre-mRNA," *The Journal of Allergy and Clinical Immunology*, vol. 147, pp. 921–932, 2021.

[17] J. P. Concordet and M. Haeussler, "CRISPOR: intuitive guide selection for CRISPR/Cas9 genome editing experiments and screens," *Nucleic Acids Research*, vol. 46, pp. W242–W245, 2018.

[18] M. Chittezhath, C. M. M. Wai, V. S. Y. Tay, M. Chua, S. R. Langley, and Y. Ali, "TLR4 signals through islet macrophages to alter cytokine secretion during diabetes," *The Journal of Endocrinology*, vol. 247, p. 87, 2020.

[19] H. Li, J. H. Yoon, H. J. Won et al., "Isotrifoliol inhibits proinflammatory mediators by suppression of TLR/NF-kappaB and TLR/MAPK signaling in LPS-induced RAW264.7 cells," *International Immunopharmacology*, vol. 45, pp. 110–119, 2017.

[20] Y. Wang, X. Song, Z. Li, and B. Liu, "Long non-coding RNAs in coronary atherosclerosis," *Life Sciences*, vol. 211, pp. 189–197, 2018.

[21] D. A. Chistiakov, D. A. Kashirskikh, V. A. Khotina, A. V. Grechko, and A. N. Orekhov, "Immune-inflammatory responses in atherosclerosis: the role of myeloid cells," *Journal of Clinical Medicine*, vol. 8, 2019.

[22] C. J. Perry, A. R. Munoz-Rojas, K. M. Meeth et al., "Myeloid-targeted immunotherapies act in synergy to induce inflammation and antitumor immunity," *The Journal of Experimental Medicine*, vol. 215, pp. 877–893, 2018.

[23] M. Chatterjee, D. Rath, J. Schlotterbeck et al., "Regulation of oxidized platelet lipidome: implications for coronary artery disease," *European Heart Journal*, vol. 38, pp. 1993–2005, 2017.

[24] J. Zhang, C. R. Ma, Y. Q. Hua et al., "Contradictory regulation of macrophages on atherosclerosis based on polarization, death and autophagy," *Life Sciences*, vol. 276, p. 118957, 2021.

[25] C. Wang, M. C. Petriello, B. Zhu, and B. Hennig, "PCB 126 induces monocyte/macrophage polarization and inflammation through AhR and NF-kappaB pathways," *Toxicology and Applied Pharmacology*, vol. 367, pp. 71–81, 2019.

[26] G. Wang, X. Liu, X. Li, and Y. Zhao, "Suppression of PAPP-A mitigates atherosclerosis by mediating macrophage polarization via STAT3 signaling," *Biochemical and Biophysical Research Communications*, vol. 543, pp. 29–37, 2021.

[27] T. J. Barrett, "Macrophages in atherosclerosis regression," *Arteriosclerosis, Thrombosis, and Vascular Biology*, vol. 40, pp. 20–33, 2020.

[28] F. Moroni, E. Ammirati, G. D. Norata, M. Magnoni, and P. G. Camici, "The role of monocytes and macrophages in human atherosclerosis, plaque neoangiogenesis, and atherothrombosis," *Mediators of Inflammation*, vol. 2019, Article ID 7434376, 11 pages, 2019.

[29] E. Cario, I. M. Rosenberg, S. L. Brandwein, P. L. Beck, H. C. Reinecker, and D. K. Podolsky, "Lipopolysaccharide activates distinct signaling pathways in intestinal epithelial cell lines expressing toll-like receptors," *Journal of Immunology*, vol. 164, pp. 966–972, 2000.

[30] S. Rakoff-Nahoum and R. Medzhitov, "Regulation of spontaneous intestinal tumorigenesis through the adaptor protein MyD88," *Science*, vol. 317, pp. 124–127, 2007.

[31] B. Billack, "Macrophage activation: role of toll-like receptors, nitric oxide, and nuclear factor kappa B," *American Journal of Pharmaceutical Education*, vol. 70, p. 102, 2006.

Hindawi
Mediators of Inflammation
Volume 2022, Article ID 8732360, 20 pages
https://doi.org/10.1155/2022/8732360

Review Article

Effect of Statins on Serum level of hs-CRP and CRP in Patients with Cardiovascular Diseases: A Systematic Review and Meta-Analysis of Randomized Controlled Trials

Tahmineh Kandelouei,[1] Mitra Abbasifard,[2,3] Danyal Imani,[4] Saeed Aslani,[5] Bahman Razi,[6] Mahdieh Fasihi,[4] Sajad Shafiekhani,[7,8,9] Keyhan Mohammadi,[10] Tannaz Jamialahmadi,[11] Željko Reiner,[12] and Amirhossein Sahebkar[13,14,15,16]

[1]*Department of Oncological Sciences, Huntsman Cancer Institute, University of Utah, Salt Lake City, UT 84112, USA*
[2]*Molecular Medicine Research Center, Research Institute of Basic Medical Sciences, Rafsanjan University of Medical Sciences, Rafsanjan, Iran*
[3]*Department of Internal Medicine, School of Medicine, Ali Ibn Abi Talib Hospital, Rafsanjan University of Medical Sciences, Rafsanjan, Iran*
[4]*Department of Immunology, School of Public Health, Tehran University of Medical Sciences, Tehran, Iran*
[5]*Department of Immunology, School of Medicine, Tehran University of Medical Sciences, Tehran, Iran*
[6]*Department of Hematology and Blood Transfusion, School of Medicine, Tarbiat Modares University, Tehran, Iran*
[7]*Departments of Biomedical Engineering, School of Medicine, Tehran University of Medical Sciences, Iran*
[8]*Research Center for Biomedical Technologies and Robotics, Tehran, Iran*
[9]*Students Scientific Research Center, Tehran University of Medical Sciences, Tehran, Iran*
[10]*Faculty of Pharmacy, Tehran University of Medical Sciences, Tehran, Iran*
[11]*Department of Nutrition, Faculty of Medicine, Mashhad University of Medical Sciences, Mashhad, Iran*
[12]*Department of Internal Medicine, University Hospital Center Zagreb, School of Medicine, University of Zagreb, Zagreb, Croatia*
[13]*Applied Biomedical Research Center, Mashhad University of Medical Sciences, Mashhad, Iran*
[14]*Biotechnology Research Center, Pharmaceutical Technology Institute, Mashhad University of Medical Sciences, Mashhad, Iran*
[15]*Department of Medical Biotechnology, Faculty of Medicine, Mashhad University of Medical Sciences, Mashhad, Iran*
[16]*Department of Biotechnology, School of Pharmacy, Mashhad University of Medical Sciences, Mashhad, Iran*

Correspondence should be addressed to Bahman Razi; b.razi@modares.ac.ir
and Amirhossein Sahebkar; amir_saheb2000@yahoo.com

Received 1 October 2021; Accepted 17 December 2021; Published 28 January 2022

Academic Editor: Azizah Ugusman

Background. Several studies have reported that statins have anti-inflammatory effects. Nevertheless, results of clinical trials concerning the effect of statins on the levels of C-reactive protein (CRP) and high-sensitivity CRP (hs-CRP) have been inconsistent. Therefore, we performed a systematic review and meta-analysis of randomized clinical trials (RCTs) evaluating the effect of statins on CRP and hs-CRP levels in patients with cardiovascular diseases (CVDs). *Methods*. Literature search of the major databases was performed to find eligible RCTs assessing the effect of statins on serum levels of CRP and hs-CRP from the inception until the last week of April 2021. The effect sizes were determined for weighted mean difference (WMD) and 95% confidence intervals (CI). *Results*. 26 studies were identified (3010 patients and 2968 controls) for hs-CRP and 20 studies (3026 patients and 2968 controls) for CRP. Statins reduced the serum levels of hs-CRP (WMD = −0.97 mg/L; 95% CI: -1.26 to -0.68 mg/L; $P < 0.001$) and CRP (WMD = −3.05 mg/L; 95% CI: -4.86 to -1.25 mg/L; $P < 0.001$) in patients with CVDs. Statins decreased the serum levels of hs-CRP in patients receiving both high-intensity and moderate/low-intensity treatments with these drugs. In addition, the duration of treatment longer than 10 weeks decreased hs-CRP levels. Only high-intensity

statin treatment could marginally decrease serum levels of CRP in CVDs patients. *Conclusions*. This meta-analysis showed the efficacy of statins to reduce the concentrations of CRP and hs-CRP in patients with different types of CVDs.

1. Introduction

Statins, which are 3-hydroxy-3-methylglutaryl coenzyme A (HMG-CoA) reductase inhibitors, are broadly used as lipid-lowering drugs in patients with cardiovascular diseases (CVDs) [1, 2]. Although several classes of newer agents have been introduced in recent decades, statins still remain as the cornerstone of management of dyslipidemias [3–6]. Statins interfere with cholesterol synthesis in the liver cells and, therefore, decrease the levels of total cholesterol and low-density lipoprotein cholesterol (LDL-C) in serum [7]. Statins have been associated with decreased mortality rate in patients with CVDs. On the other hand, statins have anti-inflammatory effects, and therefore, they might be beneficial in diseases related to inflammation including not only atherosclerosis [8] but also congestive heart failure (CHF) [9], nephropathy [10], central nervous system (CNS) diseases [11], autoimmune disease [12], sepsis [13], gastrointestinal diseases [14], delirium [15], COVID-19 [16], bone remodeling/osteoporosis [17], and macular degeneration [18]. However, the treatment with statins in these diseases is still not widely accepted despite a wide range of lipid-independent and pleiotropic actions [19–21].

C-reactive protein (CRP) is an acute phase protein that is part of the pentraxin protein family. It is primarily produced by liver cells and in small quantities by some other cells like vascular smooth muscle cells and macrophages. Atherosclerotic lesions also produce CRP [22]. A lot of evidence shows that inflammatory events are underlying cause in the development of cardiovascular events and atherosclerotic CVDs, such as acute coronary syndromes (ACS) [23, 24]. CRP, as a well-known marker of inflammation, has been associated with atherosclerotic plaques development as well as with destabilization of plaques and promotion of occlusive thrombi [25]. CRP has been shown to injure the glycocalyx of vascular endothelium resulting in dysfunction of endothelium which is considered to be the first step in atherogenesis [26]. CRP can induce the renin-angiotensin-aldosterone system, and it enhances the proatherogenic function of angiotensin causing functional and structural modifications of vessel walls, stiffness of vessels, vascular remodeling, and interference with the regulatory systems of blood pressure [27]. CRP also triggers the production of different matrix metalloproteinases (MMP) in macrophages and endothelial cells, and it suppresses the MMP inhibitors, causing destruction of collagen in the cap of the atherosclerotic plaque and therefore destabilization and rupture of atherosclerotic plaques [28]. Several approaches have been attempted to control inflammatory diseases by reducing the levels of serum CRP [29, 30].

Statins reduce CRP levels by different mechanisms. Several inflammatory cytokines like interleukin- (IL-) 6 are involved in the stimulation of CRP production by hepatocytes. Statins interrupt the production of IL-6 suppressing the stimulatory effect of IL-6 on the generation of CRP. It is well known that statins decrease the number of LDL particles resulting in decreased levels of highly atherogenic oxidized-LDL (ox-LDL) particles, which in turn decreases the generation of inflammatory mediators by the atherosclerotic plaques that stimulate the production of CRP. By upmodulating apoA-I, statins can suppress the expression of E-selectin, intercellular adhesion molecule-1 (ICAM-1), and vascular cell adhesion molecule-1 (VCAM-1) on the activated endothelial cells causing a decreased production of CRP-stimulating factors [31]. Moreoever, in silico findings have suggested a direct interaction between statin molecules and CRP [32].

A number of clinical trials have tried to prove the effects of statins on lowering the levels of CRP and high-sensitivity CRP (hs-CRP) in the context of preventing CVDs and cardiovascular events [33–35]. JUPITER was the first trial which prospectively assessed the effects of rosuvastatin 20 mg versus placebo on rates of cardiovascular events during a maximum follow-up of 5 years (median 1.9 years), according to on-treatment concentrations of LDL-C ($\geq$1.8 mmol/L or <1.8 mmol/L) and hs-CRP ($\geq$2 mg/L or<2 mg/L) showing that not only decreased LDL-C but also hs-CRP are indicators of successful treatment with a statin [36]. Rosuvastatin reduced LDL-C levels by 50% and hs-CRP levels by 37%. Additionally, the results of statin therapy (pravastatin) on 472 randomly selected participants in the Cholesterol and Recurrent Events (CARE) trial indicated that median CRP levels and the mean change in CRP decreased over time (5 years) among those allocated to pravastatin (median change, -17.4%; $P = 0.004$ and mean change, -0.07 mg/dL; $P = 0.002$). Those allocated to placebo median CRP levels and the mean change in CRP tended to increase (median change, +4.2%; $P = 0.2$ and mean change, +0.07 mg/dL; $P = 0.04$) [37]. However, the results of some studies were inconsistent and inconclusive [38]. In order to obtain a clear answer, we performed a systematic review and a meta-analysis of randomized controlled trials (RCTs) which evaluated the effects of statins in lowering CRP and hs-CRP levels in different types of CVDs, such as ACS, myocardial infarction (MI), coronary artery disease (CAD), unstable angina, heart failure, stable atherosclerotic plaque, and carotid artery stenting.

2. Methods

This study was performed following the Preferred Reporting Items for Systematic Reviews and Meta-Analyses (PRISMA) statement [39]. Since the study did not include any studies with human participants or animals performed by any of the authors of this article, ethical approval was not necessary. The study was designed according to the international PICOS format—Population (adults with CVDs), Intervention (statins), Comparison/Comparator (control/placebo group), Outcome (to explore whether statins change the serum level of hs-CRP and CRP), and Study design (parallel and crossover clinical trials).

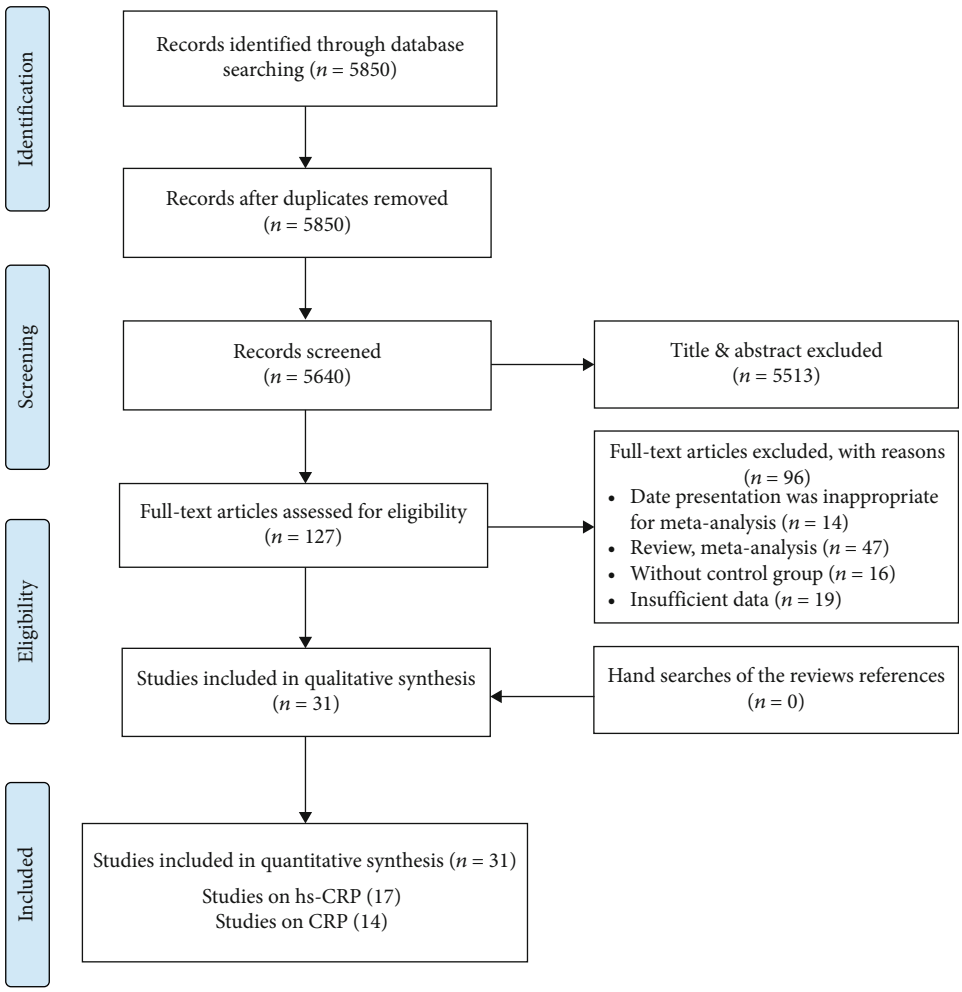

Figure 1: PRISMA flow diagram of the study selection process.

2.1. Data Sources and Search Strategy. Online literature search was performed in MEDLINE/PubMed, Scopus, and ISI Web of Science databases, and all publications evaluating the effect of statins on hs-CRP and CRP levels in patients with CVDs were analyzed until the last week of April 2021. During systematic search, the following MeSH terms and key words were used: (statins∗ OR atorvastatin OR fluvastatin OR pravastatin OR rosuvastatin OR lovastatin OR pitavastatin OR cerivastatin OR simvastatin) AND (random∗ OR "randomized controlled trial" OR "randomized trial" OR "randomized study" OR "random number") AND ("C-reactive protein" OR CRP OR "high-sensitivity C-reactive protein" OR "hs-CRP") AND ("acute coronary syndromes" OR ACS OR "coronary artery disease" OR CAD OR "heart failure" OR "myocardial infarction" OR "atherosclerosis" OR "stable angina" OR "unstable angina" OR "stable atherosclerotic plaques" OR angina). In order to increase the sensitivity of the literature search, the reference lists of eligible studies were scanned manually. Furthermore, no restrictive filter was added to the search strategy.

2.2. Inclusion and Exclusion Criteria. Trials were included in the quantitative analysis if they met the following criteria: (1) studies with randomized controlled trial (RCT) design; (2) RCTs considering the effect of statins on hs-CRP and CRP serum level in patients with CVDs; and (3) RCTs with sufficient, calculable, or convertible data regarding the mean changes of hs-CRP and CRP, along with standard deviation (SD) for both intervention and control groups. Age, gender, dose and duration of statin therapy, and number of participants in both groups were not the cause of inclusion or exclusion of studies. The publications were excluded if they were performed on animals or *in vitro* or did not report levels of hs-CRP and CRP both at starting point and at the end of treatment. Meta-analyses, case reports, book chapters, unpublished data, and gray literature (dissertations, congress abstracts, and patents) were also excluded.

2.3. Study Selection and Data Extraction. Two independent authors (TK and DI) performed a systematic search and exported the results of primary search to the Endnote X9 software. Afterwards, duplicates were removed, and the other studies were assessed by title and abstract and/or full-text. Subsequently, the data of studies that fulfilled inclusion criteria were extracted separately (TK and DI) according to a predefined extraction form as follows: the

Table 1: Demographic characteristics of the included studies.

Study author	Year	Country	Intervention/ control (sample size)	Intervention (M∗/F)/control (M∗/F)	Mean age (intervention/ control)	Intervention duration (week)	Target population	Dosage (mg/ day)	Dosage category	Hydrophilic or lipophilic	Jadad scale	Intervention name
Hs-CRP												
Luo et al.	2004	China	11/9	M = 9, F = 2/M = 6, F = 3	67.4 ± 4.5/65.7 ± 3.6	3	AMI	20	M	Lipophile	2	Simvastatin
Luo et al.	2004	China	14/16	M = 10, F = 4/M = 13, F = 3	63.2 ± 4.2/64.6 ± 7.3	3	Unstable angina	20	M	Lipophile	2	Simvastatin
Azar et al.	2005	Lebanon	44/26	NR	63 ± 8/59 ± 1	1	CAD	NR	—	—	3	Statins
Marschang et al.	2006	Austria	47/16	M = 30, F = 17/M = 6, F = 10	61 ± 2/59 ± 2	24	CAD	NR	—	—	3	Statins
Sola et al.	2006	USA	54/54	M = 33, F = 21/M = 34, F = 20	53.8 ± 5.7/55.4 ± 6.4	96	Heart failure	20	M	Lipophile	4	Atorvastatin
Yang et al. (i)	2006	China	20/20	M = 12, F = 8/M = 13, F = 7	64.2 ± 9.7/63.5 ± 9.4	1	ACS	40	L	Lipophile	3	Fluvastatin
Yang et al. (ii)	2006	China	20/20	M = 11, F = 9/M = 13, F = 7	64.1 ± 10.9/63.5 ± 9.5	1	ACS	80	M	Lipophile	3	Fluvastatin
Chan et al. (i)	2008	Taiwan	30/30	M = 24, F = 6/M = 19, F = 11	63.77 ± 12/66.13 ± 11.50	12	CAD	10	M	Lipophile	3	Atorvastatin
Chan et al. (ii)	2008	Taiwan	30/30	M = 11, F = 9/M = 13, F = 7	63.77 ± 12/66.13 ± 11.50	24	CAD	10	M	Lipophile	3	Atorvastatin
Suzuki et al. (i)	2008	Japan	10/9	NR	71 ± 8/68 ± 7	12	CAD	10	L	Lipophile	4	Fluvastatin
Suzuki et al. (ii)	2008	Japan	10/9	NR	71 ± 8/68 ± 7	12	CAD	10	L	Hydrophile	4	Pravastatin
Vasilieva et al.	2008	Russia	19/20	NR	70.1 ± 2.4	1	ACS	40	H	Lipophile	3	Atorvastatin
McMurray et al. (i)	2009	UK	777/779	M = 578, F = 199/M = 597, F = 182	72 ± 7/73.2 ± 7.2	12	Heart failure	10	M	Hydrophile	4	Rosuvastatin hs-CRP 2.0 mg/L
McMurray et al. (ii)	2009	UK	1711/1694	M = 1319, F = 392/M = 1297, F = 397	72 ± 7/73.2 ± 7.2	12	Heart failure	10	M	Hydrophile	4	Rosuvastatin hs-CRP 2.0 mg/L
Yun et al.	2009	Korea	225/220	M = 136, F = 89/M = 137, F = 83	63 ± 11/64 ± 10	1	ACS	40	H	Hydrophile	2	Rosuvastatin
Andreou et al.	2010	Greece	21/18	M = 19, F = 2/M = 16, F = 2	66 ± 11/65 ± 11	4	Heart failure	10	M	Hydrophile	3	Rosuvastatin
Dohi et al.	2010	Japan	85/84	M = 77, F = 8/M = 69, F = 5	62.8 ± 10.4/62.3 ± 10.4	24	ACS	20	M	Lipophile	3	Atorvastatin
Yun et al.	2011	Korea	237/242	M = 130, F = 107/M = 153, F = 89	63 ± 11/63 ± 11	1	ACS	NR	—	—	3	Statins
Abulhul et al.	2012	Ireland	28/28	M = 18, F = 10/M = 20, F = 8	72 ± 9/72 ± 14	24	Heart failure	40	H	Lipophile	3	Atorvastatin
Guo et al. (i)	2012	China	47/54	M = 40, F = 7/M = 48, F = 6	62.07 ± 8.51/62.64 ± 12	24	Stable atherosclerotic plaque	10	M	Lipophile	3	Atorvastatin
Guo et al. (ii)	2012	China	45/54	M = 36, F = 9/M = 48, F = 6	62.07 ± 8.51/62.64 ± 12	24	Stable atherosclerotic plaque	20	M	Lipophile	3	Atorvastatin

Table 1: Continued.

Study author	Year	Country	Intervention/ control (sample size)	Intervention (M∗/F)/control (M∗/F)	Mean age (intervention/ control)	Intervention duration (week)	Target population	Dosage (mg/ day)	Dosage category	Hydrophilic or lipophilic	Jadad scale	Intervention name
Guo et al. (iii)	2012	China	43/54	M = 41, F = 2/M = 48, F = 6	62.07 ± 8.51/62.64 ± 12	24	Stable atherosclerotic plaque	40	H	Lipophile	3	Atorvastatin
Guo et al. (iiii)	2012	China	39/54	M = 34, F = 5/M = 48, F = 6	62.07 ± 8.51/62.64 ± 12	24	Stable atherosclerotic plaque	80	H	Lipophile	3	Atorvastatin
Jiao et al. (i)	2015	China	62/64	M = 40, F = 22/M = 44, F = 20	74.9 ± 8.7/75.6 ± 7.8	1	ACS	20	H	Hydrophile	2	Rosuvastatin
Jiao et al. (ii)	2015	China	62/64	M = 40, F = 22/M = 44, F = 20	74.9 ± 8.7/75.6 ± 7.8	4	ACS	20	H	Hydrophile	2	Rosuvastatin
Qiao et al.	2019	China	82/78	M = 55, F = 27/M = 50, F = 28	65.67 ± 9.14/65.08 ± 10	2	Carotid artery stenting	40	H	Lipophile	3	Atorvastatin
CRP												
Correia et al.	2003	Brazil	18/18	M = 6, F = 12/M = 9, F = 9	66 ± 9/65 ± 12	1	ACS	80	H	Lipophile	3	Atorvastatin
Karaca et al.	2003	Turkey	46/32	NR	52/52	4	CAD	20	M	Lipophile	3	Atorvastatin
Kinlay et al. (i)	2003	USA	1186/1216	M = 774, F = 408/M = 812, F = 404	64 ± 12/64 ± 11	16	ACS	80	H	Lipophile	3	Atorvastatin
Kinlay et al. (ii)	2003	USA	555/544	NR	NR/NR	16	Unstable angina	80	H	Lipophile	3	Atorvastatin
Kinlay et al.(iii)	2003	USA	631/672	NR	NR/NR	16	MI	80	H	Lipophile	3	Atorvastatin
Ostadal et al.	2003	Czech Republic	13/17	M = 11, F = 2/M = 14, F = 3	NR/NR	1	MI	0/3	—		2	Cerivastatin
Macin et al.	2004	Argentina	44/46	M = 34, F = 10/M = 33, F = 13	61.1 ± 11.5/59.3 ± 13.4	4	ACS	40	H	Lipophile	3	Atorvastatin
Doo et al. (i)	2005	China	20/30	M = 10, F = 10/M = 15, F = 15	60 ± 9/62 ± 9	1	Unstable angina	NR	—		2	Statins
Doo et al. (ii)	2005	China	20/30	M = 10, F = 10/M = 15, F = 15	60 ± 9/62 ± 9	1	Unstable angina	NR	—		2	Statins
Li et al.	2005	China	19/17	NR	NR/NR	4	Unstable angina	20	M	Lipophile	3	Atorvastatin
Link et al. (i)	2006	Germany	18/17	NR	55.5/60	1	ACS	20	H	Hydrophile	3	Rosuvastatin
Link et al. (ii)	2006	Germany	18/17	NR	55.5/60	1	ACS	20	H	Hydrophile	3	Rosuvastatin
Link et al. (iii)	2006	Germany	18/17	NR	55.5/60	6	ACS	20	H	Hydrophile	3	Rosuvastatin
Li et al.	2007	China	18/16	M = 15, F = 3/M = 13, F = 3	NR/NR	1	Unstable angina	20	M	Lipophile	3	Simvastatin
Patti et al.	2007	Italy	86/85	M = 68, F = 18/M = 67, F = 18	67 ± 10/64 ± 11	1	ACS	80	H	Lipophile	3	Atorvastatin
Lewandowski et al. (i)	2008	Poland	39/39	M = 33, F = 6/M = 33, F = 6	55 ± 9.42/54 ± 8.86	1	ACS	40	H	Lipophile	3	Atorvastatin

Table 1: Continued.

Study author	Year	Country	Intervention/ control (sample size)	Intervention (M∗/F)/control (M∗/F)	Mean age (intervention/ control)	Intervention duration (week)	Target population	Dosage (mg/ day)	Dosage category	Hydrophilic or lipophilic	Jadad scale	Intervention name
Lewandowski et al. (ii)	2008	Poland	39/39	M = 33, F = 6/M = 33, F = 6	55 ± 9.42/54 ± 8.86	6	ACS	40	H	Lipophile	3	Atorvastatin
Nakagomi et al.	2012	Japan	63/83	M = 44, F = 19/M = 62, F = 21	66.2 ± 11.9/64.3 ± 9.9	24	Heart failure	NR	—		2	Statins
Gruzdeva et al.	2016	Russia	60/66	M = 55, F = 5/M = 58, F = 8	56.5/60.4	2	MI	20	M	Lipophile	3	Atorvastatin
Strazhesko et al.	2016	Italy	44/38	M = 34, F = 10/M = 32, F = 6	51.4 ± 1.2/59.2 ± 1.2	48	Atherosclerosis	20	M	Lipophile	3	Atorvastatin

NR: not reported; MI: myocardial infraction; ACS: acute coronary syndrome; CAD: coronary artery disease; H: high; M: moderate; L: low; M∗: male; F: female.

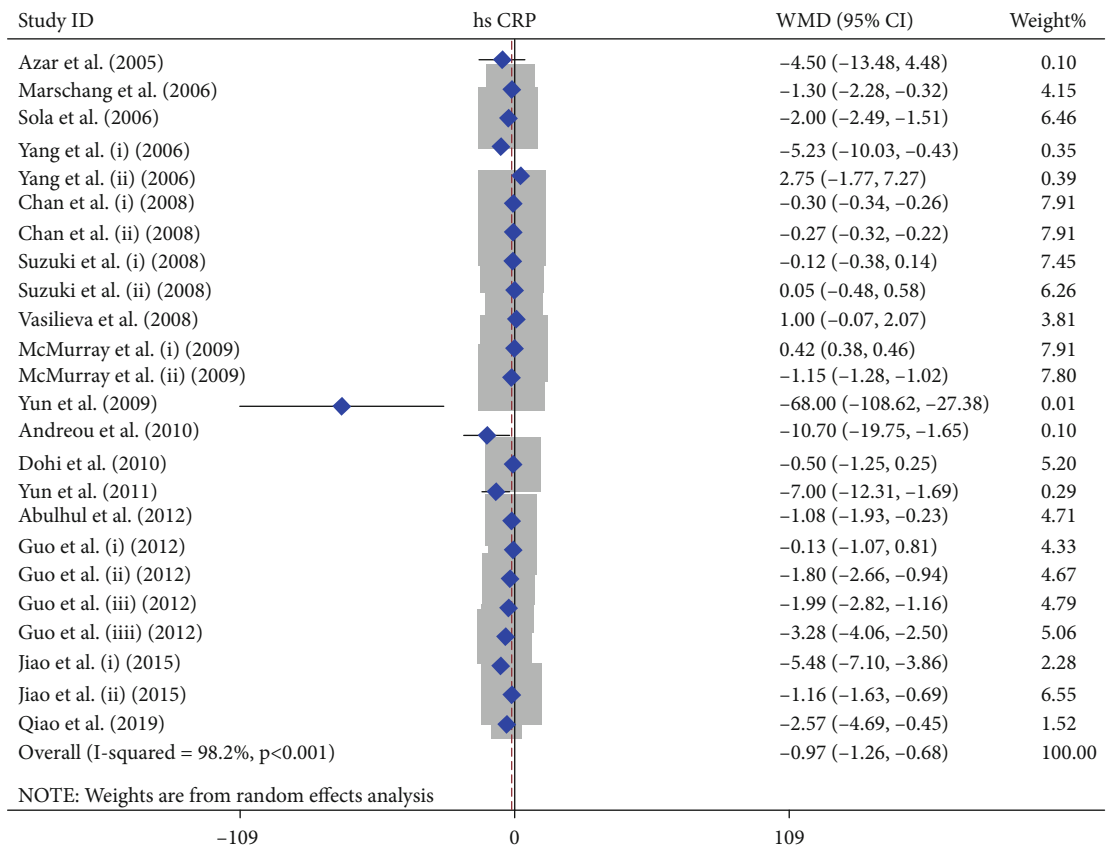

Figure 2: Forest plot presenting WMD and 95% CI for the effect of statin administration on hs-CRP (a) and CRP (b) levels in the overall population.

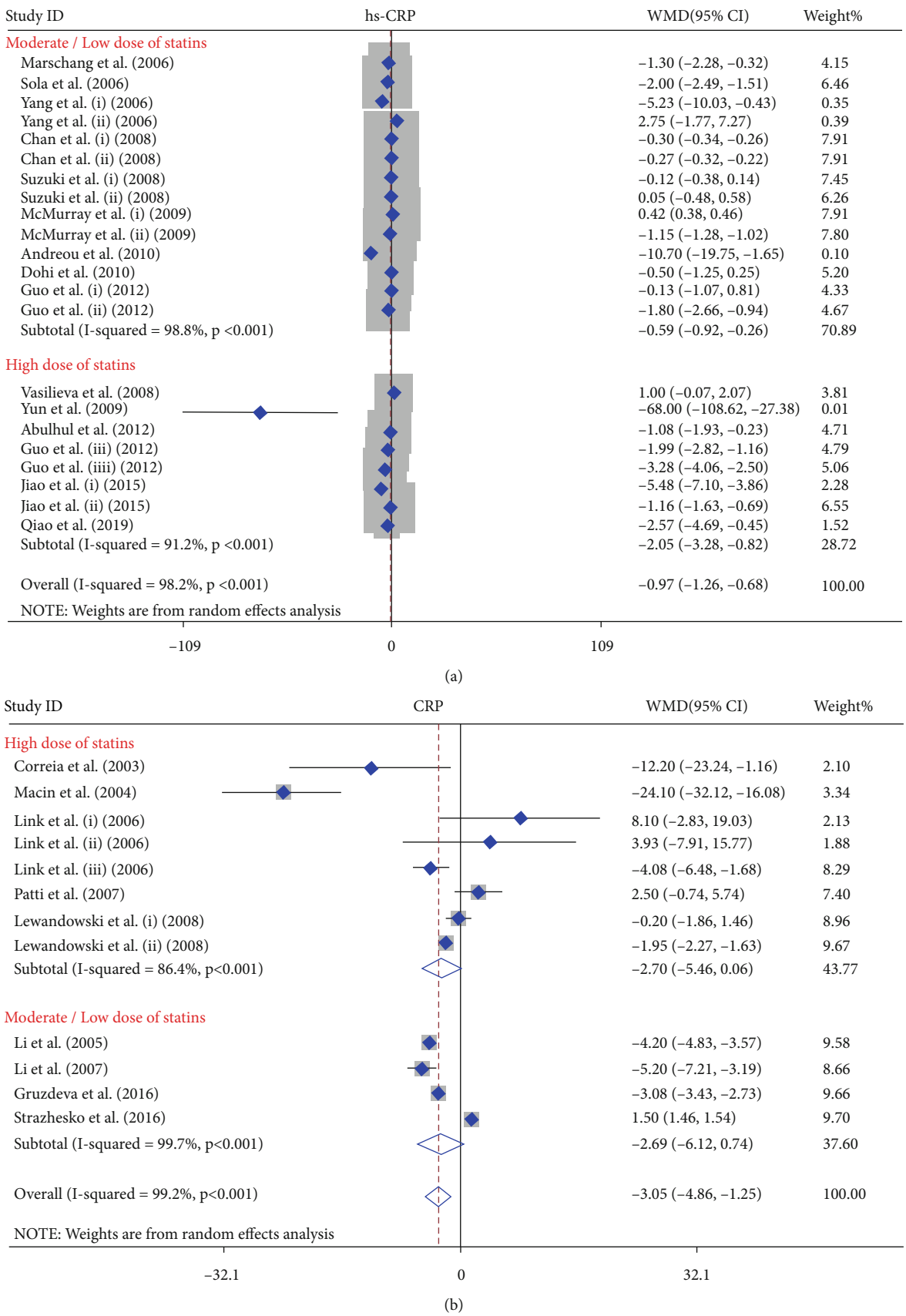

Figure 3: Forest plot presenting WMD and 95% CI for the effect of statin administration on hs-CRP and CRP levels in subgroup analysis by dose; (a) hs-CRP and (b) CRP.

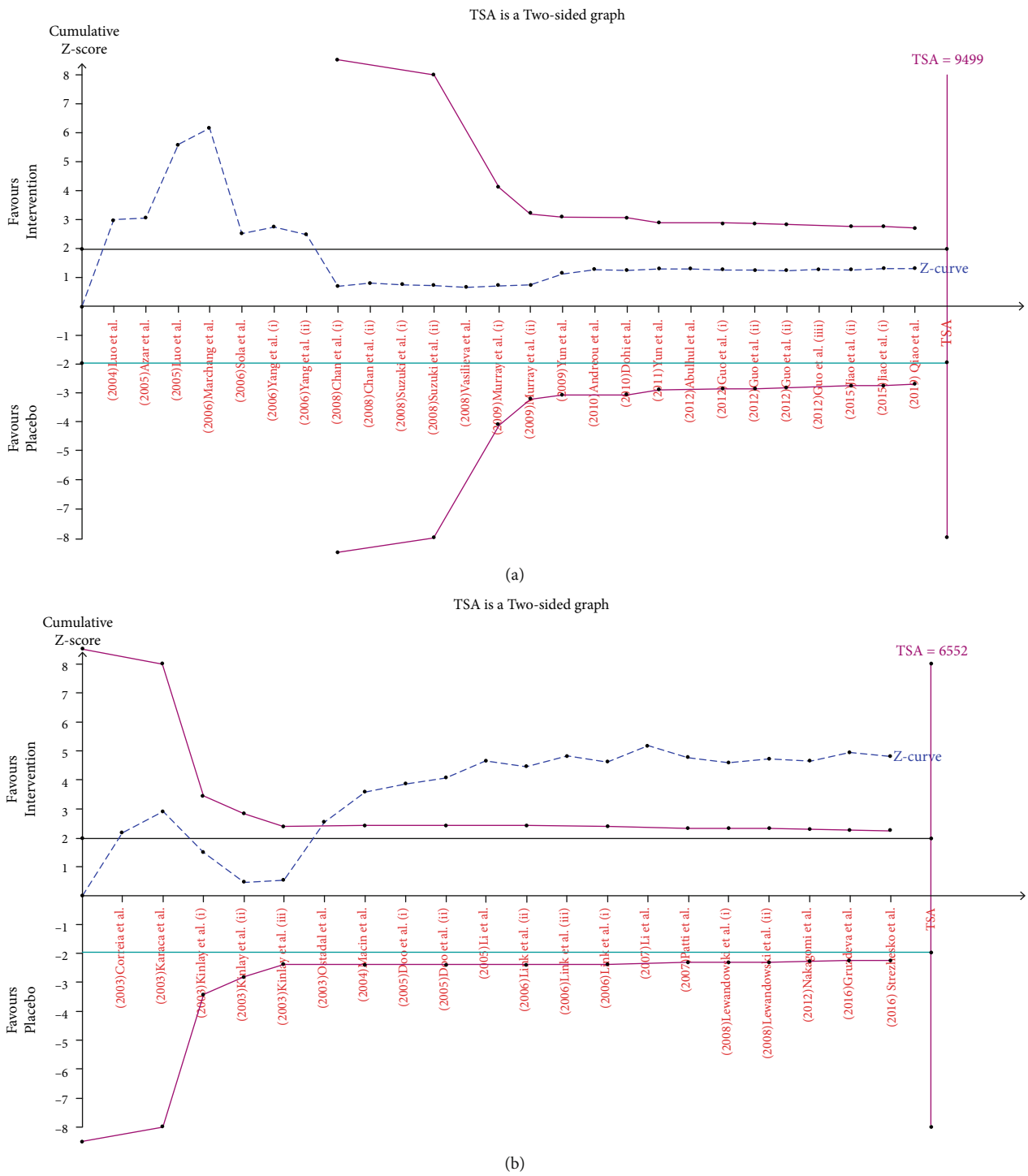

Figure 4: Trial sequence analysis of all the included studies for the effect of statin administration on the serum levels of hs-CRP (a) and CRP (b). Cumulative Z-curve (dashed blue lines), conventional boundary (green horizontal lines), trial sequential monitoring boundaries (inward sloping purple line), and required information sizes (purple vertical lines).

first author's last name, the name of the journal, year of publication, country of origin, ethnicity, study design, mean or range of age, dosage of statin (mg/day), duration of treatment (weeks), sample size, and the mean and SD of the hs-CRP and CRP levels before and after the treatment with statins. The extracted data were compared by two authors (TK and DI), and any discrepancy was resolved by consensus, and in the case in which they did not reach a definite conclusion, the data were compared with the original article.

2.4. Quality Assessment. Jadad tool was used for evaluating the quality of RCTs by assessing the randomization, blinding, and dropouts (withdrawals) [40]. This scale ranges from

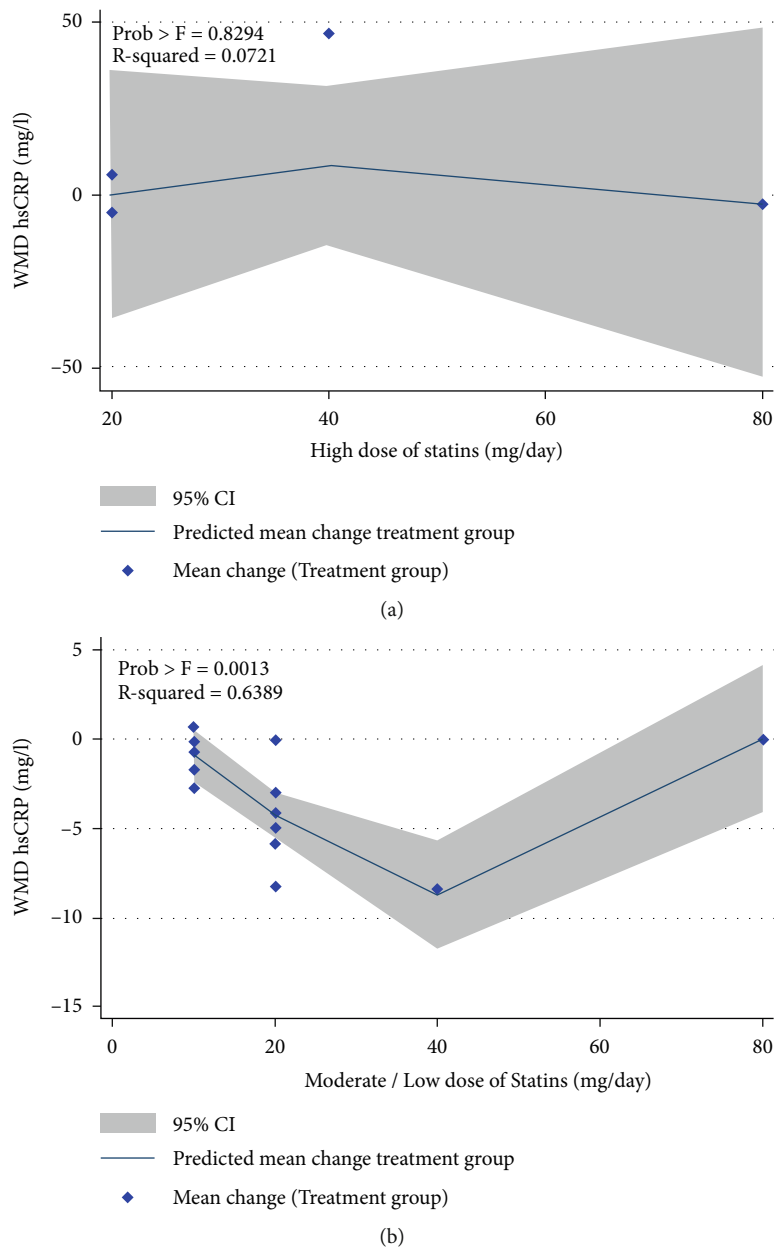

Figure 5: Nonlinear dose-response relations between dosage statin administration and WMD in hs-CRP: (a) high dose of statins and (b) moderate/low dose of statins.

0 to 5, and studies with scores ≤ 2 and ≥3 were considered low- and high-quality studies, respectively.

2.5. Statistical Analysis. The effects of treatment with statins on hs-CRP and CRP levels were expressed by weighted mean difference (WMD), with 95% confidence interval (CI) as the continuous variable. If the outcomes were reported as the median, range, mean, standard error (SE), or CI, they were converted into the mean and standard deviation (SD). Circulating hs-CRP and CRP concentrations were expressed in mg/L. The degree of heterogeneity was measured using I^2 and Cochrane's Q tests. Accordingly, heterogeneity was considered significant if I^2 was >50% and Cochrane's Q was $P < 0.10$, while $I^2 < 50\%$ and Cochrane's Q ($P > 0.10$) did not prove a heterogeneity [41, 42]. Random-effects model (REM) and fixed-effects model (FEM) were used in the presence and absence of heterogeneity, respectively. The potential publication bias was evaluated by visual inspection of asymmetry and Egger's regression test (P value less than 0.05 was considered significant) [43, 44]. Sensitivity analysis was used to express the impact of each publication on the pooled effect size by removing one study at a time. In order to find predefined source of heterogeneity, subgroup analyses and metaregression analyses were performed. Subgroup analyses were performed considering the dosage of statins (high intensity statin therapy and moderate/low intensity statin therapy) [45], treatment duration (>10 and ≤10 weeks), and characteristics of statins (hydrophilic and

Table 2: The effects of statin therapy on hs-CRP and CRP levels in overall population and subgroup analyses.

Parameter		Number of arms	Weighted mean difference	95% CI (*P* value)	Test of heterogeneity I^2 (%)	*P*
hs-CRP						
Overall		26	-0.97	-1.26, -0.68 (<0.001)	98.2	<0.001
Dosage category						
High intensity		8	-2.05	-3.28, -0.82 (<0.001)	91.2	<0.001
Treatment duration (weeks)	≤10	5	-2.20	-4.59, 0.20 (0.07)	92.7	<0.001
	>10	3	-2.13	-3.39, -0.86 (0.001)	86.1	<0.001
Hydrophilicity/lipophilicity	Hydrophilic	3	-4.19	-9.10, 0.73 (0.09)	94.4	<0.001
	Lipophilic	5	-1.55	-3.02, -0.09 (0.03)	90.8	<0.001
Moderate/low intensity		16	-0.59	-0.92, -0.26 (0.02)	98.8	<0.001
Treatment duration (weeks)	≤10	5	-3.67	-10.94, -0.43 (0.32)	79	<0.001
	>10	11	-0.57	-0.90, -0.25 (0.001)	99.1	<0.001
Hydrophilicity/lipophilicity	Hydrophilic	4	-0.41	-1.64, 0.81 (0.50)	99.4	<0.001
	Lipophilic	11	-0.49	-0.67, -0.30 (0.001)	88.1	<0.001
CRP						
Overall		20	-3.05	-4.86, -1.25 (<0.001)	99.2	<0.001
Dosage category						
High intensity		11	-2.70	-5.467, 0.06 (0.05)	86.4	<0.001
Hydrophilicity/lipophilicity	Hydrophilic	3	1.19	-7.13, 9.51 (0.77)	66.8	<0.001
	Lipophilic	8	-3.82	-7.38, -0.26 (0.03)	90.9	<0.001
Moderate intensity		5	-2.69	-6.12, 0.74 (0.12)	99.2	<0.001

lipophilic) [46]. The nonlinear potential effects for dosage and treatment duration by statins were analyzed using fractional polynomial modeling. All statistical tests for this meta-analysis were performed with STATA statistical software (version 14.0; Stata Corporation, College Station, TX, USA) and SPSS (version 23.0; SPSS, Inc. Chicago, IL, USA).

2.6. Trial Sequential Analysis. In order to minimize random errors, trial sequential analysis (TSA) was performed at a level of type-I error 5%, the statistical test power (80%), relative risk reduction (RRR) (20%), and a two-sided boundary type. When the *Z*-curve crossed the trial sequential monitoring boundaries or the required information size (RIS) line, reliability of evidence was confirmed. If the *Z*-curve did not cross the trial sequential monitoring boundaries or the RIS line, more studies were implicated.

3. Results

3.1. Study Characteristics. A total of 5850 articles were identified by the systematic literature search of databases. After excluding 210 duplicate publications and removing 5513 irrelevant publications based on titles/abstracts on 127 studies, full-text screening was performed. 96 were excluded based on the inclusion criteria because they were reviews or did not report sufficient or extractable data or did not have a control group. Finally, 31 publications were included in this meta-analysis, 17 publications (26 arms) for hs-CRP, and 14 publications (20 arms) for CRP. All included studies were performed in this century, and they were performed in different countries including China, Taiwan, Korea, Lebanon, Japan, Australia, the USA, Brazil, Argentina, the UK, Ireland, Greece, Russia, Italy, Poland, Germany, Czech Republic, and Turkey. The flow diagram of study selection is presented in Figure 1. Considering the study design, all studies were RCT. The sample size of the included studies ranged from 9 to 1216 participants, and treatment duration was between 1 to 96 weeks. Based on the Jadad scale, most of included studies received scores ≥ 3 and were considered moderate to high quality. Other characteristics of the analyzed publications are reported in Table 1.

3.2. Meta-Analyses of the Effect of Statins on the Serum Level of hs-CRP. Seventeen publications with 26 arms including 3010 participants who received statins and 2968 participants in control groups who did not receive statins or received placebo were included in this meta-analysis. Among them, 12 publications were performed in Asian countries [47–57], 4 publications in European countries [58–61], and only one study in the USA [62]. Overall population analysis showed that statins decreased the serum level of hs-CRP (WMD = −0.97 mg/L; 95% CI: -1.26 to -0.68 mg/L; $P < 0.001$; I^2: 98.2, $P_{\text{heterogeneity}} > 0.001$, Figure 2). To find more specific results, the eligible studies were stratified by dosage of statins—high-intensity statin and moderate/low-intensity statin treatment. Based on that, statins decreased the serum level of hs-CRP in both high-intensity (WMD = −2.05 mg/L; 95% CI: -3.28 to -0.82 mg/L; $P < 0.001$; I^2: 91.2, $P_{\text{heterogeneity}} > 0.001$) and moderate/low-

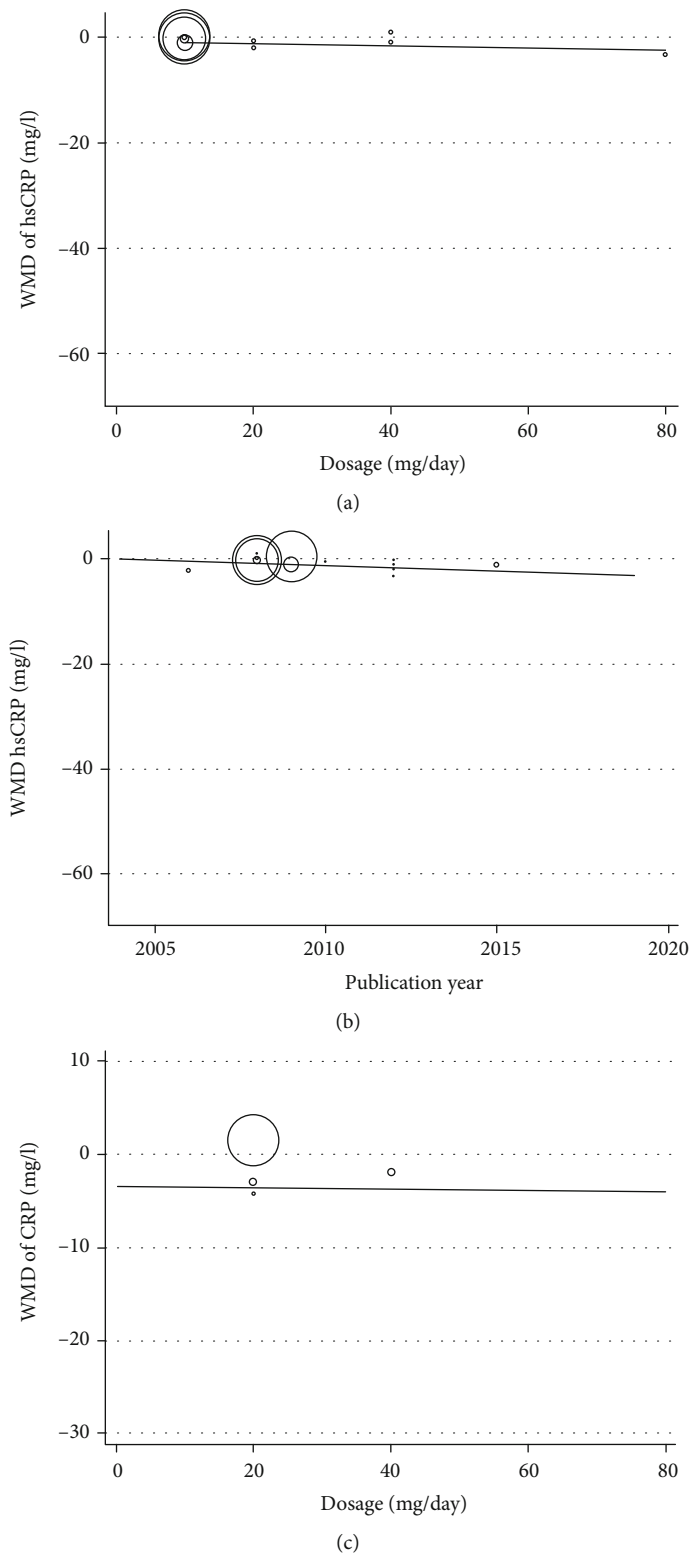

Figure 6: Continued.

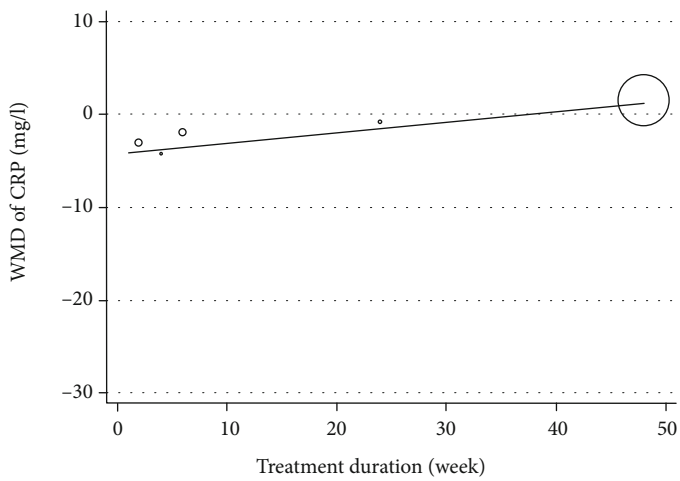

(d)

Figure 6: Random effects metaregression plots of the association between WMD of hs-CRP, CRP, and statin administration based on (a) hs-CRP (dosage), (b) hs-CRP (publication year), (c) CRP (dosage), and (d) CRP (treatment duration).

Table 3: Findings from metaregression analysis on the effects of statin therapy on hs-CRP and CRP levels.

Parameter	Coefficient	Standard error	95% CI	*P* value
Hs-CRP				
Dosage	-0.022	0.023	-0.071, 0.025	0.34
Treatment duration	-0.001	0.022	-0.047, 0.044	0.94
Publication year	-0.218	-1.72	-0.481, 0.045	1
CRP				
Dosage	-0.007	0.069	-0.219, 0.203	0.93
Treatment duration	0.116	0.138	-0.184, 0.417	0.84
Publication year	0.636	0.399	-0.234, 1.508	0.13

intensity groups (WMD = −0.59 mg/L; 95% CI: -0.92 to-0.26 mg/L; $P = 0.02$; I^2: 98.8, $P_{\text{heterogeneity}} > 0.001$). hs-CRP level in the group that was treated with high-intensity statin therapy > 10 weeks (WMD = −2.13 mg/L; 95% CI: -3.39 to -0.86 mg/L; $P = 0.001$; I^2: 86.1, $P_{\text{heterogeneity}} > 0.001$) and moderate/low-intensity statin therapy > 10 weeks (WMD = −0.57 mg/L; 95% CI: -0.90 to -0.25 mg/L; $P = 0.001$; I^2: 99.1, $P_{\text{heterogeneity}} > 0.001$) (Figure 3) was also decreased when compared with the control group. These findings were not significant for treatment duration ≤ 10 weeks in both dosage groups. Unlike hydrophilic statins, lipophilic statins significantly decreased the level of hs-CRP in both high- and moderate/low-intensity statin treatment groups. The results of TSA demonstrated that the cumulative Z-curve crossed the conventional boundary ($P = 0.05$) which confirmed the finding of meta-analysis, but it did not cross trial sequential monitoring boundaries and did not reach the required information sizes ($n = 9499$). These findings suggested that the cumulative evidence was not enough and that more studies are required for a final conclusion (Figure 4).

3.3. Dose-Response Effect of Statins on hs-CRP Concentration. The test for a nonlinear dose-response relationship was performed and demonstrated a nonlinear trend of moderate/low dose of statin treatment on hs-CRP concentration (Figure 5). The other dose and time response analyses could not confirm the presence of any significant trend on hs-CRP concentration (Table 2).

3.4. Meta-Analyses of the Effect of Statins on the Serum Level of CRP. Fourteen publications with twenty arms which included 3026 patients who were treated with statins and 2968 individuals in the control group provided data for the effect of statins on serum concentration of CRP. Among the included studies, four publications were performed on Asians [63–66], seven publications were performed on Europeans [38, 67–72], and three publications were performed on Americans [73–75]. The pooled effect indicated that treatment with statins significantly reduced CRP concentrations (WMD = −3.05 mg/L; 95% CI: -4.86 to -1.25 mg/L; $P < 0.001$; I^2: 99.2, $P_{\text{heterogeneity}} > 0.001$) (Figure 2). The studies were categorized to find influence of statin dose on CRP level. High-intensity statin therapy marginally decreased serum level of CRP (WMD = −2.70 mg/L; 95% CI: -5.46 to 0.06 mg/L; $P = 0.05$; I^2: 86.4, $P_{\text{heterogeneity}} > 0.001$) unlike moderate/low-intensity therapy (WMD = −2.69 mg/L; 95% CI: -6.12 to -0.74 mg/L; $P = 0.12$; I^2: 99.2, $P_{\text{heterogeneity}} > 0.001$) (Figure 3). The results showed that lipophilic statins are more effective in decreasing CRP level (WMD = −3.82 mg/L; 95% CI: -7.38 to -0.26 mg/L; $P = 0.03$; I^2: 90.9, $P_{\text{heterogeneity}} > 0.001$). As indicated in Figure 4, the cumulative Z-curve crossed the traditional boundary lines,

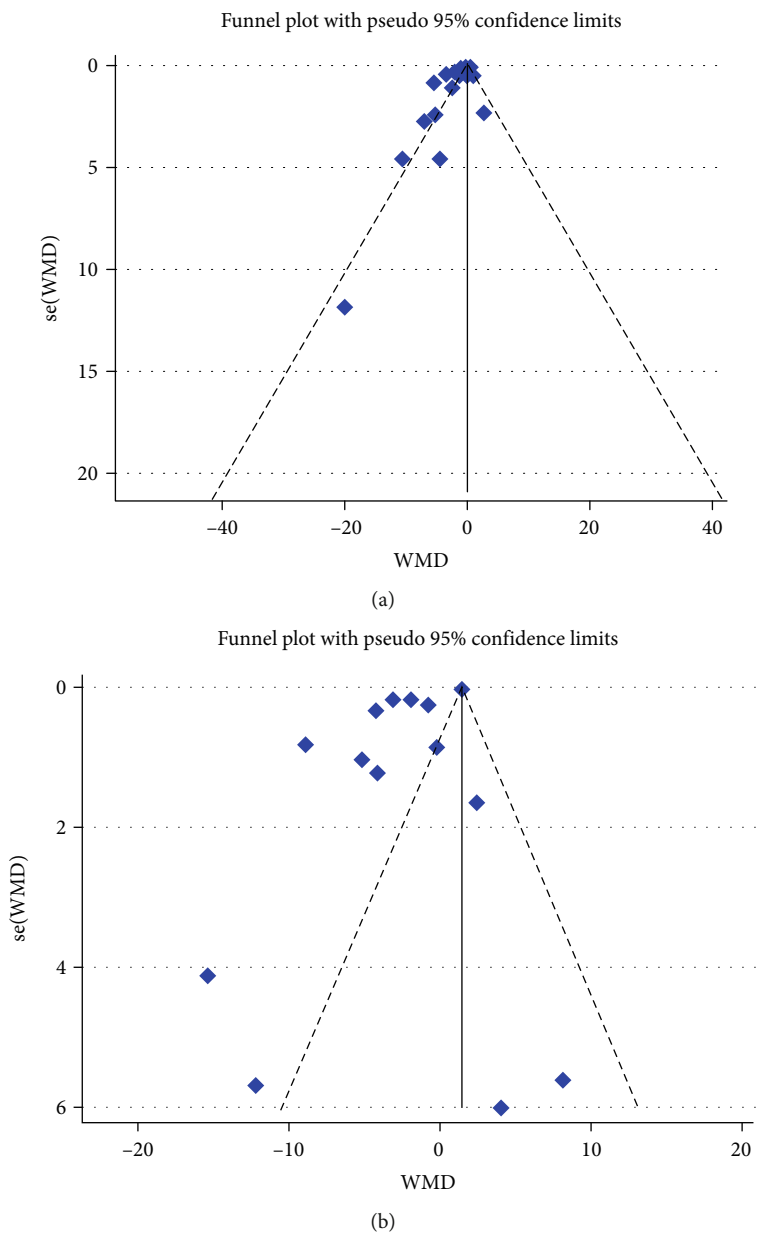

Figure 7: Funnel plot detailing publication biases in the studies included in the meta-analysis; (a) hs-CRP and (b) CRP.

and trial sequential monitoring boundary confirmed that the pooled result was reliable, although the cumulative sample size did not transcend the RIS.

3.5. Dose-Response Effect of Statins on CRP Concentration. We evaluated the dose-response relationship between the dose of statins and duration of treatment on CRP concentration. No evidence for the nonlinear relationship between CRP level and the dose of statin and duration of treatment was observed (Table 2).

3.6. Heterogeneity and Metaregression Analysis. The degree of heterogeneity was measured by I^2 and Cochrane's Q tests. A significant heterogeneity was observed in most of analyses. In these cases, REM was used. Metaregression analysis was used to find potential source of heterogeneity. However, it showed that the effect of statins on hs-CRP and CRP was not affected by treatment duration, dosage of statins, and publication year of the studies (Figure 6 and Table 3).

3.7. Publication Bias and Sensitivity Analysis. The result of Egger's linear regression test (hs-CRP [$z = 1.29, P = 0.19$] and CRP [$z = 1.98, P = 0.08$]) and funnel plots did not suggest any evidence of publication bias (Figure 7). In the sensitivity analysis of included studies, no individual study significantly affected the pooled effect size, proving the reliability of the results (Figure 8).

4. Discussion

It is well established that statins have beneficial effects on prevention of CVDs and cardiovascular events by lowering

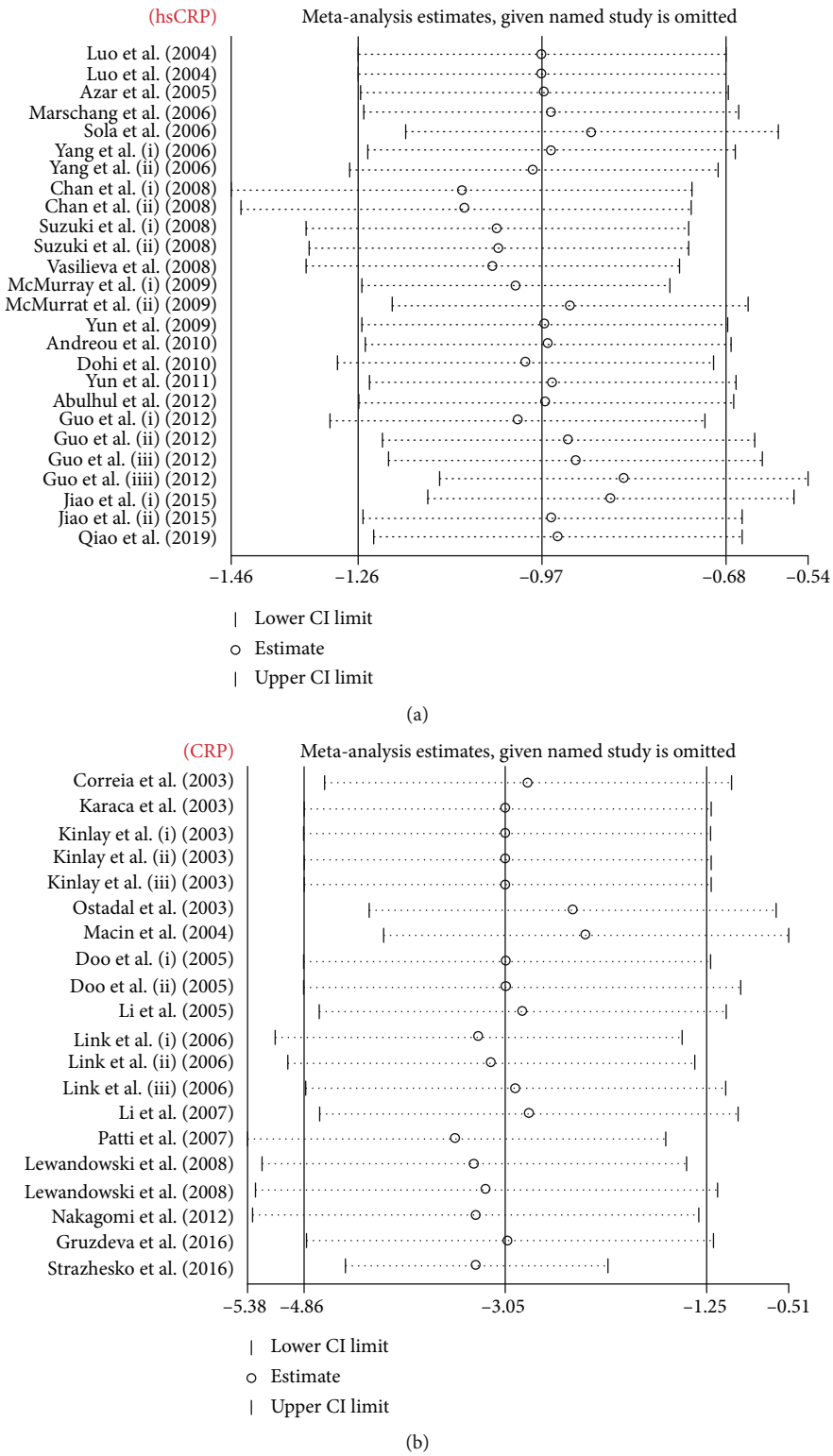

Figure 8: Leave-one-out sensitivity analyses of the statin therapy effect on serum hs-CRP (a) and CRP (b) level.

LDL-C and total cholesterol levels and having anti-inflammatory effects. Studies have proven that CRP and hs-CRP, as nonspecific markers of inflammation, are involved in the pathogenesis of CVDs. Studies have shown that reduction of LDL-C, total cholesterol levels, and markers of inflammation can reduce cardiovascular events. Elevated LDL-C is not decreased only by drugs like statins. Cicero et al. showed that red yeast rice (RYR) is among the most effective cholesterol-lowering nutraceutical which causes a reduction in LDL-C plasma levels up to 15% to

25% within 6 to 8 weeks. The decrease in LDL-C is accompanied by a proportional decrease in hs-CRP [76]. Furthermore, results of a robust meta-analysis showed that bempedoic acid is an efficient drug for lowering total cholesterol (by 15%), LDL-C (by 22.9%), apolipoprotein B (by 15.2%), and hs-CRP (by 27%) [77]. Several studies have tried to explain the role of statins in decreasing lipid levels and improving inflammation in prevention of different diseases, especially CVDs. Many of these studies had serious limitations such as little sample size, and they lacked statistical power. However, by pooling the results of different studies in a meta-analysis, it was possible to prove the effect of treatment with statins on these markers of inflammation. We performed a meta-analysis of 17 publications involving 3010 patients and 2968 controls for hs-CRP and 14 publications involving 3026 patients and 2968 controls analyzing the anti-inflammatory effects of statins by decreasing CRP and hs-CRP levels in different CVDs, including ACS, MI, CAD, unstable angina, heart failure, stable atherosclerotic plaques, and carotid artery stenting. The results indicated a significant beneficial anti-inflammatory effects of statins in patients with CVDs by decreasing the concentrations of CRP and hs-CRP in serum of these patients.

Previously, a number of meta-analyses have evaluated the effects on statins in CVDs. A most recent meta-analysis of 12 articles with 1,180 participants could not find any significant difference between patients treated with statins and those who were not treated when hs-CRP was concerned [78]. In a systematic review by Balk et al. published in 2003, statin therapy was effective in reducing levels of CRP but this effect was not dose-dependent. However, this study showed that there was no correlation between the effect of statins on CRP levels or lipids or cardiovascular outcomes [79]. Lipinski et al. in 2009 performed a meta-analysis and demonstrated that patients randomized to statins had a significant (4.2%) increase in left ventricular ejection fraction at follow-up and less hospitalizations due to deterioration of heart failure. However, treatment with statins did not affect all-cause or cardiovascular mortality in patients with heart failure [80]. A most recent study including 10,106 Finnish men without heart failure at baseline after an 8.8-year follow-up showed that several novel inflammatory biomarkers were associated with incident heart failure, suggesting early activation of respective pathways in the pathogenesis of heart failure [81]. A meta-analysis published in 2017 reported that pretreatment with statins was associated with lower levels of CRP postoperatively in patients who had coronary artery bypass graft surgery [82].

This most up-to-date meta-analysis of studies evaluating the effects of statins on CVDs indicated that statins significantly decreased levels of hs-CRP in patients with CVDs. The stratification of studies by dosage of statins suggested that statins decreased the serum levels of hs-CRP in patients who were treated with both high-intensity and moderate/low-intensity statin therapies. In addition, subgrouping based on the duration of statin treatment showed that treatment duration for more than 10 weeks decreased hs-CRP levels. Unlike hydrophilic statins, lipophilic statins significantly decreased the level of hs-CRP in both high- and moderate/low-intensity statin treatments. Regarding the influence of lipophilic statins, the findings of this meta-analysis are not in accordance with the results of Kim et al. They indicated that lipophilicity/hydrophilicity of statin did not have any effect on hs-CRP levels [83]. This study also suggests that treatment with statins significantly reduced CRP levels in CVDs patients. Considering different dosage of statins, only high-intensity statin treatment could marginally decrease the serum level of CRP in CVDs patients. Lipophilic statins were more effective in decreasing the level of CRP. The potential mechanistic role of CRP in plaque formation and subsequently an increased risk of CVDs and cardiovascular events are complex. However, theoretically, CRP could facilitate monocyte adhesion and transmigration into the vessel wall which is an early step in the atherosclerotic process. Besides, polarization of M1 macrophage by CRP is a proinflammatory trigger in plaque formation which causes macrophage infiltration in both adipose tissue and atherosclerotic lesions [84, 85].

The test for dose-response relationship between statins and levels of CRP and hs-CRP indicated a nonlinear trend of moderate/low dose of statins on hs-CRP concentration. However, no evidence for a nonlinear dose-response relationship was observed between the dose of statins and CRP level. The results of TSA for hs-CRP demonstrated that the cumulative evidence was not enough and that more studies are required for a final conclusion. Nevertheless, based on the results of TSA for CRP, trial sequential monitoring boundary indicated that the pooled result was reliable, although the cumulative sample size was lower than the expected level. Therefore, more studies are needed, at least regarding the effects of statins on hs-CRP, to prove without any doubt the beneficial effects of statins in patients with different CVDs concerning inflammatory factors.

The strength of this meta-analysis is that it included RCTs that provided the strongest level of evidence and had methodologically reliable quality. Additionally, TSA was performed for the first time in evaluating the effect of statins on CRP and hs-CRP levels and it indicated that pooled evidence concerning hs-CRP was not sufficient and that more studies are required to find a clear answer to the question about the effects of statins on hs-CRP. However, TSA results suggested that the pooled result was reliable based on the currently available data. One of the advantages of this meta-analysis was also sufficient number of studies included.

Despite our best attempt to implement a flawless systematic review and meta-analysis on the effect of statins on serum levels of hs-CRP and CRP in patients with CVDs, several limitations and caveats are still present. The first is the omission of unpublished trials with negative outcomes which is a common problem of all meta-analyses. The second problem is that heterogeneity was detected across most of our analyses. From statistical perspective, this heterogeneity describes the variability between included studies and may originate from clinical or methodological heterogeneity, from other unreported, unknown study characteristics, or may be due to chance. Therefore, to find any sources of heterogeneity and

attenuate their effects, we performed a subgroup analysis and weighted meta-regression. The results of meta-regression showed that neither the treatment duration nor dosage of statins or publication year of studies was the expected source of heterogeneity. Furthermore, the other way of dealing with statistical heterogeneity, which we used in our analysis, was to incorporate a random-effects model which typically produces more conservative estimates of the significance (a wider confidence interval) since it gives proportionately higher weights to smaller studies and lower weights to larger studies than fixed effect analysis. Third, the major limitation of this study was that no data on the effects of statins on the clinical outcomes in patients with different CVDs were analyzed.

Statins have non-lipid-lowering pleiotropic effects including anti-inflammatory, reducing the levels of free fatty acids, IL-6, and PAI-1 and improving adipokine status [86–94]. Therefore, more studies exploring these effects on CVDs should be performed. The clinical outcomes of non-lipid-lowering pleiotropic effects of statins should be more thoroughly analyzed in future studies.

5. Conclusion

It could be concluded that this meta-analysis showed that statins can be effective in reducing CRP and hs-CRP levels in patients with CVDs, particularly those with ACS, CAD, stable atherosclerotic plaques, unstable angina, and MI. The meta-analysis showed that the current level of data for evaluating the effects of statins on CRP is almost sufficient, but further studies are required in order to clearly prove the beneficial effect of statins on hs-CRP level in patients with CVDs. Finally, although statistical analysis showed robust findings because of some limitations of the study these data should be interpreted with caution.

Conflicts of Interest

ZR has received honoraria from Sanofi-Aventis; MK has received honoraria (for lectures and consultancy) from Abbott and Menarini and research funding from Amryt Pharma, Amgen, and Sanofi and has participated in clinical trials with Amgen, Medicines Company, Regeneron, and Sanofi within the last 2 years. All other authors have nothing to disclose.

References

[1] Q. Zhou and J. K. Liao, "Statins and cardiovascular diseases: from cholesterol lowering to pleiotropy," *Current Pharmaceutical Design*, vol. 15, no. 5, pp. 467–478, 2009.

[2] K. Kotseva, D. Wood, D. de Bacquer et al., "EUROASPIRE IV: a European Society of Cardiology survey on the lifestyle, risk factor and therapeutic management of coronary patients from 24 European countries," *European Journal of Preventive Cardiology*, vol. 23, no. 6, pp. 636–648, 2016.

[3] M. Ruscica, N. Ferri, R. D. Santos, C. R. Sirtori, and A. Corsini, "Lipid lowering drugs: present status and future developments," *Current Atherosclerosis Reports*, vol. 23, no. 5, p. 17, 2021.

[4] N. S. Nurmohamed, A. M. Navar, and J. J. P. Kastelein, "New and emerging therapies for reduction of LDL-cholesterol and apolipoprotein B:," *Journal of the American College of Cardiology*, vol. 77, no. 12, pp. 1564–1575, 2021.

[5] A. Sahebkar and G. F. Watts, "New therapies targeting apoB metabolism for high-risk patients with inherited dyslipidaemias: what can the clinician expect?," *Cardiovascular Drugs and Therapy*, vol. 27, no. 6, pp. 559–567, 2013.

[6] A. Sahebkar and G. F. Watts, "New LDL-cholesterol lowering therapies: pharmacology, clinical trials, and relevance to acute coronary syndromes," *Clinical Therapeutics*, vol. 35, no. 8, pp. 1082–1098, 2013.

[7] U. Rauch, J. I. Osende, J. H. Chesebro et al., "Statins and cardiovascular diseases: the multiple effects of lipid-lowering therapy by statins," *Atherosclerosis*, vol. 153, no. 1, pp. 181–189, 2000.

[8] R. Ross, "Atherosclerosis—an inflammatory disease," *The New England journal of medicine*, vol. 340, no. 2, pp. 115–126, 1999.

[9] K. Node, M. Fujita, M. Kitakaze, M. Hori, and J. K. Liao, "Short-term statin therapy improves cardiac function and symptoms in patients with idiopathic dilated cardiomyopathy," *Circulation*, vol. 108, no. 7, pp. 839–843, 2003.

[10] H. Usui, K. Shikata, M. Matsuda et al., "HMG-CoA reductase inhibitor ameliorates diabetic nephropathy by its pleiotropic effects in rats," *Nephrology, Dialysis, Transplantation*, vol. 18, no. 2, pp. 265–272, 2003.

[11] U. Laufs, M. Endres, N. Stagliano et al., "Neuroprotection mediated by changes in the endothelial actin cytoskeleton," *The Journal of Clinical Investigation*, vol. 106, no. 1, pp. 15–24, 2000.

[12] B. P. Leung, N. Sattar, A. Crilly et al., "A novel anti-inflammatory role for simvastatin in inflammatory arthritis," *Journal of Immunology*, vol. 170, no. 3, pp. 1524–1530, 2003.

[13] D. Pruefer, J. Makowski, M. Schnell et al., "Simvastatin inhibits inflammatory properties of Staphylococcus aureus alpha-toxin," *Circulation*, vol. 106, no. 16, pp. 2104–2110, 2002.

[14] B. Agarwal, S. Bhendwal, B. Halmos, S. F. Moss, W. G. Ramey, and P. R. Holt, "Lovastatin augments apoptosis induced by chemotherapeutic agents in colon cancer cells," *Clinical Cancer Research*, vol. 5, no. 8, pp. 2223–2229, 1999.

[15] Ž. Reiner, M. Hatamipour, M. Banach et al., "Statins and the COVID-19 main protease: in silico evidence on direct interaction," *Archives of Medical Science*, vol. 16, no. 3, pp. 490–496, 2020.

[16] A. Vahedian-Azimi, S. M. Mohammadi, F. Beni et al., "Improved COVID-19 ICU admission and mortality outcomes following treatment with statins: a systematic review and meta-analysis," *Archives of Medical Science*, vol. 17, no. 3, pp. 579–595, 2021.

[17] D. C. Bauer, G. R. Mundy, S. A. Jamal et al., "Use of statins and fracture," *Archives of internal medicine*, vol. 164, no. 2, pp. 146–152, 2004.

[18] R. Klein, B. E. Klein, S. C. Tomany, L. G. Danforth, and K. J. Cruickshanks, "Relation of statin use to the 5-year incidence and progression of age-related maculopathy," *Archives of Ophthalmology*, vol. 121, no. 8, pp. 1151–1155, 2003.

[19] K. Almuti, R. Rimawi, D. Spevack, and R. J. Ostfeld, "Effects of statins beyond lipid lowering: potential for clinical benefits,"

International Journal of Cardiology, vol. 109, no. 1, pp. 7–15, 2006.

[20] C. G. Mihos, A. M. Pineda, and O. Santana, "Cardiovascular effects of statins, beyond lipid-lowering properties," *Pharmacological Research*, vol. 88, pp. 12–19, 2014.

[21] A. M. Gorabi, N. Kiaie, S. Aslani, T. Sathyapalan, T. Jamialahmadi, and A. Sahebkar, "Implications on the therapeutic potential of statins via modulation of autophagy," *Oxidative medicine and cellular longevity*, vol. 2021, Article ID 9599608, 10 pages, 2021.

[22] J. Salazar, M. S. Martínez, M. Chávez et al., "C-reactive protein: clinical and epidemiological perspectives," *Cardiology Research and Practice*, vol. 2014, Article ID 605810, 10 pages, 2014.

[23] M. Mohajeri, P. T. Kovanen, V. Bianconi, M. Pirro, A. F. Cicero, and A. Sahebkar, "Mast cell tryptase - marker and maker of cardiovascular diseases," *Pharmacology & therapeutics*, vol. 199, pp. 91–110, 2019.

[24] P. Libby, "Inflammation and cardiovascular disease mechanisms," *The American Journal of Clinical Nutrition*, vol. 83, no. 2, pp. 456S–460S, 2006.

[25] W. Koenig, "High-sensitivity C-reactive protein and atherosclerotic disease: from improved risk prediction to risk-guided therapy," *International Journal of Cardiology*, vol. 168, no. 6, pp. 5126–5134, 2013.

[26] S. Devaraj, J. M. Yun, G. Adamson, J. Galvez, and I. Jialal, "C-reactive protein impairs the endothelial glycocalyx resulting in endothelial dysfunction," *Cardiovascular Research*, vol. 84, no. 3, pp. 479–484, 2009.

[27] C. M. Ferrario and W. B. Strawn, "Role of the renin-angiotensin-aldosterone system and proinflammatory mediators in cardiovascular disease," *The American Journal of Cardiology*, vol. 98, no. 1, pp. 121–128, 2006.

[28] I. Montero, J. Orbe, N. Varo et al., "C-reactive protein induces matrix metalloproteinase-1 and -10 in human endothelial cells: implications for clinical and subclinical atherosclerosis," *Journal of the American College of Cardiology*, vol. 47, no. 7, pp. 1369–1378, 2006.

[29] R. V. Jimenez and A. J. Szalai, "Therapeutic Lowering of C-Reactive Protein," *Frontiers in Immunology*, vol. 11, p. 619564, 2021.

[30] A. M. Gorabi, S. Aslani, D. Imani, B. Razi, T. Sathyapalan, and A. Sahebkar, "*Effect of resveratrol on C-reactive protein: An updated meta-analysis of randomized controlled trials*," *Phytotherapy research: PTR*, vol. 35, no. 12, pp. 6754–6767, 2021.

[31] J. C. Arévalo-Lorido, "Clinical relevance for lowering C-reactive protein with statins," *Annals of Medicine*, vol. 48, no. 7, pp. 516–524, 2016.

[32] N. Shakour, M. Ruscica, F. Hadizadeh et al., "Statins and C-reactive protein: in silico evidence on direct interaction," *Archives of Medical Science*, vol. 16, no. 6, pp. 1432–1439, 2020.

[33] P. M. Ridker, N. Rifai, M. A. Pfeffer et al., "Inflammation, pravastatin, and the risk of coronary events after myocardial infarction in patients with average cholesterol levels. Cholesterol and Recurrent Events (CARE) investigators," *Circulation*, vol. 98, no. 9, pp. 839–844, 1998.

[34] P. M. Ridker, C. P. Cannon, D. Morrow et al., "C-reactive protein levels and outcomes after statin therapy," *The New England Journal of Medicine*, vol. 352, no. 1, pp. 20–28, 2005.

[35] D. A. Morrow, J. A. de Lemos, M. S. Sabatine et al., "Clinical relevance of C-reactive protein during follow-up of patients with acute coronary syndromes in the Aggrastat-to-Zocor trial," *Circulation*, vol. 114, no. 4, pp. 281–288, 2006.

[36] P. M. Ridker, E. Danielson, F. A. Fonseca et al., "Rosuvastatin to prevent vascular events in men and women with elevated C-reactive protein," *The New England Journal of Medicine*, vol. 359, no. 21, pp. 2195–2207, 2008.

[37] P. M. Ridker, N. Rifai, M. A. Pfeffer, F. Sacks, and E. Braunwald, "Long-term effects of pravastatin on plasma concentration of C-reactive protein. The Cholesterol and Recurrent Events (CARE) investigators," *Circulation*, vol. 100, no. 3, pp. 230–235, 1999.

[38] A. Link, T. Ayadhi, M. Bohm, and G. Nickenig, "Rapid immunomodulation by rosuvastatin in patients with acute coronary syndrome," *European Heart Journal*, vol. 27, no. 24, pp. 2945–2955, 2006.

[39] M. J. Page, M. K. JE, P. M. Bossuyt et al., "The PRISMA 2021 statement: an updated guideline for reporting systematic reviews," *BMJ*, vol. 372, 2021.

[40] A. R. Jadad, R. A. Moore, D. Carroll et al., "Assessing the quality of reports of randomized clinical trials: is blinding necessary?," *Controlled Clinical Trials*, vol. 17, no. 1, pp. 1–12, 1996.

[41] R. DerSimonian and N. Laird, "Meta-analysis in clinical trials," *Controlled Clinical Trials*, vol. 7, no. 3, pp. 177–188, 1986.

[42] J. P. Higgins and S. G. Thompson, "Quantifying heterogeneity in a meta-analysis," *Statistics in Medicine*, vol. 21, no. 11, pp. 1539–1558, 2002.

[43] C. B. Begg and M. Mazumdar, "Operating characteristics of a rank correlation test for publication bias," *Biometrics*, vol. 50, no. 4, pp. 1088–1101, 1994.

[44] M. Egger, G. Davey Smith, M. Schneider, and C. Minder, "Bias in meta-analysis detected by a simple, graphical test," *BMJ*, vol. 315, no. 7109, pp. 629–634, 1997.

[45] S. M. Grundy, N. J. Stone, A. L. Bailey et al., "2018 AHA/ACC/AACVPR/AAPA/ABC/ACPM/ADA/AGS/APhA/ASPC/NLA/PCNA guideline on the management of blood cholesterol: a report of the American College of Cardiology/American Heart Association Task Force on Clinical Practice Guidelines," *Circulation*, vol. 73, no. 24, pp. e285–e350, 2019.

[46] E. Climent, D. Benaiges, and J. Pedro-Botet, "Hydrophilic or lipophilic statins?," *Frontiers in Cardiovascular Medicine*, vol. 8, article 687585, 2021.

[47] R. R. Azar, G. Badaoui, A. Sarkis et al., "Effects of _tirofiban_ and statins on high-sensitivity C-reactive protein, interleukin-6, and soluble CD40 ligand following percutaneous coronary interventions in patients with stable coronary artery disease," *The American Journal of Cardiology*, vol. 95, no. 2, pp. 236–240, 2005.

[48] K. H. Yun, M. H. Jeong, S. K. Oh et al., "The beneficial effect of high loading dose of rosuvastatin before percutaneous coronary intervention in patients with acute coronary syndrome," *International journal of cardiology*, vol. 137, no. 3, pp. 246–251, 2009.

[49] Y. Luo, D. Jiang, D. Wen, J. Yang, and L. Li, "Changes in serum interleukin-6 and high-sensitivity C-reactive protein levels in patients with acute coronary syndrome and their responses to simvastatin," *Heart and vessels*, vol. 19, no. 6, pp. 257–262, 2004.

[50] J. Yang, X. P. Li, S. P. Zhao, J. Li, J. D. Li, and X. M. Xie, "The effect of different doses of fluvastatin on inflammatory

markers in the early phase of acute coronary syndrome," *Clinica Chimica Acta*, vol. 368, no. 1-2, pp. 183–187, 2006.

[51] K. C. Chan, H. H. Chou, C. N. Huang, and M. C. Chou, "Atorvastatin administration after percutaneous coronary intervention in patients with coronary artery disease and normal lipid profiles: impact on plasma adiponectin level," *Clinical Cardiology*, vol. 31, no. 6, pp. 253–258, 2008.

[52] T. Suzuki, T. Nozawa, M. Sobajima et al., "Atorvastatin-induced changes in plasma coenzyme q10 and brain natriuretic peptide in patients with coronary artery disease," *International Heart Journal*, vol. 49, no. 4, pp. 423–433, 2008.

[53] T. Dohi, K. Miyauchi, S. Okazaki et al., "Early intensive statin treatment for six months improves long-term clinical outcomes in patients with acute coronary syndrome (extended-ESTABLISH trial): a follow-up study," *Atherosclerosis*, vol. 210, no. 2, pp. 497–502, 2010.

[54] L. Qiao, S. Wang, Q. Jia, J. Bian, Y. Fan, and X. Xu, "Clinical efficacy and safety of statin treatment after carotid artery stenting," *Artificial cells, nanomedicine, and biotechnology*, vol. 47, no. 1, pp. 3110–3115, 2019.

[55] K. H. Yun, I. S. Shin, S. N. Shin et al., "Effect of previous statin therapy in patients with acute coronary syndrome and percutaneous coronary intervention," *Korean Circulation Journal*, vol. 41, no. 8, pp. 458–463, 2011.

[56] S. Guo, R. Wang, Z. Yang, K. Li, and Q. Wang, "Effects of atorvastatin on serum lipids, serum inflammation and plaque morphology in patients with stable atherosclerotic plaques," *Experimental and Therapeutic Medicine*, vol. 4, no. 6, pp. 1069–1074, 2012.

[57] Y. Jiao, F. Hu, Z. Zhang et al., "Efficacy and safety of loading-dose rosuvastatin therapy in elderly patients with acute coronary syndromes undergoing elective percutaneous coronary intervention," *Clinical Drug Investigation*, vol. 35, no. 12, pp. 777–784, 2015.

[58] E. Abulhul, K. McDonald, R. Martos et al., "Long-term statin therapy in patients with systolic heart failure and normal cholesterol: effects on elevated serum markers of collagen turnover, inflammation, and B-type natriuretic peptide," *Clinical Therapeutics*, vol. 34, no. 1, pp. 91–100, 2012.

[59] P. Marschang, G. J. Friedrich, H. Ditlbacher et al., "Reduction of soluble P-selectin by statins is inversely correlated with the progression of coronary artery disease," *International journal of cardiology*, vol. 106, no. 2, pp. 183–190, 2006.

[60] E. Vasilieva, O. Kasyanova, and A. Shpektor, "The antiplatelet effect of atorvastatin in patients with acute coronary syndrome depends on the hs-CRP level," *Acute Cardiac Care*, vol. 10, no. 3, pp. 181–184, 2008.

[61] J. J. C. McMurray, "Effects of statin therapy according to plasma high-sensitivity C-reactive protein concentration in the Controlled Rosuvastatin Multinational Trial in Heart Failure (CORONA): a retrospective analysis," *Circulation*, vol. 2010, article e461, pp. 77–80, 2010.

[62] S. Sola, M. Q. Mir, S. Lerakis, N. Tandon, and B. V. Khan, "Atorvastatin improves left ventricular systolic function and serum markers of inflammation in nonischemic heart failure," *Journal of the American College of Cardiology*, vol. 47, no. 2, pp. 332–337, 2006.

[63] Y. C. Doo, S. J. Han, S. W. Han et al., "Effect of preexisting statin use on expression of C-reactive protein, adhesion molecules, interleukin-6, and antioxidized low-density lipoprotein antibody in patients with unstable angina undergoing coronary stenting," *Clinical cardiology*, vol. 28, no. 2, pp. 72–76, 2005.

[64] J. J. Li and C. H. Fang, "Effects of 4 weeks of atorvastatin administration on the antiinflammatory cytokine interleukin-10 in patients with unstable angina," *Clinical Chemistry*, vol. 51, no. 9, pp. 1735–1738, 2005.

[65] J.-J. Li, Y. Wang, S.-P. Nie et al., "Reduction of C-reactive protein by a single 80 mg of simvastatin in patients with unstable angina," *Clinica chimica acta*, vol. 376, no. 1-2, pp. 163–167, 2007.

[66] A. Nakagomi, Y. Seino, K. Kohashi et al., "Effects of statin therapy on the production of monocyte pro-inflammatory cytokines, cardiac function, and long-term prognosis in chronic heart failure patients with dyslipidemia," *Circulation Journal*, vol. 76, no. 9, pp. 2130–2138, 2012.

[67] M. K. Lewandowski, Z. Kornacewicz-Jach, B. Millo et al., "The influence of low dose atorvastatin on inflammatory marker levels in patients with acute coronary syndrome and its potential clinical value," *Cardiology Journal*, vol. 15, no. 4, pp. 357–364, 2008.

[68] G. Patti, V. Pasceri, G. Colonna et al., "Atorvastatin pretreatment improves outcomes in patients with acute coronary syndromes undergoing early percutaneous coronary intervention: results of the ARMYDA-ACS randomized trial," *Journal of the American College of Cardiology*, vol. 49, no. 12, pp. 1272–1278, 2007.

[69] P. Ostadal, D. Alan, P. Hajek et al., "The effect of early treatment by cerivastatin on the serum level of C-reactive protein, interleukin-6, and interleukin-8 in the patients with unstable angina and non-Q-wave myocardial infarction," *Molecular and Cellular Biochemistry*, vol. 246, no. 1-2, pp. 45–50, 2003.

[70] O. Gruzdeva, E. Uchasova, Y. Dyleva, O. Akbasheva, V. Karetnikova, and O. Barbarash, "Early effects of treatment low-dose atorvastatin on markers of insulin resistance and inflammation in patients with myocardial infarction," *Frontiers in Pharmacology*, vol. 7, p. 324, 2016.

[71] I. Karaca, E. ilkay, M. Akbulut et al., "Atorvastatin affects C-reactive protein levels in patients with coronary artery disease," *Current Medical Research and Opinion*, vol. 19, no. 3, pp. 187–191, 2003.

[72] I. D. Strazhesko, O. N. Tkacheva, D. U. Akasheva et al., "Atorvastatin therapy modulates telomerase activity in patients free of atherosclerotic cardiovascular diseases," *Frontiers in Pharmacology*, vol. 7, p. 347, 2016.

[73] S. M. Macin, E. R. Perna, E. F. Farías et al., "Atorvastatin has an important acute anti-inflammatory effect in patients with acute coronary syndrome: results of a randomized, double-blind, placebo- controlled study," *American heart journal*, vol. 149, no. 3, pp. 451–457, 2005.

[74] S. Kinlay, G. G. Schwartz, A. G. Olsson et al., "High-dose atorvastatin enhances the decline in inflammatory markers in patients with acute coronary syndromes in the MIRACL study," *Circulation*, vol. 108, no. 13, pp. 1560–1566, 2003.

[75] L. C. Correia, A. C. Spósito, J. C. Lima et al., "Anti-inflammatory effect of _atorvastatin_ (80 mg) in unstable angina pectoris and non -Q-wave acute myocardial infarction," *The American journal of cardiology*, vol. 92, no. 3, pp. 298–301, 2003.

[76] A. F. G. Cicero, F. Fogacci, and A. Zambon, "Red yeast rice for hypercholesterolemia:," *Journal of the American College of Cardiology*, vol. 77, no. 5, pp. 620–628, 2021.

[77] A. F. G. Cicero, F. Fogacci, A. V. Hernandez, and M. Banach, "Efficacy and safety of bempedoic acid for the treatment of hypercholesterolemia: a systematic review and meta-analysis," *PLoS Medicine*, vol. 17, no. 7, article e1003121, 2020.

[78] J. Jia, L. Zhang, L. Wang, C. Ji, R. Xia, and Y. Yang, "A systematic review and meta-analysis on the efficacy of statins in the treatment of atherosclerosis," *Annals of Palliative Medicine*, vol. 10, no. 6, pp. 6793–6803, 2021.

[79] E. M. Balk, J. Lau, L. C. Goudas et al., "Effects of statins on non-lipid serum markers associated with cardiovascular disease: a systematic review," *Annals of Internal Medicine*, vol. 139, no. 8, pp. 670–682, 2003.

[80] M. J. Lipinski, C. A. Cauthen, G. G. Biondi-Zoccai et al., "Meta-analysis of randomized controlled trials of statins versus placebo in patients with heart failure," *The American Journal of Cardiology*, vol. 104, no. 12, pp. 1708–1716, 2009.

[81] R. Jauhiainen, M. Jauhiainen, J. Vangipurapu et al., "Novel biomarkers associated with incident heart failure in 10 106 Finnish men," *ESC Heart Fail*, vol. 8, no. 1, pp. 605–614, 2021.

[82] J. An, F. Shi, S. Liu, J. Ma, and Q. Ma, "Preoperative statins as modifiers of cardiac and inflammatory outcomes following coronary artery bypass graft surgery: a meta-analysis," *Interactive cardiovascular and thoracic surgery*, vol. 25, no. 6, pp. 958–965, 2017.

[83] M. C. Kim, Y. Ahn, S. Y. Jang et al., "Comparison of clinical outcomes of hydrophilic and lipophilic statins in patients with acute myocardial infarction," *The Korean Journal of Internal Medicine*, vol. 26, no. 3, pp. 294–303, 2011.

[84] R. Kones, "Primary prevention of coronary heart disease: integration of new data, evolving views, revised goals, and role of rosuvastatin in management. A comprehensive survey," *Drug Design, Development and Therapy*, vol. 5, pp. 325–380, 2011.

[85] P. Libby, M. Nahrendorf, M. J. Pittet, and F. K. J. C. Swirski, "Diversity of denizens of the atherosclerotic plaque: not all monocytes are created equal," *Circulation*, vol. 117, no. 25, pp. 3168–3170, 2008.

[86] P. Chruściel, A. Sahebkar, M. Rembek-Wieliczko et al., "Impact of statin therapy on plasma adiponectin concentrations: a systematic review and meta-analysis of 43 randomized controlled trial arms," *Atherosclerosis*, vol. 253, pp. 194–208, 2016.

[87] G. Ferretti, T. Bacchetti, and A. Sahebkar, "Effect of statin therapy on paraoxonase-1 status: a systematic review and meta-analysis of 25 clinical trials," *Progress in Lipid Research*, vol. 60, pp. 50–73, 2015.

[88] S. M. Parizadeh, M. R. Azarpazhooh, M. Moohebati et al., "Simvastatin therapy reduces prooxidant-antioxidant balance: results of a placebo-controlled cross-over trial," *Lipids*, vol. 46, no. 4, pp. 333–340, 2011.

[89] A. Sahebkar, K. Kotani, C. Serban et al., "Statin therapy reduces plasma endothelin-1 concentrations: a meta-analysis of 15 randomized controlled trials," *Atherosclerosis*, vol. 241, no. 2, pp. 433–442, 2015.

[90] A. Sahebkar, C. Serban, D. P. Mikhailidis et al., "Association between statin use and plasma D-dimer levels. A systematic review and meta-analysis of randomised controlled trials," *Thrombosis and Haemostasis*, vol. 114, no. 3, pp. 546–557, 2015.

[91] A. Sahebkar, C. Serban, S. Ursoniu et al., "The impact of statin therapy on plasma levels of von Willebrand factor antigen. Systematic review and meta-analysis of randomised placebo-controlled trials," *Thrombosis and Haemostasis*, vol. 115, no. 3, pp. 520–532, 2016.

[92] M. Khalifeh, P. E. Penson, M. Banach, and A. Sahebkar, "Statins as anti-pyroptotic agents," *Archives of Medical Science*, vol. 17, no. 5, pp. 1414–1417, 2021.

[93] A. Bahrami, S. Bo, T. Jamialahmadi, and A. Sahebkar, "Effects of 3-hydroxy-3-methylglutaryl coenzyme A reductase inhibitors on ageing: molecular mechanisms," *Ageing Research Reviews*, vol. 58, article 101024, 2020.

[94] A. M. Gorabi, N. Kiaie, M. Pirro, V. Bianconi, T. Jamialahmadi, and A. Sahebkar, "Effects of statins on the biological features of mesenchymal stem cells and therapeutic implications," *Heart Failure Reviews*, vol. 26, no. 5, pp. 1259–1272, 2021.

Hindawi
Mediators of Inflammation
Volume 2021, Article ID 6609143, 13 pages
https://doi.org/10.1155/2021/6609143

Review Article

Particulate Matter-Induced Acute Coronary Syndrome: MicroRNAs as Microregulators for Inflammatory Factors

Nur Izah Ab Razak,[1] **Nor Eliani Ezani**,[2] **and Norzian Ismail**[3]

[1]*Department of Human Anatomy, Faculty of Medicine and Health Sciences, Universiti Putra Malaysia, 43400 Serdang, Malaysia*
[2]*Department of Environmental and Occupational Health, Faculty of Medicine and Health Sciences, Universiti Putra Malaysia, 43400 Serdang, Malaysia*
[3]*Department of Medicine, Faculty of Medicine and Health Sciences, Universiti Putra Malaysia, 43400 Serdang, Malaysia*

Correspondence should be addressed to Nur Izah Ab Razak; nurizah@upm.edu.my

Received 27 June 2021; Accepted 18 November 2021; Published 11 December 2021

Academic Editor: Azizah Ugusman

The most prevalent cause of mortality and morbidity worldwide is acute coronary syndrome (ACS) and its consequences. Exposure to particulate matter (PM) from air pollution has been shown to impair both. Various plausible pathogenic mechanisms have been identified, including microRNAs (miRNAs), an epigenetic regulator for gene expression. Endogenous miRNAs, average 22-nucleotide RNAs (ribonucleic acid), regulate gene expression through mRNA cleavage or translation repression and can influence proinflammatory gene expression posttranscriptionally. However, little is known about miRNA responses to fine PM ($PM_{2.5}$, PM_{10}, ultrafine particles, black carbon, and polycyclic aromatic hydrocarbon) from air pollution and their potential contribution to cardiovascular consequences, including systemic inflammation regulation. For the past decades, microRNAs (miRNAs) have emerged as novel, prospective diagnostic and prognostic biomarkers in various illnesses, including ACS. We wanted to outline some of the most important studies in the field and address the possible utility of miRNAs in regulating particulate matter-induced ACS (PMIA) on inflammatory factors in this review.

1. Introduction

Air pollution has been considered a major public health threat and has caused about seven million deaths every year, according to the World Health Organization (WHO) [1]. The complex mixture of air pollutants arises from particulate matter (PM), chemical substances, and biological materials which are emitted from a natural process (volcano, oceans, forest, etc.) or anthropogenic activities (industry or transportation) [2]. With the increasing demands of global energy, the generation of the combustion of fossil fuels, including coal, diesel fuel, gasoline, and natural gas for electricity, heating, industry, and transportation, is also increased [3]. This has resulted in the higher release of air pollutants whereby air pollution was a major burden to an individual, especially to those living in the growing economic countries [4]. Of these, it is greatly important to address air pollution issues where reducing air pollution will meet the Sustainable Development Goals (SDG) proposed by the United Nation (UN) in SDG 3, for good health and well-being [5]. Increased PM from air pollution contributes to the occurrence of acute coronary syndrome (ACS) in several studies [6]. MicroRNAs (miRNAs), a short noncoding RNA, have been observed in few studies to be dysregulated in inflammatory modulation in cardiovascular disorder exposed to PM [7–9]. The aim of this review is to look at the potential role of miRNAs in the regulation of inflammatory factors in particulate matter-induced ACS (PMIA).

The references of this narrative review paper were searched through PubMed and Google Scholar. The keywords used were particulate matter, air pollution, acute coronary syndrome, miRNA, and inflammation.

1.1. Common Air Pollutants. There is growing awareness of health outcomes related to air pollution from short- and long-term exposure to air pollutants. Many studies have reported the adverse health effects linked with heart diseases from these exposures [10–13]. This showed how crucial the air pollutants' role is in cardiovascular events and outcomes. PM can be differentiated by ranging size of aerodynamic diameter (AD) from 2.5 to 10 μm (including $PM_{2.5}$ and PM_{10}) and chemical composition (including black carbon, polycyclic aromatic hydrocarbon, and trace metals). Organic aerosol is mainly the result of anthropogenic emissions such as vehicle emissions, residential fuel combustion, and wildfires, representing a large proportion of PM. It is estimated that 180,000 (117,000 to 389,000) premature deaths were prevented from reducing anthropogenic organic aerosol between 1990 and 2012 [14]. Table 1 shows the summary of the sources of $PM_{2.5}$, PM_{10}, ultrafine particle (UFP, AD less than 0.1 μm), black carbon (BC), and polycyclic aromatic hydrocarbons (PAHs). According to a study conducted in a medium-sized Dutch city, UFP and BC concentrations in transportation zones more than doubled between 8 a.m. and 10 a.m. compared to those recorded at an urban background location [15]. In $PM_{2.5}$ containing the ultrafine fraction, PAH concentrations were 12-fold higher than $M_{2.5\text{-}0.3}$, which may be explained by combustion processes that produce ultrafine particles containing high concentrations of PAHs [16, 17]. Among the most significant ultrafine particle (UFP) sources in urbanised areas are diesel combustion and solid biomass combustion [18]. Biomarkers associated with inflammation (*CCXL2*, *EPGN*, *GREM1*, *IL-1α*, *IL-1β*, *IL-6*, *IL-24*, *EREG*, and *VEGF*) and transcription factors (NFE2L2, MAFF, HES1, FOSL1, and TGIF1) relevant for cardiovascular and lung disease are secreted in response to diesel UFP exposure [19]. According to one in vitro study, $PM_{2.5}$ increased gene alteration, DNA damage, cytotoxicity, and reactive oxygen species (ROS) in the A549 cell line, most likely due to CYP enzyme activation in response to polycyclic aromatic hydrocarbons (PAHs) adsorbed to the particle surface [20].

Air pollution is also composed of gaseous pollutants including nitrogen dioxide (NO_2), ozone (O_3), sulphur dioxide (SO_2), volatile organic compounds (VOCs), and carbon monoxide (CO). However, these gaseous pollutants except for NO_2 [21, 22] are not widely reported about their acute or chronic effect relationship with cardiovascular health compared to particulate matters (PM). Ambient NO_2 is known as a good proxy for traffic-related air pollution alongside the presence of particulate pollutants such as $PM_{2.5}$ and PM_{10} [23]. NO_2 is part of reactive gas of nitrogen oxides (NO*x*) and produced from combustion processes such as traffic emissions and power plant in the outdoor environment, whereas NO_2 is generated from unvented heaters and gas stoves in the indoor environment [24]. O_3 forms from a photochemical reaction between sunlight with the presence of its precursors such as NO_2 and VOCs which derived it as a secondary gaseous pollutant. Study from ninety largest cities in the United States by the National Morbidity, Mortality, and Air Pollution Study (NMMAPS) observed that cardiopulmonary-related mortality rose by the increment of PM_{10} within a 24-hour period [25]. In another study, daily concentration of PM_{10} was significantly having an impact on ACS incidence, higher on elderly with the highest impact on older men [6]. Moreover, increase in PM_{10} pollution was noted to have relation to rise in frequency of percutaneous coronary interventions (PCIs) in ACS patients [26].

1.2. ACS. Cardiovascular disease (CVD) is one of the main causes of mortality and morbidity [27]. One of the important causes of mortality and morbidity related to CVD is acute coronary syndrome (ACS). The estimated incidence of ACS is 141 per 100,000 population per year, and the inpatient mortality rate is approximately 7% [28, 29]. The figures are similar to many developed countries. ACS is a syndrome due to decreased blood flow in the coronary arteries that leads to ischaemia, reduction in heart function, and myocardium cell death [30]. The most common symptom is chest pain, often radiating to the left shoulder or angle of the jaw (crushing, central) and associated with nausea and sweating [31]. ACS is commonly associated with three clinical manifestations, named according to the appearance of the electrocardiogram (ECG): ST elevation myocardial infarction (STEMI, 30%), non-ST elevation myocardial infarction (NSTEMI, 25%), or unstable angina (38%) [32, 33].

ACS occurs due to atherosclerotic plaque (atheroma) rupture, fissure, or ulceration with superimposed thrombosis and coronary vasospasm. Depending on the acuteness, the degree of occlusion, and the presence of collaterals, patients can present as having UA (unstable angina), NSTEMI, or STEMI. In those who have ACS, atheroma rupture is the most found compared to atheroma erosion [34], thus causing the formation of thrombus which blocks the coronary arteries. The diagnosis of ACS requires at least two of the following: ischemic symptoms, diagnostic ECG changes, and serum cardiac marker elevation [35]. ACS often reflects a degree of damage to the coronaries by atherosclerosis. Primary prevention of atherosclerosis is controlling the risk factors: healthy eating, exercise, treatment for hypertension and diabetes, avoiding smoking, and controlling cholesterol levels [36]. The management in ACS includes medication such as antiplatelet, betablocker, ACE inhibitor, lipid lowering agent, anticoagulant, thrombolytic treatment, and invasive percutaneous coronary intervention [37]. Hazard from the exposure to particulate matters has shown to have strong association with ACS that leads to severe detrimental effects on the cardiovascular system through numerous mechanisms including increased inflammation response, oxidative stress, endothelial injury, cell apoptosis, and mitochondrial dysfunction [38]. A study reported that significant 18% increase in the risk of STEMI was linked to each 7.1 g/m^3 rise in $PM_{2.5}$ concentration before the onset of ACS [39]. MicroRNAs have been shown to contribute as biomarkers in ACS [40]. One study showed, in plasma of myocardial infarction patients, the cardiac myocyte-associated miRNAs, and miR-208b and miR-499 were significantly elevated. Both miRNAs were positively correlated with plasma troponin T, indicating that the release of both was from injured cardiomyocytes [41]. The studies may suggest that miRNAs and PM regulate the cellular pathophysiology of ACS.

Table 1: Summary of particulate matter (PM) and its composition sources.

Particulate matter (PM)	Main source of emission	Reference
$PM_{2.5}$	Traffic emissions (brake and vehicle exhaust) Industrial emissions released from power plant and oil refinery Secondary organic and inorganic aerosol	[11] ([104]; [105]; [14])
PM_{10}	Road dust and tire wear Construction activities Wildfires and windblown dust	([106]; [107])
Ultrafine particles (UFP)	Tailpipe emissions from vehicle exhaust, diesel combustion, and solid biomass burning	([106]; [11]; [18]; [108]; [88])
Black carbon (BC)	Combustion process (vehicle exhaust emissions and cookstoves)	([109]; [106])
Polycyclic aromatic hydrocarbons (PAHs)	Incomplete combustion of fossil fuels, natural combustion (forest fires and volcanic eruption), anthropogenic cause (wood, coal burning, vehicle exhaust emissions, heat and power generation)	([110]; [16]; [111]; [17])

1.3. miRNAs. miRNAs are estimated to regulate more than 60% of human protein-coding genes at the translational level [42]. These single-stranded nucleotides are the noncoding RNAs, binding to the 3′untranslated region (3′UTR), 5′ untranslated region (5′UTR), protein-coding sequence, or gene promoters that lead to degradation or repression of the mRNAs at the posttranscriptional level [43]. miRNAs are involved in various physiological processes including cell cycle, cell proliferation, and apoptosis [43]. Some of the miRNAs are reported in pathological dysregulation including cancer [44], diabetes mellitus [45], and hypertension [46]. In cardiovascular disorder, miRNAs were linked to various pathological events including ACS [40, 47, 48].

In recent years, there is substantial interest on epigenetic regulatory mechanisms at the cellular level and their association with air pollution including miRNAs [49–51]. miRNA, as one of the main epigenetic regulators, has been proposed to modulate the cellular event affected in those who were exposed to PM [7, 8, 52, 53]. The studies suggested that there are changes in miRNA expression in people that are exposed to particulate matter (PM) in air pollution. On top of that, these miRNAs are shown to have association with the genes involved in cardiovascular morbidity [8, 54, 55].

2. miRNA Profiles of Air Pollution in ACS

2.1. miRNAs and PM. $PM_{2.5}$ exposure from few hours to several weeks can stimulate morbidity and mortality due to cardiovascular disease. In contrast, reductions in PM levels are associated with declines in cardiovascular mortality [56].

A randomised crossover study was designed towards 55 healthy young adults, comparing reduced or ambient levels of indoor $PM_{2.5}$ for 2-week duration; expression of miRNA, mRNA, and protein of 10 serum cytokines was measured. Further analysis showed that higher $PM_{2.5}$ exposure was negatively associated with miR-1-3p, miR-146a-5p, miR-187-3p, miR-199a-5p, and miR-21-5p [7].

In another study, the exposure length was limited to 24 hours. Strong evidence of high expression of let-7d-5p, miR-24-3p, miR-425-5p, miR-4454, miR-4763-3p, miR-502-5p, and miR-505-3p was found after exposure to $PM_{2.5}$ [52].

Turning now to the experimental evidence on myocardial toxicity involvement, Feng et al. reported that $PM_{2.5}$ could contribute to toxicity via miR-205, by negatively regulating the IRAK2/TRAF6/NF-κB signalling pathway [55].

Furthermore, exposure to ambient $PM_{2.5}$ revealed increase level of miR-223-3p expressed in the extracellular vesicle from serum samples [57]. miR-223 was shown to be involved in endovascular inflammation and platelet activation. This serum-derived miRNAs in circulation were identified as cardiovascular mortality predictors in coronary artery disease (CAD) [58].

Li et al. reported that let-7a, miR-146a-5p, and miR-155-5p were highly expressed in respondents exposed to the elevated level of PM exposure and decreased level of interleukin-6 (IL-6) and toll-like receptor 2 (TLR2) mRNAs [9]. However, this study did not specify the type of PM and their specific changes in miRNA and mRNA expression. The experiment utilised benzo[a]pyrene-r-7,t-8,t-9,c-10-tetrahydotetrol-albumin (BPDE-Alb) adducts in serum as the internal exposure biomarker of PM in general.

Similar to the previous experiment, $PM_{2.5}$ exposure upregulated miR-146a, miR-155, and other miRNAs (miR-146b, miR-139, miR-129, miR-340, miR-691, miR-181a, miR-21-3p, and miR-21-5p), and the experiment was set up through intratracheal installation of $PM_{2.5}$ in mice. Furthermore, interleukin-4 (IL-4) was decreased. In contrast, interferon gamma (IFN-γ) was increased, and the IL-4/IFN-γ ratio was inclined to Th1 shifting. This study concluded that the acute exposure to $PM_{2.5}$ increased the mentioned miRNAs and correlates with T lymphocyte immune imbalance that stimulates Th1-biased immune response [59].

2.2. miRNAs and UFP (Ultrafine Particle). UFP is the ultrasmall and lightweight particle that has been reported to be one of occupational inhalation risks. UFP sizes range from 0.0001 to 0.1 μm [60]. The accumulation of UFP to the lung and various organs could lead to various morbidities including thrombosis, ischaemia, and cardiovascular disease [61, 62]. Acute exposure to UFP in vivo demonstrated increase in inflammation parameters and nitrate stress level, such as serum IL-6, monocyte chemoattractant protein 1 (MCP-1),

Table 2: Summary of particulate matter (PM) and related miRNAs.

Particulate matter (PM)	miRNAs	Reference
$PM_{2.5}$	miR-129, miR-139, miR-146a, miR-146b, miR-155, miR-340, miR-691, miR-181a, miR-21-3p, and miR-21-5p	[59]
	miR-1-3p, miR-146a-5p, miR-187-3p, miR-199a-5p, and miR-21-5p	[7]
	let-7d-5p, miR-24-3p, miR-425-5p, miR-4454, miR-4763-3p, miR-502-5p, and miR-505-3p	[52]
	miR-205	[55]
	miR-223-3p	[57]
PM (general)	let-7a, miR-146a-5p, and miR-155-5p	[9]
Ultrafine particle (UFP)	miR-222	[64]
	let-7a, let-7b, let-7d, let-7e, miRNA-16, miR-155, miR-24, miR-27, and miRNA-34	[60]
	miR-301b-3p and let-7c-1-3p	[63]
Black carbon (BC)	miR-135b, miR-146b, and miR-21	[67]
Polycyclic aromatic hydrocarbons (PAHs)	miR-181a, miR-181b, and miR-181d	[75]
	miR-24-3p, miR-27a-3p, miR-142-5p, and miR-28-5p and miR-150-5p	[74]
	miR-155	[8]

p47phox (known as NCF1 (neutrophil cytosolic factor 1)), and 3-NT (nitration marker). Furthermore, both of the in vivo and in vitro studies revealed upregulations of miR-301b-3p and let-7c-1-3p with the downstream targets, SMAD2, SMAD3, and transforming growth factor $\beta 1$ (TGF$\beta 1$), indicating higher risk of atherosclerosis following UFP exposure [63]. Another study reported that exposure to UFP among school children was positively associated with increased miR-222 from saliva samples [64]. miR-222 was shown to protect pathological cardiac remodelling and necessary for exercise-induced cardiomyocyte growth and proliferation [65]. It was reported that exposure to UFP for 72 hours significantly downregulates let-7a, let-7b, let-7d, let-7e, miRNA-16, and miRNA-34 with 10-fold upregulation of miR-24 and 6-fold increase in miR-27 and miR-155 expression, respectively [60].

2.3. miRNAs and BC (Black Carbon). The mortality and morbidity related to a BC-related cardiovascular event are reported to be stronger than those due to $PM_{2.5}$ [66]. High concentration of BC was observed to have relation with increased major adverse cardiovascular events in ACS patients [66]. Exposure to BC nanoparticles leads to marked increase in miR-135b and subtle changes in miR-21 and miR-146b, with RT-PCR validation [67]. miR-135b has been shown to stimulate apoptosis and inflammation, reduce cell proliferation, and inhibit macrophage function. Moreover, miR-135b inhibition was reported to increase atherosclerotic plaque development [68]. miR-21 showed increased plaque stability in ACS [69]. This miRNA also showed to have significant elevation in stable and unstable angina and as compared to control subject thus may play an important role for a new biomarker for this disease along with a strong correlation with aging [70]. Exogenous miR-21 was reported to drastically inhibit cardiomyocyte and endothelial cell apoptosis thus leading to significant improvement of cardiac function [71]. The expression of miR-146b was demonstrated to be downregulated in a myocardial infarction model in vivo as compared to the control group, whereas the in vitro experiment showed that the downregulation of miR-146b led to increased inflammatory factors and apoptosis of the vascular cells and was suggested to be associated with the PI3K/Akt/NF-κB pathway [72]. In contrast to earlier findings, however, no evidence of miRNA changes was detected through black carbon exposure through intratracheal instillation in C57BL/6 mice (Julie A [73]).

2.4. miRNA and PAHs (Polycyclic Aromatic Hydrocarbons). miR-155 expression was upregulated in human umbilical cord vein cells (HUVECs) exposed to PAH treatment. The putative gene target for miR-155 was shown to be linked to Wingless/Integrated (Wnt) and epidermal growth factor (ErbB) signalling which is important for vasculature development, thus proposing involvement of miRNA for a novel target for cardiovascular-related therapy [8]. In one study, exposure to PAHs showed significant increase in lower expression of miR-24-3p, miR-27a-3p, miR-142-5p, and miR-28-5p, through analysis of urinary 4-hydroxyphenanthrene and/or plasma BPDE-Alb. On the other hand, urinary 1-hydroxynaphthalene, 2-hydroxynaphthalene, 2-hydroxyphenanthrene, and the sum of monohydroxy-PAHs were associated with high level of miR-150-5p expression [74]. In PAH-induced hepatocarcinogenesis, miR-181a, miR-181b, and miR-181d were significantly upregulated through p38 MAPK activation [75]. The summary of specific particulate matter and related miRNAs is shown in Table 2.

3. PM Exposure and Cardiac Inflammatory Mediators

PM exposure is known to exacerbate inflammatory response through mRNA mediation [63, 76, 77], some of it through miRNA modulation [7–9]. The summary of particulate matter (PM) and related cardiac inflammatory mediators is

Table 3: Summary of particulate matter (PM) and related cardiac inflammatory mediators.

Particulate matter (PM)	Cardiac inflammatory mediators	Effect	Reference
$PM_{2.5}$	IL-1β, IL-8, IL-12, TNF-α, CRP, COX	Decrease cell viability and increase inflammatory mediators	[79]
	TNF-α	Increase inflammation and blood coagulation markers	[80]
	CD4+, CD8+, CD14+ and CD16+, IL-6, IL-1β, MCP-1, MIP-1α/β, TNF-α	Increased endothelial cell apoptosis, proinflammatory cytokines, and antiangiogenic activity contribute to pathogenic atherogenesis and acute coronary events	[82]
	TRAF6, NF-κB	Increased reactive oxygen species (ROS), increased cardiomyocyte apoptosis, stimulated inflammatory cell infiltration, and enhanced inflammatory factors in AC16 cells and heart tissue	[55]
	EDN1, F3, IL-1, IL-6, TNF, TLR2	Involved in systemic inflammation, coagulation, and vasoconstriction	[7]
Smaller PM size	IL-1β, IL-6, TNF-α	Increase inflammation marker	[81]
PM_{10}	CD14 and TLR4	Inverse association of DNA methylation of inflammatory genes in overweight and obese patients	[78]
	TNF-α	Increase inflammation and blood coagulation markers	[80]
Ultrafine particle	3-NT, CCXL2, EPGN, EREG, FOSL1, GREM1, HES1, IL-1α, IL-1β, IL-6, IL-24, NFE2L2, MAFF, MCP-1, p47phox, TGIF1, VEGF	Biological dysregulation in atherosclerosis, increase inflammation	[19]; [63])
Black carbon (BC)	F3, ICAM-1	Inflammation and thrombosis	[76]
Polycyclic aromatic hydrocarbons (PAHs)	IL-1β, IL-6, IL-10, TNF-α, IFN-γ, and hs-CRP	Inflammation and atherogenesis	[77]

shown in Table 3. In one experiment, exposure to daily PM_{10} of overweight and obese patients showed an inverse association of DNA methylation of inflammatory genes, in particular cluster of differentiation antigen 14 (CD14) and toll-like receptor 4 (TLR4), but not in tumour necrosis factor-α (TNF-α) [78]. Through in vitro study, $PM_{2.5}$ was shown to decrease cell viability and increased the expression of NF-kB1 family gene mRNA and inflammatory mediators including C-reactive protein (CRP), cyclooxygenase-2 (COX-$_2$), interleukin-1β (IL-1β), interleukin-8 (IL-8), interleukin-12 (IL-12), and TNF-α (J. [79]). In a meta-analysis finding, short-term exposure to $PM_{2.5}$ and PM_{10} had a significant association with inflammation and blood coagulation markers, TNF-α, and fibrinogen; however, the long-term exposure to both $PM_{2.5}$ and PM_{10} was not significant [80]. In another study, it was reported that the smaller the size of the PM, the more significant the association of PM exposure to inflammation markers, for example, IL-1β, IL-6, and TNF-α [81]. Exposure to $PM_{2.5}$ was also associated with increased level of proinflammatory cytokines MCP-1, macrophage inflammatory protein 1α/β (MIP-1α/β), IL-6, and IL-1β and increased level of inflammatory response, for example, CD4+, CD8+, CD14+, and CD16+ [82]. MCP-1 acts through the CCR2 receptor and is increased by chronic inflammatory condition which stimulates the adherence of monocytes to the subendothelial region of the atherogenic arterial wall [83]. This finding is supported by a Mendelian randomisation study, indicating the linkage of MCP-1 to an increased risk of coronary artery disease (CAD), myocardial infarction (MI), and ischemic stroke [84]. In several atherosclerotic studies, the inhibition of the CCR2 receptor reduced inflammatory monocyte recruitment, reduced neointimal hyperplasia, and reduced the size of atherosclerotic plaque [85–87]. One study among healthy nonsmokers exposed to ambient $PM_{2.5}$ for 24 hours demonstrated significant increase in proinflammatory cytokines (IL-6 and IL-1β) and antiangiogenic agent (TNF-α) that may contribute to endothelial dysfunction, inflammation, and platelet activation. $PM_{2.5}$ induced reactive oxygen species (ROS), increased cardiomyocyte apoptosis, stimulated inflammatory cell infiltration, and enhanced the inflammatory factors in AC16 cells and heart tissue [55]. The regulation is through $PM_{2.5}$-induced downregulation of miR-205 activating the TNF receptor-associated factor 6 (TRAF6)/nuclear transcription factor-B (NF-κB) signalling pathway, which further activated the signalling network. In the higher PM2.5 exposure, the result showed a positive association with IL-1, IL-6, and TNF [7].

Exposure to UFPs was reported to have a significant link to cardiovascular disease, such as atherosclerosis (AS) [63].

Table 4: Target inflammatory genes and miRNAs.

Target inflammatory genes	miRNAs	Related cell/organ/disease	Author
CD14	miR-199a-3p, miR-199a-5p, and miR-21-5p	RAW264.7 macrophage cell line, lipopolysaccharide-(LPS-) induced proinflammatory cytokine release, and LPS-induced septic shock	[91]
EDN1 (putative target of miRNA	miR-199	Liver sinusoidal endothelial cells (rLSEC) derived from ethanol-fed rats	[94]
IL-1β	miR-448	Autoimmune diseases	[95]
IL-6	miR-181c	INS-1 cells	[96]
IL-6	miR-410	Lupus nephritis, systemic lupus erythematosus (SLE) in kidney tissue of MRL/lpr mice	[97]
MCP-1	miR-124a	Synoviocytes from rheumatoid arthritis	[98]
TLR2	miR-146a	BLP-stimulated human THP-1 promonocytic cells, innate immune response to infection	[99]
TLR2	miR-105	Primary human keratinocytes, challenge with *Porphyromonas gingivalis* (a Gram-negative bacterium that triggers TLR-2 and TLR-4)	[100]
TLR2	miR19a/b	Rheumatoid fibroblast-like synoviocytes, rheumatoid arthritis (RA)	[101]
TNF-α	miR-181a-5p	Dendritic cells	[102]

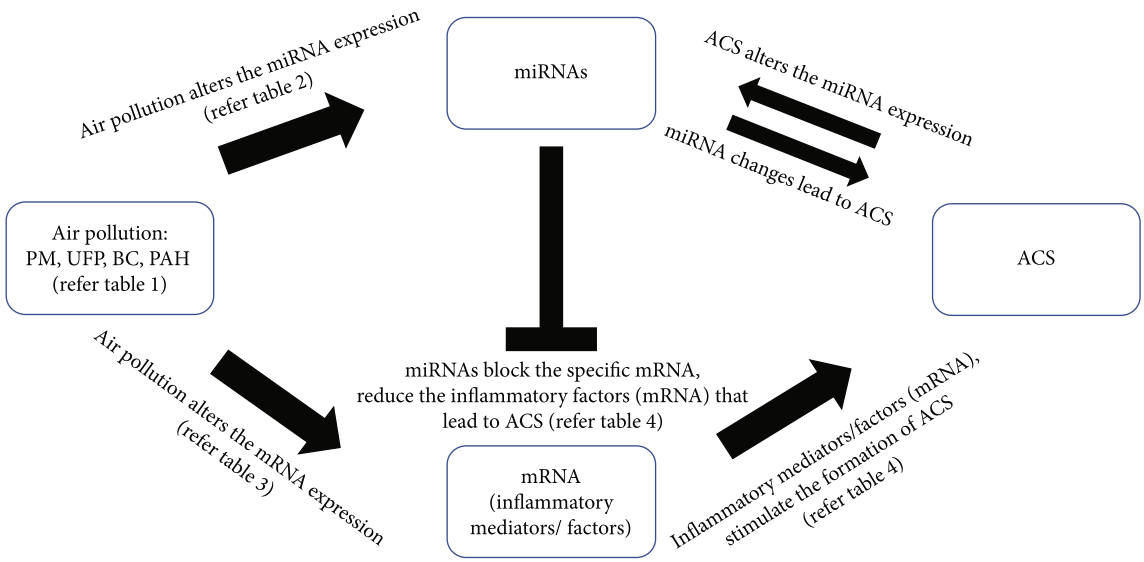

Figure 1: The summary of the mode of action of PMIA through miRNA-mRNA regulation. ACS = acute coronary syndrome; BC = black carbon; miRNA = microRNA; mRNA = messenger RNA; PAH = polycyclic aromatic hydrocarbon; PM = particulate matter; PMIA = particulate matter-induced ACS; UFP = ultrafine particle.

Mice were given an acute dose of UFPs for six days, after which they were sacrificed few days later. Postacute exposure revealed increased inflammation responses and nitrate stress, with elevated IL-6, MCP-1, p47phox, and 3-NT levels in the mouse serum compared to the untreated control. In an in vitro study, exposure to diesel UFP increased the levels of IL-6 and vascular endothelial growth factor (VEGF) in lung epithelial cells, whereas treatment of endothelial cells with diesel UFP media increased the levels of vascular cell adhesion protein 1 (VCAM-1) and intercellular adhesion molecule 1 (ICAM-1) in endothelial cells [88].

Black carbon (BC) is a traffic-related particle that is formed as a combustion by-product and has been linked to several cardiovascular adverse events, stronger than the effect of fine $PM_{2.5}$ [89]. However, this study contrasts with that of Bourdon et al.'s finding few years before who stated that intrathecal instillation of carbon black nanoparticles had no effect on cardiac gene expression [73]. This finding was supported by Dominguez-Rodriguez et al. who argue that the major adverse cardiovascular events (MACE) were detected in other PM exposure, except BC [90]. Nevertheless, BC exposure was linked to methylation of genes

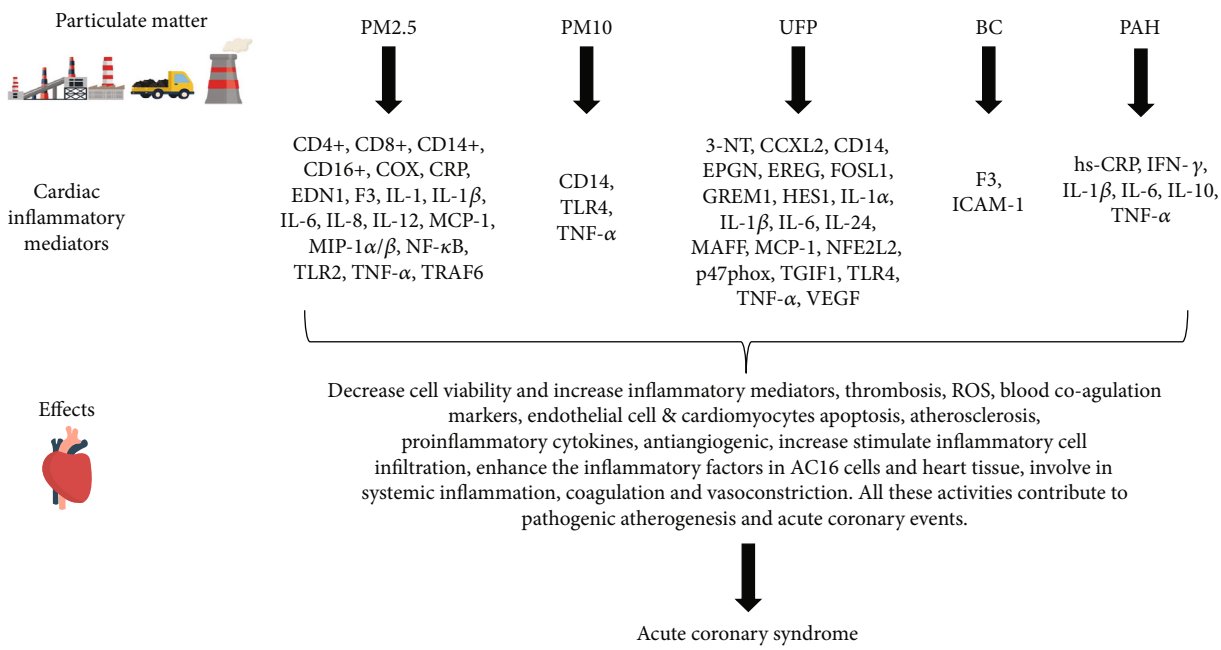

Figure 2: The mode of action of PM in inducing ACS. The PM stimulates the production cardiac inflammatory mediators that might lead to ACS. 3-NT = nitration marker; ACS = acute coronary syndrome; CCXL2 = chemokine genes; CD14 = differentiation antigen 14; CD14 + = cluster of differentiation 14 (monocyte differentiation antigen); CD16+ = cluster of differentiation 16 (monocyte differentiation antigen); CD4+ = cluster of differentiation 4 (monocyte differentiation antigen); CD8+ = cluster of differentiation 8 (monocyte differentiation antigen); COX = cyclooxygenase; CRP = C-reactive protein; EDN1 = endothelin 1 (protein-coding gene); EPGN = epithelial mitogen (protein-coding gene); EREG = epiregulin (protein-coding gene); F3 = coagulation factor III, tissue factor (protein-coding gene); FOSL1 = FOS like 1, AP-1 transcription factor subunit (protein-coding gene); GREM1 = gremlin 1, DAN family BMP antagonist (protein-coding gene); HES1 = Hes family BHLH transcription factor 1 (protein-coding gene); hs-CRP = high-sensitivity C-reactive protein; ICAM-1 = intercellular adhesion molecule 1; IFN-γ = interferon gamma; IL-1 = interleukin-1; IL-10 = interleukin-10; IL-12 = interleukin-12; IL-1α = interleukin-1α; IL-1β = interleukin-1β; IL-24 = interleukin-24; IL-6 = interleukin-6; IL-8 = interleukin-8; MAFF = MAF BZIP transcription factor F (protein-coding gene); MCP-1 = monocyte chemoattractant protein 1; MIP-1α/β = macrophage inflammatory protein-1 alpha/beta; NFE2L2 = nuclear factor erythroid 2-like 2 (protein-coding gene); NF-κB = nuclear factor kappa B; p47phox = neutrophil cytosolic factor 1 protein, encoded by NCF1; PM = particulate matter; TGIF1 = TG-interacting factor 1; TLR2 = toll-like receptor 2; TLR4 = toll-like receptor 4; TLR4 = toll-like receptor 4; TNF-α = tumour necrosis factor-α; TRAF6 = TNF receptor-associated factor 6; VEGF = vascular endothelial growth factor.

implicated in inflammation and endothelial function, through decreased coagulation factor III (*F3*) and ICAM-1 methylation [76].

1-Hydroxypyrene (1-OHP) is a biomarker for traffic-related air pollution exposure to polycyclic aromatic hydrocarbons (PAHs). In one study, urinary 1-OHP levels were higher in taxi drivers than in nonoccupationally exposed people, and it was linked to proinflammatory cytokines, for example, IL-1β, IL-6, IL-10, TNF-α, IFN-γ, and hs-CRP [77]. These higher inflammatory biomarkers were linked to the key indicators of cardiovascular morbidity.

4. miRNAs and PM-Induced Inflammation Mediators

Even though study on PM-induced cardiac inflammation mediators is limited, other experiments were performed utilising the similar genes or mediators in other system rather than focusing on the cardiovascular system. Regardless, these mediators are similar and involved in many parts of the ACS cellular pathological mechanism. For example, CD14 gene silencing was reported to significantly change the expression of 199a-3p, miR-199a-5p, and miR-21-5p in the RAW264.7 macrophage cell line [91]. Endothelin-1 (ET-1) is a peptide encoded by the ET-1 gene (EDN1). Endothelin-1 (ET-1) is a 21-amino acid polypeptide that is mainly generated by endothelial cells of the vascular system and has been shown to participate in a variety of biological processes, including inflammation, fibrosis, proliferation of vascular smooth muscle, and cardiovascular hypertrophy [92]. ET-1 is a potent vasoconstrictor in cardiac, renal, and nervous system vasculature and known to be attenuated by miRNA regulation [93]. In one study, overexpression of miR-199 inhibited ethanol-induced EDN1, and on the other hand, inhibiting miR-199 levels led to increase in ET-1 protein with the presence of ethanol [94]. IL-1 is a cumulative IL-1α and IL-1β and a potent inducer of inflammatory protein, and miR-448 reportedly enhanced the production of proinflammatory cytokine including IL-1β [95]. IL-6 is a proapoptotic and proinflammatory cytokine, secreted by inflammatory cells in response to inflammation. In IL-6-treated cells, miR-181c was significantly downregulated as

compared to control cells [96]. Other study found that miR-410 targets the 3′untranslated region (3′UTR) of IL-6; thus, increase in miR-410 reduces the IL-6 levels [97]. miR-124a is reported to bind at the 3′UTR of MCP-1 mRNA, and the upregulation of this miRNA supressed the MCP-1 protein levels [98]. Toll-like receptor 2 (TLR2) plays an important role in the activation of innate immunity, activation of the macrophage, and promotion of apoptosis. Some study reported that miR-146a [99] and miR-105 [100] downregulated the expression of TLR2. On the other hand, miR19a/b upregulated the TLR2 expression, and the increased expression of miR-19a/b by mimics significantly reduced TLR2 protein and inhibited the TLR2-triggered cytokine and kinase activities [101]. TNF-α is a proinflammatory cytokine. Luciferase reporters confirm the in silico algorithms of miR-181a-5p target 3′UTR of TNF-α, in which the miR-181a-5p mimic suppressed the TNF-α levels and the miR-181a-5p inhibitor increased its level [102]. The summary of inflammatory genes and related miRNAs is shown in Table 4.

5. Discussion and Conclusion

miRNAs bind to a specific sequence in the 3′UTR, 5′UTR, and coding sequence of their target mRNAs, resulting in translational repression, mRNA deadenylation, and decapping of the target mRNAs, respectively [103]. Therefore, we may take various viewpoints on PM exposure to miRNA and mRNA involved in inflammation and ACS (Figure 1). Firstly, this paper might suggest that PM could deter the level of mRNA involved in cardiac inflammation (Figure 2). For example, $PM_{2.5}$ was reported to increase TNF-α, CD14+, and TLR2. These mRNAs and others (Table 3) might have a significant potential role for future applications in ACS screening and biomarkers. Secondly, we would suggest specific miRNA that could be used as therapeutic tools to treat ACS. We identify several studies indicating significant miRNA functions to downregulate several inflammatory factors, such as miR-146a-5p, miR-181a, miR-199a-5p, and miR-21-5p, which target TRL2, TNF-α, and CD14, respectively (Table 4). An increase in the stated miRNAs could downregulate the genes involved in cardiac inflammation and grant future experiments and validation. Therefore, a common pathway in PMIA regulated by the miRNAs could be investigated in the future.

The findings presented here have established that PMIA has a major impact on miRNAs and vice versa. For prevention and management of ACS, PM and other hazardous substances from air pollution should be considered significant modifiable risk factors. Policymakers should strengthen the effort to reduce air pollution exposure through suitable and effective legislation significantly. The use of miRNA and mRNA in novel clinical settings offers promising potentials. Currently, multiple clinical trials are exploring miRNA profiles in various illness conditions for prognostic or diagnostic reasons. Since one miRNA can target several different mRNAs, it is important to be cautious when attributing miRNA effects to a specific mRNA. miRNAs have been well established to play a role in the regulation of inflammatory factors in ACS. However, little is known on how these miRNAs directly contribute to the modulation of PMIA. Further study should be conducted to determine the best techniques for air pollution reduction and to document the effects of these techniques on the incidence of ACS and its relationship to morbidity and mortality. It seems prudent to predict that future research investigating PMIA on miRNAs will adopt more comprehensive technology.

Abbreviations

1-OHP: 1-Hydroxypyrene
3′UTR: 3′untranslated region
3-NT: Nitration marker
5′UTR: 5′untranslated region
ACS: Acute coronary syndrome
AD: Aerodynamic diameter
Akt: Protein kinase B (PKB)
BC: Black carbon
BPDE-Alb: Benzo[a]pyrene-r-7,t-8,t-9,c-10-tetrahydotetrol-albumin
CAD: Coronary artery disease
CCR2: C-C chemokine receptor type 2
CCXL2: Chemokine genes
CD14: Differentiation antigen 14
CD14+: Cluster of differentiation 14 (monocyte differentiation antigen)
CD16+: Cluster of differentiation 16 (monocyte differentiation antigen)
CD4+: Cluster of differentiation 4 (monocyte differentiation antigen)
CD8+: Cluster of differentiation 8 (monocyte differentiation antigen)
CO: Carbon monoxide
COX: Cyclooxygenase
COX-2: Cyclooxygenase-2
CRP: C-reactive protein
CVD: Cardiovascular disease
CYP: Cytochrome P450
DNA: Deoxyribonucleic acid
ECG: Electrocardiogram
EDN1: Endothelin 1 (protein-coding gene)
EPGN: Epithelial mitogen (protein-coding gene)
ErbB: Epidermal growth factor (EGF)
EREG: Epiregulin (protein-coding gene)
ET-1: Endothelin 1
F3: Coagulation factor III, tissue factor (protein-coding gene)
FOSL1: FOS kike 1, AP-1 transcription factor subunit (protein-coding gene)
GREM1: Gremlin 1, DAN family BMP antagonist (protein-coding gene)
HES1: Hes family BHLH transcription factor 1 (protein-coding gene)
hs-CRP: High-sensitivity C-reactive protein
HUVECs: Human umbilical cord vein cells

ICAM-1: Intercellular adhesion molecule 1
IFN-γ: Interferon gamma
IL-1: Interleukin-1
IL-12: Interleukin-12
IL-1α: Interleukin-1α
IL-1β: Interleukin-1β
IL-24: Interleukin-24
IL-4: Interleukin-4
IL-6: Interleukin-6
IL-8: Interleukin-8
IL-10: Interleukin-10
IRAK2: Interleukin-1 receptor-associated kinases
MACE: Major adverse cardiovascular events
MAFF: MAF BZIP transcription factor F (protein-coding gene)
MAPK: Mitogen-activated protein kinase
MCP-1: Monocyte chemoattractant protein 1
MI: Myocardial infarction
MIP-1α: Macrophage inflammatory protein-1 alpha
MIP-1β: Macrophage inflammatory protein-1 beta
miRNAs: MicroRNAs
mRNA: Messenger RNA
NFE2L2: Nuclear factor erythroid 2-like 2 (protein-coding gene)
NF-κB: Nuclear factor kappa B
NMMAPS: National Morbidity, Mortality, and Air Pollution Study
NO_2: Nitrogen dioxide
NOx: Nitrogen oxides
NSTEMI: Non-ST elevation myocardial infarction
O_3: Ozone
p47phox: Neutrophil cytosolic factor 1 (NCF1)
PAHs: Polycyclic aromatic hydrocarbons
PI3K: Phosphatidyl-inositol-3-kinase
PM: Particulate matter
PMIA: Particulate matter-induced ACS
RNA: Ribonucleic acid
ROS: Reactive oxygen species
RT-PCR: Real-time polymerase chain reaction
SDG: Sustainable Development Goals
SMAD2: SMAD family member 2
SMAD3: SMAD family member 3
SO_2: Sulphur dioxide
STEMI: ST elevation myocardial infarction
TGFβ1: Transforming growth factor β1
TGIF1: TG-interacting factor 1
Th1: T helper type 1
TLR2: Toll-like receptor 2
TLR4: Toll-like receptor 4
TNF-α: Tumour necrosis factor-α
TRAF6: TNF receptor-associated factor 6
UA: Unstable angina
UFP: Ultrafine particle
UN: United Nation
VCAM-1: Vascular cell adhesion protein 1
VEGF: Vascular endothelial growth factor
VOCs: Volatile organic compounds
WHO: World Health Organization
Wnt: Wingless/Integrated.

Conflicts of Interest

The authors declared that they have no conflicts of interest.

References

[1] WHO, *7 million premature deaths annually linked to air pollution*, 2014, https://www.who.int/mediacentre/news/releases/2014/air-pollution/en/.

[2] EPA, U, *Greenhouse gas (GHG) emissions*, 2020, https://www.epa.gov/ghgemissions.

[3] C. Pénard-Morand and I. Annesi-Maesano, "Air pollution: from sources of emissions to health effects," *Breathe*, vol. 1, no. 2, pp. 108–119, 2004.

[4] A. J. Cohen, M. Brauer, R. Burnett et al., "Estimates and 25-year trends of the global burden of disease attributable to ambient air pollution: an analysis of data from the Global Burden of Diseases Study 2015," *Lancet*, vol. 389, no. 10082, pp. 1907–1918, 2017.

[5] United Nations, *Sustainable Development Goals*, 2015, https://www.un.org/sustainabledevelopment/health/.

[6] M. Ravljen, T. Hovelja, and D. Vavpotič, "Relationship between particulate matter pollution and acute coronary syndrome incidence," *Atmosphere*, vol. 10, no. 3, p. 103, 2019.

[7] C. Renjie, H. Li, J. Cai et al., "Fine particulate air pollution and the expression of microRNAs and circulating cytokines relevant to inflammation, coagulation, and vasoconstriction," *Environmental Health Perspectives*, vol. 126, no. 1, article 017007, 2018.

[8] X. He, Y. Chen, C. Zhang, W. Gong, X. Zhang, and S. Nie, "Polycyclic aromatic hydrocarbons from particulate matter 2.5 (PM2.5) in polluted air changes miRNA profile related to cardiovascular disease," *Medical Science Monitor*, vol. 24, pp. 5925–5934, 2018.

[9] J. Li, T. Wang, Y. Wang et al., "Particulate matter air pollution and the expression of microRNAs and pro-inflammatory genes: association and mediation among children in Jinan, China," *Journal of Hazardous Materials*, vol. 389, article 121843, 2020.

[10] R. W. Atkinson, I. M. Carey, A. J. Kent, T. P. van Staa, H. R. Anderson, and D. G. Cook, "Long-term exposure to outdoor air pollution and incidence of cardiovascular diseases," *Epidemiology*, vol. 24, no. 1, pp. 44–53, 2013.

[11] Y. Du, X. Xu, M. Chu, Y. Guo, and J. Wang, "Air particulate matter and cardiovascular disease: the epidemiological, biomedical and clinical evidence," *Journal of Thoracic Disease*, vol. 8, no. 1, pp. E8–e19, 2016.

[12] A. Peters, D. W. Dockery, J. E. Muller, and M. A. Mittleman, "Increased particulate air pollution and the triggering of myocardial infarction," *Circulation*, vol. 103, no. 23, pp. 2810–2815, 2001.

[13] C. A. Pope III, R. T. Burnett, M. J. Thun et al., "Lung cancer, cardiopulmonary mortality, and long-term exposure to fine particulate air pollution," *JAMA*, vol. 287, no. 9, pp. 1132–1141, 2002.

[14] D. A. Ridley, C. L. Heald, K. J. Ridley, and J. H. Kroll, "Causes and consequences of decreasing atmospheric organic aerosol in the United States," *Proceedings of the National Academy of Sciences*, vol. 115, no. 2, pp. 290–295, 2018.

[15] M. Zuurbier, G. Hoek, M. Oldenwening et al., "Commuters' exposure to particulate matter air pollution is affected by

mode of transport, fuel type, and route," *Environmental Health Perspectives*, vol. 118, no. 6, pp. 783–789, 2010.

[16] Y. Kawanaka, Y. Tsuchiya, S.-J. Yun, and K. Sakamoto, "Size distributions of polycyclic aromatic hydrocarbons in the atmosphere and estimation of the contribution of ultrafine particles to their lung deposition," *Environmental Science & Technology*, vol. 43, no. 17, pp. 6851–6856, 2009.

[17] Y. Landkocz, F. Ledoux, V. André et al., "Fine and ultrafine atmospheric particulate matter at a multi-influenced urban site: physicochemical characterization, mutagenicity and cytotoxicity," *Environmental Pollution*, vol. 221, pp. 130–140, 2017.

[18] L. Eleonora, G. Maurizio, C. Laura et al., "Physico-chemical properties and biological effects of diesel and biomass particles," *Environmental Pollution*, vol. 215, pp. 366–375, 2016.

[19] A. Grilli, R. Bengalli, E. Longhin et al., "Transcriptional profiling of human bronchial epithelial cell BEAS-2B exposed to diesel and biomass ultrafine particles," *BMC Genomics*, vol. 19, no. 1, p. 302, 2018.

[20] G. Maurizio, L. Eleonora, M. Michela et al., "Gene expression profiling of A549 cells exposed to Milan PM2.5," *Toxicology Letters*, vol. 209, no. 2, pp. 136–145, 2012.

[21] R. W. Atkinson, B. K. Butland, H. R. Anderson, and R. L. Maynard, "Long-term concentrations of nitrogen dioxide and mortality: a meta-analysis of cohort studies," *Epidemiology*, vol. 29, no. 4, pp. 460–472, 2018.

[22] P. Collart, D. Dubourg, A. Levêque, N. B. Sierra, and Y. Coppieters, "Short-term effects of nitrogen dioxide on hospital admissions for cardiovascular disease in Wallonia, Belgium," *International Journal of Cardiology*, vol. 255, pp. 231–236, 2018.

[23] J. R. Brook, R. T. Burnett, T. F. Dann et al., "Further interpretation of the acute effect of nitrogen dioxide observed in Canadian time-series studies," *Journal of Exposure Science & Environmental Epidemiology*, vol. 17, Supplement 2, pp. S36–S44, 2007.

[24] EPA, U, *Nitrogen dioxide (NO2) pollution*, 2016, https://www.epa.gov/no2-pollution/basic-information-about-no2#What%20is%20NO2.

[25] A. M. Francesca Dominici, M. Daniels, S. L. Zeger, and J. M. Samet, *Mortality among residents of 90 cities*, 2003, https://www.researchgate.net/profile/Antonella-Zanobetti/publication/230651495_Mortality_and_morbidity_among_eldery_residents_of_cities_with_daily_PM_measurements/links/00b7d513f5ce2f4197000000/Mortality-and-morbidity-among-eldery-residents-of-cities-with-daily-PM-measurements.pdf#page=19.

[26] R. Januszek, B. Staszczak, Z. Siudak et al., "The relationship between increased air pollution expressed as PM10 concentration and the frequency of percutaneous coronary interventions in patients with acute coronary syndromes—a seasonal differences," *Environmental Science and Pollution Research*, vol. 27, no. 17, pp. 21320–21330, 2020.

[27] MOH, *National Health and Morbidity Survey 2015 (NMRR – 14-1064-21877)*, 2015, https://www.moh.gov.my/moh/resources/nhmsreport2015vol2.pdf.

[28] MOH, *National Cardiovascular Disease Database (NCVD)*, 2015, https://www.malaysianheart.org/files/5d1998d5b6248.pdf.

[29] B. Norsa'adah and C. M. Che-Muzaini, "Association of Comorbidity and treatment with the complications of acute coronary syndrome in young patients less than 45 years," *Malaysian Journal of Medical Sciences*, vol. 25, no. 1, pp. 42–52, 2018.

[30] E. A. Amsterdam, N. K. Wenger, R. G. Brindis et al., "2014 AHA/ACC guideline for the management of patients with non-ST-elevation acute coronary syndromes: a report of the American College of Cardiology/American Heart Association Task Force on Practice Guidelines," *Journal of the American College of Cardiology*, vol. 64, no. 24, pp. e139–e228, 2014.

[31] S. Goodacre, P. Pett, J. Arnold et al., "Clinical diagnosis of acute coronary syndrome in patients with chest pain and a normal or non-diagnostic electrocardiogram," *Emergency Medicine Journal*, vol. 26, no. 12, pp. 866–870, 2009.

[32] E. D. Grech and D. R. Ramsdale, "Acute coronary syndrome: unstable angina and non-ST segment elevation myocardial infarction," *BMJ*, vol. 326, no. 7401, pp. 1259–1261, 2003.

[33] M. Torres and S. Moayedi, "Evaluation of the acutely dyspneic elderly patient," *Clinics in Geriatric Medicine*, vol. 23, no. 2, pp. 307–325, 2007.

[34] J. F. Bentzon, F. Otsuka, R. Virmani, and E. Falk, "Mechanisms of plaque formation and rupture," *Circulation Research*, vol. 114, no. 12, pp. 1852–1866, 2014.

[35] S. A. Achar, S. Kundu, and W. A. Norcross, "Diagnosis of acute coronary syndrome," *American Family Physician*, vol. 72, no. 1, pp. 119–126, 2005, https://www.aafp.org/afp/2005/0701/afp20050701p119.pdf.

[36] D. K. Arnett, R. S. Blumenthal, M. A. Albert et al., "2019 ACC/AHA guideline on the primary prevention of cardiovascular disease: a report of the American College of Cardiology/American Heart Association Task Force on Clinical Practice Guidelines," *Circulation*, vol. 140, no. 11, pp. e596–e646, 2019.

[37] E. Braunwald, E. M. Antman, J. W. Beasley et al., "ACC/AHA guidelines for the management of patients with unstable angina and non–ST-segment elevation myocardial infarction: executive summary and recommendations," *Circulation*, vol. 102, no. 10, pp. 1193–1209, 2000.

[38] X. Meng, Y. Zhang, K.-Q. Yang, Y.-K. Yang, and X.-L. Zhou, "Potential harmful effects of PM2.5 on occurrence and progression of acute coronary syndrome: epidemiology, mechanisms, and prevention measures," *International Journal of Environmental Research and Public Health*, vol. 13, no. 8, p. 748, 2016, https://www.mdpi.com/1660-4601/13/8/748.

[39] B. Gardner, F. Ling, P. K. Hopke et al., "Ambient fine particulate air pollution triggers ST-elevation myocardial infarction, but not non-ST elevation myocardial infarction: a case-crossover study," *Particle and Fibre Toxicology*, vol. 11, no. 1, 2014.

[40] F. Ahlin, J. Arfvidsson, K. G. Vargas, S. Stojkovic, K. Huber, and J. Wojta, "MicroRNAs as circulating biomarkers in acute coronary syndromes: a review," *Vascular Pharmacology*, vol. 81, pp. 15–21, 2016.

[41] M. F. Corsten, R. Dennert, S. Jochems et al., "Circulating microRNA-208b and microRNA-499 reflect myocardial damage in cardiovascular disease," *Circulation. Cardiovascular Genetics*, vol. 3, no. 6, pp. 499–506, 2010.

[42] R. C. Friedman, K. K. Farh, C. B. Burge, and D. P. Bartel, "Most mammalian mRNAs are conserved targets of microRNAs," *Genome Research*, vol. 19, no. 1, pp. 92–105, 2009.

[43] D. P. Bartel, "MicroRNAs: genomics, biogenesis, mechanism, and function," *Cell*, vol. 116, no. 2, pp. 281–297, 2004.

[44] Y. Peng and C. M. Croce, "The role of microRNAs in human cancer," *Signal Transduction and Targeted Therapy*, vol. 1, no. 1, p. 15004, 2016.

[45] J. Feng, W. Xing, and L. Xie, "Regulatory roles of microRNAs in diabetes," *International Journal of Molecular Sciences*, vol. 17, no. 10, p. 1729, 2016.

[46] X. Li, Y. Wei, and Z. Wang, "MicroRNA-21 and hypertension," *Hypertension Research*, vol. 41, no. 9, pp. 649–661, 2018.

[47] J. Y. Barraclough, M. Joan, M. V. Joglekar, A. A. Hardikar, and S. Patel, "MicroRNAs as prognostic markers in acute coronary syndrome patients-a systematic review," *Cell*, vol. 8, no. 12, 2019.

[48] M. Horváth, V. Horváthová, P. Hájek et al., "MicroRNA-331 and microRNA-151-3p as biomarkers in patients with ST-segment elevation myocardial infarction," *Scientific Reports*, vol. 10, no. 1, p. 5845, 2020.

[49] R. Alfano, Z. Herceg, T. S. Nawrot, M. Chadeau-Hyam, A. Ghantous, and M. Plusquin, "The impact of air pollution on our epigenome: how far is the evidence? (a systematic review)," *Curr Environ Health Rep*, vol. 5, no. 4, pp. 544–578, 2018.

[50] M. D. Patsouras and P. G. Vlachoyiannopoulos, "Evidence of epigenetic alterations in thrombosis and coagulation: a systematic review," *Journal of Autoimmunity*, vol. 104, article 102347, 2019.

[51] M. Tsamou, K. Vrijens, N. Madhloum, W. Lefebvre, C. Vanpoucke, and T. S. Nawrot, "Air pollution-induced placental epigenetic alterations in early life: a candidate miRNA approach," *Epigenetics*, vol. 13, no. 2, pp. 135–146, 2018.

[52] F. R. Mancini, J. E. Laine, S. Tarallo et al., "MicroRNA expression profiles and personal monitoring of exposure to particulate matter," *Environmental Pollution*, vol. 263, no. Part B, article 114392, 2020.

[53] Y. Wang and M. Tang, "Integrative analysis of mRNAs, miRNAs and lncRNAs in urban particulate matter SRM 1648a-treated EA.hy926 human endothelial cells," *Chemosphere*, vol. 233, pp. 711–723, 2019.

[54] J. Dai, W. Chen, Y. Lin, S. Wang, X. Guo, and Q. Q. Zhang, "Exposure to concentrated ambient fine particulate matter induces vascular endothelial dysfunction via miR-21," *International Journal of Biological Sciences*, vol. 13, no. 7, pp. 868–877, 2017.

[55] L. Feng, J. Wei, S. Liang, Z. Sun, and J. Duan, "miR-205/IRAK2 signaling pathway is associated with urban airborne PM2.5-induced myocardial toxicity," *Nanotoxicology*, vol. 14, no. 9, pp. 1198–1212, 2020.

[56] R. D. Brook, S. Rajagopalan, C. A. Pope III et al., "Particulate matter air pollution and cardiovascular disease: an update to the scientific statement from the American Heart Association," *Circulation*, vol. 121, no. 21, pp. 2331–2378, 2010.

[57] R. S. Rodosthenous, B. A. Coull, Q. Lu, P. S. Vokonas, J. D. Schwartz, and A. A. Baccarelli, "Ambient particulate matter and microRNAs in extracellular vesicles: a pilot study of older individuals," *Particle and Fibre Toxicology*, vol. 13, no. 1, 2015.

[58] C. Schulte, S. Molz, S. Appelbaum et al., "miRNA-197 and miRNA-223 predict cardiovascular death in a cohort of patients with symptomatic coronary artery disease," *PLoS One*, vol. 10, no. 12, article e0145930, 2015.

[59] T. Hou, J. Liao, C. Zhang, C. Sun, X. Li, and G. Wang, "Elevated expression of miR-146, miR-139 and miR-340 involved in regulating Th1/Th2 balance with acute exposure of fine particulate matter in mice," *International Immunopharmacology*, vol. 54, pp. 68–77, 2018.

[60] B. Arpit, S. Anushi, B. Neha et al., "Exposure to ultrafine particulate matter induces NF-$\kappa\beta$ mediated epigenetic modifications," *Environmental Pollution*, vol. 252, no. Part A, pp. 39–50, 2019.

[61] W. E. Cascio, E. Cozzi, S. Hazarika et al., "Cardiac and Vasular changes in mice after exposure to ultrafine particulate matter," *Inhalation Toxicology*, vol. 19, supplement 1, pp. 67–73, 2007.

[62] G. S. Downward, E. van Nunen, J. Kerckhoffs et al., "Long-term exposure to ultrafine particles and incidence of cardiovascular and cerebrovascular disease in a prospective study of a Dutch cohort," *Environmental Health Perspectives*, vol. 126, no. 12, article 127007, 2018.

[63] K. Li, J. Yan, S. Wang et al., "Acute exposure of atmospheric ultrafine particles induced inflammation response and dysregulated TGFβ/Smads signaling pathway in ApoE−/− mice," *Cardiovascular Toxicology*, vol. 21, no. 5, pp. 410–421, 2021.

[64] A. Vriens, T. S. Nawrot, N. D. Saenen et al., "Recent exposure to ultrafine particles in school children alters miR-222 expression in the extracellular fraction of saliva," *Environmental Health*, vol. 15, no. 1, 2016.

[65] X. Liu, J. Xiao, H. Zhu et al., "miR-222 is necessary for exercise-induced cardiac growth and protects against pathological cardiac remodeling," *Cell Metabolism*, vol. 21, no. 4, pp. 584–595, 2015.

[66] A. Dominguez-Rodriguez, S. Rodríguez, P. Abreu-Gonzalez, P. Avanzas, and R. A. Juarez-Prera, "Black carbon exposure, oxidative stress markers and major adverse cardiovascular events in patients with acute coronary syndromes," *International Journal of Cardiology*, vol. 188, pp. 47–49, 2015.

[67] J. A. Bourdon, A. T. Saber, S. Halappanavar et al., "Carbon black nanoparticle intratracheal installation results in large and sustained changes in the expression of miR-135b in mouse lung," *Environmental and Molecular Mutagenesis*, vol. 53, no. 6, pp. 462–468, 2012.

[68] B. W. Wu, Y. Liu, M. S. Wu et al., "Downregulation of microRNA-135b promotes atherosclerotic plaque stabilization in atherosclerotic mice by upregulating erythropoietin receptor," *IUBMB Life*, vol. 72, no. 2, pp. 198–213, 2020.

[69] W. He, L. Zhu, Y. Huang et al., "The relationship of microRNA-21 and plaque stability in acute coronary syndrome," *Medicine*, vol. 98, no. 47, article e18049, 2019.

[70] M. S. Ali Sheikh, "Diagnostic role of plasma microRNA-21 in stable and unstable angina patients and association with aging," *Cardiology Research and Practice*, vol. 2020, Article ID 9093151, 7 pages, 2020.

[71] Y. Song, C. Zhang, J. Zhang et al., "Localized injection of miRNA-21-enriched extracellular vesicles effectively restores cardiac function after myocardial infarction," *Theranostics*, vol. 9, no. 8, pp. 2346–2360, 2019.

[72] L. Zhao, X. R. Yang, and X. Han, "MicroRNA-146b induces the PI3K/Akt/NF-κB signaling pathway to reduce vascular inflammation and apoptosis in myocardial infarction by targeting PTEN," *Experimental and Therapeutic Medicine*, vol. 17, no. 2, pp. 1171–1181, 2018.

[73] J. A. Bourdon, A. T. Saber, N. R. Jacobsen et al., "Carbon black nanoparticle intratracheal instillation does not alter cardiac gene expression," *Cardiovascular Toxicology*, vol. 13, no. 4, pp. 406–412, 2013.

[74] Q. Deng, S. Huang, X. Zhang et al., "Plasma microRNA expression and micronuclei frequency in workers exposed to polycyclic aromatic hydrocarbons," *Environmental Health Perspectives*, vol. 122, no. 7, pp. 719–725, 2014.

[75] S. Mi-Kyung, P. Yong-Keun, and R. Jae-Chun, "Polycyclic aromatic hydrocarbon (PAH)-mediated upregulation of hepatic microRNA-181 family promotes cancer cell migration by targeting MAPK phosphatase-5, regulating the activation of p38 MAPK," *Toxicology and Applied Pharmacology*, vol. 273, no. 1, pp. 130–139, 2013.

[76] M. A. Bind, J. Lepeule, A. Zanobetti et al., "Air pollution and gene-specific methylation in the Normative Aging Study: association, effect modification, and mediation analysis," *Epigenetics*, vol. 9, no. 3, pp. 448–458, 2014.

[77] N. Brucker, A. M. Moro, M. F. Charão et al., "Biomarkers of occupational exposure to air pollution, inflammation and oxidative damage in taxi drivers," *Science of The Total Environment*, vol. 463-464, pp. 884–893, 2013.

[78] C. Laura, I. Simona, T. Letizia et al., "Particulate matter exposure is associated with inflammatory gene methylation in obese subjects," *Environmental Research*, vol. 152, pp. 478–484, 2017.

[79] J. Zhu, Y. Zhao, Y. Gao et al., "Effects of different components of PM2.5 on the expression levels of NF-κB family gene mRNA and inflammatory molecules in human macrophage," *International Journal of Environmental Research and Public Health*, vol. 16, no. 8, p. 1408, 2019.

[80] H. Tang, Z. Cheng, N. Li et al., "The short- and long-term associations of particulate matter with inflammation and blood coagulation markers: a meta-analysis," *Environmental Pollution*, vol. 267, article 115630, 2020.

[81] R. Chen, Z. Zhao, Q. Sun et al., "Size-fractionated particulate air pollution and circulating biomarkers of inflammation, coagulation, and vasoconstriction in a panel of young adults," *Epidemiology*, vol. 26, no. 3, pp. 328–336, 2015.

[82] C. A. Pope 3rd, A. Bhatnagar, J. P. McCracken, W. Abplanalp, D. J. Conklin, and T. O'Toole, "Exposure to fine particulate air pollution is associated with endothelial injury and systemic inflammation," *Circulation Research*, vol. 119, no. 11, pp. 1204–1214, 2016.

[83] J. Lin, V. Kakkar, and X. Lu, "Impact of MCP-1 in atherosclerosis," *Current Pharmaceutical Design*, vol. 20, no. 28, pp. 4580–4588, 2014.

[84] M. K. Georgakis, D. Gill, K. Rannikmäe et al., "Genetically determined levels of circulating cytokines and risk of stroke," *Circulation*, vol. 139, no. 2, pp. 256–268, 2019.

[85] I. Bot, N. V. Ortiz Zacarías, W. E. de Witte et al., "A novel CCR2 antagonist inhibits atherogenesis in apoE deficient mice by achieving high receptor occupancy," *Scientific Reports*, vol. 7, no. 1, 2017.

[86] C. Combadière, S. Potteaux, M. Rodero et al., "Combined inhibition of CCL2, CX3CR1, and CCR5 abrogates Ly6Chi and Ly6Clo monocytosis and almost abolishes atherosclerosis in hypercholesterolemic mice," *Circulation*, vol. 117, no. 13, pp. 1649–1657, 2008.

[87] E. A. Liehn, A. M. Piccinini, R. R. Koenen et al., "A new monocyte chemotactic protein-1/chemokine CC motif ligand-2 competitor limiting neointima formation and myocardial ischemia/reperfusion injury in mice," *Journal of the American College of Cardiology*, vol. 56, no. 22, pp. 1847–1857, 2010.

[88] B. Rossella, L. Eleonora, M. Sara, C. P. Maria, B. Cristina, and C. Marina, "The role of IL-6 released from pulmonary epithelial cells in diesel UFP- induced endothelial activation," *Environmental Pollution*, vol. 231, Part 2, pp. 1314–1321, 2017.

[89] D. E. Newby, P. M. Mannucci, G. S. Tell et al., "Expert position paper on air pollution and cardiovascular disease," *European Heart Journal*, vol. 36, no. 2, pp. 83–93, 2015.

[90] A. Dominguez-Rodriguez, P. Abreu-Gonzalez, S. Rodríguez, P. Avanzas, and R. A. Juarez-Prera, "Short-term effects of air pollution, markers of endothelial activation, and coagulation to predict major adverse cardiovascular events in patients with acute coronary syndrome: insights from AIRACOS study," *Biomarkers*, vol. 22, no. 5, pp. 389–393, 2017.

[91] L. Du, H. Rong, Y. Cheng et al., "Identification of microRNAs dysregulated in CD14 gene silencing RAW264.7 macrophage cells," *Inflammation*, vol. 37, no. 1, pp. 287–294, 2014.

[92] M. Beghetti, S. M. Black, and J. R. Fineman, "Endothelin-1 in congenital heart disease," *Pediatric Research*, vol. 57, 5 Part 2, pp. 16R–20R, 2005.

[93] M. E. Jacobs, C. S. Wingo, and B. D. Cain, "An emerging role for microRNA in the regulation of endothelin-1," *Frontiers in Physiology*, vol. 4, 2013.

[94] S. Yeligar, H. Tsukamoto, and V. K. Kalra, "Ethanol-induced expression of ET-1 and ET-BR in liver sinusoidal endothelial cells and human endothelial cells involves hypoxia-inducible factor-1alpha and microrNA-199," *Journal of Immunology*, vol. 183, no. 8, pp. 5232–5243, 2009.

[95] V. Salvi, V. Gianello, L. Tiberio, S. Sozzani, and D. Bosisio, "Cytokine targeting by miRNAs in autoimmune diseases," *Frontiers in Immunology*, vol. 10, no. 15, 2019.

[96] Y. S. Oh, G. D. Bae, E. Y. Park, and H. S. Jun, "MicroRNA-181c inhibits Interleukin-6-mediated Beta cell apoptosis by targeting TNF-α expression," *Molecules*, vol. 24, no. 7, p. 1410, 2019.

[97] D. Liu, N. Zhang, J. Zhang, H. Zhao, and X. Wang, "miR-410 suppresses the expression of interleukin-6 as well as renal fibrosis in the pathogenesis of lupus nephritis," *Clinical and Experimental Pharmacology and Physiology*, vol. 43, no. 6, pp. 616–625, 2016.

[98] Y. Nakamachi, S. Kawano, M. Takenokuchi et al., "MicroRNA-124a is a key regulator of proliferation and monocyte chemoattractant protein 1 secretion in fibroblast-like synoviocytes from patients with rheumatoid arthritis," *Arthritis and Rheumatism*, vol. 60, no. 5, pp. 1294–1304, 2009.

[99] E. M. Quinn, J. H. Wang, G. O'Callaghan, and H. P. Redmond, "MicroRNA-146a is upregulated by and negatively regulates TLR2 signaling," *PLoS One*, vol. 8, no. 4, article e62232, 2013.

[100] M. R. Benakanakere, Q. Li, M. A. Eskan et al., "Modulation of TLR2 protein expression by miR-105 in human oral keratinocytes∗," *The Journal of Biological Chemistry*, vol. 284, no. 34, pp. 23107–23115, 2009.

[101] L. Philippe, G. Alsaleh, G. Suffert et al., "TLR2 expression is regulated by microRNA miR-19 in rheumatoid fibroblast-like synoviocytes," *Journal of Immunology*, vol. 188, no. 1, pp. 454–461, 2012.

[102] J. Zhu, F.-L. Wang, H.-B. Wang et al., "TNF-α mRNA is negatively regulated by microRNA-181a-5p in maturation of dendritic cells induced by high mobility group box-1 protein," *Scientific Reports*, vol. 7, no. 1, p. 12239, 2017.

[103] W. Xu, A. San Lucas, Z. Wang, and Y. Liu, "Identifying microRNA targets in different gene regions," *BMC Bioinformatics*, vol. 15, Supplement 7, pp. 1–11, 2014.

[104] S. Decesari, J. Allan, C. Plass-Duelmer et al., "Measurements of the aerosol chemical composition and mixing state in the Po Valley using multiple spectroscopic techniques," *Atmospheric Chemistry and Physics*, vol. 14, no. 22, pp. 12109–12132, 2014.

[105] B. A. Nault, D. S. Jo, B. C. McDonald et al., "Secondary organic aerosols from anthropogenic volatile organic compounds contribute substantially to air pollution mortality," *Atmospheric Chemistry and Physics*, vol. 21, no. 14, pp. 11201–11224, 2021.

[106] F. Costabile, H. Alas, M. Aufderheide et al., "First results of the "Carbonaceous Aerosol in Rome and Environs (CARE)" experiment: beyond current standards for PM10," *Atmosphere*, vol. 8, no. 12, p. 249, 2017.

[107] B. Z. Simkhovich, M. T. Kleinman, and R. A. Kloner, "Air pollution and cardiovascular injury: epidemiology, toxicology, and mechanisms," *Journal of the American College of Cardiology*, vol. 52, no. 9, pp. 719–726, 2008.

[108] A. Nemmar, J. A. Holme, I. Rosas, P. E. Schwarze, and E. Alfaro-Moreno, "Recent advances in particulate matter and nanoparticle toxicology: a review of the in vivo and in vitro studies," *BioMed research international*, vol. 2013, Article ID 279371, 22 pages, 2013.

[109] T. C. Bond, "A technology-based global inventory of black and organic carbon emissions from combustion," *Journal of Geophysical Research*, vol. 109, D14, 2004.

[110] X. Bi, G. Sheng, P. Peng, Y. Chen, Z. Zhang, and J. Fu, "Distribution of particulate- and vapor-phase n -alkanes and polycyclic aromatic hydrocarbons in urban atmosphere of Guangzhou, China," *Atmospheric Environment*, vol. 37, no. 2, pp. 289–298, 2003.

[111] P. Rajput, M. M. Sarin, R. Rengarajan, and D. Singh, "Atmospheric polycyclic aromatic hydrocarbons (PAHs) from post-harvest biomass burning emissions in the Indo-Gangetic Plain: isomer ratios and temporal trends," *Atmospheric Environment*, vol. 45, no. 37, pp. 6732–6740, 2011.

Hindawi
Mediators of Inflammation
Volume 2021, Article ID 7042148, 13 pages
https://doi.org/10.1155/2021/7042148

Research Article

Ataxin-10 Inhibits TNF-α-Induced Endothelial Inflammation via Suppressing Interferon Regulatory Factor-1

Yong Li,[1] Qi Zhang,[2] Na Li,[3] Liting Ding,[2] Jinping Yi,[4] Yue Xiao,[5] Shibiao Chen,[1] and Xuan Huang[2]

[1]*Department of Anesthesiology, The First Affiliated Hospital of Nanchang University, Nanchang, China*
[2]*The National Engineering Research Center for Bioengineering Drugs and the Technologies, Institute of Translational Medicine, Nanchang University, Nanchang, China*
[3]*School of Future Technology, Nanchang University, Nanchang, China*
[4]*Department of Clinical Laboratory, The First Affiliated Hospital of Nanchang University, Nanchang, China*
[5]*First School of Clinical Medicine, Nanchang University, Nanchang, China*

Correspondence should be addressed to Xuan Huang; huangxuan@ncu.edu.cn

Received 29 April 2021; Accepted 1 November 2021; Published 23 November 2021

Academic Editor: AZIZAH UGUSMAN

Endothelial inflammation is a crucial event in the initiation of atherosclerosis. Here, we identify Ataxin-10 protein as a novel negative modulator of endothelial activation by suppressing IRF-1 transcription activity. The protein level of Ataxin-10 is relatively higher in human vascular endothelial cells, which can be significantly suppressed by TNF-α in both HUVECs and HLMECs. Overexpression of Ataxin-10 markedly inhibited the mRNA expressions of VCAM-1 and several cytokines including MCP-1, CXCL-1, CCL-5, and TNF-α; thus, it can also suppress monocyte adhesion to endothelial cells. Accordingly, Ataxin-10 silencing promoted endothelial inflammation. However, Ataxin-10 did not affect the MAPK/NF-κB signaling pathway stimulated by TNF-α in HUVECs. Using the yeast two-hybrid assay, we found that Ataxin-10 can directly bind to interferon regulatory factor-1 (IRF-1). Upon TNF-α stimulation, Ataxin-10 promoted the cytoplasmic localization of IRF-1, which inhibited the transcription of VCAM-1. Moreover, knockdown of IRF-1 can eliminate the effect of Ataxin-10 on the expression of VCAM-1 in HUVECs induced by TNF-α. Taken together, these results indicate that Ataxin-10 inhibits endothelial cell activation and may serve as a promising therapeutic target for some vascular inflammatory-related diseases such as atherosclerosis.

1. Introduction

Atherosclerosis is a chronic inflammatory disease characterized by local accumulation of lipid-rich plaques, which is a predominant cause of cardiovascular disorders [1]. As the pathogenesis of atherosclerosis refers to multifactorial processes, increasing evidences showed that endothelial inflammation played a pivotal role in the occurrence and progression of atherosclerosis [2]. In response to inflammation, endothelial cell (EC) activation increases proinflammatory cytokine secretion and adhesion molecule expression, ultimately resulting in endothelial dysfunction and vascular inflammation [3]. Tumor necrosis factor-α (TNF-α) is a primary pathogenic mediator of EC activation [4] and also a major prototypic proinflammatory cytokine derived from activated monocytes/macrophage [5], which is mainly related to the pathogenesis of atherosclerosis [6]. TNF-α activates multiple cellular signaling pathways, such as the classic NF-κB and MAPK pathway, to induce mRNA expression of cell adhesion molecules, including ICAM-1 (intercellular adhesion molecule 1), VCAM-1 (vascular cell adhesion molecule 1), and E-selectin, which play key roles in the crosstalk between leukocyte and endothelium [7]. Activated ECs recruit monocytes to mediate vascular inflammation, which may result in the development of atherosclerosis [8]. Besides, endothelial interferon regulatory factor 1 (IRF-1) was reported to function in the regulation of TNF-α-mediated signaling, especially VCAM-1 expression modulation [9]. Understanding

Table 1: Sequences of qPCR primers used in this study.

Primer name	Forward sequences (5′-3′)	Reverse sequences (5′-3′)
Ataxin-10	GCGGAACCGGAACTTGGATA	GCCTAAAAACTGCAGGCCAC
VCAM-1	TGTTTGCAGCTTCTCAAGCTTTT	GATGTGGTCCCCTCATTCGT
ICAM-1	AGCTTCGTGTCCTGTATGGC	TTTTCTGGCCACGTCCAGTT
VE-cadherin	ATGAGATCGTGGTGGAAGCG	TGTGTACTTGGTCTGGGTGAAG
TNF-α	TCTCGCACCCCGAGTGA	GGAGCTGCCCCTCAGCTT
MCP1	CAGCCAGATGCAATCAATGCC	TGGAATCCTGAACCCACTTCT
IL-1β	AGAAGTACCTGAGCTCGCCA	CTGGAAGGAGCACTTCATCTGT
IL-6	GGAGACTTGCCTGGTGAA	GCATTTGTGGTTGGGTCA
CXCL1	CTGGCTTAGAACAAAGGGGCT	TAAAGGTAGCCCTTGTTTCCCC
CCL-5	CGTGCCCACATCAAGGAGTA	CTTGACCTGTGGACGACTGC
CCL-7	TTGCTCAGCCAGTTGGGATTA	GCTCTCCAGCCTCTGCTTAG
CXCL-9	GAGTGCAAGGAACCCCAGTAG	AAGGGCTTGGGGCAAATTGT
β-Actin	ACGTTGCTATCCAGGCTGTG	GAGGGCATACCCCTCGTAGA

the regulation of TNF-α signaling in ECs is very important to explore these therapeutic pathways.

Spinocerebellar ataxia type 10 (SCA10) is an autosomal dominant neurologic disorder which is characterized by slowly progressive gait ataxia, nystagmus, dysarthria, epilepsy, and nonmotor symptoms [10]. It is the only known human disease to date caused by ATTCT pentanucleotide repeat expansion in the *ATXN10* gene [11]. The expanded repeats cannot disrupt gene transcription [12] but bind to hnRNP K, which results in PKC δ translocation to the mitochondria and cell apoptosis [13]. However, *ATXN10* knockout mice are embryonic lethal, suggesting that Ataxin-10 protein is indispensable for normal embryonic development.

So far, the biological function of Ataxin-10 protein is largely unknown. Besides two armadillo repeats at C-terminus, Ataxin-10 protein does not contain other functional motifs [14]. Ataxin-10 was reported to localize predominantly in the cytoplasm and can bind to β2 subunit of G-protein to activate the Ras-MAP kinase-Elk-1 cascade [15]. Ataxin-10 was found to be phosphorylated by Plk1 and Aurora B in cytokinesis [16, 17]. Moreover, Ataxin-10 interacted with O-linked β-N-acetylglucosamine transferase (OGT) to enhance intracellular glycosylation activity, indicating that Ataxin-10 might be indispensable for intracellular O-GlcNAcylation level maintenance and homeostasis [18, 19]. Accumulating evidence shows that O-GlcNAcylation is of critical importance in mediating cardiovascular function and disease [20]. Hilgers et al. demonstrated that *O*-GlcNAcylation can inhibit TNF-α-induced vascular inflammation [21]. Therefore, we speculate that Ataxin-10 may regulate TNF-α-induced endothelial inflammation.

Here, we aimed to explore the function of Ataxin-10 protein in TNF-α-stimulated endothelial cell dysfunction. Using the yeast two-hybrid assay, we identified IRF-1 as a novel interactor of Ataxin-10. Furthermore, we found that Ataxin-10 exerted its anti-inflammatory effect via suppressing IRF-1 translocation to the nucleus, which resulted in reduced VCAM-1 expression and monocyte adherent. This study demonstrates a new role for Ataxin-10 in the modulation of inflammation and endothelial functions.

2. Materials and Methods

2.1. Reagents. Recombinant human TNF-α (94948-59-1) was bought from Sigma-Aldrich. VCAM-1 (sc-13160), ICAM-1 (sc-1511-R), Ataxin-10 (sc-271233), and β-actin (sc-1616) antibodies were purchased from Santa Cruz Biotechnology. IκBα (4812), phospho-IκBα (2859), phospho-p65 (3033), p65 (8242), phospho-IKKα/β (2078), IKKα (11930), IKKβ (8943), phospho-ERK1/2 (4370), ERK1/2 (4695), phospho-JNK (4668), JNK (9252), phospho-p38 (4511), p38 (8690), phospho-C-Jun (2361), C-Jun (9165), Flag (8146), VE-cadherin (2158), IRF-1 (8478), α-tubulin (2125), and TBP (8515) antibodies were obtained from Cell Signaling Technology. siRNAs targeting *ATXN10* (sc-60218) were purchased from Santa Cruz Biotechnology. qPCR primers were from Integrated DNA Technologies, Inc.

2.2. Cell Culture and Transfection. All human primary vascular ECs including human aortic ECs (HAECs), human coronary artery ECs (HCAECs), human dermal microvascular ECs (HDMECs), human lung microvascular ECs (HLMECs), and human umbilical vein ECs (HUVECs) were purchased from Lonza Walkersville Inc. maintained in EGM™ Endothelial Cell Growth Medium BulletKit™ or EGM™-2 Endothelial Cell Growth Medium-2 BulletKit™ according to the manufacturer's instruction. For the present study, cells less than passage five were used for the experiment. THP-1 cells (human acute monocytic leukemia cell) were obtained from ATCC and cultured in 10% FBS (Sigma-Aldrich) RPMI 1640 medium (Corning), 1% penicillin/streptomycin (Invitrogen), and 0.05 mmol/L 2-mercaptoethanol (Sigma Aldrich). HEK293T cells were bought from ATCC and seeded in Dulbecco's modified Eagle's medium supplemented with 10% FBS and 1% penicillin/streptomycin (Invitrogen). Transfection of Ataxin-10

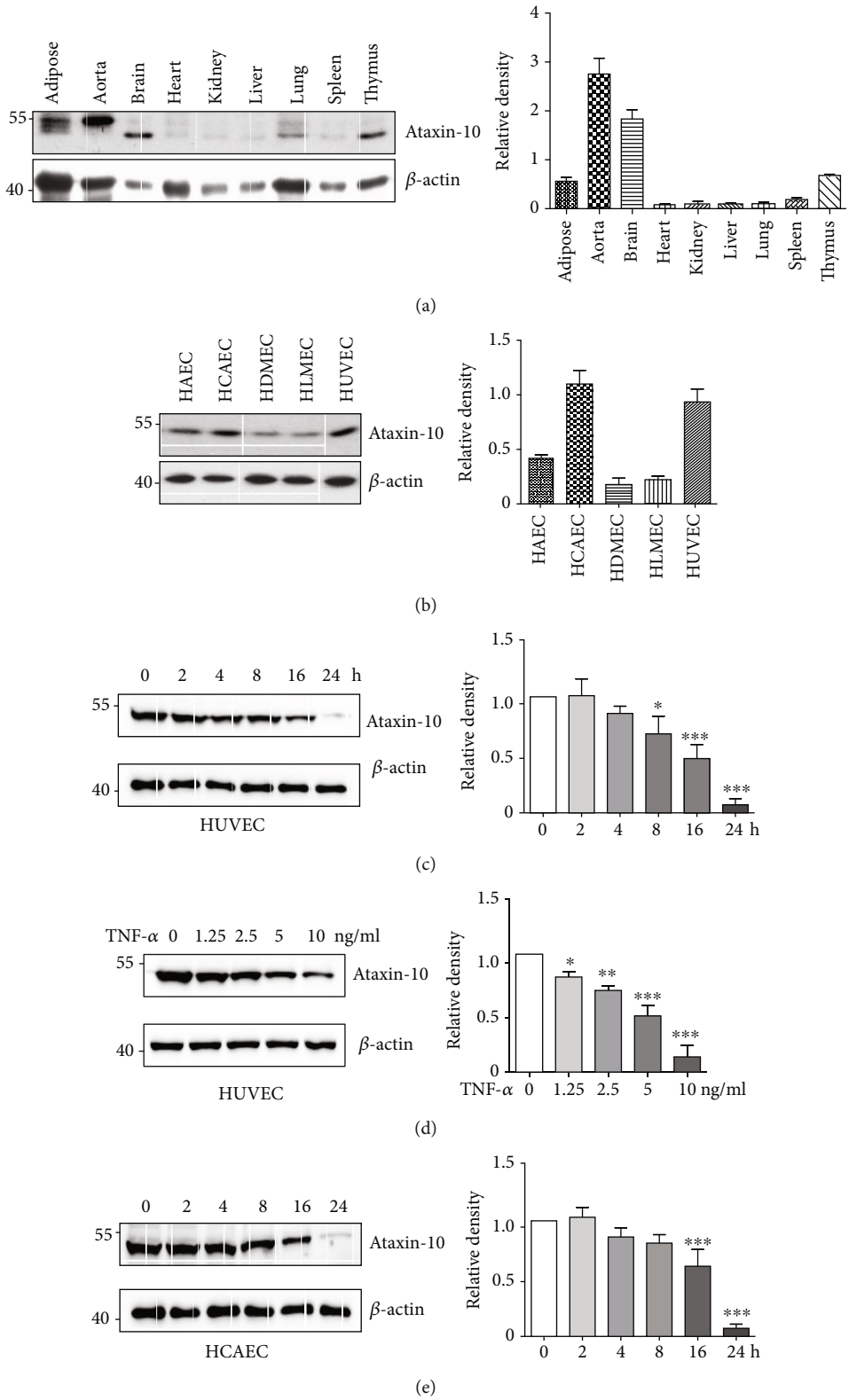

Figure 1: Continued.

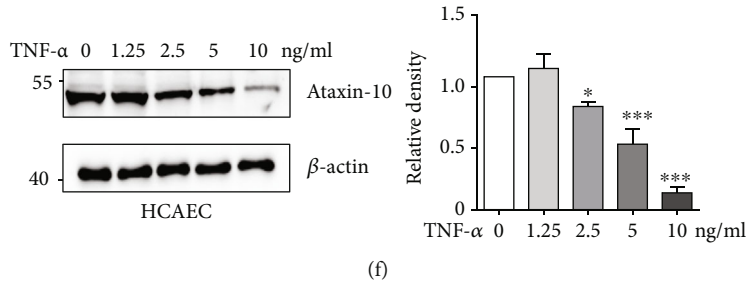

Figure 1: Expression of Ataxin-10 in endothelial cells. (a) Representative images of Western blotting for detection of the expression of Ataxin-10 in mouse tissues including adipose, aorta, brain, heart, kidney, liver, lung, spleen, and thymus. β-Actin was provided as a loading control. (b) Representative images of Western blotting for detection of the expression of Ataxin-10 in human primary vascular endothelial cells. (c, d) HUVEC or (e, f) HCAEC was stimulated with TNF-α for different time intervals and doses as indicated. Cell lysates were collected for Western blotting analysis. Quantification of the bands was carried out using Gel-Pro Analyzer software, and results were presented as "fold changes" at the right side of the bands.

vector and siRNA into HUVECs transiently was performed by electroporation using Nucleofector device and Nucleofector kits for HUVEC (Lonza) as described [22, 23]. After 24 h, 10 ng/mL TNF-α was added to the cells for indicated times, and cell lysates were collected and detected by Western blotting.

2.3. Western Blotting and Immunoprecipitation. Mouse tissue (twelve-week-old male C57BL/6) and cells were homogenized in the lysis buffer containing a protease inhibitor cocktail (Sigma-Aldrich) as described previously [22]. Samples with equal total protein amounts (20–50 μg) were separated by electrophoresis in SDS-PAGE and then transferred to the NC membrane (Corning). The membranes were blocked in 5% nonfat milk PBST (PBS with 0.1% Tween-20) for 20-30 min and then incubated with specific primary antibody overnight at 4°C with gentle shaking. After washing with PBST for three times, the blots were then incubated with secondary antibody for 2-4 h at room temperature. Bands were detected using a chemiluminescent detection kit according to the protocol (Pierce). The results were normalized to β-actin. The relative band density of the blots was determined with Gel-Pro analyzer software. For immunoprecipitation (IP) assays, proteins were extracted with lysis buffer and subjected to IP with Ataxin-10 or IRF-1 antibody as described previously [22].

2.4. qPCR. Total RNA from HUVECs was extracted using TRIzol (Invitrogen) according to the manufacturer's instructions. Then, 1 μg RNA was reverse-transcribed to cDNA using the PrimeScript™ RT reagent kit with gDNA Eraser (TAKARA). Quantitative real-time PCR (qPCR) was performed in 96-well plate format using TB Green® *Premix Ex Taq*™ II (TAKARA) on ViiA-7 real-time PCR system instrument (ABI). Each reaction was performed in triplicate. As an internal control, the results were normalized to β-actin transcript. Fold changes were determined from cycle threshold values using the $2^{-\Delta\Delta CT}$ method. Sequences of the primers used here are listed in Table 1.

2.5. Yeast Two-Hybrid Screening. The yeast two-hybrid screening assay was performed as recommended by the manufacturer of the Matchmaker Gold Yeast Two-Hybrid System as described previously [24]. cDNA of *ATXN10* gene was cloned into the pGBKT7 vector as the bait and subsequently transformed into the yeast strain Y2HGold. The Y2HGold yeast strain was then mated with Y187 yeast strain containing a Universal Human Mate & Plate™ Library (Clontech Laboratories). Blue yeast colonies growing on SD/-Ade/-His/-Leu/-Trp/X-α-Gal (QDO/X/A) medium were regarded as positive candidates, and PCR was performed for the positive cDNA clones using the T7 sequencing primer followed by sequencing to identify candidate genes.

2.6. Isolation of Nuclear and Cytoplasm Extracts. The cytoplasm and nuclear portion were collected and separated using the Cell Fractionation Kit (Cell Signaling Technology, Inc) as previously described [25]. Briefly, cells were harvested and washed with ice-cold PBS and centrifuged at 350 g for 5 min. 500 μL cytoplasmic isolation buffer was added to the pellet to fully suspend it. The suspension was kept on ice for over 5 min and then centrifuged for 5 min at 500 g. The cytoplasm in the supernatant fraction was moved to a pre-chilled tube and stored on ice. The pellet fraction was resuspended in 500 μL membrane isolation buffer, vortexed for 15 s, then incubated on ice for 5 min, and centrifuged for 5 min at 8000 g. The pellet fraction was resuspended in 250 μL cytoskeleton/nucleus isolation buffer and sonicated for 5 s. After centrifugation for 10 min at 16000 g, the supernatant including the nuclear fraction can be collected for the subsequent experiments.

2.7. Monocyte Adhesion Assay. The monocyte adhesion assay was carried out as previously described [22, 23]. After 24 h of transfection, cells were seeded and cultured in a 6-well plate until they reached about 85% confluence. Then, HUVECs were treated with TNF-α (10 ng/mL) for 8 h and washed with PBS twice. After labeling with fluorescein isothiocyanate via a PKH67 fluorescent staining kit (Zynaxis, Inc.), 5×10^5 THP-1 cells were added into each well and incubated for 1 h in a 37°C incubator. Unbound cells were removed gently by washing with cold PBS. Adhesive THP-1 cells were determined using a fluorescence microscope,

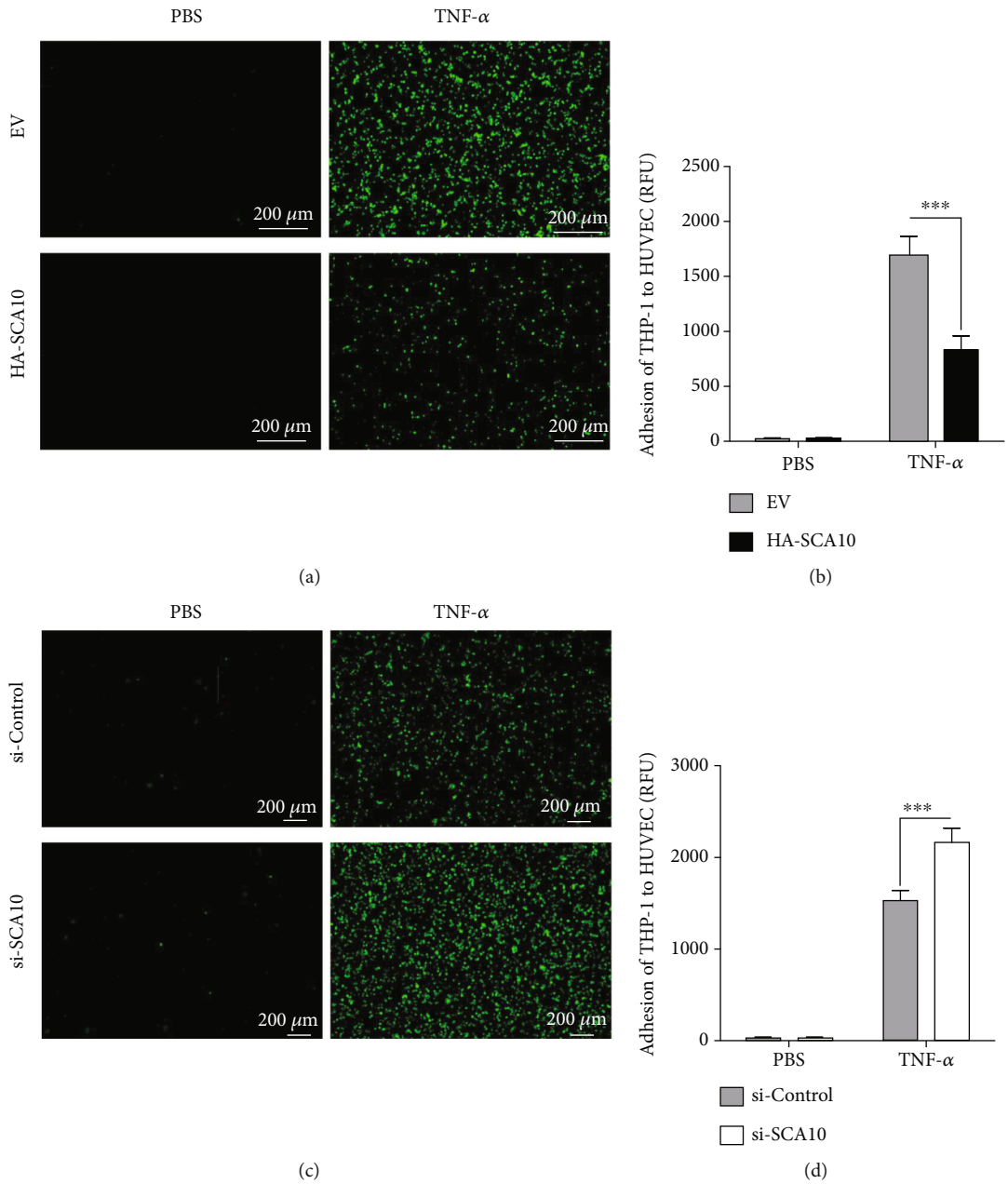

Figure 2: Effects of Ataxin-10 on the adhesion of THP-1 monocytes to TNF-α-treated HUVECs. (a, c) Photographs (×200 magnification) of PKH67 fluorescent labeled monocytes (THP-1 cells, green) adhering to HUVECs. (b, d) Quantitative data analysis revealed significant increases in adhesion of THP-1 cells to the HUVEC monolayer. The data are representative of 6 independent experiments. $^{***}p < 0.001$ vs. TNF-α treated control group. (a, b) Ataxin-10 or empty vector (EV) was transfected transiently into HUVECs; 48 h later, cells were incubated with or without TNF-α (10 ng/mL) for 8 h. Then, fluorescence-labeled THP-1 cells were added to the activated HUVECs for 1 h. After being washed carefully by PBS, adherent cells were visualized, photographed, and counted. (c, d) The HUVECs transfected with si-control or si-Ataxin-10 were treated with TNF-α (10 ng/mL) for 8 h and incubated with PKH67 fluorescent labeled monocytes for 1 h. Adhesive cells were visualized, photographed, and counted as well.

and the numbers were read out by the Cytation 3 Cell Imaging Multimode Reader (Biotek Instruments).

2.8. Statistical Analysis. Data are expressed as the means ± standard deviation (SD) of at least three independent experiments. Differences between groups were assessed by two-tailed Student's t-test not assuming equal variance between groups using GraphPad Prism 5.0 software. Statistical significance was defined as $p < 0.05$.

3. Results

3.1. Proinflammatory Cytokine TNF-α Significantly Decreases Ataxin-10 Expression in ECs. Since the expression and

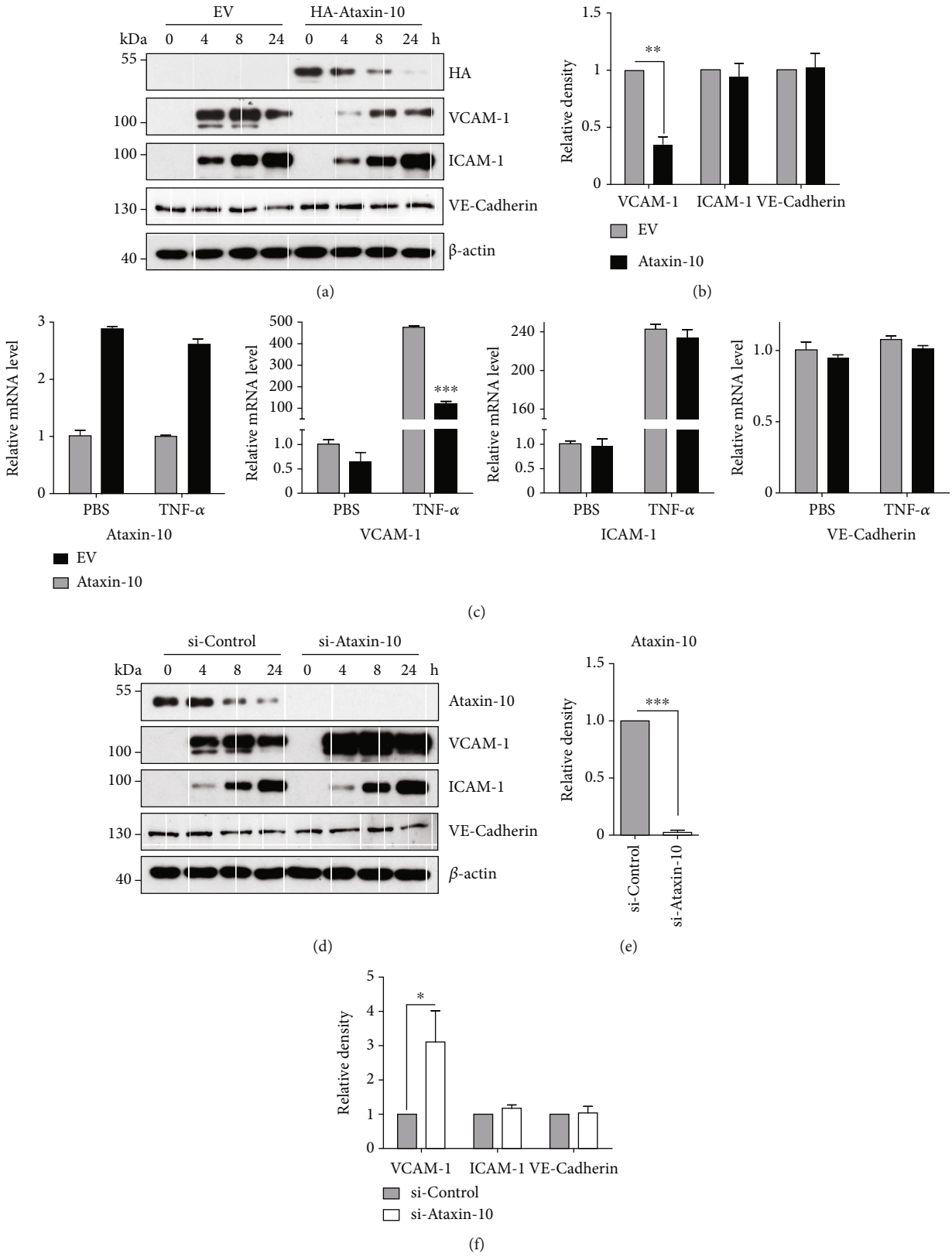

Figure 3: Continued.

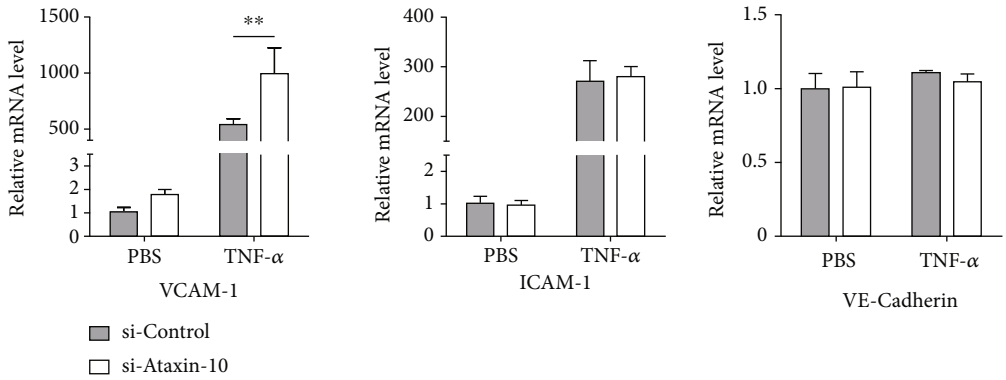

(g)

Figure 3: Effects of Ataxin-10 on adhesion molecule expressions in TNF-α-activated HUVECs. (a, d) Representative images of Western blotting for the detection of indicated protein expression. (a) HUVECs were transfected with either EV or HA-Ataxin-10 for 48 h, followed by stimulation with TNF-α (10 ng/mL) for the indicated times. Total cell lysates were used for immunoblotting analysis with appropriate antibodies (right panel). (b) Densitometry analysis of 3 independent experiments is shown as the relative ratio of each protein after TNF-α treatment (8 h) and normalized to β-actin. (c) HUVECs were transiently transfected with HA-Ataxin-10 or empty vector (EV) for 48 h. Then, cells were incubated with TNF-α (10 ng/mL) or PBS (as controls) for another 4 h. qPCR assays were performed to determine the mRNA levels of Ataxin-10 and adhesive molecules. $^{***}p < 0.001$ vs. EV control group. (d) Ataxin-10 siRNAs or control siRNAs were transfected transiently into HUVECs. 48 h later, transfected cells were stimulated with TNF-α (10 ng/mL) for 0, 4, 8, and 24 h. Protein levels of VCAM-1, ICAM-1, and VE-cadherin were determined. Relative fold changes of Ataxin-10 (e) or adhesion proteins (f) after TNF-α stimulation (8 h) were confirmed by densitometry and normalized to β-actin. $^{*}p < 0.05$ and $^{***}p < 0.001$ vs. si-control group. (g) Ataxin-10 siRNAs/control siRNAs were transfected into endothelial cells. 24 h later, cells were incubated with TNF-α (10 ng/mL) or PBS (as controls) for another 4 h. qPCR assays were performed to determine the mRNA levels of adhesive molecules. $^{**}p < 0.001$ vs. si-control group.

function of Ataxin-10 in vascular endothelial cells were never reported, we first detected the protein expression of Ataxin-10 in a variety of mouse tissues (adipose, aorta, brain, heart, kidney, liver, lung, spleen, and thymus) and primary ECs (HAEC, HCAEC, HDMEC, HLMEC, and HUVEC). As shown in Figure 1(a), Ataxin-10 was expressed highest in the aorta among the indicated mouse tissues. Of note, the observed molecular weight (MW) of Ataxin-10 was larger in the aorta and adipose than that in the brain and thymus (Figure 1(a)), suggesting that Ataxin-10 may have posttranslational modifications in different tissues. In fact, it was reported that Ataxin-10 could be phosphorylated and O-linked glycosylated [16–18]. Ataxin-10 can be detected in all cultured primary ECs, with higher expression in HCAEC and HUVEC (Figure 1(b)). Moreover, the expression of Ataxin-10 was further inhibited by TNF-α in HCAECs or HUVECs in both time-dependent and dose-dependent manners (Figures 1(c)–1(f)). These results indicated that Ataxin-10 may be relevant to the regulation of vascular endothelial activation in response to TNF-α stimulation.

3.2. Ataxin-10 Inhibits Human Monocyte Adherence to TNF-α-Activated HUVECs. Since the adhesion of inflammatory monocytes to endothelial cells is an important step in the development of atherosclerosis, we evaluated the possible role of Ataxin-10 on TNF-α-induced monocyte adhesion. We previously reported that TNF-α stimulation can markedly increase THP-1 cell adhesion to HUVECs [22, 23]. Therefore, the monocyte adhesion assay was performed after incubating with TNF-α for 8 h as described in Materials and Methods. As shown in Figure 2, THP-1 adhesion was minimal in unstimulated HUVECs, but treatment with TNF-α resulted in a marked increase of monocyte adhesion to endothelial cells. However, knocking down Ataxin-10 expression by siRNA dramatically promoted the TNF-α-induced adhesion between the THP-1 cells and HUVECs (Figures 2(c) and 2(d)). In contrast, overexpression of Ataxin-10 significantly inhibited the recruitment of THP-1 to activated HUVECs (Figures 2(a) and 2(b)), suggesting that Ataxin-10 has a specific inhibitory effect on monocyte adhesion induced by TNF-α to endothelial cells.

3.3. Ataxin-10 Suppresses VCAM-1 Expression in HUVECs. Cell adhesion is under the control of several adhesion molecules on the endothelial cell surface [8]. VCAM-1 and ICAM-1 are shown to represent predominant adhesive forces of endothelial cells under cytokine stimulation [8]. In order to explore the possible molecular mechanism of Ataxin-10 on THP-1 cell adhesion, ICAM-1 and VCAM-1 expressions were evaluated by Western blotting and qPCR. HUVECs were transiently transfected with Ataxin-10 plasmids or empty vectors for 24 h, and then, cells were treated with TNF-α for endothelial cell activation. The expression of adhesion molecules was detected by Western blotting and qPCR. Results of Figures 3(a) and 3(b) showed that TNF-α evoked a marked increase in VCAM-1 and ICAM-1 expression compared to the control group; overexpression of Ataxin-10 significantly reduced the VCAM-1 protein levels but did not affect ICAM-1 and VE-cadherin expression. Consistently, Ataxin-10 overexpression also suppressed the mRNA level of VCAM-1 but not ICAM-1 and VE-cadherin (Figure 3(c)). Next, we sought to confirm its

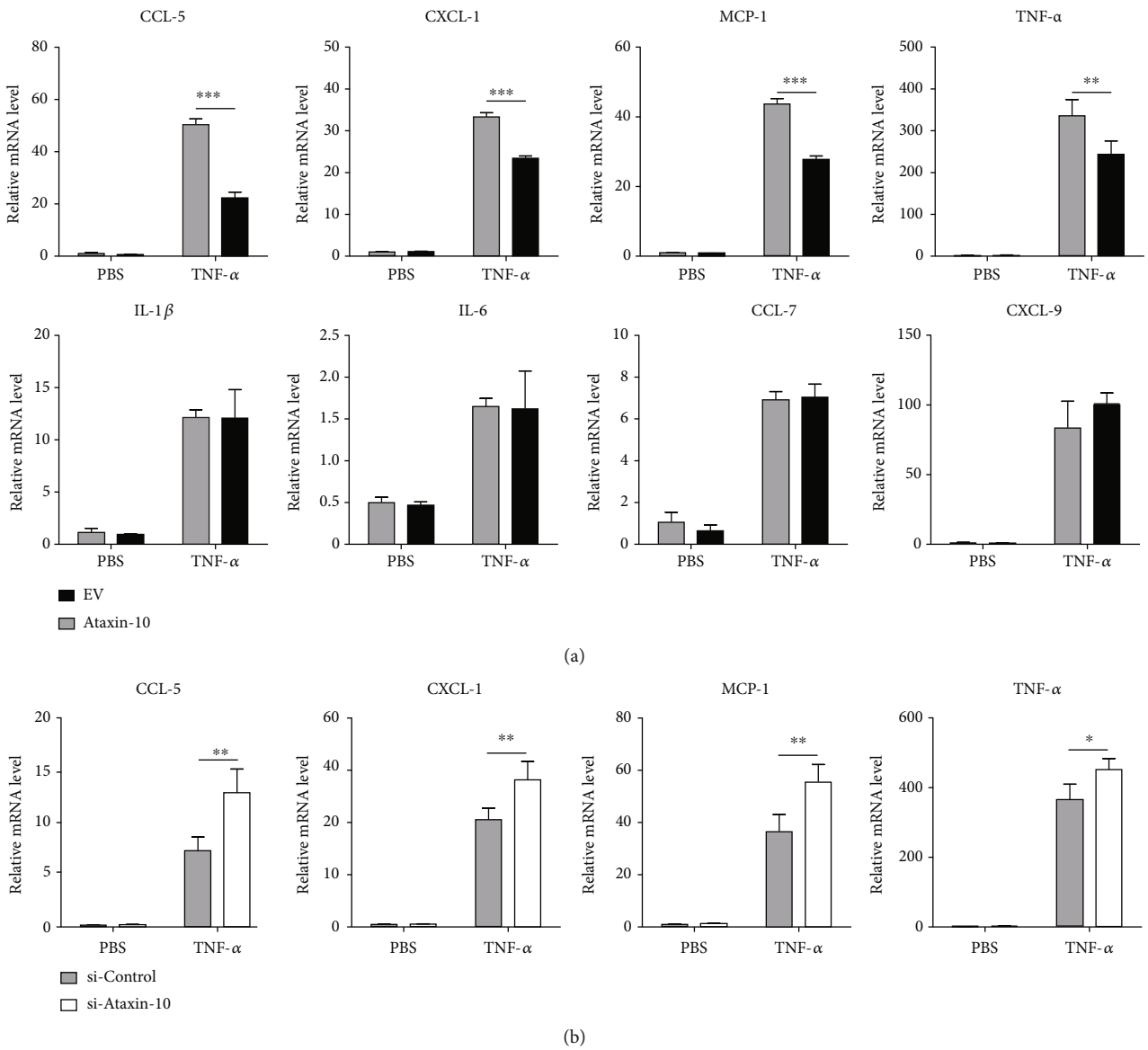

Figure 4: Effects of Ataxin-10 on chemokine/cytokine expression in TNF-α-stimulated HUVECs. (a) HUVECs were transfected with either EV or HA-Ataxin-10 for 48 h, followed by incubation with TNF-α (10 ng/mL) for 4 h. Relative mRNA levels of IL-1β, IL-6, CCL-5, CCL-7, CXCL-9, CXCL-1, MCP-1, and TNF-α were detected by qPCR, with β-actin as an internal control. $^{**}p < 0.01$ and $^{***}p < 0.001$ vs. EV. (b) Ataxin-10 was knocked down using siRNA and then stimulated with TNF-α for 4 h. mRNA levels of CCL-5, CXCL-1, MCP-1, and TNF-α were determined by qPCR. $^{*}p < 0.05$ and $^{**}p < 0.01$ vs. si-control group.

function by determining the role of endogenous Ataxin-10 using siRNA. Confluent HUVECs were transfected with either a control siRNA duplex or a human Ataxin-10 specific siRNA. Treatment with Ataxin-10 siRNA effectively suppressed Ataxin-10 protein levels (Figures 3(d) and 3(e)). As expected, Ataxin-10 knockdown significantly promoted VCAM-1 expression in TNF-α-induced HUVECs (Figures 3(d), 3(f), and 3(g)). Neither ICAM-1 nor VE-cadherin were affected by Ataxin-10 knockdown (Figures 3(d), 3(f), and 3(g)). Taken together, these data indicate that Ataxin-10 specifically inhibited VCAM-1 expression induced by TNF-α in HUVECs.

3.4. Ataxin-10 Inhibits TNF-α-Induced Cytokine/Chemokine Production in HUVECs. Upon TNF-α stimulation, endothelial cells produce proinflammatory mediators, which cause more monocytes to be recruited [26]. These proinflammatory mediators are reported to aggravate endothelial dysfunction [27]. As presented in Figure 4(a), exposure of HUVECs to TNF-α for 4 h significantly induced the expression of the cytokine/chemokine (including MCP-1, TNF-α, CXCL-1, IL-1β, IL-6, CCL-5, CCL-7, and CXCL-9). However, the expression of several TNF-α-induced chemokines (MCP-1, CXCL-1, and CCL-5) and cytokine TNF-α was markedly suppressed in HUVECs transfected with HA-Ataxin-10 (Figure 4(a)). IL-1β, IL-6, CCL-7, and CXCL-9 were not influenced by Ataxin-10 (Figure 4(a)). To further verify the regulation of these genes by Ataxin-10, a knockdown approach was applied. Ataxin-10 knockdown

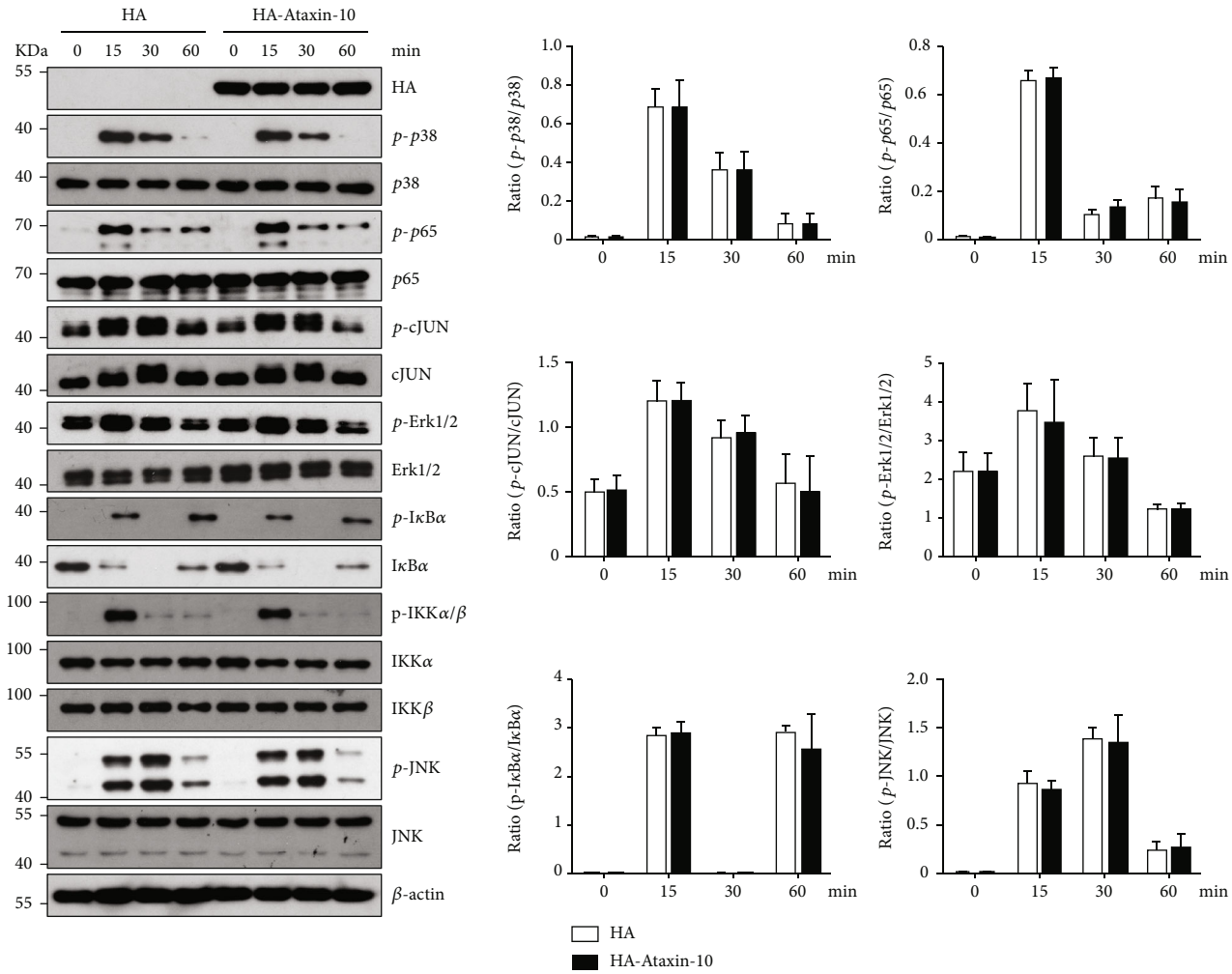

Figure 5: Effect of Ataxin-10 on MAPK/NF-κB signaling pathway in TNF-α-stimulated HUVECs. HA-Ataxin-10 or empty vector was transfected into HUVECs and then stimulated with TNF-α for the indicated times, and whole cell lysates were prepared and harvested for immunoblotting. Blots for activated p38 (phospho-p38 Thr180/Tyr182), activated p65 (phospho-p65S536), activated c-JUN (phospho-c-JUN Ser63), activated ERK (phospho-ERK T202/Y204), activated IκBα (phospho-IκBαSer32), activated IKKα/β (phospho-IKKα/βSer176/Ser177), and activated JNK (phospho-JNK T183/Y185) are shown. Internal loading is shown by antiactin or reprobing membranes with antibodies to total p38, p65, c-JUN, ERK1/2, IκBα, IKKα, IKKβ, and JNK immunoblotting. The bands of Western blotting were quantified by Gel-Pro Analyzer software, and the results were presented as fold changes at the right side of the bands.

markedly increased the mRNA levels of MCP-1, CXCL-1, CCL-5, and TNF-α in HUVECs stimulated with TNF-α (Figure 4(b)). Again, IL-1β, IL-6, CCL-7, and CXCL-9 expressions were not altered (data not shown). In a word, these data identify Ataxin-10 as a negative regulator of cytokine/chemokine expression in HUVECs.

3.5. Ataxin-10 Does Not Affect the MAPK and NF-κB Signaling Pathways Inactivating HUVECs. As we all know, MAPK/NF-κB cascade plays a critical role in the pathogenesis of atherosclerosis by modulating a series of adhesion molecules and inflammation-related genes including VCAM-1 [28]. Accordingly, we examined whether Ataxin-10 affects the MAPK/NF-κB signaling pathway activated by TNF-α in HUVECs. After transfection with HA-Ataxin-10 or empty vector (EV) for 24 h, the HUVECs were treated with TNF-α for different time intervals (Figure 5). As expected, TNF-α stimulation induced the phosphorylation of p38, c-JUN, Erk1/2, IκBα, IKKα/β, JNK, and p65 during these experimental intervals (Figure 5). However, overexpression of Ataxin-10 did not affect TNF-α-induced phosphorylation of the above proteins involved in the MAPK/NF-κB signaling pathway (Figure 5).

3.6. Ataxin-10 Inhibits IRF-1 Activity to Suppress TNF-α-Induced VCAM-1 in HUVECs. To gain a mechanistic understanding of the function of Ataxin-10 in TNF-α-induced endothelial activation, we performed yeast two-hybrid technology to screen the interaction protein of Ataxin-10. The bait vector (pGBKT7-Ataxin-10) was successfully transformed to Y2HGold (Figure 6(a)), which has no cytotoxic effect and no self-activation (data not shown). From initial putative positive colonies in the screen from the human cDNA library, one of them was identified by sequence

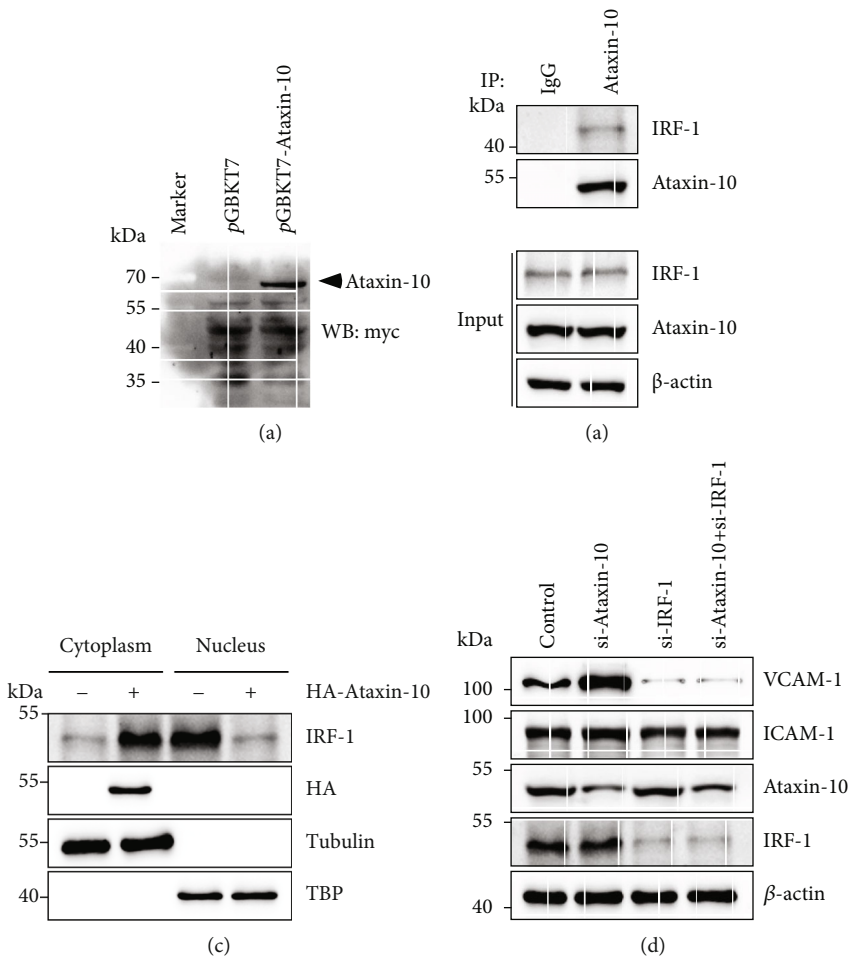

Figure 6: Ataxin-10 binds to and inhibits IRF-1 to suppress TNF-α-induced VCAM-1 in HUVECs. (a) Cell lysates were harvested from Y2HGold yeast strain transfected with pGBKT7 or pGBKT7-Ataxin-10. The expression of Ataxin-10 was detected by Western blotting. (b) HUVECs were treated with 10 ng/mL TNF-α for 2 hours. Immunoprecipitation experiment was performed with Ataxin-10 antibody and IgG (control), showing specific interaction between Ataxin-10 and IRF-1 in HUVECs. (c) Western blotting analysis of endogenous IRF-1 subcellular localization in HUVECs transfected with empty vector of HA-Ataxin-10. The purity and equal loading of cytoplasmic fractions and nuclear fractions were confirmed by tubulin and TBP, respectively. (d) HUVECs were transfected with Ataxin-10 siRNA or IRF-1 siRNA or both and then treated with TNF-α (10 ng/mL) for 8 hours. VCAM-1 and ICAM-1 protein levels were detected by Western blotting.

analysis as IRF-1. To further verify the interaction between Ataxin-10 and IRF-1, a co-IP assay was performed. Since TNF-α stimulation of HUVECs led to a significant increase in IRF-1 protein [29], HUVECs were treated with TNF-α for 2 hours; then, cells were collected for protein extraction, and the cell lysates were incubated with specific anti-Ataxin-10 antibody or normal IgG. The result showed that Ataxin-10 was coimmunoprecipitated together with IRF-1 (Figure 6(b)). In addition, TNF-α triggered nuclear translocation and activation of IRF1 in endothelial cells [9]. As shown in Figure 6(c), quantification of protein levels by densitometry indicated that ~90% of the IRF-1 protein present in TNF-α-treated HUVECs localized to the nucleus. Overexpression of Ataxin-10 significantly decreased nuclear accumulation of IRF-1 (Figure 6(c)). It is reported that Ataxin-10 is mainly cytoplasmic [14]. These data suggested that Ataxin-10 may bind and sequester IRF-1 in the cytoplasm, thereby inhibiting the transcription activity of IRF-1. Using siRNA to knock down the expression of IRF-1, it can eliminate the effect of Ataxin-10 on VCAM-1 expression in HUVECs induced by TNF-α (Figure 6(d)). Taken together, Ataxin-10 selectively inhibits TNF-α-induced VCAM-1 expression in HUVECs through an IRF-1-dependent mechanism.

4. Discussion

Monocytes adhere to endothelial cells and then migrate to the subendothelial layer, which is a pivotal event in the early pathogenesis of atherosclerosis [30]. This is a strictly regulated process mediated by the expression of a variety of chemokines and adhesion molecules [8, 31]. Inflammatory stimuli, including TNF-α and other cytokines, result in endothelial cell activation and the induction of adhesive molecules [7]. Sustained adhesion and migration lead to excessive infiltration of monocytes into the arterial intima,

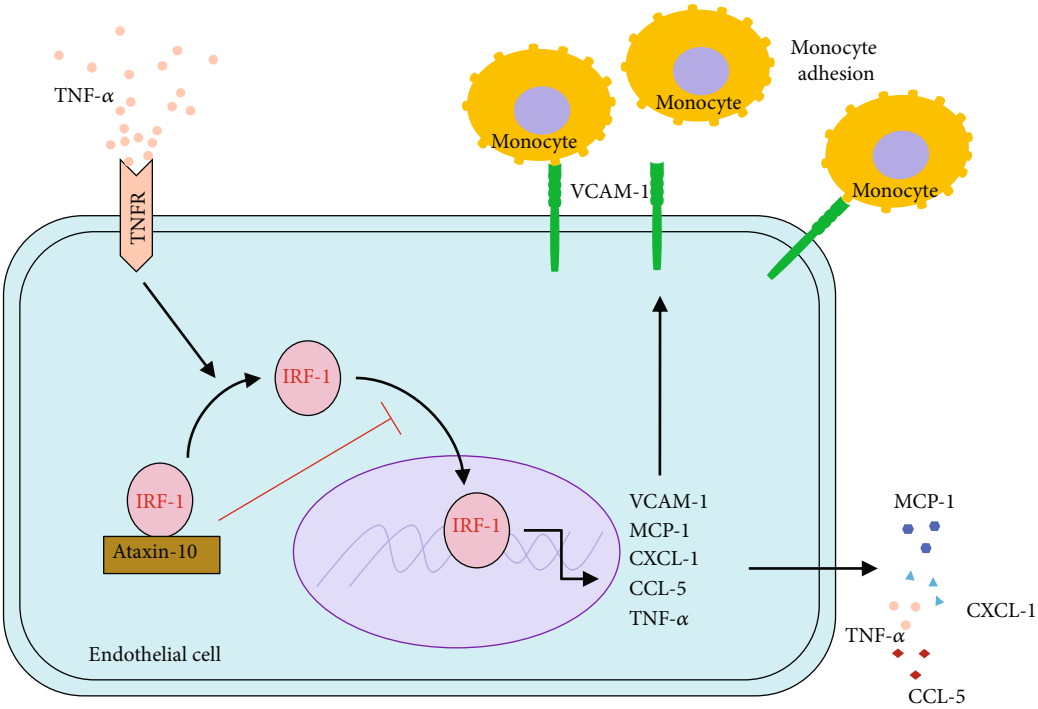

Figure 7: Graphic depiction of how Ataxin-10 suppresses TNF-α-induced VCAM-1 in endothelial cells via sequestering cytoplasmic IRF-1.

the release of inflammatory factors, and lipid overload, which finally aggravates the instability of plaque [30]. Therefore, understanding the potential mechanism of monocyte-endothelial adherence will help to take effective strategies to prevent and treat atherosclerosis. This study proved that Ataxin-10 could reduce THP-1-HUVEC adhesion via inhibiting VCAM-1 expression. The VCAM-1 expression on the endothelial cell surface contributes to the monocyte recruitment to endothelial cells [23, 32]. Thus, Ataxin-10 may be a potential target for preventing the progression of vascular inflammatory diseases, such as atherosclerosis.

Considering the critical role of VCAM-1 in the development of atherosclerosis, considerable attention has been devoted to clarifying the regulation of VCAM-1 by cytokine in the endothelium. Ataxin-10 could inhibit TNF-α-induced VCAM-1 expression in HUVECs as well as its mRNA level, suggesting that Ataxin-10 may regulate VCAM-1 transcription. As MAPKs and NF-κB both play significant roles in the regulation of VCAM-1 expression, we first examined whether Ataxin-10 affects VCAM-1 transcription via these signaling pathways. However, Ataxin-10 did not affect the MAPK or NF-κB cascade in TNF-α-activated HUVECs. Through a comprehensive approach encompassing yeast two-hybrid technologies, our studies revealed that Ataxin-10 can interact with IRF-1, resulting in sequestration of IRF-1 in the cytoplasm and blocking the entry of IRF-1 into the nucleus. IRF-1 has been proved to regulate the expression of VCAM-1 [9]. It was reported that constitutively bound IRF-1 regulated by TNF-α is indispensable for the optimal expression of VCAM-1, which can associate with NF-κB to yield a maximal response [33]. Our results indicate that regulation of Ataxin-10 in IRF-1 activity rather than MAPK/NF-κB signaling pathway plays a leading role in determining the VCAM-1 expression pattern observed in response to TNF-α stimuli in endothelial cells.

An overexpression of inflammatory cytokines/chemokines can induce cell adhesion, migration, angiogenesis, and vascular permeability to aggravate atherosclerosis [31]. In this study, Ataxin-10 significantly reduced the mRNA expressions of MCP-1, CXCL-1, CCL-5, and TNF-α in TNF-α-stimulated HUVECs. However, the mRNA expressions of IL-1β, IL-6, CCL-7, and CXCL-9 were not obviously changed. It is known that the transcription of MCP-1, CXCL-1, CCL-5, and TNF-α was regulated by IRF-1 [34–36]. Therefore, Ataxin-10 attenuated cytokine/chemokine production in TNF-α-activated endothelial cells dependent on IRF-1 transcriptional activity.

5. Conclusions

In summary, our data demonstrate a novel role for Ataxin-10 in the regulation of TNF-α-induced endothelial inflammation via suppressing IRF-1 (Figure 7). Our results revealed that Ataxin-10 attenuated proinflammatory changes induced by TNF-α in endothelial cells, which was related to downregulation of cytokines and chemokines (MCP-1, CXCL-1, CCL-5, and TNF-α) together with VCAM-1, resulting in a reduction in endothelial-monocyte adhesion. Interestingly, Ataxin-10 suppressed TNF-α-induced VCAM-1 expression but not ICAM-1/VE-cadherin expression and reduced the nuclear localization of IRF1. Our results show that the anti-inflammatory effects of Ataxin-10 are exerted on endothelial cells through suppression of IRF-1 activation.

Data Availability

The data used to support the findings of this study are available from the corresponding author upon request.

Conflicts of Interest

The authors declare that they have no conflicts of interest.

Acknowledgments

This work was supported by grants from the National Natural Science Foundation of China (31760329, 31960147, 82160133, 32170793, and 81660390) and Research and Training Fund for Young Talents in the First Affiliated Hospital of Nanchang University (YFYPY202003).

References

[1] J. Frostegard, "Immunity, atherosclerosis and cardiovascular disease," *BMC Medicine*, vol. 11, no. 1, p. 117, 2013.

[2] J. Moriya, "Critical roles of inflammation in atherosclerosis," *Journal of Cardiology*, vol. 73, no. 1, pp. 22–27, 2019.

[3] M. A. Gimbrone Jr. and G. Garcia-Cardena, "Endothelial cell dysfunction and the pathobiology of atherosclerosis," *Circulation Research*, vol. 118, no. 4, pp. 620–636, 2016.

[4] J. S. Pober, "Endothelial activation: intracellular signaling pathways," *Arthritis Research*, vol. 4, Supplement 3, pp. S109–S116, 2002.

[5] N. Parameswaran and S. Patial, "Tumor necrosis Factor-α signaling in macrophages," *Critical Reviews in Eukaryotic Gene Expression*, vol. 20, no. 2, pp. 87–103, 2010.

[6] G. E. McKellar, D. W. McCarey, N. Sattar, and I. B. McInnes, "Role for TNF in atherosclerosis? Lessons from autoimmune disease," *Nature Reviews Cardiology*, vol. 6, no. 6, pp. 410–417, 2009.

[7] L. A. Madge and J. S. Pober, "TNF signaling in vascular endothelial cells," *Experimental and Molecular Pathology*, vol. 70, no. 3, pp. 317–325, 2001.

[8] E. Galkina and K. Ley, "Vascular adhesion molecules in atherosclerosis," *Arteriosclerosis, Thrombosis, and Vascular Biology*, vol. 27, no. 11, pp. 2292–2301, 2007.

[9] D. Venkatesh, T. Ernandez, F. Rosetti et al., "Endothelial TNF Receptor 2 Induces IRF1 Transcription Factor-Dependent Interferon-β Autocrine Signaling to Promote Monocyte Recruitment," *Immunity*, vol. 38, no. 5, pp. 1025–1037, 2013.

[10] H. A. Teive, R. P. Munhoz, W. O. Arruda, S. Raskin, L. C. Werneck, and T. Ashizawa, "Spinocerebellar ataxia type 10 - A review," *Parkinsonism & Related Disorders*, vol. 17, no. 9, pp. 655–661, 2011.

[11] T. Matsuura, T. Yamagata, D. L. Burgess et al., "Large expansion of the ATTCT pentanucleotide repeat in spinocerebellar ataxia type 10," *Nature Genetics*, vol. 26, no. 2, pp. 191–194, 2000.

[12] M. Wakamiya, T. Matsuura, Y. Liu et al., "The role of ataxin 10 in the pathogenesis of spinocerebellar ataxia type 10," *Neurology*, vol. 67, no. 4, pp. 607–613, 2006.

[13] M. C. White, R. Gao, W. Xu et al., "Inactivation of hnRNP K by expanded intronic AUUCU repeat induces apoptosis via translocation of PKCδ to mitochondria in spinocerebellar ataxia 10," *PLoS Genetics*, vol. 6, no. 6, article e1000984, 2010.

[14] P. Marz, A. Probst, S. Lang et al., "Ataxin-10, the Spinocerebellar Ataxia Type 10 Neurodegenerative Disorder Protein, Is Essential for Survival of Cerebellar Neurons," *The Journal of Biological Chemistry*, vol. 279, no. 34, pp. 35542–35550, 2004.

[15] M. Waragai, S. Nagamitsu, W. Xu, Y. J. Li, X. Lin, and T. Ashizawa, "Ataxin 10 induces neuritogenesis via interaction with G-protein β2 subunit," *Journal of Neuroscience Research*, vol. 83, no. 7, pp. 1170–1178, 2006.

[16] J. Li, J. Wang, W. Hou et al., "Phosphorylation of Ataxin-10 by polo-like kinase 1 is required for cytokinesis," *Cell Cycle*, vol. 10, no. 17, pp. 2946–2958, 2011.

[17] J. Tian, C. Tian, Y. Ding et al., "Aurora B-dependent phosphorylation of Ataxin-10 promotes the interaction between Ataxin-10 and Plk1 in cytokinesis," *Scientific Reports*, vol. 5, no. 1, p. 8360, 2015.

[18] S. S. Andrali, P. Marz, and S. Ozcan, "Ataxin-10 interacts with O-GlcNAc transferase OGT in pancreatic β cells," *Biochemical and Biophysical Research Communications*, vol. 337, no. 1, pp. 149–153, 2005.

[19] P. März, J. Stetefeld, K. Bendfeldt et al., "Ataxin-10 Interacts with *O*-Linked β-*N*-Acetylglucosamine Transferase in the Brain," *The Journal of Biological Chemistry*, vol. 281, no. 29, pp. 20263–20270, 2006.

[20] J. N. Wright, H. E. Collins, A. R. Wende, and J. C. Chatham, "O-GlcNAcylation and cardiovascular disease," *Biochemical Society Transactions*, vol. 45, no. 2, pp. 545–553, 2017.

[21] R. H. Hilgers, D. Xing, K. Gong, Y. F. Chen, J. C. Chatham, and S. Oparil, "AcuteO-GlcNAcylation prevents inflammation-induced vascular dysfunction," *American Journal of Physiology Heart and Circulatory Physiology*, vol. 303, no. 5, pp. H513–H522, 2012.

[22] X. Huang, Y. Li, X. Li, D. Fan, H. B. Xin, and M. Fu, "TRIM14 promotes endothelial activation via activating NF-κB signaling pathway," *Journal of Molecular Cell Biology*, vol. 12, no. 3, pp. 176–189, 2020.

[23] Y. Li, X. Huang, F. Guo et al., "TRIM65 E3 ligase targets VCAM-1 degradation to limit LPS-induced lung inflammation," *Journal of Molecular Cell Biology*, vol. 12, no. 3, pp. 190–201, 2020.

[24] Y. Wang, Y. Li, G. Hu et al., "Nek2A phosphorylates and stabilizes SuFu: a new strategy of Gli2/Hedgehog signaling regulatory mechanism," *Cellular Signalling*, vol. 28, no. 9, pp. 1304–1313, 2016.

[25] Y. Li, W. Sun, F. Saaoud et al., "miR155 modulates vascular calcification by regulating Akt-FOXO3a signalling and apoptosis in vascular smooth muscle cells," *Journal of Cellular and Molecular Medicine*, vol. 25, no. 1, pp. 535–548, 2021.

[26] S. Čejková, I. Králová Lesná, and R. Poledne, "Monocyte adhesion to the endothelium is an initial stage of atherosclerosis development," *Cor et Vasa*, vol. 58, no. 4, pp. e419–e425, 2016.

[27] Y. Shao, Z. Cheng, X. Li, V. Chernaya, H. Wang, and X. F. Yang, "Immunosuppressive/anti-inflammatory cytokines directly and indirectly inhibit endothelial dysfunction–a novel mechanism for maintaining vascular function," *Journal of Hematology & Oncology*, vol. 7, no. 1, p. 80, 2014.

[28] A. O. Jackson, M. A. Regine, C. Subrata, and S. Long, "Molecular mechanisms and genetic regulation in atherosclerosis," *IJC Heart & Vasculature*, vol. 21, pp. 36–44, 2018.

[29] S. Lechleitner, J. Gille, D. R. Johnson, and P. Petzelbauer, "Interferon enhances tumor necrosis factor-induced vascular cell adhesion molecule 1 (CD106) expression in human

endothelial cells by an interferon-related factor 1-dependent pathway," *The Journal of Experimental Medicine*, vol. 187, no. 12, pp. 2023–2030, 1998.

[30] I. Hilgendorf, F. K. Swirski, and C. S. Robbins, "Monocyte fate in atherosclerosis," *Arteriosclerosis, Thrombosis, and Vascular Biology*, vol. 35, no. 2, pp. 272–279, 2015.

[31] A. Hanna and N. G. Frangogiannis, "Inflammatory cytokines and chemokines as therapeutic targets in heart failure," *Cardiovascular Drugs and Therapy*, vol. 34, no. 6, pp. 849–863, 2020.

[32] H. E. Chuluyan, L. Osborn, R. Lobb, and A. C. Issekutz, "Domains 1 and 4 of vascular cell adhesion molecule-1 (CD106) both support very late activation antigen-4 (CD49d/CD29)-dependent monocyte transendothelial migration," *Journal of Immunology*, vol. 155, no. 6, 1995.

[33] A. S. Neish, M. A. Read, D. Thanos, R. Pine, T. Maniatis, and T. Collins, "Endothelial interferon regulatory factor 1 cooperates with NF-kappa B as a transcriptional activator of vascular cell adhesion molecule 1," *Molecular and Cellular Biology*, vol. 15, no. 5, pp. 2558–2569, 1995.

[34] A. Yarilina, K. H. Park-Min, T. Antoniv, X. Hu, and L. B. Ivashkiv, "TNF activates an IRF1-dependent autocrine loop leading to sustained expression of chemokines and STAT1-dependent type I interferon-response genes," *Nature Immunology*, vol. 9, no. 4, pp. 378–387, 2008.

[35] A. J. Valente, J. F. Xie, M. A. Abramova, U. O. Wenzel, H. E. Abboud, and D. T. Graves, "A complex element regulates IFN-gamma-stimulated monocyte chemoattractant protein-1 gene transcription," *Journal of Immunology*, vol. 161, no. 7, pp. 3719–3728, 1998.

[36] R. Karki, B. R. Sharma, E. Lee et al., "Interferon regulatory factor 1 regulates PANoptosis to prevent colorectal cancer," *JCI insight*, vol. 5, no. 12, 2020.

Hindawi
Mediators of Inflammation
Volume 2021, Article ID 4504431, 17 pages
https://doi.org/10.1155/2021/4504431

Research Article

Cholinergic Elicitation Prevents Ventricular Remodeling via Alleviations of Myocardial Mitochondrial Injury Linked to Inflammation in Ischemia-Induced Chronic Heart Failure Rats

Yang Zhao,[1,2] Huaxin Sun,[1,2] Kai Li,[1,2] Luxiang Shang,[3] Xiaoyan Liang,[1,2] Hang Yang,[1,2] Zhenyu Dong,[1,2] Jiasuoer Xiaokereti,[1,2] Shuai Shang,[1,2] Qina Zhou,[1,2] Xianhui Zhou,[1,2] Ling Zhang,[1] Yanmei Lu,[1,2] and Baopeng Tang[1,2]

[1]*Xinjiang Key Laboratory of Cardiac Electrophysiology and Remodeling, First Affiliated Hospital of Xinjiang Medical University, Urumqi 830011, China*
[2]*Department of Pacing and Electrophysiology, First Affiliated Hospital of Xinjiang Medical University, Urumqi 830011, China*
[3]*Department of Cardiology, The First Affiliated Hospital of Shandong First Medical University & Shandong Provincial Qianfoshan Hospital, Shandong Medicine and Health Key Laboratory of Cardiac Electrophysiology and Arrhythmia, Jinan, China*

Correspondence should be addressed to Ling Zhang; ydzhangling@126.com, Yanmei Lu; 18909917855@189.cn, and Baopeng Tang; tangbaopeng111@163.com

Received 21 August 2021; Accepted 20 October 2021; Published 20 November 2021

Academic Editor: Amilia Aminuddin

Background. Cholinergic anti-inflammatory pathway (CAP) is implicated in cardioprotection in chronic heart failure (CHF) by downregulating inflammation response. Mitochondrial injuries play an important role in ventricular remodeling of the CHF process. Herein, we aim to investigate whether CAP elicitation prevents ventricular remodeling in CHF by protecting myocardial mitochondrial injuries and its underlying mechanisms. *Methods and Results*. CHF models were established by ligation of anterior descending artery for 5 weeks. Postoperative survival rats were assigned into 5 groups: the sham group (sham, $n = 10$), CHF group (CHF, $n = 11$), Vag group (CHF+vagotomy, $n = 10$), PNU group (CHF+PNU-282987 for 4 weeks, $n = 11$), and Vag+PNU group (CHF+vagotomy+PNU-282987 for 4 weeks, $n = 10$). The antiventricular remodeling effect of cholinergic elicitation was evaluated in vivo, and H9C2 cells were selected for the TNF-α gradient stimulation experiment in vitro. In vivo, CAP agitated by PNU-282987 alleviated the left ventricular dysfunction and inhibited the energy metabolism remodeling. Further, cholinergic elicitation increased myocardium ATP levels and reduced systemic inflammation. CAP induction alleviates macrophage infiltration and cardiac fibrosis, of which the effect is counteracted by vagotomy. Myocardial mitochondrial injuries were ameliorated by CAP activation, including the reserved ultrastructural integrity, declining ROS overload, reduced myocardial apoptosis, and enhanced mitochondrial fusion. In vitro, TNF-α intervention significantly exacerbated the mitochondrial damage in H9C2 cells. *Conclusion*. CAP elicitation effectively improves ischemic ventricular remodeling by suppressing systemic and cardiac inflammatory response, attenuating cardiac fibrosis and potentially alleviating the mitochondrial dysfunction linked to hyperinflammation reaction.

1. Introduction

Chronic heart failure (CHF), one of the most life-threatening public health problems, has resulted in many global economic and living burdens. Ischemic events such as myocardial infarction (MI) have been acknowledged as the most common etiology of CHF [1]. Due to its intricate pathogenesis, over 30% of patients with normalized pharmacological therapies or mechanotherapy still experience deteriorations in cardiac function and poor prognosis during long-term follow-up [2, 3]. Hence, it is meaningful to explore additional available therapeutic strategies.

CHF secondary to the ischemia generally results in adverse cardiac remodeling [4]. Current knowledge suggests

that a sustained inflammatory response resulting from the initial myocardial injury, as well as the maladaptive cardiac energy metabolism due to mitochondrial dysfunction, jointly participate in decompensated ventricular remodeling [5–7]. Notably, chronic inflammation mediated by immune cells or proinflammatory cytokines has a close association with mitochondrial dysfunction [8]. For instance, a recent study reported that tumor necrosis factor α (TNF-α) preconditioning directly induced mitochondrial fragmentation and increased membrane potential and reactive oxygen species (ROS) overproduction in cardiomyocytes [9]. Moreover, mitochondrial-related damage accelerates inflammatory response in turn by activating the NLR family pyrin domain containing 3 (NLRP3) inflammasomes and downstream regulators of the immune signaling pathway like toll-like receptors (TLRs) [10, 11]. In short, the detrimental crosstalk between myocardial mitochondrial injury and hyperinflammation may further establish a damaging pathophysiological cycle and facilitate the ventricular remodeling [12].

The cholinergic anti-inflammatory pathway (CAP) is an endogenous self-protective mechanism connecting the autonomic neural reflex to immune regulation. Activating alpha 7 nicotinic acetylcholine receptors (α7nAChRs) expressed on macrophages or monocytes mediates a decrease in the transcription of downstream proinflammatory cytokines in the context of an intact vagal nerve [13–15]. Emerging evidence showed that cholinergic stimulation was able to improve cardiac remodeling and hemodynamics in the post-infarction rats, and this effect was reversed by the peripheral blockade of α7nAChR [16]. Other studies demonstrated the beneficial effect of activating the CAP on the arrhythmogenic substrate with ischemic cardiomyopathy, and the underlying mechanisms rely on the inflammation resolution and cardiac fibrosis attenuation [17, 18]. There are no ongoing studies regarding whether CAP elicitation ameliorates the myocardial mitochondrial injuries in the postinfarction state. Here, we aimed to study the following: (1) to verify the effect of cholinergic stimulation on ventricular remodeling especially in the cardiac energy metabolism state, in CHF models; (2) to ascertain the role of CAP activation in mitochondrial dysfunction in CHF; and (3) to uncover the potential mechanisms related to the cardioprotective effect of stimulating CAP.

2. Methods

2.1. Ethics Statement. All animal experiments were approved by the Animal Ethics Committee of the First Affiliated Hospital of Xinjiang Medical University (Approval Number: IACUC-20200318-74). All studies were conducted under the Basel Declaration and in accordance with the criteria of the Association for Assessment and Accreditation of Laboratory Care (AAALAC).

2.2. Animal Preparation. Eighty male purebred specific pathogen-free (SPF) Sprague-Dawley (SD) rats (5 months old), weighing 250-300 g, were purchased from the Animal Laboratory Center of Xinjiang Medical University. The animals were reared in rat cages under SPF-grade normalized laboratory conditions (12-hour light/dark cycle, 22°C, 45% humidity) with available food and water. Postoperative surviving rats were divided into 5 groups according to reduced left ventricular (LV) ejection fraction values (LVEF < 50%) with the following different interventions: sham group (thoracotomy only, $n = 10$), CHF group (coronary artery ligation for 5 weeks, $n = 11$), CHF+Vag group (CHF with right cervical vagotomy, $n = 10$), CHF+PNU group (CHF rats treated with PNU-282987, $n = 11$), CHF+Vag+PNU group (postvagotomy CHF rats treated with PNU-282987 administration, $n = 10$).

2.3. Surgical Procedures

2.3.1. MI Establishment. All operations were carried out in a laminar flow room under aseptic conditions. Before all the invasive manipulations, each rat was generally administered 1 ml of sodium pentobarbital (2 mg/100 ml) to induce anesthesia and atropine (0.05 mg/kg) to prevent airway secretions. A multichannel physiology recorder (Lead-7000 EP CONTROL, Sichuan, China) was used to monitor the intraoperative heart rate. The anesthetized rats were fixed on a bubble brick and placed in the right lateral position. A cannula with an outer diameter of 2.5 mm (Jinkou 2.5 mm, Yu Yan Instruments, Shanghai), which was connected to the animal respirator (Ugo Basile 5025), was used for tracheal intubation with a tidal volume of 8 ml/kg. The left ventricle was exposed after thoracotomy at the left third intercostal space. The left anterior descending (LAD) branch was ligated approximately 2–3 mm below the left atrial appendage (LAA) with a 7–0 polyglactin suture. The successful MI model was determined by the ST-segment alterations from the II-lead of the ECG during a postoperative half hour. After the surgery, 50 mg of pethidine and 400 U of penicillin were administered intramuscularly for analgesia and infection prevention, respectively [19].

2.3.2. Vagotomy. We subjected CHF rats to the right cervical vagotomy during anesthesia in the fifth week. The skin was incised along the right cervical line before the blunt dissection of the subcutaneous muscle layer. The right cervical vagal nerve was located in the carotid sheath, meticulously isolated by a glass needle, and cut off with ceramic scissors [20]. After the vagotomy, the incised skin was closed with interrupted sutures, and the rats were individually housed.

2.3.3. Cholinergic Elicitation. PNU-282987, a selective α7nAChR agonist (APExBIO, No. B7007, USA) was dissolved in 0.2% DMSO organic solvent and thoroughly oscillated at 37°C until the particles had completely dissociated. Cholinergic stimulation was conducted for 4 weeks with PNU-282987 (1 mg/kg) via a slow intraperitoneal injection for 2 minutes in the CHF rats [17].

2.4. Echocardiography. Transthoracic echocardiography was performed weekly beginning in the first postinfarction week and lasting until the fifth week. Echocardiographic examination was implemented with a Philips HD11XE transthoracic Doppler ultrasound imaging system (Philips Inc., Bothell, WA, USA) as described in our previous work [21]. The

short-axis views of the left ventricle were recorded by two-dimensional M-mode tracing at the level of the papillary muscle. The main measured indices were as follows: LV end-diastolic dimension (LVEDd), LVEF, and LV fraction shortening (LVFS). At least three consecutive cardiac beats were measured for every result.

2.5. Enzyme-Linked Immunosorbent Assay (ELISA). The plasma levels of inflammatory factors, metabolic indices, and brain natriuretic peptide (BNP) were detected by ELISA. Whole blood samples were obtained from the canthus veins of rats and stored in the EDTA tubes after the completion of in vivo interventions for standby. The plasma was collected after centrifugation at 3000 r for 15 minutes. The levels of TNF-α, IL-1β, IL-6 (Multi Science Biotech, China, 70-EK382/3-96, 70-EK301B/3-96, 70-EK306/3-96), insulin (INS), BNP (Cusabio, China, CSB-E05070r, CSB-E07972r), glucose (Glu), and nonesterified fatty acid (NEFA) (Nanjing Jiancheng Bioengineering Institute, China, F006-1-1, A042-2-1) were measured with ELISA kits according to the manufacturer instructions. Absorbance (OD) value determination was performed at wavelengths of 450 nm and 570 nm within 30 minutes after the addition of termination fluid. The calibrated OD value was obtained by subtracting the measured value at 570 nm from the OD value at 450 nm.

2.6. Transmission Electron Microscopy (TEM). The animals were euthanized by overdose anesthesia at the end of this experiment. Tissues were collected from the peripheral infarction area of the LV lateral wall. Each specimen was trimmed to approximately 1 mm^3 size and directly immersed in precooled 2.5% glutaraldehyde at 4°C overnight (Sbjbio, China, SBJ-0639M). Then, the fixed specimens were subjected to gradient dehydration in an acetone solution, uranium acetate staining, and lead citrate staining as described in our previous study [22]. The ultrastructure of cardiomyocytes was observed by a JEM-100 CXII TEM (JEOL, Japan, 80 kV), and images were captured at 500x magnification.

2.7. Adenosine Triphosphate (ATP) Concentration Determination. Fresh tissue samples were prepared, homogenized, and centrifuged to extract the supernatant (3000 r/min, 15 minutes). The LV myocardium ATP levels were examined by an ATP assay kit (Nanjing Jiancheng Bioengineering Institute, China, A095-1-1) according to the product instructions. OD values of the tested samples were measured at a wavelength of 636 nm, and ATP concentrations were calculated based on the standard curve.

2.8. Histology Study. LV tissues were cut into small pieces, fixed with 4% paraformaldehyde, and embedded in paraffin. Hematoxylin-eosin (HE) staining, Masson's trichrome staining, and picrosirius red staining were performed on the 5 μm thick histological sections to analyze LV fibrosis in the light of our previous method [23]. Eight paraffin blocks per group were taken for the tissue slide preparation and 9 separate bright field microscopic images per animal were quantified. The degree of fibrosis was analyzed by ImageJ software version 1.8.0. The fibrosis size was defined as the proportion of the collagen-positive area in the total myocardial area.

2.9. Immunohistochemistry. Tissue paraffin blocks of different groups were selected to be sliced and subjected to specimen preparation, antigen repair, and background sealing. Primary antibodies against CD68 (ab125212, Abcam, Cambridge, UK) and CD163 (ab182422, Abcam, Cambridge, UK) were added to the tissue sections and detected by the goat anti-rabbit IgG (H&L) secondary antibodies (ab150077, Abcam, Cambridge, UK). Similar to the quantitative method in histology, immunoreactivity was expressed as the entire positive staining area per square millimeter and was calculated manually by ImageJ software version 1.8.0.

2.10. Terminal Deoxynucleotidyl Transferase dUTP Nick End Labeling (TUNEL) Staining. LV peri-infarct myocardial tissue was embedded in paraffin and routinely sliced into 5 μm sections for TUNEL staining. After a series of processes including deparaffinization, rehydration, and cell transparency, 50 μl of the TUNEL mixture was added to the sections according to the instructions for the kit (No.11684817910, Roche, USA). Subsequently, the sections were incubated with converter pods for 30 minutes at 37°C, and DAB color reagent was used for chromogenic detection. Analysis of the apoptosis rate, which reflected the myocardial apoptosis level, was performed by selecting eight slides in each group randomly and then taking photos manually by laser scanning confocal microscopy (LSCM). The proportion of apoptotic cardiomyocytes was also measured using Image-Pro Plus software version 6.0.

2.11. Cell Culture and Treatment. H9C2(2-1) cells (Cell Bank, Chinese Academy of Sciences) were incubated in 90% DMEM medium (12800017, GIBCO) containing $NaHCO_3$ (1.5 g/l) and supplemented with 10% high-quality FBS (HN-FBS-50, HAKATA). All cell lines were cultured in a 5% CO_2 atmosphere at 37°C. Cell viability was measured by a cell growth curve, and cell proliferation was evaluated by the CCK-8 growth curve. Different concentrations of TNF-α (0, 5, 10, 20, 30, and 50 ng/ml) were used for choosing the optimal concentration in vitro treatment of cell lines. Untreated H9C2 cells were added as a comparison control group.

2.12. Flow Cytometry

2.12.1. ROS Measurements. Intercellular ROS were detected by flow cytometry. Ventricular tissues were ground and filtered through a sieve to prepare a single-cell suspension. H9C2 cell lines were collected from the 6-well plates. Both the cell suspension and H9C2 cells were incubated with 2 ml phosphate-buffered saline (PBS) and 2 μl of dichlorodihydrofluorescein diacetate (DCFH-DA) for 30 minutes. Next, all resuspended cells were transferred to a luciferase microplate reader (VLB000D2, Thermo Fisher) to acquire the fluorescence intensity. The optimum fluorescence excitation and emission wavelengths were set at 500 nm and 525 nm, respectively.

2.12.2. Mitochondrial Membrane Potential (MMP) Measurement. After being centrifuged for 5 minutes at 1000 r, H9C2 cells were resuspended in JCI-1 staining fluid,

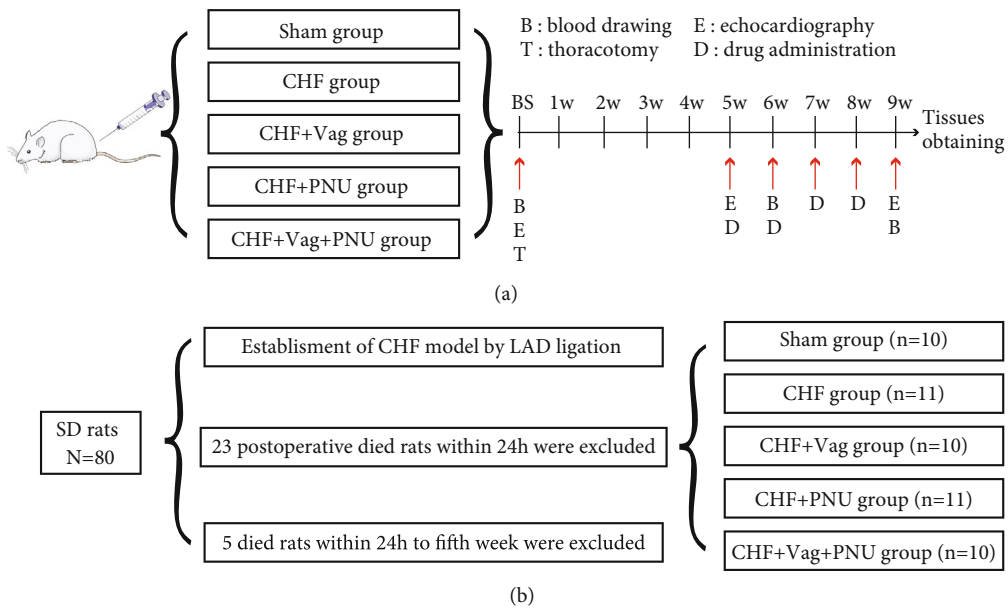

Figure 1: Flow chart of the experiment process: (a) study protocol diagram; (b) grouping criterion.

incubated at 37°C for 20 minutes, and washed twice with precooled PBS. Then, we added 500 μl cells resuspended in PBS and passed the sediments through a 200-filter mesh to prepare a single-cell suspension. TNF-α-induced MMP levels were assessed with 30 minutes using flow cytometry.

2.12.3. Mitochondrial Permeability Transition Pore (mPTP) Measurement. The cells were lysed in a lysis buffer, preliminarily transferred, and centrifuged. Then, we added 1 ml of calcein AM staining solution to 10 ml of assay buffer, and the mixture was used to resuspend the cells. Moreover, a tube of cells in 1 ml of PBS was used as the negative control group. The single-cell suspension was prepared as previously mentioned. mPTP assessments were also achieved by flow cytometry.

2.12.4. Apoptosis Evaluation. The acquisition and collection of cells from tissue and cell lines were similar to the procedures described for measuring ROS. The single-cell suspension was prepared by adding 500 μl of 1x binding buffer to resuspend the cells, which were passed through a 200-filter mesh. Five microliters of Annexin V-PE and 10 μl of 7-AAD were added to each tube. After gentle mixing and 10 minutes of rest at 4°C, flow cytometry was performed within 30 minutes.

2.13. Western Blotting. Excised ventricular tissues were promptly transferred to liquid nitrogen, and tissue homogenate was prepared. Tissue and cell samples were lysed with 200 μl of RIPA lysis buffer with protease inhibitors and mixed adequately on a shaker for 1 hour. The supernatant was collected after high-speed centrifugation for 15 minutes at 15000 rpm. Protein concentrations were determined by a BCA assay kit (23235, Thermo Fisher). The quantified protein was mixed with 5x loading buffer and boiled for 5 minutes at 100°C. Electrophoresis was performed using a 10% SDS-PAGE separation gel. Semidry transfer was carried out on the PVDF membrane for 60 minutes at 100 V. Then, 5% BSA powder sealant was used to seal the membrane. After incubating overnight at 4°C with primary antibodies, we incubated the membrane with diluted secondary antibodies at room temperature for 1 hour. Finally, the chemiluminescence reagent was selected for coloration. H9C2 cells were rapidly scraped from the culture dish surface rapidly. Three tissue samples and 4 cell samples per group (25 cm^2 cell culture flasks) were used for western blotting quantification. Every blot was conducted in duplicate. The following primary antibodies were used: anti-caspase-3 (ab184787, Abcam, Cambridge, MA, USA), anti-Bcl-2 (ab59348, Abcam, Cambridge, MA, USA), anti-Bax (ab182734, Abcam, Cambridge, MA, USA), anti-Drp1 (ab184247, Abcam, Cambridge, MA, USA), anti-Fis1 (ab71498, Abcam, Cambridge, MA, USA), anti-Mfn1 (ab221661, Abcam, Cambridge, MA, USA), anti-Mfn2 (ab124773, Abcam, Cambridge, MA, USA), anti-Opa1 (ab157457, Abcam, Cambridge, MA, USA), anti-α7nAChR (ab182442, Abcam, Cambridge, MA, USA), anti-NF-κB (ab16502, Abcam, Cambridge, MA, USA), antiphosphorylated NF-κB (ab86299, Abcam, Cambridge, MA, USA), anti-JAK2 (ab108596, Abcam, Cambridge, MA, USA), antiphosphorylated JAK2 (ab32101, Abcam, Cambridge, MA, USA), anti-STAT3 (ab68153, Abcam, Cambridge, MA, USA), and antiphosphorylated STAT3 (ab76315, Abcam, Cambridge, MA, USA).

2.14. Statistical Analysis. All raw data were input into Excel version 2007 and were analyzed by SPSS version 26.0. Continuous variables between the control and the TNF-α group are described by means ± standard deviations and were analyzed by Student's t -tests. Univariate ANOVA with Bonferroni post hoc comparisons was used to analyze the differences in cardiac function parameters, circulating marker levels, local immune infiltration degrees, fibrosis

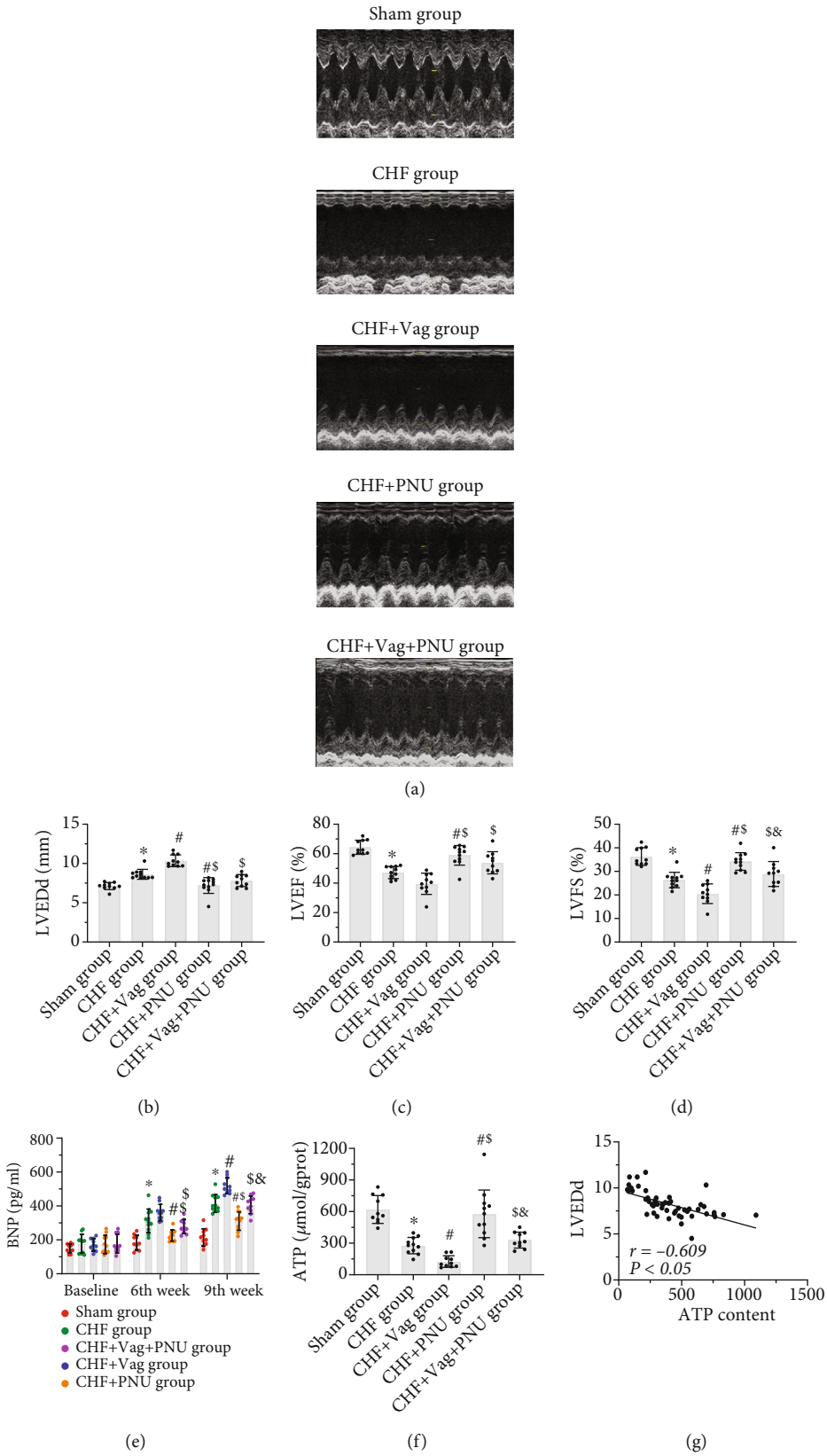

Figure 2: Continued.

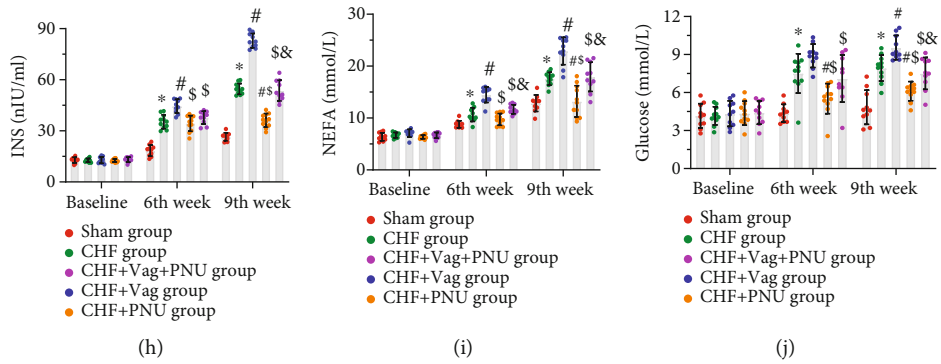

Figure 2: Effects of cholinergic elicitation on cardiac dysfunction and cardiac energy metabolism alterations. Representative M-mode echocardiogram of short-axis views from five groups (a). Comparisons of LVEDd (b), LVEF (c), LVFS (d), and ATP (F) among five groups. Correlation between LVEDd values of the 9th week and ATP contents (g). Differences of BNP (e), INS (h), NEFA (i), and glucose (j) among five groups at baseline, the 6th week, and the 9th week. $^{*}P < 0.05$ vs. Sham group. $^{\#}P < 0.05$ vs. CHF group. $^{\$}P < 0.05$ vs. CHF+Vag group. $^{\&}P < 0.05$ vs. CHF+PNU group. LVEDd: left ventricular end-diastolic dimension; LVEF: left ventricular ejection fraction; LVFS: left ventricular fraction shortening; BNP: brain natriuretic peptide; ATP: adenosine triphosphate; INS: insulin; NEFA: nonesterified fatty acid.

and apoptosis extents, and protein expression levels among the five groups. Correlations between LVEDd and the levels of IL-1β, IL-6, TNF-α, and ATP levels were analyzed by Pearson's correlation coefficient. Statistical significance was defined as a 2-tailed P value < 0.05.

3. Results

3.1. Cholinergic Elicitation Restored Cardiac Dysfunction and Myocardial Energy Metabolism Alterations. All experimental procedures were conducted according to the study protocol (Figure 1(a)). In this study, the postoperative mortality of rats was approximately 30% (Figure 1(b)). Typical M-mode ultrasound schematic diagrams are shown in Figure 2(a). For echocardiographic data during the 9th week, the LVEDd was enlarged in the CHF group in comparison to that in the sham group, and this parameter was further increased in the Vag group while decreased in the PNU group ($P < 0.05$, Figure 2(b)). The LVEF and LVFS values obviously declined in the Vag group. Compared to those in the CHF group, both the LVEF and LVFS values were larger in the sham and PNU groups ($P < 0.05$, Figures 2(c) and 2(d)). As shown in the Vag+PNU group, vagotomy counteracted the protective effect of PNU on LVFS but not LVEDd or LVEF ($P < 0.05$, Figure 2(d)). The exact values of the echocardiographic parameters are displayed in Supplemental Table 1. The decline in intramyocardial ATP contents in the CHF state was prevented by PNU treatment and was exacerbated by vagal mutilation ($P < 0.05$, Figure 2(f)). Correlation analysis showed that the ATP level negatively moderately correlated with LVEDd ($r = -0.609$, $P < 0.05$, Figure 2(g)). The changes in BNP, INS, NEFA, and Glu levels in the five groups showed a consistent trend with LVEDd from the 6th week to the 9th week, which was enhanced by vagotomy and weakened by PNU administration. Until the 9th week, compared with those in the PNU group, four indicator values in the Vag+PNU group increased (Figure 2(e) and Figures 2(h)–2(j)).

3.2. Cholinergic Elicitation Inhibited Systemic Inflammation and Cardiac Macrophage Infiltration in the Postinfarct Phase. The levels of three cytokines (IL-1β, IL-6, and TNF-α) that participate in the systemic inflammatory response are shown in Figures 3(e)–3(i). As expected, the plasma levels of these three proinflammatory factors in plasma were lowered by one week of PUN administration but were increased by vagotomy, and this trend persisted until the 9th week. Pearson's correlation analysis showed the moderate positive correlations between IL-1β, IL-6, and TNF-α and LVEDd (IL-1β: $r = 0.691$, $P < 0.05$; IL-6: $r = 0.717$, $P < 0.05$; TNF-α: $r = 0.824$, $P < 0.05$, Figures 3(f)–3(j)). Immunohistochemical staining was used to evaluate the abundance of local macrophages in the myocardium. As presented in Figures 3(a) and 3(b), $CD68^{+}$ and $CD163^{+}$ macrophages, which represented the M1-like and M2-like phenotypes, respectively, were mostly found in the peri-infarction border areas at the 9th week post-MI. Quantitative analysis demonstrated that the number of $CD68^{+}$ macrophages increased in the Vag group and decreased in the PNU group, whereas the numbers of $CD163^{+}$ macrophages peaked in both the Vag and PNU groups ($P < 0.05$). The impact of PNU cure on macrophage infiltration was counteracted by vagotomy to some extent ($P < 0.05$, Figures 3(c) and 3(d)).

3.3. Cholinergic Elicitation Suppressed Cardiac Fibrosis. Four typical pathological changes were detected by HE staining and are shown in the Supplementary Figures online. As displayed in Figure S1A, some cardiomyocytes were covered by the accumulated inflammatory cells in a cross-sectional view. The vast formation of connective tissue in the perivascular space is presented in Figure S1B. In Figure S1C, a mass of fibrous tissue hyperplasia was accompanied by few inflammatory cells distributed around the myocardial interstitial substance. Figure S1D shows that the disrupted cardiomyocytes were replaced by the extensive production and deposition of fibrous tissue. HE staining shows scar regions in the five groups (Figure 4(a)). The Masson's trichrome staining and picrosirius red staining were performed to identify the differences in collagen deposition among the five groups. The

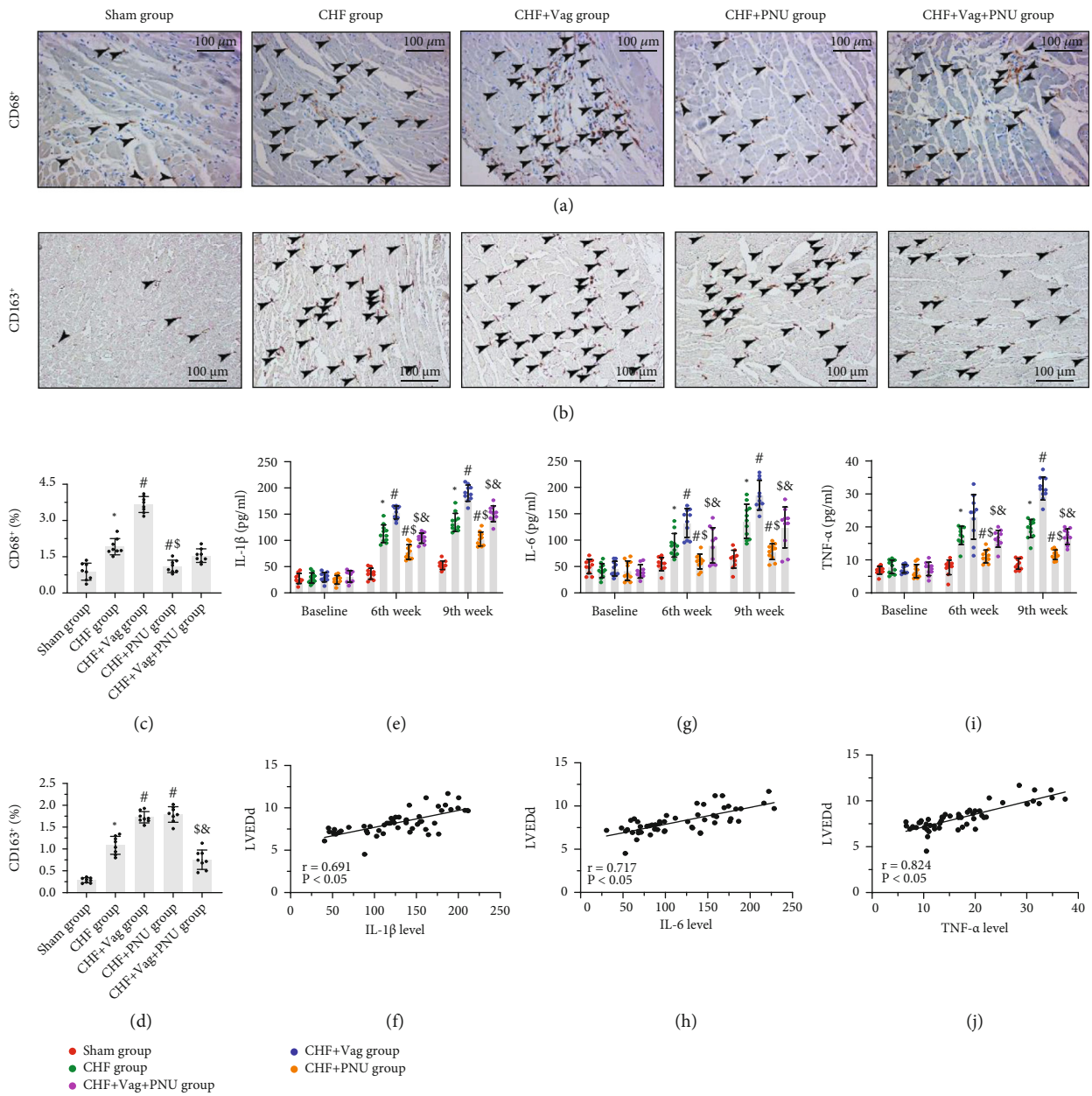

Figure 3: Effects of cholinergic elicitation on systemic inflammation and cardiac macrophage infiltration. Typical images of $CD68^+$ staining (a) (×20) and $CD163^+$ staining (b) (×20) among five groups. Quantitative analysis of immunohistochemical results (c, d). Comparisons of IL-1β (e), IL-6 (g), and TNF-α (i) among five groups at three time points at baseline, the 6th week, and the 9th week. Correlations of LVEDd values of the 9th week with IL-1β (f), IL-6 (h), and TNF-α (j) levels of the 9th week. $^{*}P < 0.05$ vs. Sham group. $^{\#}P < 0.05$ vs. CHF group. $^{\$}P < 0.05$ vs. CHF+Vag group. $^{\&}P < 0.05$ vs CHF+PNU group. IL-1β: interlukin-1β; IL-6: interlukin-6; TNF-α: tumor necrosis factor α.

Masson's trichrome staining showed that there were no significant differences in the total collagen areas between the CHF and Vag groups ($P < 0.05$, Figure 4(b)). However, as shown in the picrosirius red-stained sections, chronic infarction/ischemia induced collagen accumulation, which were reduced by PNU administration and were augmented by vagotomy ($P < 0.05$, Figure 4(c)).

3.4. Cholinergic Elicitation Alleviated Mitochondrial-Dependent Apoptosis. TUNEL staining was used to assess myocardial apoptosis. As shown in Figure 5(a), the number of brown DIG-d-UTP-stained brown cells, which represented apoptotic cells, was markedly increased in CHF and Vag groups and decreased in the PNU group ($P < 0.05$, Figures 5(a) and 5(b)). Three proteins related to the mitochondrial apoptotic pathway were tested by western blotting. Quantitative analysis showed that the expression levels of caspase-3 and Bax were elevated in the CHF phase and were further upregulated by vagus transection and downregulated by PNU treatments. In contrast, the relative expression of Bcl-2 was reduced in the Vag group and augmented in the PNU group ($P < 0.05$, respectively, Figures 5(c)–5(g)).

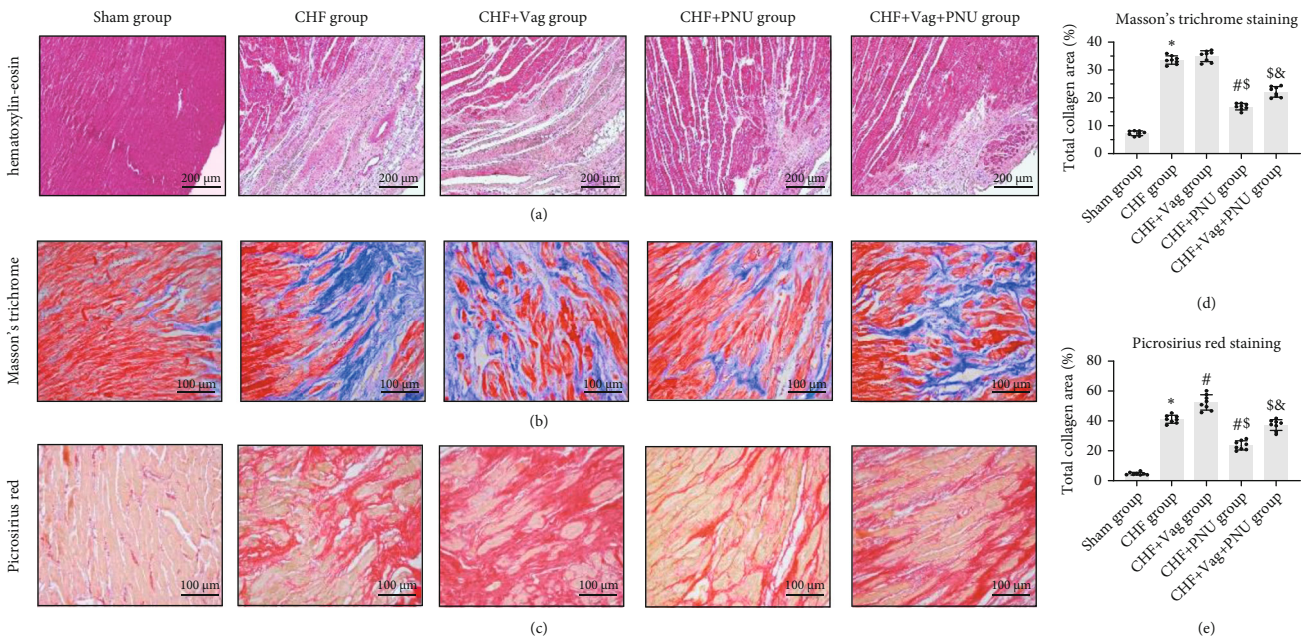

Figure 4: Effects of cholinergic elicitation on cardiac fibrosis. Representative images of scar ranges by HE staining in five groups (a) (×10). Masson's trichrome staining and picrosirius red staining of left ventricular noninfarct sections in five groups (b, c) (×20). Quantitative statistics of collagen contents (d, e). $^{*}P < 0.05$ vs. Sham group. $^{\#}P < 0.05$ vs. CHF group. $^{\$}P < 0.05$ vs. CHF+Vag group. $^{\&}P < 0.05$ vs. CHF+PNU group.

3.5. Cholinergic Elicitation Attenuated the Myocardial Ultrastructural Changes. Cardiomyocyte ultrastructural changes are shown in Figure 6. In the sham group, the well-defined mitochondria and intact sarcomeres were arranged regularly, and there were clear Z-lines. The abundant mitochondria are shown in the detailed panel. However, a panel of the CHF group showed the damaged mitochondria scattered among snatchy Z-lines tangled with the disorganized myofibers. In the CHF group, most mitochondria were present with dissociated myofibers near a few distinct lipid droplets. Similarly, a large area of impaired mitochondria accompanied by broken fibers was present in the CHF+Vag group. Furthermore, a reduction in mitochondria, the disappearance of inner and outer membranes, the absence of cristae, and mitochondrial vacuolization were clearly observed. In the CHF+PNU group, lipid droplets were surrounded by lysosomes, and most mitochondria maintained regular morphologies with slightly swollen mitochondrial cristae. Finally, the CHF+Vag+PNU group exhibited distorted cristae and discontinuous membranes.

3.6. Cholinergic Elicitation Blunted the Myocardial Mitochondrial Injury. Typical flow cytometry images are shown in Figure 7(a). Quantitative analysis demonstrated that ROS levels increased in the Vag group and decreased in the PNU group ($P < 0.05$, Figure 7(b)). PNU treatment significantly downregulated mitochondrial fission-related proteins, such as Fis1, and upregulated fusion-related proteins as Mfn1 and Opa1, in comparison to those postvagotomy. However, the expression levels of other mitochondrial fission-related protein as Drp1 and fusion-related protein as Mfn2 showed insignificant differences among five groups ($P > 0.05$, Figures 8(a)–8(f)). The expression of membrane receptor α7nAchR was downregulated by vagotomy and was partially counteracted by PNU administration ($P < 0.05$, Figure 8(g)). Besides, vagotomy obviously lowered the expression levels of phosphorylated transcription factors NF-κB and STAT3, which were rescued by PNU treatment ($P < 0.05$, Figures 8(i) and 8(m)). On the contrary, the protein levels of both NF-κB, JAK2, phosphorylated JAK2, and STAT3 were not altered among five groups ($P > 0.05$, Figures 8(h) and 8(j)–8(l)).

3.7. TNF-α Mediated Mitochondrial Injury in Cardiomyocytes in a Concentration-Dependent Manner. A TNF-α gradient experiment was performed to determine a target concentration for in vitro experiments. Growth curve of H9C2 cells was depicted in Figure 9(a). With increasing concentrations of TNF-α from 0 ng/ml to 50 ng/ml, intercellular ROS production increased (Figure 9(b)). TNF-α at 50 ng/ml was chosen for the optimal intervention concentration in vitro study. As anticipated, compared with the control group, TNF-α induced cardiomyocyte apoptosis and facilitated the reduction in MMP and opening of the mPTP without affecting cell proliferations (Figure 9(c), $P > 0.05$; Figures 9(d)–9(f), $P < 0.05$, respectively). Consistent with the western blot results at the tissue level, TNF-α stimulation significantly inhibited mitochondrial fusion-related markers such as Mfn1 and Opa1 ($P < 0.05$, Figure 9(g)).

4. Discussion

The major findings of the present study were as follows: (1) CAP activation ameliorated the impaired cardiac function, reduced the LV dilatation, and restored abnormal Glu and lipid metabolism in the chronic infarction phase; (2) CAP

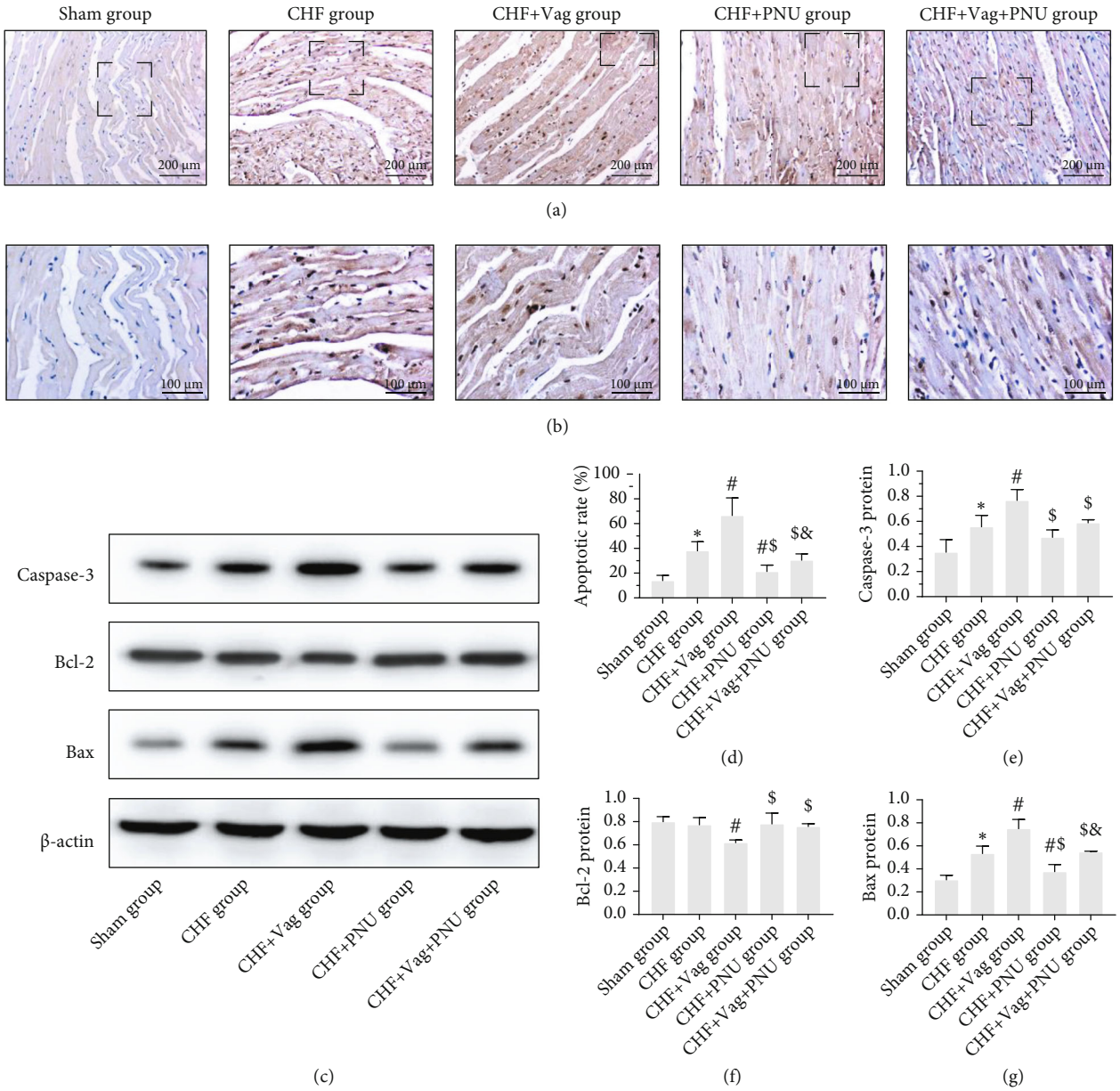

Figure 5: Effects of cholinergic elicitation on mitochondrial-dependent apoptosis. Representative images and detailed drawings of TUNEL staining among five groups ((a) ×10; (b) ×20). Western blot results for caspase-3, Bcl-2, and Bax of five groups (c). Quantitative statistical results of apoptotic rate (d) and relative expression levels of apoptosis-related proteins (e–g). $^{*}P < 0.05$ vs. Sham group. $^{\#}P < 0.05$ vs. CHF group. $^{\$}P < 0.05$ vs. CHF+Vag group. $^{\&}P < 0.05$ vs. CHF+PNU group. Bcl-2: B cell leukemia/lymphoma 2; Bax: Bcl-2-associated X.

induction mitigated systemic and local cardiac inflammatory response and suppressed myocardial fibrosis; (3) CAP elicitation prevented the mitochondrial dysfunction by inhibiting mitochondria-dependent apoptosis, ameliorating ROS overload, and promoting mitochondrial fusion; and (4) the phosphorylation of STAT3 and NF-κB in cardiomyocytes was involved in the cardioprotective effect of positively modulating the CAP (Figure 10).

Clinically, CHF challenged by MI tends to be a consequence of cardiac pathologic remodeling during the postinfarction late phase [24]. First, in order to simulate the pathophysiological features of ischemic HF, we established the postinfarction CHF models, which successfully mimicked the hallmarks including the altered ventricular structure, the impaired pump function, and disordered energy metabolism after a five-week cardiac remodeling period [25, 26].

Then, in order to examine the macroscopic effect of CAP modulation on cardiac dysfunction and energy metabolism state, we bidirectionally manipulated CAP activities with PNU treatment and vagotomy in the 6th week. Coinciding with previous results regarding the salutary effect of cholinergic induction on cardiac dysfunction [27–29], we demonstrated that activating the CAP improved ventricular structural remodeling and mechanical function, as evidenced by echocardiographic parameters and BNP levels.

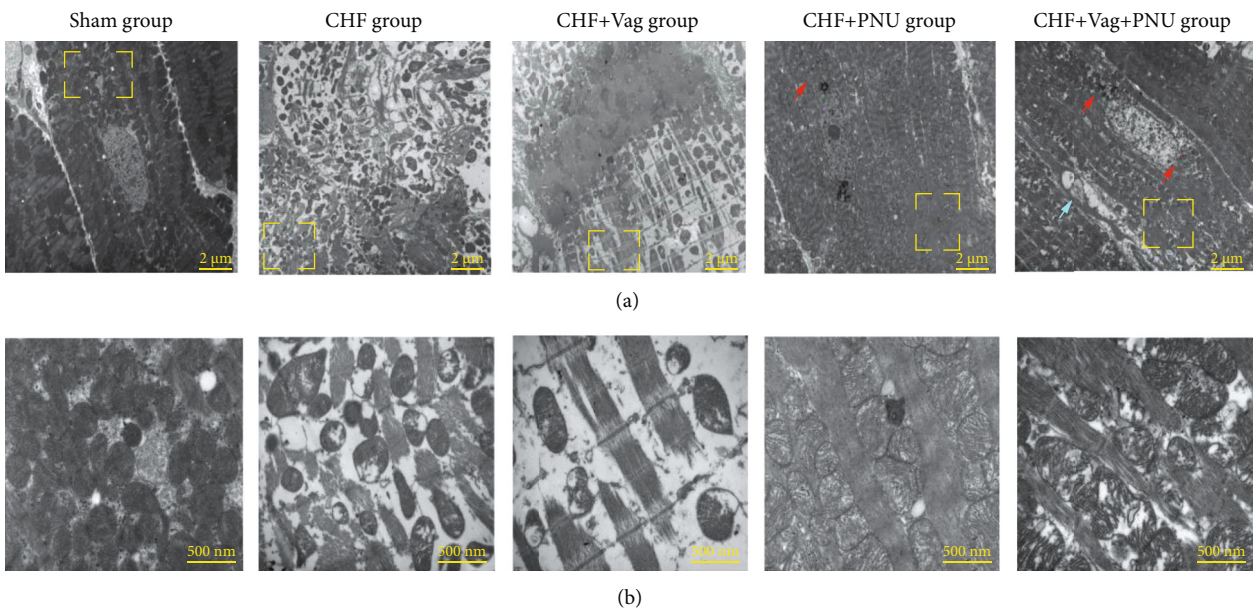

Figure 6: Effects of cholinergic elicitation on cardiomyocyte ultrastructural alterations. General observation (a) (×5000) and detailed view (b) (×30000) of transmission electron microscopy among five groups. Red arrow: mitophagy of autolysosome phase; green arrow: mitophagy of phagophore phase; blue arrow: mitophagy of mitophagolysosome phase.

For the first time, to our knowledge, we reported that the levels of INS, NEFAs, and Glu continuously increased in CHF rats, which was partly inhibited by CAP stimulation and exacerbated by vagotomy. To explain this result, physiological evidence suggested that enhanced lipolysis induced by hypersympathetic activities worsened the reduction in Glu uptake and increased insulin resistance in advanced HF [30]. It was verified that cholinergic elicitation can modulate autonomic nerve activity and especially suppress sympathetic activities in many cases [31, 32]. In addition, we found that insufficient ATP levels were moderately correlated with LV expansion, and an improved energy supply was achieved by targeting the CAP. From these observations, we hypothesized that mitochondria, which link substrate utilization and ATP production, may be essential for the protective effect of cholinergic stimulation.

Next, we focused on the three key pathophysiological responses to HF progress (inflammation, fibrosis, and mitochondrial injury) to describe the detailed beneficial effects of cholinergic elicitation. Solid evidence suggests that a prolonged inflammatory response challenged by myocardial injury, namely, chronic inflammation, is implicated in pathological cardiac remodeling and also has the crosstalk with cardiac fibrosis and mitochondrial injuries [33–35]. In our study, the systemic inflammatory reaction in the postinfarction stage was mitigated by activating the CAP but intensified by unilateral vagotomy, as proven by serum proinflammatory cytokine levels. The levels of IL-1β, IL-6, and TNF-α changed from the first week after intervention, which suggested a rapid anti-inflammatory effect of cholinergic stimulation. However, circulatory cytokine levels are susceptible to the anti-inflammatory effect of peripheral organs when the CAP is activated and fails to reflect the regional cardiac inflammation [36, 37]. Thus, immunohistochemistry was performed to examine cardiac macrophage infiltration. In a prior study, stimulating the CAP was shown to promote the transformation of Ly-6C^{high} macrophages to Ly-6C^{low} macrophages in the late infarction phase [17]. Similarly, our results showed that cholinergic evocation reduced the accumulation of M1 macrophages and increased M2 macrophages infiltration in the peri-infarct area. A reasonable explanation for this result is that anti-inflammatory cytokines released from M2 macrophages limit the activation and proliferation of M1 macrophages [38]. Interestingly, a question originating from our study is why M1 and M2 macrophages maintain the high abundances in the Vag group. This effect may occur because the biological functions of recruited macrophages at injured sites as proinflammation or repair are dependent on microenvironmental stress [39]; that is, the enhanced macrophage plasticity synchronously tends to the proinflammation and anti-inflammation preponderances in the absence of vagus [40]. In terms of the pathological results, upregulating the CAP ameliorated cardiac fibrosis in the peri-infarction area, while vagus transection partially offsets this protective effect. Previous evidence supported that macrophage polarization plays an important role in the process of cardiac fibrosis [41]. In our study, the decrease in M1 macrophages induced by cholinergic elicitation may mediate attenuation of extracellular matrix remodeling by downregulating the expression of matrix metalloproteinase, TNF-α, and IL-1 [42].

Most importantly, we reported the ameliorative effect of CAP activation on mitochondrial injuries under CHF conditions for the first time. In the context of chronic inflammation, detrimental cytokines such as TNF-α trigger mitochondrial dysfunction via inducing ROS overproduction and further beget a series of downstream events as apoptosis and hyperinflammation [8]. Mitochondria-mediated apoptosis relies on the inhibition of Bcl-2 and the activation

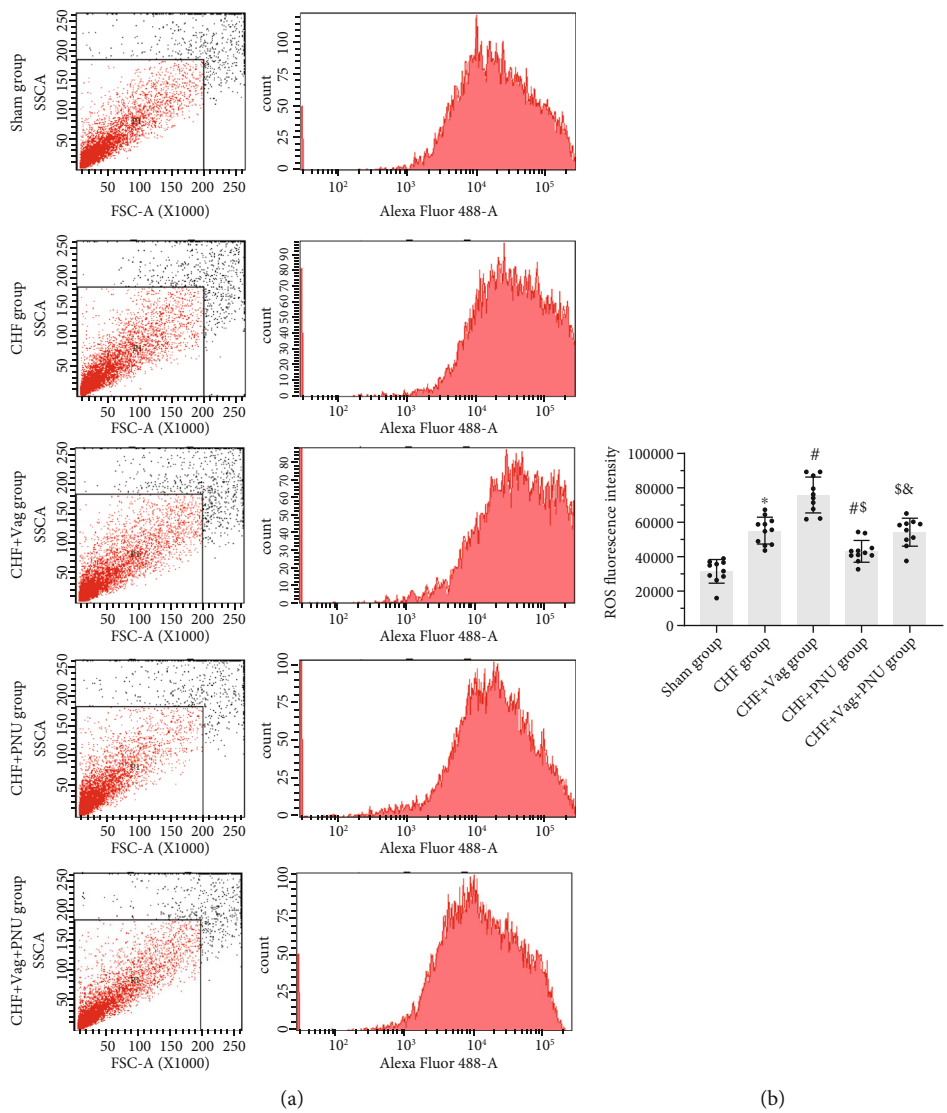

Figure 7: Effects of cholinergic elicitation on cardiac ROS production. Typical images of ROS production by flow cytometry among five groups (a) and the related quantitative analysis (b). $^{*}P < 0.05$ vs. Sham group. $\#P < 0.05$ vs. CHF group. $\$P < 0.05$ vs. CHF+Vag group. $^{\&}P < 0.05$ vs. CHF+PNU group.

of Bax and caspase-3/7 [43]. Here, we observed a decline in ROS overload in the PNU group and the alleviation of cardiomyocyte apoptosis, especially the mitochondria-mediated apoptosis, according to changes in mitochondrial apoptosis-related proteins such as caspase-3, Bcl-2, and Bax. Different periods of ongoing mitophagy were discovered by TEM, including the segregation of damaged mitochondria and degradation mediated by lysosomes. Regrettably, no further investigation was conducted in allusion to mitophagy in the present study. It has been widely reported that steady mitochondrial dynamics confer extensive advantages to mitochondrial biogenesis and cellular events [44]. Thereupon, we detected the changes in key proteins implicated in mitochondrial dynamics under CAP initiation. Confusingly, the expression of both Mfn1 and Opa1 was upregulated in the PNU group and downregulated in the Vag group, while Fis1 but not Drp1 expression changed after cholinergic interventions. We merely speculated that CAP induction potentially drove more healthy mitochondrial fragments toward rebirth through mitochondrial fusion mediated by Mfn1 and Opa1 [45], but the exact mechanisms remain unclear.

In consideration of the beneficial effect of CAP elicitation, numerous studies have focused on the activated JAK/STAT3 pathway and NF-κB/HMGB1/RAGE pathway in immune cells [46]. Our study suggested that the activation of STAT3 and inactivation of NF-κB were implicated in the cardioprotective effects of CAP stimulation, possibly due to the negative modulations of these two transcription factors on downstream phenotypes like inflammation, apoptosis, and MPTP activities, through the signaling cascade triggered by TNF-α/TNFR [47].

Finally, an in vitro cell experiment was performed to validate the association of mitochondrial injury with proinflammatory cytokines. As expected, together with the reductions in MMP and mPTP opening, the major event of mitochondrial apoptosis [48] was increased markedly when

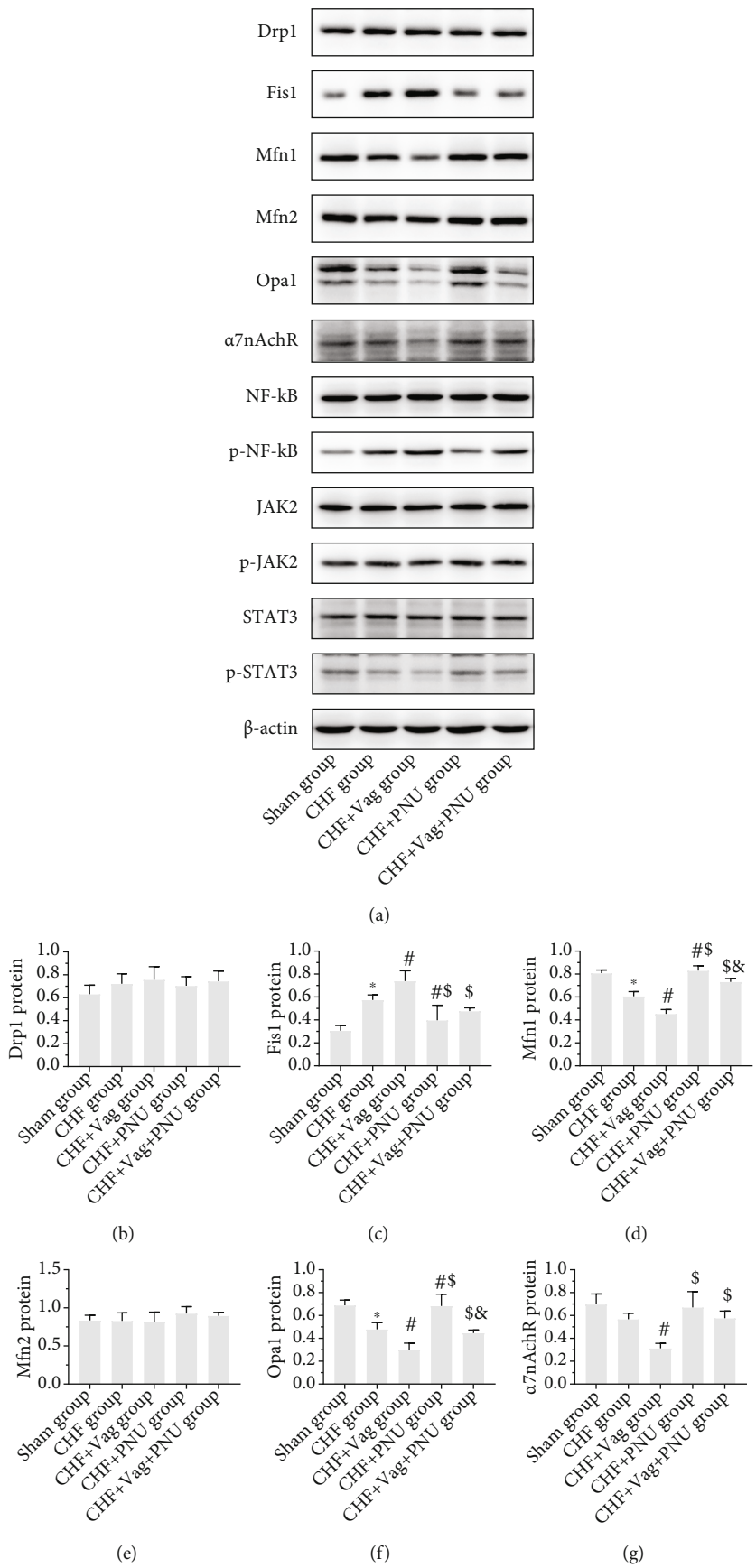

Figure 8: Continued.

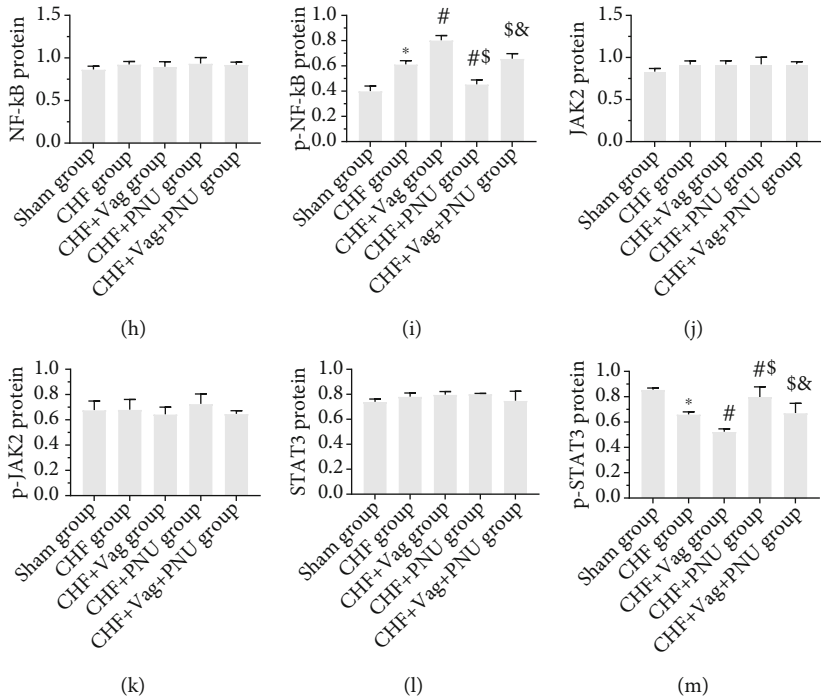

Figure 8: Effects of cholinergic elicitation on myocardial mitochondrial dynamics and the activities of NF-κB and JAK2/STAT3 pathway. Western blot results and quantitative statistics for Drp1, Fis1, Mfn1, Mfn2, Opa1, α7nAChR, NF-κB, P-NF-κB, JAK2, P-JAK2, STAT3, and p-STAT3 (a–m). $^{*}P < 0.05$ vs. Sham group. $^{\#}P < 0.05$ vs. CHF group. $^{\$}P < 0.05$ vs. CHF+Vag group. $^{\&}P < 0.05$ vs. CHF+PNU group. Drp1: dynamin-related protein 1; Fis1: fission, mitochondrial 1; Mfn1: mitofusin 1; Mfn2: mitofusin 2; Opa1: OPA1 mitochondrial dynamin-like GTPase; α7nAChR: α7-nicotinic acetylcholine receptor; NF-κB: nuclear factor kappa B; p-NF-KB: phosphorylated nuclear factor kappa B; JAK2: Janus kinase 2; p-JAK2: phosphorylated Janus kinase 2; STAT3: signal transducer and activator of transcription 3; p-STAT3: phosphorylated signal transducer and activator of transcription 3.

cells were exposed to the exogenous TNF-α. These results are consistent with other findings, as evidenced by the enhanced mitochondrial apoptosis in the CHF and Vag groups in vivo. Consistently, the expression of mitochondrial fusion-related proteins as Mfn1 and Opa1 was downregulated when challenged by TNF-α. However, we observed that TNF-α had no effect on cell proliferations. The present in vitro experiment may imitate a systemic scenario in which hyperinflammation contributes to mitochondrial dysfunction and accelerates a vicious pathophysiological cycle.

5. Limitations

There were a few limitations in our study. First, to highlight the protective effect of cholinergic elicitation at any one time point, we ignored the influences of time factor on several repeated measurement data and used univariate ANOVA to analyze effects of indicators such as metabolisms and cytokines. Second, the method of CAP modulation was based on the methods of previously published work, and it was still unclear whether the different degrees of activating or inhibiting the CAP had different effects on the expected outcome. Third, the results of the cell experiment only explained the detrimental impact of exogenous proinflammatory cytokine on mitochondria and indirectly indicated that eliciting the CAP prevented mitochondrial injury linked to inflammation. However, a better design should be aimed at investigating the protective effect of CAP induction on HF cell models. Fourth, our results merely affirmed the protective role of CAP stimulation on CHF induced by MI, but the therapeutic effects on cardiac remodeling caused by other pathogenic factors, such as hypertrophy and cardiotoxicity, remain unknown. Fifth, our results were inclined to the onefold observations of efficacy produced by eliciting CAP and the descriptions of altered pathophysiological phenomena, whereas the key target of cholinergic stimulation in ameliorating mitochondrial dysfunction and the exact molecular mechanisms were still not elucidated.

6. Clinical Implications

Two emerging clinical trials announced that the applications of IL-1β inhibitors and sodium glucose cotransporter-2 inhibitors significantly lowered the hospitalization for HF and all-cause mortality among CHF patients. These inspiring results indicated the feasibility and potential use of anti-inflammatory agents and improved cardiac energy metabolism therapies in CHF fields [49–51]. Certainly, the anti-inflammatory effects of CAP elicitation against various diseases, such as rheumatoid arthritis and ulcerative colitis, have been proven by strong evidence, but few researchers have focused on cholinergic activation to cure CHF [52]. Numerous treatment strategies targeting the CAP including neuromodulation as well as drug administration have been preliminarily applied to clinical practice and have shown the helpful curative effects in cardiovascular diseases

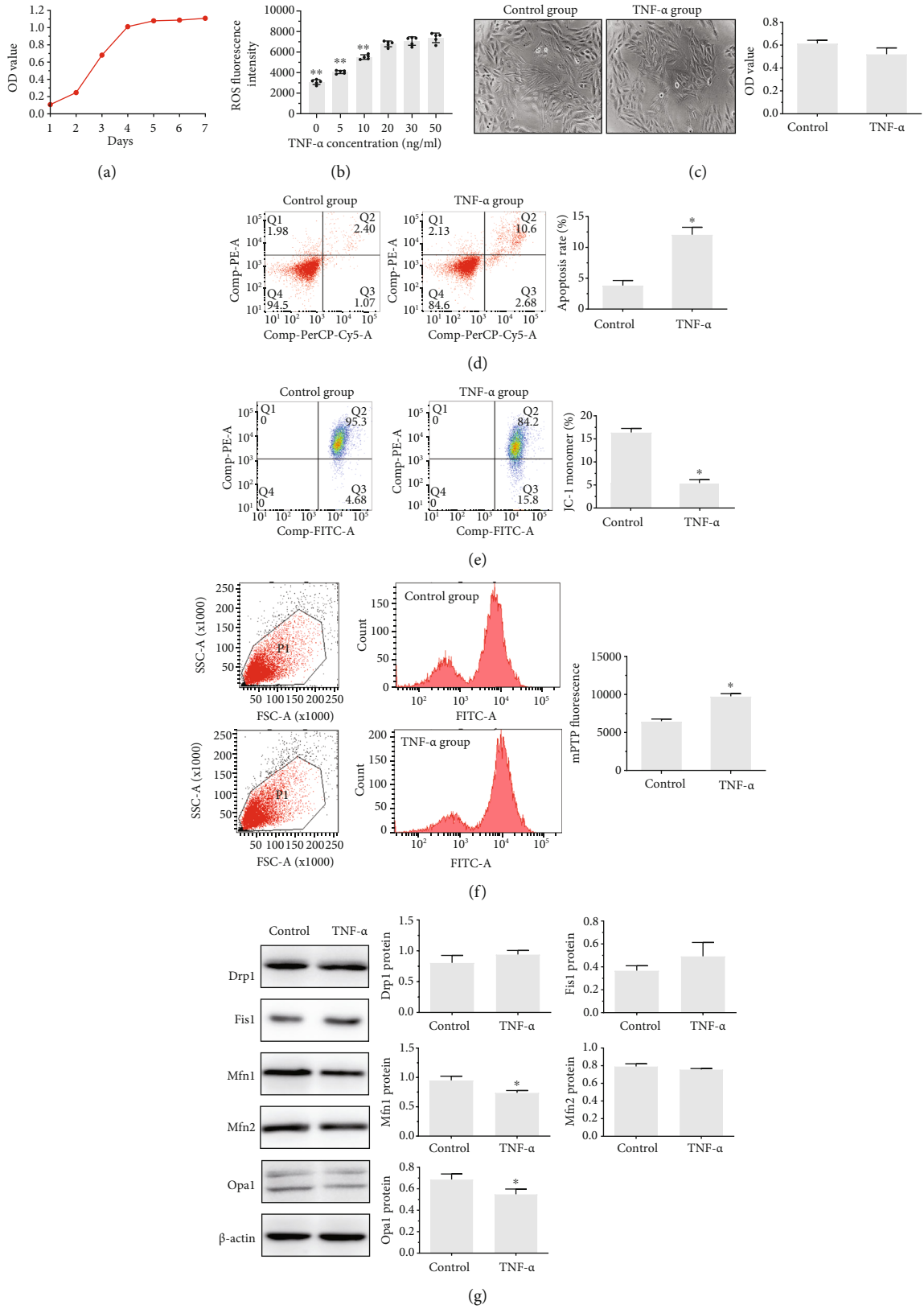

Figure 9: Impacts of TNF-α exposure on mitochondrial function of H9C2 cell lines. Evaluation of cell variability by cell growth curve (a). Screening of the optimal TNF-α-disposed concentration by ROS fluorescence intensity detections (b). Detections of cell proliferation by CCK-8 assay (c). Measurements of apoptosis rate, MMP, and mPTP by flow cytometry (d–f). Results of mitochondrial dynamics-related proteins between control and experimental groups by western blot (g). $^{*}P < 0.05$ vs. control group. ROS: reactive oxygen; MMP: mitochondrial membrane potential; mPTP: mitochondrial permeability transition pore.

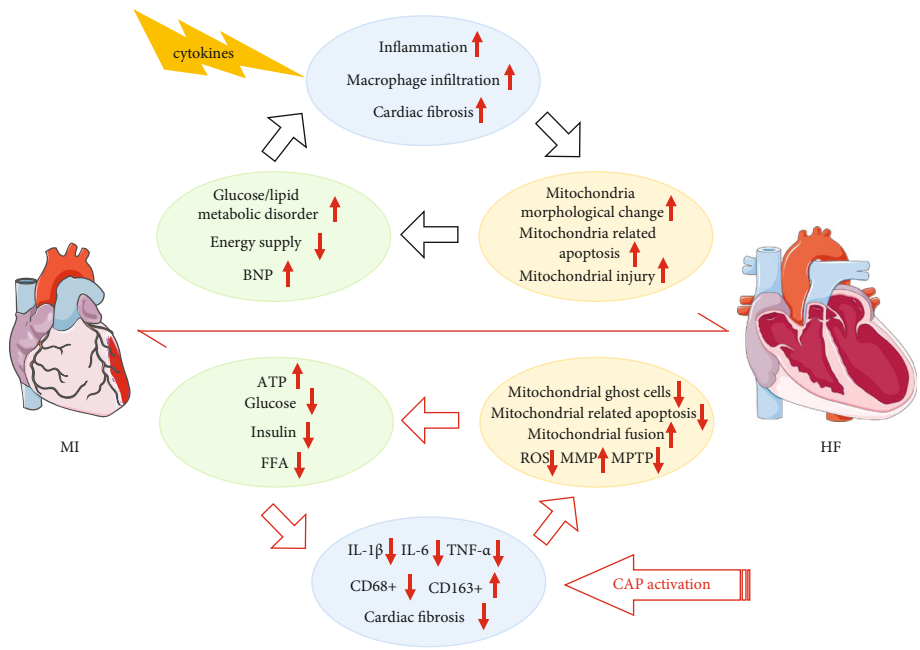

Figure 10: A schematic diagram of the cardioprotection of cholinergic elicitation to heart failure induced by MI. During the period of postinfarction heart advance into heart failure, chronic inflammation response induced by initial proinflammatory cytokines begets a detrimental pathophysiological circle through disturbing the mitochondrial biogenesis and eventually contributes to the ventricular remodeling. Such aforementioned vicious circle may be partly interrupted by cholinergic elicitation.

[53–55]. Spurred by our promising results, further studies should focus more on the clinical translation of cholinergic elicitation in CHF populations.

7. Conclusion

This study provides evidence that cholinergic elicitation exerts a salutary effect by suppressing the production of proinflammatory cytokines, attenuating cardiac fibrosis, and potentially ameliorating inflammation-linked myocardial mitochondrial injuries. These alterations above are associated with the holistic inflammation resolution, systemic energy metabolism balance, and improvements in cardiac dysfunction.

Data Availability

The datasets of this study are available from the corresponding authors on demand.

Conflicts of Interest

The authors declare that they have no conflicts of interest.

Authors' Contributions

B.T., Y.L., L.Z., and H.S. were responsible for the conception of this work. Y.Z., K.L., and H.S. were responsible for the acquisition, analysis, or interpretation of the data for the work. Y.Z., H.S., and K.L. were responsible for the drafting of the manuscript of the work. L.S., X.L., H.Y., Z.D., X.J., S.S., Q.Z., and H.Z. were responsible for revisions for important intellectual content. All authors who qualify for authorship have approved the manuscript for submission. Yang Zhao, Huaxin Sun, and Kai Li contributed equally to this work.

Acknowledgments

We are thankful for the experimental rats that were sacrificed for this study. We thank Dr. Yazhen Zong, Shiyao Chu, and other colleagues of the animal center at Xinjiang Medical University for the assistance. This work was funded by the National Natural Science Foundation (81660071, 81873488, 82060069) and the Provincial and Ministry Co-Construction of the Open Project of the State Key Laboratory (SKL-HIDCA-2019-42).

Supplementary Materials

Supplementary 1. Figure S1: typical pathologic changes in the myocardium. Inflammation infiltration (A); perivascular fibrosis (B); reactive fibrosis (C); reparative fibrosis (D).

Supplementary 2. Table 1: $*P < 0.05$ vs. sham group at the same point in time, $^{\#}P < 0.05$ vs. CHF group at the same point in time. LVEDd: left ventricular end-diastolic diameter; LVEDs: left ventricular end-systolic diameter; LVPWd: left ventricular posterior wall thickness at the end of diastole; LVPWs: left ventricular posterior wall thickness at the end of systole; LVEF: left ventricular ejection fraction; LVFS: left ventricular fraction shortening.

References

[1] R. S. Velagaleti, M. J. Pencina, J. M. Murabito et al., "Long-term trends in the incidence of heart failure after myocardial infarction," *Circulation*, vol. 118, no. 20, pp. 2057–2062, 2008.

[2] F. Zannad, W. Gattis Stough, P. Rossignol et al., "Mineralocorticoid receptor antagonists for heart failure with reduced ejection fraction: integrating evidence into clinical practice," *European Heart Journal*, vol. 33, no. 22, pp. 2782–2795, 2012.

[3] M. Merlo, D. Stolfo, M. Anzini et al., "Persistent recovery of normal left ventricular function and dimension in idiopathic dilated cardiomyopathy during long-term follow-up: does real healing exist?," *Journal of the American Heart Association*, vol. 4, no. 1, 2015.

[4] M. C. Bahit, A. Kochar, and C. B. Granger, "Post-myocardial infarction heart failure," *JACC: Heart Failure*, vol. 6, no. 3, pp. 179–186, 2018.

[5] P. C. Westman, M. J. Lipinski, D. Luger et al., "Inflammation as a driver of adverse left ventricular remodeling after acute myocardial infarction," *Journal of the American College of Cardiology*, vol. 67, no. 17, pp. 2050–2060, 2016.

[6] X.-H. Ning, J. Zhang, J. Liu et al., "Signaling and expression for mitochondrial membrane proteins during left ventricular remodeling and contractile failure after myocardial infarction," *Journal of the American College of Cardiology*, vol. 36, 2016.

[7] S. Kaimoto, A. Hoshino, M. Ariyoshi et al., "Activation of PPAR-α in the early stage of heart failure maintained myocardial function and energetics in pressure-overload heart failure," *American Journal of Physiology. Heart and Circulatory Physiology*, vol. 312, no. 2, pp. H305–H313, 2017.

[8] A. Aimo, V. Castiglione, C. Borrelli et al., "Oxidative stress and inflammation in the evolution of heart failure: from pathophysiology to therapeutic strategies," *European Journal of Preventive Cardiology*, vol. 27, no. 5, pp. 494–510, 2020.

[9] M. Buoncervello, S. Maccari, B. Ascione et al., "Inflammatory cytokines associated with cancer growth induce mitochondria and cytoskeleton alterations in cardiomyocytes," *Journal of Cellular Physiology*, vol. 234, no. 11, pp. 20453–20468, 2019.

[10] P. Gurung, J. R. Lukens, and T. D. Kanneganti, "Mitochondria: diversity in the regulation of the NLRP3 inflammasome," *Trends in Molecular Medicine*, vol. 21, no. 3, pp. 193–201, 2015.

[11] S. M. Cloonan and A. M. Choi, "Mitochondria: sensors and mediators of innate immune receptor signaling," *Current Opinion in Microbiology*, vol. 16, no. 3, pp. 327–338, 2013.

[12] C. S. Dela Cruz and M. J. Kang, "Mitochondrial dysfunction and damage associated molecular patterns (DAMPs) in chronic inflammatory diseases," *Mitochondrion*, vol. 41, pp. 37–44, 2018.

[13] S. Guarini, D. Altavilla, M. M. Cainazzo et al., "Efferent vagal fibre stimulation blunts nuclear Factor-κB activation and protects against hypovolemic hemorrhagic shock," *Circulation*, vol. 107, no. 8, pp. 1189–1194, 2003.

[14] W. J. de Jonge, E. P. van der Zanden, F. O. The et al., "Erratum: Stimulation of the vagus nerve attenuates macrophage activation by activating the Jak2-STAT3 signaling pathway," *Nature Immunology*, vol. 6, no. 9, p. 954, 2005.

[15] B. Lu, K. Kwan, Y. A. Levine et al., "α7 nicotinic acetylcholine receptor signaling inhibits inflammasome activation by preventing mitochondrial DNA release," *Molecular Medicine*, vol. 20, no. 1, pp. 350–358, 2014.

[16] M. Li, C. Zheng, T. Kawada et al., "Impact of peripheral α7-nicotinic acetylcholine receptors on cardioprotective effects of donepezil in chronic heart failure rats," *Cardiovascular Drugs and Therapy*, vol. 35, 2014.

[17] Z. H. Lin, Y. C. Li, S. J. Wu et al., "Eliciting α7-nAChR exerts cardioprotective effects on ischemic cardiomyopathy via activation of AMPK signalling," *Journal of Cellular and Molecular Medicine*, vol. 23, no. 7, pp. 4746–4758, 2019.

[18] Q. Wang, M. Zhang, G. Torres et al., "Metformin suppresses diabetes-accelerated atherosclerosis via the inhibition of Drp1-mediated mitochondrial fission," *Diabetes*, vol. 66, no. 1, pp. 193–205, 2017.

[19] J. Hu, M. Ji, C. Niu et al., "Effects of renal sympathetic denervation on post-myocardial infarction cardiac remodeling in rats," *PLoS One*, vol. 7, no. 9, 2012.

[20] S. J. Wu, Z. W. Shi, X. Wang et al., "Activation of the cholinergic anti-inflammatory pathway attenuated angiotension II-dependent hypertension and renal injury," *Frontiers in Pharmacology*, vol. 12, 2021.

[21] L. Shang, L. Zhang, M. Shao et al., "Elevated β1-adrenergic receptor autoantibody levels increase atrial fibrillation susceptibility by promoting atrial fibrosis," *Frontiers in Physiology*, vol. 11, 2020.

[22] B. G. Nasi-Er, Z. Wenhui, S. Hua Xin et al., "Vagus nerve stimulation reduces ventricular arrhythmias and increases ventricular electrical stability," *Pacing and Clinical Electrophysiology*, vol. 42, 2018.

[23] H. L. Wang, X. H. Zhou, Z. Q. Li et al., "Prevention of atrial fibrillation by using sarcoplasmic reticulum calcium ATPase pump overexpression in a rabbit model of rapid atrial pacing," *Medical Science Monitor*, vol. 23, pp. 3952–3960, 2017.

[24] M. M. Bostan, C. Stătescu, L. Anghel, I. L. Șerban, E. Cojocaru, and R. Sascău, "Post-myocardial infarction ventricular remodeling biomarkers-the key link between pathophysiology and clinic," *Biomolecules*, vol. 10, no. 11, p. 1587, 2020.

[25] R. Knöll, G. Iaccarino, G. Tarone et al., "Towards a redefinition of 'cardiac hypertrophy' through a rational characterization of left ventricular phenotypes: a position paper of the working group 'Myocardial Function' of the ESC," *European Journal of Heart Failure*, vol. 13, no. 8, pp. 811–819, 2011.

[26] D. Murashige, C. Jang, M. Neinast et al., "Comprehensive quantification of fuel use by the failing and nonfailing human heart," *Science*, vol. 370, no. 6514, pp. 364–368, 2020.

[27] "Intracerebroventricular infusion of donepezil prevents cardiac remodeling and improves the prognosis of chronic heart failure rats," *The Journal of Physiological Sciences*, vol. 70, no. 1, 2020.

[28] Y. Mao, T. Tokudome, I. Kishimoto et al., "Endogenous ghrelin attenuates pressure overload-induced cardiac hypertrophy via a cholinergic anti-inflammatory pathway," *Hypertension*, vol. 65, no. 6, pp. 1238–1244, 2015.

[29] S. J. Wu, Y. C. Li, Z. W. Shi et al., "Alteration of cholinergic anti-inflammatory pathway in rat with ischemic cardiomyopathy-modified electrophysiological function of heart," *Journal of the American Heart Association*, vol. 6, 2015.

[30] E. Tanai and S. Frantz, "Pathophysiology of heart failure," *Comprehensive Physiology*, vol. 6, 2011.

[31] A. Kobrzycka, P. Napora, B. L. Pearson, K. Pierzchała-Koziec, R. Szewczyk, and M. Wieczorek, "Peripheral and central compensatory mechanisms for impaired vagus nerve function during peripheral immune activation," *Journal of Neuroinflammation*, vol. 16, no. 1, 2019.

[32] O. C. Bezerra, C. M. França, J. A. Rocha et al., "Cholinergic stimulation improves oxidative stress and inflammation in experimental myocardial infarction," *Scientific Reports*, vol. 7, no. 1, 2017.

[33] L. Bacmeister, M. Schwarzl, S. Warnke et al., "Inflammation and fibrosis in murine models of heart failure," *Basic Research in Cardiology*, vol. 114, no. 3, 2019.

[34] R. Medzhitov, "Origin and physiological roles of inflammation," *Nature*, vol. 454, no. 7203, pp. 428–435, 2008.

[35] R. Zhou, A. S. Yazdi, P. Menu, and J. Tschopp, "A role for mitochondria in NLRP3 inflammasome activation," *Nature*, vol. 469, no. 7329, pp. 221–225, 2011.

[36] G. Matteoli, P. J. Gomez-Pinilla, A. Nemethova et al., "A distinct vagal anti-inflammatory pathway modulates intestinal muscularis resident macrophages independent of the spleen," *Gut*, vol. 63, no. 6, pp. 938–948, 2014.

[37] G. Vida, G. Peña, E. A. Deitch, and L. Ulloa, "α7-cholinergic receptor mediates vagal induction of splenic norepinephrine," *Journal of Immunology*, vol. 186, no. 7, pp. 4340–4346, 2011.

[38] D. T. Ploeger, N. A. Hosper, M. Schipper, J. A. Koerts, S. de Rond, and R. A. Bank, "Cell plasticity in wound healing: paracrine factors of M1/M2 polarized macrophages influence the phenotypical state of dermal fibroblasts," *Cell Communication and Signaling: CCS*, vol. 11, no. 1, p. 29, 2013.

[39] C. Zhao, A. C. Mirando, R. J. Sové, T. X. Medeiros, B. H. Annex, and A. S. Popel, "A mechanistic integrative computational model of macrophage polarization: implications in human pathophysiology," *PLoS Computational Biology*, vol. 15, no. 11, 2019.

[40] J. A. Rocha, S. P. Ribeiro, C. M. França et al., "Increase in cholinergic modulation with pyridostigmine induces anti-inflammatory cell recruitment soon after acute myocardial infarction in rats," *American Journal of Physiology. Regulatory, Integrative and Comparative Physiology*, vol. 310, no. 8, pp. R697–R706, 2016.

[41] M. Hulsmans, F. Sam, and M. Nahrendorf, "Monocyte and macrophage contributions to cardiac remodeling," *Journal of Molecular and Cellular Cardiology*, vol. 93, pp. 149–155, 2016.

[42] N. G. Frangogiannis, "Cardiac fibrosis: cell biological mechanisms, molecular pathways and therapeutic opportunities," *Molecular Aspects of Medicine*, vol. 65, pp. 70–99, 2019.

[43] D. P. Del Re, D. Amgalan, A. Linkermann, Q. Liu, and R. N. Kitsis, "Fundamental mechanisms of regulated cell death and implications for heart disease," *Physiological Reviews*, vol. 99, no. 4, pp. 1765–1817, 2019.

[44] D. C. Chan, "Mitochondrial dynamics and its involvement in disease," *Annual Review of Pathology*, vol. 15, no. 1, pp. 235–259, 2020.

[45] D. A. Kubli and Å. B. Gustafsson, "Mitochondria and Mitophagy," *Circulation Research*, vol. 111, no. 9, pp. 1208–1221, 2012.

[46] S. A. Wazea, W. Wadie, A. K. Bahgat, and H. S. El-Abhar, "Galantamine anti-colitic effect: Role of alpha-7 nicotinic acetylcholine receptor in modulating Jak/STAT3, NF-κB/HMGB1/RAGE and p -AKT/Bcl-2 pathways," *Scientific Reports*, vol. 8, no. 1, 2018.

[47] P. Kleinbongard, R. Schulz, and G. Heusch, "TNFα in myocardial ischemia/reperfusion, remodeling and heart failure," *Heart Failure Reviews*, vol. 16, no. 1, pp. 49–69, 2011.

[48] T. Nakagawa, S. Shimizu, T. Watanabe et al., "Cyclophilin D-dependent mitochondrial permeability transition regulates some necrotic but not apoptotic cell death," *Nature*, vol. 434, no. 7033, pp. 652–658, 2005.

[49] B. M. Everett, J. H. Cornel, M. Lainscak et al., "Anti-inflammatory therapy with canakinumab for the prevention of hospitalization for heart failure," *Circulation*, vol. 139, no. 10, pp. 1289–1299, 2019.

[50] Y. Lytvyn, P. Bjornstad, J. A. Udell, J. A. Lovshin, and D. Z. I. Cherney, "Sodium glucose cotransporter-2 inhibition in heart Failure," *Circulation*, vol. 136, no. 17, pp. 1643–1658, 2017.

[51] M. M. JJ, S. D. Solomon, S. E. Inzucchi et al., "Dapagliflozin in patients with heart failure and reduced ejection fraction," *The New England Journal of Medicine*, vol. 381, 2017.

[52] A. F. Salvador, K. A. de Lima, and J. Kipnis, "Neuromodulation by the immune system: a focus on cytokines," *Nature Reviews. Immunology*, vol. 21, no. 8, pp. 526–541, 2021.

[53] H. Park, H. Park, D. Mun et al., "Sympathetic nerve blocks promote anti-inflammatory response by activating the JAK2-STAT3-mediated signaling cascade in rat myocarditis models: a novel mechanism with clinical implications," *Heart Rhythm*, vol. 15, no. 5, pp. 770–779, 2018.

[54] L. Yu, B. Huang, S. S. Po et al., "Low-Level Tragus Stimulation for the Treatment of Ischemia and Reperfusion Injury in Patients With ST-Segment Elevation Myocardial Infarction: A Proof- of-Concept Study," *JACC. Cardiovascular Interventions*, vol. 10, no. 15, pp. 1511–1520, 2017.

[55] S. J. Wu, Z. H. Lin, Y. Z. Lin et al., "Dexmedetomidine exerted anti-arrhythmic effects in rat with ischemic cardiomyopathy via upregulation of connexin 43 and reduction of fibrosis and inflammation," *Frontiers in Physiology*, vol. 11, 2020.

Hindawi
Mediators of Inflammation
Volume 2021, Article ID 1376859, 11 pages
https://doi.org/10.1155/2021/1376859

Research Article

Characterization of Transverse Aortic Constriction in Mice Based on the Specific Recruitment of Leukocytes to the Hypertrophic Myocardium and the Aorta Ascendens

Jan Lukas Kleiner,[1] Odilia Köpke,[2] Anton Faron,[3] Yunyang Zhang,[1] Jan Cornelssen,[1] Mark Coburn,[1] Stilla Frede,[1] Lars Eichhorn,[1] and Christina Katharina Weisheit[1]

[1]*Department of Anesthesiology and Intensive Care Medicine, University Hospital Bonn, Germany*
[2]*Department of Obstetrics and Gynecology, Marienhospital, Bonn, Germany*
[3]*Department of Diagnostic and Interventional Radiology, University Hospital Bonn, Germany*

Correspondence should be addressed to Christina Katharina Weisheit; christina.weisheit@ukbonn.de

Received 1 July 2021; Revised 7 September 2021; Accepted 13 October 2021; Published 3 November 2021

Academic Editor: Simon Kennedy

Transverse aortic constriction (TAC) is a model that mimics pressure overload-induced left ventricular (LV) hypertrophy in mice. Alterations in immune cell functionality can promote cardiac and vascular remodeling. In the present study, we characterized the time course in innate immune cell dynamics in response to TAC in the different tissues of mice. It was determined whether TAC induces a characteristic leukocyte-driven immune response in the myocardium, aorta ascendens and descendens, spleen, blood, and draining lymph nodes supported by cytokine-driven chemotaxis in mice at 3, 6, and 21 days following surgery. We used complex flow cytometry staining combinations to characterize the various innate immune cell subsets and a multiplex array to determine cytokine concentrations in the serum. The results of the current study indicated that leukocytes accumulate in the myocardium and aorta ascendens in response to TAC. The leukocyte dynamics in the myocardium were dominated by the Ly6C^{low} macrophages with an early accumulation, whereas the response in the aorta ascendens was characterized by a long-lasting proinflammatory phenotype driven by Ly6C^{high} macrophages, neutrophils, and activated DCs. In contrast to the high-pressure environment of the aorta ascendens, the tissue of the aorta descendens did not react to TAC with any leukocyte increase. The levels of proinflammatory cytokines in the blood were elevated in response to TAC, indicating a systemic reaction. Moreover, our findings strongly suggest that cardiac macrophages could origin from splenic pools and reach the site of the inflammation via the blood. Based on the current findings, it can be concluded that the high-pressure conditions in the aorta ascendens cause a characteristic immune response, dominated by the accumulation of leukocytes and the activation of DCs that varies in comparison to the immune cell dynamics in the myocardium and the aorta descendens.

1. Introduction

Chronic pressure overload induces left ventricular (LV) hypertrophy and consequently results in congestive heart failure. This process is driven by the immune response and is known to influence the outcome and quality of life. In sterile inflammations, the innate immune system is activated by danger-associated molecular patterns (DAMPs) that are released by injured or necrotic cells and damaged extracellular matrix. DAMPs can activate the response of leukocytes via toll-like receptor signaling [1]. Our recent studies indicated that LV hypertrophy induced by pressure overload provokes an immune response which is dominated by anti-inflammatory macrophages [2]. These cardiac Ly6C^{low} CX3CR1^{+} macrophages contribute to myocardial hypertrophy and impaired heart function following pressure overload in a mouse model of transverse aortic constriction (TAC) [3].

As previously shown, our TAC model causes LV hypertrophy and heart failure in mice [3]. Moreover, we assume

that the narrowing of the aortic lumen provokes a high-pressure (in front of the constriction) and a low-pressure part (behind the constriction) of the aorta that are characterized by a specific leukocyte response. The TAC model can be used to analyze the high-pressure and low-pressure parts of the aortic tissue in the same animal. The aim of the present is to further investigate the local and systemic inflammatory response induced by TAC. Besides, the present study investigates not only the immune response in the myocardium but also the ongoing inflammatory processes in the aorta, spleen, lymph nodes, and blood.

The most important cells of the innate immune system involved in cardiac remodeling processes are monocytes/-macrophages, neutrophils, and dendritic cells (DCs) [4]. Murine monocytes and macrophages can be classified by either the $Ly6C^{low}$ or $Ly6C^{high}$ surface expression in the patrolling monocytes or anti-inflammatory macrophages ($Ly6C^{low}$ in mice and $CD14^{low}CD16^{+}$ in humans), which survey the vascular lumen, clear cellular debris, and contribute to remodeling processes, as well as in the inflammatory monocytes and macrophages ($Ly6C^{high}$ in mice and $CD14^{high}CD16^{-}$ in humans), which secrete a variety of pro-inflammatory cytokines and maintain inflammation [5, 6]. Our previous work had shown that these two distinct macrophage subsets cross-talked and orchestrated the immune defense against bacterial urinary tract infection, by regulating neutrophil migration into the infected uroepithelium [7]. In the context of cardiovascular diseases, we elucidated the influence of pattern recognition receptors expressed by cardiac macrophages and circulating leukocytes to cardiac remodeling following myocardial infarction and pressure overload induced LV hypertrophy, using our TAC model [2, 3, 8, 9].

We recently published that cardiac macrophages do not replenish by local proliferation in response to pressure overload-induced LV hypertrophy but appear to be recruited via the chemotaxis of CCL2 to the site of the myocardial inflammation [3]. In this context, the source of the recruited monocytes has not been further investigated.

Under steady-state conditions, the resident cardiac DCs represent approximately 1% of the total cardiac leukocytes and can be divided into $CD103^{+}$ and $CD11b^{+}$ cells in a model of viral myocarditis [10]. In the context of MI, the DCs infiltrated the infarcted heart, internalized locally released cardiomyocyte-derived antigens, and migrated into the mediastinal lymph nodes, where they presented antigen-derived peptides and stimulated T cells [11].

In the present study, we focused on the dynamics of leukocyte accumulation in the myocardium as well as in the ascending and descending parts of the aorta, spleen, lymph nodes, and blood to characterize the potential remote immunologic effects of TAC-induced cardiac hypertrophy.

2. Materials and Methods

2.1. Mice. Female C57BL/6J mice aged 10-14 weeks were purchased from Charles River (Wilmington, MA, USA). The mice were kept under specific pathogen-free conditions in isolated, ventilated cages with free access to water and food. All animal experiments were approved by the governmental ethics board at the Ministry of Nature, Environment and Consumer Protection of the German state of North Rhine Westphalia (LANUV Recklinghausen permit numbers 84-02.04.2011.A313, 84-02.04.2016.A374) and were supervised by the central animal facilities of the medical faculty of Bonn (HET, Venusberg-Campus 1, Bonn, Germany). All surgical interventions were performed under anesthesia and analgesia as described below, and all efforts were made to minimize the suffering of the mice.

2.2. Transverse Aortic Constriction (TAC). TAC was performed as published previously [2]. In short, mice were anesthetized with isoflurane (2 vol%) and intubated with an intubation cannula (OD 1.2 mm). The respiratory rate was set to 150/min and the tidal volumes to 8-10 ml/kg body weight using a small animal ventilator (Harvard Apparatus; Holliston, MA, USA). A 27 G spacer was used to standardize the degree of aortic constriction. The sham control animals underwent intubation and surgery except that the suture around the aorta was not tight. For postoperative pain management, buprenorphine was administered (0.1 μg/g subcutaneously) every 8 h for the next 3 days after surgery. The mice were sacrificed 3, 6, and 21 days following surgical intervention.

2.3. Flow Cytometry. The immune cells were isolated from the blood, spleen, lymph node, aorta, and LV tissue. Peripheral blood (100 μl) was collected in tubes with ethylenediaminetetraacetic acid (EDTA) (Sigma Aldrich, St. Louis, MO, USA). The spleen tissue and lymph nodes were mechanically homogenized and filtered via 80 μm meshes. The spleen samples and blood were treated with RBC lysis buffer (Thermo Fisher Scientific, Waltham, MA, USA) to eliminate erythrocytes. Whole hearts were flushed with PBS, and the heart tissue and parts of the aorta were minced into small pieces using a single-edged blade and digested in gently agitated RPMI medium with 1 mg/ml collagenase 2 (Sigma Aldrich) and 1 mg/ml DNAse I (Sigma Aldrich) at 37°C for 60 min.

Unspecific Fc-receptor binding was blocked incubating the cells with anti-mouse CD16/32 (BD Biosciences, Franklin Lakes, NJ, USA) for 10 min at 4°C. The cells were stained with anti-mouse fluorochrome-conjugated antibodies in panel-appropriate combinations in the dark for 20 min at 4°C with following antibody clones from Thermo Fisher (Waltham, MA, USA), (i.e., CD45 (30-F11), CD11b (ITGAM), CD115 (c-fms), F4/80 (BM-8), Ly6C (HK1.4), Ly6G (1A8)) and BioLegend (San Diego, CA, USA) (i.e., CD103 (2E7), CD11c (Cr4)). We performed live/dead staining using Hoechst 33258 in a dilution of 1 μl/100 ml (Thermo Fisher). Flow cytometry was performed on a BD Canto and a BD LSR Fortessa, and the data were analyzed using the Flow-Jo software (BD Bioscience).

2.4. Cytokine Measurement. The cytokine concentrations in the serum of the mice were measured using a custom-made FlowCytomix Multiple Analyte Detection System (Thermo Fisher, formerly eBioscience). This bead-based

immunoassay for the simultaneous detection of the cytokines in one sample was performed according to the manufacturer's instructions. As suggested by the manufacturer, 25 μl of mouse serum was used. The data were evaluated using the FlowCytomix Pro Software.

2.5. Statistical Analysis. Appropriate assumptions of the data (e.g., normal distribution or similar variation between experimental groups) were examined before the statistical tests were conducted. Student's *t*-tests were performed whenever two groups were compared, whereas one-way or two-way analyses of variance followed by Tukey's test were performed for multiple comparisons. The analysis was performed using Prism 8 (GraphPad Software, Inc., La Jolla, CA, USA). The results were provided as mean ± standard deviation (SD) unless noted otherwise; a P value of < 0.05 was considered statistically significant.

3. Results

3.1. The Effect of TAC on the Immune Responses in the Myocardium and the High-Pressure and Low-Pressure Parts of the Aorta. Our recent studies highlighted that LV hypertrophy caused by pressure overload induces a complex immune response in the myocardium [2]. Moreover, we focused on the immune response in the LV tissue and did not investigate the systemic or remote immune response. In the present study, we examined the migration pattern of immune cells to the ascending and descending parts of the aorta, draining lymph nodes, blood, spleen, and LV tissue in response to TAC, which has not been determined systematically in previous studies.

In this project, we performed TAC or sham surgery and analyzed the immune response in the course of the disease at 3, 6, and 21 days after intervention (Figure 1(a)). Our model of TAC induced LV hypertrophy was evaluated by calculating the heart-weight/body-weight-index of the mice. Hypertrophy of the hearts becomes significant at days 6 and 21 after TAC compared to the controls (Figure 1(b)). In addition to the myocardium, we investigated the immune cell dynamics in the ascending and descending parts of the aorta, draining lymph nodes, spleen, and blood, which allowed us to describe the migration and recruitment processes provoked by TAC (Figure 1(c)). The immune cell subsets and activation markers were determined via flow cytometry. Our gating strategy was based on the guidelines for the use of flow cytometry in immunology [12] and was optimized and refined with the help of our flow cytometry core facility (Figure 1(d) and Supplemental Figure 1).

The characterization of the immune cell composition in the myocardium indicated a significant increase in the proportion of immune cells at all three time points (Figure 2(a)). The percentage of neutrophils and Ly6C^{low} macrophages was significantly elevated at days 3 and 6 after TAC compared with the controls (Figures 2(b) and 2(d)). The Ly6C^{high} macrophages significantly accumulated only at day 3 after TAC compared to controls (Figure 2(c)). Next, it was determined whether and how our model of TAC-induced LV hypertrophy affected the high-pressure and low-pressure parts of the aorta to determine specific immunological signatures.

Flow cytometry analyses performed at days 3, 6, and 21 after TAC or sham surgery revealed that TAC surgery directly influenced the immune reaction in the ascending aortic tissue compared with that in the descending part of the aorta. The immune response in the ascending part of the aorta was characterized by a significant increase in CD45^{+} immune cells at days 3, 6, and 21 after TAC compared to controls. The increase in CD45^{+} immune cells was significantly higher at day 6 compared to day 3 indicating that the inflammation increases in the first 6 days (Figure 2(e)). Especially neutrophils and Ly6C^{high} macrophages invaded the aortic tissue in the high-pressure environment, reaching the level of significance at all three time points in comparison with the sham animals (Figures 2(f) and 2(g)). The Ly6C^{low} macrophages significantly increased in response to TAC at days 3 and 6 compared with controls decreasing to sham level at day 21 (Figure 2(h)). In the LV tissue, the neutrophils and Ly6C^{low} macrophages dominated the immune response with significantly elevated cell proportions at days 3 and 6 after TAC compared with the control groups, a situation which was mirrored in the ascending part of the aorta. The Ly6C^{high} macrophage levels were significantly increased at day 3 only in the myocardium, whereas the reaction in the aorta ascendens lasted for 21 days (Figures 2(c) and 2(g)). In the descending part of the aorta, a significant increase in immune cells was observed only at day 6 after TAC compared with day 3 which we could not directly break down to any of the analyzed innate immune cell subsets (Figure 2(i)). The proportion of the different leukocyte subsets did not vary in response to TAC (Figures 2(j)–2(l)). The descending part of the aorta did not reflect the immune response of the myocardium but reacted to the surgical intervention and maybe changes in the blood flow f.e. turbulences that may result in an increase in immune cells in general.

3.2. TAC Provokes an Immune Response in Spleen and Blood. Certainly, monocytes and macrophages play important roles in the orchestration and maintenance of the cardiac inflammation in the development of pressure overload-induced LV hypertrophy. Our recent findings demonstrated that CCL2-driven chemotaxis plays an important role in the recruitment of cardiac macrophages to the site of cardiac injury [3]. The remote activation of the splenic immune response provoked by TAC has not been systematically studied yet. In post-MI inflammation and remodeling, it is already known that cardiac macrophages originate mostly from splenic pools and are transported via the blood to the site of the inflammation [13]. However, the immune response in MI and LV hypertrophy with a biphasic response after MI differs from the chronic response with dominating Ly6C^{low} macrophages in the myocardium after TAC [2]. Considering this, we determined whether the immune cell composition of the spleen and blood is affected from TAC, and whether the splenic myeloid cell pool might serve as a source to supply the cardiac immune response in our TAC model.

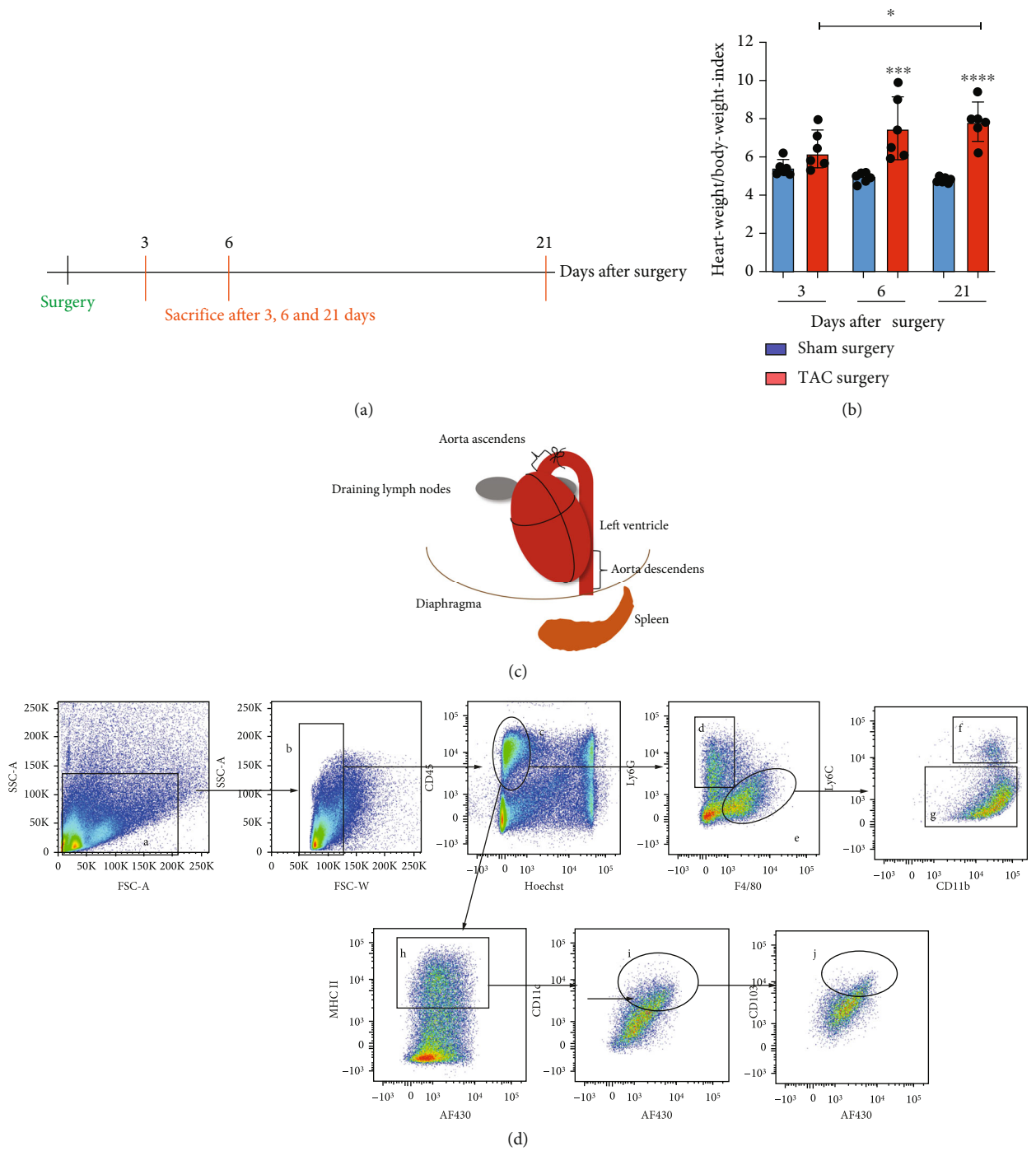

Figure 1: Methodological procedure and definition of the immune cell subsets. (a) We sacrificed the mice 3, 6, and 21 days after TAC or sham surgery. (b) Heart-weight/body-weight-index in mg/g was calculated 3, 6, and 21 days after TAC or sham surgery. (c) In addition to the LV tissue, we analyzed the tissue of the aorta ascendens, aorta descendens, spleen, blood, and heart draining lymph nodes. (d) The gating strategy for flow cytometry analyses was performed as illustrated for the tissue of the aorta ascendens. All cell-like events (a) were isolated by using the forward scatter area versus sideward scatter area. Doublets were excluded using forward scatter area versus sideward scatter width (b). We defined the living immune cells (c), using CD45 staining versus Hoechst staining. The $CD45^+$ immune cells were further classified by staining for the surface markers Ly6G and F4/80 to determine neutrophils (d) and macrophages (e). Next, we checked for the Ly6C surface expression of the macrophage population as a function of CD11b to differentiate between the $Ly6C^{high}$ (f) and the $Ly6C^{low}$ macrophages (g). We analyzed the DC compartment based on the population of the $CD45^+$ cells (c) and stained for MHC-II to identify $MHC\text{-}II^+$ immune cells (h). We used CD11c as a function of the autofluorescence channel AF430 for the definition of classical dendritic cells (i). The cDCs were further discriminated according to the CD103 surface expression (j).

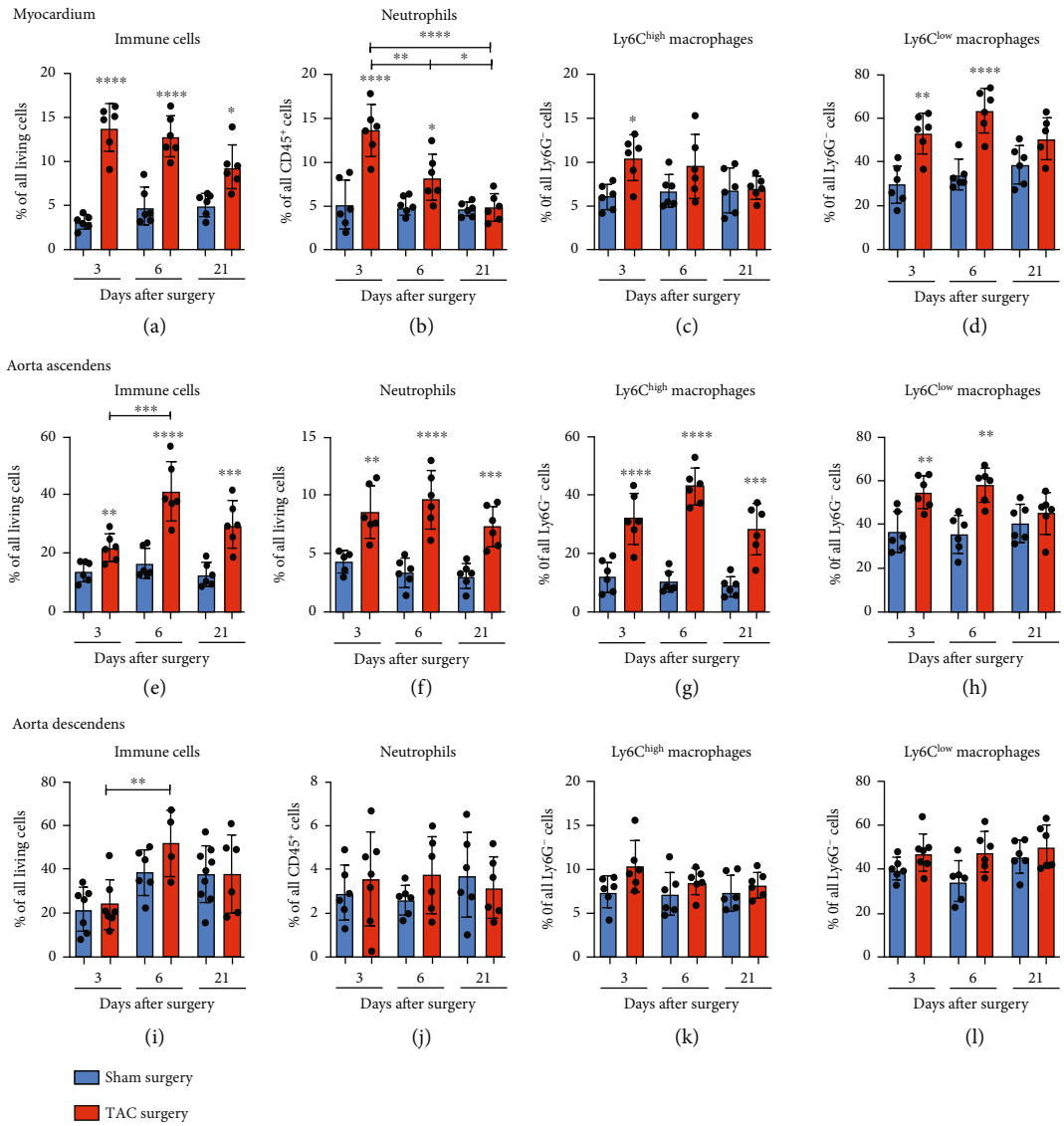

Figure 2: Innate immune response in the myocardium and the ascending and descending parts of the aorta. (a)–(l) The $CD45^+$ immune cells, neutrophils, $Ly6C^{low}$, and $Ly6C^{high}$ macrophages in the tissue of the LV, the aorta ascendens and descendens of the mice were quantified via flow cytometry. The particular cell subsets were defined as follows: neutrophils as $CD45^+$ $F4/80^-$ $Ly6G^+$ and macrophages as $CD45^+$ $F4/80^+$ $Ly6G^-$. Moreover, the $Ly6C^{high}$ and $Ly6C^{low}$ macrophages were further discriminated according to the respective Ly6C surface expression. *The above individual columns indicate the significant differences between the TAC and respective sham group; $^*P < 0.05$, $^{**}P < 0.01$, $^{***}P < 0.001$, and $^{****}P < 0.0001$.

The results of the present study showed a decrease in splenic immune cells at day 6 after TAC compared with the sham group, not reaching the level of significance (Figure 3(a)). The kinetics of the $Ly6C^{low}$ macrophages in the spleen showed a significant increase at day 3 compared with the sham controls and both other time points that were paralleled by an increase in DCs (Figures 3(d) and 3(e)). The first increase of splenic $Ly6C^{low}$ macrophages was followed by a decline to sham level at days 6 and 21 after TAC (Figure 3(d)). The quantification of splenic $Ly6C^{high}$ macrophages and neutrophils did not reveal any changes following TAC (Figures 3(b) and 3(c)). These findings showed that there is a remote reaction of the immune system in the spleen triggered by TAC.

From the spleen, the immune cells are transported via the circulation to the site of inflammation and injury. We suggested that TAC provoked changes in the amount of immune cells in the blood caused by the release of monocytes from the spleen for the recruitment of monocytes to the injured heart. Our flow cytometry-based quantification approach revealed a significant increase only in the population of the $Ly6C^{low}$ monocytes at day 3 after TAC compared with the sham group (Figure 4(d)). No significant increase was detectable at days 6 and 21 after TAC. The reaction of neutrophils did not alter in response to TAC, and the observed changes in the immune cell subsets did not cause alterations of the total immune cell compartment (Figure 4(a)). In addition to the flow cytometry studies,

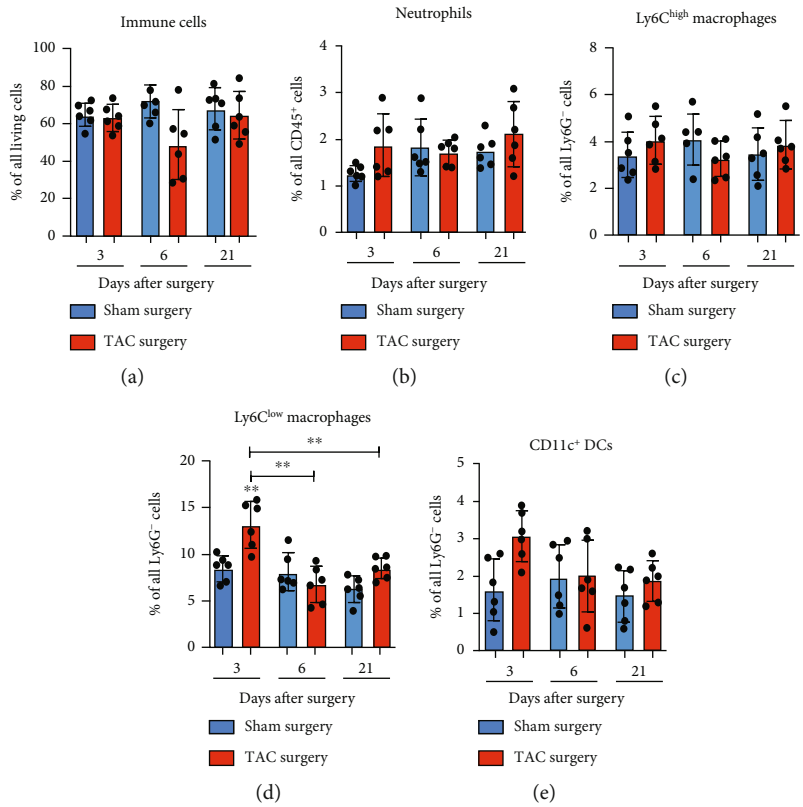

Figure 3: Innate immune response in the spleen. (a)–(e) The $CD45^+$ immune cells, neutrophils, and $Ly6C^{low}$ and $Ly6C^{high}$ macrophages, and DCs in the spleen of the mice were quantified via flow cytometry. The particular cell subsets were defined as follows: neutrophils as $CD45^+$ $F4/80^-$ $Ly6G^+$ and macrophages as $CD45^+$ $F4/80^+$ $Ly6G^-$. Moreover, the $Ly6C^{high}$ and $Ly6C^{low}$ macrophages were further discriminated according to the respective Ly6C surface expression, and the DCs were defined as $CD45^+$ $F4/80^-$ $Ly6G^-$and $CD11c^+$. *The above individual columns indicate the significant differences between the TAC and respective sham group; $^*P < 0.05$, and $^{**}P < 0.01$.

we determined the levels of proinflammatory cytokines in the serum of TAC and sham mice as indicators of systemic inflammation. The results of the current study indicated a significant increase in IL-6 and IL-1b at day 3 after TAC compared with the control group (Figures 4(e) and 4(f)). The concentration of TNF-a was significantly elevated at days 3 and 6 in response to TAC compared with the sham group (Figure 4(g)). This data demonstrated a systemic immunological reaction reflected in the blood by an increase in proinflammatory cytokines.

The analysis of draining lymph nodes with regard to changes in the leukocyte composition did not exhibit noteworthy changes in response to TAC (data not shown).

3.3. Dendritic Cells Are Activated in Response to TAC in the Myocardium and Aorta Ascendens. Recently, a published work demonstrated that TAC-induced LV hypertrophy is associated with the accumulation of $CD11c^+$ $MHC\text{-}II^+$ cells in the LV, spleen, and blood [14]. Based on these findings, we decided to take a closer look at both the DC activation pattern and subtypes in the myocardium, aorta ascendens and descendens, and draining lymph nodes.

Our analyses revealed that the percentage of $MHC\text{-}II^+$ cells was significantly elevated in the myocardium 3 and 6 days after TAC compared with the respective control group (Figure 5(a)). These $MHC\text{-}II^+$ cells were further subdivided into classical DCs according to the CD11c surface expression. The amount of classical DCs (cDCs) significantly increased at day 6 compared with that at days 3 and 21 after TAC and the respective controls (Figure 5(b)). However, the activation of these cells in the myocardium, measured by CD86 MFI, did not show any changes in response to TAC (Figure 5(c)). Since the majority of the aortic $CD11c^+$ $MHC\text{-}II^+$ DCs showed no staining for E-cadherin ligand CD103, a small $CD103^+$ DC population could be confined in the myocardium (Figure 5(d)). In our model, the $CD103^+$ DCs increased at days 3 and 6 after TAC compared with the control groups. At day 21, the increase in $CD103^+$ DCs returned to the initial level (Figure 5(d)).

In addition to the myocardium, we examined the DC response in the ascending, high-pressure part of the aorta. In response to TAC, we observed a significant increase in $MHC\text{-}II^+$ cells at day 3 after TAC compared with the sham group (Figure 5(e)). The proportion of cDCs was significantly elevated at days 3 and 6 after TAC compared with the respective sham animals and presented with an earlier onset compared with our observations in the myocardium (Figure 5(f)). We determined a significant increase in the activation marker CD86 at day 3 after TAC compared with the sham group and with the TAC groups at

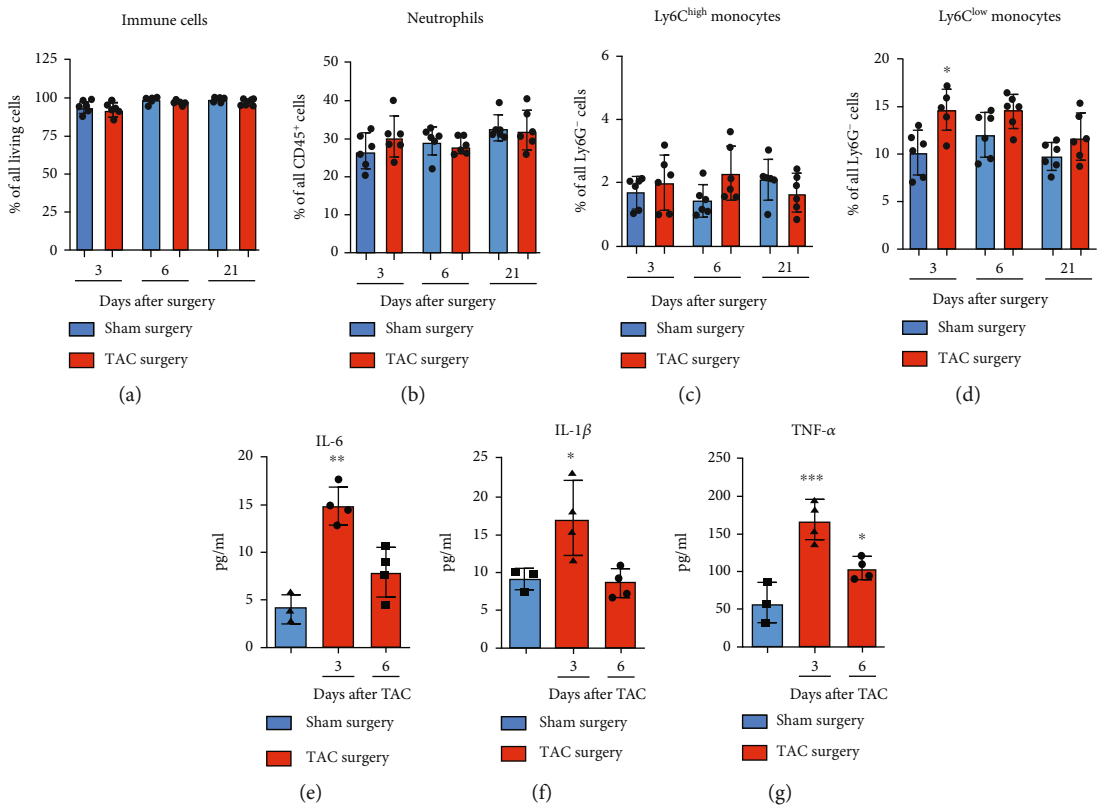

Figure 4: Innate immune cell quantification and cytokine levels in response to TAC in the blood. (a)–(d) The $CD45^+$ immune cells, neutrophils, and $Ly6C^{low}$ and $Ly6C^{high}$ monocytes in the blood of the mice were quantified using flow cytometry. The particular cell subsets were defined as follows: neutrophils as $CD45^+$ $CD115^-$ $Ly6G^+$ and monocytes as $CD45^+$ $CD115^+$ $Ly6G^-$. In addition, the $Ly6C^{high}$ and $Ly6C^{low}$ monocytes were further discriminated according to the respective Ly6C surface expression. (e)–(g) The cytokine levels of IL-6, IL-1β, and TNF-α in the serum of the mice were measured at days 3 and 6 after TAC or after day 3 after sham surgery. *The above individual columns indicate the significant differences between the TAC and respective sham group; $^*P < 0.05$, $^{**}P < 0.01$, and $^{***}P < 0.001$.

days 6 and 21 in the aorta ascendens (Figure 5(g)). The CD86 MFI indicated a higher activity level of cDCs in the aorta ascendens after TAC (mean: 5501-8004) compared with that in the myocardium (mean: 3447-4414) (Figures 5(k), 5(g), and 5(o) and Supplementary Figure 2). The amount of $CD103^+$ DCs was significantly increased in response to TAC at day 6 compared with the control group and the 21-day TAC group in the aorta ascendens (Figure 5(h)).

In the tissue of the aorta descendens, less changes were observed in the population of DCs. The findings of the present study showed a significant increase in MHC-II^+ cells at day 6 after TAC compared with the sham group (Figure 5(i)). The kinetics of cDCs and DC86 MFI did not reach the level of significance at any time point (Figures 5(j) and 5(k)). The mean of the CD86 expression pattern did not exceed the mean of 3513 at day 6 after TAC, which represents a low activation level compared to the CD86 MFI measured on the surface of the cDCs in the aorta ascendens and the draining lymph nodes (Figures 5(c) and 5(g) and Supplementary Figure 2). However, we determined a significant increase in $CD103^+$ DCs at day 3 after TAC compared with the sham group (Figure 5(l)).

The examination of the draining lymph nodes with focus on the DC dynamics in response to TAC revealed a significant increase in cDCs at day 3 after TAC compared with the respective control group and the 21-day TAC group (Figure 5(n)). CD86 MFI was significantly elevated at day 3 after TAC in comparison with the respective control group and presented with a higher activation level (mean: 6428 at day 6 to 8519 at day 3) compared with the myocardium and the aorta descendens (Figure 5(o)).

This finding indicated an influence of TAC on the population of DCs and the activation status as well as on the DC subsets in the myocardium, aorta ascendens and descendens, and draining lymph nodes.

4. Discussion

In the present project, we further investigated the immune response in the myocardium, aortic tissue, spleen, blood, and lymph nodes following TAC in mice. TAC is a commonly and frequently used animal model for the examination of pressure overload-induced LV hypertrophy. Relevant systemic immunological reactions following TAC

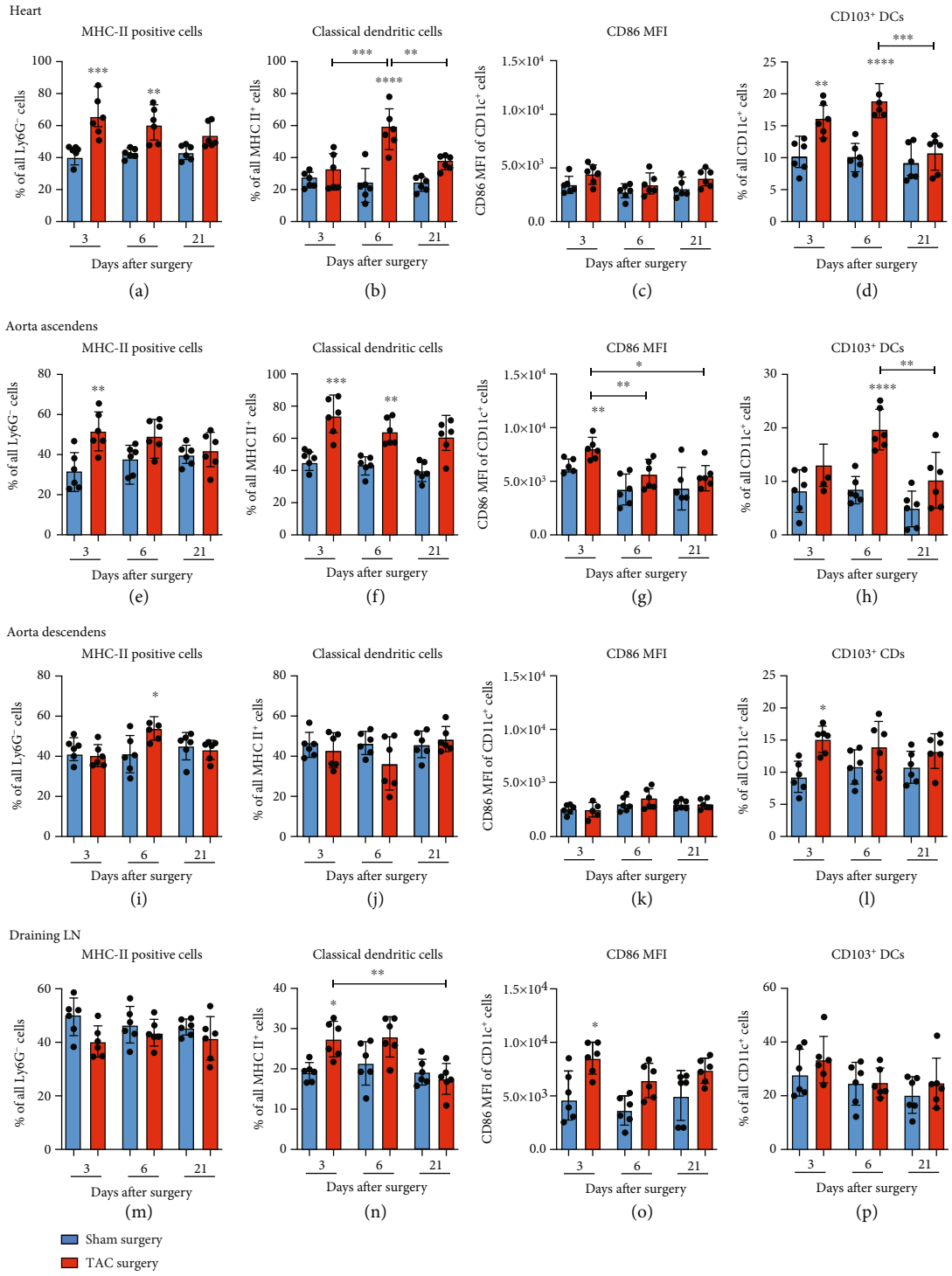

Figure 5: TAC provoked the response of the DC compartment in the myocardium, aorta ascendens, aorta descendens, and draining lymph nodes. (a)–(p) The total of the MHC-II$^+$ cells was determined from the fraction of CD45$^+$ Ly6G$^-$ cells. The population of cDCs was defined using the CD11c surface staining. CD86 MFI was calculated from the population of all cDCs. The population of CD103$^+$ cDCs was determined based on the results of the CD103 surface staining. *The above individual columns indicate the significant differences between the TAC and respective sham group; $^*P < 0.05$, $^{**}P < 0.01$, $^{***}P < 0.001$, and $^{****}P < 0.0001$.

induction are of great interest in the field of cardiovascular research [15]. Alterations in the immune cell activity and quantity can promote cardiac remodeling and functional outcome [16]. Herein, we characterized the time course in innate immune cell dynamics in response to TAC in the different tissues of mice. We investigated whether TAC induces a characteristic leukocyte-driven immune response in the myocardium, aorta ascendens and descendens, spleen,

blood, and draining lymph nodes supported by cytokine-driven chemotaxis in mice in the course of the disease.

The results of the current study indicated that the dynamics of immune cells and neutrophils and Ly6C^{high} and Ly6C^{low} macrophage accumulation in the myocardium were mirrored in the aorta ascendens which is directly affected by the increase in blood pressure after TAC. We observed significantly increased amount of leukocytes at all three time points following TAC in the myocardium and the tissue of the aorta ascendens, highlighting a chronic inflammation in a duration of 21 days. The TAC model allowed the simultaneous analysis of the aortic tissue in a high- and low-pressure environment in front of and behind the knot of the suture.

We assume that the early accumulation of macrophages at day 3 in the spleen reflects the systemic inflammation in response to TAC and the decline in macrophages compared to day 3 after TAC could mirror the release of these cells to the circulation. Unfortunately, our data did not indicate a significant increase in monocytes in the blood at day 6 after TAC. This might be because monocytes were recruited from the circulation maybe in the same amount as they are released from the spleen. This observation underlined the hypothesis that in LV hypertrophy the invading monocytes were released from the spleen and transported via the blood to the site of inflammation similar to the replenishment of monocytes following MI [13]. Our recently published findings demonstrated that the peak of inflammatory activity is at day 3 and is paralleled by the high levels of CCL2 in the myocardium, a chemokine, which is known to attract CCR2^{+} monocytes from the circulation [3]. Besides, we could already show by means of BrdU analyses that there is no local proliferation of macrophages in the myocardium in response to TAC [3]. This supports the idea that macrophages are recruited to the heart in the development of LV hypertrophy. Moreover, the present study investigated the systemic immune response expressed by the increased levels of proinflammatory cytokines in the serum of the mice. The findings that we already published were focused on elucidating the cytokine expression pattern in the myocardium following TAC and confirmed the newly acquired data [3]. We suggest that tissue-resident endothelial and immune cells account for the increase in proinflammatory cytokines and induce a systemic immune response to attract immune cells in response to TAC.

The analysis of the DC dynamics in the myocardium, aortic tissue, blood, lymph nodes, and spleen in response to TAC allows to determine the role of DCs in the modulation of sterile inflammations. Moreover, we identified the DCs based on the surface staining of F4/80, CD11c, MHC-II, and CD103. In the myocardium, the MHC-II^{+} CD11c^{+} DCs have accumulated following TAC and peaked at day 6, whereas in the aorta ascendens, the proportion of DCs significantly increased already at day 3, and the aortic DCs presented with a significantly higher activation level based on CD86 MFI in comparison with the DCs isolated in the myocardium and aorta descendens. This finding indicates that inflammation and the high-pressure environment in the ascending part of the aorta in our TAC model induced a DC response that was more pronounced than that in the myocardium. The chronic remote inflammation induced in the heart provoked a later onset of the DC response with less activated DCs. We assume that the increase in DCs in the aorta ascendens, which is highly affected by the onset of high-pressure after TAC, contributed to the inflammation process maybe through the breakdown of vascular tolerance as in Kawasaki disease [17]. The finding confirming that CD86 expression was much higher in the DCs found in the aorta ascendens than in the myocardium or the aorta descendens supported the hypothesis that DCs are highly involved in vascular inflammation in response to TAC. The higher activation level of CD11c^{+} cDCs in control animals suggests a reaction to the sham intervention f.e. at day 3 in the sham group but might also indicate that CD86 expression is elevated under steady-state conditions in the lymph nodes. Additionally, in the group of the MHC II^{+} CD11c^{+} DCs, we observed 15% to 20% of CD103^{+} DCs after TAC in the myocardium and the aorta ascendens. CD103, a ligand for E-cadherin expressed by most epithelial cells and also a marker for CD11b^{-} DCs in many tissues, was shown to originate from the aortic sinus [18], a region which was directly affected by the TAC surgery in our model. In the draining lymph nodes, we observed a relevant increase in the population of cDCs and at day 3 an early elevation in cell activation. We hypothesize that the DC response in the draining lymph nodes played a critical role in the orchestration of the immune response following TAC in the aorta and the myocardium and contributed to T cell activation. T cells are known to promote nonischemic heart failure, and the specific antigen recognition of CD4 T cells appears to be crucial for the progression from compensated cardiac hypertrophy to heart failure [19].

Our analyses of the aorta descendens did not reveal any significant changes in the immune response following TAC which might be due to the fact that the tissue was not directly and even remotely affected.

The TAC model used in this project mirrors the situation of patients suffering from diseases such as chronic arterial hypertension or aortic valve stenosis that result in LV hypertrophy. It was considered that the acute onset of pressure overload in the TAC model did not perfectly reflect the patients' clinical course in which the pressure overload slowly evolves over the years leading to LV hypertrophy and heart failure. Despite the limitations of the current study, the model of TAC in mice has been extensively used to examine signaling pathways that contribute to adverse cardiac remodeling and hypertrophy in the context of pressure overload [15]. The observations collected in this study promote a model that can be used to compare high-pressure and low-pressure conditions in the aortic tissue in parallel in the same animal.

5. Conclusion

Based on the findings of the current study, it is likely that the monocytes that have accumulated in response to TAC in the myocardium originate from splenic pools and reach the site of the inflammation via the blood driven by chemotaxis. The

high-pressure conditions in the aorta ascendens cause a characteristic immune response, dominated by the accumulation of leukocytes that varies depending on the immune cell dynamics in the myocardium and the aorta descendens.

Abbreviations

DAMPs: Danger-associated molecular patterns
DC: Dendritic cell
FACS: Fluorescence-activated cell sorting
IL: Interleukin
LV: Left ventricle
MFI: Mean Fluorescence Intensitiy
MHC: Major histocompatibility complex
MI: Myocardial infarction
TAC: Transverse aortic constriction
Wt: Wild-type mice (C57BL/6).

Data Availability

The authors confirm that the data supporting the findings of this study are available within the article [and/or] its supplementary material.

Conflicts of Interest

The authors declare no competing financial interests.

Authors' Contributions

CKW, LE, JC, and SF conceived and designed the experiments. JLK, YZ, OK, and AF performed the experiments. CKW, JLK, SF, OK, and AF analyzed the data. CKW, JLK, SF, and MC wrote the manuscript.

Acknowledgments

The authors thank the Anesthesia lab Bonn for their helpful contributions. We acknowledge the support of the Flowcytometry Core Facility and the House for Experimental Therapy (HET) of the medical faculty of Bonn University. C. K. W. is funded by the Deutsche Forschungsgemeinschaft (DFG, German Research Foundation) (Grant no. 397484323, project no. 426093965).

Supplementary Materials

Supplemental Figure 1: fluorescence minus one (FMO) controls of CD11c and CD103 staining in addition to Figure 1. Supplemental Figure 2: direct comparison of CD86 MFI of $CD11c^+$ cells in heart, aorta ascendens, aorta descendens, and lymph node in addition to Figure 5. *(Supplementary Materials)*

References

[1] L. Lin and A. A. Knowlton, "Innate immunity and cardiomyocytes in ischemic heart disease," *Life Sciences*, vol. 100, no. 1, pp. 1–8, 2014.

[2] C. Weisheit, Y. Zhang, A. Faron et al., "Ly6C(low) and not Ly6C(high) macrophages accumulate first in the heart in a model of murine pressure-overload," *PLoS One*, vol. 9, no. 11, article e112710, 2014.

[3] C. K. Weisheit, J. L. Kleiner, M. B. Rodrigo et al., "CX3CR1 is a prerequisite for the development of cardiac hypertrophy and left ventricular dysfunction in mice upon transverse aortic constriction," *PLoS One*, vol. 16, no. 1, article e0243788, 2021.

[4] Y. Zhang, W. Wen, and H. Liu, "The role of immune cells in cardiac remodeling after myocardial infarction," *Journal of Cardiovascular Pharmacology*, vol. 76, no. 4, pp. 407–413, 2020.

[5] C. Auffray, D. Fogg, M. Garfa et al., "Monitoring of blood vessels and tissues by a population of monocytes with patrolling behavior," *Science*, vol. 317, no. 5838, pp. 666–670, 2007.

[6] M. Nahrendorf, F. K. Swirski, E. Aikawa et al., "The healing myocardium sequentially mobilizes two monocyte subsets with divergent and complementary functions," *Journal of Experimental Medicine*, vol. 204, no. 12, pp. 3037–3047, 2007.

[7] M. Schiwon, C. Weisheit, L. Franken et al., "Crosstalk between sentinel and helper macrophages permits neutrophil migration into infected uroepithelium," *Cell*, vol. 156, no. 3, pp. 456–468, 2014.

[8] H. Ehrentraut, S. Felix Ehrentraut, O. Boehm et al., "Tlr4 deficiency protects against cardiac pressure overload induced hyperinflammation," *PLoS One*, vol. 10, no. 11, article e0142921, 2015.

[9] H. Ehrentraut, C. Weber, S. Ehrentraut et al., "The toll-like receptor 4-antagonist eritoran reduces murine cardiac hypertrophy," *European Journal of Heart Failure*, vol. 13, no. 6, pp. 602–610, 2011.

[10] X. Clemente-Casares, S. Hosseinzadeh, I. Barbu et al., "A $CD103^+$ Conventional Dendritic Cell Surveillance System Prevents Development of Overt Heart Failure during Subclinical Viral Myocarditis," *Immunity*, vol. 47, no. 5, pp. 974–989.e8, 2017.

[11] I. Santos-Zas, J. Lemarie, A. Tedgui, and H. Ait-Oufella, "Adaptive immune responses contribute to post-ischemic cardiac remodeling," *Frontiers in Cardiovascular Medicine*, vol. 5, p. 198, 2019.

[12] A. Cossarizza, H. D. Chang, A. Radbruch et al., "Guidelines for the use of flow cytometry and cell sorting in immunological studies," *European Journal of Immunology*, vol. 47, no. 10, pp. 1584–1797, 2017.

[13] F. K. Swirski, M. Nahrendorf, M. Etzrodt et al., "Identification of splenic reservoir monocytes and their deployment to inflammatory sites," *Science*, vol. 325, no. 5940, pp. 612–616, 2009.

[14] H. Wang, D. Kwak, J. Fassett et al., "Role of bone marrow-derived CD11c(+) dendritic cells in systolic overload-induced left ventricular inflammation, fibrosis and hypertrophy," *Basic Research in Cardiology*, vol. 112, no. 3, p. 25, 2017.

[15] L. Bacmeister, M. Schwarzl, S. Warnke et al., "Inflammation and fibrosis in murine models of heart failure," *Basic Research in Cardiology*, vol. 114, no. 3, p. 19, 2019.

[16] Y. Zaidi, E. G. Aguilar, M. Troncoso, D. V. Ilatovskaya, and K. Y. DeLeon-Pennell, "Immune regulation of cardiac fibrosis post myocardial infarction," *Cellular Signalling*, vol. 77, p. 109837, 2021.

[17] S. J. Inder, Y. V. Bobryshev, S. M. Cherian et al., "Immunophenotypic analysis of the aortic wall in Takayasu's arteritis:

involvement of lymphocytes, dendritic cells and granulocytes in immuno- inflammatory reactions," *Cardiovascular Surgery*, vol. 8, no. 2, pp. 141–148, 2000.

[18] J. H. Choi, C. Cheong, D. B. Dandamudi et al., "Flt3 signaling-dependent dendritic cells protect against atherosclerosis," *Immunity*, vol. 35, no. 5, pp. 819–831, 2011.

[19] F. Laroumanie, V. Douin-Echinard, J. Pozzo et al., "CD4+ T cells promote the transition from hypertrophy to heart failure during chronic pressure overload," *Circulation*, vol. 129, no. 21, pp. 2111–2124, 2014.

Hindawi
Mediators of Inflammation
Volume 2021, Article ID 6889733, 12 pages
https://doi.org/10.1155/2021/6889733

Research Article

The Predictive role of Neutrophil-to-Lymphocyte Ratio (NLR) and Mean Platelet Volume-to-Lymphocyte Ratio (MPVLR) for Cardiovascular Events in Adult Patients with Acute Heart Failure

Teeranan Angkananard,[1] **Teeraporn Inthanoo**,[2] **Suchat Sricholwattana**,[1] **Nattapun Rattanajaruskul**,[1] **Arthit Wongsoasu**,[1] **and Worawut Roongsangmanoon**[1]

[1]*Division of Cardiovascular Medicine, Department of Medicine, Faculty of Medicine, HRH Princess Maha Chakri Sirindhorn Medical Center, Srinakharinwirot University, Nakhon Nayok, Thailand*
[2]*Department of Medicine, Faculty of Medicine, HRH Princess Maha Chakri Sirindhorn Medical Center, Srinakharinwirot University, Nakhon Nayok, Thailand*

Correspondence should be addressed to Teeranan Angkananard; teeranan@g.swu.ac.th

Received 2 July 2021; Revised 22 August 2021; Accepted 16 September 2021; Published 11 October 2021

Academic Editor: Amilia Aminuddin

Introduction. The inflammatory response plays a potential role for the pathogenesis and adverse outcomes of heart failure (HF). We aimed to explore the predictive role of baseline neutrophil-to-lymphocyte ratio (NLR) and mean platelet volume-to-lymphocyte ratio (MPVLR) on cardiovascular events (CVEs) in patients hospitalized with acute HF. *Materials and Methods*. A retrospective cohort study was conducted in 321 patients with HF between January 2017 and December 2019. The association between their NLR, MPVLR, and combined NLR and MPVLR and CVEs, rehospitalization for HF, in-hospital death, and a composite outcome was explored by survival analysis using a Cox proportional hazard model. They were separately investigated and compared with the area under the receiver operating characteristics curve (AUC). *Results*. Up to the end of the 3-year follow-up, 96 (29.9%) had CVEs, 106 (33.0%) died, 62 (19.3%) were rehospitalized with HF, and 21 (6.5%) died during admission. The NLR and MPVLR were significantly associated with CVEs (adjusted HR for NLR ≥ 3.29, 3.11; 95% CI, 1.98-4.89; MPVLR ≥ 8.57, 2.86; 95% CI, 1.87-4.39), readmissions for HF (adjusted HR for NLR ≥ 3.58, 2.70; 95% CI, 1.58-4.61; MPVLR ≥ 6.43, 2.84; 95% CI,1.59-5.07), in-hospital mortality (adjusted HR for NLR ≥ 3.29, 9.54; 95% CI, 2.19-41.40; MPVLR ≥ 8.57, 7.87; 95% CI, 2.56-24.19), and composite outcome (adjusted HR for NLR ≥ 3.32, 4.76; 95% CI, 3.29-6.89; MPVLR ≥ 7.07, 3.64; 95% CI, 2.58-5.15). The AUC of NLR and MPVLR for CVEs were 0.67 (95% CI, 0.61-0.72) and 0.63 (95% CI, 0.58-0.69). Combined NLR and MPVLR increased the AUC to 0.77 (95% CI, 0.72-0.83) with statistical significance. *Conclusion*. The elevated NLR and MPVLR on admission in patients with acute HF were independently associated with worse CVEs, rehospitalization for HF, in-hospital death, and composite outcomes. These economical biomarkers should be considered in the management and follow-up care of patients with acute HF.

1. Introduction

Heart failure (HF) is a common and serious condition with a global prevalence of 64.3 million [1]. The prevalence is predicted to increase rapidly by 46% from 2012 to 2030 [2]. The 1-year and 5-year mortality rates after HF hospitalization are reported to be as high as 22% and 42.3%, respectively [2]. Therefore, using biomarkers to predict HF outcomes may benefit HF management and reduce the mortality rate.

The inflammatory response plays a potential role in the pathogenesis and adverse remodeling process in patients with both acute and chronic HF [3, 4]. Neutrophil- and T-cell-derived enzymes and cytokines can cause myocardial damage, negative left ventricular remodeling, and disease

progression in both HF with reduced ejection fraction and HF with preserved ejection fraction [5]. In addition, platelets are involved in hemostasis, thrombosis, and inflammation and are thus important in disease occurrence. It has been shown that inflammatory processes are regulated by the platelet-induced activation of blood leukocytes, which influences the pathophysiology and progression of chronic HF [6, 7].

The neutrophil-to-lymphocyte ratio (NLR) is an emerging biomarker useful for predicting the risk and prognosis of cardiovascular diseases [8–10]. Thus, its usefulness has been recognized in risk stratification and has been shown to be cost-effective for patients with cardiovascular (CV) disease [11]. Previous studies have demonstrated the relationship between NLR and acute and chronic HF, including their associated complications, severity, and prognosis [12]. A recent meta-analysis [10] also supported the prognostic role of the NLR for all-cause mortality in patients with HF. NLR has a similar prognostic power as the N-terminal probrain B-type natriuretic peptide (NT-Pro, BNP) for major cardiovascular events (CVEs), particularly in elderly patients with HF [13].

Furthermore, the mean platelet volume (MPV), a known biomarker of both proinflammatory and prothrombotic conditions [14, 15], has been found to be an independent variable for predicting in-hospital and 6-month mortality [16] and HF-related hospitalization outcomes in patients with HF [17]. However, all-cause mortality outcomes include both CV and non-CV deaths. No study has thus far investigated the prognostic role of NLR, MPV, MPV to lymphocyte ratio (MPVLR), and combined NLR and MPVLR for a particular outcome of CV mortality and CVEs in patients hospitalized with acute HF (AHF). Hence, we aimed to explore the predictive role of them on CVEs in adult patients with AHF.

2. Materials and Methods

2.1. Study Design and Data Collection. We conducted a retrospective cohort study using the electronic medical records of consecutive patients with acute HF admitted to the H.R.H Maha Chakri Sirindhorn Medical Center of Srinakharinwirot University between January 1, 2017, and December 31, 2019. Patients included in the study must have been admitted with a principal diagnosis of HF and underwent transthoracic echocardiography. Exclusion criteria included a history of hematologic disease, severe infection, cancer, or recent corticosteroid use within 3 months prior to admission. HF was classified into three groups according to the HF guidelines of the European Society of Cardiology [2]; that is, HF with preserved ejection fraction was defined as left ventricular ejection fraction (LVEF) $\geq 50\%$ while HF with reduced ejection fraction was defined as LVEF $< 40\%$. Patients with LVEF between 40% and 49% were categorized as having HF with midrange ejection fraction.

The primary outcome was a combined CVEs of CV death and hospitalization due to HF; acute coronary syndrome (ACS), including ST-segment elevation myocardial infarction, non-ST elevation myocardial infarction, and unstable angina; acute stroke or cerebrovascular accident; and cardiac arrhythmia. The secondary outcomes included readmission for HF, in-hospital death, and a composite outcome of CVEs and all-cause mortality. Patient data were collected at the index of hospitalization and included demographics, initial vital signs (respiratory rate (RR), pulse rate, and systolic and diastolic blood pressure), New York Heart Association (NYHA) functional classification, concomitant CV diseases, laboratory findings, current medication, electrocardiographic and echocardiogram findings, current medication, clinical course, and length of hospital stay. Clinical outcomes during admission and after discharge were collected from electronic medical records and telephone consults.

NLR was calculated by dividing absolute neutrophil counts by absolute lymphocyte counts derived from automated cell counters. MPVLR was computed by dividing the MPV by absolute lymphocyte counts. Both NLR and MPVLR were classified into two groups using different optimal cut-off values for each outcome. To define the optimal cut-off values of NLR and MPVLR, the receiver operating characteristic curve-based method of the Youden index was used. These cut-off points optimized the differentiating capability of the NLR and MPVLR when an equal weight was given to the sensitivity and specificity [18, 19]. Using data from a previous study [20], the calculation for a sample size revealed that at least 305 patients were needed to achieve a power of 0.8 and a type I error of 0.05.

2.2. Statistical Analyses. Continuous variables are expressed as the mean with standard deviation or the median with interquartile range (IQR) and were compared between CVEs and each outcome using the Student t-test or Mann-Whitney U test, depending on the data distribution. Categorical variables are shown as frequencies and percentages and were compared between groups of outcomes using the chi-square test. Survival probability was assessed using Kaplan–Meier estimation. The relationship between the NLR and MPVLR groups, CVEs, and composite outcomes was compared using a log-rank test. Survival analysis with the Cox proportional hazard model was used to identify factors associated with the NLR and MPVLR groups according to individual outcomes. Hazard ratios (HRs) and their 95% confidence intervals (CIs) were calculated to explore the strength of association between the studied factors (NLR and MPVLR), confounders, and outcomes using Breslow's method for handling ties.

The set of possible confounders for each outcome based on background knowledge and clinical practice was individually considered in the univariate analysis. Variables with a P value < 0.1 in the univariate analysis were considered in the multivariate analysis. We excluded the variables that had high missing data (>10%) from the analysis (51.7% magnesium, 57% phosphorus, 42.1% albumin, 50.8% troponin, and 86.3% NT-pro-BNP). The forward selection was used to identify the significant variables for each outcome and the studied factors (NLR and MPVLR). However, MPV was not included in the multivariate model because it was part of our studied factor (MPVLR). The final variables were included in the Cox regression multivariate models for each outcome.

Both NLR and MPVLR were found to have equal ability to predict the risks of our outcomes; thus, we converted them into a combined NLR and MPVLR using a point-based risk score. It was derived from the β-coefficients of the final Cox regression multivariate model of individual outcomes (Appendix). We applied categorical NLR and MPVLR for each outcome with different cut-off values (NLR: 3.29, MPVLR: 8.57 for CVEs and in-hospital death outcomes; NLR: 3.58, MPVLR: 6.43 for rehospitalization for HF; and NLR: 3.32, MPVLR: 7.07 for the composite outcome). The predictive abilities of NLR, MPVLR, and combined NLR and MPVLR were separately evaluated and compared in each outcome with respect to the area under the receiver operating characteristic curve (AUC) [21].

All P values were two-sided, and a value of less than 0.05 was considered significant. All analyses were performed using STATA version 16.1 (StataCorp; College Station, Texas, United States). The study protocols were reviewed and approved by the Institutional Review Board Committee of Srinakharinwirot University (SWUEC-365/2562E) in April 2020.

3. Results

3.1. Baseline Characteristics of the Patients with HF Stratified by CVEs. Table 1 shows the demographic, clinical, and laboratory data of the 321 patients with HF. The majority were elderly (62.2%), with a mean age of 67.4 ± 14.9 years, and nearly half of them were men (44.9%). Hypertension, diabetes, dyslipidemia, history of coronary heart disease, history of stroke, and atrial fibrillation (AF) were present in 85.7%, 56.4%, 58.6%, 41.1%, 16.2%, and 23.1%, respectively. The baseline vitals were as follows: body mass index (BMI), 24.1 ± 5.6 kg/m^2; blood pressure (BP), 142.2 ± 27.7/82.3 ± 16.9 mmHg; mean BP, 102.2 ± 19.1 mmHg; initial pulse rate, 92.3 ± 20.6 beats per minute; initial RR, 24 breaths per minute; and LVEF, 45.4 ± 16.9%. All patients suffered from HF with NYHA class III (57.0%) and IV (42.9%). The baseline laboratory results were as follows: baseline NLR, 3.2 (IQR: 2.3, 5.0); MPV, 10.4 ± 0.9 fL; and MPVLR, 7.5 ± 4.9. The absolute lymphocyte count, MPV, NLR, and MPVLR are substantial predictors of CVEs.

3.2. Survival Analysis. Up to the end of the 3-year follow-up, 320 patients had a median follow-up time of 23 months (IQR: 2, 33 months). Of these, 96 patients (29.9%) had CVEs, 106 (33.0%) died, 62 (19.3%) were rehospitalized with HF, and 21 (6.5%) died at the time of admission. The incidence rate of CVEs was 60.57 per 1,000 population per year. Fifty percent of patients with HF were free of the composite outcome at approximately 39.8 months. The log-rank tests of equality across NLR and MPVLR groups for prediction of CVEs had a P value of <0.001 (Figures 1(a) and 1(b)); thus, the NLR and MPVLR groups were included as potential candidates for the final model. Tables 2 and 3 show that the univariate analyses using the Cox proportional hazard models were stratified by CVEs after HF inception. BMI; history of stroke; initial mean BP; initial RR; NYHA class IV; concomitant AF; ACS; valvular heart disease (VHD); prescribed angiotensin-converting enzymes inhibitors; and baseline NLR, MPV, MPVLR, and PLR were statistically significant covariates of CVE outcomes. In the multivariate analysis, initial RR, NYHA class IV, concomitant AF, ACS, and VHD were considerable variables with CVEs when the studied factors were NLR ≥ 3.29 (adjusted HR, 3.11; 95% CI, 1.98–4.89), MPVLR ≥ 8.57 (adjusted HR, 2.86; 95% CI, 1.87–4.39), or combined NLR and MPVLR (adjusted HR, 2.72; 95% CI, 2.15–3.43 (data not shown)).

For readmission for HF outcome, NYHA class IV, concomitant ACS, prescribed beta-blocker during hospitalization, and anemic status were significant variables in the multivariate Cox proportional hazard model (Table 3). The adjusted HR was 2.70 (95% CI, 1.58–4.61), 2.84 (95% CI,1.59–5.07), and 2.73 (95% CI, 1.93–3.85) for NLR ≥ 3.58 , MPVLR ≥ 6.43, and combined NLR and MPVLR, respectively. NYHA class IV, initial systolic BP, and RR were significant factors associated with in-hospital mortality in patients with HF. The adjusted HRs were 9.54 (95% CI, 2.19–41.40), 7.87 (95% CI, 2.56–24.19), and 1.05 (95% CI, 1.03–1.07) for NLR ≥ 3.29, MPVLR ≥ 8.57, and combined NLR and MPVLR, respectively. In addition, NYHA class IV, concomitant AF, ACS, and BMI were significant variables associated with the composite outcome, with adjusted HRs of 4.76 (95% CI, 3.29–6.89), 3.64 (95% CI, 2.58–5.15), and 2.60 (95% CI, 2.17–3.12) for NLR ≥ 3.32, MPVLR ≥ 7.07, and combined NLR and MPVLR, respectively.

3.3. AUC Analyses of NLR, MPVLR, and Combined NLR and MPVLR for Each Outcome. The receiver operating characteristic curves of NLR, MPVLR, and combined NLR and MPVLR for each outcome are illustrated in Figure 2. The AUC of NLR and MPVLR for CVEs were 0.67 (95% CI, 0.61–0.72) and 0.63 (95% CI, 0.58–0.69). Combining NLR and MPVLR increased the AUC value to 0.77 (95% CI, 0.72–0.83) with statistical significance. Likewise, combining NLR and MPVLR substantially strengthened the AUC value for predicting readmission for HF and in-hospital mortality (0.72 (95% CI, 0.65–0.79, $P < 0.05$) and 0.92 (95% CI, 0.88–0.96, $P = 0.03$). For the composite outcome, the AUC of NLR, MPVLR, and combined NLR and MPVLR were 0.80 (95% CI, 0.75–0.85), 0.78 (95% CI, 0.72–0.83), and 0.83 (95% CI, 0.79–0.88), respectively (Table 4). However, combining both the NLR and MPVLR did not significantly improve its performance in predicting the composite outcome ($P = 0.07$).

4. Discussion

This study evaluated the predictive role of the NLR and MPVLR on CVEs, readmission for HF, in-hospital death, and composite outcomes of patients hospitalized with AHF. During the 3-year follow-up, higher levels of NLR and MPVLR at baseline were independently associated with all outcomes after discharge. Notably, combining both NLR and MPVLR improved the ability to portend CVEs, readmission for HF, and in-hospital mortality than individual NLR or MPVLR.

Table 1: Baseline characteristics of patients with heart failure, stratified by cardiovascular events.

Characteristics	Mean (SD)	CVEs ($N = 96$)	No CVEs ($N = 225$)	z/X^2	P value[a]
Male sex, N (%)	144 (44.9)	40 (41.7)	104 (46.2)	-0.62	0.53
Age (years)	67.4 (14.9)	69.5 (13.6)	66.5 (15.4)	1.80	0.07
BW (kg)	61.7 (15.9)	58.4 (12.2)	63.2 (17.2)	2.48	0.01
Height (cm)	159.7 (8.9)	159.9 (8.9)	159.7 (8.9)	-0.24	0.81
BMI (kg/m^2)	24.1 (5.6)	22.8 (4.3)	24.7 (5.9)	-2.70	<0.05
BMI class, N (%)					
<18.5 kg/m^2	33 (10.3)	12 (12.5)	21 (9.3)		
18.5-24.9 kg/m^2	172 (53.6)	60 (62.5)	112 (49.8)	7.56	0.06
25.0-29.9 kg/m^2	79 (24.6)	16 (16.7)	63 (28.0)		
30.0 kg/m^2	37 (11.5)	8 (8.3)	29 (12.9)		
Hypertension, N (%)	275 (85.7)	79 (82.3)	196 (87.1)	-1.11	0.27
Diabetes mellitus, N (%)	181 (56.4)	52 (54.2)	129 (57.3)	-0.28	0.78
Dyslipidemia, N (%)	188 (58.6)	56 (58.3)	132 (58.7)	0.03	0.98
Coronary heart disease, N (%)	132 (41.1)	73 (55.3)	59 (44.7)	1.69	0.09
Cerebrovascular accident, N (%)	52 (16.2)	24 (25.0)	28 (12.4)	2.81	<0.05
CKD stage, N (%)					
Stage 1	166 (51.7)	49 (51.0)	117 (52.0)		
Stage 2	10 (3.1)	3 (3.1)	7 (3.1)		
Stage 3	50 (15.6)	14 (14.6)	36 (16.0)	3.20	0.53
Stage 4	32 (9.9)	14 (14.6)	18 (8.0)		
Stage 5	63 (19.6)	16 (16.7)	47 (20.9)		
Alcohol consumption*, N (%)					
Never	247 (82.1)	79 (84.9)	168 (80.8)		
Quit	35 (11.6)	10 (10.8)	25 (12.0)	0.96	0.62
Current	19 (6.3)	4 (4.3)	15 (7.2)		
Smoking*, N (%)					
Never	223 (73.4)	75 (79.8)	148 (70.5)		
Quit	59 (19.4)	15 (15.9)	44 (20.9)	3.89	0.14
Current	22 (7.2)	4 (4.3)	18 (8.6)		
Rhythm, N (%)					
Sinus	247 (76.9)	64 (66.7)	183 (81.3)	7.66	<0.05
Atrial fibrillation	74 (23.1)	32 (33.3)	42 (18.7)		
LVEF (%)	45.4 (16.9)	45.2 (16.9)	45.5 (17.0)	-0.07	0.94
Type of HF, N (%)					
HFrEF	127 (39.6)	37 (38.5)	90 (40.0)	0.03	0.87
HFmEF	39 (12.2)	13 (13.5)	26 (11.6)	0.19	0.66
HFpEF	155 (48.3)	46 (47.9)	82 (48.4)	0.00	0.96
SBP (mmHg)	142.2 (27.7)	138.6 (28.2)	143.7 (27.4)	-1.79	0.07
DBP (mmHg)	82.3 (16.9)	80.0 (18.3)	83.2 (16.3)	-1.85	0.06
Mean BP (mmHg)	102.2 (19.1)	99.6 (19.8)	103.4 (18.7)	-1.96	0.05
Pulse rate (bpm)	92.3 (20.6)	93.4 (25.4)	91.8 (18.3)	0.87	0.38
Respiratory rate (per min)	23.6 (4.3)	24.5 (4.3)	23.2 (4.2)	2.77	<0.05
NYHA classification, N (%)					
III	183 (57.0)	39 (40.6)	144 (64.0)	3.99	<0.05
IV	138 (42.9)	57 (59.4)	81 (36.0)		
Comorbidity, N (%)					
Acute coronary syndrome	43 (13.4)	22 (22.9)	21 (9.3)	3.13	<0.05
Valvular heart disease[b]	57 (17.8)	25 (26.0)	32 (14.2)	2.41	0.02

Table 1: Continued.

Characteristics	Mean (SD)	CVEs ($N = 96$)	No CVEs ($N = 225$)	z/X^2	P value[a]
Cardiomyopathy (CM)	181 (56.4)	55 (57.3)	126 (56.0)		
Ischemic CM	87 (27.1)	31 (32.3)	56 (24.9)		
Nonischemic CM	50 (15.6)	11 (11.5)	39 (17.3)	2.79	0.41
Hypertensive CM	44 (13.7)	13 (13.5)	31 (13.8)		
HT emergency	32 (9.9)	7 (7.3)	25 (11.1)	-1.11	0.27
Medication, N (%)					
Statin	235 (73.2)	75 (78.1)	160 (71.1)	1.19	0.23
Beta-blocker	182 (56.7)	60 (62.5)	122 (54.2)	1.19	0.24
ACEIs	101 (31.5)	22 (22.9)	79 (35.1)	-2.19	0.03
ARBs	55 (17.1)	20 (20.8)	35 (15.6)	1.26	0.21
Aspirin	177 (55.1)	54 (56.3)	123 (54.7)	0.33	0.74
P2Y12 inhibitors	92 (28.7)	32 (33.3)	60 (26.7)	2.18	0.34
Diuretics	224 (69.8)	60 (62.5)	164 (72.9)	-1.90	0.06
Lab					
WBC, $\times 10^3$, median (IQR) (cells/mL)	8.20 (6.4, 10.4)	8.6 (6.7, 10.4)	8.1 (6.4, 10.0)	-0.66	0.51
Neutrophil (%)	68.0 (11.0)	71.6 (10.7)	66.5 (10.8)	3.89	<0.001
Neutrophil count, $\times 10^3$, median (IQR) (cells/mL)	5.4 (4.3, 7.1)	6.1 (4.6, 7.4)	5.1 (4.0, 7.0)	-0.36	0.72
Lymphocyte (%)	22.5 (10.6)	19.2 (9.9)	23.9 (10.6)	-3.87	<0.001
Lymphocyte count, $\times 10^3$, median (IQR) (cells/mL)	1.7 (1.1, 2.4)	1.3 (0.9, 2.0)	1.8 (1.2, 2.4)	-2.07	0.04
NLR, median (IQR)	3.2 (2.3, 5.0)	5.0 (3.4)	3.6 (2.7)	4.25	<0.001
Q1 (NLR < 3.29)	2.2 (0.7)	1.9 (0.7)	2.3 (0.7)	5.24	<0.001
Q2 (NLR ≥ 3.29)	5.9 (3.3)	6.2 (3.3)	5.8 (3.3)		
Platelets, ×103 (cells/mL)	254.7 (92.4)	251.3 (94.5)	256.1 (91.6)	-0.50	0.61
Hb (g/dL)	10.7 (2.6)	10.7 (2.5)	10.7 (2.7)	-0.08	0.94
Anemia[c]	245 (76.3)	74 (77.1)	171 (76.0)	0.32	0.75
MPV (fL)*	10.4 (0.9)	10.7 (1.0)	10.3 (0.9)	2.80	0.005
MPVLR*	7.5 (4.9)	9.0 (5.7)	6.9 (4.5)	3.92	<0.001
Q1 (MPVLR < 8.57)	5.0 (1.9)	5.1 (2.0)	5.0 (1.8)	5.12	<0.001
Q2 (MPVLR ≥ 8.57)	13.6 (4.9)	13.4 (5.3)	13.9 (4.6)		
BUN, median (IQR) (mg/dL)	24.9 (18.1, 43.5)	25.5 (18.8, 40.5)	24.6 (16.9, 43.9)	-0.15	0.89
Creatinine, median (IQR), mg/dL	1.5 (1.1, 2.7)	1.5 (1.1, 2.6)	1.5 (1.0, 2.8)	-0.23	0.82
Sodium (mmol/L)	136.2 (8.0)	136.4 (4.0)	136.2 (9.2)	0.17	0.86
Potassium, median (IQR) (mmol/L)	4.0 (3.6, 4.4)	4.0 (3.6, 4.4)	4.0 (3.6, 4.5)	-0.36	0.72
Magnesium (mg/dL)*	2.1 (0.4)	2.0 (0.5)	2.1 (0.3)	-0.13	0.89
Phosphorous (mmol/L)*	4.1 (1.3)	4.3 (1.4)	4.1 (1.2)	0.64	0.52
Albumin (g/dL)*	3.5 (0.5)	3.4 (0.5)	3.5 (0.6)	-1.10	0.27
Troponin, median (IQR), (ng/mL)*	57.7 (20.0, 172.0)	115.0 (55.0, 410.5)	40.0 (16.0, 137.0)	1.47	0.14
NT-pro-BNP ($\times 10^3$), median (IQR) (pg/mL)*	5.2 (2.6-13.6)	9.9 (4.5, 14.1)	4.2 (1.7, 12.7)	0.92	0.36

Data are reported by mean ± SD or count (%); IQR: interquartile range. Abbreviations: CVEs: cardiovascular events; BW: body weight; BMI: body mass index; CKD: chronic kidney disease; LVEF: left ventricular ejection fraction; HFrEF: heart failure with reduced ejection fraction; HFmEF: heart failure with midrange ejection fraction; HFpEF: heart failure with preserved ejection fraction; SBP: systolic blood pressure; DBP: diastolic blood pressure; NYHA: the New York Heart Association Functional Classification; ACEIs: angiotensin-converting enzyme inhibitors; ARBs: angiotensin-II receptor antagonists; WBC: white blood cell; NLR: neutrophil-lymphocyte ratio; Hb: hemoglobin; MPV: mean platelet volume; MPVLR: MPV-to-lymphocyte ratio; NT-pro-BNP: N-terminal pro-B-type natriuretic peptide. *Missing data: alcohol consumption = 6.2%, smoking = 5.3%, MPV and MPVLR = 5.9%, magnesium = 51.7%, phosphorous = 57%, albumin = 42.1%, troponin = 50.8%, and NT − pro − BNP = 86.3%. [a]Using t-test for continuous variables and χ^2 test for categorical variables. [b]Valvular heart disease (VHD): mitral valve disease (5.3%), aortic valve disease (9.9%), others (2.5%). [c]Anemia: Hb < 13 g/dL in men and Hb < 12 g/dL in women.

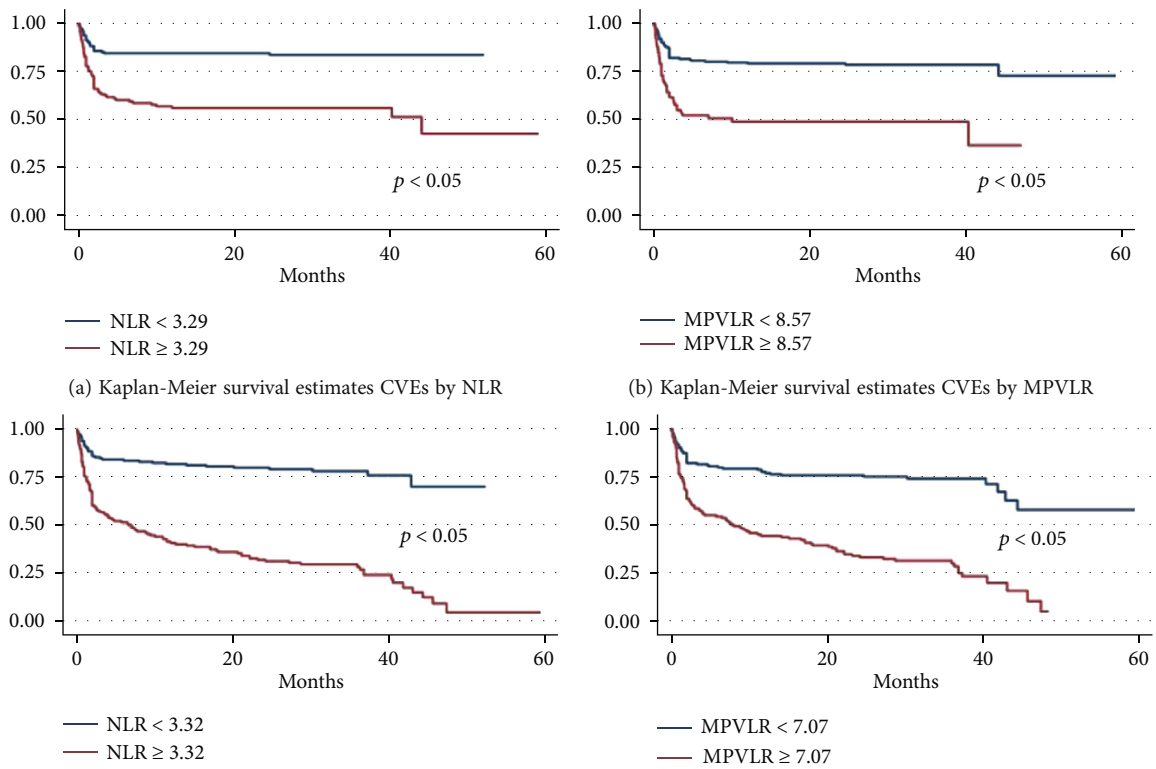

(a) Kaplan-Meier survival estimates CVEs by NLR

(b) Kaplan-Meier survival estimates CVEs by MPVLR

(c) Kaplan-Meier survival estimates composite outcome by NLR

(d) Kaplan-Meier survival estimates composite outcome by MPVLR

Figure 1: Kaplan-Meier survival estimation of NLR and MPVLR for cardiovascular events and a composite outcome.

The findings of this study correspond with the results from other published studies. In a previous prospective study of patients with acute decompensated HF, elevated NLR was associated with higher rates of in-hospital, 3-year mortality after discharge [22, 23], and heart transplantation risk [23]. A prior meta-analysis conducted by Wang et al. [10] also supported the predictive role of the NLR for all-cause mortality in patients with HF. All-cause mortality in this study includes both CV and non-CV deaths; however, no study has evaluated a particular outcome of CV mortality and CVEs in patients with AHF. Moreover, no study has investigated the prognostic role of NLR, MPVLR, and combined NLR and MPVLR for CV mortality and CVEs in adult patients hospitalized with AHF. Thus, this study was the first analysis of the capability of them, to predict an imperative CV outcome in patients with AHF.

The association between high NLR levels and worse CV outcomes in patients with HF could be explained by the activation of neutrophils from inflammatory and autonomic responses [24]. The release of proteolytic cytokines, such as acid phosphatase, elastase, and myeloperoxidase leads to an excess of free radicals which may cause myocardial injury. The neutrophil-derived enzyme myeloperoxidase has been studied in the context of ischemic myocardial damage [25, 26] and advanced HF [27], which is a potential mediator of impaired myocardial remodeling and poor prognosis. Furthermore, the elevation of ventricular filling pressure in patients with HF produces splanchnic congestion, which may affect the enteral loss of lymphocytes [28] and promote bacterial endotoxin translocation from the gut into the systemic circulation [29]. The levels of cortisol and tumor necrosis factor-1 during stress and immunologic response are also enhanced, which induces a diminished number of lymphocytes. Moreover, the release of cytokines, such as tumor necrosis factor-1, from the activation of the immunologic response may diminish lymphocyte counts [30]. The mouse model study supports the finding that T-cells can inhibit the development of intimal thickening and the proliferation of smooth muscle cells, endothelial cells, and fibroblasts by secretion of interferon-gamma [30]. Therefore, tissue healing is inhibited during the phase of T-cell activation and immune responses after injury.

In addition, MPV has been found to be an independent variable for predicting in-hospital and 6-month mortality [16] and HF-related hospitalization outcomes in patients with HF [17]. However, it was a good predictor of CVE, in-hospital death, and readmission for HF, but not for total mortality in our study. It has become evident that MPV is an indicator of both proinflammatory and prothrombotic conditions. The possible mechanism of MPV accompanying HF may be the MPV indicating the platelet size and function. The size of platelets in the circulation is correlated with the intensity of systemic inflammation [31]. Some genetic factors play a possible role in the regulation of MPV in inflammation and thrombosis [32]. Moreover, prior evidence derived from both retrospective and prospective studies proposes that a large platelet size and high MPV are predictors of established CV risk factors [31, 33] and

Table 2: Univariate and multivariate analysis with a Cox proportional hazard model of risk factors for cardiovascular events of patients with heart failure.

Variables	Univariate analysis						Multivariate analysis (NLR)				Multivariate analysis (MPVLR)				Multivariate analysis (NLR and MPVLR)			
	β	HR	Z	95% CI Lower	95% CI Upper	P value	HR	95% CI Lower	95% CI Upper	P value	HR	95% CI Lower	95% CI Upper	P value	HR	95% CI Lower	95% CI Upper	P value
NLR																		
NLR < 3.29	1	1				<0.05	1			<0.05					1			<0.05
NLR ≥ 3.29	1.19	3.30	5.24	2.11	5.16		3.11	1.98	4.89						2.42	1.46	4.01	
MPVLR																		
MPVLR < 8.57	1					<0.05					1			<0.05	1			<0.05
MPVLR ≥ 8.57	1.08	2.93	5.12	1.94	4.42						2.86	1.87	4.39		1.95	1.22	3.10	
BMI	-0.06	0.94	-2.70	0.90	0.98	<0.05												
CVA	0.67	1.95	2.81	1.22	3.10	<0.05												
Rhythm																		
Sinus	1	1				<0.05	1			0.02	1			<0.05	1			0.05
Atrial fibrillation	0.63	1.88	2.89	1.22	2.89		1.76	1.12	2.78		2.86	1.87	4.39		1.60	1.00	2.56	
Mean BP	-0.01	0.99	-1.96	0.98	1.00	0.05												
Respiratory rate	0.05	1.06	2.77	1.02	1.09	<0.05	1.05	1.00	1.09	0.04	1.05	1.00	1.09	0.03	1.05	1.00	1.09	0.04
NYHA																		
III	1	1				<0.05	1				1			<0.05	1			<0.05
IV	0.84	2.32	3.99	1.53	3.49		2.21	1.45	3.38	<0.05	2.14	1.39	3.31		2.16	1.40	3.34	
Etiology																		
ACS	0.77	2.17	3.13	1.33	3.52	<0.05	2.17	1.32	3.57	<0.05	2.41	1.46	3.96	<0.05	2.33	1.41	3.86	<0.05
VHD	0.57	1.77	2.41	1.11	2.81	0.02	1.71	1.06	2.75	0.03	1.71	1.04	2.79	0.03	1.83	1.12	2.98	0.02
Medication																		
ACEIs	-0.54	0.58	-2.19	0.36	0.94	0.03												
PLR	0.002	1.00	3.09	1.001	1.003	<0.05												
MPV	0.27	1.31	2.80	1.08	1.58	<0.05												

Abbreviations: NLR: neutrophil-lymphocyte ratio; MPVLR: mean platelet volume-to-lymphocyte ratio; CI: confidential interval; HR: hazard ratio; BMI: body mass index; CVA: cerebrovascular accident; BP: blood pressure; NYHA: New York Heart Association Classification; ACS: acute coronary syndrome; VHD: valvular heart disease; ACEIs: angiotensin-converting enzyme inhibitors; PLR: platelet to lymphocyte ratio; MPV: mean platelet volume.

Table 3: Association of NLR and MPVLR with a prognosis of subsequent cardiovascular events and mortality in patients with heart failure.

Outcome	Number of events	Crude HR	95% CI	*P* value	Adjusted HR	95% CI	*P* value
Cardiovascular events[a]							
NLR < 3.29	27	1 (reference)	1 (reference)	<0.001	1 (reference)	1 (reference)	<0.001
NLR ≥ 3.29	69	3.30	2.11-5.16		3.11	1.98-4.89	
MPVLR < 8.57	48	1 (reference)	1 (reference)	<0.001	1 (reference)	1 (reference)	<0.001
MPVLR ≥ 8.57	44	2.93	1.94-4.42		2.86	1.87-4.39	
Rehospitalization for HF[b]							
NLR < 3.58	26	1 (reference)	1 (reference)	0.002	1 (reference)	1 (reference)	<0.001
NLR ≥ 3.58	36	2.23	1.34-3.69		2.70	1.58-4.61	
MPVLR < 6.43	25	1 (reference)	1 (reference)	0.020	1 (reference)	1 (reference)	<0.001
MPVLR ≥ 6.43	35	1.84	1.10-3.08		2.84	1.59-5.07	
In-hospital death[c]							
NLR < 3.29	3	1 (reference)	1 (reference)	0.002	1 (reference)	1 (reference)	0.003
NLR ≥ 3.29	18	10.62	2.46-45.81		9.54	2.19-41.40	
MPVLR < 8.57	4	1 (reference)	1 (reference)	<0.001	1 (reference)	1 (reference)	<0.001
MPVLR ≥ 8.57	15	10.43	3.45-31.55		7.87	2.56-24.19	
Composite outcome[d]							
NLR < 3.32	38	1 (reference)	1 (reference)	<0.001	1 (reference)	1 (reference)	<0.001
NLR ≥ 3.32	119	4.82	3.34-6.96		4.76	3.29-6.89	
MPVLR < 7.07	50	1 (reference)	1 (reference)	<0.001	1 (reference)	1 (reference)	<0.001
MPVLR ≥ 7.07	100	3.50	2.49-4.92		3.64	2.58-5.15	

Abbreviations: NLR: neutrophil-lymphocyte ratio; MPVLR: mean platelet volume-to-lymphocyte ratio; CI: confidential interval; HR: hazard ratio; HF: heart failure; NYHA: New York Heart Association; ACS: acute coronary syndrome. [a]A multivariate Cox proportional hazard model adjusted for NYHA classification, ACS, heart rhythm, initial respiratory rate, and underlying valvular heart disease (VHD). [b]A multivariate Cox proportional hazard model adjusted for NYHA classification, ACS, taking beta-blocker, and anemia. [c]A multivariate Cox proportional hazard model adjusted for NYHA classification, initial systolic blood pressure, and initial respiratory rate. [d]A multivariate Cox proportional hazard model adjusted for NYHA classification, ACS, heart rhythm, and body mass index.

thrombotic events in several CV and venous disorders, such as coronary artery disease, myocardial infarction, restenosis after percutaneous coronary intervention, cerebrovascular disease, AF, venous thromboembolism, and mortality [14, 15, 34]. Some biomarkers of inflammation are associated with HF [35], and platelet size is increased in both acute decompensated and chronic HF [16, 17, 36].

Our study had several strengths. This was the first to analyse the prognostic factors for CV outcomes in patients with AHF using routinely measured biomarkers (NLR, MPVLR, and combined NLR and MPVLR) by automated cell counters. The combination of the NLR and MPVLR had better performance for predicting CVEs and composite outcomes. A previous study reported a higher cut-off value of NLR to predict the mortality outcome compared to ours (NLR 5 to 7) [22], in which its performance was not reported. Additionally, HF is an endpoint of untreated CV disorders. As such, our study included those as confounding factors in the multivariate analysis, that is, concomitant AF, ACS, and significant VHD, and still found a significant association between the level of NLR and MPVLR, and CVEs. These results support the role of inflammation in the development and progression of different etiologies of HF. Therefore, NLR and MPVLR are potentially cost-effective biomarkers for the prediction of short- and long-term CVE outcomes and follow-up care of patients with HF.

This study had some limitations. This study was a retrospective cohort analysis that could not collect and evaluate the variation of NLR and MPVLR on clinical outcomes over a follow-up period. It was also based on a single center and was restricted to patients with AHF requiring hospitalization, which may have introduced bias. Our analysis did not include some potential confounders, such as concomitant inflammation, malignancy, and genetic factors, because of our limited data. Due to many missing data (86.3%), B-type natriuretic peptide and/or NT-pro-BNP were not analyzed in the study. However, a recent study revealed that the NLR was comparable with NT-pro-BNP as a prognostic marker in elderly patients with chronic HF [13]. Therefore, the varying cut-off values of NLR for HF outcomes between studies is a possible barrier to its application in clinical practice. Further studies are needed to explore the specific cut-off values of NLR and MPVLR for predicting HF outcomes in both acute and chronic HF settings.

Our findings demonstrated that 13.4% of patients with AHF had ACS as a precipitating factor, and the percentages of those with CVEs had ACS as their comorbidity was significantly higher than those without CVEs (Table 1). We also

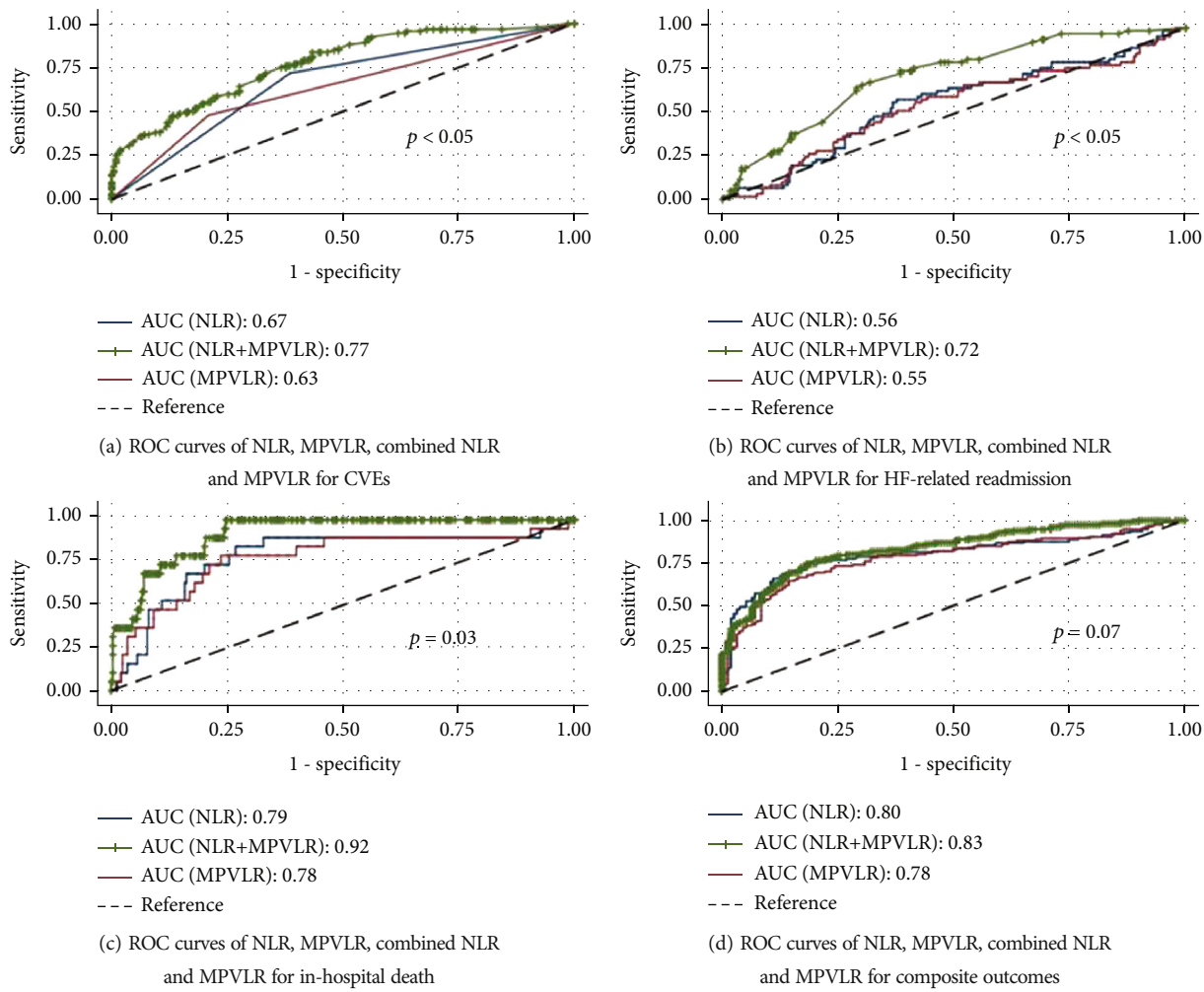

Figure 2: Receiver operating characteristics curves and AUC of NLR, MPVLR, and combined NLR and MPVLR for each outcome.

Table 4: Area under the receiver operating characteristics curve (AUC) stratified according to each outcome.

Variables	AUC	95% CI	Sensitivity (%)	Specificity (%)	*P* value
Cardiovascular events					
NLR	0.67	0.61-0.72	75.2	66.1	
MPVLR	0.63	0.58-0.69	45.3	79.7	<0.05
Combined NLR and MPVLR	0.77	0.72-0.83	84.6	58.7	
Rehospitalization					
NLR	0.56	0.48-0.64	61.2	61.0	
MPVLR	0.55	0.46-0.63	60.2	57.1	<0.05
Combined NLR and MPVLR	0.72	0.65-0.79	82.1	60.8	
In-hospital mortality					
NLR	0.79	0.66-0.91	87.5	70.8	
MPVLR	0.78	0.65-0.90	79.6	75.7	0.03
Combined NLR and MPVLR	0.92	0.88-0.96	88.7	85.5	
Composite outcome					
NLR	0.80	0.75-0.85	71.6	86.8	
MPVLR	0.78	0.72-0.83	62.8	91.1	0.07
Combined NLR and MPVLR	0.83	0.79-0.88	79.8	84.7	

Abbreviations: NLR: neutrophil-lymphocyte ratio; MPVLR: mean platelet volume-to-lymphocyte ratio; CI: confidential interval.

found ACS to be a significant confounding factor for CVE outcomes in the univariate and multivariate analyses. Similar to real-world data, AHF is a frequent consequence of ACS, which has an incidence of 6% to >45% [37], and their combination is associated with a poor prognosis [38]. Cardiac biomarkers of myocardial injury in patients with AHF in the absence of ACS are frequently raised and remain a diagnostic dilemma for those with ACS on admission; therefore, a diagnosis differentiating myocardial infarction and injury should be established in all patients with AHF [37]. Given our study's retrospective design, we were not able to confirm an associated ACS condition in all subjects with AHF. Further prospective studies focusing on ACS diagnosis of patients with AHF and prognostic differences between those with ACS on and during admission are also needed. Lastly, the new universal definition and classification of HF have just been launched [38], and additional studies on patients with HF with improved ejection fraction should be conducted.

5. Conclusion

Our study demonstrated that elevated NLR and MPVLR on admission in patients with AHF were independently associated with worse CVEs, rehospitalization for HF, in-hospital death, and composite outcomes of CVEs and all-cause mortality. NLR ≥ 3.29 and MPVLR ≥ 8.57 were also significant predictors for CVEs and in-hospital mortality. Interestingly, combining both NLR and MPVLR had superior performance compared to individual NLR or MPVLR. These economic biomarkers should be considered in the management and follow-up care of patients with AHF. Based on our single-center, retrospective cohort study, we recommend exploring this relationship and determining the optimal cut-off values of NLR and MPVLR for patients with both acute and chronic HF using other well-designed datasets.

Appendix

Calculation of Combined NLR and MPVLR

Combined NLR and MPVLR was derived from β-coefficients of the final Cox regression multivariate model of the individual outcome as shown below (abbreviations: NLR: neutrophil-lymphocyte ratio; MPVLR: mean platelet volume-to- lymphocyte ratio; NYHA: New York Heart Association; ACS: Acute coronary syndrome; VHD: valvular heart disease; RR: respiratory rate; SBP: systolic blood pressure; BMI: body mass index).

(i) C_{CVE} (combined NLR and MPVLR of CVE) = [(0.89 × NLR) + (0.67 × MPVLR) + (0.77 × NYHA) + (0.85 × ACS) + (0.60 × VHD) + (0.47 × rhythm) + (0.05 × RR)]

(ii) $C_{\mathrm{HF\ rehospitalization}}$ (combined NLR and MPVLR of HF rehospitalization) = [(0.67 × NLR) + (0.68 × MPVLR) + (0.58 × NYHA) + (1.05 × ACS) + (0.77 × BetaBlocker use) − (0.79 × anemia)]

(iii) $C_{\mathrm{InhospDeath}}$ (combined NLR and MPVLR of in − hospital death) = [(1.62 × NLR) + (1.51 × MPVLR) + (2.05 × NYHA) − (0.03 × SBP) + (0.14 × RR)]

(iv) $C_{\mathrm{Composite}}$ (combined NLR and MPVLR of composite outcome) = [(1.22 × NLR) + (0.76 × MPVLR) + (0.65 × NYHA) + (0.52 × ACS) + (0.36 × rhythm) − (0.04 × BMI)]

For the categorical variables of ACS, VHD, BetaBlocker use, and anemia, the patients were assigned the value 1 for the category they belong to and 0 for the other categories, whereas those with variables of NYHA class IV, AF rhythm, NLR, and MPVLR equal or above cut-offs were designated as 1 and 0 for the others. Different cut-off values for categorical NLR and MPVLR of each outcome are as follows: NLR = 3.29 and MPVLR = 8.57 for CVEs and in-hospital death outcomes; NLR = 3.58 and MPVLR = 6.43 for rehospitalization for HF; and NLR = 3.32 and MPVLR = 7.07 for the composite outcome.

Data Availability

The data used to support the findings of this study are included within the article.

Conflicts of Interest

The authors declare that there is no conflict of interest regarding the publication of this article.

Acknowledgments

The authors are grateful to Assoc. Prof. Dr. Sasivimol Rattanasiri, a lecturer of the Department of Clinical Epidemiology and Biostatistics, Faculty of Medicine, Ramathibodi Hospital, Mahidol University, Thailand, for statistical analysis. We would also like to thank Editage (http://www.editage.com) for English language editing.

References

[1] A. Groenewegen, F. H. Rutten, A. Mosterd, and A. W. Hoes, "Epidemiology of heart failure," *European Journal of Heart Failure*, vol. 22, no. 8, pp. 1342–1356, 2020.

[2] S. S. Virani, A. Alonso, H. J. Aparicio et al., "Heart disease and stroke Statistics-2021 Update: A Report From the American Heart Association," *Circulation*, vol. 143, no. 8, pp. e254–e743, 2021.

[3] C. Riehle and J. Bauersachs, "Key inflammatory mechanisms underlying heart failure," *Herz*, vol. 44, no. 2, pp. 96–106, 2019.

[4] L. Adamo, C. Rocha-Resende, S. D. Prabhu, and D. L. Mann, "Reappraising the role of inflammation in heart failure," *Nature Reviews Cardiology*, vol. 17, no. 5, pp. 269–285, 2020.

[5] D. L. Mann, "Innate immunity and the failing heart," *Circulation Research*, vol. 116, no. 7, pp. 1254–1268, 2015.

[6] A. T. Franco, A. Corken, and J. Ware, "Platelets at the interface of thrombosis, inflammation, and cancer," *Blood*, vol. 126, no. 5, pp. 582–588, 2015.

[7] N. Glezeva, J. F. Gilmer, C. J. Watson, and M. Ledwidge, "A central role for monocyte–platelet interactions in heart failure," *Journal of Cardiovascular Pharmacology and Therapeutics*, vol. 21, no. 3, pp. 245–261, 2015.

[8] T. Angkananard, T. Anothaisintawee, M. McEvoy, J. Attia, and A. Thakkinstian, "Neutrophil lymphocyte ratio and cardiovascular disease risk: a systematic review and meta-analysis," *BioMed Research International*, vol. 2018, Article ID 2703518, 11 pages, 2018.

[9] Y. Xu, H. Fang, Z. Qiu, and X. Cheng, "Prognostic role of neutrophil-to-lymphocyte ratio in aortic disease: a meta-analysis of observational studies," *Journal of Cardiothoracic Surgery*, vol. 15, no. 1, p. 215, 2020.

[10] X. Wang, X. Fan, S. Ji, A. Ma, and T. Wang, "Prognostic value of neutrophil to lymphocyte ratio in heart failure patients," *Clinica Chimica Acta*, vol. 485, pp. 44–49, 2018.

[11] D. Martínez-Urbistondo, A. Beltrán, O. Beloqui, and A. Huerta, "El indice neutrofilo/linfocito como marcador de disfuncion sistemica endotelial en sujetos asintomaticos," *Nefrología (English Edition)*, vol. 36, no. 4, pp. 397–403, 2016.

[12] C. Delcea, C. A. Buzea, and G. A. Dan, "The neutrophil to lymphocyte ratio in heart failure: a comprehensive review," *Romanian Journal of Internal Medicine*, vol. 57, no. 4, pp. 296–314, 2019.

[13] W. Yan, R. J. Li, Q. Jia, Y. Mu, C. L. Liu, and K. L. He, "Neutrophil-to-lymphocyte ratio compared to N-terminal pro-brain natriuretic peptide as a prognostic marker of adverse events in elderly patients with chronic heart failure," *Journal of Geriatric Cardiology*, vol. 14, no. 2, pp. 127–134, 2017.

[14] N. Sansanayudh, T. Anothaisintawee, D. Muntham, M. McEvoy, J. Attia, and AmmarinThakkinstian, "Mean platelet volume and coronary artery disease: a systematic review and meta-analysis," *International Journal of Cardiology*, vol. 175, no. 3, pp. 433–440, 2014.

[15] G. Tekin, Y. K. Tekin, N. Sivri, and E. Yetkin, "Mean platelet volume in patients with nonvalvular atrial fibrillation," *Blood Coagulation & Fibrinolysis*, vol. 24, no. 5, pp. 537–539, 2013.

[16] H. Kandis, H. Ozhan, S. Ordu et al., "The prognostic value of mean platelet volume in decompensated heart failure," *Emergency Medicine Journal*, vol. 28, no. 7, pp. 575–578, 2011.

[17] H. Kaya, M. Kutay Yıldırımlı, R. Kurt, O. Beton, and M. Birhan Yilmaz, "Mean platelet volume as a predictor of heart failure-related hospitalizations in stable heart failure outpatients with sinus rhythm," *Acta Cardiologica Sinica*, vol. 33, no. 3, pp. 292–300, 2017.

[18] D. Faraggi, "The effect of random measurement error on receiver operating characteristic (ROC) curves," *Statistics in Medicine*, vol. 19, no. 1, pp. 61–70, 2000.

[19] M. Cattaneo, P. Malighetti, and D. Spinelli, "Estimating receiver operative characteristic curves for time-dependent outcomes: the Stroccurve package," *The Stata Journal*, vol. 17, no. 4, pp. 1015–1023, 2017.

[20] S. Uthamalingam, E. A. Patvardhan, S. Subramanian et al., "Utility of the neutrophil to lymphocyte ratio in predicting long-term outcomes in acute decompensated heart failure," *The American Journal of Cardiology*, vol. 107, no. 3, pp. 433–438, 2011.

[21] F. E. Harrell Jr., R. M. Califf, D. B. Pryor, K. L. Lee, and R. A. Rosati, "Evaluating the yield of medical tests," *Journal of the American Medical Association*, vol. 247, no. 18, pp. 2543–2546, 1982.

[22] J. H. Cho, H.-J. Cho, H.-Y. Lee et al., "Neutrophil-lymphocyte ratio in patients with acute heart failure predicts in-hospital and long-term mortality," *Journal of Clinical Medicine*, vol. 9, no. 2, p. 557, 2020.

[23] V. A. Benites-Zapata, A. V. Hernandez, V. Nagarajan, C. A. Cauthen, R. C. Starling, and W. H. Wilson Tang, "Usefulness of neutrophil-to-lymphocyte ratio in risk stratification of patients with advanced heart failure," *The American Journal of Cardiology*, vol. 115, no. 1, pp. 57–61, 2015.

[24] T. Abo and T. Kawamura, "Immunomodulation by the autonomic nervous system: therapeutic approach for cancer, collagen diseases, and inflammatory bowel diseases," *Therapeutic Apheresis and Dialysis*, vol. 6, no. 5, pp. 348–357, 2002.

[25] M. Mollenhauer, K. Friedrichs, M. Lange et al., "Myeloperoxidase mediates postischemic arrhythmogenic ventricular remodeling," *Circulation Research*, vol. 121, no. 1, pp. 56–70, 2017.

[26] M. el Kazzi, B. S. Rayner, B. Chami, J. M. Dennis, S. R. Thomas, and P. K. Witting, "Neutrophil-mediated cardiac damage after acute myocardial infarction: significance of defining a new target cell type for developing cardioprotective drugs," *Antioxidants and Redox Signaling*, vol. 33, no. 10, pp. 689–712, 2020.

[27] W. H. W. Tang, W. Tong, R. W. Troughton et al., "Prognostic value and echocardiographic determinants of plasma myeloperoxidase levels in chronic heart failure," *Journal of the American College of Cardiology*, vol. 49, no. 24, pp. 2364–2370, 2007.

[28] D. L. Battin, S. Ali, A. U. Shahbaz et al., "Hypoalbuminemia and lymphocytopenia in patients with decompensated biventricular failure," *The American Journal of the Medical Sciences*, vol. 339, no. 1, pp. 31–35, 2010.

[29] A. Krack, R. Sharma, H. R. Figulla, and S. D. Anker, "The importance of the gastrointestinal system in the pathogenesis of heart failure," *European Heart Journal*, vol. 26, no. 22, pp. 2368–2374, 2005.

[30] A. Castro, V. Bemer, A. Nóbrega, A. Coutinho, and P. Truffa-Bachi, "Administration to mouse of endotoxin from gram-negative bacteria leads to activation and apoptosis of T lymphocytes," *European Journal of Immunology*, vol. 28, no. 2, pp. 488–495, 1998.

[31] A. Yuri Gasparyan, L. Ayvazyan, D. P. Mikhailidis, and G. D. Kitas, "Mean platelet volume: a link between thrombosis and inflammation?," *Current Pharmaceutical Design*, vol. 17, no. 1, pp. 47–58, 2011.

[32] C. Meisinger, H. Prokisch, C. Gieger et al., "A genome-wide association study identifies three loci associated with mean platelet volume," *American Journal of Human Genetics*, vol. 84, no. 1, pp. 66–71, 2009.

[33] S. G. Chu, R. C. Becker, P. B. Berger et al., "Mean platelet volume as a predictor of cardiovascular risk: a systematic review and meta-analysis," *Journal of Thrombosis and Haemostasis*, vol. 8, no. 1, pp. 148–156, 2010.

[34] A. Icli, F. Aksoy, Y. Turker et al., "Relationship between mean platelet volume and pulmonary embolism in patients with deep vein thrombosis," *Heart, Lung and Circulation*, vol. 24, no. 11, pp. 1081–1086, 2015.

[35] R. S. Vasan, L. M. Sullivan, R. Roubenoff et al., "Inflammatory markers and risk of heart failure in elderly subjects without prior myocardial infarction: the Framingham Heart Study," *Circulation*, vol. 107, no. 11, pp. 1486–1491, 2003.

[36] I. Chung, A. Choudhury, and G. Y. H. Lip, "Platelet activation in acute, decompensated congestive heart failure," *Thrombosis Research*, vol. 120, no. 5, pp. 709–713, 2007.

[37] V.-P. Harjola, J. Parissis, J. Bauersachs et al., "Acute coronary syndromes and acute heart failure: a diagnostic dilemma and high-risk combination. A statement from the Acute Heart Failure Committee of the Heart Failure Association of the European Society of Cardiology," *European Journal of Heart Failure*, vol. 22, no. 8, pp. 1298–1314, 2020.

[38] D. D. McManus, M. Chinali, J. S. Saczynski et al., "30-year trends in heart failure in patients hospitalized with acute myocardial infarction," *The American Journal of Cardiology*, vol. 107, no. 3, pp. 353–359, 2011.

Hindawi
Mediators of Inflammation
Volume 2021, Article ID 3698386, 13 pages
https://doi.org/10.1155/2021/3698386

Research Article

Loss of GATA4 C-Terminus by p.S335X Mutation Modulates Coronary Artery Vascular Smooth Muscle Cell Phenotype

Ting-Yan Yu,[1,2] Xin-Xin Chen,[3] Qing-Wen Liu,[1] Fang-Fang Ma,[1] Hong-Lang Huang,[4] Lei Zhou,[1] and Wei Zhang[4]

[1]*Department of Cardiology, The First Affiliated Hospital of Nanjing Medical University, Nanjing, 210029 Jiangsu, China*
[2]*Department of Echocardiography, The Second Affiliated Hospital of Zhejiang University, Hangzhou, 310009 Zhejiang, China*
[3]*Department of Cardiology, The Affiliated Hospital of Jiangsu University, Zhenjiang, 212001 Jiangsu, China*
[4]*Xiamen Key Laboratory of Cardiac Electrophysiology, Xiamen Institute of Cardiovascular Diseases, The First Affiliated Hospital of Xiamen University, School of Medicine, Xiamen University, Xiamen, 361003 Fujian, China*

Correspondence should be addressed to Lei Zhou; zhoulei@njmu.edu.cn and Wei Zhang; zhangw@xmu.edu.cn

Received 5 July 2021; Accepted 17 August 2021; Published 11 September 2021

Academic Editor: Azizah Ugusman

Coronary artery disease (CAD) has been the leading cause of morbidity and mortality worldwide, and its pathogenesis is closely related with the proliferation and migration of vascular smooth muscle cell (VSMC). We previously reported a truncated GATA4 protein lacking C-terminus induced by p.S335X mutation in cardiomyocyte from ventricular septal defect (VSD) patients. However, it is still unclear whether GATA4 p.S335X mutation could influence the development of CAD. GATA4 wild-type (WT) and p.S335X mutant (MU) overexpression plasmids were constructed and transfected transiently into rat coronary artery smooth muscle cell (RCSMC) to observe the proliferative and migratory abilities by MTS and wound healing assay, respectively. PCR array was used to preliminarily detect the expression of phenotypic modulation-related genes, and QRT-PCR was then carried out to verify the screened differentially expressed genes (DEGs). The results showed that, when stimulated by fetal bovine serum (10%) for 24 h or tumor necrosis factor-α (10 or 30 ng/ml) for 10 or 24 h, deletion of GATA4 C-terminus by p.S335X mutation in GATA4 enhanced the proliferation of RCSMC, without alteration of the migration capability. Twelve DEGs, including Fas, Hbegf, Itga5, Aimp1, Cxcl1, Il15, Il2rg, Il7, Tnfsf10, Il1r1, Irak1, and Tlr3, were screened and identified as phenotypic modulation-related genes. Our data might be beneficial for further exploration regarding the mechanisms of GATA4 p.S335X mutation on the phenotypic modulation of coronary VSMC.

1. Introduction

Coronary artery disease (CAD) is an atherosclerotic disease affecting the global human health and has been found to be the leading cause of death in both developed and developing countries [1]. Vascular smooth muscle cell (VSMC) is a major cell type presenting at all stages of atherosclerosis [2]. Unlike skeletal muscle cells or cardiomyocytes, VSMCs are not terminally differentiated and hence maintain phenotypic plasticity [3]. Under normal physiological conditions, VSMCs present as the contractile phenotype located in media and exhibit extremely low proliferative rate, as well as synthetic activity [4]. However, in the presence of environmental stimuli, such as inflammatory mediators, growth factors, and mitogens, VSMCs dedifferentiate into synthetic phenotype and lose the ability to contract, but migrate, proliferate, and accumulate into the intima [5]. VSMC dedifferentiation produces extracellular matrix and participates in fibrous cap formation [6] and subsequently accelerates the process of atherosclerosis ultimately [7].

The zinc finger transcription factor GATA4 belongs to an evolutionarily conserved GATA family, which consists of six members [8]. The importance of GATA4 is well appreciated in congenital heart diseases (CHDs) and some other cardiac malformations, such as myocardial hypoplasia, double outlets of the right ventricle, and common

atrioventricular canal [9]. However, recent studies have found that GATA4 is also associated with the development of CAD. It has been revealed that GATA4 gene transcription was significantly enhanced in the peripheral blood mononuclear cells (PBMCs) in patients with severe stable CAD [10]. Further study suggested that, the higher expression of GATA4 was probably related to the increased GATA4 gene promoter activity affected by the DNA variants within its promoter in patients with acute myocardial infraction (AMI) [11]. Moreover, two single-nucleotide polymorphisms (SNPs), rs1062219 and rs804280, were unequivocally identified as risk variants for CAD, both of which were also linked to the development of CHDs [12]. We previously detected a p.S335X mutation in GATA4 in ventricular septal defect (VSD) patients, which could lead to truncated GATA4 protein lacking a conservative region at C-terminus [13]. The deletion of GATA4 C-terminus might induce VSD by suppressed cardiomyocyte proliferation and enhanced cell apoptosis [14]. Accordingly, we wonder whether the C-terminal deletion induced by p.S335X mutation in GATA4 also contribute to the development of CAD.

GATA4 was found to be an important regulator of coronary vasculature in the murine heart. It has been reported that conditional overexpression of GATA4 increased myocardial capillary and small conducting vessel densities, as well as increased coronary flow reserve [15]. Furthermore, the peri-infarct intramyocardial delivery of GATA4 vector prior to the ligation of left anterior descending coronary artery significantly increased the number of capillaries and reduced the infarct size [16]. GATA4 could not only target directly to the angiogenic factor vascular endothelial growth factor-A (VEGF-A) to promote angiogenesis but also interact with the transcriptional regulator friend of GATA2 (FOG2). GATA4-FOG2 would synergistically regulate a broad panel of angiogenesis-related genes to promote the formation of coronary vascular plexus [17]. Besides, GATA4 has also been revealed to participate in the regulation of VSMC proliferation and migration [18, 19]. However, the possible role of GATA4 p.S335X in the proliferation and migration of VSMC in coronary artery has not been studied so far. In the present study, a rat coronary artery smooth muscle cell (RCSMC) culture model overexpression p.S335X mutant of GATA4 was established in vitro. The proliferation and migration of RCSMC was validated, and the altered expression of important phenotypic modulation-related genes was assessed.

2. Materials and Methods

2.1. Cell Culture and Transient Transfection. RCSMCs (BNCC, Beijing, China) were cultured in DMEM (Gibco, Grand Island, NY, USA) supplemented with 10% fetal bovine serum (FBS; US origin, Gibco, Grand Island, NY, USA) and 1% penicillin and streptomycin (MP Biomedicals, Solon, OH, USA) at 37°C in a humidified atmosphere of 5% CO_2. RCSMC in each well was transfected using Lipofectamine 2000 reagent (Invitrogen, Carlsbad, CA, USA) according to manufacturer's protocol.

2.2. Western Blot. Western blot samples were lysed within RIPA buffer (Pierce, Rockford, IL, USA) containing protease inhibitors. Then, the same amount of proteins was resolved by SDS-PAGE and PVDF membranes (Millipore, Bedford, MA, USA). After blocking with 5% skim milk for one hour, the blots were incubated with primary antibody GATA4 (Abcam, Cambridge, UK) overnight and then with horseradish peroxidase-conjugated secondary antibody for another one hour. Finally, protein bands were visualized using the Western blotting detection kit (Millipore, Bedford, MA, USA) and quantified with Image Pro Plus version 6 software (Media Cybernetics, Rockville, MD, USA).

2.3. QRT-PCR. Total RNA was extracted from RCSMC by Buffer RZ (Tiangen, Beijing, China) and then reversed into cDNAs using Transcriptor Fast Quant RT Kit (Tiangen, Beijing, China) following manufacturer's protocol. The obtained cDNAs were then mixed with primers and Fast SYBR Green Master Mix (Applied Biosystems, Vilnus, Lithuania) to carry out QRT-PCR by ABI 7500 PCR machine (Applied Biosystems, Foster City, CA, USA). Data was analyzed using $2^{-\Delta\Delta Ct}$ method and normalized to Rat Actb expression. The primers were listed in supplemental Table S1 and all primers were synthesized by Sangon Biotech (Shanghai, China).

2.4. MTS Assay. Cell proliferation assay was conducted by using CellTiter 96® Aqueous One Solution Cell Proliferation kit (MTS, Promega, USA). After 24-hour transfection and 4-hour starvation, RCSMCs were seeded at $(2-3)\times 103$ cells /well in 96-well plates and then incubated at 37°C in a humidified atmosphere of 5% CO_2 overnight. After cultivation in 100 μl medium containing different drug concentrations for 10 or 24 h, 20 μl MTS were added into each well and incubated in cell incubator for 4 hours. The absorbance was read at 490 nm on a microplate reader (Infinite M1000 Pro, Tecan, Switzerland).

2.5. Wound Healing Assay. After transfection, RCSMCs were seeded in 6-well plates at 2×10^7 cells/well and incubated at 37°C in a humidified atmosphere of 5% CO_2 overnight. When the degree of cell fusion reached above 90%, wounds were produced by a sterile 200 μl plastic pipette tips. Cells were further cultured with medium containing different drug concentrations and allowed to migrate into the denuded area for 24 h. Images were acquired by microscope (Leica, Germany) at 4×40 magnification.

2.6. PCR Array Analysis. The total RNA samples were extracted by RNeasy Plus Mini Kit (Qiagen, Helden, Germany) according to manufacturer's protocol. cDNA synthesis was performed on 1 μg RNA in a 10 μl sample volume using the RT^2 First Strand Kit (Qiagen, Frederick, MD, USA) as recommended by manufacturer's protocol. Then, the obtained cDNAs were mixed with RT^2 SYBR Green qPCR Mastermix (Qiagen, Frederick, MD, USA) to perform RT^2 Profiler PCR Array (Qiagen, Frederick, MD, USA) by ABI-7500 machine (Applied Biosystems, Foster City, CA, USA). All data from the PCR array experiments were

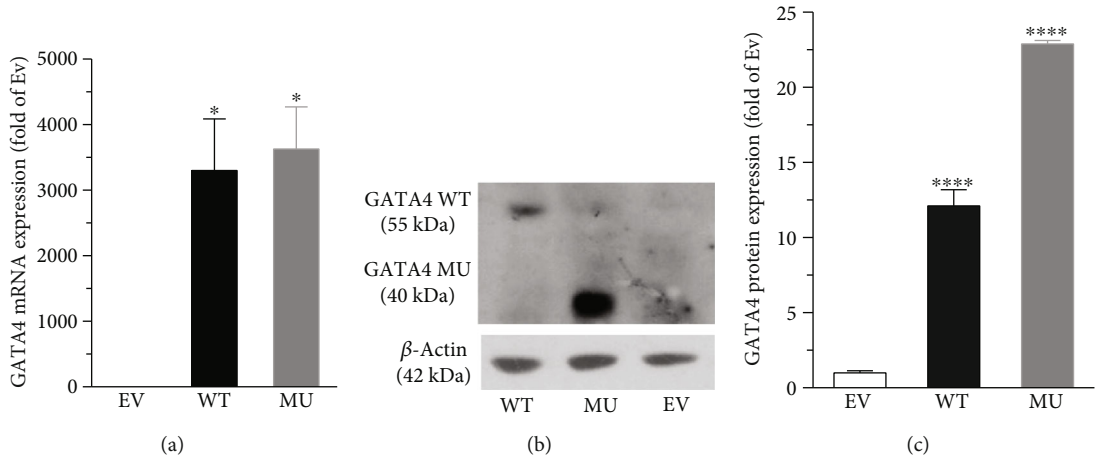

Figure 1: The transfection of plasmids pcDNA6-GATA4-WT and pcDNA-GATA4-MU. (a) QRT-PCR results demonstrated the successful transfection and expression of GATA4 mRNA in RCSMCs. One-way ANOVA, $^{*}P < 0.05$ versus EV, $n = 3$. (b) Western blot results showed the expression of GATA4 in WT group (55 KDa) and MU group (40 KDa, truncated form). (c) Semiquantitative analysis of Western blot results. One-way ANONA, $^{****}P < 0.0001$ versus EV, $n = 3$.

analyzed by Qiagen GeneGlobe Data Analysis Center Web Portal (https://geneglobe.qiagen.com/cn/analyze).

2.7. Statistical Analysis. Data were expressed as means ± SEM from at least three independent experiments. Differences between groups were analyzed by Prism 6 software (GraphPad, La Jolla, CA, USA). One-way ANOVA with Fisher's LSD test was used for comparison of data in more than two groups. $P < 0.05$ was considered to be statistically significant.

3. Results

3.1. Establishment of RCSMC Culture Model Overexpressing GATA4 WT and MU. RCSMC is a kind of long spindle cell, with adherent growth and typical characteristics of smooth muscle cell. Plasmids pcDNA6-GATA4-WT and pcDNA-GATA4-MU have been constructed, representing GATA4 full length sequence and GATA4 p.S335X mutant sequence. The latter could result in deletion of GATA4 C-terminus [13]. The plasmids were transfected into RCSMC for 24 h to establish GATA4 WT and MU overexpression models. QRT-PCR and Western blot were then used to evaluate the transfection efficiency. QRT-PCR results showed that the expression of GATA4 mRNA in WT and MU groups was significantly higher than that in GATA4 empty vector (EV) group ($P < 0.05$, Figure 1(a)), indicating the successful transfection of GATA4 WT and MU plasmids. Western blot results demonstrated that deletion of GATA4 C-terminus induced by p.S335X mutation decreased the molecular weight of target protein in MU group (40 KDa) compared to that in WT (55 KDa), i.e., the GATA4 protein was truncated (Figures 1(b) and 1(c)).

3.2. Deletion of GATA4 C-Terminus Enhanced RCSMC Proliferation. MTS assay kit was used to detect the viability of RCSMC. The results showed that the viability of RCSMC in MU group in the presence of 10% FBS was significantly higher than that in WT group ($P < 0.05$, Figure 2(a)), suggesting enhanced proliferation of cells in MU group.

To further confirm the effect of GATA4 C-terminal deletion on the proliferation capability of RCSMC, we adopted different concentrations of the proinflammatory cytokine tumor necrosis factor-α (TNF-α, 10 and 30 ng/ml) under serum-free condition. Cells in WT group showed higher viability compared to that in EV group in case of TNF-α 10 ng/ml for 24 h, and 30 ng/ml for 10 and 24 h. Impressively, C-terminal deletion by p.S335X mutation (MU) in GATA4 further enhanced the viability of cells compared to that in WT group regardless of the TNF-α concentration (10 or 30 ng/ml) or duration of drug administration (10 or 24 h) ($P < 0.05$, Figures 2(b)–2(g)). These data suggested that the C-terminus of GATA4 might exert a negative regulatory effect on RCSMC proliferation, whose deletion may play a vital role in RCSMC proliferation.

3.3. Migration of RCSCM Was Not Significantly Modulated by GATA4 MU. Wound healing assay was performed to evaluate the migration ability of RCSMC in GATA4 WT, MU and, EV groups. The results showed that, after additional 10% of FBS to the culture medium for 24 h, the wound healing rates of cells in WT, MU, and EV groups were all around 45%, with no significant difference between the groups, respectively (Figures 3(a) and 3(b)). Neither did the administration of TNF-α (10 and 30 ng/ml) for 10 or 24 h induce significant changes in the migration of RCSMCs in the present settings (Figures 3(c)–3(k)).

3.4. Screening and Verification of Phenotypic Modulation-Related Genes Regulated by the Deletion of GATA4 C-Terminus. Since p.S335X mutation-induced GATA4 C-terminal deletion showed potent effects on the proliferation of RCSMC, a high-throughput PCR analysis (RT^2 Profiler RT-PCR Array) was performed to detect the expression profile of phenotypic modulation-related genes. The scatter plots taking 2 folds of gene regulation as the threshold value

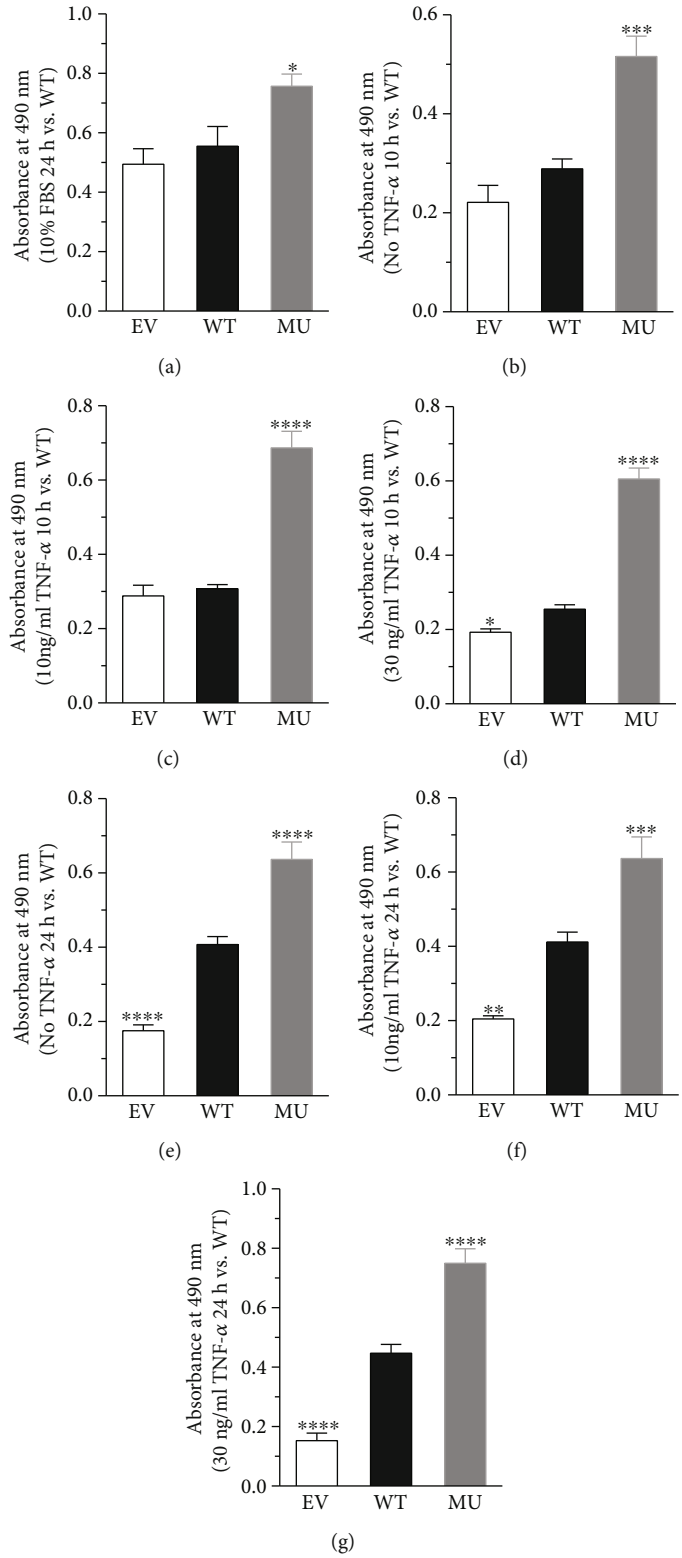

Figure 2: Deletion of GATA4 C-terminus enhanced RCSMC proliferation. The effects of GATA4 WT and MU overexpression on RCSMC proliferation was detected by MTS. The cells were treated with (a) 10% FBS for 24 h, (b–d) TNF-α (10 or 30 ng/ml) for 10 h, and (e–g) TNF-α (10 or 30 ng/ml) for 24 h. One-way ANOVA, $^{*}P < 0.05$, $^{***}P < 0.001$, $^{****}P < 0.0001$ versus WT, $n = 3$.

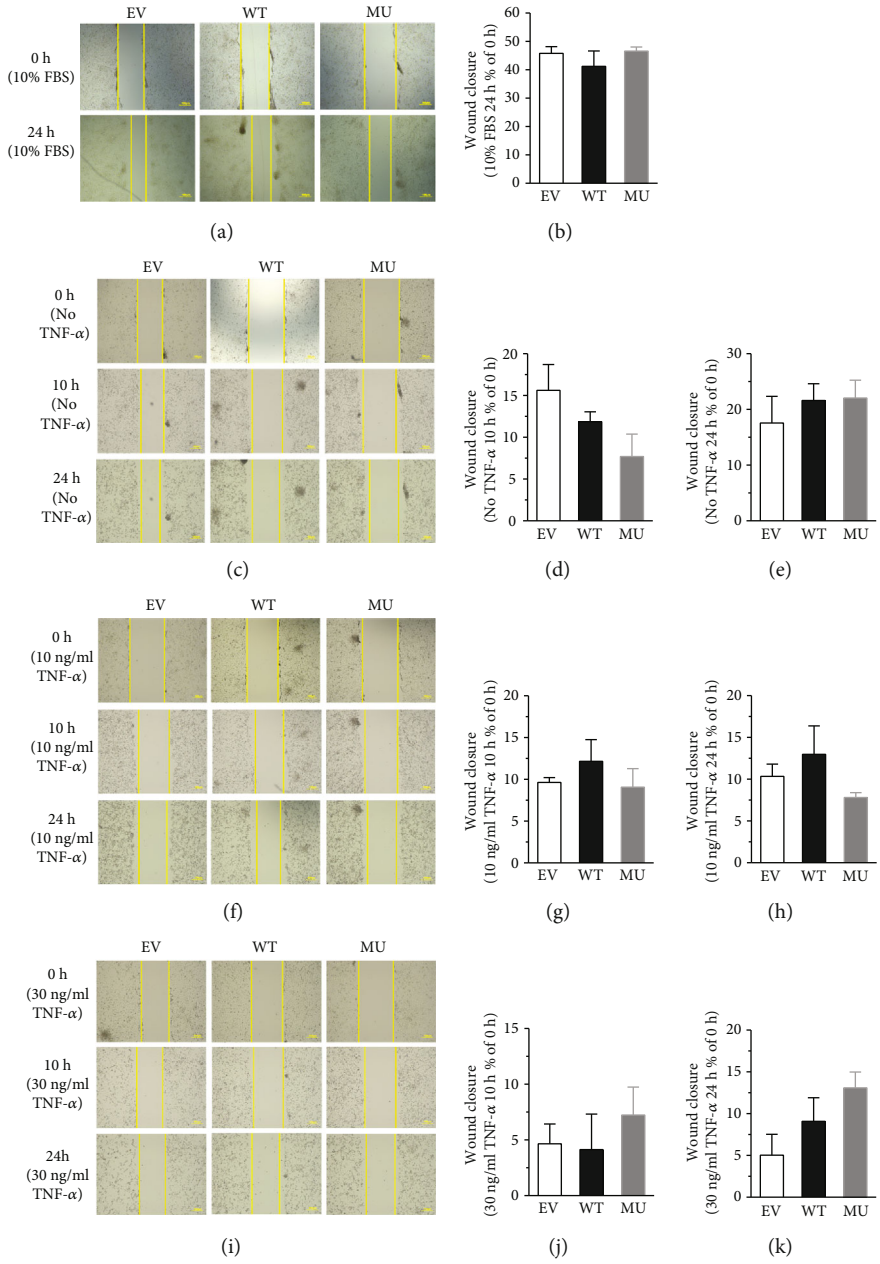

Figure 3: Deletion of GATA4 C-terminus did not alter RCSMC migration. Wound healing assay was adopted to observe the migratory rate of RCSMC. The quantitative analysis of wound healing assay was presented by the wound closure rate relative to the initial distance. Magnification: 4×40. (a, b) Representative images of migrated cells incubated with 10% FBS taken at 0 and 24 h after injury. One-way ANOVA, $P > 0.05$ versus WT, $n = 3$. (c–k) Representative images of migrated cells stimulated by TNF-α (10 or 30 ng/ml) taken at 0, 10, and 24 h after injury. One-way ANOVA, $P > 0.05$ versus WT, $n = 4$.

are shown in Figure 4 ((a–c), rat atherosclerosis PCR array (PARN-038Z); (d–f), rat inflammatory cytokines and receptors PCR array (PARN-011Z); and (g–i), rat nuclear factor-κB (NF-κB) pathway PCR array (PARN-025Z), respectively).

Subsequently, differentially expressed genes (DEGs) in WT and MU groups in comparison with EV group were screened and listed in Figure 5. In rat atherosclerosis PCR array (Figure 5(a)), Abca1, Bax, Bcl2, Bcl2a1, Cd44, Fabp3, Hbegf, Lypla1, Ptgs1, Selplg, Tgfb2, Tnc, and Vegfa had reverse trend between WT and MU groups, while the trends of Bcl2l1, Bid, Birc3, Cxcl1, Fas, Fn1, Itga2, Itga5, Lif, Nfkb1, Nr1h3, Ppard, and Sod1 were consistent. In rat inflammatory cytokines and receptors PCR array (Figure 5(b)), the DEGs with opposite tendency were Aimp1, Ccl5, Ccl6, Cxcl1, Cxcl9, Cxcr5, Il15, Il1rn, Spp1, and Tnfsf10, while the DEGs on the same trend were Bmp2, Ccl7, Ccr1, Ccr10, Cx3cl1, Cxcl12, Il2rg, Il33, Il6r, Il7, Mif, Nampt, and Tnfsf13b. In rat NF-κB pathway PCR array (Figure 5(c)), Akt1, Atf1, Atf2, Bcl10, Cflar, Chuk, Crebbp, Egr1, F2r, Icam1, Irak1, Irf1, Nfkb1, Raf1, Rela, Tbk1, Timp1, Tlr2, Tlr3, Tlr6, Tnfrs10b, Tradd, and Traf6 were

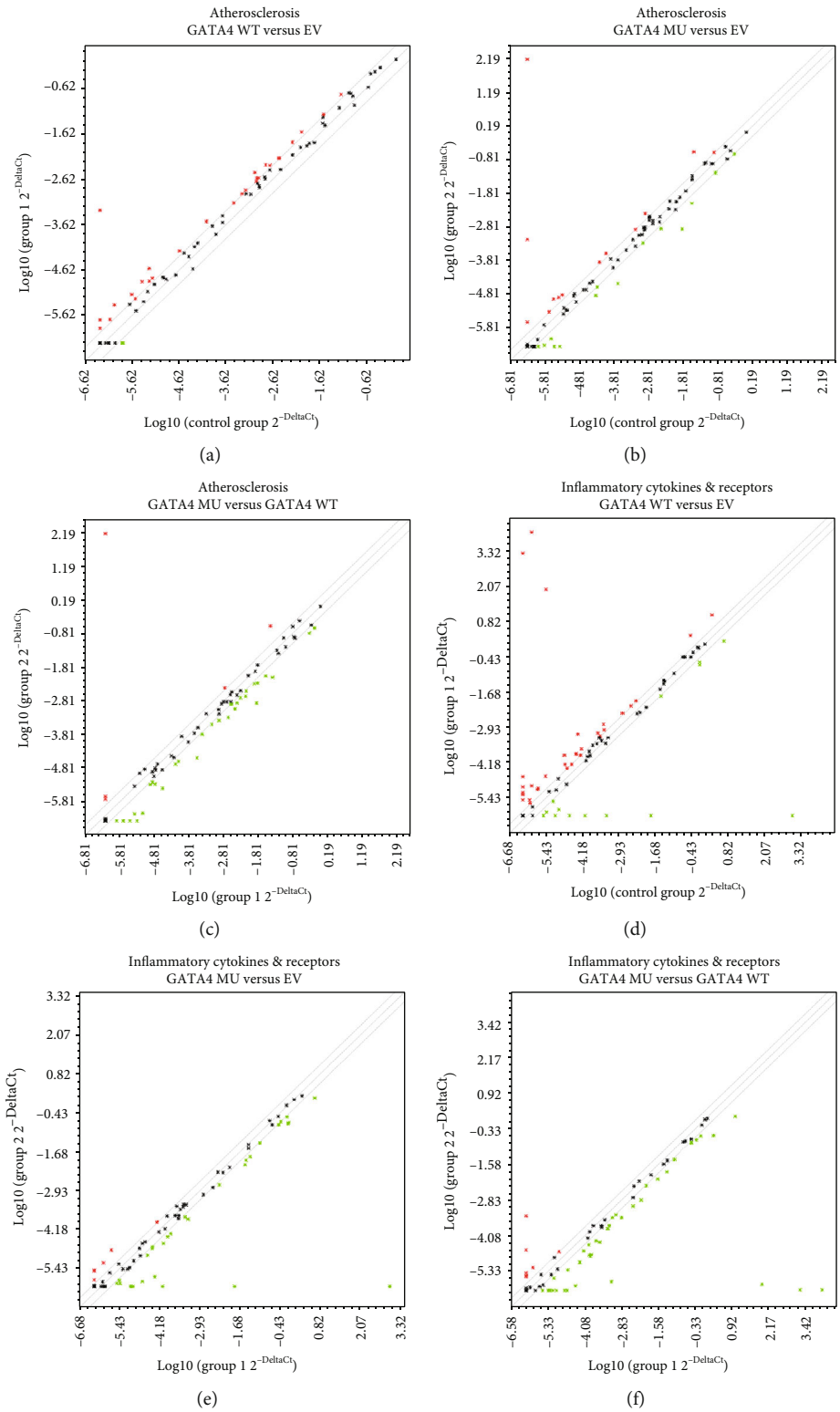

Figure 4: Continued.

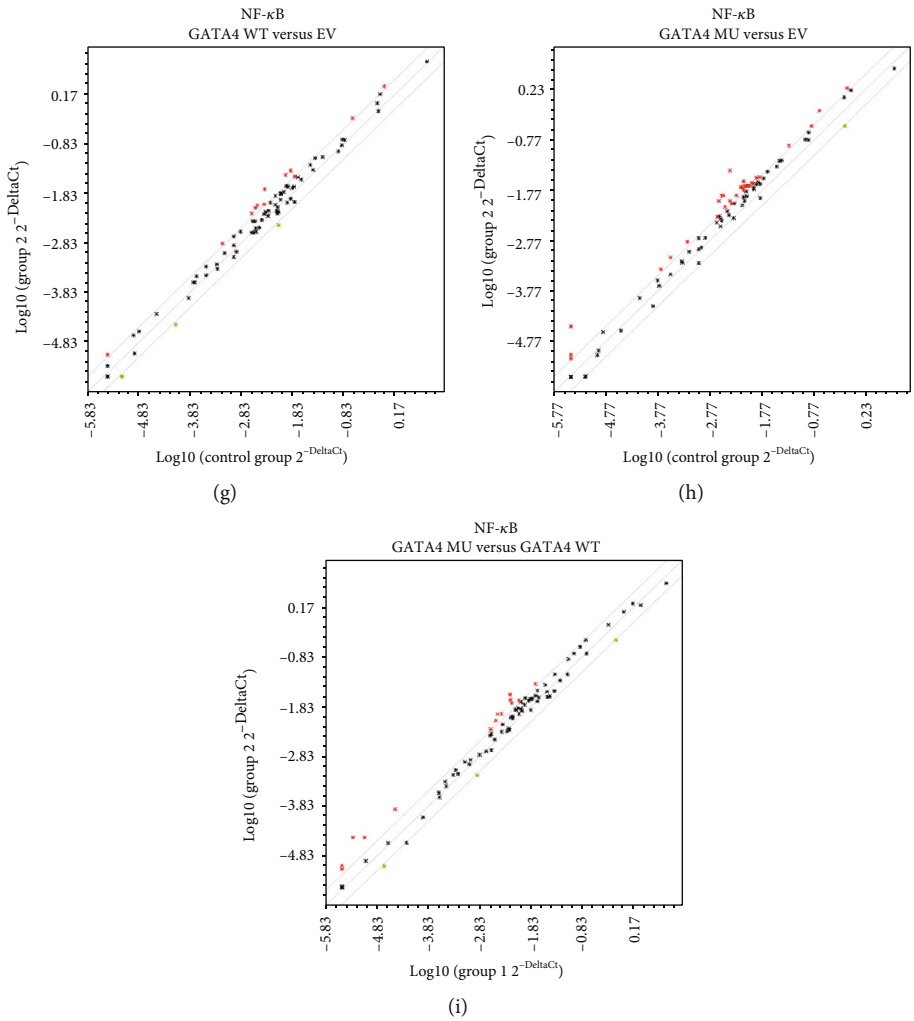

Figure 4: The scatter plots of PCR array results. (a–c) Rat atherosclerosis; (d–f) rat inflammatory cytokines and receptors; (g–i) rat NF-κB. Fold change ≥ 2 was taken as the threshold value. (a, d, and g) WT versus EV; (b, e, and h) MU versus EV; (c, f, and i) MU versus WT.

with the consistent tendency, while Ccl5, Il1r1, Myd88, Nfkb2, Ripk1, and Tnfrsf1a had opposite trend.

As per the previous reports, we further selected part of the DEGs which are closely linked to the phenotypic modulation of VSMC and verified their expression by using QRT-PCR (Figure 6). Particularly, the expression of Fas and Hbegf was markedly lower in MU group compared to that in WT group. Aimp1, Cxcl1, and Tnfsf10 had higher expression in MU group compared to that in WT group, while the expression of Il15 and Il7 was lower. Analogously, the expression of Il1r1, Irak1, and Tlr3, was decreased in MU group versus WT group. These data suggested that the above-mentioned genes might be regulated by GATA4 C-terminus.

4. Discussion

In the present study, the deletion of GATA4 C-terminus by p.S335X mutation enhanced RCSMC proliferation, without alteration of migration in the cell culture model in vitro. Twelve DEGs including Fas, Hbegf, Itga5, Aimp1, Cxcl1, Il15, Il2rg, Il7, Tnfsf10, Il1r1, Irak1, and Tlr3 were screened and identified as phenotypic modulation-related genes that might be regulated by GATA4 and its C-terminus. Our data could provide a clue for further exploration for the molecular mechanisms of GATA4 on the modulation of VSMC phenotype.

Previously, GATA4 has been proven to regulate the proliferation capability of a variety of cell types, such as cardiomyocytes, small intestinal epithelial cells, follicular granulosa cells, and leukemia lymphocytes [20–24]. However, regarding the VSMC, only two studies concerning human pulmonary artery SMCs and mouse aortic SMCs were reported so far [18, 19]. Since the proliferation of VSMC is a vital phenotypic modulation characteristic in VSMC dedifferentiation and is closely linked to atherosclerosis [5, 7], we wondered if GATA4 account for the development of CAD via regulating the proliferation of coronary artery VSMC. Hence, we firstly adopted RCSMC overexpressing GATA4 WT or MU as cell culture model. The expression level of MU protein was higher than WT (Figure 1(c)), possibly because of the different plasmids used or the difference in transfection efficacy. The cell viability of RCSMC was significantly increased by MU in the presence of different stimuli

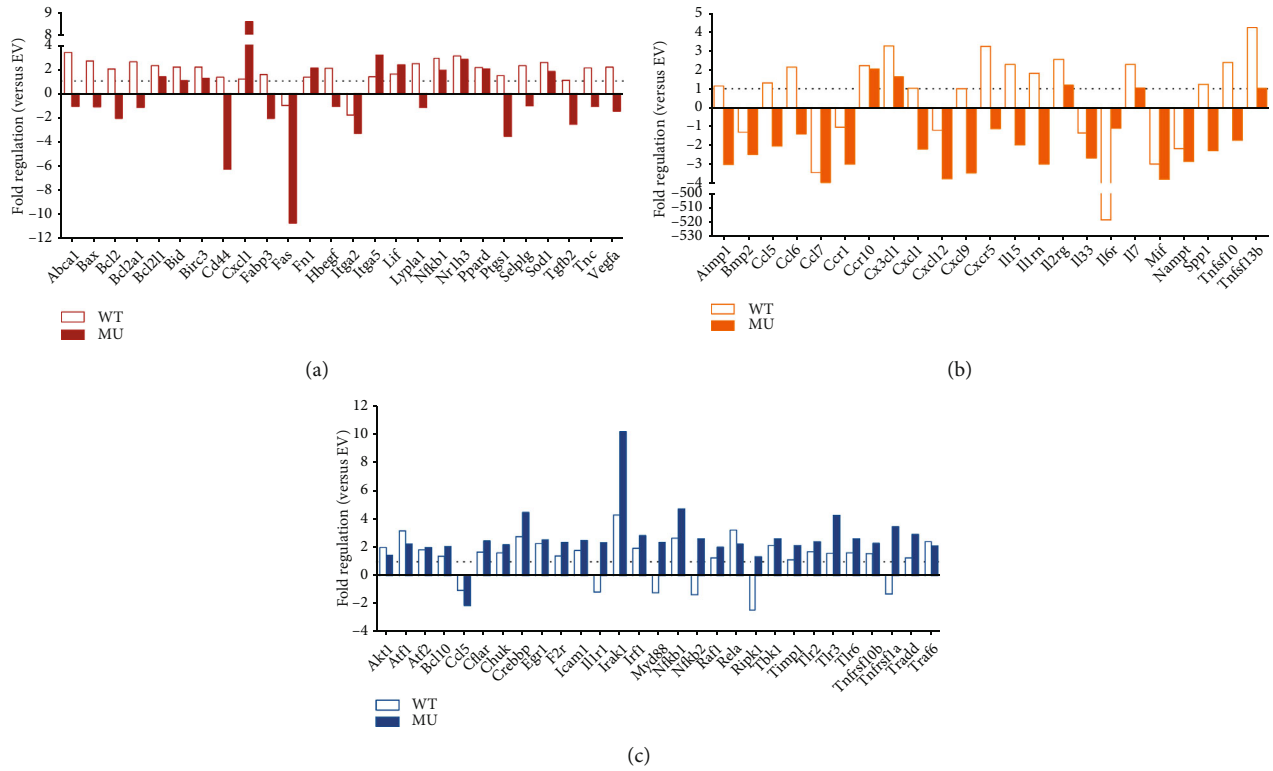

Figure 5: The fold regulation of differential expression genes (DEGs) in WT and MU groups compared to EV group. (a) Rat atherosclerosis-related DEGs. (b) Rat inflammatory cytokines and receptor-related DEGs. (c) Rat NF-κB pathway-related DEGs.

(10% FBS for 24 h, or TNF-α 10 or 30 ng/ml for 10 or 24 h) (Figure 2), demonstrating that the deletion of GATA4 C-terminus by p.S335X mutation could enhance proliferation of RCMSC. It is likely that GATA4 protein could exert bidirectional regulatory effects on cell proliferation, i.e., the C-terminus of GATA4 could possibly protect VSMC against TNF-α-induced proliferation to some extent. Such findings extended the current knowledge about the function of GATA4 C-terminus, whose deletion not only promoted the apoptosis of cardiomyocyte [13, 14], and also enhanced the proliferation of RCSMC that might contribute to the development of CAD.

Migration is another important characteristic of phenotypic modulation in the process of VSMC dedifferentiation. Our data showed that the migratory rates of RCSMCs among WT, MU, and EV groups yielded no significant difference in the presence of different stimuli (10% FBS for 24 h, or TNF-α 10 or 30 ng/ml for 10 or 24 h) (Figure 3), indicating the ineffectiveness of GATA4 C-terminal deletion on RCSMC migration under such experimental conditions. Rabinovitch and co-authors reported that the migration of pulmonary artery SMC could be stimulated by S100A4/Mts1 depending on the phosphorylation of GATA4 [18]. Previous studies found that 10% FBS and TNF-α 10-100 ng/ml were efficient for the migration of aortic VSMC [25–28]. However, in our experiments, neither WT nor MU exerted significant effect on the migratory capability of RCSMC and that might be resulted from the different cell types.

To further explore the possible molecules involved in the effects of GATA4 C-terminal deletion on RCSMC proliferation, a panel of phenotypic modulation-related genes was screened by using PCR array. Subsequently, QRT-PCR was performed to confirm the changed expression of the following: Fas, Hbegf, Itga5, Aimp1, Cxcl1, Il15, Il2rg, Il7, Tnfsf10, Il1r1, Irak1, and Tlr3. These genes are considered to be associated with atherosclerosis and vascular inflammatory response during the pathogenesis of cardiovascular disorders including CAD.

Fas, also known as CD95 or APO-1, is a member of the TNF/nerve growth factor superfamily and can induce cell proliferation by stimulating the formation of death-inducing signaling complex (DISC). The latter activates the mitogen-activated protein kinase (MAPK) family, as well as NF-κB. In addition, Fas ligands can also induce ligand-dependent epidermal growth factor (EGF) receptor activation and phosphorylation, triggering cell proliferation through extracellular-signal regulated kinases (ERK)1/2 signaling pathway [29]. Hbegf belongs to the EGF family and is known to induce VSMC proliferation by autophosphorylation of EGF receptors, followed by the activation of PI3K-Akt, MAPK, and janus kinase-signal transducer and activator of transcription (JAK-STAT) pathways [30, 31]. Itga5, a member of integrin α chain family, binds predominantly with integrin β1 and functions in cell surface adhesion and signaling [32]. It has been reported that Itga5 could enhance the proliferation of human periodontal ligament stem cells (PDLSCs) via PI3K-Akt and MEK1/2/ERK1/2 pathways [33]. As per our QRT-PCR results (Figure 6), the expressions of Fas and Hbegf were both lower in MU group compared to that in WT group, implying that the deletion of

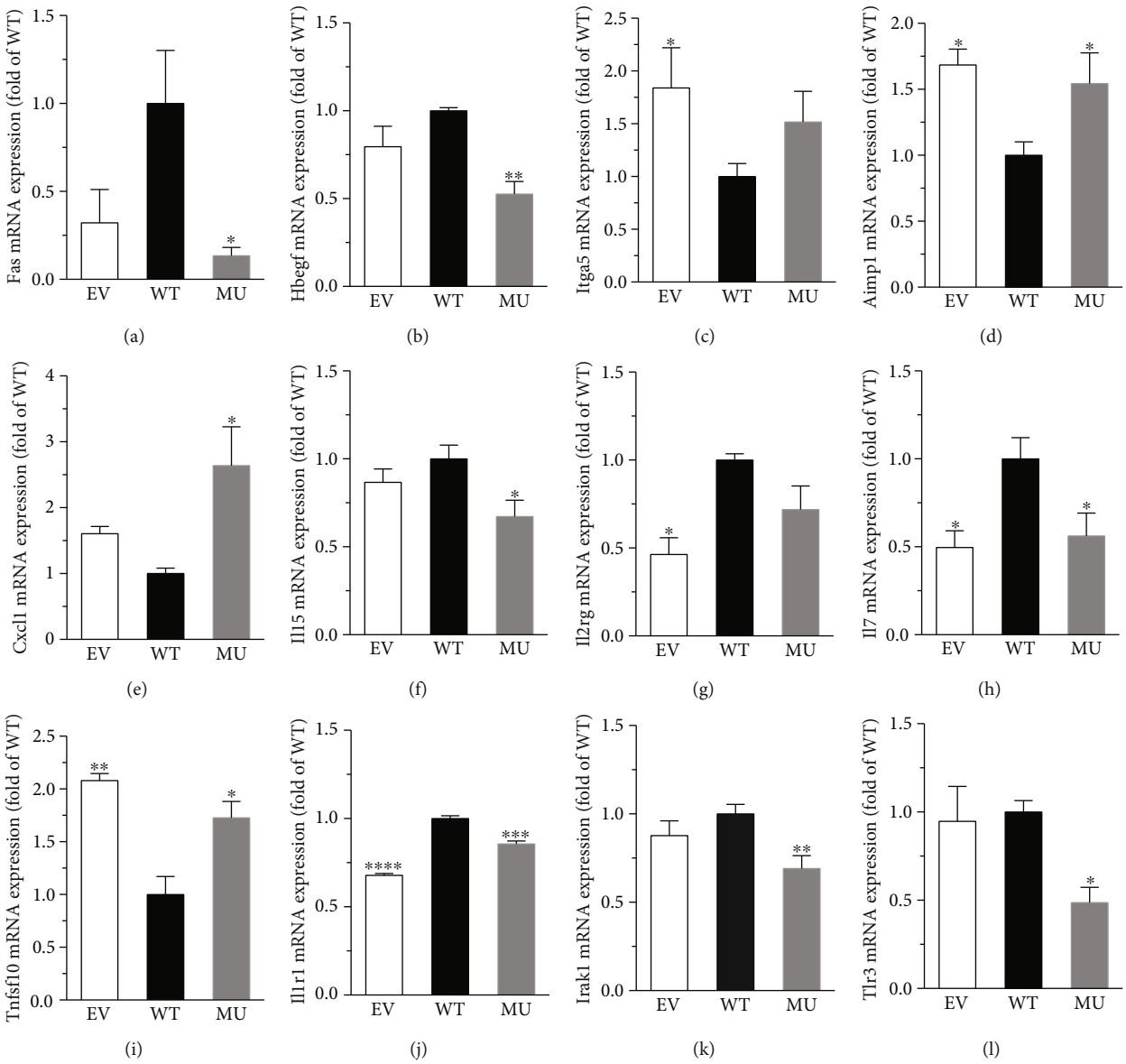

Figure 6: QRT-PCR verification of the screened DEGs. (a) Fas; (b) Hbegf; (c) Itga5; (d) Aimp1; (e) Cxcl1; (f) Il15; (g) Il2rg; (h) Il7; (i) Tnfsf10; (j) Il1r1; (k) Irak1; (l) Tlr3. One-way ANOVA, $^{*}P < 0.05$, $^{**}P < 0.01$, $^{***}P < 0.001$, $^{****}P < 0.0001$ versus WT, $n = 7$.

GATA4 C-terminus might inhibit their expressions. Additionally, Itga5 expression was higher in EV group and was not significantly different in WT and MU group, indicating that the C-terminus of GATA4 was not required for the regulation of Itga5.

Aimp1 is a cytokine involved in the regulation of angiogenesis, immune activation, and fibroblast proliferation. Aimp1 could promote the proliferation of human bone marrow-derived mesenchymal stem cells by activating the β-catenin/TCF complex via FGFR2-mediated activation of Akt [34]. Another study focused on intimal hyperplasia and found a significant upregulation of Aimp1, as well as Cxcl1, at the early stage of arterial injury in rat model [35]. Cxcl1, also known as growth-related oncogene protein-α (GRO-α), is a chemotactic cytokine. TNF-α could stimulate Cxcl1 release from human umbilical vein endothelial cells (HUVECs) through JNK-mediated Cxcl1 mRNA expression and p38 MAPK- and PI3K-mediated Cxcl1 secretory processes, and the recombinant Cxcl1 secreted by HUVECs enhanced cell proliferation in turn [36]. Conversely, another study pointed out that recombinant Cxcl1 induced by cyclic mechanical stretch (CMS) in a JNK-dependent manner failed to impact the proliferation of rat aortic smooth muscle cells (RASMCs) [37]. Tnfsf10, also named after TRAIL, is a member of a subset of the TNF receptor superfamily [38]. It has been reported that Tnfsf10 could promote the proliferation of VSMC via the activation of ERK1/2, Akt, and NF-κB [39–41]. Il15, Il7, and Il2rg are different subtypes of interleukins. Il15 has been detected in atherosclerosis plaques as a proinflammatory cytokine and could attenuate SMC proliferation possibly via inhibiting the chemokine receptor CX3CR1 [42, 43]. Il7 is a hematopoietic factor

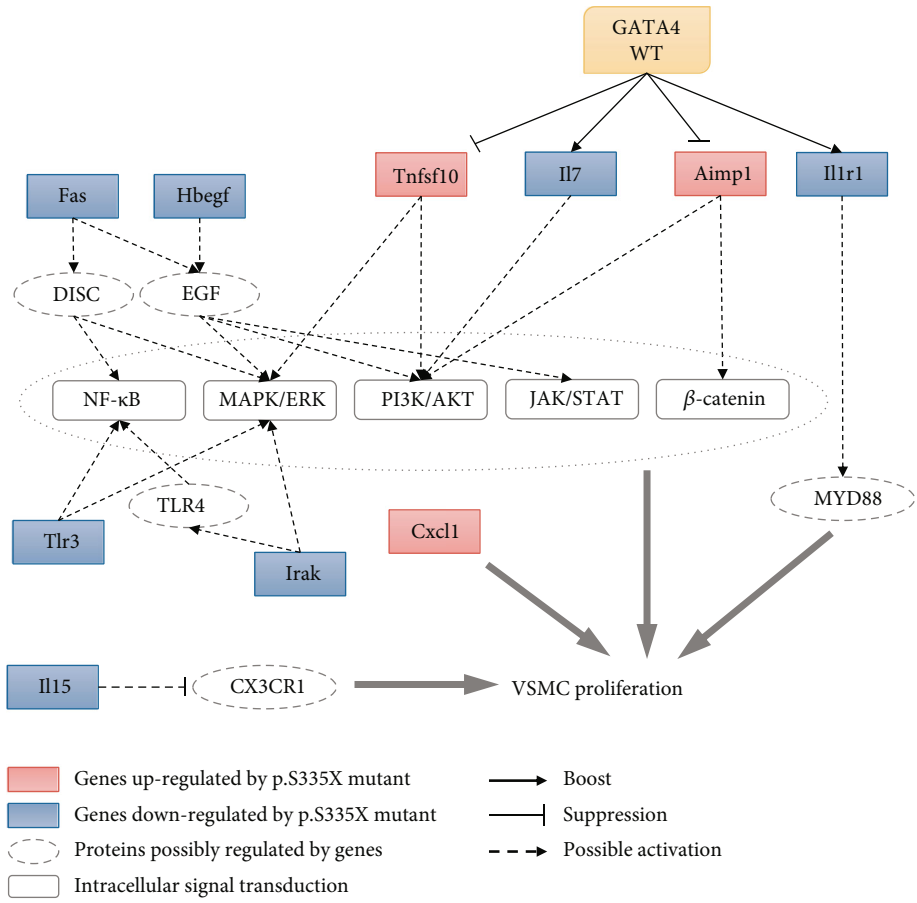

Figure 7: A schema illustrating the potential relationship between the regulation of RCSMC phenotype by GATA4 WT and MU and the DEGs and possible intracellular signals.

secreted by mesenchymal cells in the bone marrow and thymus, whose variant Il7δ5 could induce human breast cancer cell proliferation and cell cycle progression in a PI3K-Akt-dependent manner [44]. IL2RG encoded by Il2rg is an important signaling component of many cytokine receptors, including those of Il1, Il4, Il7, Il9, Il15, and Il21. A case report in Japan showed that, an atypical γc deficiency in IL2RG might be related with the occurrence of EBV-associated γδ T-cell lymphoproliferative disorder [45]. In our study, the expression of Aimp1, Cxcl1, and Thfsf10 was significantly higher in MU groups than that in WT groups, while the trends of Il15 and Il7 were opposite, suggesting that GATA4 C-terminus might target to the above-mentioned genes. Moreover, Il2rg expression was lower in EV group and was comparable between WT ang MU groups, implying that GATA4 might not regulate the expression of Il2rg through its C-terminus.

Encoded by Il1r1, IL-1 receptor 1 (IL-1R1) protein could be bound by Il-1β to recruit the molecular adaptor myeloid differentiation primary response protein 88 (MyD88) and thus induce IL-1, IL-6, and TNF-α synthesis through NF-κB activation. It has been reported that the IL-1R1/MyD88 signaling was involved in pulmonary vessel remodeling [46]. Gomez et al. observed smaller lesions nearly devoid of SMC and a fibrous cap in SMC-specific Il1r1 KO mice [47], indicating the close relationship between Il1r1 and atherosclerosis. Protein IRAK1 encoded by Irak1 has been reported to regulate VSMC proliferation in carotid arteries with IRAK4 via the TLR4/NF-κB signaling pathway [48]. Protein kinase C (PKC)-ε-IRAK–ERK axis also played important roles in the process of VSMC proliferation and neointimal hyperplasia mediated by IRAK1 [49]. Tlr3 is a member of the TLR family and can bind to double-strand RNA to regulate vascular remodeling [50]. It could evoke a proinflammatory and proliferative phenotype in human VSMC, probably mediated by ERK1/2 and NF-κB signaling [51]. The expression of Il1r1, Irak1, and Tlr3 in MU group was lower than that in WT group, indicating that the deletion of GATA4 C-terminus could suppress their expressions.

The above-mentioned DEGs regulated by the deletion of GATA4 C-terminus had the potential to regulate the proliferation of VSMC or other cell types through MAPK family (P38, JNK1/2, and ERK1/2), NF-κB, PI3K-Akt, and JAK-STAT pathways. A schema was provided in Figure 7 in order to illustrate the potential relationship between the regulation of RCSMC phenotype by GATA4 WT and MU and the DEGs and possible intracellular signals. However, whether such pathways are responsible for the phenotypic modulation of RCSMC by GATA-4 C-terminus still remained unclear. Further in-depth mechanism studies are required

to elucidate the exact signaling pathway(s) that account for the effects of GATA4 under both in vitro and in vivo conditions.

5. Conclusions

We herein reported that the deletion of GATA4 C-terminus induced by p.S335X mutation could enhance the proliferation but not the migration of RCSMC in vitro under certain stimulation. Twelve DEGs, including Fas, Hbegf, Itga5, Aimp1, Cxcl1, Il15, Il2rg, Il7, Tnfsf10, Il1r1, Irak1, and Tlr3, were screened and identified as phenotypic modulation-related genes that might be targeted by GATA4 and its C-terminus in the regulation of RCSMC proliferation. Our findings could provide a new sight and might be beneficial for the further mechanism study concerning CAD associated with GATA4 mutation.

Data Availability

The data used to support the findings of this study are available from the corresponding author upon request.

Conflicts of Interest

The authors have no conflict of interests to declare.

Authors' Contributions

Ting-Yan Yu and Xin-Xin Chen contributed equally to this work.

Acknowledgments

This study was supported by the National Natural Science Foundation of China (81970732 and 81570332 to LZ) and Medical Health Science and Technology Project of Xiamen, China (3502Z20194001 to WZ).

Supplementary Materials

Supplemental Table S1: primer sequences for QRT-PCR. *(Supplementary Materials)*

References

[1] A. K. Malakar, D. Choudhury, B. Halder, P. Paul, A. Uddin, and S. Chakraborty, "A review on coronary artery disease, its risk factors, and therapeutics," *Journal of Cellular Physiology*, vol. 234, no. 10, pp. 16812–16823, 2019.

[2] G. L. Basatemur, H. F. Jørgensen, M. C. H. Clarke, M. R. Bennett, and Z. Mallat, "Vascular smooth muscle cells in atherosclerosis," *Nature Reviews Cardiology*, vol. 16, no. 12, pp. 727–744, 2019.

[3] D. A. Chistiakov, A. N. Orekhov, and Y. V. Bobryshev, "Vascular smooth muscle cell in atherosclerosis," *Acta Physiologica*, vol. 214, no. 1, pp. 33–50, 2015.

[4] A. Frismantiene, M. Philippova, P. Erne, and T. J. Resink, "Cadherins in vascular smooth muscle cell (patho)biology: quid nos scimus?," *Cellular Signalling*, vol. 45, pp. 23–42, 2018.

[5] G. Wang, L. Jacquet, E. Karamariti, and Q. Xu, "Origin and differentiation of vascular smooth muscle cells," *The Journal of Physiology*, vol. 593, no. 14, pp. 3013–3030, 2015.

[6] D. Gomez and G. K. Owens, "Smooth muscle cell phenotypic switching in atherosclerosis," *Cardiovascular Research*, vol. 95, no. 2, pp. 156–164, 2012.

[7] M. R. Bennett, S. Sinha, and G. K. Owens, "Vascular smooth muscle cells in atherosclerosis," *Circulation Research*, vol. 118, no. 4, pp. 692–702, 2016.

[8] Y. Zhang, F. Ai, J. Zheng, and B. Peng, "Associations of Gata4 genetic mutations with the risk of congenital heart disease: a meta-analysis," *Medicine*, vol. 96, no. 18, article e6857, 2017.

[9] Z. Zhao, Y. Zhan, W. Chen, X. Ma, W. Sheng, and G. Huang, "Functional analysis of rare variants of Gata4 identified in Chinese patients with congenital heart defect," *Genesis*, vol. 57, no. 11-12, article e23333, 2019.

[10] J. E. Kontaraki, G. E. Kochiadakis, M. E. Marketou et al., "Early cardiac gene transcript levels in peripheral blood mononuclear cells reflect severity in stable coronary artery disease," *Hellenic Journal of Cardiology*, vol. 55, no. 2, pp. 119–125, 2014.

[11] J. Chen, S. Wang, S. Pang, Y. Cui, B. Yan, and R. Hawley, "Functional genetic variants of the Gata4 gene promoter in acute myocardial infarction," *Molecular Medicine Reports*, vol. 19, no. 4, pp. 2861–2868, 2019.

[12] N. P. Muiya, S. M. Wakil, A. I. Tahir et al., "A study of the role of Gata4 polymorphism in cardiovascular metabolic disorders," *Human Genomics*, vol. 7, no. 1, p. 25, 2013.

[13] C. Cheng, Y. Lin, F. Yang et al., "Mutational screening of affected cardiac tissues and peripheral blood cells identified novel somatic mutations in Gata4 in patients with ventricular septal defect," *Journal of Biomedical Research*, vol. 25, no. 6, pp. 425–430, 2011.

[14] F. Yang, M. Wu, Y. Li et al., "Mutation P.S335x in Gata4 reduces its DNA binding affinity and enhances cell apoptosis associated with ventricular septal defect," *Current Molecular Medicine*, vol. 13, no. 6, pp. 993–999, 2013.

[15] J. Heineke, M. Auger-Messier, J. Xu et al., "Cardiomyocyte Gata4 functions as a stress-responsive regulator of angiogenesis in the murine heart," *The Journal of Clinical Investigation*, vol. 117, no. 11, pp. 3198–3210, 2007.

[16] J. Rysä, O. Tenhunen, R. Serpi et al., "Gata-4 is an angiogenic survival factor of the infarcted heart," *Circulation. Heart Failure*, vol. 3, no. 3, pp. 440–450, 2010.

[17] B. Zhou, Q. Ma, S. W. Kong et al., "Fog2 is critical for cardiac function and maintenance of coronary vasculature in the adult mouse heart," *The Journal of Clinical Investigation*, vol. 119, no. 6, pp. 1462–1476, 2009.

[18] A. Lawrie, E. Spiekerkoetter, E. C. Martinez et al., "Interdependent serotonin transporter and receptor pathways regulate S100a4/Mts1, a gene associated with pulmonary vascular disease," *Circulation Research*, vol. 97, no. 3, pp. 227–235, 2005.

[19] K. Jeong, J.-H. Kim, J. M. Murphy et al., "Nuclear focal adhesion kinase controls vascular smooth muscle cell proliferation and neointimal hyperplasia through Gata4-mediated cyclin D1 transcription," *Circulation Research*, vol. 125, no. 2, pp. 152–166, 2019.

[20] B. M. Kohlnhofer, C. A. Thompson, E. M. Walker, and M. A. Battle, "Gata4 regulates epithelial cell proliferation to control intestinal growth and development in mice," *Cellular and Molecular Gastroenterology and Hepatology*, vol. 2, no. 2, pp. 189–209, 2016.

[21] M. K. Singh, Y. Li, S. Li et al., "Gata4 and Gata5 cooperatively regulate cardiac myocyte proliferation in mice," *The Journal of Biological Chemistry*, vol. 285, no. 3, pp. 1765–1772, 2010.

[22] C. Misra, S. W. Chang, M. Basu, N. Huang, and V. Garg, "Disruption of myocardial Gata4 and Tbx5 results in defects in cardiomyocyte proliferation and atrioventricular septation," *Human Molecular Genetics*, vol. 23, no. 19, pp. 5025–5035, 2014.

[23] E. Efimenko, M. B. Padua, N. L. Manuylov, S. C. Fox, D. A. Morse, and S. G. Tevosian, "The transcription factor Gata4 is required for follicular development and normal ovarian function," *Developmental Biology*, vol. 381, no. 1, pp. 144–158, 2013.

[24] Q. Han, X. Xu, J. Li et al., "Gata4 is highly expressed in childhood acute lymphoblastic leukemia, promotes cell proliferation and inhibits apoptosis by activating Bcl2 and Mdm2," *Molecular Medicine Reports*, vol. 16, no. 5, pp. 6290–6298, 2017.

[25] S. Lu, H. Liu, L. Lu et al., "Wisp1 overexpression promotes proliferation and migration of human vascular smooth muscle cells via Akt signaling pathway," *European Journal of Pharmacology*, vol. 788, pp. 90–97, 2016.

[26] L. Meng, W. Xu, L. Guo, W. Ning, and X. Zeng, "Paeonol inhibits the proliferation, invasion, and inflammatory reaction induced by TNF-α in vascular smooth muscle cells," *Cell Biochemistry and Biophysics*, vol. 73, no. 2, pp. 495–503, 2015.

[27] H. Li, Y. Cheng, T. Simoncini, and S. Xu, "17β-Estradiol inhibits TNF-α-induced proliferation and migration of vascular smooth muscle cells via suppression of trail," *Gynecological Endocrinology*, vol. 32, no. 7, pp. 581–586, 2016.

[28] S. Chen, Y. Ding, W. Tao, W. Zhang, T. Liang, and C. Liu, "Naringenin inhibits TNF-α induced VSMC proliferation and migration via induction of HO-1," *Food and Chemical Toxicology*, vol. 50, no. 9, pp. 3025–3031, 2012.

[29] E. Brint, G. O'Callaghan, and A. Houston, "Life in the Fas lane: differential outcomes of Fas signaling," *Cellular and Molecular Life Sciences*, vol. 70, no. 21, pp. 4085–4099, 2013.

[30] K.-S. Lee, J.-H. Park, S. Lee, H.-J. Lim, H.-E. Choi, and H.-Y. Park, "Hb-Egf induces delayed Stat3 activation via Nf-Kappab mediated Il-6 secretion in vascular smooth muscle cell," *Biochimica et Biophysica Acta (BBA) - Molecular Cell Research*, vol. 1773, no. 11, pp. 1637–1644, 2007.

[31] S. Lee, H.-J. Lim, H.-Y. Park, K.-S. Lee, J.-H. Park, and Y. Jang, "Berberine inhibits rat vascular smooth muscle cell proliferation and migration in vitro and improves neointima formation after balloon injury in vivo: Berberine improves neointima formation in a rat model," *Atherosclerosis*, vol. 186, no. 1, pp. 29–37, 2006.

[32] L. Feng, J. Ma, H. Ji, Y. Liu, and W. Hu, "Mir-330-5p Suppresses glioblastoma cell proliferation and invasiveness through targeting Itga5," *Bioscience Reports*, vol. 37, no. 3, article BSR20170019, 2017.

[33] H. Wang, J. Li, X. Zhang et al., "Priming integrin alpha 5 promotes the osteogenic differentiation of human periodontal ligament stem cells due to cytoskeleton and cell cycle changes," *Journal of Proteomics*, vol. 179, pp. 122–130, 2018.

[34] S. Y. Kim, W. S. Son, M. C. Park et al., "Ars-interacting multifunctional protein 1 induces proliferation of human bone marrow-derived mesenchymal stem cells by accumulation of beta-catenin via fibroblast growth factor receptor 2-mediated activation of Akt," *Stem Cells and Development*, vol. 22, no. 19, pp. 2630–2640, 2013.

[35] A. Fedorov, A. Kostareva, J. Raud, J. Roy, U. Hedin, and A. Razuvaev, "Early changes of gene expression profiles in the rat model of arterial injury," *Journal of Vascular and Interventional Radiology*, vol. 25, no. 5, pp. 789–796, 2014.

[36] J. Zhao, Y. Nishimura, A. Kimura et al., "Chemokines protect vascular smooth muscle cells from cell death induced by cyclic mechanical stretch," *Scientific Reports*, vol. 7, no. 1, p. 16128, 2017.

[37] H.-m. Lo, T.-h. Lai, C.-h. Li, and W.-b. Wu, "Tnf-alpha induces Cxcl1 chemokine expression and release in human vascular endothelial cells in vitro via two distinct signaling pathways," *Acta Pharmacologica Sinica*, vol. 35, no. 3, pp. 339–350, 2014.

[38] S. P. Cullen and S. J. Martin, "Fas and trail 'death receptors' as initiators of inflammation: implications for cancer," *Seminars in Cell & Developmental Biology*, vol. 39, pp. 26–34, 2015.

[39] P. Secchiero, C. Zerbinati, E. Rimondi et al., "Trail promotes the survival, migration and proliferation of vascular smooth muscle cells," *Cellular and Molecular Life Sciences*, vol. 61, no. 15, pp. 1965–1974, 2004.

[40] M. M. Kavurma, M. Schoppet, Y. V. Bobryshev, L. M. Khachigian, and M. R. Bennett, "TRAIL Stimulates Proliferation of Vascular Smooth Muscle Cells via Activation of NF-κB and Induction of Insulin-like Growth Factor-1 Receptor$*$," *Journal of Biological Chemistry*, vol. 283, no. 12, pp. 7754–7762, 2008.

[41] J. Chan, L. Prado-Lourenco, L. M. Khachigian, M. R. Bennett, B. A. Di Bartolo, and M. M. Kavurma, "Trail promotes Vsmc proliferation and neointima formation in a Fgf-2-, Sp1 phosphorylation-, and Nfkappab-dependent manner," *Circulation Research*, vol. 106, no. 6, pp. 1061–1071, 2010.

[42] M. Cercek, M. Matsumoto, H. Li et al., "Autocrine role of vascular Il-15 in intimal thickening," *Biochemical and Biophysical Research Communications*, vol. 339, no. 2, pp. 618–623, 2006.

[43] S. Iwasaki, S. Minamisawa, U. Yokoyama et al., "Interleukin-15 inhibits smooth muscle cell proliferation and hyaluronan production in rat ductus arteriosus," *Pediatric Research*, vol. 62, no. 4, pp. 392–398, 2007.

[44] D. Pan, B. Liu, X. Jin, and J. Zhu, "Il-7 splicing variant Il-7δ5 induces human breast cancer cell proliferation via activation of Pi3k:Akt pathway," *Biochemical and Biophysical Research Communications*, vol. 422, no. 4, pp. 727–731, 2012.

[45] K. Tanita, A. Hoshino, K.-I. Imadome et al., "Epstein-Barr virus-associated $\gamma\delta$ T-cell lymphoproliferative disorder associated with hypomorphic Il2rg mutation," *Frontiers in Pediatrics*, vol. 7, no. 15, 2019.

[46] A. Parpaleix, V. Amsellem, A. Houssaini et al., "Role of interleukin-1 receptor 1/Myd88 signalling in the development and progression of pulmonary hypertension," *European Respiratory Journal*, vol. 48, no. 2, pp. 470–483, 2016.

[47] D. Gomez, R. A. Baylis, B. G. Durgin et al., "Interleukin-1beta has atheroprotective effects in advanced atherosclerotic lesions of mice," *Nature Medicine*, vol. 24, no. 9, pp. 1418–1429, 2018.

[48] S. Bai, D. Li, Z. Zhou et al., "Interleukin-1 receptor-associated kinase 1:4 as a novel target for inhibiting neointimal formation after carotid balloon injury," *Journal of Atherosclerosis and Thrombosis*, vol. 22, no. 12, pp. 1317–1337, 2015.

[49] M. Jain, A. Singh, V. Singh, and M. K. Barthwal, "Involvement of interleukin-1 receptor-associated kinase-1 in vascular smooth muscle cell proliferation and neointimal formation after rat carotid injury," *Arteriosclerosis, Thrombosis, and Vascular Biology*, vol. 35, no. 6, pp. 1445–1455, 2015.

[50] D. Farkas, A. A. R. Thompson, A. R. Bhagwani et al., "Toll-like receptor 3 is a therapeutic target for pulmonary hypertension," *American Journal of Respiratory and Critical Care Medicine*, vol. 199, no. 2, pp. 199–210, 2019.

[51] X. Yang, V. Murthy, K. Schultz, J. B. Tatro, K. A. Fitzgerald, and D. Beasley, "Toll-like receptor 3 signaling evokes a proinflammatory and proliferative phenotype in human vascular smooth muscle cells," *American Journal of Physiology-Heart and Circulatory Physiology*, vol. 291, no. 5, pp. H2334–H2343, 2006.

Hindawi
Mediators of Inflammation
Volume 2021, Article ID 9661752, 12 pages
https://doi.org/10.1155/2021/9661752

Review Article

The Effects of Statin Dose, Lipophilicity, and Combination of Statins plus Ezetimibe on Circulating Oxidized Low-Density Lipoprotein Levels: A Systematic Review and Meta-Analysis of Randomized Controlled Trials

Tannaz Jamialahmadi,[1,2] Fatemeh Baratzadeh,[3] Željko Reiner,[4] Luis E. Simental-Mendía,[5] Suowen Xu,[6] Andrey V. Susekov,[7] Raul D. Santos,[8] and Amirhossein Sahebkar[9,10]

[1]*Department of Food Science and Technology, Quchan Branch, Islamic Azad University, Quchan, Iran*
[2]*Department of Nutrition, Faculty of Medicine, Mashhad University of Medical Sciences, Mashhad, Iran*
[3]*School of Pharmacy, Mashhad University of Medical Sciences, Mashhad, Iran*
[4]*Department of Internal Medicine, University Hospital Centre Zagreb, School of Medicine, University of Zagreb, Zagreb, Croatia*
[5]*Biomedical Research Unit, Mexican Social Security Institute, Durango, Mexico*
[6]*Division of Life Sciences and Medicine, University of Science and Technology of China, Hefei, China*
[7]*GBOU DPO Russian Medical Academy for Postgraduate Medical Education Ministry of Health, Moscow, Russia*
[8]*Lipid Clinic Heart Institute (Incor), University of São Paulo, Medical School Hospital, São Paulo, Brazil*
[9]*Applied Biomedical Research Center, Mashhad University of Medical Sciences, Mashhad, Iran*
[10]*Biotechnology Research Center, Pharmaceutical Technology Institute, Mashhad University of Medical Sciences, Mashhad, Iran*

Correspondence should be addressed to Amirhossein Sahebkar; amir_saheb2000@yahoo.com

Received 23 June 2021; Accepted 19 August 2021; Published 6 September 2021

Academic Editor: Dominik Skiba

Background. Elevated plasma low-density lipoprotein cholesterol (LDL-C) is the main risk factor for atherosclerotic cardiovascular disease (ASCVD). Statins are the drugs of choice for decreasing LDL-C and are used for the prevention and management of ASCVD. Guidelines recommend that subjects with high and very high ASCVD risk should be treated with high-intensity statins or a combination of high-intensity statins and ezetimibe. The lipophilicity or hydrophilicity (solubility) of statins is considered to be important for at least some of their LDL-C lowering independent pleiotropic effects. Oxidative modification of LDL (ox-LDL) is considered to be the most important atherogenic modification of LDL and is supposed to play a crucial role in atherogenesis and ASCVD outcomes. *Objective*. The aim of this systematic review and meta-analysis was to find out what are the effects of statin intensity, lipophilicity, and combination of statins plus ezetimibe on ox-LDL. *Methods*. PubMed, Scopus, Embase, and Web of Science were searched from inception to February 5, 2021, for randomized controlled trials (RCTs). Two independent and blinded authors evaluated eligibility by screening the titles and abstracts of the studies. Risk of bias in the studies included in this meta-analysis was evaluated according to the Cochrane instructions. Meta-analysis was performed using Comprehensive Meta-Analysis (CMA) V2 software. Evaluation of funnel plot, Begg's rank correlation, and Egger's weighted regression tests were used to assess the presence of publication bias. *Results*. Among the 1427 published studies identified by a systematic databases search, 20 RCTs were finally included in the systematic review and meta-analysis. A total of 1874 patients are included in this meta-analysis. This meta-analysis suggests that high-intensity statin treatment is associated with a significant decrease in circulating concentrations of ox-LDL when compared with low-to-moderate treatment (SMD: -0.675, 95% CI: -0.994, -0.357, $p < 0.001$; I^2: 55.93%). There was no difference concerning ox-LDL concentration between treatments with hydrophilic and lipophilic statins (SMD: -0.129, 95% CI: -0.330, -0.071, $p = 0.206$; I^2: 45.3%), but there was a significant reduction in circulating concentrations of ox-LDL associated with statin plus ezetimibe combination therapy when compared with statin monotherapy (SMD: -0.220, 95% CI: -0.369, -0.071, $p = 0.004$; I^2: 0%). *Conclusion*. High-dose statin or combination of statins with ezetmibe reduces plasma ox-LDL in comparison low-to-moderate intensity statin therapy alone. Statin lipophilicity is not associated with reduction in ox-LDL plasma concentrations.

1. Introduction

It has been well known for many decades that elevated plasma level of low-density lipoprotein cholesterol (LDL-C) is the most important risk factor for atherosclerotic cardiovascular disease (ASCVD) [1, 2]. For almost four decades, statins are the drugs of choice for treating elevated LDL-C and are used for primary and secondary prevention of ASCVD [3, 4]. Besides, these drugs have been identified to exert several pleiotropic effects relevant to cardiovascular health and improvement of noncardiovascular diseases [5–10]. Both the 2019 European Society of Cardiology (ESC)/European Atherosclerosis Society (EAS) Guidelines for the Management of Dyslipidemias and 2018 American Heart Association (AHA)/American College of Cardiology (ACC) Multisociety Guideline on the Management of Blood Cholesterol recommend that patients with ASCVD, severe hypercholesterolemia, familial hypercholesterolemia, or diabetes should be treated aggressively with high-intensity statins or a combination of high-intensity statins and ezetimibe in order to achieve improved ASCVD outcomes [11, 12]. High-intensity statins were defined as atorvastatin 40-80 mg/day or rosuvastatin 20-40 mg/day. The results of some most recently published studies have confirmed such an approach [13–15]. Unfortunately, most of these high and very-high risk patients in real life do not receive high-intensity lipid lowering therapy [4, 16].

Lipophilic statins include atorvastatin, simvastatin, lovastatin, fluvastatin, cerivastatin, and pitavastatin, while hydrophilic statins include rosuvastatin and pravastatin [17]. The lipophilicity or hydrophilicity of statins is important for their pharmacokinetics and pharmacodynamics, and these characteristics are considered to be crucial for at least some of their LDL-C lowering independent pleiotropic effects [18]. Statin lipophilicity might be important because of its association with hepatoselectivity since lipophilic statins undergo oxidative biotransformation by the CYP450 in hepatocytes and therefore are susceptible to drug-drug interactions and might passively and nonselectively pass through the membranes of nonhepatic tissues thus theoretically having a possible role in some adverse effects of statins, e.g., myopathy [19]. On the other hand, hydrophilic statins employ carrier-mediated mechanisms for uptake, which could reduce their ability to have non-lipid-lowering pleiotropic effects on extrahepatic tissues, and they are excreted largely in an unchanged form [17]. However, in randomized trials and in real-world clinical setting, these differences concerning the effects of statins on myopathy risk have not been proven [20].

Oxidative modification of LDL particles (ox-LDL) is for more than a quarter of century considered to be the most important atherogenic modification of LDL and is supposed to play a crucial role in atherogenesis and ASCVD outcomes [21–23]. This is not only due to the role of ox-LDL in atherosclerotic plaque formation [24] but also because ox-LDL participate in destabilization of the existing atherosclerotic plaques by inducing matrix degradation, fissuring of the plaque and thrombus formation on this site thus causing clinical manifestations such as myocardial infarction (MI) and unstable angina [25].

Nevertheless, there are not many studies analyzing the possible association of statin lipophilicity with plasma ox-LDL concentration neither; it is clear whether there is any association between statin intensity and plasma ox-LDL concentration. Furthermore, the association between the uses of ezetimibe, a cholesterol absorption inhibitor, and plasma ox-LDL is not totally set. Apparently, ezetimibe could protect against the oxidative stress induced by ox-LDL [26]. However, in animal experiments, no significant correlations between atherosclerotic plaque areas and serum concentrations of ox-LDL were proven [27].

Therefore, the aim of this systematic review and meta-analysis was to dissect the effects of statins intensity, lipophilicity, and combination of statins plus ezetimibe on plasma ox-LDL.

2. Methods

2.1. Search Strategy. This systematic review and meta-analysis was designed according to the 2009 guidelines preferred reporting items for systematic reviews and meta-analysis (PRISMA) statement guidelines [28]. PubMed, Scopus, Embase, and Web of Science were searched from inception to February 5th using the following keywords in titles and abstracts (also in combination with MESH terms): ("Hydroxymethylglutaryl-CoA Reductase Inhibitors" OR simvastatin OR rosuvastatin OR atorvastatin OR pravastatin OR pitavastatin OR mevastatin OR fluvastatin OR lovastatin) AND ("oxidized low density lipoprotein" OR "oxidized LDL" OR OxLDL OR ox-LDL OR "oxidized Low-Density Lipoprotein" OR "minimally modified oxidized-LDL" OR MM-LDL OR MMLDL OR "malondialdehyde-low density lipoprotein" OR "malondialdehyde low density lipoprotein" OR MDA-LDL OR MDALDL OR "MDA-LDL IgM" OR "MDA-LDL IgG" OR "autoantibodies against oxidized low-density lipoprotein" OR "autoantibodies against oxidized low density lipoprotein" OR AuAb-oxLDL OR "antibodies against oxidized LDL" OR Anti-oxLDL).

2.2. Study Selection. Clinical studies were included if they met the following inclusion criteria: (i) randomized controlled trial with either parallel or cross-over design, (ii) the studies which investigated the impact of statin intensity (i.e., high- versus low-to-moderate-intensity statin), (iii) statin lipophilicity (lipophilic versus hydrophilic statins) or (iv) adding ezetimibe to statin therapy versus statin monotherapy on plasma ox-LDL concentrations, and (v) presentation of sufficient information at baseline and at the end of follow-up in each group or studies providing the net change values. The exclusion criteria are as follows: (i) nonrandomized trials, (ii) uncontrolled trials, (iii) observational studies with case-control, cross-sectional, or cohort design, (iv) noncomparative studies with statins versus a neutral arm, and (iv) lack of sufficient information at baseline or follow-up.

2.3. ox-LDL Assay Methods. In most of the included studies, serum ox-LDL was measured using enzyme-linked immunosorbent assay (ELISA) methods. Three studies used Mercodia ox-LDL kit (Mercodia, Uppsala, Sweden) [29–31],

two studies used Mercodia, Inc. kit (Winston-Salem, North Carolina, USA) [32, 33], two studies used SRL kit (Tokyo, Japan) [34, 35], one study used R&D Systems Inc. kit (Minneapolis, Minnesota, USA) [36], one study used Immundiagnostik kit (Bensheim, Germany) [37], three studies used Kyowa Medex MX kit (Kyowa Medex, Inc., Tokyo) [38–40], one study used Daiichi kit (Sekisui Medical, Tokyo, Japan) [41], two studies used Biomedica kit (Wien, Austria) [42, 43], one study used TPI Corporation kit (Johnson City, TN) [44], and four studies did not mention the methods used or assay kits [45–48].

2.4. Data Extraction. After removal of duplicate studies, two independent and blinded authors (FB and TJ) evaluated eligibility by screening of the titles and abstracts of the studies. Full reports of the potentially eligible studies were then obtained and evaluated. Any disagreements were resolved by discussion with a third author (AS) until reaching a consensus. Eligible studies were reviewed, and the following data were abstracted: (1) the name of first author, (2) year of publication, (3) study design, (4) type of statin used in the study, (5) dose of statin, (6) treatment duration, (7) patients characteristics, and (8) plasma ox-LDL concentrations.

2.4.1. Quality Assessment. Risk of bias in the studies included in this meta-analysis was evaluated according to the Cochrane instruction [28]. Selection bias, performance bias, attrition bias, detection bias, reporting bias, and other sources of bias were estimated to be high, low, or unclear in each of the included studies.

2.5. Quantitative Data Synthesis. Meta-analysis was performed using the Comprehensive Meta-Analysis (CMA) V2 software (Biostat, NJ) [49]. Information regarding sample size, means, and standard deviations from each group were extracted to calculate standardized mean differences (SMDs). We applied SMD because of the different metrics used to assay and report plasma ox-LDL values. Effect size was calculated as follows: (measure at the end of follow-up in the treatment group − measure at baseline in the treatment group) − (measure at the end of follow-up in the control group − measure at baseline in the control group). A random effects model (using DerSimonian-Laird method) and the generic inverse variance weighting method were used to compensate for the heterogeneity of studies in terms of study design, treatment duration, and the characteristics of the studied populations [50]. If the outcome measures were reported in median and range (or 95% confidence interval (CI)), mean and SD values were estimated using the method described by Hozo et al. [51]. Where only the standard error of the mean (SEM) was reported, SD was estimated using the following formula: $SD = SEM \times \text{sqrt}(n)$, where n is the number of subjects. Effect sizes were expressed as standard mean difference (SMD) and 95% CI. In order to evaluate the influence of each study on the overall effect size, a sensitivity analysis was conducted using the leave-one-out method (i.e., removing one study each time and repeating the analysis) [52, 53].

2.5.1. Metaregression. LDL changes were entered into a random effects metaregression model to explore their association with the estimated effect size.

2.5.2. Publication Bias. Evaluation of funnel plot, Begg's rank correlation, and Egger's weighted regression tests were used to assess the presence of publication bias in the meta-analysis. When there was an evidence of funnel plot asymmetry, potentially missing studies were imputed using the "trim and fill" method [54].

2.5.3. Results. Among the 1427 published studies identified by a systematic databases search, 130 were found to be potentially relevant following assessment of titles and abstracts. Of those, 77 studies were excluded after careful evaluation (3 studies were cross-sectional, 24 studies were nonrandomized clinical trials, 34 studies did not report sufficient data, and 16 studies were not comparative according to inclusion criteria). However, from remaining 53 studies , 33 studies were not placebo-controlled. Therefore, 20 RCTs were finally included in the systematic review and meta-analysis (Table 1). The study selection process is shown in Figure 1.

3. Results

3.1. Effects of Statin Intensity on Circulating Concentrations of ox-LDL. Meta-analysis of data from 4 trials including 381 patients suggested a significant decrease in circulating concentrations of ox-LDL after high-intensity statin treatment vs. low-to-moderate intensity (SMD: -0.675, 95% CI: -0.994, -0.357, $p < 0.001$; I^2: 55.93%) (Figure 2(a)). The reduction in circulating concentrations of ox-LDL was robust in the leave-one-out sensitivity analysis (Figure 2(b)).

3.2. Effects of Statin Lipophilicity on Circulating Concentrations of ox-LDL. Meta-analysis of data from 10 trials including 795 patients showed that plasma ox-LDL (SMD: -0.129, 95% CI: -0.330, -0.071, $p = 0.206$; I^2: 45.3%) levels were not significantly different between patients treated with hydrophilic and lipophilic statins (Figure 3(a)). This finding was robust in the leave-one-out sensitivity analysis (Figure 3(b)).

3.3. Effects of Statin/Ezetimibe Combination Therapy vs. Statin Monotherapy on Circulating Concentrations of ox-LDL. Meta-analysis of data from 7 trials including 698 patients suggested a significant reduction in circulating concentrations of ox-LDL following statin/ezetimibe combination therapy vs. statin monotherapy (SMD: -0.220, 95% CI: -0.369, -0.071, $p = 0.004$; I^2: 0%) (Figure 4(a)). The reduction in circulating concentrations of ox-LDL with statin/ezetimibe combination therapy was robust in the leave-one-out sensitivity analysis (Figure 4(b)).

3.3.1. Metaregression. Random effects metaregression was performed to assess the impact of changes in LDL concentration on the circulating concentrations of ox-LDL lowering activity of statins. The results suggested a significant association between the changes in circulating concentrations of

Table 1: Characteristics of studies measuring circulating concentrations of oxidized LDL.

Study, year	Study design	Follow-up	Treatment	Control	Clinical outcome ox-LDL	MDA-LDL	Patients	No. of patients
van Tits et al., 2006 [29]	Randomized double-blind study	2 years	A 80 mg/day	S 40 mg/day	Significant decrease in plasma level of ox-LDL	—	Patients with heterozygous familial hypercholesterolemia	115
Puccetti et al., 2011 [45]	Prospective, randomized, double-blind study	8 weeks	A 20 mg/day	R 10 mg/day	Significant decrease in plasma level of ox-LDL	—	Hypercholesterolemic patients	60
Tsutamoto et al., 2011 [38]	Randomized double-blind open-label study	6 months	A 5 mg/day	R 2.5 mg/day	Significant decrease in plasma level of ox-LDL in the A group but not in the R group	—	CHF patients with dilated cardiomyopathy	63
Aydin et al., 2015 [37]	Randomized active-controlled study	4 weeks	A 80 mg/day	R 20 mg/day	Significant decrease in plasma level of ox-LDL	—	STEMI	90
Altunkeser et al., 2019 [42]	Randomized active-controlled study	4 weeks	A 80 mg/day	R 40 mg/day	Significant decrease in plasma level of ox-LDL	—	ACS	106
Tunçez et al., 2019 [43]	Randomized active-controlled study	4 weeks	A 80 mg/day	R 40 mg/day	Significant decrease in plasma level of ox-LDL	—	AMI	63
Gavazzoni et al., 2017 [36]	Single-center, prospective, randomized, blinded open-label study	1 month	A 80 mg/day	A 20 mg/day	Significant decrease in plasma level of ox-LDL	—	STEMI	52
Soran et al., 2018 [31]	Double-blind randomized study	12 months	A 80 mg/day	A 10 mg/day	Significant decrease in plasma level of ox-LDL	—	T2DM with microalbuminuria or proteinuria	119
Huang et al., 2012 [44]	Double-blind randomized study	12 months	A 40 mg/day	A 10 mg/day	Significant decrease in plasma level of ox-LDL	—	Patients with ischemic cardiomyopathy	95
Tamura et al., 2003 [34]	Randomized crossover study	8 weeks	A 10 mg/day	P 10 mg/day	—	Significant decrease in plasma level of MDA-LDL	Hypercholesterolemic patients	34
Tsutamoto et al., 2009 [39]	Randomized active-controlled study	4 months	S 5 mg/day	R 2.5 mg/day	Significant decrease in plasma level of ox-LDL in the R group but not in the S group	—	Patients with nonischaemic CHF	71
Moutzouri et al., 2013 [30]	Prospective, randomized, open-label, blinded endpoint study	12 weeks	S 40 mg/day	R 10 mg/day	Significant decrease in plasma level of ox-LDL	—	Hypercholesterolemic patients	100
				S 10 mg/day + Ez 10 mg/day	Significant decrease in plasma level of ox-LDL		Hypercholesterolemic patients	108
		12 weeks	P 10 mg/day	F 20 mg/day		—		16

Table 1: Continued.

Study, year	Study design	Follow-up	Treatment	Control	Clinical outcome ox-LDL	MDA-LDL	Patients	No. of patients
Inami et al., 2004 [40]	Prospective, randomized active-controlled study				Significant decrease in plasma level of ox-LDL		Hypercholesterolemic patients	
Toribio et al., 2017 [32]	Double-blind, active-controlled, parallel-group comparative study	52 weeks	Pi 4 mg/day	P 40 mg/day	Significant decrease in plasma level of ox-LDL	—	HIV-infected patients with dyslipidemia	192
Pesaro et al., 2012 [33]	Randomized, double-blind, active-controlled study	6 weeks	S 80 mg/day	S 20 mg/day + Ez 10 mg/day	Significant decrease in plasma level of ox-LDL	—	CAD	78
Uemura et al., 2012 [35]	Randomized open-label crossover study	12 weeks	A 20 mg/day	A 10 mg/day + Ez 10 mg/day	—	Decrease in plasma level of MDA-LDL	Abnormal glucose tolerance and CAD	39
Wu et al., 2018 [46]	Randomized active-controlled study	12 weeks	A 40 mg/day	A 20 mg/day + Ez 10 mg/day	Significant decrease in plasma level of ox-LDL	—	ASCVD	98
Torimoto et al., 2013 [41]	Randomized open-label study	12 weeks	R 5 mg/day	R 2.5 mg/day + Ez 10 mg/day	—	Significant decrease in plasma level of MDA-LDL	T2DM	75
Sakuma et al., 2019 [47]	Randomized crossover study	3 months	Double dose of statin	Ez 10 mg + baseline dose of statin	—	Significant decrease in plasma level of MDA-LDL	CAD	42
Takase et al., 2017 [48]	Multicenter, prospective, randomized, open-label, blinded-end point study	6-8 months	Statin monotherapy	Ez 10 mg/d + statin	—	Significant change in plasma level of MDA-LDL	CAD patients after coronary stenting	258

A: atorvastatin; ASCVD: atherosclerotic cardiovascular disease; ACS: acute coronary syndrome; AMI: acute myocardial infarction; CAD: coronary artery disease; CHF: Congestive heart failure; EZ: ezetimibe; F: fluvastatin; MDA-LDL: malondialdehyde modified low-density lipoprotein; ox-LDL: oxidized low-density lipoprotein; P: pravastatin; Pi: pitavastatin; R: rosuvastatin; S: simvastatin; T2DM: type 2 diabetes.

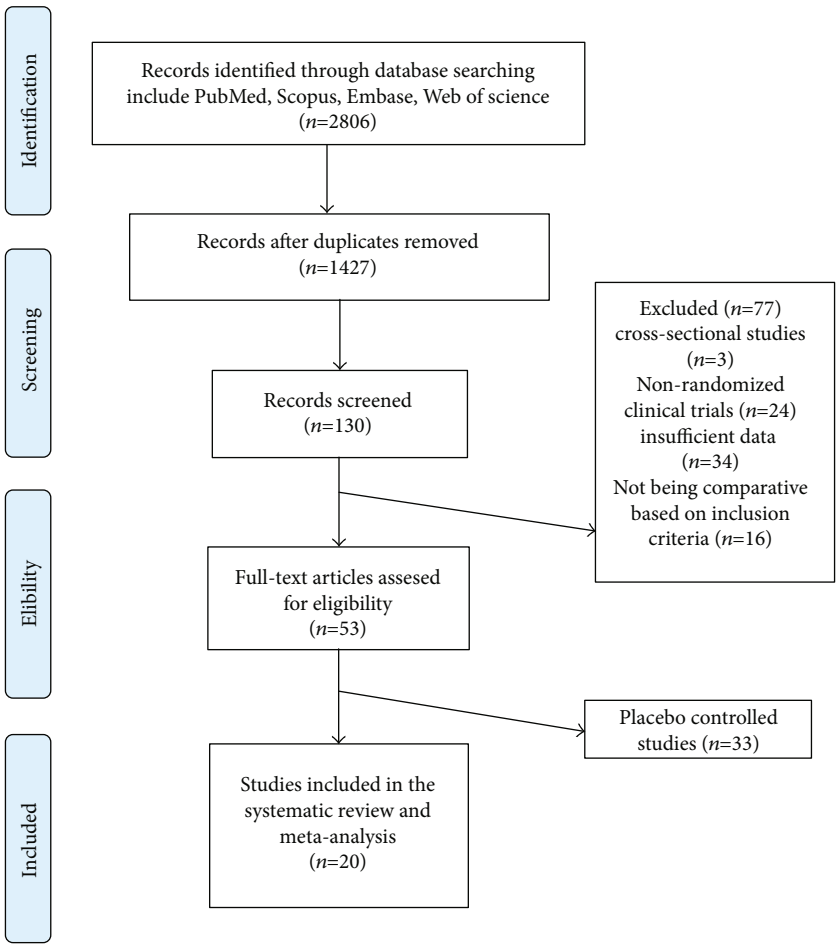

Figure 1: Flow chart of the number of studies identified and included into the meta-analysis.

Study name	Std diff in means	Standard error	Variance	Lower limit	Upper limit	Z-value	p-value
Van Tits et. al, 2006	−0.430	0.189	0.036	−0.800	−0.061	−2.281	0.023
Gavazzoni et. al, 2017	−0.895	0.291	0.085	−1.465	−0.324	−3.075	0.002
Huang et. al, 2012	−1.059	0.219	0.048	−1.488	−0.629	−4.832	0.000
Soran et. al, 2018	−0.441	0.186	0.034	−0.804	−0.077	−2.375	0.018
Meta analysis	−0.675	0.163	0.026	−0.994	−0.357	−4.153	0.000

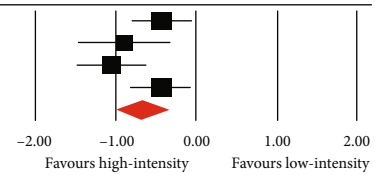

(a)

Study name	Point	Standard error	Variance	Lower limit	Upper limit	Z-value	p-value
Van Tits et. al, 2006	−0.776	0.208	0.043	−1.184	−0.367	−3.724	0.000
Gavazzoni et. al, 2017	−0.628	0.196	0.038	−1.013	−0.244	−3.203	0.001
Huang et. al, 2012	−0.516	0.123	0.015	−0.756	−0.275	−4.204	0.000
Soran et. al, 2018	−0.773	0.211	0.045	−1.187	−0.360	−3.662	0.000
Meta analysis	−0.675	0.163	0.026	−0.994	−0.357	−4.153	0.000

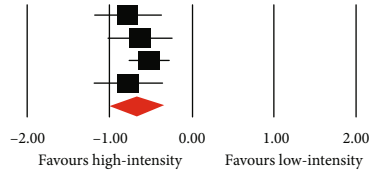

(b)

Figure 2: (a) Forest plot displaying standardized mean difference and 95% confidence intervals for the impact of high-intensity statin treatments on circulating concentrations of oxidized LDL. (b) Leave-one-out sensitivity analyses for the impact of high-intensity statin treatment on circulating concentrations of oxidized LDL.

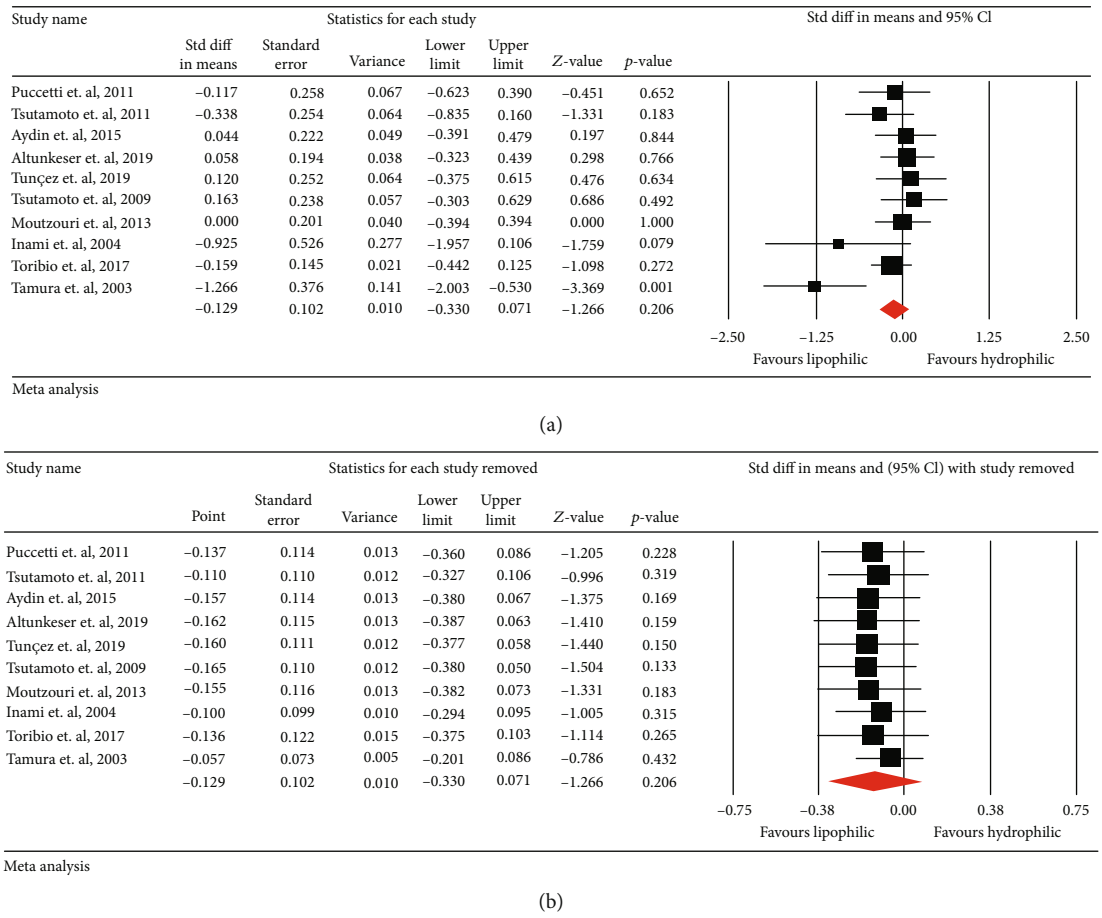

Figure 3: (a) Forest plot displaying standardized mean difference and 95% confidence intervals for the impact of lipophilic statin treatments on oxidized LDL. (b) Leave-one-out sensitivity analyses for the impact of lipophilic statin treatments on circulating concentrations of oxidized LDL.

ox-LDL and delta LDL (slope: 0.024; 95% CI: 0.017, 0.030; $p < 0.001$) (Figure 5).

3.3.2. Publication Bias. Considering the inclusion of 10 RCTs in the meta-analysis of statin lipophilicity, publication bias was assessed using funnel plot. The funnel plot on the association between statin lipophilicity and plasma ox-LDL levels is shown in Figure 6. Although the funnel plot was asymmetric on visual inspection, the "trim and fill" method did not suggest any potentially missing study indicative of publication bias. Moreover, Egger's linear regression test (intercept = −2.38, standard error = 1.28; 95%CI = −5.35, −0.57, $t = 1.85$, df = 8, two-tailed $p = 0.1$) and Begg's rank correlation test (Kendall's Tau with continuity correction = −0.31, $z = 1.25$, two-tailed p value = 0.21) did not suggest any publication bias.

4. Discussion

Findings of this meta-analysis indicate that high-intensity statin treatment is associated with a significant decrease in circulating concentrations of ox-LDL when compared with low-to-moderate treatment. There were no differences concerning ox-LDL concentrations between treatments with hydrophilic and lipophilic statins, but there was a significant reduction in circulating concentrations of ox-LDL associated with statin plus ezetimibe combination therapy when compared with statin monotherapy. We also explored the association between magnitudes of changes in plasma ox-LDL and LDL-C levels in the studies included in meta-analysis using random effects metaregression. Overall, a significant association was found between alterations in plasma ox-LDL and LDL-C concentrations. Delayed clearance of LDL in hypercholesterolemic people increases the likelihood for circulating LDL to be changed, contributing to the onset and progression of atherosclerosis [55].

ox-LDL is implicated on the pathophysiology of atherosclerosis, and there is evidence that its plasma levels are associated with the risk of ASCVD events [56]. Indeed, plasma ox-LDL correlates positively with LDL-cholesterol concentrations [57]. Therefore, it is reasonable to infer that reduction in the latter would affect plasma ox-LDL. Some studies had shown that statin treatment decreases ox-LDL levels [58–60]. However, to the best of our knowledge, so far no meta-analysis has been published showing whether there are any differences between high-intensity statin treatment and low-to-moderate treatment on ox-LDL levels. In an early study when normolipemic patients were treated

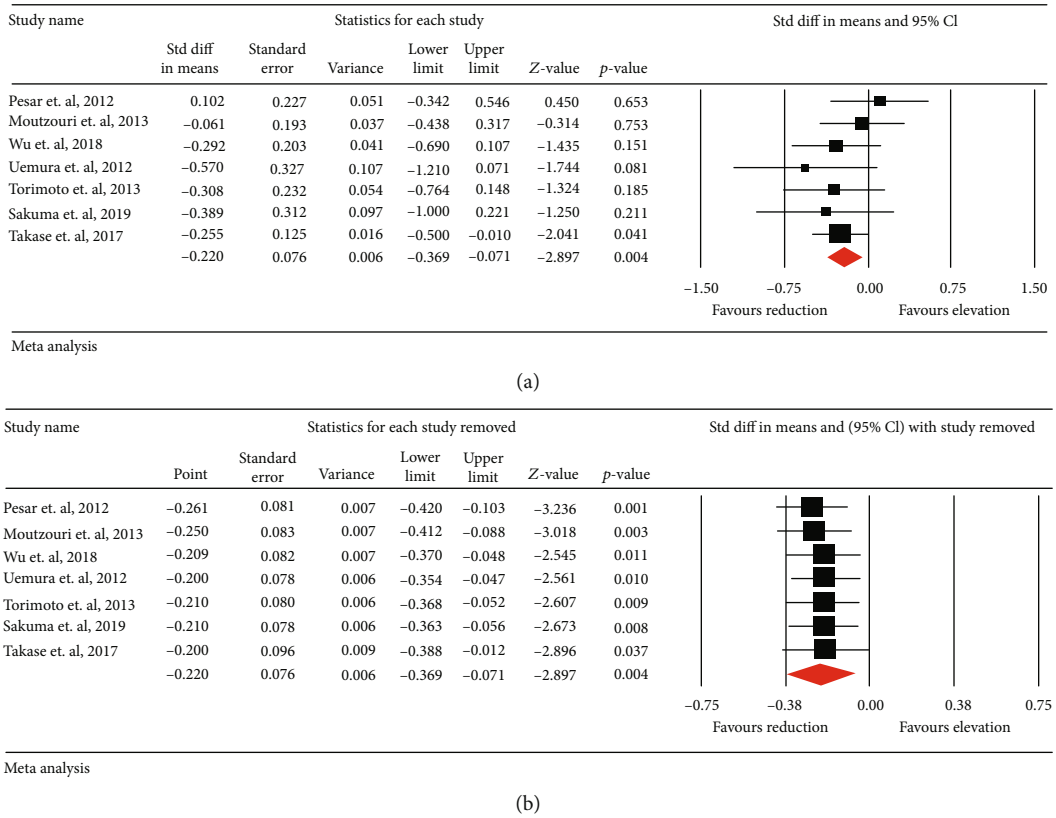

Figure 4: (a) Forest plot displaying standardized mean difference and 95% confidence intervals for the impact of statin/ezetimibe combinational therapy vs statin monotherapy on oxidized LDL. (b) Leave-one-out sensitivity analyses for the impact of statin/ezetimibe combinational therapy vs statin monotherapy on circulating concentrations of oxidized LDL.

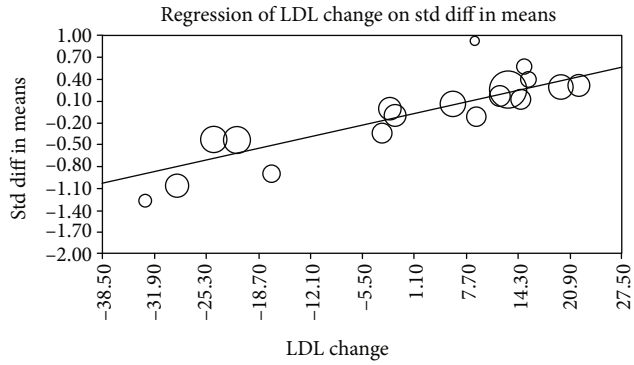

Figure 5: Random effects metaregression for assessing the effect of delta LDL.

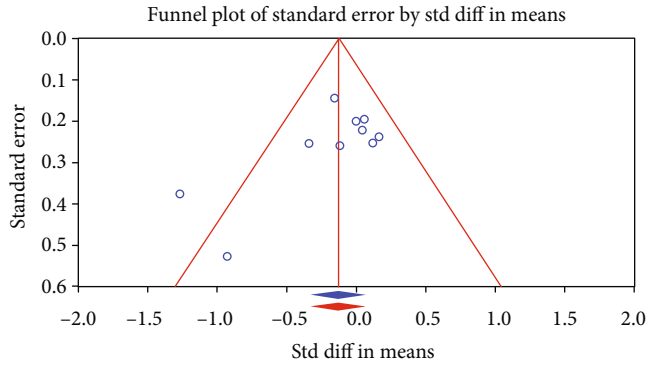

Figure 6: Funnel plot detailing publication bias in the studies reporting the impact of statin lipophilicity on circulating concentrations of oxidized LDL.

with a high dose of atorvastatin, this resulted in a decrease of autoantibodies against ox-LDL [61]. More recently, it has been shown that high-dose atorvastatin and rosuvastatin caused similar decreases in ox-LDL levels [42]. Nevertheless, it has to be mentioned that in a small study on hemodialysis patients on a low dose of a less potent statin (simvastatin 20 mg/day), a significant decrease of ox-LDL also occurred, but in this study, the result was not compared with a higher dose of a more potent statin [62]. The results of this meta-analysis indicate that high-intensity statin treatment is associated with a significant decrease in circulating concentrations of ox-LDL when compared with low-to-moderate treatment may be of clinical importance. Indeed, there is indisputable evidence that high-intensity statin therapy not only further reduces LDL-cholesterol but also prevents more ASCVD events in comparison with low-dose statins [63]. It is conceivable that greater reductions in ox-LDL may could have contributed to that.

There is evidence suggesting that statin solubility could have played a role in the reduction in ASCVD events in

patients with diabetes or those undergoing chronic dialysis [64, 65]. However, studies did not present the results of the effects of lipophilic and hydrophilic statins on ox-LDL. Previous studies suggested that there were no differences concerning ox-LDL concentrations between treatments with lipophilic and hydrophilic statins. Our meta-analysis confirms and expands these previous findings. Indeed, benefits of statin therapy on ASCVD are in theory related to their potency in reducing plasma LDL-cholesterol rather than aspects pertaining to statin solubility in water or lipids [63].

One important finding of this meta-analysis was that the combination of statin with ezetimibe was associated with greater reductions in circulating concentrations of ox-LDL when compared with statin monotherapy. It has been shown in the IMPROVE-IT study that a combination of simvastatin a statin plus ezetimibe decreased the risk of ACVD events better in comparison with simvastatin monotherapy. In that study, the benefit was proportional to LDL-cholesterol reduction [66]. However, no meta-analysis has been performed to ascertain whether such a combination therapy could have a beneficial effect on ox-LDL [65–67]. Considering the role that ox-LDL plays in atherogenesis, the findings of this study are intuitively in agreement with those of IMPROVE-IT; however, similar to high-dose statin if further ox-LDL lowering prevents ASCVD events needs to be proven.

Despite including apparently the most adequate studies in the literature with a low risk of bias and the homogeneity of study results, this meta-analysis has some limitations: (1) the meta-analysis of data on the effects of statin intensity on circulating concentrations of ox-LDL included only four trials with 381 patients and therefore these results should be interpreted with caution; (2) although in most of the included studies serum ox-LDL was measured using enzyme-linked immunosorbent assay (ELISA) method, in some studies, other assays/-kits were used; and (3) individual rather than study level data would have provided more robust results.

5. Conclusions

Based on the results of this meta-analysis, it could be concluded that high-intensity statin treatment is associated with a significant decrease in circulating concentrations of ox-LDL when compared with low-to-moderate statin treatment. There was no difference concerning ox-LDL concentration between treatments with hydrophilic and lipophilic statins, but there was a significant reduction in circulating concentrations of ox-LDL associated with statin plus ezetimibe combination therapy when compared with statin monotherapy. These findings should have mechanistic implications to explain the additional benefits of high-intensity and statin ezetimibe combination in comparison with low-to-moderate-statin therapy alone when prevention of ASCVD events is concerned.

Data Availability

There is no primary raw data associated with this review article.

Conflicts of Interest

RDS has received honoraria related to speaker activities, consulting, or research from Abbott, Aché, Astra Zeneca, Amgen, EMS, Esperion, Getz Pharma, Kowa, Merck SA, MSD, Novo Nordisk, Novartis, Pfizer, PTC Therapeutics, and Sanofi. Other authors have no competing interests to disclose.

Authors' Contributions

Fatemeh Baratzadeh and Željko Reiner contributed equally to this work and as the first author.

References

[1] European Association for Cardiovascular Prevention & Rehabilitation, Z. Reiner, A. L. Catapano et al., "ESC/EAS guidelines for the management of dyslipidaemias: the task force for the management of dyslipidaemias of the European Society of Cardiology (ESC) and the European Atherosclerosis Society (EAS)," *European heart journal*, vol. 32, no. 14, pp. 1769–1818, 2011.

[2] I. Graham, M.-T. Cooney, D. Bradley, A. Dudina, and Z. Reiner, "Dyslipidemias in the prevention of cardiovascular disease: risks and causality," *Current cardiology reports*, vol. 14, no. 6, pp. 709–720, 2012.

[3] Ž. Reiner, "Statins in the primary prevention of cardiovascular disease," *Nature Reviews Cardiology*, vol. 10, no. 8, pp. 453–464, 2013.

[4] Ž. Reiner, G. de Backer, Z. Fras et al., "Lipid lowering drug therapy in patients with coronary heart disease from 24 European countries - Findings from the EUROASPIRE IV survey," *Atherosclerosis*, vol. 246, pp. 243–250, 2016.

[5] G. Ferretti, T. Bacchetti, and A. Sahebkar, "Effect of statin therapy on paraoxonase-1 status: A systematic review and meta-analysis of 25 clinical trials," *Progress in Lipid Research*, vol. 20, pp. 50–73, 2015.

[6] C. Serban, A. Sahebkar, S. Ursoniu et al., "A systematic review and meta-analysis of the effect of statins on plasma asymmetric dimethylarginine concentrations," *Scientific Reports*, vol. 5, no. 1, 2015.

[7] A. Sahebkar, C. Serban, D. P. Mikhailidis et al., "Association between statin use and plasma d-dimer levels: A systematic review and meta-analysis of randomised controlled trials," *Thrombosis and Haemostasis*, vol. 114, no. 3, pp. 546–557, 2015.

[8] A. Sahebkar, C. Serban, S. Ursoniu et al., "The impact of statin therapy on plasma levels of von Willebrand factor antigen: Systematic review and meta-analysis of Randomised placebo-controlled trials," *Thrombosis and Haemostasis*, vol. 115, no. 3, pp. 520–532, 2016.

[9] A. Bahrami, N. Parsamanesh, S. L. Atkin, M. Banach, and A. Sahebkar, "Effect of statins on toll-like receptors: a new insight to pleiotropic effects," *Pharmacological Research*, vol. 135, pp. 230–238, 2018.

[10] H. Mollazadeh, E. Tavana, G. Fanni et al., "Effects of statins on mitochondrial pathways," *Journal of Cachexia, Sarcopenia and Muscle*, vol. 12, no. 2, pp. 237–251, 2021.

[11] F. Mach, C. Baigent, A. L. Catapano et al., "2019 ESC/EAS guidelines for the management of dyslipidaemias: lipid

modification to reduce cardiovascular risk," *European heart journal*, vol. 41, no. 1, pp. 111–188, 2020.

[12] S. M. Grundy, N. J. Stone, and for the Guideline Writing Committee for the 2018 Cholesterol Guidelines, "2018 cholesterol clinical practice guidelines: synopsis of the 2018 American Heart Association/American College of Cardiology/multisociety cholesterol guideline," *Annals of internal medicine*, vol. 170, no. 11, pp. 779–783, 2019.

[13] J. Ha, B. Lee, J. M. Park et al., "Escalation of liPid-lOwering therapy in patientS wiTh vascular disease receiving HIGH-intensity statins: the retrospective POST-HIGH study," *Scientific Reports*, vol. 11, no. 1, article 88416, pp. 8884–8888, 2021.

[14] F. Schiele, N. Quignot, A. Khachatryan et al., "Clinical impact and room for improvement of intensity and adherence to lipid lowering therapy: Five years of clinical follow-up from 164,565 post- myocardial infarction patients," *International Journal of Cardiology*, vol. 332, pp. 22–28, 2021.

[15] E. Desjobert, V. Tea, F. Schiele et al., "Évolution clinique avec des statines de forte intensite selon le risque atherothrombotique apres un infarctus du myocarde (a partir des registres FAST-MI)," *Archives of Cardiovascular Diseases*, vol. 114, no. 2, pp. 88–95, 2021.

[16] G. de Backer, P. Jankowski, K. Kotseva et al., "Management of dyslipidaemia in patients with coronary heart disease: results from the ESC-EORP EUROASPIRE V survey in 27 countries," *Atherosclerosis*, vol. 285, pp. 135–146, 2019.

[17] M. Schachter, "Chemical, pharmacokinetic and pharmacodynamic properties of statins: an update," *Fundamental & clinical pharmacology*, vol. 19, no. 1, pp. 117–125, 2005.

[18] C. Murphy, E. Deplazes, C. G. Cranfield, and A. Garcia, "The role of structure and biophysical properties in the pleiotropic effects of statins," *International journal of molecular sciences*, vol. 21, no. 22, p. 8745, 2020.

[19] C. W. Fong, "Statins in therapy: understanding their hydrophilicity, lipophilicity, binding to 3-hydroxy-3-methylglutaryl-CoA reductase, ability to cross the blood brain barrier and metabolic stability based on electrostatic molecular orbital studies," *European journal of medicinal chemistry*, vol. 85, pp. 661–674, 2014.

[20] I. Simic and Z. Reiner, "Adverse effects of Statins - Myths and reality," *Current pharmaceutical design*, vol. 21, no. 9, pp. 1220–1226, 2015.

[21] R. Wu and A. Lefvert, "Autoantibodies against oxidized low density lipoproteins (oxLDL): characterization of antibody isotype, subclass, affinity and effect on the macrophage uptake of oxLDL," *Clinical & Experimental Immunology*, vol. 102, no. 1, pp. 174–180, 1995.

[22] K. Nishi, H. Itabe, M. Uno et al., "Oxidized LDL in carotid plaques and plasma associates with plaque instability," *Arteriosclerosis, thrombosis, and vascular biology*, vol. 22, no. 10, pp. 1649–1654, 2002.

[23] D. Steinberg and J. L. Witztum, "Is the oxidative modification hypothesis relevant to human atherosclerosis? Do the antioxidant trials conducted to date refute the hypothesis?," *Circulation*, vol. 105, no. 17, pp. 2107–2111, 2002.

[24] J. Borén, M. J. Chapman, R. M. Krauss et al., "Low-density lipoproteins cause atherosclerotic cardiovascular disease: pathophysiological, genetic, and therapeutic insights: a consensus statement from the European Atherosclerosis Society Consensus Panel," *European heart journal*, vol. 41, no. 24, pp. 2313–2330, 2020.

[25] C. Chen and D. B. Khismatullin, "Oxidized low-density lipoprotein contributes to atherogenesis via co-activation of macrophages and mast cells," *PLoS One*, vol. 10, no. 3, article e0123088, 2015.

[26] J. Qin, L. L. Wang, Z. Y. Liu, Y. L. Zou, Y. J. Fei, and Z. X. Liu, "Ezetimibe protects endothelial cells against oxidative stress through Akt/GSK-3β pathway," *Current medical science*, vol. 38, no. 3, pp. 398–404, 2018.

[27] C. Tie, K. Gao, N. Zhang et al., "Ezetimibe attenuates atherosclerosis associated with lipid reduction and inflammation inhibition," *PLoS One*, vol. 10, no. 11, article e0142430, 2015.

[28] J. P. T. G. S. Higgins, *Handbook for Systematic Reviews of Interventions. Version 5.0.2 ed*, The Cochrane Collaboration, London, 2009.

[29] L. J. van Tits, T. M. van Himbergen, H. L. Lemmers, J. de Graaf, and A. F. Stalenhoef, "Proportion of oxidized LDL relative to plasma apolipoprotein B does not change during statin therapy in patients with heterozygous familial hypercholesterolemia," *Atherosclerosis*, vol. 185, no. 2, pp. 307–312, 2006.

[30] E. Moutzouri, E. N. Liberopoulos, C. C. Tellis, H. J. Milionis, A. D. Tselepis, and M. S. Elisaf, "Comparison of the effect of simvastatin versus simvastatin/ezetimibe versus rosuvastatin on markers of inflammation and oxidative stress in subjects with hypercholesterolemia," *Atherosclerosis*, vol. 231, no. 1, pp. 8–14, 2013.

[31] H. Soran, Y. Liu, S. Adam et al., "A comparison of the effects of low- and high-dose atorvastatin on lipoprotein metabolism and inflammatory cytokines in type 2 diabetes: results from the Protection Against Nephropathy in Diabetes with Atorvastatin (PANDA) randomized trial," *Journal of Clinical Lipidology*, vol. 12, no. 1, pp. 44–55, 2018.

[32] M. Toribio, K. V. Fitch, L. Sanchez et al., "Effects of pitavastatin and pravastatin on markers of immune activation and arterial inflammation in HIV," *AIDS*, vol. 31, no. 6, pp. 797–806, 2017.

[33] A. E. P. Pesaro, C. V. Serrano, J. L. Fernandes et al., "Pleiotropic effects of ezetimibe/simvastatin vs. high dose simvastatin," *International Journal of Cardiology*, vol. 158, no. 3, pp. 400–404, 2012.

[34] A. Tamura, T. Watanabe, and M. Nasu, "Effects of atorvastatin and pravastatin on malondialdehyde-modified LDL in hypercholesterolemic patients," *Circulation Journal*, vol. 67, no. 10, pp. 816–820, 2003.

[35] Y. Uemura, M. Watarai, H. Ishii et al., "Atorvastatin 10 mg plus ezetimibe 10 mg compared with atorvastatin 20 mg: Impact on the lipid profile in Japanese patients with abnormal glucose tolerance and coronary artery disease," *Journal of Cardiology*, vol. 59, no. 1, pp. 50–56, 2012.

[36] M. Gavazzoni, E. Gorga, G. Derosa, P. Maffioli, M. Metra, and R. Raddino, "High-dose atorvastatin versus moderate dose on early vascular protection after ST-elevation myocardial infarction," *Drug Design, Development and Therapy*, vol. 11, pp. 3425–3434, 2017.

[37] M. U. Aydin, N. Aygul, B. B. Altunkeser, A. Unlu, and A. Taner, "Comparative effects of high-dose atorvastatin versus moderate-dose rosuvastatin on lipid parameters, oxidized-LDL and inflammatory markers in ST elevation myocardial infarction," *Atherosclerosis*, vol. 239, no. 2, pp. 439–443, 2015.

[38] T. Tsutamoto, H. Sakai, K. Ibe et al., "Effect of atorvastatin vs. rosuvastatin on cardiac sympathetic nerve activity in non-

diabetic patients with dilated cardiomyopathy," *Circulation Journal*, vol. 75, no. 9, pp. 2160–2166, 2011.

[39] T. Tsutamoto, M. Yamaji, C. Kawahara et al., "Effect of simvastatin vs. rosuvastatin on adiponectin and haemoglobin A1c levels in patients with non-ischaemic chronic heart failure," *European Journal of Heart Failure*, vol. 11, no. 12, pp. 1195–1201, 2009.

[40] S. Inami, K. Okamatsu, M. Takano et al., "Effects of statins on circulating oxidized low-density lipoprotein in patients with hypercholesterolemia," *Japanese Heart Journal*, vol. 45, no. 6, pp. 969–975, 2004.

[41] K. Torimoto, Y. Okada, H. Mori et al., "Efficacy of combination of ezetimibe 10 mg and rosuvastatin 2.5 mg versus rosuvastatin 5 mg monotherapy for hypercholesterolemia in patients with type 2 diabetes," *Lipids in Health and Disease*, vol. 12, no. 1, p. 137, 2013.

[42] B. B. Altunkeser, A. Tuncez, B. Ozturk et al., "Comparative effects of high-dose atorvastatin versus rosuvastatin on lipid parameters, oxidized low-density lipoprotein, and proprotein convertase subtilisin kexin 9 in acute coronary syndrome," *Coronary Artery Disease*, vol. 30, no. 4, pp. 285–290, 2019.

[43] A. Tunçez, B. B. Altunkeser, B. Öztürk et al., "Comparative effects of atorvastatin 80 mg and rosuvastatin 40 mg on the levels of serum endocan, chemerin, and galectin-3 in patients with acute myocardial infarction," *Anatolian Journal of Cardiology*, vol. 22, no. 5, pp. 240–249, 2019.

[44] B. Huang, Y. Cheng, Q. Xie et al., "Effect of 40 mg versus 10 mg of atorvastatin on oxidized low-density lipoprotein, high-sensitivity C-reactive protein, circulating endothelial-derived microparticles, and endothelial progenitor cells in patients with ischemic cardiomyopathy," *Clinical cardiology*, vol. 35, no. 2, pp. 125–130, 2012.

[45] L. Puccetti, F. Santilli, A. L. Pasqui et al., "Effects of atorvastatin and rosuvastatin on thromboxane-dependent platelet activation and oxidative stress in hypercholesterolemia," *Atherosclerosis*, vol. 214, no. 1, pp. 122–128, 2011.

[46] N. Q. Wu, Y. L. Guo, C. G. Zhu et al., "Comparison of statin plus ezetimibe with double-dose statin on lipid profiles and inflammation markers," *Lipids in Health and Disease*, vol. 17, no. 1, p. 265, 2018.

[47] M. Sakuma, S. Toyoda, R. Hashimoto et al., "Add-on ezetimibe treatment to low-dose statins vs medium-intensity statin monotherapy in coronary artery disease patients with poorly controlled dyslipidemia," *Hypertension Research*, vol. 42, no. 12, pp. 1923–1931, 2019.

[48] S. Takase, T. Matoba, S. Nakashiro et al., "Ezetimibe in combination with statins ameliorates endothelial dysfunction in coronary arteries after Stenting," *Arteriosclerosis, Thrombosis, and Vascular Biology*, vol. 37, no. 2, pp. 350–358, 2017.

[49] M. Borenstein, L. Hedges, J. Higgins, and H. Rothstein, *Comprehensive meta-analysis, version 2 biostat*, Englewood NJ, 2005.

[50] A. J. Sutton, K. R. Abrams, D. R. Jones, D. R. Jones, T. A. Sheldon, and F. Song, *Methods for meta-Analysis in Medical Research*, Wiley Chichester, 2000.

[51] S. P. Hozo, B. Djulbegovic, and I. Hozo, "Estimating the mean and variance from the median, range, and the size of a sample," *BMC medical research methodology*, vol. 5, no. 1, pp. 1–10, 2005.

[52] Lipid and Blood Pressure Meta-analysis Collaboration (LBPMC) Group, M. Banach, C. Serban et al., "Impact of statin therapy on coronary plaque composition: a systematic review and meta-analysis of virtual histology intravascular ultrasound studies," *BMC medicine*, vol. 13, no. 1, pp. 1–21, 2015.

[53] M. Banach, C. Serban, S. Ursoniu et al., "Statin therapy and plasma coenzyme Q10 concentrations–A systematic review and meta-analysis of placebo-controlled trials," *Pharmacological Research*, vol. 99, pp. 329–336, 2015.

[54] S. Duval and R. Tweedie, "Trim and fill: a simple funnel-plot–based method of testing and adjusting for publication bias in meta-analysis," *Biometrics*, vol. 56, no. 2, pp. 455–463, 2000.

[55] D. Steinberg and J. L. Witztum, "Oxidized low-density lipoprotein and atherosclerosis," *Arteriosclerosis, thrombosis, and vascular biology*, vol. 30, no. 12, pp. 2311–2316, 2010.

[56] S. Gao, D. Zhao, M. Wang et al., "Association between circulating oxidized LDL and atherosclerotic cardiovascular disease: a meta-analysis of observational studies," *Canadian Journal of Cardiology*, vol. 33, no. 12, pp. 1624–1632, 2017.

[57] N.-W. Tsai, L.-H. Lee, C.-R. Huang et al., "Statin therapy reduces oxidized low density lipoprotein level, a risk factor for stroke outcome," *Critical Care*, vol. 18, no. 1, pp. R16–R18, 2014.

[58] T. Janatuinen, J. Knuuti, J. O. Toikka et al., "Effect of pravastatin on low-density lipoprotein oxidation and myocardial perfusion in young adults with type 1 diabetes," *Arteriosclerosis, Thrombosis, and Vascular Biology*, vol. 24, no. 7, pp. 1303–1308, 2004.

[59] J. Rodenburg, M. N. Vissers, A. Wiegman et al., "Oxidized low-density lipoprotein in children with familial hypercholesterolemia and unaffected siblings: effect of pravastatin," *Journal of the American College of Cardiology*, vol. 47, no. 9, pp. 1803–1810, 2006.

[60] E. Nou, M. T. Lu, S. E. Looby et al., "Serum oxidized low-density lipoprotein decreases in response to statin therapy and relates independently to reductions in coronary plaque in patients with HIV," *AIDS*, vol. 30, no. 4, pp. 583–590, 2016.

[61] A. M. Kuklinska, B. Mroczko, W. J. Musial et al., "Influence of atorvastatin on blood pressure control in treated hypertensive, normolipemic patients - an open, pilot study," *Blood pressure*, vol. 19, no. 4, pp. 260–266, 2010.

[62] A. M. Abdel Magid, M. M. Abbassi, E. E. M. Iskander, O. Mohamady, and S. F. Farid, "Randomized comparative efficacy and safety study of intermittent simvastatin versus fenofibrate in hemodialysis," *Journal of comparative effectiveness research*, vol. 6, no. 5, pp. 413–424, 2017.

[63] Cholesterol Treatment Trialists' (CTT) Collaboration, C. Baigent, L. Blackwell et al., "Efficacy and safety of more intensive lowering of LDL cholesterol: a meta- analysis of data from 170 000 participants in 26 randomised trials," *Lancet*, vol. 376, no. 9753, pp. 1670–1681, 2010.

[64] S. W. Wang, L. C. Li, C. H. Su, Y. H. Yang, T. W. Hsu, and C. N. Hsu, "Association of statin and its lipophilicity with cardiovascular events in patients receiving chronic dialysis," *Clinical pharmacology and therapeutics*, vol. 107, no. 6, pp. 1312–1324, 2020.

[65] S. Y. Li, H. H. Chen, C. L. Lin, S. Y. Yeh, and C. H. Kao, "The different cardiovascular outcomes between long-term efficacy of hydrophilic and lipophilic statin therapy in both Asian diabetic sexes," *Dose-response : a publication of International Hormesis Society*, vol. 17, no. 3, 2019.

[66] C. P. Cannon, M. A. Blazing, R. P. Giugliano et al., "Ezetimibe added to statin therapy after acute coronary syndromes," *The*

New England journal of medicine, vol. 372, no. 25, pp. 2387–2397, 2015.

[67] J. Lee, U. Egolum, H. Parihar, M. Cooley, and H. Ling, "Effect of ezetimibe added to high-intensity statin therapy on low-density lipoprotein cholesterol levels: a meta-analysis," *Cardiology research*, vol. 12, no. 2, pp. 98–108, 2021.

Hindawi
Mediators of Inflammation
Volume 2021, Article ID 7712587, 12 pages
https://doi.org/10.1155/2021/7712587

Review Article

The Biological Disease-Modifying Antirheumatic Drugs and the Risk of Cardiovascular Events: A Systematic Review and Meta-Analysis

Suiyuan Hu,[1] Chu Lin,[1] Xiaoling Cai,[1] Xingyun Zhu,[1] Fang Lv,[1] Lin Nie,[2] and Linong Ji[1]

[1]*Department of Endocrinology and Metabolism, Peking University People's Hospital, Beijing, China*
[2]*Department of Endocrinology and Metabolism, Beijing Airport Hospital, Beijing, China*

Correspondence should be addressed to Xiaoling Cai; dr_junel@sina.com and Linong Ji; prof_jilinong@aliyun.com

Received 6 July 2021; Accepted 18 August 2021; Published 31 August 2021

Academic Editor: Dominik Skiba

Objective. To assess the association between the use of biological disease-modifying antirheumatic drugs (bDMARDs) and the risk of cardiovascular events in patients with systemic inflammatory conditions. *Methods*. Eligible cohort studies or randomized controlled trials (RCTs) from inception to January 2021 were included. Pooled odds ratios (ORs) with 95% confidence intervals (CIs) for cardiovascular outcomes were calculated in the fixed- and random-effects model accordingly. Associated factors with risks of cardiovascular events were also studied in sensitivity analyses and metaregression analyses. *Results*. Compared with non-bDMARD users, the risks of myocardial infarction (MI) (OR = 0.74, 95% CI, 0.63 to 0.87), heart failure (OR = 0.84, 95% CI, 0.74 to 0.95), cardiovascular (CV) death (OR = 0.62, 95% CI, 0.40 to 0.95), all-cause mortality (OR = 0.64, 95% CI, 0.58 to 0.70), and 3P-MACE (composite endpoint of MI, stroke, and CV death) (OR = 0.69, 95% CI, 0.53 to 0.89) were significantly reduced in bDMARD users, which were mainly driven by the risk reduction in patients with rheumatoid arthritis (RA). TNF-α inhibitors exhibited consistent benefits in reducing the risks of MI, heart failure, CV death, all-cause mortality, and 3P-MACE. Moreover, the risks of heart failure, CV death, all-cause mortality, and 3P-MACE were significantly reduced in bDMARD users with follow-up over one year. *Conclusions*. The use of bDMARDs might be associated with the reduced risks of CV events, especially in patients with RA. The CV events might be less frequent in bDMARD users with TNF-α inhibitors or follow-up over one year. More investigations are needed to validate conclusions.

1. Introduction

Cardiovascular disease (CVD) is the leading cause of death worldwide [1]. With accumulated evidence [2–5], the presence of chronic inflammation was proposed to play an important role in cardiovascular (CV) risk. It was suggested that inflammation might modify traditional CV risk factors such as lipids [2], which were involved in the pathogenesis of atherosclerosis [3], promoting endothelial dysfunction and microvascular disease [4, 5]. Therefore, this spurred researchers to seek therapeutics that target inflammation to reduce CV events. Inspiringly, encouraging results from the recent anti-inflammatory trials in population with CVD, such as CANTOS [6] and LoDoCo2 [7], indicated that anti-inflammatory treatments might provide CV protective effects.

Meanwhile, several systemic inflammatory diseases have been found to be associated with excess CV risk. It was revealed that cardiovascular disease accounted for the largest proportion of excess mortality in rheumatoid arthritis (RA) [8]. What is more, individuals with systemic lupus erythematosus (SLE) were observed to have increased incidence of ischemic stroke or myocardial infarction (MI) [9], which were also found in patients with psoriasis and other inflammatory diseases [10]. It is putative that the excess CV risk in many inflammatory diseases might be mediated through the persistent inflammation and oxidative stress [11].

As a fundamental therapy for systemic inflammatory diseases, anti-inflammatory agents were commonly used, among which biological disease-modifying antirheumatic drugs (bDMARDs) developed rapidly and were gradually applied in clinical management in the past two decades, for their potent anti-inflammatory effects and specific targets. Besides the prompt and sustained efficacy in disease remission and the safety of bDMARDs in systemic inflammatory conditions [12–14], cardioprotective effects were found in tumor necrosis factor-α (TNF-α) inhibitor treatment [15–18] in patients with RA and psoriasis and were also suggested in certain biological agents, such as tocilizumab and rituximab [19–21]. Meanwhile, some agents like adalimumab and ustekinumab might be associated with the increased risk of cardiovascular events [18, 22–24] Therefore, the cardiovascular effects of bDMARDs have yet to be definitive.

In order to reveal the association between the use of bDMARDs and the risks of cardiovascular events in patients with systemic inflammatory conditions, we designed and performed a systematic review and meta-analysis, with the aim to evaluate whether treatments with bDMARDs would reduce the risk of cardiovascular events in patients with systemic inflammatory conditions.

2. Methods

2.1. Study Design and Electronic Literature Search Strategy. According to the recommendations from the Cochrane Handbook for Systematic Reviews for meta-analysis, we conducted systematic searches in PubMed, Medline, Embase, the Cochrane Central Register of Controlled Trials, and Clinicaltrial.gov for studies of bDMARD published from inception to January 2021. The search strategies included the following search terms: bDMARD, biological therapy, biological agent, RA, SLE, psoriasis, cardiovascular risk, cardiovascular event, cardiovascular disease, TNF-α inhibitor, infliximab, etanercept, adalimumab, certolizumab, golimumab, IL (receptor) inhibitor, anakinra, tocilizumab, CD17 inhibitor, secukinumab, brodalumab, ixekizumab, CD23 inhibitor, risankizumab, tildrakizumab, guselkumab, CD22 inhibitor, epratuzumab, CD12/23inhibitor, briakinumab, ustekinumab, CD20 antibody, CD20 inhibition, rituximab, belimumab, blisibimod, atacicept, tabalumab, sifalimumab, CD80/86 inhibition, abatacept, interferon receptor antibody, anifrolumab, observational study, cohort study, and RCT. We also screened reference lists of relevant articles in order not to miss any possibly eligible study.

2.2. Selection of Articles, Data Extraction, and Quality Assessment. The inclusion criteria for the meta-analysis were as follows: (1) cohort studies or randomized controlled trials (RCTs) with presented outcomes of cardiovascular events between bDMARD users and non-bDMARD users; (2) studies conducted in systemic inflammatory conditions including RA, SLE, and psoriasis. The exclusion criteria were as follows: (1) studies without presented outcomes of cardiovascular events; (2) studies with bDMARDs in both treatment arms; (3) studies with participants less than 18 years old. Two investigators (SH and CL) performed the study selection independently. A third investigator (FL) reexamined the selected results. Every disagreement would be pointed out and resolved by a joint discussion until a consensus was reached.

Study data was abstracted from eligible RCTs and cohorts by two investigators (SH and CL), including first author, publication year, study design, numbers of participants, age, disease duration, drug exposure, history of CVD, incidence of cardiovascular events, and any available efficacy endpoint reported in the studies. If data on cardiovascular events could not be accessed in both original articles and supplementary materials, the investigators would search from Clinicaltrial.gov website with the unique registered NCT number. Qualities of the observational studies were evaluated by using the Newcastle-Ottawa Scale, and qualities of RCTs were evaluated by using the Cochrane risk of bias tool. A third investigator (FL) confirmed the accuracy of the abstractions and study quality evaluation. Any disagreement would be resolved by a joint discussion until a consensus was reached.

2.3. Definition of Clinical Outcomes. In this meta-analysis, we set up two composite CV endpoints, which consisted of a three-point major adverse cardiovascular event (3P-MACE, including myocardial infarction (MI), stroke, and CV death) and a four-point major adverse cardiovascular event (4P-MACE, including 3P-MACE and heart failure). In addition, we separately analyzed MI, stroke, CV death, heart failure, and all-cause mortality as individual CV outcomes.

2.4. Statistical Analysis. Results of the meta-analysis were presented by the odds ratio (OR) along with the 95% confidence interval (CI). Higgins I^2 statistics were used to evaluate the heterogeneity between different studies, when an I^2 value > 50% indicates a high level of heterogeneity. A fixed-effects model was used for low level of heterogeneity, and a random-effects model was used for high level of heterogeneity. Metaregression analyses were performed to evaluate whether age, sex, disease duration, concomitant medication, and efficacy endpoints were associated with the risk of cardiovascular events. Statistical analyses were performed by the Review Manager statistical software package (Version 5.3, Nordic Cochrane Center, Copenhagen, Denmark). Metaregression analyses were performed by STATA, version 11.0 (STATA, College Station, TX, USA). All statistical analyses with P value < 0.05 were considered statistically significant.

3. Results

3.1. Characteristics of Included Studies. In all, 72 studies were included (38 studies with RA, 21 studies with psoriasis, and 13 studies with SLE), with 55 RCTs and 17 cohort studies, respectively (Figure 1). The enrolled systemic inflammatory conditions were RA, psoriasis, and SLE. Baseline characteristics of included studies are summarized in Table S1-S2. This

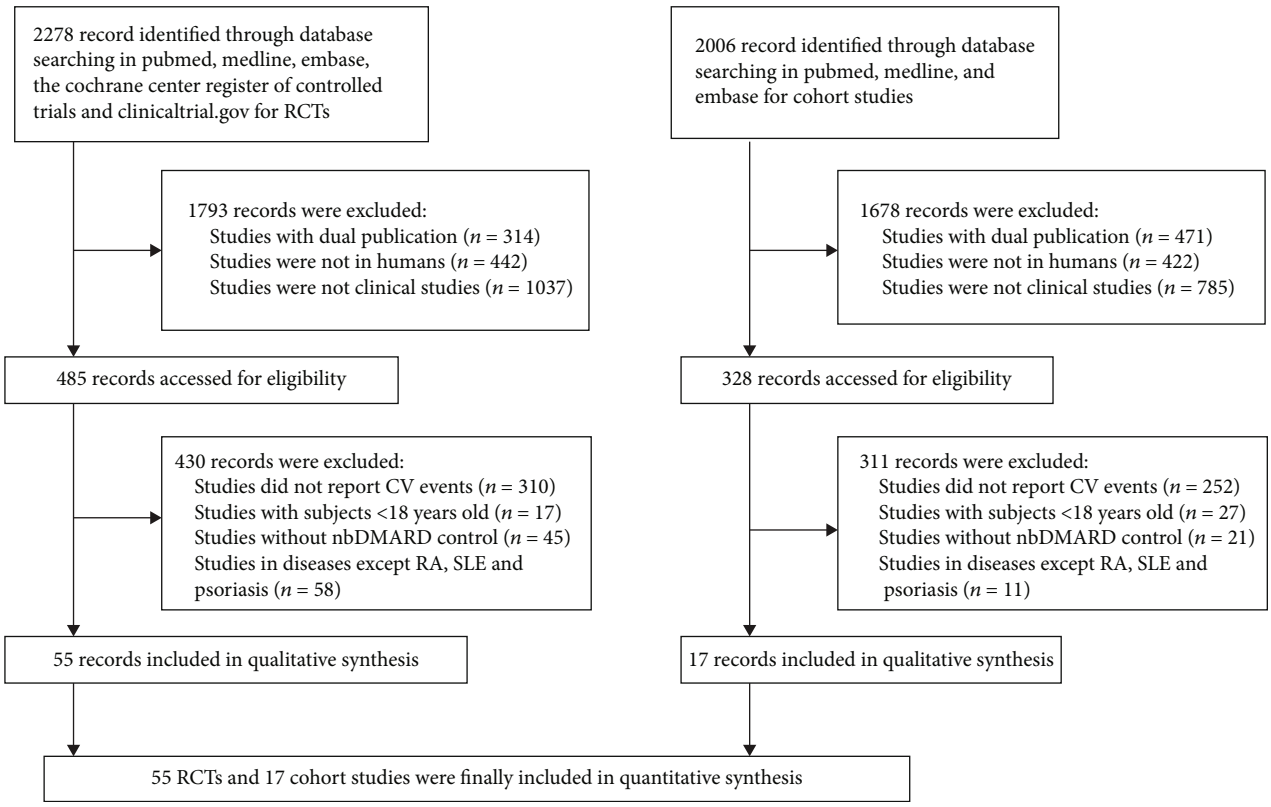

Figure 1: Flowchart of included studies.

meta-analysis was registered in the PROSPERO platform as CRD42020207140.

The risk of bias for RCT was systematically evaluated by the Cochrane tool (Table S3). There were 14 RCTs with unclear risk of selection bias (random sequence generation), 1 RCT with high risk and 7 RCTs with unclear risk of selection bias (allocation concealment), 2 RCTs with high risk and 1 RCT with unclear risk of performance bias, and 19 RCTs with high risk and 2 RCTs with unclear risk of attrition bias. The included cohort studies were of relatively high quality as Newcastle-Ottawa Scale suggested (Table S4). The funnel plots for individual and composite CV endpoints generally displayed even distributions (Figure S1).

3.2. The Association between the Use of bDMARDs and the Risk of CV Events. Overall, compared with non-bDMARDs users, the risks of MI (OR = 0.74, 95% CI, 0.63 to 0.87, I^2 = 0%), heart failure (OR = 0.84, 95% CI, 0.74 to 0.95, I^2 = 21%), CV death (OR = 0.62, 95% CI, 0.40 to 0.95, I^2 = 0%), and all-cause mortality (OR = 0.64, 95% CI, 0.58 to 0.70, I^2 = 38%) were significantly reduced in bDMARD users (Figure 2), which were mainly driven by the results of cohort studies (Tables 1–4).

When stratified by the systemic inflammatory conditions, subgroup analyses showed significant reduction in risks of MI (OR = 0.74, 95% CI, 0.63 to 0.87, I^2 = 31%), heart failure (OR = 0.83, 95% CI, 0.73 to 0.95, I^2 = 41%), CV death (OR = 0.60, 95% CI, 0.38 to 0.96, I^2 = 4%), and all-cause mortality (OR = 0.64, 95% CI, 0.49 to 0.85, I^2 = 63%) in bDMARD users with RA compared with non-bDMARD users (Tables 1–4).

When stratified by different drug categories, it was indicated that when compared with non-bDMARD users, the risks of MI (OR = 0.74, 95% CI, 0.63 to 0.88, I^2 = 27%), heart failure (OR = 0.83, 95% CI, 0.73 to 0.95, I^2 = 43%), CV death (OR = 0.53, 95% CI, 0.33 to 0.86, I^2 = 0%), and all-cause mortality (OR = 0.63, 95% CI, 0.47 to 0.84, I^2 = 66%) were significantly decreased in TNF-α inhibitor users. However, no statistically significant differences of the risks of CV events were found in other subtypes of bDMARDs (Tables 1–4).

When stratified by the follow-up period, compared with non-bDMARD users, the risks of MI (OR = 0.73, 95% CI, 0.61 to 0.87, I^2 = 37), heart failure (OR = 0.80, 95% CI, 0.69 to 0.93, I^2 = 38%), CV death (OR = 0.46, 95% CI, 0.28 to 0.77, I^2 = 0%), and all-cause mortality events (OR = 0.62 , 95% CI, 0.48 to 0.80, I^2 = 42%) were less frequent in bDMARD users with a follow-up period longer than one year. However, such risk reductions were not observed in patients with a follow-up period less than one year (Tables 1–4).

As for history of CVD and its comorbidities, the results showed that risk of MI was mainly reduced in strata with lower percentage of previous CVD, diabetes, and dyslipidemia (Table 1). The risk of all-cause mortality was mainly reduced in strata with lower percentage of previous CVD and dyslipidemia (Table 4).

Study or subgroup	bDMARDs Events	bDMARDs Total	non-bDMARDs Events	non-bDMARDs Total	Weight	Odds ratio M-H, Fixed, 95% CI
Cohort study RA dixon 2007-TNF a inhibitor	63	8659	17	2170	8.1%	0.93 [0.54, 1.59]
Cohort study RA geborek 2002-entanercept	4	166	0	103	0.2%	5.73 [0.31, 107.58]
Cohort study RA greenberg 2010-TNF a vs MTX	4	4684	17	4969	4.9%	0.25 [0.08, 0.74]
Cohort study RA greenberg 2010-TNF a vs nonMTX	4	4684	5	1785	2.2%	0.30 [0.08, 1.13]
Cohort study RA jacobsson 2005-TNF a inhibitor	6	531	33	543	9.7%	0.18 [0.07, 0.43]
Cohort study RA low 2017-TNF a inhibitor	194	11200	58	3058	26.9%	0.91 [0.68, 1.23]
Cohort study RA morgan 2014-entanercept	65	3529	69	2864	22 4%	0.76 [0.54, 1.07]
Cohort study RA solomon 2013-TNF a inhibitor	39	11587	38	8656	13.0%	0.77 [0.49, 1.20]
Ps blauvelt 2015-secu	1	118	0	59	0.2%	1.52 [0.06, 37.86]
Ps blauvelt 2017-ada	1	334	0	174	0.2%	1.57 [0.06, 38.73]
Ps blauvelt 2017-guse	1	329	0	174	0.2%	1.59 [0.06, 39.33]
Ps deodhar 2018-guse	1	100	0	49	0.2%	1.49 [0.06, 37.31]
Ps gordon 2012-briakinumab	3	981	0	484	0.2%	3.47 [0.18, 67.23]
Ps gottlieb 2009-ustek	0	76	1	70	0.5%	0.30 [0.01, 7.56]
Ps griffiths 2015 lxeki	0	771	1	193	0.7%	0.08 [0.00, 2.05]
Ps kavanaugh 2017-goli	1	241	0	239	0.1%	2.99 [0.12, 73.70]
Ps krueger 2007-ustek	2	256	0	64	0.2%	1.27 [0.06, 26.72]
Ps lebwohl 2015-broda2	1	1253	0	315	0.2%	0.76 [0.03, 18.59]
Ps leonardi 2008-ustek	1	511	0	255	0.2%	1.50 [0.06, 36.99]
Ps mease 2014-certo	1	273	0	136	0.2%	1.50 [0.06, 37.13]
Ps nakagawa 2016-broda	1	113	0	38	0.2%	1.03 [0.04, 25.73]
Ps papp 2013-secu	0	103	2	22	1.2%	0.04 [0.00, 0.86]
Ps reich 2017-ada	1	248	0	248	0.1%	3.01 [0.12, 74.30]
Ps reich 2017-tildra	1	617	0	155	0.2%	0.76 [0.03, 18.66]
RA burmester 2016-tcz vs MTX	1	292	0	282	0.2%	2.91 [0.12, 71.67]
RA burmester 2016-tcs vs PBO	4	579	0	282	0.2%	4.42 [0.24, 82.34]
RA emery 2008-etn	0	279	1	268	0.5%	0.32 [0.01, 8.01]
RA emery 2008-tcz	0	338	1	160	0.6%	0.16 [0.01, 3.88]
RA NCT01519791-czp	2	659	0	217	0.2%	1.65 [0.08, 34.59]
RA smolen 2009-gol	1	304	0	155	0.2%	1.54 [0.06, 37.95]
RA St clair 2004-ifx	5	749	2	291	0.9%	0.97 [0.19, 5.03]
RA weinblatt 1999-etn	0	59	1	30	0.6%	0.17 [0.01, 4.18]
RA westhovens 2006-ifx	2	721	0	361	0.2%	2.51 [0.12, 52.46]
RA westhovens 2009-abatacept	0	256	1	253	0.5%	0.33 [0.01, 8.09]
RA yamamoto 2014-ctz	1	239	0	77	0.2%	0.97 [0.04, 24.18]
SLE furie 2011-belimumab	2	544	2	275	0.8%	0.50 [0.07, 3.60]
SLE ginzler 2014-belimumab	1	336	1	113	0.4%	0.33 [0.02, 5.39]
SLE isenberg 2015-atacicept	1	301	3	154	1.2%	0.17 [0.02, 1.63]
SLE khamashta 2016-sifalimumab	2	323	0	108	0.2%	1.69 [0.08, 35.42]
SLE navarra 2011-belimumab	0	578	1	287	0.6%	0.17 [0.01, 4.07]
SLE rovin 2012-rituximab	1	73	0	71	0.1%	2.96 [0.12, 73.84]
Total (95% Cl)		57989		30207	100.0%	0.74 [0.63, 0.87]
Total events	418		254			

Heterogeneity: $Chi^2 = 39.26$, df = 40 (P = 0.50); $I^2 = 0\%$
Test for overall effect: Z = 3.68 (P = 0.0002)

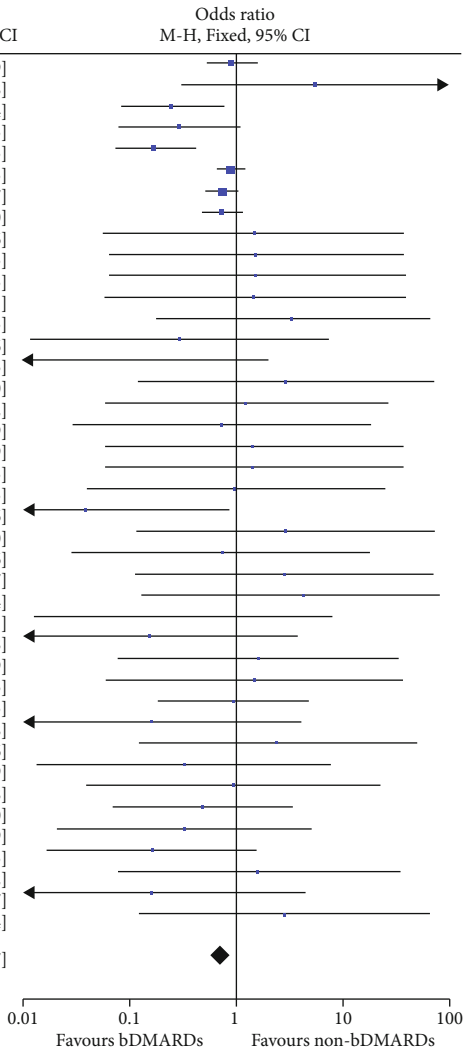

(a) Myocardial infarction

Figure 2: Continued.

Study or subgroup	bDMARDs Events	bDMARDs Total	non-bDMARDs Events	non-bDMARDs Total	Weight	Odds ratio M-H, Fixed, 95% CI
Cohort study RA carmona 2007-TNF a inhibitor	5	789	28	789	5.3%	0.17 [0.07, 0.45]
Cohort study RA cole 2007-TNF a inhibitor	7	103	8	100	1.4%	0.84 [0.29, 2.41]
Cohort study RA curtis 2007-entanercept	1	808	1	983	0.2%	1.22 [0.08,19.48]
Cohort study RA curtis 2007-infliximab	4	330	1	983	0.1%	12.05 [1.34, 108.19]
Cohort study RA jacobsson 2005-TNF a inhibitor	0	531	12	543	2.4%	0.04 [0.00, 0.68]
Cohort study RA morgan 2014-entanercept	28	3529	36	2864	7.5%	0.63 [0.38, 1.03]
Cohort study RA setoguchi 2008 with HF	33	225	101	808	7.2%	1.20 [0.79, 1.84]
Cohort study RA setoguchi 2008 without HF	26	777	126	3783	7.9%	1.00 [0.65, 1.54]
Cohort study RA solomon 2012-TNF a inhibitor	111	11587	84	8685	18.2%	0.99 [0.74, 1.32]
Cohort study RA wolfe 2004-TNF a inhibitor	180	5832	281	7339	46.1%	0.80 [0.66, 0.97]
PS baluvelt 2017-ada	1	334	0	174	0.1%	1.57 [0.06, 38.73]
PS gordon 2018-risan	1	294	0	98	0.1%	1.01 [0.04, 24.92]
PS kavanaugh 2017-goli	0	241	1	239	0.3%	0.33 [0.01, 8.12]
RA burmester 2016-tcz vs MTX	2	579	0	295	0.1%	2.53 [0.12, 52.92]
RA burmester 2016-tcz vs PBO	2	579	0	282	0.1%	2.45 [0.12, 51.12]
RA kay 2008-gol	1	137	0	34	0.2%	0.76 [0.03, 19.02]
RA NCT01519791-czp	1	659	0	217	0.1%	0.99 [0.04, 24.41]
RS St clair 2004-ifx	2	749	0	291	0.1%	1.95 [0.09, 40.74]
RA van de putte 2004-ada	1	434	0	110	0.2%	0.76 [0.09, 40.74]
RA westhovens 2006-ifx	2	721	0	361	0.1%	2.51 [0.12, 52.46]
RA westhovens 2009-abatacept	0	256	1	253	0.3%	0.33 [0.01, 8.09]
SLE furie 2011-belimumab	1	544	0	275	0.1%	1.52 [0.06, 37.45]
SLE furie 2014-abatacept	2	198	0	100	0.1%	2.56 [0.12, 53.77]
SLE isenberg 2016-tabalumab	3	775	0	387	0.1%	3.51 [0.18, 68.15]
SLE merrill 2011-rituximab	2	169	0	88	0.1%	2.64 [0.13, 55.63]
SLE merrill 2016-tabalumab	3	745	4	376	1.0%	0.38 [0.08, 1.69]
SLE morand 2020-anifrolumab	0	180	1	182	0.3%	0.34 [0.01, 8.28]
Total (95% Cl)		32105		30636	100.0%	0.84 [0.74, 0.95]
Total events	419		685			

Heterogeneity: $Chi^2 = 33.04$, df = 26 (P = 0.16); $I^2 = 21\%$
Test for overall effect: Z = 2.73 (P = 0.0006)

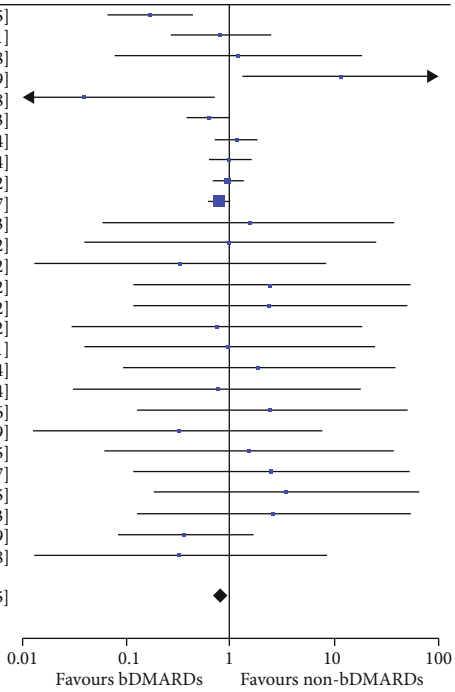

(b) Heart failure

Study or subgroup	bDMARDs Events	bDMARDs Total	non-bDMARDs Events	non-bDMARDs Total	Weight	Odds ratio M-H, Fixed, 95% CI
Cohort study RA carmona 2007-TNF a inhibitor	7	789	17	789	32.1%	0.41 [0.17, 0.99]
Cohort study RA greenberg 2010-TNF a vs MTX	5	4684	8	4684	14.8%	0.66 [0.22, 2.03]
Cohort study RA greenberg 2010-TNF a vs nonMTX	5	4684	4	1785	11.0%	0.48 [0.13, 1.77]
Cohort study RA jacobsson 2005-TNF a inhibitor	2	531	12	543	22.6%	0.17 [0.04, 0.74]
Ps gordon 2012-briakinumab	1	981	0	484	1.3%	1.48 [0.06, 36.46]
Ps mease 2014-certo	1	273	0	136	1.3%	1.50 [0.06, 37.13]
Ps paa 2008-ustek	1	820	0	410	1.3%	1.50 [0.06, 36.67]
Ps papp 2013-secu	0	103	1	22	4.7%	0.07 [0.00, 1.76]
RA genovese 2005-abatacept	1	258	0	133	1.2%	1.56 [0.06, 38.44]
RA jones 2010-tcz	2	288	0	284	1.0%	4.97 [0.24, 103.88]
RA kim 2012-etn	1	197	0	103	1.2%	1.58 [0.06, 36.13]
Ra NCT01519791-czp	1	659	0	217	1.4%	0.99 [0.04, 24.41]
RA St clair 2004-ifx	1	749	0	219	1.4%	1.17 [0.05, 28.76]
RA weisman 2007-etn	4	266	1	269	1.9%	4.09 [0.45, 36.85]
RA westhovens 2009-abatacept	1	256	0	253	1.0%	2.98 [0.12, 73.41]
SLE furie 2010-blisibimod	1	277	1	269	1.9%	0.97 [0.06, 15.60]
Total (95% Cl)		15815		10957	100.0%	0.62 [0.40, 0.95]
Total events	34		44			

Heterogeneity: $Chi^2 = 13.12$, df = 15 (P = 0.59); $I^2 = 0\%$
Test for overall effect: Z = 2.17 (P = 0.03)

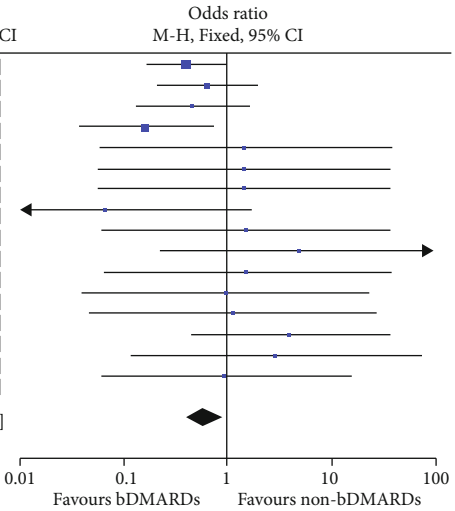

(c) Cardiovascular death

Figure 2: Continued.

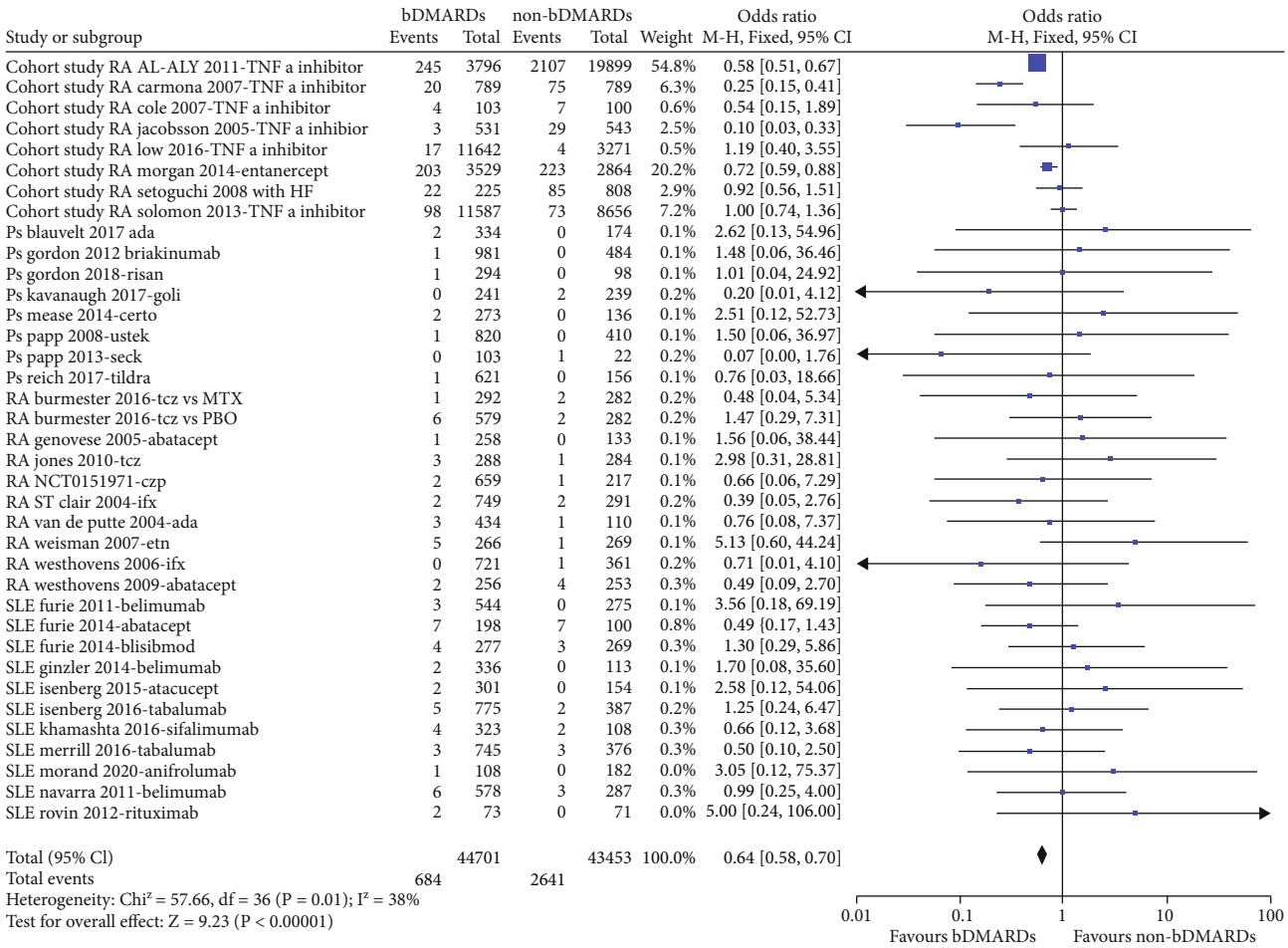

(d) All-cause mortality

Figure 2: The associations between the use of bDMARD and cardiovascular endpoint.

However, bDMARDs did not reduce the risk of stroke in patients with RA, SLE, and psoriasis when compared with non-bDMARD treatment. Subsequent sensitivity analyses did not reveal any significant association concerning the risk of stroke either (Table S5).

Furthermore, compared with non-bDMARDs, the use of bDMARDs was significantly associated with reduced risk of the composite endpoint of 3P-MACE in patients with systemic inflammatory conditions (OR = 0.69, 95% CI, 0.53 to 0.89, $I^2 = 0\%$). Subgroup analyses indicated the reduced risk of the composite endpoint of 3P-MACE in patients with RA (OR = 0.64, 95% CI, 0.47 to 0.88, $I^2 = 0\%$), in patients with TNF-α treatment (OR = 0.61, 95% CI, 0.45 to 0.84, $I^2 = 0\%$), and in patients with follow-up duration more than one year (OR = 0.59, 95% CI, 0.43 to 0.80, $I^2 = 0\%$) (Table S6). Similarly, the risk of 3P-MACE was also reduced in strata with lower percentage of previous CVD, diabetes, hypertension, and dyslipidemia. However, the risk of 4P-MACE was not significantly decreased in bDMARD users when compared with non-bDMARD users (OR = 0.99, 95% CI, 0.72 to 1.35, $I^2 = 0\%$) (Table S6).

3.3. Associated Factors with the Risks of CV Events in bDMARD Treatment. Data from the metaregression analysis showed that patient age was positively associated with risks of 3P-MACE ($\beta = 0.278$, 95% CI, 0.071 to 0.486) and 4P-MACE ($\beta = 0.255$, 95% CI, 0.039 to 0.471) in patients with RA who used bDMARDs (Table S7), but not in other diseases or cohort studies. No significant associations were found between the baseline characteristics of patients (sex, disease duration, body mass index, weight, ever smoking, etc.), or comorbidities (previous CV event, diabetes mellitus, hypertension, dyslipidemia, etc.), or changes in inflammatory indicators (CRP and ESR), and the risks of CV events in bDMARD users in metaregression analyses (Table S7). Additionally, no significant associations were found between the efficacy indicators such as DAS28 remission, ACR, BILAG, SRI response rate, SLEDAI, or PASI and the risks of CV events in bDMARD users (Table S7).

4. Discussion

By synthesizing the existing evidence from RCTs and cohort studies, we found that comparing with non-bDMARDs, the

Table 1: Sensitivity analyses for the use of bDMARD and incidence of myocardial infarction in patients with systemic inflammatory conditions.

Endpoint	Subgroup		Participant (bDMARD/control)	OR	95% CI	*P* value	I^2
Myocardial infarction							
	Total		57989/30207	0.74	0.63, 0.87	*0.002*	0
	Study type	Cohort	45040/24148	0.63	0.43, 0.91	*0.01*	66
		RCT	12949/6059	0.79	0.47, 1.31	0.36	0
	Disease type	RA	49510/26524	0.74	0.63, 0.87	*0.0004*	31
		Ps	6324/2675	0.90	0.45, 1.80	0.77	0
		SLE	2155/1008	0.49	0.19, 1.28	0.14	0
	Drug type	TNF-α inhibitor	49141/26344	0.74	0.63, 0.88	*0.0006*	27
		IL-17 inhibitor	2358/627	0.31	0.10, 1.00	0.05	3
		IL-23 inhibitor	1046/378	1.25	0.20, 7.94	0.82	0
		IL-12/23 inhibitor	1824/873	1.30	0.33, 5.21	0.71	0
		IL-6 receptor inhibitor	1209/724	1.48	0.35, 6.33	0.60	23
		B cell inhibition	2155/1008	0.49	0.19, 1.28	0.14	0
		T cell inhibition	256/253	0.33	0.01, 8.09	0.50	NA
	Follow-up duration	>1 year	38143/17825	0.73	0.61, 0.87	*0.0006*	37
		<1 year	19846/12382	0.78	0.55, 1.11	0.17	0
	Previous CVD*	<30%	42707/21393	0.78	0.63, 0.96	0.02	34
		30-50%	981/484	3.47	0.18, 67.23	0.41	NA
	Diabetes	<30%	44874/24045	0.61	0.42, 0.88	*0.009*	68
		30-50%	981/484	3.47	0.18, 67.23	0.41	NA
	Hypertension	<30%	29227/11982	0.66	0.39, 1.11	0.12	60
		30-50%	16097/12004	0.77	0.59, 1.01	0.06	0
	Dyslipidemia	<30%	9368/6754	0.27	0.11, 0.62	*0.002*	0
		30-50%	11587/8656	0.77	0.49, 1.20	0.24	NA
		>50%	12568/9140	0.81	0.52, 1.25	0.34	0

*Previous cardiovascular disease includes ischemia heart disease, coronary heart disease, angina, myocardial infarction, congestive heart failure, atrial fibrillation, and cerebrovascular disease. bDMARD: biological disease-modifying antirheumatic drug; CVD: cardiovascular disease; IFN: interferon; IL: interleukin; MACE: major adverse cardiovascular event; NA: not applicable; Ps: psoriasis; RCT: randomized controlled trial; RA: rheumatoid arthritis; SLE: systemic lupus erythematosus; TNF: tumor necrosis factor.

use of bDMARDs might be associated with reduced risks of MI, heart failure, CV death, all-cause mortality, and 3P-MACE in patients with systemic inflammatory conditions, especially for patients with RA. Moreover, subgroup analyses suggested that the cardioprotective effect of bDMARDs might be prominent in TNF-α inhibitor users and patients with follow-up over one year.

This is a state-of-art meta-analysis of biological therapy concerning the risk of CV events in patients with systemic inflammatory diseases. The new insights from this study might give researchers some hints to explore optimal biological therapeutic approaches for better CV prognosis and inspire event-driven clinical trials for CV evaluation of bDMARDs in the future.

Actually, multiple epidemiological studies have implicated the pivotal link between inflammation and cardiovascular events [11, 25–28]. Systemic inflammatory and soluble immune mechanisms (circulating antibodies, immune complexes, and complement activation products) were reported to be involved in accelerating vessel pathology in atherosclerosis [26, 27]. Furthermore, previous studies reported numerous mutual molecular pathways with the pathogenesis of atherosclerosis and persistent inflammation in the development of autoimmune diseases. For example, inflammasome infiltration has been demonstrated to play an indispensable role in the pathological progression of multiple cardiovascular diseases [28]. The formation and activation of inflammatory complex such as NLPR3 inflammasome have been noted in both inflammatory and cardiovascular diseases. And subsequent secretion of interleukin- (IL-) 1 might in turn facilitate the disease development and progression. Moreover, critical proinflammatory cytokines such as IL-6, C-reactive protein (CRP), and tumor necrosis factor (TNF-α) not only play a pivotal role in the inflammatory cascade and evolution of rheumatic diseases but also are independent predictors of CVD [11, 29]. Hence, it is plausible that excess CV risk could be observed in systemic inflammatory diseases. Targeting the mutual pathogenic mechanism, intensive anti-inflammatory therapy might have the potent to achieve disease remission and reduce the risk of cardiovascular events in patients with systemic inflammatory conditions. Fortunately, our study has just favorably responded to this scientific hypothesis within such context.

Table 2: Sensitivity analyses for the use of bDMARD and incidence of heart failure in patients with systemic inflammatory conditions.

Endpoint	Subgroup		Participant (bDMARD/control)	OR	95% CI	*P* value	I^2
Heart failure							
	Total		32105/30636	0.84	0.74, 0.95	*0.006*	21
	Study type	Cohort	24511/26848	0.81	0.60, 1.11	0.19	67
		RCT	6725/3248	1.03	0.49, 2.18	0.93	0
	Disease type	RA	28625/28688	0.83	0.73, 0.95	*0.006*	41
		Ps	869/511	0.78	0.14, 4.33	0.78	0
		SLE	2611/1408	0.98	0.40, 2.42	0.96	0
	Drug type	TNF-α inhibitor	27786/28274	0.83	0.73, 0.95	*0.005*	43
		IL-23 inhibitor	294/98	1.01	0.04, 24.92	1.00	NA
		IL-6 receptor inhibitor	1158/574	2.49	0.29, 21.35	0.41	0
		B cell inhibition	2233/1126	0.97	0.34, 2.72	0.95	0
		T cell inhibition	454/353	1.00	0.15, 6.61	1.00	0
		IFN receptor antibody	180/182	0.34	0.01, 8.28	0.50	NA
	Follow-up duration	>1 year	18357/20935	0.80	0.69, 0.93	*0.003*	38
		<1 year	13748/9672	0.99	0.75, 1.30	0.93	0
	Previous CVD*	<30%	17575/175/73	0.95	0.77, 1.17	0.62	38
		30-50%	169/88	2.64	0.13, 55.63	0.53	NA
		>50%	225/808	1.20	0.79, 1.84	0.39	NA
	Diabetes	<30%	15647/12092	0.69	0.35, 1.36	0.28	72
		30-50%	1002/4591	1.10	0.81, 1.49	0.53	0
	Hypertension	30-50%	15116/11549	0.83	0.53, 1.28	0.39	59
		>50%	1002/4591	1.10	0.81, 1.49	0.53	0
	Dyslipidemia	>50% (all available studies)	12589/13276	1.04	0.84, 1.28	0.71	0

*Previous cardiovascular disease includes ischemia heart disease, coronary heart disease, angina, myocardial infarction, congestive heart failure, atrial fibrillation, and cerebrovascular disease. bDMARD: biological disease-modifying antirheumatic drug; CVD: cardiovascular disease; IFN: interferon; IL: interleukin; MACE: major adverse cardiovascular event; NA: not applicable; Ps: psoriasis; RCT: randomized controlled trial; RA: rheumatoid arthritis; SLE: systemic lupus erythematosus; TNF: tumor necrosis factor.

As for disease subtypes, our sensitivity analysis showed that remarkable cardiovascular benefits were observed especially in patients with RA. Consistent with our results, accumulated clinical data favored anti-inflammatory therapies, including bDMARDs, in reducing the cardiovascular risk of RA [8]. However, studies concerning the cardiovascular protective effect of bDMARDs in SLE were limited. Targeting the IFN pathway might yield a promising therapeutic response since IFN was viewed as a major pathogenetic determinant in lupus-related atherosclerosis [30]. In psoriasis, indeed, several studies also suggested a cardioprotective effect of certain biologic agents [16–18, 31]. A recent meta-analysis found that the CV events were less frequent in patients with psoriasis receiving biological therapies targeting IL-17 and IL-23 [32].

Compared with the current available literatures, in addition to patients with RA, we conducted additional analyses in patients with psoriasis and lupus. Unfortunately, we did not see any positive results in these two diseases in our analysis. In our study, it was noted that the sample size of patients with SLE was much less than the patients with RA. One of the possible reasons for the negative results in psoriasis and SLE might be that current sample size and exam power were not enough to validate the cardioprotective effects. Another reason might be associated with the extent of treatment response. Studies on psoriasis suggested that patients with no response to biologic therapy might show minimal reduction in MACE risk [17, 18]. What is more, it was reported that no significant improvement of vascular inflammation was shown in patients with adalimumab treatment [22], and it was also reported that ustekinumab might have the potent to increase the risk of MACE [24]. In addition, the studies on lupus and psoriasis included in this meta-analysis were generally short-term RCTs, and we included few cohort studies related to SLE and psoriasis. While in our analyses, positive results mostly appeared in cohort studies. Therefore, longer follow-up studies are needed to further clarify the long-term effects of CVD.

Several studies demonstrated the associations between TNF-α inhibitors and improved CV outcomes, which were consistent with our results. A meta-analysis previously estimated a 30% reduction in risk of cardiovascular events with TNF-α inhibitors in RA, with protective effect specifically for MI and stroke [15]. The use of TNF-α inhibitor was found to be correlated with improved blood pressure [33], reduced aortic stiffness [34], and improved left ventricular mass index on echocardiography [35]. Possible mechanisms might rely on the quantitative and functional changes in lipids and the improvements in endothelial dysfunction and oxidative stress. It was reported that long-term use of

Table 3: Sensitivity analyses for the use of bDMARD and incidence of cardiovascular death in patients with systemic inflammatory conditions.

Endpoint	Subgroup	Participant (bDMARD/control)	OR	95% CI	*P* value	I^2
Cardiovascular death						
Total		15815/10957	0.62	0.40, 0.95	*0.03*	0
Study type	Cohort	10688/8086	0.40	0.23, 0.69	*0.001*	0
	RCT	5127/2871	1.54	0.69, 3.46	0.29	0
Disease type	RA	13361/9636	0.60	0.38, 0.96	*0.03*	4
	Ps	2177/1052	0.71	0.18, 2.85	0.63	0
	SLE	277/269	0.97	0.06, 15.60	0.98	NA
Drug type	TNF-α inhibitor	12832/9102	0.53	0.33, 0.86	*0.01*	0
	IL-17 inhibitor	103/22	0.07	0.00, 1.76	0.11	NA
	IL-12/23 inhibitor	1801/894	1.49	0.16, 14.37	0.73	0
	IL-6 receptor inhibitor	288/284	4.97	0.24, 103.88	0.30	NA
	B cell inhibition	277/269	0.97	0.06, 15.60	0.98	NA
	T cell inhibition	514/386	2.17	0.23, 20.91	0.50	0
Follow-up duration	>1 year	12629/9116	0.46	0.28, 0.77	*0.003*	0
	<1 year	3186/1841	1.62	0.62, 4.20	0.32	0
Previous CVD*	<30%	9368/6754	0.58	0.25, 1.38	0.22	0
	30-50%	981/484	1.48	0.06, 36.46	0.81	NA
Diabetes	<30% (all available studies)	10880/7781	0.42	0.21, 0.83	*0.01*	0
Hypertension	<30%	9368/6754	0.58	0.25, 1.38	0.22	0
	30-50%	981/484	1.48	0.06, 36.46	0.81	NA
Dyslipidemia	<30%	9368/6754	0.58	0.25, 1.38	0.22	0
	>50%	981/484	1.48	0.06, 36.46	0.81	NA

*Previous cardiovascular disease includes ischemia heart disease, coronary heart disease, angina, myocardial infarction, congestive heart failure, atrial fibrillation, and cerebrovascular disease. bDMARD: biological disease-modifying antirheumatic drug; CVD: cardiovascular disease; IFN: interferon; IL: interleukin; MACE: major adverse cardiovascular event; NA: not applicable; Ps: psoriasis; RCT: randomized controlled trial; RA: rheumatoid arthritis; SLE: systemic lupus erythematosus; TNF: tumor necrosis factor.

TNF-α inhibitor was associated with an increase in HDL, total cholesterol, and triglycerides, while a decrease in apolipoprotein B/A and stable LDL as well as total cholesterol/HDL [36]. Moreover, in RA patients, infliximab treatment led to sustained increases in paraoxonase and arylesterase activities of PON-1 on HDL-cholesterol molecules, which may improve HDL antiatherogenic capacity by increasing the antioxidative properties of HDL [37].

Apart from TNF-α inhibitor, CV effects of other bDMARDs were less characterized. A multidatabase cohort study indicated that tocilizumab use had a similar risk of cardiovascular events versus TNF-α inhibitor use in patients with RA [19]. Likewise, it was observed that tocilizumab could improve qualitative and functional lipid parameters [38], endothelial function, and oxidative stress [39]. Similarly, improved macro- and microvascular endothelial function and beneficial effects on cholesterol profile were found in small case series of rheumatoid arthritis with rituximab users [20, 21]. Although they may contribute to favorable cardiovascular and metabolic profile, these drugs were not suggested to achieve cardiovascular risk reductions yet in our meta-analysis.

A Danish cohort study, examining the rate of CV events (CV death, MI, and stroke) in 6,902 patients with severe psoriasis, indicated the use of IL-12/23 inhibitor ustekinumab was not associated with reduced CV event rates [23]. Likewise, a meta-analysis of 22 RCTs reported no significant difference in the rate of MACE between anti-IL-12/IL-23 antibody treatments and placebo [18]. Another review found that patients with over-4-year treatment of ustekinumab had a decrease risk in MACE while no effects on MACE were observed with short-term use of ustekinumab [40]. Certainly, with increasing use of non-TNF-α-inhibitor bDMARDs, more attention is needed for their cardiovascular profiles.

5. Limitations

Our meta-analysis also has several limitations. First, we included both RCTs and cohort studies in our analyses, and subgroup analyses showed that positive results were mainly driven by the result from cohort studies, while we did not observe significant CV risk reduction in RCT strata. Thus, the heterogeneity lying in different study designs and population might compromise the reliability of our results. Therefore, we conducted the sensitivity analyses and metaregression to control the potential bias. But there is no denying that the data should be interpreted with caution, since the unmeasured confounding factors in cohort studies would undermine the confidence of the conclusion.

Table 4: Sensitivity analyses for the use of bDMARD and all-cause mortality in patients with systemic inflammatory conditions.

Endpoint	Subgroup		Participant (bDMARD/control)	OR	95% CI	*P* value	I^2
All-cause mortality							
	Total		44701/43453	0.64	0.58, 0.70	*<0.0001*	38
	Study type	Cohort	32202/36930	0.60	0.44, 0.82	*0.002*	82
		RCT	12499/6523	0.91	0.61, 1.35	0.65	0
	Disease type	RA	36704/39412	0.64	0.49, 0.85	*0.002*	63
		Ps	36677/1719	0.80	0.26, 2.45	0.70	0
		SLE	4330/2322	0.93	0.54, 1.59	0.79	0
	Drug type	TNF-α inhibitor	35879/38727	0.63	0.47, 0.84	*0.002*	66
		IL-6 receptor inhibitor	1159/848	1.36	0.43, 4.31	0.60	0
		IL-17 inhibitor	103/22	0.07	0.00, 1.76	0.11	NA
		IL-23 inhibitor	915/254	0.87	0.09, 8.43	0.91	0
		IL-12/23 inhibitor	1801/894	1.49	0.16, 14.3	0.73	0
		B cell inhibition	3952/2040	1.11	0.59, 2.09	0.74	0
		T cell inhibition	712/486	0.53	0.22, 1.28	0.16	0
		IFN receptor antibody	180/182	3.05	0.12, 75.37	0.50	NA
	Follow-up duration	>1 year	27480/31921	0.62	0.48, 0.80	*0.0002*	42
		<1 year	17221/11532	1.02	0.77, 1.35	0.90	0
	Previous CVD*	<30%	27880/15353	0.81	0.69, 0.95	*0.01*	15
		30-50%	4777/20383	0.58	0.51, 0.67	*<0.0001*	0
		>50%	225/808	0.92	0.56, 1.51	0.75	NA
	Diabetes	<30%	27289/15334	0.68	0.40, 1.14	0.14	80
		30-50%	5002/21191	0.68	0.47, 0.98	*0.04*	0
	Hypertension	<30%	11642/3271	1.19	0.40, 3.55	0.75	NA
		30-50%	16097/12004	0.80	0.68, 0.94	*0.007*	39
		>50%	4021/20707	0.69	0.45, 1.06	0.09	68
	Dyslipidemia	30-50%	3529/2864	0.72	0.59, 0.88	*0.001*	NA
		>50%	116589/29847	0.80	0.53, 1.19	0.26	76

*Previous cardiovascular disease includes ischemia heart disease, coronary heart disease, angina, myocardial infarction, congestive heart failure, atrial fibrillation, and cerebrovascular disease. bDMARD: biological disease-modifying antirheumatic drug; CVD: cardiovascular disease; IFN: interferon; IL: interleukin; MACE: major adverse cardiovascular event; NA: not applicable; Ps: psoriasis; RCT: randomized controlled trial; RA: rheumatoid arthritis; SLE: systemic lupus erythematosus; TNF: tumor necrosis factor.

However, since most of included RCTs were not specially designed for cardiovascular evaluation, the synthesized evidence from prospective cohort studies still gave us useful clues for the link between bDMARDs and CV risk reduction. More investigations, such as Cardiovascular Outcome Trials for bDMARDs, should be designed and conducted to validate the aforementioned associations in the future. Second, although we tried our best to collect every available data, the indicators reflecting the alteration of inflammation, such as CRP and ESR, were rarely reported. Furthermore, since the efficacy endpoints varied in different diseases, we were unable to assess the association between disease remission and the risks of CV events uniformly. Moreover, the percentage of participants with history of CVD and its relevant comorbidities was generally low in the included studies. Whether patients with systemic inflammatory conditions who also have established CVD still benefit from bDMARD treatment requires more investigations. Since the included studies were not primarily designed for cardiovascular evaluation, the administration of cardio- and vasculoprotective drugs like angiotensin-converting enzyme inhibitor, β-blocker, and anticoagulant was rarely reported, whose influence on patients with bDMARD treatment should be further evaluated in the future.

6. Conclusions

According to our meta-analysis, the use of bDMARDs might be associated with reduced risks of CV events in patients with systemic inflammatory conditions, especially for patients with RA. The CV events might be less frequent in TNF-α inhibitor users and in bDMARD users with follow-up over one year.

Data Availability

All data relevant to the study are included in the article or uploaded as supplementary information. No more additional data are available.

Additional Points

Highlights. (i) This is a comprehensive evaluation regarding the use of bDMARD and CV risk. (ii) The use of bDMARD might be associated with reduced risk of CV events. (iii) The risk reductions were mainly observed in patients with rheumatoid arthritis. (iv) The risk was lower in patients with TNF-α inhibitors or follow-up over one year. (v) Such associations need to be validated by well-designed event-driven trials.

Disclosure

The funding agencies had no roles in the study design, data collection or analysis, decision to publish, or preparation of the manuscript.

Conflicts of Interest

LJ has received fees for lecture presentations and for consulting from AstraZeneca, Merck, Metabasis, MSD, Novartis, Eli Lilly, Roche, Sanofi-Aventis, and Takeda. There is no other support from any organization for the submitted work other than that described above.

Authors' Contributions

LJ and XC conceptualized this study and designed the systematic review protocol; SH, CL, and FL performed the study selection and data extraction; CL and XC performed the statistical analyses; SH, CL, and XC prepared the outlines and wrote the manuscript. All authors contributed to the critical revision of manuscript drafts. Suiyuan Hu and Chu Lin contributed equally to the manuscript.

Acknowledgments

This work was supported by the Beijing Natural Science Foundation (No. 7202216) and the National Natural Science Foundation of China (No. 81970698 and No. 81970708). We thank the doctors, nurses, and technicians for their practical during the study at the Department of Endocrinology and Metabolism in Peking University People's Hospital.

Supplementary Materials

Figure S1: funnel plots of analyses for individual and composite CV endpoints. Table S1: baseline characteristics of included randomized controlled trials. Table S2: baseline characteristics of included cohort studies. Table S3: evaluation for risk of bias in included RCTs. Table S4: evaluation for risk of bias in included cohort studies. Table S5: sensitivity analyses for the use of bDMARD and incidence of stroke in patients with systemic inflammatory conditions. Table S6: sensitivity analyses for the use of bDMARD and incidence of composite endpoints in patients with systemic inflammatory conditions. Table S7: metaregression analysis of the association between the use of bDMARDs and the risks of CV events. *(Supplementary Materials)*

References

[1] P. Joseph, D. Leong, M. McKee et al., "Reducing the global burden of cardiovascular disease, part 1: the epidemiology and risk factors," *Circulation Research*, vol. 121, no. 6, pp. 677–694, 2017.

[2] K. P. Liao, T. Cai, V. S. Gainer et al., "Lipid and lipoprotein levels and trend in rheumatoid arthritis compared to the general population," *Arthritis Care & Research*, vol. 65, no. 12, pp. 2046–2050, 2013.

[3] P. Libby, "Role of inflammation in atherosclerosis associated with rheumatoid arthritis," *The American Journal of Medicine*, vol. 121, no. 10, pp. S21–S31, 2008.

[4] W. Foster, D. Carruthers, G. Y. H. Lip, and A. D. Blann, "Inflammation and microvascular and macrovascular endothelial dysfunction in rheumatoid arthritis: effect of treatment," *The Journal of Rheumatology*, vol. 37, no. 4, pp. 711–716, 2010.

[5] O. Ciftci, S. Yilmaz, S. Topcu et al., "Impaired coronary microvascular function and increased intima-media thickness in rheumatoid arthritis," *Atherosclerosis*, vol. 198, no. 2, pp. 332–337, 2008.

[6] P. M. Ridker, B. M. Everett, T. Thuren et al., "Antiinflammatory therapy with canakinumab for atherosclerotic disease," *The New England Journal of Medicine*, vol. 377, no. 12, pp. 1119–1131, 2017.

[7] S. M. Nidorf, A. T. L. Fiolet, A. Mosterd et al., "Colchicine in patients with chronic coronary disease," *The New England Journal of Medicine*, vol. 383, no. 19, pp. 1838–1847, 2020.

[8] B. R. England, G. M. Thiele, D. R. Anderson, and T. R. Mikuls, "Increased cardiovascular risk in rheumatoid arthritis: mechanisms and implications," *BMJ*, vol. 361, 2018.

[9] Y. Liu and M. J. Kaplan, "Cardiovascular disease in systemic lupus erythematosus: an update," *Current Opinion in Rheumatology*, vol. 30, no. 5, pp. 441–448, 2018.

[10] A. A. Manolis, T. A. Manolis, H. Melita, and A. S. Manolis, "Psoriasis and cardiovascular disease: the elusive link," *International Reviews of Immunology*, vol. 38, no. 1, pp. 33–54, 2019.

[11] A. Abou-Raya and S. Abou-Raya, "Inflammation: a pivotal link between autoimmune diseases and atherosclerosis," *Autoimmunity Reviews*, vol. 5, no. 5, pp. 331–337, 2006.

[12] A. Kerschbaumer, A. Sepriano, J. S. Smolen et al., "Efficacy of pharmacological treatment in rheumatoid arthritis: a systematic literature research informing the 2019 update of the EULAR recommendations for management of rheumatoid arthritis," *Annals of the Rheumatic Diseases*, vol. 79, no. 6, pp. 744–759, 2020.

[13] A. Sepriano, A. Kerschbaumer, J. S. Smolen et al., "Safety of synthetic and biological DMARDs: a systematic literature review informing the 2019 update of the EULAR recommendations for the management of rheumatoid arthritis," *Annals of the Rheumatic Diseases*, vol. 79, no. 6, pp. 760–770, 2020.

[14] A. Ruyssen-Witrand, R. Perry, C. Watkins et al., "Efficacy and safety of biologics in psoriatic arthritis: a systematic literature review and network meta-analysis," *RMD Open*, vol. 6, no. 1, article e001117, 2020.

[15] C. Roubille, V. Richer, T. Starnino et al., "The effects of tumour necrosis factor inhibitors, methotrexate, non-steroidal anti-inflammatory drugs and corticosteroids on cardiovascular events in rheumatoid arthritis, psoriasis and psoriatic arthritis:

a systematic review and meta-analysis," *Annals of the Rheumatic Diseases*, vol. 74, no. 3, pp. 480–489, 2015.

[16] J. J. Wu and K. Y. Poon, "Tumor necrosis factor inhibitor therapy and myocardial infarction risk in patients with psoriasis, psoriatic arthritis, or both," *Journal of Drugs in Dermatology*, vol. 13, no. 8, pp. 932–934, 2014.

[17] K. Abuabara, H. Lee, and A. B. Kimball, "The effect of systemic psoriasis therapies on the incidence of myocardial infarction: a cohort study," *The British Journal of Dermatology*, vol. 165, no. 5, pp. 1066–1073, 2011.

[18] C. Ryan, C. L. Leonardi, J. G. Krueger et al., "Association between biologic therapies for chronic plaque psoriasis and cardiovascular events: a meta-analysis of randomized controlled trials," *JAMA*, vol. 306, no. 8, pp. 864–871, 2011.

[19] S. C. Kim, D. H. Solomon, J. R. Rogers et al., "Cardiovascular safety of tocilizumab versus tumor necrosis factor inhibitors in patients with rheumatoid arthritis: a multi-database cohort study," *Arthritis & Rhematology*, vol. 69, no. 6, pp. 1154–1164, 2017.

[20] P. Y. Hsue, R. Scherzer, C. Grunfeld et al., "Depletion of B-cells with rituximab improves endothelial function and reduces inflammation among individuals with rheumatoid arthritis," *Journal of the American Heart Association*, vol. 3, no. 5, article e001267, 2014.

[21] H. G. Raterman, H. Levels, A. E. Voskuyl, W. F. Lems, B. A. Dijkmans, and M. T. Nurmohamed, "HDL protein composition alters from proatherogenic into less atherogenic and proinflammatory in rheumatoid arthritis patients responding to rituximab," *Annals of the Rheumatic Diseases*, vol. 72, no. 4, pp. 560–565, 2013.

[22] R. Bissonnette, F. Harel, J. G. Krueger et al., "TNF-α antagonist and vascular inflammation in patients with psoriasis vulgaris: a randomized placebo-controlled study," *The Journal of Investigative Dermatology*, vol. 137, no. 8, pp. 1638–1645, 2017.

[23] O. Ahlehoff, L. Skov, G. Gislason et al., "Cardiovascular outcomes and systemic anti-inflammatory drugs in patients with severe psoriasis: 5-year follow-up of a Danish nationwide cohort," *Journal of the European Academy of Dermatology and Venereology*, vol. 29, no. 6, pp. 1128–1134, 2015.

[24] K. Papp, A. B. Gottlieb, L. Naldi et al., "Safety surveillance for ustekinumab and other psoriasis treatments from the Psoriasis Longitudinal Assessment and Registry (PSOLAR)," *Journal of Drugs in Dermatology*, vol. 14, no. 7, pp. 706–714, 2015.

[25] P. M. Ridker, M. Cushman, M. J. Stampfer, R. P. Tracy, and C. H. Hennekens, "Inflammation, aspirin, and the risk of cardiovascular disease in apparently healthy men," *The New England Journal of Medicine*, vol. 336, no. 14, pp. 973–979, 1997.

[26] V. Pasceri and E. T. Yeh, "A tale of two diseases: atherosclerosis and rheumatoid arthritis," *Circulation*, vol. 100, no. 21, pp. 2124–2126, 1999.

[27] R. Ross, "Atherosclerosis — An inflammatory disease," *The New England Journal of Medicine*, vol. 340, no. 2, pp. 115–126, 1999.

[28] W. Zhou, C. Chen, Z. Chen et al., "NLRP3: a novel mediator in cardiovascular disease," *Journal of Immunology Research*, vol. 2018, Article ID 5702103, 8 pages, 2018.

[29] P. A. Bacon and J. N. Townend, "Nails in the coffin: increasing evidence for the role of rheumatic disease in the cardiovascular mortality of rheumatoid arthritis," *Arthritis and Rheumatism*, vol. 44, no. 12, pp. 2707–2710, 2001.

[30] M. F. Denny, S. Thacker, H. Mehta et al., "Interferon-alpha promotes abnormal vasculogenesis in lupus: a potential pathway for premature atherosclerosis," *Blood*, vol. 110, no. 8, pp. 2907–2915, 2007.

[31] O. Ahlehoff, L. Skov, G. Gislason et al., "Cardiovascular disease event rates in patients with severe psoriasis treated with systemic anti-inflammatory drugs: a Danish real-world cohort study," *Journal of Internal Medicine*, vol. 273, no. 2, pp. 197–204, 2013.

[32] L. Cui, R. Chen, S. Subedi et al., "Efficacy and safety of biologics targeting IL-17 and IL-23 in the treatment of moderate-to-severe plaque psoriasis: a systematic review and meta-analysis of randomized controlled trials," *International Immunopharmacology*, vol. 62, pp. 46–58, 2018.

[33] N. B. Klarenbeek, S. M. van der Kooij, T. J. Huizinga et al., "Blood pressure changes in patients with recent-onset rheumatoid arthritis treated with four different treatment strategies: a post hoc analysis from the BeSt trial," *Annals of the Rheumatic Diseases*, vol. 69, no. 7, pp. 1342–1345, 2010.

[34] K. Angel, S. A. Provan, H. L. Gulseth, P. Mowinckel, T. K. Kvien, and D. Atar, "Tumor necrosis Factor-α antagonists improve aortic stiffness in patients with inflammatory Arthropathies," *Hypertension*, vol. 55, no. 2, pp. 333–338, 2010.

[35] C. I. Daïen, P. Fesler, G. du Cailar et al., "Etanercept normalises left ventricular mass in patients with rheumatoid arthritis," *Annals of the Rheumatic Diseases*, vol. 72, no. 6, pp. 881–887, 2013.

[36] C. I. Daïen, Y. Duny, T. Barnetche, J. P. Daurès, B. Combe, and J. Morel, "Effect of TNF inhibitors on lipid profile in rheumatoid arthritis: a systematic review with meta-analysis," *Annals of the Rheumatic Diseases*, vol. 71, no. 6, pp. 862–868, 2012.

[37] C. Popa, L. J. van Tits, P. Barrera et al., "Anti-inflammatory therapy with tumour necrosis factor alpha inhibitors improves high-density lipoprotein cholesterol antioxidative capacity in rheumatoid arthritis patients," *Annals of the Rheumatic Diseases*, vol. 68, no. 6, pp. 868–872, 2009.

[38] A. C. Strang, R. J. Bisoendial, R. S. Kootte et al., "Pro-atherogenic lipid changes and decreased hepatic LDL receptor expression by tocilizumab in rheumatoid arthritis," *Atherosclerosis*, vol. 229, no. 1, pp. 174–181, 2013.

[39] P. Ruiz-Limón, R. Ortega, I. Arias de la Rosa et al., "Tocilizumab improves the proatherothrombotic profile of rheumatoid arthritis patients modulating endothelial dysfunction, NETosis, and inflammation," *Translational Research*, vol. 183, pp. 87–103, 2017.

[40] J. Hugh, A. S. van Voorhees, R. I. Nijhawan et al., "From the Medical Board of the National Psoriasis Foundation: the risk of cardiovascular disease in individuals with psoriasis and the potential impact of current therapies," *Journal of the American Academy of Dermatology*, vol. 70, no. 1, pp. 168–177, 2014.

Hindawi
Mediators of Inflammation
Volume 2021, Article ID 9450843, 11 pages
https://doi.org/10.1155/2021/9450843

Research Article

Silencing IL12p35 Promotes Angiotensin II-Mediated Abdominal Aortic Aneurysm through Activating the STAT4 Pathway

Lanlan Wang,[1,2] Chengyun Hu,[3] Yongfei Dong,[4] Feibiao Dai,[3] Yongxia Xu,[1] Yumeng Dai,[2] Lijie Shao,[2] and Defa Zhu[1]

[1]*Department of Geriatric Endocrinology, The First Affiliated Hospital of Anhui Medical University, Hefei 230032, China*
[2]*Department of Geriatric Endocrinology, The First Affiliated Hospital of USTC, Division of Life Sciences and Medicine, University of Science and Technology of China, Hefei, Anhui 230001, China*
[3]*Department of Anesthesiology, The First Affiliated Hospital of USTC, Division of Life Sciences and Medicine, University of Science and Technology of China, Hefei, Anhui 230001, China*
[4]*Department of Neurosurgery, The First Affiliated Hospital of USTC, Division of Life Sciences and Medicine, University of Science and Technology of China, Hefei, Anhui 230001, China*

Correspondence should be addressed to Defa Zhu; zdfa0168@sina.com

Received 24 April 2021; Accepted 1 July 2021; Published 27 July 2021

Academic Editor: Amilia Aminuddin

Background and Purpose. Abdominal aortic aneurysm (AAA) is a chronic inflammatory disorder and the important causes of death among men over the age of 65 years. Interleukin-12p35 (IL12p35) is an inflammatory cytokine that participates in a variety of inflammatory diseases. However, the role of IL12p35 in the formation and development of AAA is still unknown. *Experimental Approach*. Male apolipoprotein E-deficient (Apoe$^{-/-}$) mice were generated and infused with 1.44 mg/kg angiotensin II (Ang II) per day. We found that IL12p35 expression was noticeably increased in the murine AAA aorta and isolated aortic smooth muscle cells (SMCs) after Ang II stimulation. IL12p35 silencing promoted Ang II-induced AAA formation and rupture in Apoe$^{-/-}$ mice. IL12p35 silencing markedly increased the expression of inflammatory cytokines, including IL-1β, IL-6, and tumor necrosis factor-α (TNF-α), in both the serum and AAA aorta. Additionally, IL12p35 silencing exacerbated SMC apoptosis in Apoe$^{-/-}$ mice after Ang II infusion. IL12p35 silencing significantly increased signal transducer and activator of transcription (STAT) 4 phosphorylation levels in AAA mice, and STAT4 knockdown abolished the IL12p35-mediated proinflammatory response and SMC apoptosis. *Interpretation*. Silencing IL12p35 promotes AAA formation by activating the STAT4 pathway, and IL12p35 may serve as a novel and promising therapeutic target for AAA treatment.

1. Introduction

Abdominal aortic aneurysm (AAA) is a chronic inflammatory disorder and one of the important causes of death among men over the age of 65 years [1, 2]. AAA is defined as localized enlargement of the abdominal aorta to a diameter of at least 50% greater than its normal size or an aorta that measures greater than 30 mm in diameter [3]. Epidemiological data have shown that the incidence rate of AAA is approximately 1.4%~12.4% and directly causes 150,000~200,000 deaths each year worldwide due to AAA rupture [4, 5]. In addition, the mortality rate of AAA exceeds 80% after rupture despite surgical advancements [3, 6]. Effective pharmacotherapies for halting the growth and rupture of AAA or delaying the need for surgical repair are currently lacking.

Although the pathogenesis of AAA is complex, degeneration of the aortic media has been proven to be a crucial hallmark of AAA pathology [7, 8]. High numbers of smooth muscle cells (SMCs), elastic fiber fragmentation, and excessive collagen and proteoglycan accumulation are the main characteristics of medial degeneration and are key factors in AAA dilation and rupture [9, 10]. In addition, the inflammatory response, oxidative stress, SMC apoptosis, and proteolytic degradation of aortic wall connective tissue have all

been associated with the development of AAA [11, 12]. Accordingly, the pharmacological regulation of these processes represents a promising strategy to control the progression of AAA.

Interleukin-12 (IL-12) is a pleiotropic cytokine with multiple immunomodulatory effects and is composed of p35 and p40 subunits [13, 14]. The biological effect mediated by IL-12 is closely associated with signal transducer and activator of transcription (STAT) signaling, specifically STAT4 [15, 16]. IL-12 has been identified as an important inflammation-related cytokine involved in the regulation of several cardiovascular diseases, including myocardial infarction [17], atherosclerosis [18], and hypertension [19]. Recent studies have demonstrated that IL12p40 deficiency accelerates pathological matrix remodeling and promotes the development of AAA [20, 21]. However, the direct role of IL12p35 in the development of AAA had not yet been determined. In this study, we identified the role of IL12p35 in the development of AAA and attempted to elucidate the possible mechanism.

2. Materials and Methods

2.1. Animals and Animal Model. Nine- to eleven-week-old male apolipoprotein E-deficient ($Apoe^{-/-}$) mice generated on a C57BL/6J background were purchased from Hunan SJA Laboratory Co., Ltd. (Hunan, China) and housed under pathogen-free conditions pm a 12-h light/dark cycle. All animal protocols were approved by the Animal Care and Use Committee of Anhui Medical University.

To silence IL12p35 in vivo, adeno-associated viruses (AAVs) carrying IL12p35 shRNA (AAV-shIL12p35) and scramble RNA (AAV-shRNA) were constructed and generated by Shandong Vigenebio Co., Ltd. (Shandong, China). The mice were randomly assigned to two groups and received injections of AAV-shIL12p35 (1×1011 vector genomes) and AAV-shRNA (1×1011 vector genomes) via the tail vein. After 4 weeks, all mice were implanted with osmotic pumps and received a continuous subcutaneous infusion of angiotensin II (Ang II) or saline as described previously [22]. In brief, the animals were anesthetized and then placed in a prone position on a heating pad. Next, an Alzet osmotic pump (Model 2004, USA) loaded with Ang II (1.44 mg/kg per day, Calbiochem, USA) or saline was implanted subcutaneously in the nape of the neck. After 4 weeks, murine aortas and blood samples were collected to perform further analyses.

2.2. Ultrasonic Imaging. Upon completion of Ang II infusion, the mice were anesthetized, and ultrasound analysis of the abdominal aorta was performed using a Vevo 2100 System (Visual Sonics, Canada) equipped with a linear array ultrasound transducer. The maximum aortic diameters of the mice were measured three times by an investigator who was blinded to the group information.

2.3. Aneurysm Quantification. For aneurysm analysis, the aortas were isolated, and the periadventitial tissue was removed. The maximal aortic diameter was measured using the ImageJ software (NIH, USA). Aneurysm formation was identified as an enlargement >50% of the diameter compared with that of mice without Ang II infusion as described previously [23]. In addition, the incidence of aneurysms and the survival rate were monitored and calculated. Two colleagues who were blinded to the group information carried out the aneurysm quantification analysis.

2.4. Histological Analysis. Murine aortas were fixed with 4% paraformaldehyde and embedded in paraffin. Serial sections (7 μm) were created and analyzed as previously described [24]. Hematoxylin and eosin (H&E) staining was performed to assess aortic morphology. Elastin staining was performed to assess elastin degradation. In addition, a commercially available terminal deoxynucleotidyl transferase dUTP nick-end labeling (TUNEL) detection kit was used to assess SMC apoptosis.

2.5. Cell Culture and Treatments. Aortic SMCs were isolated from $Apoe^{-/-}$ mice and cultured in DMEM supplemented with 10% fetal bovine serum (FBS) as previously described [25]. Then, SMCs were transfected with si-IL12p35 in the presence or absence of Ang II (1 μmol/L) for 24 h. To knockdown STAT4, SMCs were transfected with si-STAT4 using Lipofectamine 2000 (Thermo Fisher Scientific, USA) in accordance with the manufacturer's instructions.

2.6. Quantitative Real-Time PCR (qRT-PCR). Total RNA was extracted from aortic tissues or cultured aortic SMCs using an RNeasy kit (Qiagen, Germany), and 2-μg aliquots of total RNA were used for first-strand cDNA synthesis using reverse transcriptase (TaKaRa, Japan) according to the manufacturer's recommendation. qRT-PCR was performed using a SYBR Green RT-PCR kit (TaKaRa, Japan), and β-actin was used to normalize gene expression. The primer sequences are shown in Table 1.

2.7. Western Blot Analysis. Total protein was extracted from abdominal aortic tissues or cultured aortic SMCs using RIPA buffer according to the manufacturer's instructions. Then, the protein samples were loaded onto SDS-PAGE gels and electrophoretically transferred to an Immobilon-P membrane. The membranes were probed with primary antibodies at 4°C overnight, after which the membranes were incubated with secondary antibodies. Finally, the membranes were visualized, and the density of each target protein band was normalized to the corresponding density of the β-actin band.

2.8. Enzyme-Linked Immunosorbent Assay (ELISA). Mouse blood was collected and separated by centrifugation to prepare serum. Then, the concentrations of IL-1β, IL-6, and tumor necrosis factor- (TNF-) α in the serum samples were measured using ELISA kits (Arigo Biolaboratories, China) according to the manufacturer's protocols.

2.9. Statistical Analysis. The data are presented as the means ± standard deviation (SD). Continuous data were examined by the Shapiro-Wilk test for normality. After confirming variance equality between different groups, statistical comparisons between 2 groups were performed using Student's t-tests, whereas significant comparisons between

Table 1: Primers used for qRT-PCR.

Gene	Direction	Primer
IL12p35	Forward	AGTTTGGCCAGGGTCATTCC
	Reverse	TCTCTGGCCGTCTTCACCAT
IL-1β	Forward	GCAACTGTTCCTGAACTCAACT
	Reverse	ATCTTTTGGGGTCCGTCAACT
IL-6	Forward	CTGCAAGAGACTTCCATCCAG
	Reverse	AGTGGTATAGACAGGTCTGTTGG
TNF-α	Forward	CCCTCACACTCAGATCATCTTCT
	Reverse	GCTACGACGTGGGCTACAG
β-Actin	Forward	TATTGGCAACGAGCGGTTCC
	Reverse	GGCATAGAGGTCTTTACGGATGT

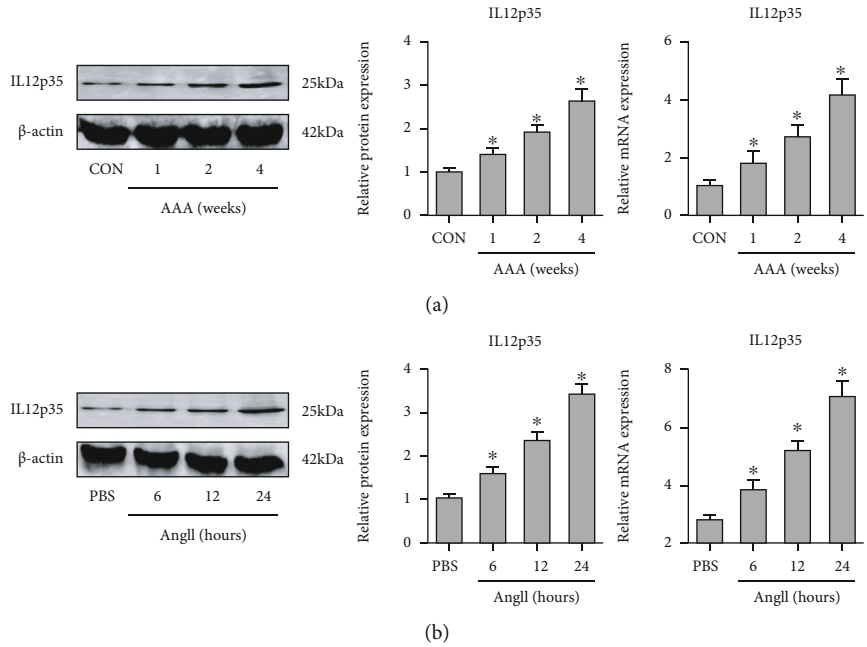

Figure 1: IL12p35 expression is increased in the murine AAA aorta and isolated aortic SMCs. (a) Western blots and PCR analysis of IL12p35 expression in murine aortic samples ($n = 5$ per group). (b) Western blots and PCR analysis of IL12p35 expression in isolated aortic SMCs ($n = 5$ per group). $^*P < 0.05$, compared with the control or PBS group.

multiple groups were performed using one-way analysis of variance (ANOVA)with post hoc Bonferroni's tests. For variables with a nonnormal distribution, the nonparametric Mann–Whitney U test was performed to assess the differences between the 2 groups. In addition, the AAA incidence in each group was compared using Fisher's exact test. Kaplan-Meier analysis was performed to assess the survival rate using the log-rank test. P values less than 0.05 were considered significant.

3. Results

3.1. IL12p35 Expression Is Increased in Murine AAA Aorta and Isolated Aortic SMCs. We first examined IL12p35 expression in the murine AAA aorta and aortic SMCs. IL12p35 protein levels were progressively elevated in the aorta from 1 to 4 weeks after Ang II infusion in the experimental AAA model mice compared with control mice (1.4-, 1.9-, and 2.6-fold at 1, 2, and 4 weeks, respectively) (Figure 1(a)). In addition, IL12p35 mRNA levels gradually increased in murine AAA aorta (Figure 1(a)). Consistent with this finding, increased IL12p35 levels were also detected in isolated aortic SMCs after Ang II stimulation (Figure 1(b)).

3.2. IL12p35 Silencing Promotes Ang II-Induced AAA Formation and Rupture. To investigate the functional role of IL12p35 in AAA, the mice were given injections of AAV-shIL12p35 via the tail vein to silence IL12p35 in vivo (Figure 2(a)). After 4 weeks of chronic Ang II infusion, aortic rupture-induced mortality was higher in the AAV-shIL12p35 group than in the AAV-shRNA group (40.0% versus 16.0%) (Figure 2(b)). The AAA incidence was higher in the AAV-shIL12p35 group than in the AAV-shRNA group after Ang II infusion (84.0% versus 52.0%) (Figure 2(c)). In

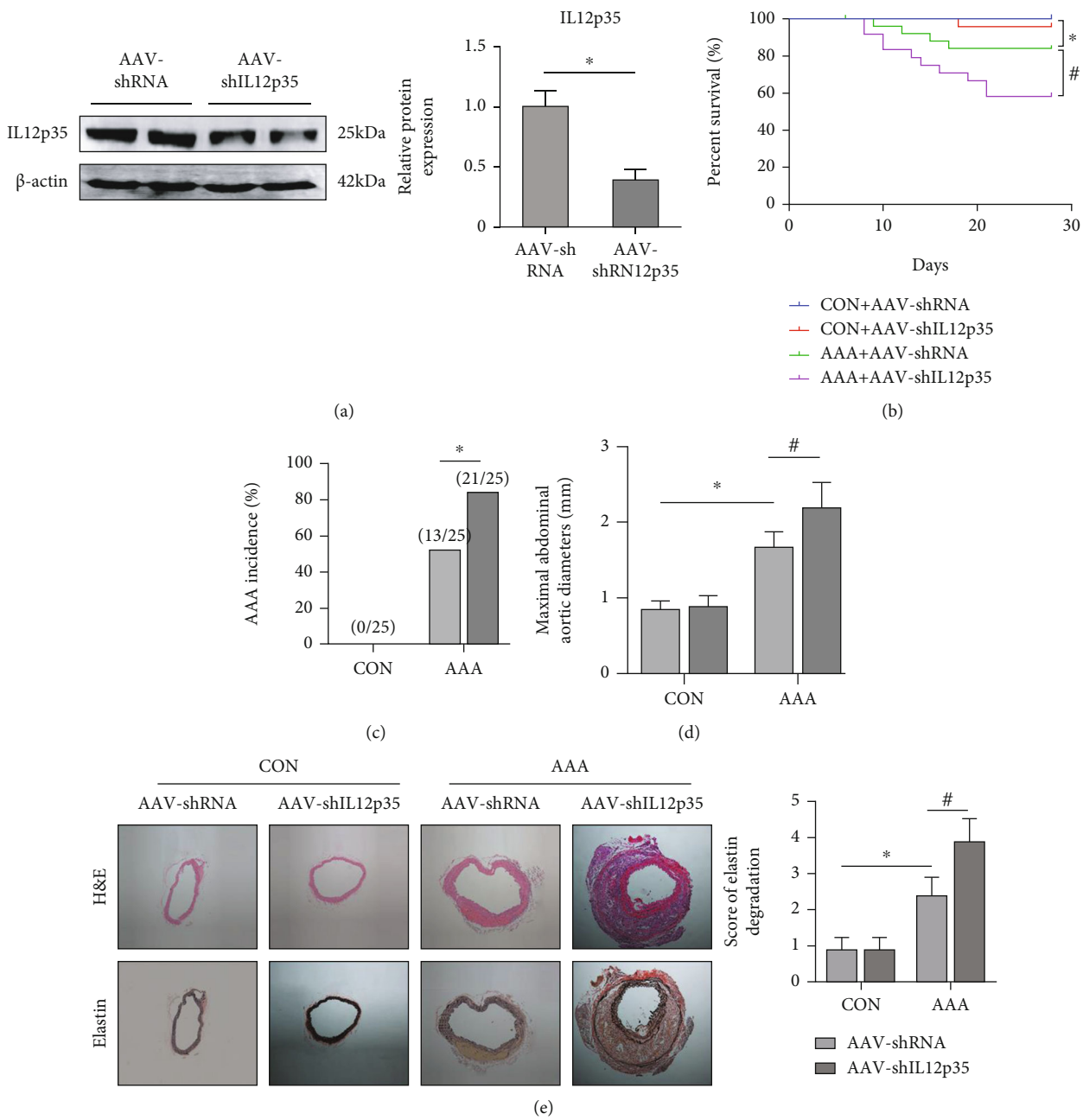

Figure 2: IL12p35 silencing promotes Ang II-induced AAA formation and rupture. (a) Western blot analysis of IL12p35 expression after AAV-shIL12p35 injection in mice ($n = 5$ per group). (b) The survival curves of mice in the four groups ($n = 25$ per group). (c) The rupture rates of mice in the four groups ($n = 25$ per group). (d) Maximal abdominal aortic diameters of mice in the four groups ($n = 10$ per group). (e) Representative H&E and elastin staining in the four groups of mice ($n = 8$ per group). $^{*}P < 0.05$ compared with the control group; $^{\#}P < 0.05$ compared with the AAA group.

addition, IL12p35 silencing also increased the maximal aortic diameter and elastin degradation score after Ang II infusion (Figures 2(d) and 2(e)).

3.3. IL12p35 Silencing Exacerbates the Inflammatory Response after Ang II Infusion. Compared with those in the control group, serum concentrations of inflammatory cytokines, including IL-1β, IL-6, and TNF-α, in the AAA group were significantly increased, while IL12p35 silencing further increased the serum levels of these cytokines (Figures 3(a)–3(c)). Furthermore, IL12p35 silencing also increased the mRNA expression of IL-1β, IL-6, and TNF-α in aortic tissues after Ang II infusion (Figures 3(d)–3(f)).

3.4. IL12p35 Silencing Exacerbates SMC Apoptosis after Ang II Infusion. The TUNEL staining results showed that IL12p35 silencing further increased SMC apoptosis after Ang II infusion (Figure 4(a)). The Western blot results also showed that the expression of Bcl-2 was significantly decreased and that the expression of Bax was significantly

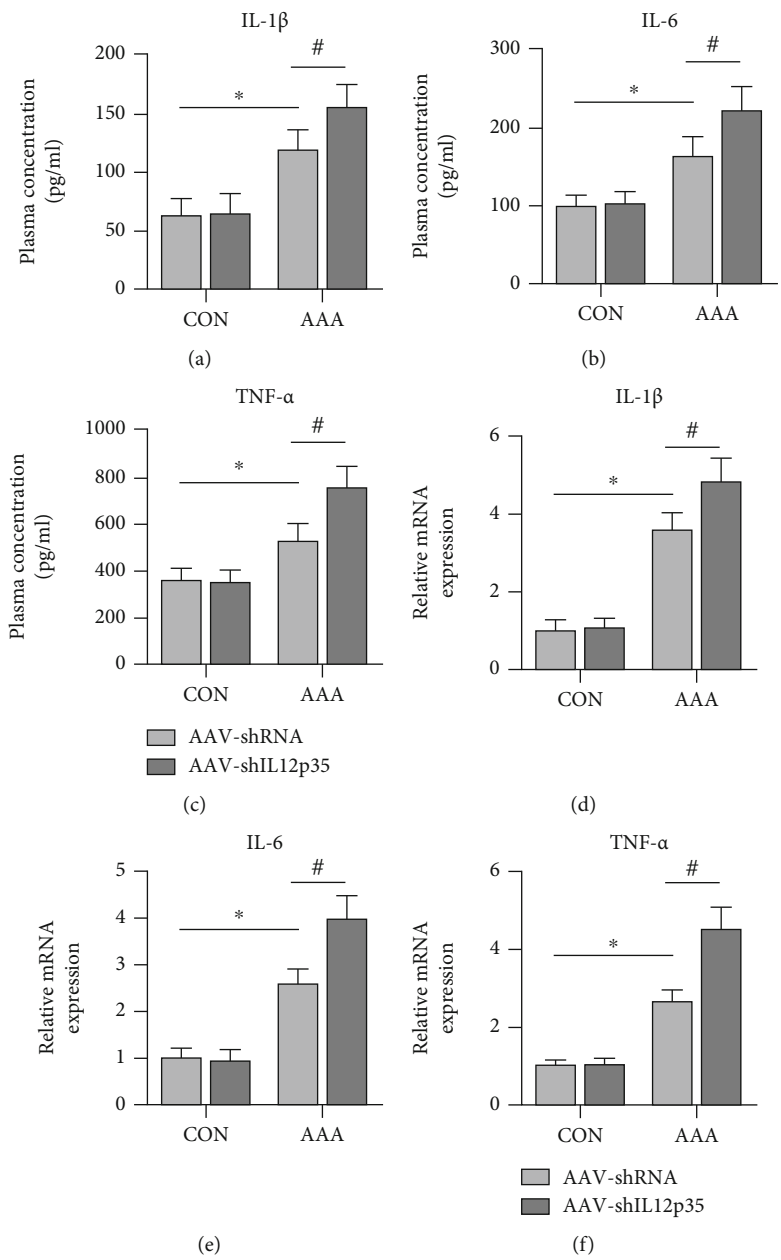

Figure 3: IL12p35 silencing exacerbates the inflammatory response after Ang II infusion. (a–c) ELISA analysis of serum IL-1β, IL-6, and TNF-α levels of mice in the four groups ($n = 8$ per group). (d–f) PCR analysis of IL-1β, IL-6, and TNF-α mRNA expression in murine aortic samples ($n = 8$ per group). $^{*}P < 0.05$ compared with the control group; $^{\#}P < 0.05$ compared with the AAA group.

increased in the AAA group compared with the control group (Figure 4(b)). However, IL12p35 silencing further reduced Bcl-2 expression and increased Bax expression after Ang II infusion (Figure 4(b)).

3.5. IL12p35 Silencing Activates the STAT4 Signaling Pathway. We further investigated the molecular mechanisms by which IL12p35 affected the development of AAA. The results showed that Ang II infusion significantly increased the phosphorylation of STAT1 (2.3-fold), STAT3 (2.1-fold), STAT4 (1.9-fold), and STAT5 (1.9-fold) (Figures 5(a)–5(d)). In addition, IL12p35 silencing further increased the expression of p-STAT4 (2.9-fold) but did not affect the expression of p-STAT1, p-STAT3, or p-STAT5 (Figure 5(a)–5(d)).

3.6. IL12p35 Silencing Exacerbates the Ang II-Induced Inflammatory Response and SMC Apoptosis. To investigate the functional role of IL12p35 in AAA, SMCs were transfected with si-IL12p35 to silence IL12p35 (Figure 6(a)). The results showed that Ang II stimulation significantly increased the mRNA expression of IL-1β, IL-6, and TNF-α, while IL12p35 silencing further increased the expression of those inflammatory markers (Figures 6(b)–6(d)). In addition,

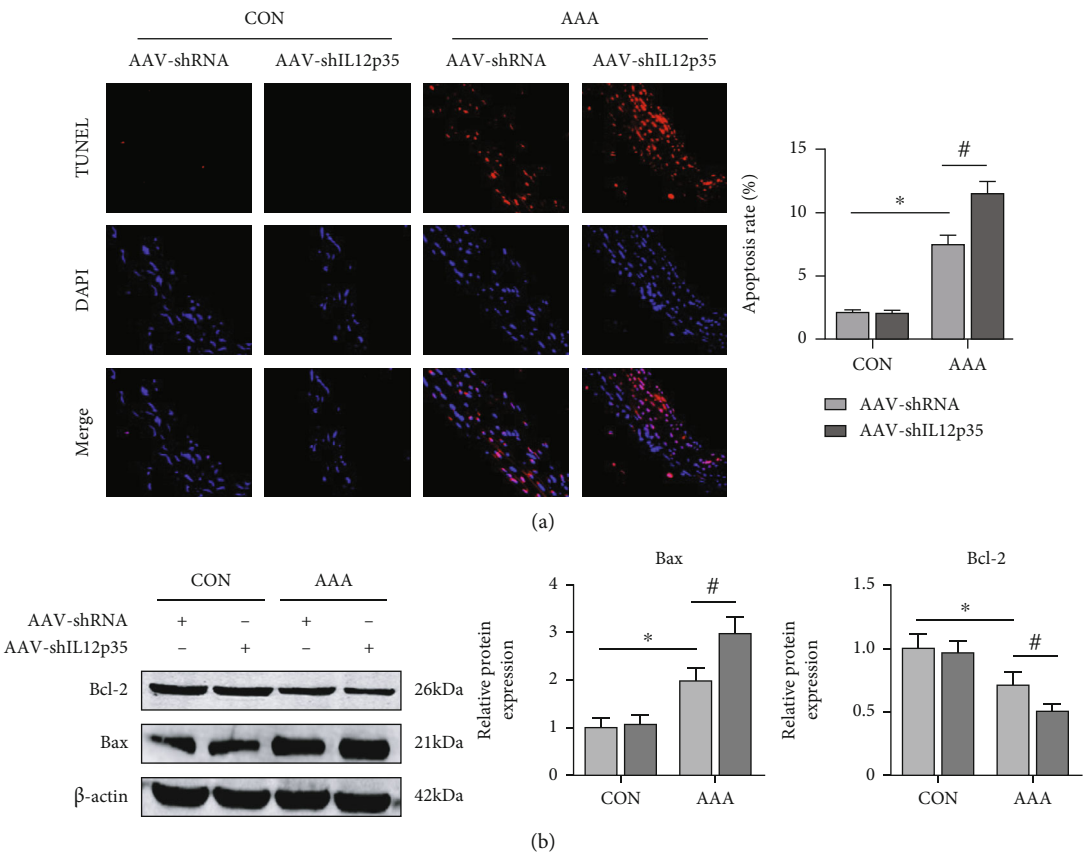

Figure 4: IL12p35 silencing exacerbates SMC apoptosis after Ang II infusion. (a) Representative TUNEL staining in the four groups of mice ($n = 8$ per group). (b) Western blot analysis of the protein levels of Bcl-2 and Bax in the aortas of the four groups ($n = 5$ per group). $^{*}P < 0.05$ compared with the control group; $^{\#}P < 0.05$ compared with the AAA group.

IL12p35 silencing further significantly enhanced Ang II-induced SMC apoptosis by decreasing Bcl-2 expression and increasing Bax expression (Figure 6(e)).

3.7. STAT4 Silencing Abolishes IL12p35-Mediated Inflammatory Responses and SMC Apoptosis. To further confirm the effect of the STAT4 signaling pathway on IL12p35-mediated inflammatory responses and SMC apoptosis, cells were transfected with si-STAT4 to silence STAT4 expression in vitro (Figure 7(a)). The results showed that STAT4 silencing abolished the IL12p35-mediated proinflammatory effects by decreasing IL-1β, IL-6, and TNF-α mRNA expression (Figures 7(b)–7(d)). In addition, STAT4 silencing attenuated IL12p35-mediated SMC apoptosis by increasing Bcl-2 expression and decreasing Bax expression (Figure 7(e)).

4. Discussion

In the present study, we identified the role of IL12p35 in exacerbating the growth and rupture of AAA. We provided direct evidence that IL12p35 expression was noticeably increased in the murine AAA aorta and aortic SMCs after Ang II stimulation. In addition, IL12p35 silencing promoted Ang II-induced AAA formation and rupture in Apoe$^{-/-}$ mice by activating the inflammatory response and SMC apoptosis. Moreover, the deterioration caused by IL12p35 silencing was associated with STAT4 activation. These findings suggest that IL12p35 could be a promising target to control the progression of AAA.

In our study, the murine AAA model was induced by subcutaneous infusion of Ang II into Apoe$^{-/-}$ mice for 4 weeks. This model mimics some of the pathological features of human AAA, such as aortic rupture, inflammation, and important risk factors, and it is also technically appropriate for operations [26, 27]. Based on these advantages, this has become one of the main methods used to induce AAA in mice [28, 29]. In the present study, we successfully established an AAA model in Apoe$^{-/-}$ mice, and the results showed that IL12p35 expression was noticeably increased in the murine AAA aorta and isolated aortic SMCs after Ang II stimulation. To further investigate the role of IL12p35 in the development of AAA, we utilized AAV transfection to silence IL12p35 expression in AAA mice, and the results showed that silencing IL12p35 increased AAA formation and rupture-induced mortality. In addition, IL12p35 silencing also increased the maximal aortic diameter and elastin degradation score after Ang II infusion.

Although the pathogenesis of AAA is complex, inflammatory responses have been proven to be crucial in the formation of AAA [30, 31]. Many clinical studies and animal experiments have confirmed that extensive inflammatory cell infiltration occurs in both the media and adventitia and is

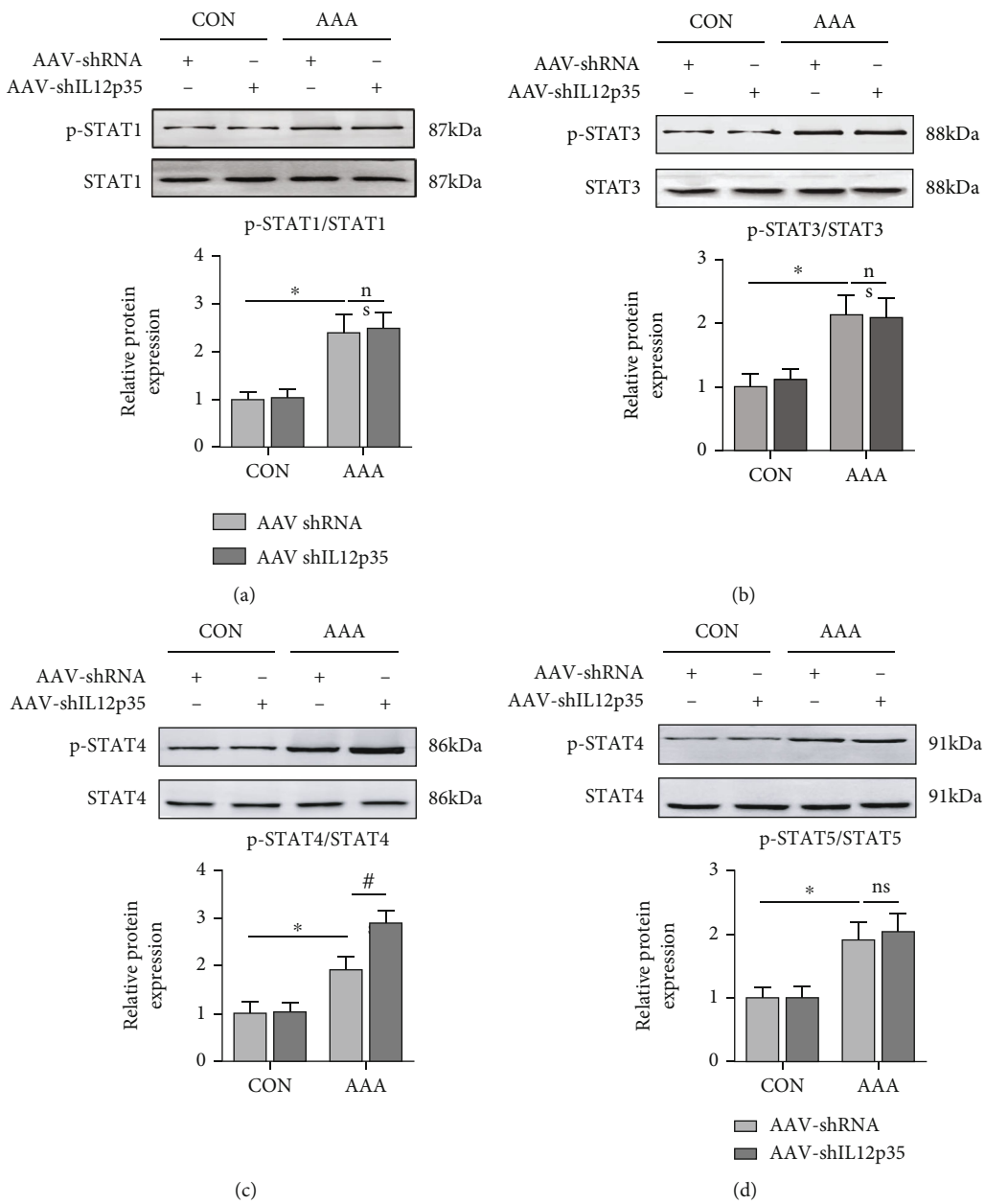

Figure 5: IL12p35 silencing activates the STAT4 signaling pathway. (a–d) Western blot analysis of the protein levels of p-STAT1, STAT1, p-STAT3, STAT3, p-STAT4, STAT4, p-STAT5, and STAT5 in the aortas of the four groups ($n = 5$ per group). $^{*}P < 0.05$ compared with the control group; $^{\#}P < 0.05$ compared with the AAA group.

associated with increased aneurysm diameter [32, 33]. In addition, these infiltrating cells also secrete various inflammatory cytokines, such as IL-1β[34], IL-6 [35], and TNF-α [36], which further drive inflammatory responses and ultimately lead to AAA rupture. Studies have suggested that reducing the activation of these proinflammatory cytokines could inhibit the formation and progression of AAA [34–37]. Thus, it is clear that therapeutic drugs targeting the inflammatory response can be very effective in improving AAA.

Current literatures have described that IL12p35 is an important inflammation-related cytokines involved in the regulation of several inflammation-related diseases [38]. Thus, we investigated the effect of IL12p35 silencing on the inflammatory response in the development of AAA. In line with data from previous research, our results showed that serum and aortic levels of IL-1β, IL-6, and TNF-α in the AAA group were significantly increased compared with those in the control group, while IL12p35 silencing further increased the expression of these cytokines. In addition, IL12p35 silencing also increased the IL-1β, IL-6, and TNF-α levels in isolated aortic SMCs after Ang II stimulation. These results suggested that IL12p35 silencing promotes Ang II-induced AAA formation by exacerbating the inflammatory response.

SMCs are one of the most important cellular components of the aortic wall and play a pivotal role in maintaining

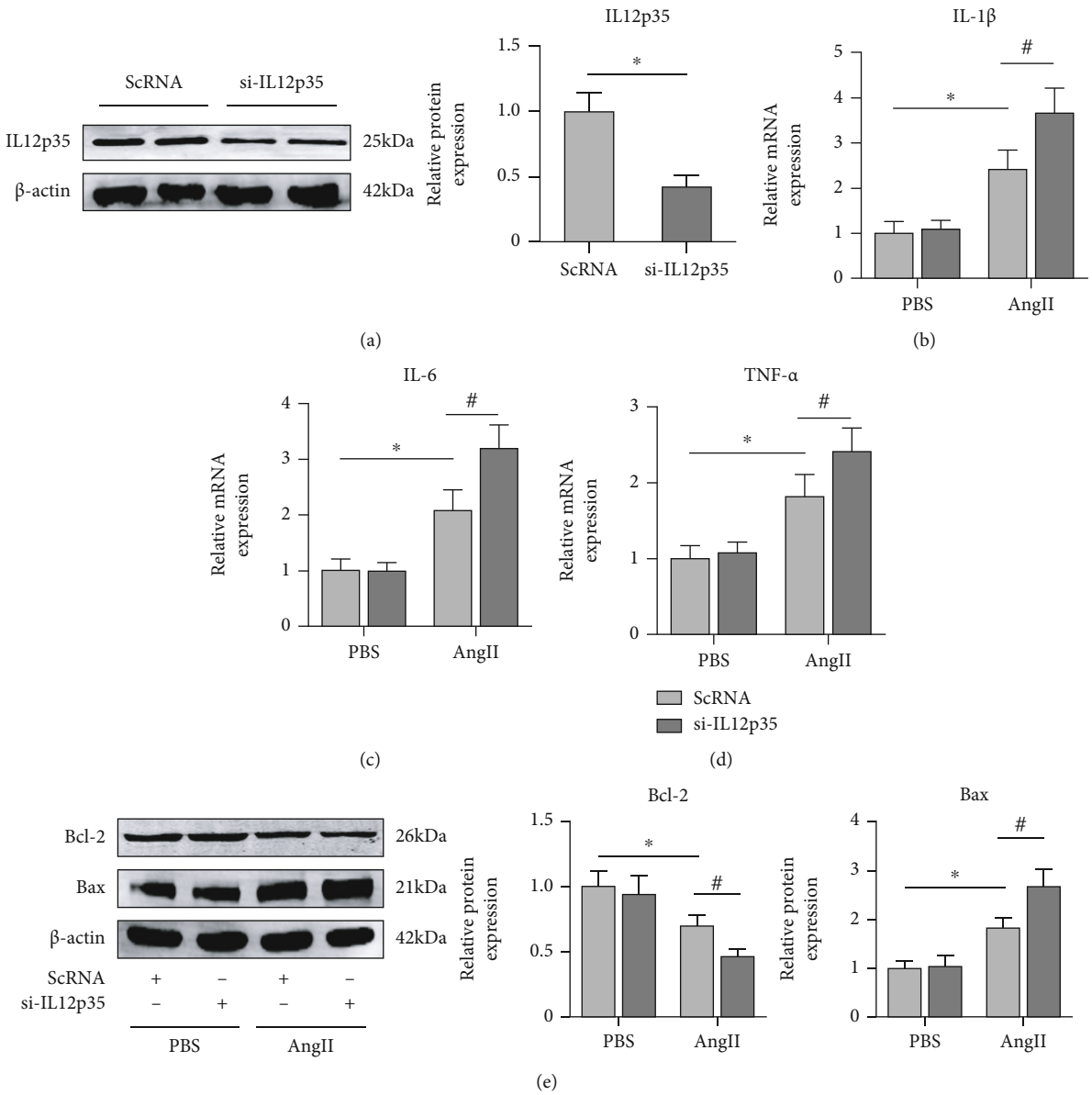

Figure 6: IL12p35 silencing exacerbates the Ang II-induced inflammatory response and SMC apoptosis. (a) Western blot analysis of IL12p35 expression after transfection with si-IL12p35 ($n = 5$ per group). (b–d) PCR analysis of IL-1β, IL-6, and TNF-α mRNA expression in the four groups ($n = 6$ per group). (e) Western blot analysis of the protein levels of Bcl-2 and Bax in the four groups ($n = 5$ per group). $^{*}P < 0.05$ compared with the PBS group; $^{\#}P < 0.05$ compared with the Ang II group.

normal aortic structure and homeostasis [39]. SMCs can synthesize and secrete extracellular matrix proteins and induce aortic wall remodeling in response to increased hemodynamic pressure [39, 40]. A large number of studies have shown that AAA formation is associated with the loss of SMCs due to enhanced apoptosis [41]. In addition, the inflammatory response has been shown to be responsible for SMC apoptosis [42]. Thus, we examined whether IL12p35 affected SMC apoptosis during the development of AAA. The results indicated that the expression of Bax was upregulated and that the expression of Bcl-2 was lower in the AAA group than in the control group. The TUNEL staining results also showed that the apoptosis rates of SMCs in the AAA group were significantly increased compared with those in the control group, and these effects were further augmented by IL12p35 silencing. In addition, these results further confirmed the in vitro results, indicating that the effect of IL12p35 silencing was associated with exacerbation of SMC apoptosis.

Signaling through the STAT pathway is an important regulator of vascular diseases, including hypertension [43], atherosclerosis [44], pulmonary hypertension [45], and AAA [46]. An accumulating body of evidence has indicated that STAT signaling is activated during the early stage of AAA and mediates the inflammatory response, oxidative stress, and SMC apoptosis [47, 48]. Extensive data have also

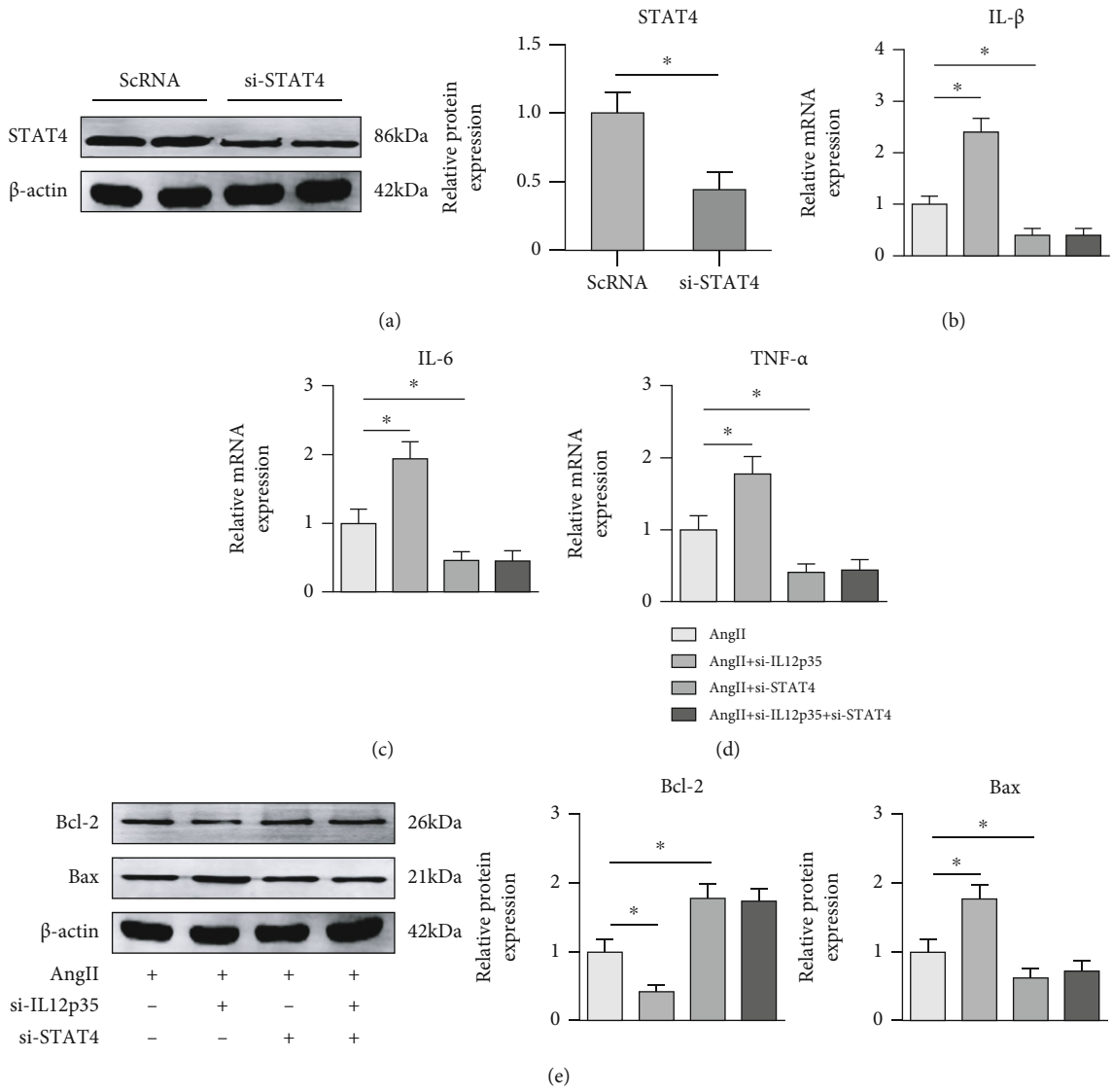

Figure 7: STAT4 silencing abolishes IL12p35-mediated inflammatory responses and SMC apoptosis. (a) Western blot analysis of STAT4 expression after transfection with si-STAT4 ($n = 4$ per group). (b–d) PCR analysis of IL-1β, IL-6, and TNF-α mRNA expression in the four groups ($n = 6$ per group). (e) Western blot analysis of the protein levels of Bcl-2 and Bax in the four groups ($n = 4$ per group). $^*P < 0.05$ compared with the Ang II group.

demonstrated that the biological effect mediated by IL-12 is closely associated with STAT signaling, including STAT1, STAT3, STAT4, and STAT5 [49, 50]. Thus, we examined whether IL12p35 affected specific STAT transcription factors during the development of AAA. In the present study, we found that IL12p35 silencing did not affect STAT1, STAT3, or STAT5 phosphorylation but induced STAT4 phosphorylation during the development of AAA. Moreover, STAT4 knockdown nearly abolished the IL12p35 silencing-induced increase in the inflammatory response and SMC apoptosis after Ang II stimulation. Taken together, these results showed that STAT4 activation is critical for IL12p35 silencing-mediated inflammatory responses and SMC apoptosis, which may contribute to AAA formation and rupture.

In summary, our work provides preliminary evidence clarifying the role of IL12p35 in the development of AAA. Silencing of IL12p35 increased AAA formation and rupture in Apoe$^{-/-}$ mice by activating the STAT4 pathway. Our findings suggest that IL12p35 may serve as a novel and promising therapeutic target for AAA treatment.

Data Availability

The datasets generated and/or analyzed during the current study are available from the corresponding author on reasonable request in compliance with ethical standards.

Conflicts of Interest

The authors declare that they have no conflicts of interest.

Acknowledgments

This study was supported by a grant from the Major Special Science and Technology Project of Anhui Province (No.18030801134).

References

[1] N. Sakalihasan, R. Limet, and O. D. Defawe, "Abdominal aortic aneurysm," *Lancet*, vol. 365, no. 9470, pp. 1577–1589, 2005.

[2] D. Martinez-Lopez, E. Camafeita, L. Cedo et al., "APOA1 oxidation is associated to dysfunctional high-density lipoproteins in human abdominal aortic aneurysm," *eBioMedicine*, vol. 43, pp. 43–53, 2019.

[3] J. Golledge, "Abdominal aortic aneurysm: update on pathogenesis and medical treatments," *Nature Reviews. Cardiology*, vol. 16, no. 4, pp. 225–242, 2019.

[4] U. K. Sampson, P. E. Norman, F. G. Fowkes et al., "Global and regional burden of aortic dissection and aneurysms: mortality trends in 21 world regions, 1990 to 2010," *Global Heart*, vol. 9, no. 1, pp. 171–180, 2014.

[5] E. Bossone and K. A. Eagle, "Epidemiology and management of aortic disease: aortic aneurysms and acute aortic syndromes," *Nature Reviews Cardiology*, vol. 18, no. 5, pp. 331–348, 2021.

[6] L. Zhong, X. He, H. Song et al., "METTL3 induces AAA development and progression by modulating N6-methyladenosine-dependent primary miR34a processing," *Molecular Therapy - Nucleic Acids*, vol. 21, pp. 394–411, 2020.

[7] A. Kopacz, E. Werner, A. Grochot-Przęczek et al., "Simvastatin Attenuates Abdominal Aortic Aneurysm Formation Favoured by Lack of Nrf2 Transcriptional Activity," *Oxidative Medicine and Cellular Longevity*, vol. 2020, Article ID 6340190, 16 pages, 2020.

[8] X. Xu, F. Zhang, Y. Lu et al., "Silencing of NONO inhibits abdominal aortic aneurysm in apolipoprotein E-knockout mice via collagen deposition and inflammatory inhibition," *Journal of Cellular and Molecular Medicine*, vol. 23, no. 11, pp. 7449–7461, 2019.

[9] R. A. Quintana and W. R. Taylor, "Cellular mechanisms of aortic aneurysm formation," *Circulation Research*, vol. 124, no. 4, pp. 607–618, 2019.

[10] A. Lopez-Candales, D. R. Holmes, S. Liao, M. J. Scott, S. A. Wickline, and R. W. Thompson, "Decreased vascular smooth muscle cell density in medial degeneration of human abdominal aortic aneurysms," *The American Journal of Pathology*, vol. 150, no. 3, pp. 993–1007, 1997.

[11] H. Chai, Z. H. Tao, Y. C. Qi et al., "IKK epsilon deficiency attenuates angiotensin II-induced abdominal aortic aneurysm formation in mice by inhibiting inflammation, oxidative stress, and apoptosis," *Oxidative Medicine and Cellular Longevity*, vol. 2020, Article ID 3602824, 16 pages, 2020.

[12] P. Ren, D. Wu, R. Appel et al., "Targeting the NLRP3 inflammasome with inhibitor MCC950 prevents aortic aneurysms and dissections in mice," *Journal of the American Heart Association*, vol. 9, no. 7, article e014044, 2020.

[13] G. Trinchieri, "Interleukin-12 and the regulation of innate resistance and adaptive immunity," *Nature Reviews. Immunology*, vol. 3, no. 2, pp. 133–146, 2003.

[14] M. W. Teng, E. P. Bowman, J. J. McElwee et al., "IL-12 and IL-23 cytokines: from discovery to targeted therapies for immune- mediated inflammatory diseases," *Nature Medicine*, vol. 21, no. 7, pp. 719–729, 2015.

[15] D. Bastian, Y. Wu, B. C. Betts, and X. Z. Yu, "The IL-12 cytokine and receptor family in graft-vs.-host disease," *Frontiers in Immunology*, vol. 10, p. 988, 2019.

[16] D. A. Vignali and V. K. Kuchroo, "IL-12 family cytokines: immunological playmakers," *Nature Immunology*, vol. 13, no. 8, pp. 722–728, 2012.

[17] M. V. Zykov, O. L. Barbarash, V. V. Kashtalap, A. G. Kutikhin, and L. S. Barbarash, "Interleukin-12 serum level has prognostic value in patients with ST-segment elevation myocardial infarction," *Heart & Lung*, vol. 45, no. 4, pp. 336–340, 2016.

[18] R. Posadas-Sanchez and G. Vargas-Alarcon, "Innate immunity in coronary disease. The role of interleukin-12 cytokine family in atherosclerosis," *Revista de Investigación Clínica*, vol. 70, no. 1, pp. 5–17, 2018.

[19] J. Ye, Y. Wang, Z. Wang et al., "The expression of IL-12 family members in patients with hypertension and its association with the occurrence of carotid atherosclerosis," *Mediators of Inflammation*, vol. 2020, Article ID 2369279, 10 pages, 2020.

[20] N. Sharma, R. Dev, A. M. Belenchia et al., "Deficiency of IL12p40 (interleukin 12 p 40) promotes Ang II (angiotensin II)-induced abdominal aortic aneurysm," *Arteriosclerosis, Thrombosis, and Vascular Biology*, vol. 39, no. 2, pp. 212–223, 2019.

[21] N. Sharma and C. P. Hans, "Interleukin 12p40 deficiency promotes abdominal aortic aneurysm by activating CCN2/MMP2 pathways," *Journal of the American Heart Association*, vol. 10, no. 3, article e017633, 2021.

[22] X. Meng, J. Yang, K. Zhang et al., "Regulatory T cells prevent angiotensin II-induced abdominal aortic aneurysm in apolipoprotein E knockout mice," *Hypertension*, vol. 64, no. 4, pp. 875–882, 2014.

[23] X. Qin, L. He, M. Tian et al., "Smooth muscle-specific Gsα deletion exaggerates angiotensin II-induced abdominal aortic aneurysm formation in mice in vivo," *Journal of Molecular and Cellular Cardiology*, vol. 132, pp. 49–59, 2019.

[24] F. Xue, J. Yang, J. Cheng et al., "Angiotensin-(1-7) mitigated angiotensin II-induced abdominal aortic aneurysms in apolipoprotein E-knockout mice," *British Journal of Pharmacology*, vol. 177, no. 8, pp. 1719–1734, 2020.

[25] J. Kong, K. Zhang, X. Meng, Y. Zhang, and C. Zhang, "Dose-dependent bidirectional effect of angiotensin IV on abdominal aortic aneurysm via variable angiotensin receptor stimulation," *Hypertension*, vol. 66, no. 3, pp. 617–626, 2015.

[26] H. Li, X. Qin, J. Yang et al., "Smooth muscle-specific LKB1 deletion exaggerates angiotensin II-induced abdominal aortic aneurysm in mice," *Journal of Molecular and Cellular Cardiology*, vol. 130, pp. 131–139, 2019.

[27] S. Wang, C. Zhang, M. Zhang et al., "Activation of AMP-activated protein kinase α2 by nicotine instigates formation of abdominal aortic aneurysms in mice in vivo," *Nature Medicine*, vol. 18, no. 6, pp. 902–910, 2012.

[28] H. Song, T. Xu, X. Feng et al., "Itaconate prevents abdominal aortic aneurysm formation through inhibiting inflammation via activation of Nrf2," *eBioMedicine*, vol. 57, p. 102832, 2020.

[29] X. Chen, Y. Li, J. Xiao et al., "Modulating neuro-immune-induced macrophage polarization with topiramate attenuates experimental abdominal aortic aneurysm," *Frontiers in Pharmacology*, vol. 11, p. 565461, 2020.

[30] X. Meng, J. Yang, M. Dong et al., "Regulatory T cells in cardiovascular diseases," *Nature Reviews. Cardiology*, vol. 13, no. 3, pp. 167–179, 2016.

[31] J. Kong, Y. Zhang, S. Liu et al., "Melatonin attenuates angiotensin II-induced abdominal aortic aneurysm through the down-regulation of matrix metalloproteinases," *Oncotarget*, vol. 8, no. 9, pp. 14283–14293, 2017.

[32] I. O. Peshkova, G. Schaefer, and E. K. Koltsova, "Atherosclerosis and aortic aneurysm – is inflammation a common denominator?," *The FEBS Journal*, vol. 283, no. 9, pp. 1636–1652, 2016.

[33] M. A. Dale, M. K. Ruhlman, and B. T. Baxter, "Inflammatory cell phenotypes in AAAs: their role and potential as targets for therapy," *Arteriosclerosis, Thrombosis, and Vascular Biology*, vol. 35, no. 8, pp. 1746–1755, 2015.

[34] A. K. Meher, M. Spinosa, J. P. Davis et al., "Novel role of IL (interleukin)-1β in neutrophil extracellular trap formation and abdominal aortic aneurysms," *Arteriosclerosis, Thrombosis, and Vascular Biology*, vol. 38, no. 4, pp. 843–853, 2018.

[35] M. Nishihara, H. Aoki, S. Ohno et al., "The role of IL-6 in pathogenesis of abdominal aortic aneurysm in mice," *PLoS One*, vol. 12, no. 10, article e185923, 2017.

[36] R. Batra, M. K. Suh, J. S. Carson et al., "IL-1β (interleukin-1β) and TNF-α (tumor necrosis factor-α) impact abdominal aortic aneurysm formation by differential effects on macrophage polarization," *Arteriosclerosis, Thrombosis, and Vascular Biology*, vol. 38, no. 2, pp. 457–463, 2018.

[37] D. Yan, H. Ma, W. Shi et al., "Bazedoxifene attenuates abdominal aortic aneurysm formation via downregulation of interleukin-6/glycoprotein 130/signal transducer and activator of transcription 3 signaling pathway in apolipoprotein E-knockout mice," *Frontiers in Pharmacology*, vol. 11, p. 392, 2020.

[38] I. M. Dambuza, C. He, J. K. Choi et al., "IL-12p35 induces expansion of IL-10 and IL-35-expressing regulatory B cells and ameliorates autoimmune disease," *Nature Communications*, vol. 8, no. 1, p. 719, 2017.

[39] R. Chakraborty, F. Z. Saddouk, A. C. Carrao, D. S. Krause, D. M. Greif, and K. A. Martin, "Promoters to study vascular smooth muscle," *Arteriosclerosis, Thrombosis, and Vascular Biology*, vol. 39, no. 4, pp. 603–612, 2019.

[40] A. Frismantiene, M. Philippova, P. Erne, and T. J. Resink, "Smooth muscle cell-driven vascular diseases and molecular mechanisms of VSMC plasticity," *Cellular Signalling*, vol. 52, pp. 48–64, 2018.

[41] R. W. Thompson, S. Liao, and J. A. Curci, "Vascular smooth muscle cell apoptosis in abdominal aortic aneurysms," *Coronary Artery Disease*, vol. 8, no. 10, pp. 623–632, 1997.

[42] M. C. Clarke, S. Talib, N. L. Figg, and M. R. Bennett, "Vascular smooth muscle cell apoptosis induces interleukin-1-directed inflammation: effects of hyperlipidemia-mediated inhibition of phagocytosis," *Circulation Research*, vol. 106, no. 2, pp. 363–372, 2010.

[43] A. W. Johnson, D. A. Kinzenbaw, M. L. Modrick, and F. M. Faraci, "Small-molecule inhibitors of signal transducer and activator of transcription 3 protect against angiotensin II-induced vascular dysfunction and hypertension," *Hypertension*, vol. 61, no. 2, pp. 437–442, 2013.

[44] N. Adhikari, N. Charles, U. Lehmann, and J. L. Hall, "Transcription factor and kinase-mediated signaling in atherosclerosis and vascular injury," *Current Atherosclerosis Reports*, vol. 8, no. 3, pp. 252–260, 2006.

[45] D. Yerabolu, A. Weiss, B. Kojonazarov et al., "Targeting Jak-Stat signaling in experimental pulmonary hypertension," *American Journal of Respiratory Cell and Molecular Biology*, vol. 64, no. 1, pp. 100–114, 2021.

[46] M. Liao, J. Xu, A. J. Clair, B. Ehrman, L. M. Graham, and M. J. Eagleton, "Local and systemic alterations in signal transducers and activators of transcription (STAT) associated with human abdominal aortic aneurysms," *The Journal of Surgical Research*, vol. 176, no. 1, pp. 321–328, 2012.

[47] J. Xiao, Z. Wei, X. Chen et al., "Experimental abdominal aortic aneurysm growth is inhibited by blocking the JAK2/STAT3 pathway," *International Journal of Cardiology*, vol. 312, pp. 100–106, 2020.

[48] M. J. Eagleton, J. Xu, M. Liao, B. Parine, G. M. Chisolm, and L. M. Graham, "Loss of STAT1 is associated with increased aortic rupture in an experimental model of aortic dissection and aneurysm formation," *Journal of Vascular Surgery*, vol. 51, no. 4, pp. 951–961, 2010, 961.

[49] W. T. Watford, B. D. Hissong, J. H. Bream, Y. Kanno, L. Muul, and J. J. O'Shea, "Signaling by IL-12 and IL-23 and the immunoregulatory roles of STAT4," *Immunological Reviews*, vol. 202, no. 1, pp. 139–156, 2004.

[50] E. D. Tait Wojno, C. A. Hunter, and J. S. Stumhofer, "The Immunobiology of the interleukin-12 family: room for discovery," *Immunity*, vol. 50, no. 4, pp. 851–870, 2019.

Hindawi
Mediators of Inflammation
Volume 2021, Article ID 4977209, 9 pages
https://doi.org/10.1155/2021/4977209

Review Article

Cardiovascular Effects Mediated by HMMR and CD44

Kinga Jaskuła,[1] Mariusz Sacharczuk,[1,2] Zbigniew Gaciong,[3] and Dominik S. Skiba[1]

[1]*Department of Experimental Genomics, Institute of Genetics and Animal Biotechnology, Polish Academy of Sciences, Postępu 36A, Jastrzebiec, Poland*
[2]*Faculty of Pharmacy with the Laboratory Medicine Division, Department of Pharmacodynamics, Medical University of Warsaw, Centre for Preclinical Research and Technology, Banacha 1B, Warsaw, Poland*
[3]*Department of Internal Medicine, Hypertension and Vascular Diseases, Medical University of Warsaw, Banacha 1A, Warsaw, Poland*

Correspondence should be addressed to Dominik S. Skiba; d.skiba@igbzpan.pl

Received 27 May 2021; Accepted 7 June 2021; Published 10 July 2021

Academic Editor: Elena Dozio

Cardiovascular disease (CVD) is the leading cause of death worldwide. The most dangerous life-threatening symptoms of CVD are myocardial infarction and stroke. The causes of CVD are not entirely clear, and new therapeutic targets are still being sought. One of the factors involved in CVD development among vascular damage and oxidative stress is chronic inflammation. It is known that hyaluronic acid plays an important role in inflammation and is regulated by numerous stimuli, including proinflammatory cytokines. The main receptors for hyaluronic acid are CD44 and RHAMM. These receptors are membrane proteins that differ in structure, but it seems that they can perform similar or synergistic functions in many diseases. Both RHAMM and CD44 are involved in cell migration and wound healing. However, their close association with CVD is not fully understood. In this review, we describe the role of both receptors in CVD.

1. Introduction

Cardiovascular disease (CVD) is a main cause of death globally, causing an estimated 17.9 million deaths annually. CVD is a general term for a group of heart and blood vessel diseases including coronary heart disease, cerebrovascular disease, and peripheral arterial disease. Late manifestations of CVD are heart attack and stroke mainly caused by previous vascular damage. Chronic inflammation is one of the causes of vascular damage or narrowing [1]. CD44 plays an important role in both inflammation and vascular injury [2]. Inflammation is associated with increased vascular permeability, recruitment of inflammatory cells, and release of inflammatory mediators. The cascade of inflammatory reactions can alter blood flow in the altered tissues by inflammatory cells infiltrating vascular tissues and releasing proteases, cytokines, and reactive oxygen species, which trigger vasoconstriction or relaxation [3], neointimal growth [4], and angiogenesis and tissue remodeling [5, 6]. The main ligand for the CD44 receptor is hyaluronic acid (HA) which binds also to RHAMM (hyaluronan-mediated motility receptor) [7]. HA is regulated by numerous stimuli, including proinflammatory cytokines [8]. Thus, the local production of cytokines within inflammatory lesions in the vessels increases the expression of HA on endothelial cells facilitating CD44-HA interactions and hence causing extravasation of inflammatory cells [9]. The role of CD44 in cardiovascular disease is well described; however, the role of another RHAMM receptor in CVDs is little known. This review discusses the role of both receptors in CVDs and their connections.

2. CD44 and RHAMM: Structure and Expression

CD44 is a widely expressed cellular adhesion molecule that serves as the major receptor for components of the extracellular matrix (ECM) [10]. Apart from HA, CD44 binds other carbohydrate ligands, such as heparan sulfate [11], as well as noncarbohydrate ligands: collagen and osteopontin [12]. CD44 occurs as a series of isoforms with molecular weights ranging from 85 to over 200 kDa [13]. The most commonly

expressed CD44 receptor is the 85-90 kDa glycoprotein which represents the standard CD44 molecule which does not contain products with spliced exon variants [14]. CD44 is structurally and functionally polymorphic. Its gene consists of at least 20 exons, of which 12 can be alternatively spliced. The heterogeneity of the protein is mainly due to the variable splicing of 10 exons encoding the extracellular region located between the invariant HA-binding domain at the NH2 terminus and the membrane proximal extracellular domain [15]. The most common isoform of CD44, called standard form (CD44s), does not contain any exon variants. It consists of a large extracellular domain of 248 amino acids, a 21-amino acid segment encompassing the membrane, and a relatively short cytoplasmic part of 72 amino acids [16]. The *CD44* gene contains 20 exons, of which exons 1-5, 15-17, and 19 encode the CD44 isoform, while exons 6.6a and 7-14 (also designated as vl-v10) are alternatively spliced to generate variant isoforms with insertion into the membrane proximal region of the extracellular domain between amino acids 202 and 203. The amino terminal region is relatively conserved in mammalian species (about 85% homology) and contains a hyaluronan-binding domain, while the membrane proximal region is relatively unconservative (about 35-45% sequence similarity between species) and has several sites for glycosylation and chondroitin sulfate attachment [17, 18]. The transmembrane domain ensures a way to interact with cofactors and adapter proteins and to direct the influx of lymphocytes [19]. The intracellular domain of CD44 has short- and long-tail configurations and performs nuclear localization functions for the regulation of transcription [20].CD44 is expressed in a variety of cell types (Figures 1(a) and 1(b)), including lymphocytes, macrophages, erythrocytes, fibroblasts, neurons, epithelial cells, and endothelial cells [18]. CD44 supports the adhesion of leukocytes to endothelial cells [10], induces the secretion of chemokines from macrophages, and regulates the proliferation and migration of vascular smooth muscle cells [21].

In contrast to CD44, the main hyaluronan receptor, RHAMM, is less well studied and mainly is involved in cell locomotion. It was firstly described by Turley et al. [22, 23] and soon was linked to *ras* transformation and tumor progression [24]. The *HMMR* gene encodes an 85 kDa protein—RHAMM—with an extensive helix structure and a basic globular domain at the amino terminus [25]. It has approximately 35% protein sequence homology to KIF15, a member of the kinesin family [26]. RHAMM does not contain a signal peptide for export via the Golgi apparatus and the endoplasmic reticulum [7]. RHAMM is a member of the hyaladherin protein family, has two hyaluronan-binding domains, and interacts with it through 9–11-amino acid basic motifs [27]. The extracellular part of RHAMM activates signaling cascades that control the expression of cell cycle genes and genes related to cell motility [28, 29]. The intracellular domain of RHAMM is required for the formation of the mitotic spindle and may play a role in the direction of cell motility [30]. The *HMMR* gene is located on the human chromosome 5q33.2 and contains 18 exons [31]. RHAMM, also described as CD168, does not have a transmembrane domain but is anchored by the glycosylphosphatidylinositol (GPI) group in the plasma membrane where it can interact with CD44 and participate in many cell functions, including cell motility, wound healing, and modification of the Ras signaling cascade. Interestingly, RHAMM does not contain a signal peptide and is believed to be transported to the cell surface by unconventional transport mechanisms where it binds to the cell surface by docking to HA synthase [32] and, like CD44, transmits signals affecting cell mobility [27]. It has been shown that RMAMM interacts with hyaluronan in an ionic manner via a 35-amino acid basic C-terminal region, which can be further subdivided into two motifs of 10 and 11 amino acids, respectively [33]. RHAMM is present on the cell surface, in the cytoplasm, and in the nucleus of different types of cells [25] and regulates cell movement and proliferation [24, 25]. RHAMM under physiological conditions is poorly expressed on various cell types (Figures 1(a) and 1(b)) such as lymphocytes, smooth muscle cells, macrophages, and fibroblasts; however, its expression rises in pathological conditions [34, 35].

Although CD44 and RHAMM have different primary amino acid sequences and although CD44 is conservatively expressed in cells and RHAMM is tightly regulated, both receptors possess transforming properties that may be related to their ability to promote motility [34, 36]. Research indicates that during inflammation, wound healing, and tumor formation, cell migration is mediated by CD44 and may require RHAMM surface expression [36]. This means that these receptors may act synergistically in some diseases.

3. Atherosclerosis and Vascular Inflammation

Atherosclerosis is an inflammatory disease of the walls of large and medium arteries. Its etiology is not fully understood, but there are several factors influencing its development. Chronic inflammation and increased levels of low-density lipoprotein (LDL) in the blood play a major role in the development of atherosclerosis. Abnormal blood flow in the vessels can cause increased wall tension and promote the production of proteoglycans by arterial smooth muscle cells (SMCs), which can bind and retain lipoprotein molecules, facilitating their oxidative modification, thereby promoting an inflammatory response at lesion sites [38]. Vascular endothelial cells become activated by proinflammatory stimuli and begin to express selective adhesion molecules on the surface, which recruit monocytes and T lymphocytes and which are likely to be involved in the recruitment of blood-borne cells for atherosclerotic lesions [39, 40].

Atherosclerosis at the developed stage is characterized by the formation of atherosclerotic plaque containing macrophages, dendritic cells (DC), foam cells, lymphocytes, and other inflammatory cells. In advanced age, atherosclerotic plaque calcifications appear [41]. Not only the vascular wall is affected but also the adventitia and adipose tissue attached to the vessel express some degree of inflammation which may precede vascular dysfunction [42, 43]. Dendritic cells and lymphocytes are found in the adventitia and perivascular adipose tissue of normal arteries, but their number is significantly increased in the atherosclerotic arteries [43]. Under

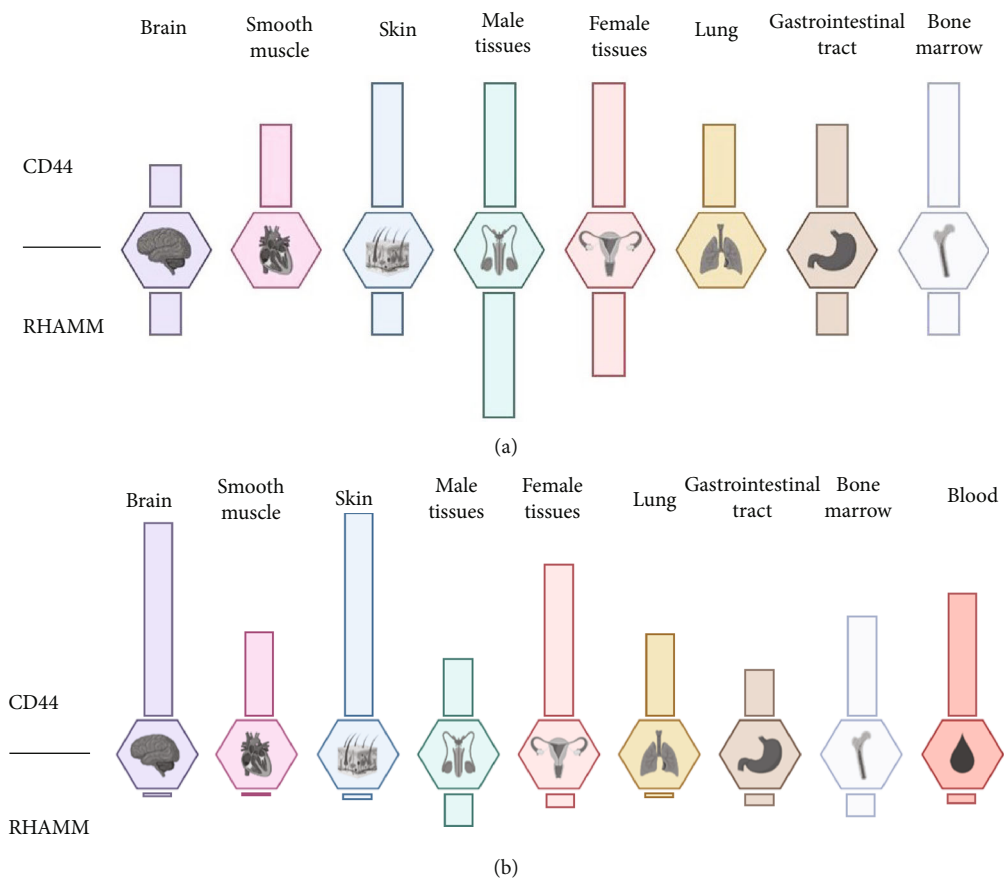

Figure 1: Protein (a) and mRNA (b) expression of CD44. Prepared on the basis of data from the Human Protein Atlas [37]. Protein expression reported with the units: not detected, low, medium, and high. mRNA expression reported as normalized expression (NX) combined from three transcriptomics datasets (HPA, GTEx, and FANTOM5). Created with BioRender.com.

internal atherosclerotic lesions, leukocytes organize themselves into clusters resembling tertiary lymphoid tissue [44]. These features of atherosclerotic plaques illustrate that atherosclerosis is a complex disease in which many elements of the vascular, metabolic, and immune systems take part. Atherosclerotic changes result from inflammatory triggers, subsequent release of various cytokines, proliferation of smooth muscle cells, synthesis of the connective tissue matrix, and accumulation of macrophages and lipids [39, 45, 46]. In those processes, CD44 and RHAMM may play an important role (Figure 2).

Numerous studies suggest that the CD44 cell adhesion molecule may promote atherosclerosis by mediating the recruitment of inflammatory cells into platelets and activation of vascular cells [47, 48]. In the atherosclerosis model of apoE$^{-/-}$ mice, vascular expression of CD44 was highest in areas prone to damage [48, 49]. This was confirmed in human studies where CD44 was present in areas of human atherosclerotic plaques, rich in macrophages, and susceptible to rupture, compared to healthy vascular tissues [50, 51]. Elevated expression of CD44 correlated with a 10-fold increase in the secretion of proinflammatory cytokines such as interleukin-1β (IL-1β) and IL-6 by endothelial cells and macrophages. These cytokines in turn increased CD44 expression [50, 51]. Such a positive feedback loop may exacerbate arteriosclerosis, leading to plaque instability. The elimination of CD44 in mice with the apoE knockout led to a significant reduction in aortic lesions and a reduction in the number of macrophages present in the lesions by 90% [48]. Moreover, gene expression profiling in the aorta of CD44 knockout mice compared to a wild type led to the discovery that CD44 regulates focal adhesion formation, extracellular matrix deposition, and angiogenesis, critical processes for atherosclerosis [49]. To investigate the mechanism by which CD44 controls atherosclerosis, bone marrow chimeras were generated using bone marrow transplant from a wild type (WT) and CD44-null donor to apoE$^{-/-}$ and apoE$^{-/-}$ CD44$^{-/-}$. The expression of CD44 in both the vascular and bone marrow cells contributed to the development of changes in the apoE$^{-/-}$ model. It means that CD44, on both the resident and recruited cells, is essential for its full proatherogenic effect *in vivo* [47]. Moreover, the CD44 deletion also favored an increase in fibrotic lesions in apoE$^{-/-}$ CD44$^{-/-}$ mice compared to apoE$^{-/-}$ mice, which indicates that CD44 also regulates the lesion composition and influences the stability of atherosclerotic plaques [47].

So far, RHAMM has not been directly associated with atherosclerosis, but it is known that it plays a vital role in inflammation, an important factor in the pathogenesis of atherosclerosis [36]. It has been shown that RHAMM interacts with growth factor receptors such as PDGFR [52], TGF-β receptor I [53], or bFGFR [54]. Growth factors regulate the function of ERK signaling and are responsible for the regulation of cell proliferation and differentiation [52]. In

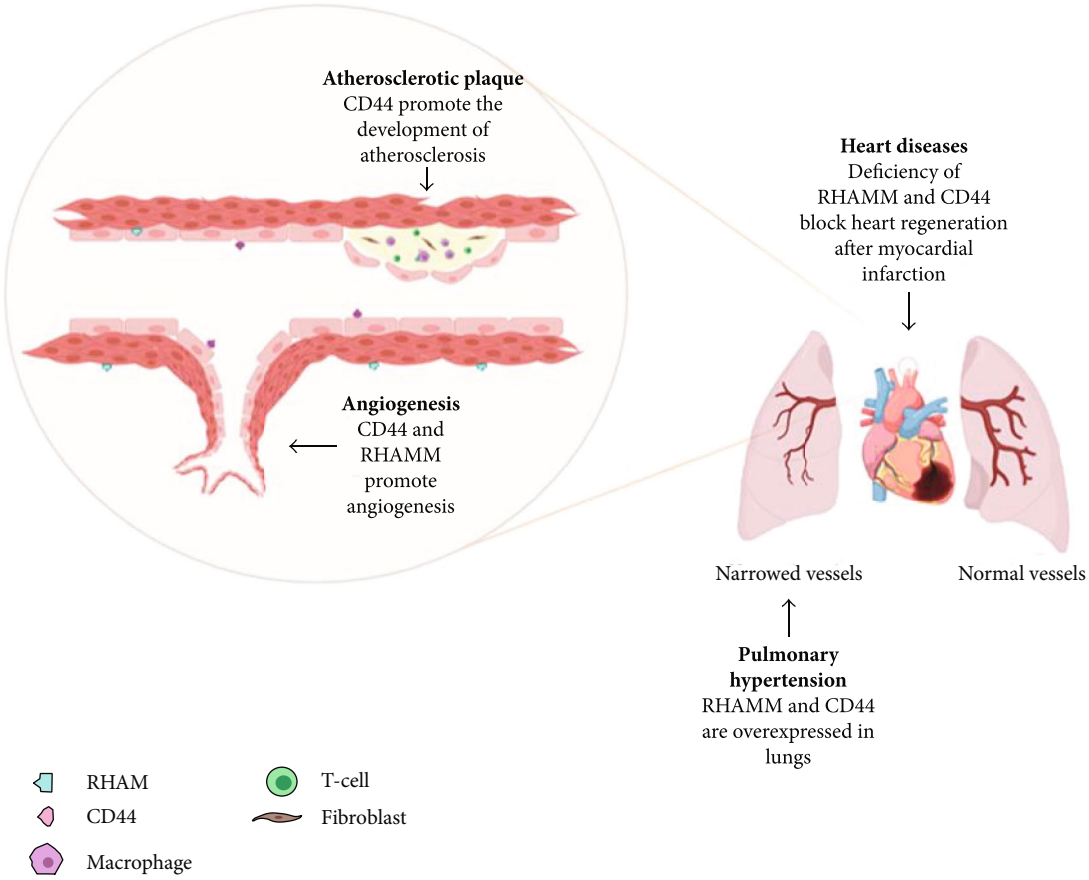

Figure 2: Diagram describing the role of RHAMM and CD44 receptors in the cardiovascular system. Created with BioRender.com.

addition, ERK signaling has been shown to play a role in altering cholesterol homeostasis in human macrophages [55]. By interacting, RHAMM takes part in the mobility necessary for the inflammation by activating ERK1/2/MAPK. Nuclear RHAMM is also associated with the ERK1/2/MAP kinase, which mediates the activation of PAI-1 and MMP-9, which are involved in cell mobility and inflammation [56]. RHAMM also participates in HA-dependent regulation. HA is produced during tissue damage, causing activation of inflammatory cells to induce innate immune response and regulation of the behavior of epithelial cells and fibroblasts [57–59]. Additional confirmation of the importance of RHAMM is the fact that the use of a 15-mer peptide with homology to RHAMM-binding sequences has been shown to block HA signaling and reduce inflammation and fibrogenesis [60].

Macrophages in atherosclerotic plaque formation play a fundamental role [61]. Macrophages colonizing the atherosclerotic plaque have a reduced migration capacity, which leads to the maintenance of inflammation and further progression into the atherosclerotic plaque [62]. Moreover, they participate in the intake and accumulation of lipoproteins. Cholesterol uptake by macrophages leads to their transformation to foam cells in the vascular wall. At this stage of atherosclerosis, fatty streaks are observed in the vasculature. The RHAMM receptor is expressed on macrophages. In a rat model of acute lung damage, the expression of RHAMM and HA is increased in macrophages responding to intratracheal injury [63, 64]. Moreover, *Hmmr*$^{-/-}$ transgenic mice have been shown to exhibit reduced macrophage chemotaxis [65]. Another element essential in the development of atherosclerotic lesions includes vascular smooth muscle cells (VSMCs). VSMCs, under the influence of vascular damage, are able to change the quiescent "contractile" phenotype into a "proinflammatory" phenotype. Activated VSMCs can effectively multiply and migrate, helping to repair vascular walls. However, in the chronic inflammation that occurs in atherosclerosis, VSMCs are misregulated, leading to extracellular matrix formation in the plaque areas [66]. Research has shown that RHAMM can be an important element in these processes. *In vitro* studies have shown that HA mediates VSMC migration through CD44 and RHAMM receptors as well as VSMC proliferation but only through the CD44 receptor [2, 67, 68]. On the basis of the culture of bovine vascular smooth muscle cells, an increase in RHAMM expression was observed after scratch wound assay. It was concluded that vascular damage leads to an increase in RHAMM expression and is localized in the VSMC at the edge of the lesion [68].

4. Ischemic Heart Disease

Ischemic heart disease is one of the most common causes of death in developed countries. After myocardial infarction

(MI), billions of cardiomyocytes undergo apoptosis, pyroptosis, and necrosis, resulting in a noncontractile collagen scar that reduces heart function [69]. The mammalian heart's ability to replace lost cardiomyocytes is limited, while adult zebrafish (*Danio rerio*) can successfully regenerate the heart following apical ventricular amputation throughout its lifetime [70, 71]. A key factor in the regeneration process in zebrafish is the ability of preexisting cardiomyocytes to proliferate after organ damage [72–74].

After analyzing the proteomic changes following ventricular apex resection in adult zebrafish, increased expression of the RHAMM was identified. It was also investigated that after zebrafish ventricular resection, the area of scar tissue was significantly larger in the RHAMM knockdown fish, suggesting that the RHAMM knockdown blocked heart regeneration. The importance of hyaluronic acid in the regeneration of the heart was also determined. It was found that after inhibition of HA synthesis, after ventricular resection in zebrafish, significant scar tissue was still present compared to minimal or no scar tissue in controls [75].

Studies on the role of CD44 in regeneration after MI have shown a correlation between inflammatory mediators and CD44 in regulating the inflammatory response, repairing the heart, and differentiating the heart fibroblasts after MI [76]. Studies in CD44-deficient mice that underwent myocardial infarction showed prolonged inflammation, reduced collagen deposition in scars, decreased myofibroblast infiltration, and decreased TGF-β signaling [77]. Following acute MI, IL-6 has been shown to enhance CD44 and HA synthase (HAS-1 and HAS-2) expression in cardiac fibroblasts, resulted in a matrix rich in HA. As a result, proinflammatory cytokines and the expression of smooth muscle α-actin were induced through CD44-HA interactions. This interaction, together with circulating IL-6, changed the nature of the ECM, modulated the differentiation of cardiac fibroblasts, and promoted the immune responses [78].

5. Vascular Remodeling

Restrictive remodeling assumes that SMCs reorganize the ECM, while the factors causing constrained remodeling compared to external remodeling remain poorly defined [79]. The contraction of the vessel wall is similar to that of a cutaneous wound. SMCs repopulate the sites of vascular damage and cause the production and remodeling of the ECM, which changes the geometry of the vessel wall. It is known that matrix remodeling depends in part on direct adhesion interactions of ECM cells. In *in vitro* studies on SMCs, HA consistently increased the adhesion of SMCs to collagen-precoated plates and blocking or removing RHAMM weakened SMC adhesion to collagen with or without exogenous HA [80]. That suggests that the endogenous production of HA is sufficient to activate RHAMM. RHAMM activation by HA significantly influences the adhesive interactions between SMC and ECM and contributes to remodeling of the wall and narrowing of the lumen after carotid artery ligation [80]. RHAMM-blocking strategies at sites of vascular injury may be potentially useful in the prevention of clinical restenosis.

The role that CD44 plays in remodeling, for example, after angioplasty, is unclear. Available data published on that topic does not clearly indicate whether CD44 may be a remodeling factor or may play a protective role by inhibiting neointimal formation [81, 82]. However, studies have shown that the deficiency of the *CD44* gene significantly enhanced neointimal hyperplasia, which suggests that the *CD44* gene is involved in the process of pathological remodeling and may play a protective role. The remodeling response to injury involves circulating cells that arise from the bone marrow as well as cells from the local artery wall. Compared with damaged femoral arteries in $CD44^{+/+}$ mice, $CD44^{-/-}$ mice showed significantly greater femoral vascular remodeling. In remodeled femoral arteries from $CD44^{-/-}$ mice, no significant changes were observed in CD44 expression when compared to intact arteries. After the use of low-mass weight (LMW) heparin, the damaged arteries showed a significant reduction in neointimal thickness and a significant increase in CD44 expression. This suggests that CD44 may be the route by which LMW heparin diminishes the remodeling process [83].

6. Angiogenesis

Angiogenesis is the formation of new blood vessels from existing vessels (Figure 2). It can occur in a pathological form in the context of circulatory diseases or cancer and in a physiological form in the case of tissue ischemia, wound healing, etc. [84]. To investigate the involvement of CD44 in blood vessel formation, *in vivo* angiogenesis was studied in CD44-deficient mice [85]. Initial studies were performed in a model in which vessels develop around and within subcutaneously implanted Matrigel plugs containing B16 murine melanoma tumor cells as a source of angiogenic growth factors. Vascularization of the plugs was observed in wild-type animals, but not in CD44 knockout mice, confirming the involvement of CD44 in the pathological formation of blood vessels [86]. In addition, in a mouse oral carcinogenesis model, after implantation of Matrigel plugs with suspended cancer cells into the dorsal chamber of the skin fold, $CD44^{+/+}$ mice showed a higher microvascular density than $CD44^{-/-}$ [87]. It has also been shown that inhibition of CD44 reduces the adhesion of endothelial cells (EC) to HA immobilized on the plastic surface [54]. This means that an increase in CD44 expression may allow the adhesion of the EC to the components of the ECM, which is one of the processes enabling the formation of new blood vessels [1]. Whether CD44 plays a role in physiological angiogenesis has also been investigated. Wound closure in animals with the CD44 knockout was shown to be delayed within 1 to 3 days after wounding, relative to wild-type animals. Vascular density at the edge of the wounds on day 3 was reduced by around 20% in $CD44^{-/-}$ animals compared to wild-type mice. This means that the lack of CD44 results in an early delay in skin wound closure, which is associated with reduced neovascularization of the injured tissue. The above results thus confirmed that CD44 may be involved in physiological angiogenesis [86]. The differentiation and organization of EC in blood vessels is a critical step in angiogenesis [88]. To

investigate the role of RHAMM receptors in blood vessel formation, the effect of anti-RHAMM antibodies on EC function and *in vivo* angiogenesis was determined. Using the endothelial tube formation model on Matrigel, anti-RHAMM antibodies were found to inhibit tube formation by human endothelial cells. It was also investigated that the use of an anti-RHAMM antibody in a mouse model of angiogenesis significantly reduced the vascularization of the plugs [54].

7. Idiopathic Pulmonary Arterial Hypertension

Idiopathic pulmonary arterial hypertension (IPAH) is a disorder characterized by persistent elevated pulmonary arterial pressure with unknown causes [89]. The primary mechanism of IPAH is pulmonary vascular remodeling involving pre- and intra-acinar arteries, such as stenotic lesions and complex lesions characterized by plexiform lesions (Figure 2) [90]. The plexiform injury has been studied in relation to idiopathic pulmonary arterial hypertension as a marker of the severity or rapid progression of pulmonary hypertension [91], but it also contributed to the pathogenesis of the disease. Studies have shown that CD44 was frequently expressed in plexiform lung lesions in IPAH patients and was mainly located in endothelial cells that make up the microvasculature of the lesions and surrounding T lymphocytes. However, CD44 was not found in any of the vascular cells of normal pulmonary arteries. This suggests that CD44 is involved in the pathogenesis of idiopathic pulmonary arterial hypertension [92]. The role of RHAMM in pulmonary hypertension is not fully understood. However, studies have shown that loss of PPARγ (peroxisome proliferator-activated receptor γ) is associated with pulmonary hypertension [93]. It has been shown that PPARγ expression is significantly reduced in plexiform lesions in humans with PH. Reduced PPARγ expression was also demonstrated in vascular lesions in a rat model of severe pulmonary hypertension [94]. It has also been investigated that by pharmacological inhibition of PPARγ, RHAMM was upregulated in pulmonary arterial endothelial cells in a sheep model of pulmonary hypertension. The increased expression of RHAMM was also confirmed in human pulmonary microvascular endothelial cells (HMVEC) with PPARγ depletion. These results suggest that HMMR plays a large role in hypertension but it would be worthwhile to conduct more research in this area [95].

8. Conclusions

CD44 and RHAMM mediate different cardiovascular effects in normal and pathological conditions. Herein, we discussed the role of these receptors not only in cardiovascular diseases such as atherosclerosis, pulmonary hypertension, and ischemic heart disease but also in cardiovascular processes such as vascular inflammation, vascular remodeling, and angiogenesis. Expression of RHAMM in contrast to CD44 is relatively low in vascular cells and blood. However, RHAMM expression rises in pathological conditions. Expression of CD44 was found to be upregulated in areas prone to atherosclerosis. The important role of RHAMM in atherosclerosis development is its role in the motility of the immune cells. The gained ability of migration mediated by RHAMM allows cells to the inflammatory response. This process is important also in other conditions where vascular remodeling is present. In conditions after myocardial infarction, CD44 and RHAMM help in wound healing by reorganization of the extracellular matrix and collagen deposition. Inhibition or lack of RHAMM or CD44 blocks angiogenesis in both the physiological and pathological conditions. Summarizing the role of both described receptors is similar apart from its different role in vascular remodeling. However, the RHAMM receptor is significantly less studied in cardiovascular diseases.

Conflicts of Interest

The authors declare that there are no conflicts of interest.

Acknowledgments

This work was supported by the National Science Centre, Poland (project numbers 2019/35/D/NZ5/02820 and 2014/15/B/NZ5/03566).

References

[1] G. W. Sullivan, I. J. Sarembock, and J. Linden, "The role of inflammation in vascular diseases," *Journal of Leukocyte Biology*, vol. 67, no. 5, pp. 591–602, 2000.

[2] M. Jain, Q. He, W. S. Lee et al., "Role of CD44 in the reaction of vascular smooth muscle cells to arterial wall injury," *The Journal of Clinical Investigation*, vol. 97, no. 3, pp. 596–603, 1996.

[3] A. B. Peitzman, B. G. Harbrecht, A. O. Udekwu, T. R. Billiar, E. Kelly, and R. L. Simmons, "Hemorrhagic shock," *Current Problems in Surgery*, vol. 32, no. 11, pp. 925–1002, 1995.

[4] G. K. Hansson, "Immunological control mechanisms in plaque formation," in *Arteriosclerosis*, vol. 89, Dr. Dietrich Steinkopff Verlag GmbH and Co. KG, 1994.

[5] R. L. Wilensky, K. L. March, I. Gradus-Pizlo, G. Sandusky, N. Fineberg, and D. R. Hathaway, "Vascular injury, repair, and restenosis after percutaneous transluminal angioplasty in the atherosclerotic rabbit," *Circulation*, vol. 92, no. 10, pp. 2995–3005, 1995.

[6] F. Mach, U. Schönbeck, R. P. Fabunmi et al., "T lymphocytes induce endothelial cell matrix metalloproteinase expression by a CD40L-dependent mechanism: implications for tubule formation," *The American Journal of Pathology*, vol. 154, no. 1, pp. 229–238, 1999.

[7] J. Jiang, R. Casalegno-Garduno, H. Chen, A. Schmitt, M. Schmitt, and C. A. Maxwell, "Multifunctional proteins bridge mitosis with motility and cancer with inflammation and arthritis," *ScientificWorldJournal*, vol. 10, pp. 1244–1257, 2010.

[8] H. J. Cao, H. S. Wang, Y. Zhang, H. Y. Lin, R. P. Phipps, and T. J. Smith, "Activation of human orbital fibroblasts through CD40 engagement results in a dramatic induction of hyaluronan synthesis and prostaglandin endoperoxide H synthase-2 expression," *The Journal of Biological Chemistry*, vol. 273, no. 45, pp. 29615–29625, 1998.

[9] E. Puré and C. A. Cuff, "A crucial role for CD44 in inflammation," *Trends in Molecular Medicine*, vol. 7, no. 5, pp. 213–221, 2001.

[10] A. I. Khan, S. M. Kerfoot, B. Heit et al., "Role of CD44 and hyaluronan in neutrophil recruitment," *Journal of Immunology*, vol. 173, no. 12, pp. 7594–7601, 2004.

[11] S. Jalkanen and M. Jalkanen, "Lymphocyte CD44 binds the COOH-terminal heparin-binding domain of fibronectin," *The Journal of Cell Biology*, vol. 116, no. 3, pp. 817–825, 1992.

[12] G. F. Weber, S. Ashkar, M. J. Glimcher, and H. Cantor, "Receptor-ligand interaction between CD44 and osteopontin (Eta-1)," *Science*, vol. 271, no. 5248, pp. 509–512, 1996.

[13] S. Goodison, V. Urquidi, and D. Tarin, "CD44 cell adhesion molecules," *Molecular Pathology*, vol. 52, no. 4, pp. 189–196, 1999.

[14] A. Aruffo, I. Stamenkovic, M. Melnick, C. B. Underhill, and B. Seed, "CD44 is the principal cell surface receptor for hyaluronate," *Cell*, vol. 61, no. 7, pp. 1303–1313, 1990.

[15] M. P. Martegani, F. Del Prete, A. Gasbarri, P. G. Natali, and A. Bartolazzi, "Structural variability of CD44v molecules and reliability of immunodetection of CD44 isoforms using mAbs specific for CD44 variant exon products," *The American Journal of Pathology*, vol. 154, no. 1, pp. 291–300, 1999.

[16] G. Borland, J. A. Ross, and K. Guy, "Forms and functions of CD44," *Immunology*, vol. 93, no. 2, pp. 139–148, 1998.

[17] C. M. Isacke and H. Yarwood, "The hyaluronan receptor, CD44," *The International Journal of Biochemistry & Cell Biology*, vol. 34, no. 7, pp. 718–721, 2002.

[18] S. Ilangumaran, B. Borisch, and D. C. Hoessli, "Signal transduction via CD44: role of plasma membrane microdomains," *Leukemia & Lymphoma*, vol. 35, no. 5-6, pp. 455–469, 1999.

[19] K. Williams, K. Motiani, P. V. Giridhar, and S. Kasper, "CD44 integrates signaling in normal stem cell, cancer stem cell and (pre)metastatic niches," *Experimental Biology and Medicine*, vol. 238, no. 3, pp. 324–338, 2013.

[20] I. Okamoto, Y. Kawano, H. Tsuiki et al., "CD44 cleavage induced by a membrane-associated metalloprotease plays a critical role in tumor cell migration," *Oncogene*, vol. 18, no. 7, pp. 1435–1446, 1999.

[21] C. M. McKee, M. B. Penno, M. Cowman et al., "Hyaluronan (HA) fragments induce chemokine gene expression in alveolar macrophages: the role of HA size and CD44," *The Journal of Clinical Investigation*, vol. 98, no. 10, pp. 2403–2413, 1996.

[22] E. A. Turley and J. Torrance, "Localization of hyaluronate and hyaluronate-binding protein on motile and non- motile fibroblasts," *Experimental Cell Research*, vol. 161, no. 1, pp. 17–28, 1985.

[23] E. A. Turley, D. Moore, and L. J. Hayden, "Characterization of hyaluronate binding proteins isolated from 3T3 and murine sarcoma virus transformed 3T3 cells," *Biochemistry*, vol. 26, no. 11, pp. 2997–3005, 1987.

[24] C. L. Hall, B. Yang, X. Yang et al., "Overexpression of the hyaluronan receptor RHAMM is transforming and is also required for *H-ras* transformation," *Cell*, vol. 82, no. 1, pp. 19–28, 1995.

[25] C. Hardwick, K. Hoare, R. Owens et al., "Molecular cloning of a novel hyaluronan receptor that mediates tumor cell motility," *The Journal of Cell Biology*, vol. 117, no. 6, pp. 1343–1350, 1992.

[26] C. A. Maxwell, J. J. Keats, M. Crainie et al., "RHAMM is a centrosomal protein that interacts with dynein and maintains spindle pole stability," *Molecular Biology of the Cell*, vol. 14, no. 6, pp. 2262–2276, 2003.

[27] B. Yang, B. L. Yang, R. C. Savani, and E. A. Turley, "Identification of a common hyaluronan binding motif in the hyaluronan binding proteins RHAMM, CD44 and link protein," *The EMBO Journal*, vol. 13, no. 2, pp. 286–296, 1994.

[28] Slevin, "Oligosaccharides of hyaluronan induce angiogenesis through distinct CD44 and RHAMM-mediated signalling pathways involving Cdc2 and γ-adducin," *International Journal of Oncology*, vol. 35, no. 4, p. 35, 2009.

[29] S. Mohapatra, X. Yang, J. A. Wright, E. A. Turley, and A. H. Greenberg, "Soluble hyaluronan receptor RHAMM induces mitotic arrest by suppressing Cdc2 and cyclin B1 expression," *The Journal of Experimental Medicine*, vol. 183, no. 4, pp. 1663–1668, 1996.

[30] R. Silverman-Gavrila, L. Silverman-Gavrila, G. Hou, M. Zhang, M. Charlton, and M. P. Bendeck, "Rear polarization of the microtubule-organizing center in neointimal smooth muscle cells depends on PKCα, ARPC5, and RHAMM," *The American Journal of Pathology*, vol. 178, no. 2, pp. 895–910, 2011.

[31] C. Wang, J. Entwistle, G. Hou, Q. Li, and E. A. Turley, "The characterization of a human _RHAMM_ cDNA: conservation of the hyaluronan- binding domains," *Gene*, vol. 174, no. 2, pp. 299–306, 1996.

[32] L. Klewes, E. A. Turley, and P. Prehm, "The hyaluronate synthase from a eukaryotic cell line," *The Biochemical Journal*, vol. 290, no. 3, pp. 791–795, 1993.

[33] B. Yang, L. Zhang, and E. A. Turley, "Identification of two hyaluronan-binding domains in the hyaluronan receptor RHAMM," *The Journal of Biological Chemistry*, vol. 268, no. 12, pp. 8617–8623, 1993.

[34] L. M. Pilarski, A. Masellis-Smith, A. R. Belch, B. Yang, R. C. Savani, and E. A. Turley, "RHAMM, a receptor for hyaluronan-mediated motility, on normal human lymphocytes, thymocytes and malignant B cells: a mediator in B cell malignancy?," *Leukemia & Lymphoma*, vol. 14, no. 5-6, pp. 363–374, 1994.

[35] C. Tolg, S. R. Hamilton, K. A. Nakrieko et al., "Rhamm-/-fibroblasts are defective in CD44-mediated ERK1,2 motogenic signaling, leading to defective skin wound repair," *The Journal of Cell Biology*, vol. 175, no. 6, pp. 1017–1028, 2006.

[36] S. Misra, V. C. Hascall, R. R. Markwald, and S. Ghatak, "Interactions between hyaluronan and its receptors (CD44, RHAMM) regulate the activities of inflammation and cancer," *Frontiers in Immunology*, vol. 6, p. 201, 2015.

[37] M. Uhlen, L. Fagerberg, B. M. Hallstrom et al., "Tissue-based map of the human proteome," *Science*, vol. 347, no. 6220, article 1260419, 2015.

[38] D. E. Andreou and I. Andreadou, "Atherosclerosis: an inflammatory disease," *New England Journal of Medicine*, vol. 340, no. 2, pp. 115–126, 1999.

[39] M. A. Crowther, "Pathogenesis of atherosclerosis," *Hematology. American Society of Hematology. Education Program*, vol. 2005, no. 1, pp. 436–441, 2005.

[40] G. K. Hansson, "Inflammation, atherosclerosis, and coronary artery disease," *The New England Journal of Medicine*, vol. 352, no. 16, pp. 1685–1695, 2005.

[41] C. Weber and H. Noels, "Atherosclerosis: current pathogenesis and therapeutic options," *Nature Medicine*, vol. 17, no. 11, pp. 1410–1422, 2011.

[42] E. Galkina, A. Kadl, J. Sanders, D. Varughese, I. J. Sarembock, and K. Ley, "Lymphocyte recruitment into the aortic wall before and during development of atherosclerosis is partially L-selectin dependent," *The Journal of Experimental Medicine*, vol. 203, no. 5, pp. 1273–1282, 2006.

[43] D. S. Skiba, R. Nosalski, T. P. Mikolajczyk et al., "Anti-atherosclerotic effect of the angiotensin 1-7 mimetic AVE0991 is mediated by inhibition of perivascular and plaque inflammation in early atherosclerosis," *British Journal of Pharmacology*, vol. 174, no. 22, pp. 4055–4069, 2017.

[44] P. Srikakulapu, D. Hu, C. Yin et al., "Artery tertiary lymphoid organs control multilayered territorialized atherosclerosis B-cell responses in aged ApoE-/- mice," *Arteriosclerosis, Thrombosis, and Vascular Biology*, vol. 36, no. 6, pp. 1174–1185, 2016.

[45] C. Weber, A. Zernecke, and P. Libby, "The multifaceted contributions of leukocyte subsets to atherosclerosis: lessons from mouse models," *Nature Reviews. Immunology*, vol. 8, no. 10, pp. 802–815, 2008.

[46] G. K. Hansson and P. Libby, "The immune response in atherosclerosis: a double-edged sword," *Nature Reviews. Immunology*, vol. 6, no. 7, pp. 508–519, 2006.

[47] L. Zhao, E. Lee, A. M. Zukas et al., "CD44 expressed on both bone marrow-derived and non-bone marrow-derived cells promotes atherogenesis in ApoE-deficient mice," *Arteriosclerosis, Thrombosis, and Vascular Biology*, vol. 28, no. 7, pp. 1283–1289, 2008.

[48] C. A. Cuff, D. Kothapalli, I. Azonobi et al., "The adhesion receptor CD44 promotes atherosclerosis by mediating inflammatory cell recruitment and vascular cell activation," *The Journal of Clinical Investigation*, vol. 108, no. 7, pp. 1031–1040, 2001.

[49] L. Zhao, J. A. Hall, N. Levenkova et al., "CD44 regulates vascular gene expression in a proatherogenic environment," *Arteriosclerosis, Thrombosis, and Vascular Biology*, vol. 27, no. 4, pp. 886–892, 2007.

[50] D. Hägg, S. Sjöberg, L. M. Hultén et al., "Augmented levels of CD44 in macrophages from atherosclerotic subjects: a possible IL-6-CD44 feedback loop?," *Atherosclerosis*, vol. 190, no. 2, pp. 291–297, 2007.

[51] A. Krettek, G. K. Sukhova, U. Schönbeck, and P. Libby, "Enhanced expression of CD44 variants in human atheroma and abdominal aortic aneurysm: possible role for a feedback loop in endothelial cells," *The American Journal of Pathology*, vol. 165, no. 5, pp. 1571–1581, 2004.

[52] S. Zhang, M. C. Y. Chang, D. Zylka, S. Turley, R. Harrison, and E. A. Turley, "The hyaluronan receptor RHAMM regulates extracellular-regulated kinase∗," *The Journal of Biological Chemistry*, vol. 273, no. 18, pp. 11342–11348, 1998.

[53] D. Park, Y. Kim, H. Kim et al., "Hyaluronic acid promotes angiogenesis by inducing RHAMM-TGFβ receptor interaction via CD44-PKCδ," *Molecules and Cells*, vol. 33, no. 6, pp. 563–574, 2012.

[54] R. C. Savani, G. Cao, P. M. Pooler, A. Zaman, Z. Zhou, and H. M. DeLisser, "Differential involvement of the hyaluronan (HA) receptors CD44 and receptor for HA-mediated motility in endothelial cell function and angiogenesis," *The Journal of Biological Chemistry*, vol. 276, no. 39, pp. 36770–36778, 2001.

[55] N. Li, J. E. McLaren, D. R. Michael, M. Clement, C. A. Fielding, and D. P. Ramji, "ERK is integral to the IFN-γ–mediated activation of STAT1, the expression of key genes implicated in atherosclerosis, and the uptake of modified lipoproteins by human macrophages," *Journal of Immunology*, vol. 185, no. 5, pp. 3041–3048, 2010.

[56] C. Tolg, J. B. McCarthy, A. Yazdani, and E. A. Turley, "Hyaluronan and RHAMM in wound repair and the "cancerization" of stromal tissues," *BioMed Research International*, vol. 2014, Article ID 103923, 18 pages, 2014.

[57] M. Slevin, J. Krupinski, J. Gaffney et al., "Hyaluronan-mediated angiogenesis in vascular disease: uncovering RHAMM and CD44 receptor signaling pathways," *Matrix Biology*, vol. 26, no. 1, pp. 58–68, 2007.

[58] D. Jiang, J. Liang, J. Fan et al., "Regulation of lung injury and repair by toll-like receptors and hyaluronan," *Nature Medicine*, vol. 11, no. 11, pp. 1173–1179, 2005.

[59] N. Itano, F. Atsumi, T. Sawai et al., "Abnormal accumulation of hyaluronan matrix diminishes contact inhibition of cell growth and promotes cell migration," *Proceedings of the National Academy of Sciences of the United States of America*, vol. 99, no. 6, pp. 3609–3614, 2002.

[60] C. Tolg, S. R. Hamilton, E. Zalinska et al., "A RHAMM mimetic peptide blocks hyaluronan signaling and reduces inflammation and fibrogenesis in excisional skin wounds," *The American Journal of Pathology*, vol. 181, no. 4, pp. 1250–1270, 2012.

[61] K. J. Moore, F. J. Sheedy, and E. A. Fisher, "Macrophages in atherosclerosis: a dynamic balance," *Nature Reviews. Immunology*, vol. 13, no. 10, pp. 709–721, 2013.

[62] G. J. Randolph, "Mechanisms that regulate macrophage burden in atherosclerosis," *Circulation Research*, vol. 114, no. 11, pp. 1757–1771, 2014.

[63] A. Zaman, Z. Cui, J. P. Foley et al., "Expression and role of the hyaluronan receptor RHAMM in inflammation after bleomycin injury," *American Journal of Respiratory Cell and Molecular Biology*, vol. 33, no. 5, pp. 447–454, 2005.

[64] R. C. Savani, G. Hou, P. Liu et al., "A role for hyaluronan in macrophage accumulation and collagen deposition after bleomycin-induced lung injury," *American Journal of Respiratory Cell and Molecular Biology*, vol. 23, no. 4, pp. 475–484, 2000.

[65] J. P. Foley, D. Lam, H. Jiang et al., "Toll-like receptor 2 (TLR2), transforming growth factor-β, hyaluronan (HA), and receptor for HA-mediated motility (RHAMM) are required for surfactant protein A-stimulated macrophage chemotaxis∗,," *The Journal of Biological Chemistry*, vol. 287, no. 44, pp. 37406–37419, 2012.

[66] D. A. Chistiakov, A. N. Orekhov, and Y. V. Bobryshev, "Vascular smooth muscle cell in atherosclerosis," *Acta Physiologica*, vol. 214, no. 1, pp. 33–50, 2015.

[67] K. G. Maier, B. Sadowitz, S. Cullen, X. Han, and V. Gahtan, "Thrombospondin-1-induced vascular smooth muscle cell migration is dependent on the hyaluronic acid receptor CD44," *American Journal of Surgery*, vol. 198, no. 5, pp. 664–669, 2009.

[68] R. C. Savani, C. Wang, B. Yang et al., "Migration of bovine aortic smooth muscle cells after wounding injury: the role of hyaluronan and RHAMM," *The Journal of Clinical Investigation*, vol. 95, no. 3, pp. 1158–1168, 1995.

[69] J. Schaper, "Ultrastructural changes of the myocardium in regional ischaemia and infarction," *European Heart Journal*, vol. 7, suppl B, pp. 3–9, 1986.

[70] K. D. Poss, L. G. Wilson, and M. T. Keating, "Heart regeneration in zebrafish," *Science*, vol. 298, no. 5601, pp. 2188–2190, 2002.

[71] J. Itou, H. Kawakami, T. Burgoyne, and Y. Kawakami, "Life-long preservation of the regenerative capacity in the fin and heart in zebrafish," *Biol Open*, vol. 1, no. 8, pp. 739–746, 2012.

[72] C. Jopling, E. Sleep, M. Raya, M. Martí, A. Raya, and J. C. I. Belmonte, "Zebrafish heart regeneration occurs by cardiomyocyte dedifferentiation and proliferation," *Nature*, vol. 464, no. 7288, pp. 606–609, 2010.

[73] K. Kikuchi, J. E. Holdway, A. A. Werdich et al., "Primary contribution to zebrafish heart regeneration by *gata4*$^{+}$ cardiomyocytes," *Nature*, vol. 464, no. 7288, pp. 601–605, 2010.

[74] C. L. Lien, M. Schebesta, S. Makino, G. J. Weber, and M. T. Keating, "Gene expression analysis of zebrafish heart regeneration," *PLoS Biology*, vol. 4, no. 8, pp. e260–e296, 2006.

[75] M. A. Missinato, K. Tobita, N. Romano, J. A. Carroll, and M. Tsang, "Extracellular component hyaluronic acid and its receptor Hmmr are required for epicardial EMT during heart regeneration," *Cardiovascular Research*, vol. 107, no. 4, pp. 487–498, 2015.

[76] M. Suleiman, N. Abdulrahman, H. Yalcin, and F. Mraiche, "The role of CD44, hyaluronan and NHE1 in cardiac remodeling," *Life Sciences*, vol. 209, pp. 197–201, 2018.

[77] P. Huebener, T. Abou-Khamis, P. Zymek et al., "CD44 is critically involved in infarct healing by regulating the inflammatory and fibrotic response," *Journal of Immunology*, vol. 180, no. 4, pp. 2625–2633, 2008.

[78] J. Müller, S. Gorressen, M. Grandoch et al., "Interleukin-6-dependent phenotypic modulation of cardiac fibroblasts after acute myocardial infarction," *Basic Research in Cardiology*, vol. 109, no. 6, p. 440, 2014.

[79] R. L. Geary, S. T. Nikkari, W. D. Wagner, J. K. Williams, M. R. Adams, R. H. Dean et al., "Wound healing: a paradigm for lumen narrowing after arterial reconstruction," *Journal of Vascular Surgery*, vol. 27, no. 1, pp. 96–108, 1998.

[80] X. Ma, J. D. Pearce, D. B. Wilson, W. P. English, M. S. Edwards, and R. L. Geary, "Loss of the hyaluronan receptor RHAMM prevents constrictive artery wall remodeling," *Journal of Vascular Surgery*, vol. 59, no. 3, pp. 804–813, 2014.

[81] J. A. Travis, M. G. Hughes, J. M. Wong, W. D. Wagner, and R. L. Geary, "Hyaluronan enhances contraction of collagen by smooth muscle cells and adventitial fibroblasts," *Circulation Research*, vol. 88, no. 1, pp. 77–83, 2001.

[82] A. E. Vendrov, N. R. Madamanchi, Z. S. Hakim, M. Rojas, and M. S. Runge, "Thrombin and NAD(P)H oxidase-mediated regulation of CD44 and BMP4-Id pathway in VSMC, restenosis, and atherosclerosis," *Circulation Research*, vol. 98, no. 10, pp. 1254–1263, 2006.

[83] G. Zhao, R. S. Shaik, H. Zhao, J. Beagle, S. Kuo, and C. A. Hales, "Low molecular weight (LMW) heparin inhibits injury-induced femoral artery remodeling in mouse via upregulating CD44 expression," *Journal of Vascular Surgery*, vol. 53, no. 5, pp. 1359–1367.e3, 2011.

[84] L. Chen, C. Fu, Q. Zhang, C. He, F. Zhang, and Q. Wei, "The role of CD44 in pathological angiogenesis," *The FASEB Journal*, vol. 34, no. 10, pp. 13125–13139, 2020.

[85] P. Teder, R. W. Vandivier, D. Jiang et al., "Resolution of lung inflammation by CD44," *Science*, vol. 296, no. 5565, pp. 155–158, 2002.

[86] G. Cao, R. C. Savani, M. Fehrenbach et al., "Involvement of endothelial CD44 during _in vivo_ angiogenesis," *The American Journal of Pathology*, vol. 169, no. 1, pp. 325–336, 2006.

[87] N. Ludwig, M. J. Szczepanski, A. Gluszko et al., "CD44(+) tumor cells promote early angiogenesis in head and neck squamous cell carcinoma," *Cancer Letters*, vol. 467, pp. 85–95, 2019.

[88] E. L. Pardue, S. Ibrahim, and A. Ramamurthi, "Role of hyaluronan in angiogenesis and its utility to angiogenic tissue engineering," *Organogenesis*, vol. 4, no. 4, pp. 203–214, 2008.

[89] L. J. Rubin, "Primary pulmonary hypertension," *The New England Journal of Medicine*, vol. 336, no. 2, pp. 111–117, 1997.

[90] G. G. Pietra, F. Capron, S. Stewart et al., "Pathologic assessment of vasculopathies in pulmonary hypertension," *Journal of the American College of Cardiology*, vol. 43, no. 12, pp. S25–S32, 2004.

[91] G. G. Pietra, W. D. Edwards, J. M. Kay et al., "Histopathology of primary pulmonary hypertension. A qualitative and quantitative study of pulmonary blood vessels from 58 patients in the National Heart, Lung, and Blood Institute, Primary Pulmonary Hypertension Registry," *Circulation*, vol. 80, no. 5, pp. 1198–1206, 1989.

[92] K. Ohta-Ogo, H. Hao, H. Ishibashi-Ueda et al., "CD44 expression in plexiform lesions of idiopathic pulmonary arterial hypertension," *Pathology International*, vol. 62, no. 4, pp. 219–225, 2012.

[93] R. E. Nisbet, R. L. Sutliff, and C. M. Hart, "The role of peroxisome proliferator-activated receptors in pulmonary vascular disease," *PPAR Research*, vol. 2007, 10 pages, 2007.

[94] S. Ameshima, H. Golpon, C. D. Cool et al., "Peroxisome proliferator-activated receptor gamma (PPARγ) expression is decreased in pulmonary hypertension and affects endothelial cell growth," *Circulation Research*, vol. 92, no. 10, pp. 1162–1169, 2003.

[95] J. Tian, A. Smith, J. Nechtman et al., "Effect of PPARγ inhibition on pulmonary endothelial cell gene expression: gene profiling in pulmonary hypertension," *Physiological Genomics*, vol. 40, no. 1, pp. 48–60, 2009.

Hindawi
Mediators of Inflammation
Volume 2021, Article ID 3002439, 10 pages
https://doi.org/10.1155/2021/3002439

Research Article

Polymorphism of CD14 Gene Is Associated with Adverse Outcome among Patients Suffering from Cardiovascular Disease

Susanne Schulz,[1] Martin Zielske,[1] Sascha Schneider,[1] Britt Hofmann,[2] Hans-Günter Schaller,[1] Axel Schlitt,[3,4] and Stefan Reichert[1]

[1]*Department of Operative Dentistry and Periodontology, Martin Luther University of Halle-Wittenberg, Germany*
[2]*Department of Cardiac Surgery, Mid-German Heart Centre of the University Hospital Halle (Saale), Martin Luther University of Halle-Wittenberg, Germany*
[3]*Department of Internal Medicine III, Heart Centre of the University Clinics Halle (Saale), Martin Luther University of Halle-Wittenberg, Germany*
[4]*Department for Cardiology, Paracelsus Harzklinik Bad Suderode, Germany*

Correspondence should be addressed to Susanne Schulz; susanne.schulz@medizin.uni-halle.de

Received 12 April 2021; Revised 28 May 2021; Accepted 8 June 2021; Published 8 July 2021

Academic Editor: Dominik Skiba

Background. The biological link between severe periodontitis and cardiovascular disease is well established. Both complex inflammatory diseases are influenced by genetic background. Therefore, the impact of genetic variations of receptors of the innate immune system—(Toll-like receptors (TLRs)) TLR2, TLR4, cluster of differentiation 14 (CD14), and the transcription factor nuclear factor-*κB* (NF-κB)—was investigated. *Materials and Methods.* In this study (ClinicalTrials.gov identifier: NCT01045070), 1002 cardiovascular (CV) patients were included. In a 3-year follow-up period, new vascular events were assessed. SNPs in CD14 (rs2569190), NF-*κB* (rs28362491), TLR2 (rs5743708), and TLR4 (rs4986790) were genotyped. The impact of these genetic variants on severe periodontitis as well as on CV outcome was assessed. *Results.* All investigated genetic variants were not associated with preexisting CV events or severe periodontitis in CV patients. In Kaplan-Meier survival analyses, the CT genotype of CD14 single-nucleotide polymorphism (SNP) rs2569190 was shown to be an independent predictor for combined CV endpoint (log rank: $p = 0.035$; cox regression; hazard ratio: 1.572; $p = 0.044$) as well as cardiovascular death (log rank: $p = 0.019$; cox regression; hazard ratio: 1.585; $p = 0.040$) after three years of follow-up. *Conclusions.* SNPs in CD14, NF-*κB*, TLR2, and TLR4 are no risk modulators for preexisting CV events or severe periodontitis in CV patients. The CT genotype of CD14 SNP rs2569190 provides prognostic value for further CV events within 3 years of follow-up.

1. Introduction

The immune system consists of a multitude of innate immune receptors to recognize pathogens. Among these receptors, pattern recognition receptors (PRRs), including the Toll-like receptors (TLRs) and cluster of differentiation 14 (CD14), have long been established to play a key role in the host defense system [1, 2]. In particular, lipopolysaccharides (LPS) are recognized by TLRs, which are localised in the membranes of immune cells and are the first receptors to be activated in the interaction between pathogen and host interaction [3]. TLR2 is capable of recognizing lipoproteins and peptidoglycans from both Gram-positive and Gram-negative bacteria, as well as LPS and lipoteichoic acid from Gram-positive bacteria [4]. On the other hand, TLR4, in the interaction with the cluster of differentiation (CD14), is able to recognize LPS from Gram-negative bacteria [4]. In the course of the thereby initiated signal transduction cascade, many mediators are produced which contribute to the control of infection. Among these mediators, transcription factor nuclear factor-*κB* (NF-*κB*) is an important control element that is able to promote the immune response by releasing further proinflammatory cytokines [1].

It was shown that in addition to immune cells, cells such as fibroblasts including oral fibroblasts, epithelial cells, and

endothelial cells can also contribute to the activation of innate immunity via PRRs [3, 5]. In this context, PRRs, including TLRs and CD14, as well as downstream signal transduction cascades have been implicated in pathogen recognition during periodontal infection [6]. Furthermore, activation of PRRs triggers the inflammatory response in various physiological systems, including the cardiovascular (CV) system. PRRs including downstream signal transduction cascades have been discussed as key contributors to the progression of various CV diseases including, e.g., atherosclerosis and heart failure [3].

A biologically plausible connection between periodontal and CV diseases has been assumed for many years [7]. PRRs and the downstream signal transduction cascade could be provided a biologically appropriate link between these two diseases. Among other things, a common genetic predisposition is discussed as an interface between both diseases [8]. The focus of this study will be on genetic variants of PRR candidate genes CD14, TLR2, TLR4, and NF-*κB* as a representative of downstream regulation. The main attention will be given to functionally important genetic variants for which an association with both diseases could be suspected. In the CD14 gene, a promoter polymorphism (rs2569190; c.-260C/T) was shown to be associated with increased transcriptional activity resulting in higher levels of soluble CD14 [9]. In the TLR4 gene, the SNP rs4986790 (Asp299Gly) was described to be associated with functional alterations that predispose individuals to respond less sensitively to LPS and to have an increased susceptibility to pathogenic bacterial infections [10–12]. SNP rs5743708 in the TLR2 gene (Arg753Gly) has been implicated in reducing the capability of TLR2 to target bacterial cell wall components [13]. In the NK-*κB* gene, the rs28362491 SNP represents a 4 bp ATTG insertion/deletion variation at position −94 bp of the promoter. This polymorphic site has been reported to have a major impact on gene expression, with deletion of ATTG resulting in reduced promoter activity [14]. Due to their functional consequences, all described SNPs are highly involved in the immune response and could thus represent a possible link between periodontal and cardiovascular diseases. And indeed, in a variety of case-control studies as well as in meta-analyses, their impact on periodontitis as well as CV diseases was assessed (CD14 [15–17], NF-*κB* [14, 18, 19], TLR2 [20, 21], and TLR4 [4, 22, 23]).

However, the significance of these SNPs in linking periodontitis and CV diseases has not been at the focus of investigations to date. Based on the data available, we assessed in our study the impact of SNPs in TLR2 (rs5743708), TLR4 (rs4986790), CD14 (rs2569190), and NF-*κB* (rs28362491), on severe periodontitis as well as on the incidence of new CV events within a three year follow-up in a cohort of CV patients.

2. Materials and Methods

2.1. Cohort of Cardiovascular Patients. The present investigation is a substudy of the longitudinal cohort study "Periodontitis and Coronary Heart Disease (CHD)" ClinicalTrials.gov identifier: NCT01045070. A total of 1002 coronary patients of the Department of Internal Medicine III were included in the study consecutively from October 2009 to February 2011. The inclusion and exclusion criteria for coronary patients, including periodontal and cardiovascular examinations, and determination of biochemical parameters have already been described in detail [24]. Therefore, it will only be briefly addressed here. All patients were at least 18 years old and of Caucasian descent. They have been suffering from ≥50% stenosis of a main coronary artery (angiographically proven). All patients had at least 4 of their own teeth.

The exclusion criteria applied were inability to give written informed consent, pregnancy, subgingival scaling, root planning during the last 6 months, antibiotic therapy during the last 3 months, current alcohol or drug abuse, and medication of drugs that potentially cause gingival hyperplasia (e.g., hydantoin, nifedipine, and cyclosporin A).

All patients underwent a standardized cardiovascular and dental examination and were evaluated for biochemical peculiarities. Regarding cardiovascular parameters, the left ventricular ejection fraction was assessed and serum parameters including haemoglobin, interleukin-6, C-reactive protein, low-density lipoprotein, high-density lipoprotein, triglycerides, and creatinine were measured. The dental examination comprised of determining the plaque index and bleeding on probing after 30 seconds at four sites around each tooth. Both maximal clinical probing depth (PD = distance between gingival margin and the bottom of the pocket) and maximum clinical attachment loss (CAL = distance between the cementoenamel junction and the bottom of the pocket) were taken at six sites around each tooth applying a pressure-sensitive dental probe UNC 15 (0.2N) (Aesculap, Tuttlingen, Germany). For calculating the mean values, the maximum values for each tooth were considered.

According to the periodontitis classification of Tonetti and Claffey, the coronary patients were evaluated regarding their severity of periodontitis [25]. A severe periodontitis case was diagnosed if ≥30% of the teeth that were present showed a proximal attachment loss of ≥5 mm. A periodontitis case was considered as the presence of proximal attachment loss of ≥3 mm in ≥2 nonadjacent teeth. All remaining coronary patients exhibit no periodontitis.

After 3 years, a follow-up was performed from November 2013 until January 2015. Data regarding the predefined combined endpoint (myocardial infarction, stroke/transient ischemic attack (TIA), cardiac death, and death caused by stroke) were collected. Using a standardized questionnaire, the patients (or relatives or patient's physicians) were interviewed by mail or phone. If follow-up information could not be obtained from these persons, civil registration offices were contacted and information about current address or date of death was requested.

2.2. Genetic Investigations. The genomic DNA was isolated from leucocytes of venous blood using QIAamp® blood extraction kit (QIAGEN, Hilden, Germany) in accordance with the manufacturer's manual.

For genotyping, specific restriction fragment length polymorphism (RFLP) analyses were established for all SNPs (Table 1).

Table 1: Genotyping methods applied for SNPs in CD14, NF-κB, TLR2, and TLR4.

Gene	SNP	Primer 5′➔3′	Reference sequence	Restriction enzyme
CD14	rs2569190	Forward: gtg cca aca gat gag gtt cac Reverse: cct cct ctg tga acc ctg atc ac	AF097335	HaeIII
NF-κB	rs28362491	Forward: tgc tgc ctg cgt tcc ccg acc atc g Reverse: ccc gca ggg gcc gcg gcg tcc ag	AF213884S1	TaqαI
TLR2	rs5743708	Forward: cat tcc cca gcg ctt ctg caa gct cc Reverse: gga acc tag gac ttt atc gca gct	NM 003264	MspI
TLR4	rs4986790	Forward: gat tag cat act tag acta ct acc tcc atg Reverse: gat caa ctt ctg aaa aag cat tcc cac	NM 138554	NcoI

2.3. Statistical Analyses. Statistical analyses were carried out using the SPSS software 25.0 (SPSS Inc., Chicago, Illinois). Values of $p < 0.05$ were considered to be significant. Metric data were tested for normal distribution using the Kolmogorov-Smirnov test. Categorical variables were documented as percentage and plotted in contingency tables and evaluated using the chi-square test and Yates continuity correction. If the expected cell frequency was <5, Fisher's exact test was applied.

For survival, evaluation Kaplan-Meier analyses with log-rank tests were applied. Confounding effects on survival (adjusted hazard ratios) were investigated using Cox regression.

3. Results

In the present longitudinal cohort study, 1002 patients were prospectively involved. Clinical characteristics of the patients are displayed in Table 2. 953 individuals could be evaluated in the 3-year follow-up (follow-up time: 152.9 ± 49.5 weeks). This corresponded to a dropout rate of 4.9% after three years of follow-up. The total incidence of the combined endpoint was 16.4% (stroke/TIA: $n = 23$, myocardial infarction: $n = 33$, cardiovascular death: $n = 93$, and death from stroke: $n = 7$).

3.1. Possible Association of the Genetic Background and the Prevalence of Periodontitis. Possible associations between SNPs in CD14 (rs2569190), NF-κB (rs28362491), TLR2 (rs5743708), and TLR4 (rs4986790) and the occurrence of severe periodontitis were investigated in the cohort of CV patients. Codominant, dominant, recessive genetic models for all SNPs were tested. In addition, possible associations between allele distribution and severe periodontitis were also included in the assessment. Here, we could not demonstrate any significant associations between genetic markers and the severity of periodontitis (Table 3).

3.2. Genetic Characteristics and the Cardiovascular Prognosis in the 3-Year Follow-Up. The impact of SNPs in CD14 (rs2569190), NF-κB (rs28362491), TLR2 (rs5743708), and TLR4 (rs4986790) on the incidence of combined endpoint defined as CV death, death from stroke, MI, and stroke/TIA was evaluated. In bivariate analyses without taking survival time into account, neither the genotype nor the allele distribution was shown to be associated with the adverse CV outcome (Table 4). However, when survival time as well as further genetic models were considered, a different conclusion was obtained. After Kaplan-Meier analysis and log-rank test, the CT genotype of rs2569190 in the CD14 gene was as a prognostic marker for the combined endpoint ($p = 0.035$) (Figure 1(a)). Carriers of the CT genotype had a considerably poorer prognosis than CC + TT genotype carriers (incidence of combined endpoint: CT: 18.9% vs. CC + TT 13.5%, $p = 0.036$). Taking established cardiovascular risk factors, including increasing age, male gender, body mass index, diabetes mellitus, hypertension, and hypercholesterolemia, as well as severe periodontitis into consideration, the CT genotype was proven as an independent risk modulator of the combined endpoint (HR = 1.572, $p = 0.044$) (Table 5(a)). A detailed examination of the CV endpoint showed that the CT genotype had a particular impact on CV death (Kaplan-Meier analysis including log-rank test: $p = 0.019$, Figure 1(b)). Considering further CV risk markers in Cox regression analysis, the hazard ratio for the CT genotype measured 1.585 ($p = 0.040$) (Table 5(b)).

In this study, increasing age (HR = 1.063, $p < 0.001$) and diabetes mellitus (HR = 2.366, $p < 0.001$) were shown to be additional significant predictors for adverse cardiovascular events (combined endpoint and cardiovascular death (Table 5).

All other genetic combinations of the SNPs investigated in the study did not show prognostic value for combined endpoint.

4. Discussion

The focus of this longitudinal cohort study was to examine the influence of SNPs in PRR genes and a gene of the downstream signal transduction cascade on severe periodontitis and to assess their prognostic significance for future CV events in patients with angiographically proven significant stenosis.

4.1. SNPs and Severe Periodontitis. In this cohort of CV patients, no significant associations between SNPs in CD14 (rs2569190), NF-κB (rs28362491), TLR2 (rs5743708), and TLR4 (rs4986790) and the prevalence of severe periodontitis was proven considering codominant, dominant, and recessive genetic models as well as allele distribution. The studies conducted so far on the possible association of genetic variants in PRRs as well as NF-κB and periodontitis are very heterogeneous.

Considering SNP rs2569190 in the CD14 gene, an association of this SNP with periodontitis could be shown in highly selected case-control studies [26–28]. But in contrast, other

Table 2: Demographical and anamnestic parameters, previous history of diseases, biochemical parameters, and dental parameters of the CV patients.

	CV patients $n = 1002$
Demographical and anamnestic parameters	
Age (years), median ($25^{th}/75^{th}$ IQR)	68.9 (59.8/75)
Male gender (%)	74.0
Current smoking (%)	11.9
Body mass index (kg/m^2), median ($25^{th}/75^{th}$ IQR)	28.1 (25.3/30.9)
History of	
Diabetes mellitus (%)	35.7
Hypertension (%)	87.7
MI (%)	38.8
Stroke/TIA (%)	12.7
Peripheral artery disease (%)	9.6
Dyslipoproteinemia (%)	58.8
Severe periodontitis* (%)	47.4
CV disease known by anamnesis (%)	74.3
CV disease family history (%)	39.8
Biochemical parameters	
C-Reactive protein (mg/l), median ($25^{th}/75^{th}$ IQR)	8.7 (3.4/31.6)
Leukocytes (Gpt/l), median ($25^{th}/75^{th}$ IQR)	7.8 (6.4/9.7)
Interleukin 6 (pg/ml), median ($25^{th}/75^{th}$ IQR)	7.4 (3.7/15.8)
Creatinine (mmol/l), median ($25^{th}/75^{th}$ IQR)	87 (73/107)
Total cholesterol (mmol/l), median ($25^{th}/75^{th}$ IQR)	4.3 (3.7/5.3)
HDL cholesterol (mmol/l), median ($25^{th}/75^{th}$ IQR)	1.0 (0.8/1.2)
LDL cholesterol (mmol/l), median ($25^{th}/75^{th}$ IQR)	2.6 (2.0/3.3)
Triglycerides (mmol/l), median ($25^{th}/75^{th}$ IQR)	1.4 (1.0/1.9)
Periodontal parameters	
Plaque index, median ($25^{th}/75^{th}$ IQR)	0.8 (0.5/1.4)
Clinical attachment loss (mm), median ($25^{th}/75^{th}$ IQR)	4 (3.2/5.1)
Bleeding on probing (%), median ($25^{th}/75^{th}$ IQR)	5.6 (1.9/12.5)
Missing teeth (except 8th) (n), median ($25^{th}/75^{th}$ IQR)	11.0 (5.0/19.0)

*Approximal attachment loss of ≥5 mm in ≥30% of the teeth present. Continuous variables were presented as median ($25^{th}/75^{th}$ interquartiles (IQR)); TIA: transient ischemic attack; MI: myocardial infarction.

case-control studies did not confirm this association [29, 30]. However, in meta-analyses, no association of rs2569190 in the CD14 gene with periodontitis could be confirmed [15, 31]. Furthermore, applying stratified analysis by ethnicity and the severity of periodontitis, no significant associations were assessed between CD14 SNP rs2569190 and periodontitis [15, 31]. Investigating the impact of these SNPs on the occurrence of aggressive or chronic periodontitis, a meta-analysis was performed [17]. And again, no significant genetic impact could be evaluated.

Although the importance of NF-κB in the immune response is undisputed, only few case-control studies have been conducted to investigate possible association of the SNP rs28362491 with periodontitis. The study situation is very inconsistent. Whereas, for example, Toker et al. [19] could not show any association of the SNP with periodontitis and Schulz et al. [18] demonstrated that del/del genotype carriers suffered more frequently from aggressive periodontitis.

Recently, case-control studies on the significance of the SNP rs5743708 in the TLR2 gene in periodontitis were summarized in a meta-analysis [20]. In this analysis, no association of this SNP and periodontitis, including disease-specific subgroup analysis (aggressive, chronic periodontitis), was confirmed. However, ethnic stratification revealed an indication that the SNP is associated with periodontitis in Asians [32].

Regarding rs4986790 in the TLR4 gene, the study situation is also heterogeneous. However, it should be emphasized that meta-analyses have not confirmed the association of this SNP in the TLR4 gene with periodontitis, even after stratification for ethnicity and disease severity [31, 33]. In contrast, in a meta-analysis by Chrzęszczyk et al. [34], this SNP was shown to be in association with chronic periodontitis. Furthermore, specific studies have shown that this genetic variant is associated with the occurrence of periodontitis in male [4] and with periodontitis in the presence of *P. gingivalis* infection [35].

All the meta-analyses or case-control studies presented so far have in common that no study evaluated possible associations between these genetic variants and periodontal diseases in a cohort of CV patients. Since periodontitis as a chronic inflammatory disease is characterized by a complex interaction of different mechanisms, factors interrelating with the immune system (e.g., cardiovascular diseases) must be considered as confounding modulators [7]. For this reason, patients of the present study might be particularly predisposed for periodontal inflammation due to their existing CV disease. Consequently, the current genetic results cannot be compared with the studies presented.

4.2. SNPs and the Cardiovascular Prognosis in the 3-Year Follow-Up. Because of their important role in CV disease, we hypothesized that SNPs in PRRs (CD14, TLR2, and TLR4 gene) and the NF-κB gene might also have a prognostic value for further CV events.

SNP rs2569190 located in the promoter of the CD14 gene has been shown to modulate inflammatory stimulation by regulating CD14 gene expression and the concentration of soluble CD14 (sCD14) in plasma [36]. Because of these functional effects in the context of the immune response, the SNP has been attributed an important role in inflammatory diseases.

In a genome-wide association study, the CD14 locus was shown to be associated with CV disease [37]. In particular, the SNP rs2569190 was related to the occurrence of CV

Table 3: Association of genotype and allele distribution of SNPs in CD14, NF-κB, TLR2, and TLR4 and periodontal disease severity.

	All patients	No or mild periodontitis	Severe periodontitis	p value
CD14: rs2569190				
	$n = 928$	$n = 487$	$n = 441$	
CC (%)	30.4	29.8	31.1	
CT (%)	46.6	44.8	48.5	0.182
TT (%)	23.0	25.4	20.4	
	$n = 1856$	$n = 974$	$n = 882$	
C (%)	53.7	52.2	55.3	0.186
T (%)	46.3	47.8	44.7	
NF-κB: rs28362491				
	$n = 927$	$n = 487$	$n = 440$	
II (%)	33.0	31.8	34.3	
ID (%)	51.4	51.5	51.1	0.581
DD (%)	15.6	16.6	14.6	
	$n = 1854$	$n = 974$	$n = 880$	
I (%)	58.7	57.6	59.9	0.341
D (%)	41.3	42.4	40.1	
TLR2: rs5743708				
	$n = 939$	$n = 493$	$n = 446$	
AA (%)	94.5	93.7	95.3	
AG (%)	5.4	6.1	4.7	0.389*
GG (%)	0.1	0.2	0	
	$n = 1878$	$n = 986$	$n = 892$	
A (%)	97.2	96.8	97.6	0.305
G (%)	2.8	3.2	2.4	
TLR4: rs4986790				
	$n = 942$	$n = 494$	$n = 448$	
AA (%)	91.4	92.7	90.0	
AG (%)	8.4	7.1	9.8	0.237*
GG (%)	0.2	0.2	0.2	
	$n = 1884$	$n = 988$	$n = 896$	
A (%)	95.6	96.3	94.9	0.175
G (%)	4.4	3.7	5.1	

*Fisher's exact test.

diseases in case-control studies as well as meta-analysis [16, 38, 39]. In meta-analyses, the TT genotype and T allele of rs2569190 have been associated with ischemic heart diseases [38] and the susceptibility and development of cardiovascular disease [16], particularly in the East Asian population but not European population. In accordance with these studies, we also did not demonstrate a genetic influence of CD14 SNP rs2569190 on the incidence of cardiovascular preexisting conditions (stroke, myocardial infarction, and peripheral arterial disease) in the present European cohort of CV patients.

However, the focus of the present study should be on the impact of SNPs on CV prognosis. In the presented study, the CT genotype of CD14 SNP rs2569190 was demonstrated to be associated with an adverse CV outcome in relation to the combined CV endpoint (log-rank: $p = 0.035$; cox regression; hazard ratio: 1.572; $p = 0.044$) as well as cardiovascular death (log-rank: $p = 0.019$; cox regression; hazard ratio: 1.585; $p = 0.040$) after three years of follow-up.

So far, only few data are known about a possible prognostic significance of the SNP rs2569190 with regard to the cardiovascular outcome. In a study by Porsch-Ozcürümez et al., T allele carriers were shown to have a 3.6-fold higher risk for nonlethal CV events (log-rank test = 0.029) in a 4-year follow-up period [40]. In contrast, in the present study, the TT genotype or T allele was not proven to be independent predictors for CV prognosis. Although the inclusion criteria of this study were comparable to those of the present study (≥50% stenosis of a main coronary artery; CV patients of a similar geographical region: Central Germany, Saxony-Anhalt),

Table 4: Association of genotype and allele distribution of SNPs in CD14. NF-κB. TLR2 and TLR4 and occurrence of combined endpoint (stroke/TIA. myocardial infarction. Cardiovascular death. Death from stroke).

	All patients	No or mild periodontitis	Severe periodontitis	*p* value
CD14: rs2569190				
	n = 881	*n* = 740	*n* = 141	
CC (%)	30.6	31.9	24.1	
CT (%)	46.2	44.6	54.6	0.074
TT (%)	23.2	23.5	21.3	
	n = 1762	*n* = 1480	*n* = 282	
C (%)	53.7	54.2	51.4	0.429
T (%)	46.3	45.8	48.6	
NF-κB: rs28362491				
	n = 880	*n* = 738	*n* = 142	
II (%)	32.7	33.5	28.9	
ID (%)	51.4	50.9	53.5	0.537
DD (%)	15.9	15.6	17.6	
	n = 1760	*n* = 1476	*n* = 284	
I (%)	58.4	58.9	55.6	0.332
D (%)	41.6	41.1	44.4	
TLR2: rs5743708				
	n = 892	*n* = 749	*n* = 143	
AA (%)	94.5	94.4	95.1	
AG (%)	5.4	5.5	4.9	1.000*
GG (%)	0.1	0.1	0	
	n = 1784	*n* = 1498	*n* = 286	
A (%)	97.2	97.1	97.6	0.840
G (%)	2.8	2.9	2.4	
TLR4: rs4986790				
	n = 895	*n* = 751	*n* = 144	
AA (%)	91.2	91.5	89.6	
AG (%)	8.6	8.3	10.4	0.590*
GG (%)	0.2	0.2	0.0	
	n = 1790	*n* = 1502	*n* = 288	
A (%)	95.5	95.6	94.8	0.650
G (%)	4.5	4.4	5.2	

*Fisher's exact test.

the CV endpoints differed. While Porsch-Ozcürümez et al. defined nonlethal CV events as endpoints in the present study, cardiovascular death and death from stroke were also included as endpoints. Furthermore, the enrolled patients in the present study were $n = 1002$, which is significantly higher than the number of patients in the study of Porsch-Ozcürümez et al. ($n = 69$).

SNP rs28362491 in the ubiquitous transcription factor NF-κB was reported to be involved in the expression of immune-modulating genes due to its impact on NF-κB gene transcription [41]. Therefore, this SNP has been implicated in inflammatory diseases including cardiovascular diseases [14]. In the meta-analysis by Wang et al., the deletion allele was shown to be associated with CV diseases even after stratification by ethnicity and gender [14]. However, a corresponding association could not be confirmed in the present study in the cohort of CV patients. The SNPs including all genetic models were independent of stroke, myocardial infarction, and peripheral arterial disease. However, when comparing the studies, it is important to note that the present study only included patients with a history of cardiovascular disease (inclusion criterion: ≥50% stenosis of a main coronary artery). Furthermore, it was shown that this SNP has no predictive power for an adverse CV outcome in the present study. As this issue has not been addressed in previous studies, no comparisons with the existing evidence can be provided here.

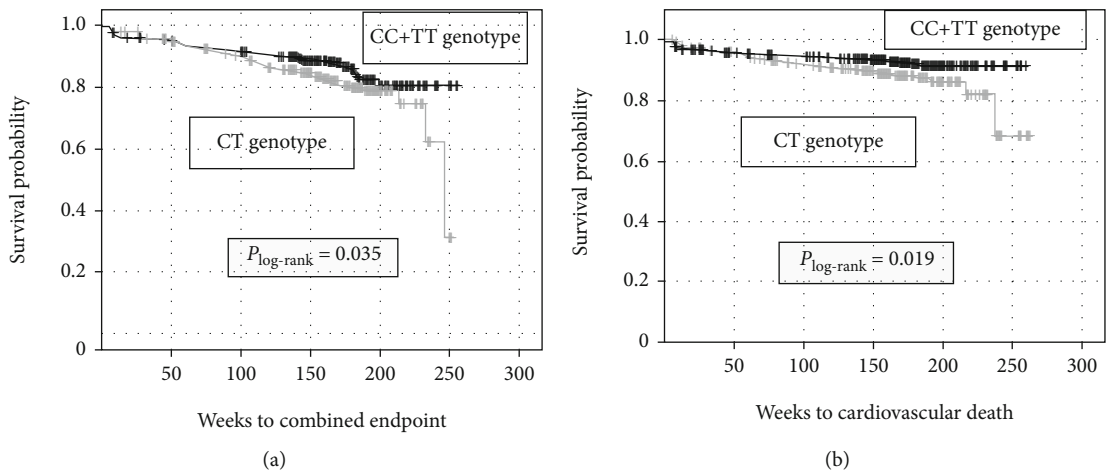

Figure 1: Kaplan-Meier plot for the incidence of the (a) combined endpoint (stroke/TIA, myocardial infarction, cardiovascular death, and death from stroke) and (b) cardiovascular death within a 3-year follow-up period according genotype distribution of CD14 SNP rs2569190. Statistical comparison was made by the log-rank test.

Table 5: Cox regression analysis evaluating the hazard ratio (HR) of the CT genotype of CD14 SNP rs2569190 for the incidence of the (a) combined endpoint (stroke/TIA, myocardial infarction, cardiovascular death, and death from stroke) and (b) cardiovascular death within a 3-year follow-up period (adjusted for age, gender, smoking, body mass index, hypertension, hyperlipoproteinemia, diabetes, and severe periodontitis).

Confounding variables	Hazard ratio	95% lower	CI upper	P values
(a) Endpoint: stroke/TIA, myocardial infarction, cardiovascular death, and death from stroke				
CT genotype rs2569190	*1.572*	*1.012*	*2.439*	*0.044*
Age	1.063	1.035	1.092	<0.001
Diabetes	2.366	1.501	3.729	<0.001
Male gender	1.302	0.784	2.162	0.309
Current smoking	1.572	0.469	5.262	0.463
Hypertension	1. 413	0.706	2.828	0.329
Hyperlipoproteinemia	1.037	0.657	1.636	0.876
Severe periodontitis	1.121	0.721	1.742	0.613
(b) Endpoint: cardiovascular death				
CT genotype rs2569190	*1.585*	*1.020*	*2.500*	*0.040*
Age	1.063	1.035	1.092	<0.001
Diabetes	2.366	1.501	3.729	<0.001
Male gender	1.280	0.772	2.125	0.339
Current smoking	1.563	0.467	5.233	0.469
Hypertension	1. 411	0.705	2.825	0.331
Hyperlipoproteinemia	1.052	0.6668	1.658	0.826
Severe periodontitis	1.116	0.717	1.736	0.626

TLR2 is involved immune response due to its recognition of many pathogen-associated molecular patterns. The SNP rs5743708 has been described to have immediate functional significance regarding altered signaling [42] and might be implicated in inflammatory diseases [21]. A few studies were conducted in order to evaluate the possible association between this SNP and CV diseases; however, results are controversial. Whereas Golovkin et al. did not reveal a genetic influence on infective endocarditis [21], Guven et al. reported on an association with CV susceptibility in Turkish patients [43]. However, in the present study, an influence on cardiovascular burden (stroke, myocardial infarction, and peripheral arterial disease) could not be confirmed in the cohort of CV patients of Central Germany. Since the inclusion criteria of the present study were comparable to those of Guven et al., ethnic characteristics could possibly play a role in the discrepancy of the results.

With regard to a possible prognostic CV power of this SNP, only limited evidence is available so far. Hamann et al. were able to prove an influence of this SNP on restenosis and recommended the inclusion of the SNP in the individual CV profile for risk stratifying as well as for preventive and therapeutic measures [44]. In the present study, however, the influence of this genetic factor on the CV outcome could not be confirmed. The reason for these differences could be found in the follow-up period, which was only 6 months in the study by Hamann et al. and 3 years in the present study. On the other hand, different CV endpoints were referred to (restenosis; present study: CV death, death from stroke, MI, and stroke/TIA).

The TLR4 SNP rs4986790 has been implicated in attenuation of receptor signaling and diminishing the inflammatory response to Gram-negative pathogens. Therefore, its impact on inflammatory diseases including CV diseases was assessed in different studies [23, 45, 46]. But here, as well, the study evidence is very heterogeneous. In an early study by Kiechl et al., investigating 810 individuals, an association of this SNP with CV disease was shown [45]. By contrast, Morange et al. demonstrated that this SNP is not a significant predictor of the CV risk in healthy individuals [46]. These data are in line with the results of two meta-analyses based on 12 and 20 case-control studies, in which nonassociation of this SNP with CV diseases was proven [23, 47]. And also, in the present study, no correlation between this genetic variant and the occurrence of preexisting CV diseases could be shown. Furthermore, SNP rs4986790 in the TLR4 gene has not been associated with cardiovascular prognosis in this study cohort. This result is in line with early studies which demonstrated that in patients with documented CV disease, this SNP was no predictor of future CV events [48] and was not associated with an increased risk of target vessel revascularization or angiographic restenosis after percutaneous coronary intervention [49].

4.3. Limitations of the Study. The presented study was performed as a longitudinal cohort study. It was conducted to establish assumptions of the possible prognostic value of genetic variants of CD14 (rs2569190), NF-*κB* (rs28362491), TLR2 (rs5743708), and TLR4 (rs4986790) on adverse CV events during a 3-year follow-up period. Considering the study design, the verification of these assumptions is not realizable. The results of the current study are representative for coronary patients in Central Germany and cannot be generally extrapolated to the overall population or other patient cohorts. Furthermore, it is advisable to verify the study results in an additional study.

In the 3-year follow-up, the combined CV endpoint (stroke/TIA, myocardial infarction, CV death, and death from stroke) was investigated. These data were obtained from existing medical records or from civil record offices or by interviewing patients or their relatives (standardized questionnaire, telephone interview). Thus, it is possible that false information from patients or their relatives cannot be excluded due to possible personal incorrect interpretations of the state of health.

5. Conclusions

(1) At baseline, SNPs in TLR2 (rs5743708), TLR4 (rs4986790), CD14 (rs2569190), and NF-*κB* (rs28362491) were not associated with the occurrence of severe periodontitis in CV patients

(2) In the 3-year follow-up, the CT genotype of CD14 SNP rs2569190 was proven to be an independent prognostic marker for further cardiovascular events, especially cardiovascular death, considering classical cardiovascular risk factors. All other genetic variants included in the study (NF-*κB* (rs28362491), TLR2 (rs5743708), and TLR4 (rs4986790)) had no predictive cardiovascular value

Confirmation of the prognostic value of the CD14 SNP rs2569190 for CV disease should be obtained in further studies. Potentially, this SNP could complement the individual CV risk profile. Integration of stable genetic markers in the CV risk profile assists in the identification of higher risk patients and supports the improvement of individualized therapy.

Data Availability

All data are available on request from the corresponding author (Susanne Schulz, Martin Luther University Halle-Wittenberg, Medical Faculty, Department of Operative Dentistry and Periodontology, Magdeburger Str. 16, 06112 Halle (Saale), Germany).

Ethical Approval

All investigations were carried out in accordance with the ethical guidelines of the "Declaration of Helsinki" and its amendment in "Tokyo and Venice." The study was approved by the ethics committee of the Martin Luther University of Halle-Wittenberg on 16.11.2016 (approval number: 2016-86).

Consent

Informed written consent was obtained from each patient.

Conflicts of Interest

The authors declare that they have no conflict of interest.

Authors' Contributions

S. Schulz and S. Reichert equally contributed to this work, designed the study, conducted statistical data analysis, confirmed the accuracy of the data, and drafted the manuscript. Dental examinations were performed under the instructions of S. Reichert and H-G. Schaller. Clinical investigations were carried out under the supervision of B. Hofmann and A. Schlitt. M. Zielske and S. Schneider conducted the genetic analyses under the instruction of S. Schulz. All authors have read and agreed to the published version of the manuscript. All authors have given their consent for publication.

Acknowledgments

We would like to thank all the patients with coronary heart disease for their cooperation. The study was supported by a grant from the Deutsche Herzstiftung, Frankfurt am Main, Germany (F/34/08), and by an unrestricted grant from HAIN-Diagnostica®, Nehren, Germany. We acknowledge the financial support of the Open Access Publication Fund of the Martin Luther University Halle-Wittenberg.

References

[1] K. Lucas and M. Maers, "Role of the Toll like receptor (TLR) radical cycle in chronic inflammation: possible treatments targeting the TLR4 pathway," *Molecular Neurobiology*, vol. 48, no. 1, pp. 190–204, 2013.

[2] C. R. Pinheiro, A. L. Coelho, C. E. de Oliveira et al., "Recognition of Candida albicans by gingival fibroblasts: the role of TLR2, TLR4/CD14, and MyD88," *Cytokine*, vol. 106, pp. 67–75, 2018.

[3] R. I. Jaén, A. Val-Blasco, P. Prieto et al., "Innate immune receptors, key actors in cardiovascular diseases," *JACC: Basic to Translational Science*, vol. 5, no. 7, pp. 735–749, 2020.

[4] J. M. V. Zacarias, J. B. de Alencar, P. Y. Tsuneto et al., "The influence of TLR4, CD14, OPG, and RANKL polymorphisms in periodontitis: a case-control study," *Mediators of Inflammation*, vol. 2019, Article ID 4029217, 10 pages, 2019.

[5] A. Matucci, E. Maggi, and A. Vultaggio, "Cellular and humoral immune responses during tuberculosis infection: useful knowledge in the era of biological agents," *The Journal of Rheumatology. Supplement*, vol. 91, pp. 17–23, 2014.

[6] B. Song, Y. L. Zhang, L. J. Chen et al., "The role of Toll-like receptors in periodontitis," *Oral Diseases*, vol. 23, no. 2, pp. 168–180, 2017.

[7] M. Sanz, A. Marco Del Castillo, S. Jepsen et al., "Periodontitis and cardiovascular diseases: consensus report," *Journal of Clinical Periodontology*, vol. 47, no. 3, pp. 268–288, 2020.

[8] G. Aarabi, T. Zeller, H. Seedorf et al., "Genetic susceptibility contributing to periodontal and cardiovascular disease," *Journal of Dental Research*, vol. 96, no. 6, pp. 610–617, 2017.

[9] T. D. LeVan, J. W. Bloom, T. J. Bailey et al., "A common single nucleotide polymorphism in the CD14 promoter decreases the affinity of Sp protein binding and enhances transcriptional activity," *Journal of Immunology*, vol. 167, no. 10, pp. 5838–5844, 2001.

[10] N. C. Arbour, E. Lorenz, B. C. Schutte et al., "TLR4 mutations are associated with endotoxin hyporesponsiveness in humans," *Nature Genetics*, vol. 25, no. 2, pp. 187–191, 2000.

[11] C. Schmitt, A. Humeny, C. M. Becker, K. Brune, and A. Pahl, "Polymorphisms of TLR4: rapid genotyping and reduced response to lipopolysaccharide of TLR4 mutant alleles," *Clinical Chemistry*, vol. 48, no. 10, pp. 1661–1667, 2002.

[12] D. M. Agnese, J. E. Calvano, S. J. Hahm et al., "Human Toll-like receptor 4 mutations but not CD14 polymorphisms are associated with an increased risk of Gram-negative infections," *The Journal of Infectious Diseases*, vol. 186, no. 10, pp. 1522–1525, 2002.

[13] N. W. Schroder, C. Hermann, L. Hamann, U. B. Gobel, T. Hartung, and R. R. Schumann, "High frequency of polymorphism Arg753Gln of the Toll-like receptor-2 gene detected by a novel allele-specific PCR," *Journal of Molecular Medicine*, vol. 81, no. 6, pp. 368–372, 2003.

[14] Y. Wang, B. Wu, M. Zhang, H. Miao, and J. Sun, "Significant association between rs28362491 polymorphism in NF-κB1 gene and coronary artery disease: a meta-analysis," *BMC Cardiovascular Disorders*, vol. 20, no. 1, p. 278, 2020.

[15] C. Chen, X. Fan, S. Yu et al., "Association between periodontitis and gene polymorphisms of hBD-1 and CD14: a meta-analysis," *Archives of Oral Biology*, vol. 104, pp. 141–149, 2019.

[16] J. J. Xu, K. Q. Liu, Z. M. Ying et al., "Effect of CD14 polymorphisms on the risk of cardiovascular disease: evidence from a meta-analysis," *Lipids in Health and Disease*, vol. 18, no. 1, p. 74, 2019.

[17] M. X. Han, C. Ding, and H. M. Kyung, "Genetic polymorphisms in pattern recognition receptors and risk of periodontitis: evidence based on 12,793 subjects," *Human Immunology*, vol. 76, no. 7, pp. 496–504, 2015.

[18] S. Schulz, L. Hierse, W. Altermann et al., "The del/del genotype of the nuclear factor-kappaB -94ATTG polymorphism and its relation to aggressive periodontitis," *Journal of Periodontal Research*, vol. 45, no. 3, pp. 396–403, 2010.

[19] H. Toker, E. P. Görgün, and E. M. Korkmaz, "Analysis of IL-6, IL-10 and NF-κB gene polymorphisms in aggressive and chronic periodontitis," *Central European Journal of Public Health*, vol. 25, no. 2, pp. 157–162, 2017.

[20] C. Shan, A. Aisaiti, Z. P. Wu, T. T. Wang, and J. Zhao, "Association of TLR-2 gene polymorphisms with the risk of periodontitis: a meta-analysis," *Disease Markers*, vol. 6, Article ID 9353958, 2020.

[21] A. S. Golovkin, A. V. Ponasenko, A. E. Yuzhalin et al., "An association between single nucleotide polymorphisms within _TLR_ and _TREM-1_ genes and infective endocarditis," *Cytokine*, vol. 71, no. 1, pp. 16–21, 2015.

[22] S. H. Jin, X. Y. Guan, W. H. Liang, G. H. Bai, and J. G. Liu, "TLR4 polymorphism and periodontitis susceptibility: a meta-analysis," *Medicine (Baltimore)*, vol. 95, no. 36, article e4845, 2016.

[23] R. Chen, N. Gu, Y. Gao, and W. Cen, "TLR4 Asp299Gly (rs4986790) polymorphism and coronary artery disease: a meta-analysis," *PeerJ*, vol. 26, no. 3, article e1412, 2015.

[24] S. Schulz, H. Lüdike, M. Lierath et al., "C-reactive protein levels and genetic variants of CRP as prognostic markers for combined cardiovascular endpoint (cardiovascular death, death from stroke, myocardial infarction, and stroke/TIA)," *Cytokine*, vol. 88, pp. 71–76, 2016.

[25] M. S. Tonetti and N. Claffey, "European Workshop in Periodontology group C, advances in the progression of periodontitis and proposal of definitions of a periodontitis case and disease progression for use in risk factor research. Group C consensus report of the 5th European Workshop in Periodontology," *Journal of Clinical Periodontology*, vol. 32, pp. 210–213, 2005.

[26] D. Ishaan, H. Parthasarathy, D. Ponnaiyan, and A. Tadepalli, "TheCD14 rs2569190 TT genotype is associated with chronic periodontitis," *Genetic Testing and Molecular Biomarkers*, vol. 21, no. 9, pp. 560–564, 2017.

[27] M. Folwaczny, J. Glas, H. P. Török, K. Fricke, and C. Folwaczny, "The CD14 -159C-to-T promoter polymorphism in periodontal disease," *Journal of Clinical Periodontology*, vol. 31, no. 11, pp. 991–995, 2004.

[28] M. L. Laine, S. A. Morré, L. S. Murillo, A. J. van Winkelhoff, and A. S. Peña, "CD14 and TLR4 gene polymorphisms in adult

periodontitis," *Journal of Dental Research*, vol. 84, no. 11, pp. 1042–1046, 2005.

[29] S. Schulz, N. Zissler, W. Altermann et al., "Impact of genetic variants of CD14 and TLR4 on subgingival periodontopathogens," *International Journal of Immunogenetics*, vol. 35, no. 6, pp. 457–464, 2008.

[30] L. I. Holla, D. Buckova, A. Fassmann, T. Halabala, A. Vasku, and J. Vacha, "Promoter polymorphisms in the CD14 receptor gene and their potential association with the severity of chronic periodontitis," *Journal of Medical Genetics*, vol. 39, no. 11, pp. 844–848, 2002.

[31] J. Zheng, T. Hou, L. Gao et al., "Association between CD14 gene polymorphism and periodontitis: a meta-analysis," *Critical Reviews in Eukaryotic Gene Expression*, vol. 23, no. 2, pp. 115–123, 2013.

[32] G. Zhu, C. Li, Z. Cao, E. F. Corbet, and L. Jin, "Toll-like receptors 2 and 4 gene polymorphisms in a Chinese population with periodontitis," vol. 39, Quintessence International, Berlin, Germany:1985, 2008.

[33] G. G. Song, J. H. Kim, and Y. H. Lee, "Toll-like receptor (TLR) and matrix metalloproteinase (MMP) polymorphisms and periodontitis susceptibility: a meta-analysis," *Molecular Biology Reports*, vol. 40, no. 8, pp. 5129–5141, 2013.

[34] D. Chrzęszczyk, T. Konopka, and M. Ziętek, "Polymorphisms of Toll-like receptor 4 as a risk factor for periodontitis: meta-analysis," *Advances in Clinical and Experimental Medicine*, vol. 24, no. 6, pp. 1059–1070, 2015.

[35] R. M. Sellers, J. B. Payne, F. Yu, L. V. TD, C. Walker, and T. R. Mikuls, "TLR4 Asp299Gly polymorphism may be protective against chronic periodontitis," *Journal of Periodontal Research*, vol. 51, no. 2, pp. 203–211, 2016.

[36] T. Griga, W. Klein, J. T. Epplen, U. Hebler, A. Stachon, and B. May, "CD14 expression on monocytes and soluble CD14 plasma levels in correlation to the promotor polymorphism of the endotoxin receptor CD14 gene in patients with inactive Crohn's disease," *Hepato-Gastroenterology*, vol. 52, pp. 808–811, 2004.

[37] A. P. Reiner, E. M. Lange, N. S. Jenny et al., "Soluble CD14: genomewide association analysis and relationship to cardiovascular risk and mortality in older adults," *Arteriosclerosis, Thrombosis, and Vascular Biology*, vol. 33, no. 1, pp. 158–164, 2013.

[38] H. F. Zhang, B. L. Zhong, W. L. Zhu et al., "CD14 C-260T gene polymorphism and ischemic heart disease susceptibility: a HuGE review and meta-analysis," *Genetics in Medicine*, vol. 11, no. 6, pp. 403–408, 2009.

[39] T. A. Nakada, W. Takahashi, E. Nakada, T. Shimada, J. A. Russell, and K. R. Walley, "Genetic polymorphisms in sepsis and cardiovascular disease: do similar risk genes suggest similar drug targets?," *Chest*, vol. 155, no. 6, pp. 1260–1271, 2019.

[40] M. Porsch-Ozcürümez, J. Hucke, S. Westphal, J. A. Hubácek, G. Schmitz, and C. Luley, "Post-hoc analysis on the CD14 C(-260)T promoter polymorphism and coronary heart disease," *Physiological Research*, vol. 56, no. 6, pp. 727–733, 2007.

[41] A. S. Karban, T. Okazaki, C. I. Panhuysen et al., "Functional annotation of a novel NFKB1 promoter polymorphism that increases risk for ulcerative colitis," *Human Molecular Genetics*, vol. 13, no. 1, pp. 35–45, 2004.

[42] U. Buwitt-Beckmann, H. Heine, K. H. Wiesmüller et al., "TLR1- and TLR6-independent recognition of bacterial lipopeptides," *The Journal of Biological Chemistry*, vol. 281, no. 14, pp. 9049–9057, 2006.

[43] M. Guven, Z. Ismailoglu, B. Batar et al., "The effect of genetic polymorphisms of TLR2 and TLR4 in Turkish patients with coronary artery disease," *Gene*, vol. 558, no. 1, pp. 99–102, 2015.

[44] L. Hamann, A. Gomma, N. W. Schröder et al., "A frequent Toll-like receptor (TLR)-2 polymorphism is a risk factor for coronary restenosis," *Journal of Molecular Medicine*, vol. 83, no. 6, pp. 478–485, 2005.

[45] S. Kiechl, E. Lorenz, M. Reindl et al., "Toll-like receptor 4 polymorphisms and atherogenesis," *New England Journal of Medicine*, vol. 347, no. 3, pp. 185–192, 2002.

[46] P. E. Morange, L. Tiret, N. Saut et al., "TLR4/Asp299Gly, CD14/C-260T, plasma levels of the soluble receptor CD14 and the risk of coronary heart disease: the PRIME study," *European Journal of Human Genetics*, vol. 12, no. 12, pp. 1041–1049, 2004.

[47] B. W. Wu, J. Zhu, H. M. Shi, B. Jin, and Z. C. Wen, "Association between Toll-like receptor 4 Asp299Gly polymorphism and coronary heart disease susceptibility," *Brazilian Journal of Medical and Biological Research*, vol. 50, no. 9, article e6306, 2017.

[48] S. M. Boekholdt, W. R. Agema, R. J. Peters et al., "Variants of Toll-like receptor 4 modify the efficacy of statin therapy and the risk of cardiovascular events," *Circulation*, vol. 107, no. 19, pp. 2416–2421, 2003.

[49] M. A. Beijk, S. M. Boekholdt, S. Z. Rittersma et al., "Toll-like receptor 4 gene polymorphisms show no association with the risk of clinical or angiographic restenosis after percutaneous coronary intervention," *Pharmacogenetics and Genomics*, vol. 20, no. 9, pp. 544–552, 2010.